LEABHARLANN CHOLÁISTE NA TRÍONÓIDE, BAILE ÁTHA CLIATH | TRINITY COLLEGE LIBRARY DUBLIN
Ollscoil Átha Cliath | The University of Dublin

Terms and Conditions of Use of Digitised Theses from Trinity College Library Dublin

Copyright statement

All material supplied by Trinity College Library is protected by copyright (under the Copyright and Related Rights Act, 2000 as amended) and other relevant Intellectual Property Rights. By accessing and using a Digitised Thesis from Trinity College Library you acknowledge that all Intellectual Property Rights in any Works supplied are the sole and exclusive property of the copyright and/or other IPR holder. Specific copyright holders may not be explicitly identified. Use of materials from other sources within a thesis should not be construed as a claim over them.

A non-exclusive, non-transferable licence is hereby granted to those using or reproducing, in whole or in part, the material for valid purposes, providing the copyright owners are acknowledged using the normal conventions. Where specific permission to use material is required, this is identified and such permission must be sought from the copyright holder or agency cited.

Liability statement

By using a Digitised Thesis, I accept that Trinity College Dublin bears no legal responsibility for the accuracy, legality or comprehensiveness of materials contained within the thesis, and that Trinity College Dublin accepts no liability for indirect, consequential, or incidental, damages or losses arising from use of the thesis for whatever reason. Information located in a thesis may be subject to specific use constraints, details of which may not be explicitly described. It is the responsibility of potential and actual users to be aware of such constraints and to abide by them. By making use of material from a digitised thesis, you accept these copyright and disclaimer provisions. Where it is brought to the attention of Trinity College Library that there may be a breach of copyright or other restraint, it is the policy to withdraw or take down access to a thesis while the issue is being resolved.

Access Agreement

By using a Digitised Thesis from Trinity College Library you are bound by the following Terms & Conditions. Please read them carefully.

I have read and I understand the following statement: All material supplied via a Digitised Thesis from Trinity College Library is protected by copyright and other intellectual property rights, and duplication or sale of all or part of any of a thesis is not permitted, except that material may be duplicated by you for your research use or for educational purposes in electronic or print form providing the copyright owners are acknowledged using the normal conventions. You must obtain permission for any other use. Electronic or print copies may not be offered, whether for sale or otherwise to anyone. This copy has been supplied on the understanding that it is copyright material and that no quotation from the thesis may be published without proper acknowledgement.

Exploring the Role of Lipoxygenases in Oesophageal Cancer and the Anti-Angiogenic Potential of Novel Lipoxygenase Inhibitors

A dissertation submitted to Trinity College Dublin, The University of Dublin
for the degree of Doctor of Philosophy

Gillian Moore

Under the supervision of Dr. Graham P. Pidgeon

Departmental Head: Prof. John V. Reynolds

Department of Surgery
School of Medicine
Trinity College Dublin

2016

TRINITY LIBRARY
0 8 MAR 2017
DUBLIN

Thesis 11214

Declaration

I declare that this thesis has not been submitted as an exercise for a degree at this or any other university and it is entirely my own work.

I agree to deposit this thesis in the University's open access institutional repository or allow the library to do so on my behalf, subject to Irish Copyright Legislation and Trinity College Library conditions of use and acknowledgement.

Summary

Over the past decade there has been a dramatic increase in the incidence of oesophageal cancer in Ireland, which has the third highest incidence rate in Europe. This is mainly due to rising numbers of the oesophageal adenocarcinoma (OAC) subtype which is strongly associated with obesity. Despite major improvements to patient outcomes through more advanced chemo-radiation therapy regimes, fewer than 20% of oesophageal cancer patients remain alive 5 years after their diagnosis. Clearly, this cancer represents a burden to the Irish health system and a challenge to clinicians and scientists alike. Thus an increased understanding of the molecular mechanisms underlying this cancer is invaluable and will lead to the identification of novel biomarkers, for both the earlier detection and molecular therapeutic targeting of this disease.

5-lipoxygenase (5-LO) and platelet-type 12-lipoxygenase (12-LO) are two enzymes involved in the metabolism of arachidonic acid to pro-inflammatory bioactive lipids signalling molecules known as eicosanoids. Both 5-LO and 12-LO and their metabolites have been linked to cancer with roles in inflammation, tumourigenesis, angiogenesis and survival reported. The overall aim of this thesis was to explore the role of 5-LO and 12-LO in OAC, which is poorly understood. The clinical significance of 5-LO and 12-LO activity in OAC was investigated in a number of different human biological sample types including OAC biopsy RNA, tumour tissue microarrays (TMA) and serum. Given the newly emerged role of 5-LO signalling in metabolic syndrome and obesity, a role of 5-LO in obesity-associated OAC was also explored in OAC tumour and fat tissue.

A significant limitation of 12-LO studies in cancer is the current dearth of selective inhibitors to investigate the effect of blocking this enzyme pathway. Recently a number of selective 5-LO and 12-LO small molecule inhibitors with different structural derivatives were identified by high-throughput screening. In this thesis the anti-angiogenic potential of these compounds was explored using *in vivo* and *in vitro* models of angiogenesis. Aside from the direct targeting of angiogenesis in growing vessels, anti-angiogenic therapies in cancer may also elicit effects by the alternate suppression of pro-angiogenic signalling by cancer cells. To this effect, this thesis explored the efficacy of novel 5-LO and 12-LO inhibitors as both anti-cancer and anti-angiogenic agents using an *in vitro* OAC cell culture model and an *ex vivo* OAC tumour biopsy model.

Significant associations between 5-LO or 12-LO expression and clinical parameters identified in the TMA study reflect an earlier OAC tumour phenotype. For example 5-LO

stromal staining was associated with lower T-stage and a history of Barrett's metaplasia suggesting an involvement in the state of chronic inflammation preceding cancer development. Similarly, OAC 12-LO epithelial and stromal expression was significantly associated with lower T-stage and shorter tumour length, while western blotting revealed higher 12-LO expression in tissue biopsied adjacent to the tumour compared to the tumour mass itself. Thus indicating that 5-LO and 12-LO signalling may be involved in tumour initiation. A significant association between OAC tumour or omental adipose tissue derived 5-LO expression, or LTB4 serum levels, and patient obesity status was observed and may suggest a novel involvement in obesity-driven disease. Interestingly 5-LO stromal expression was associated with hot spots of microvessel density in the tumour and a number of immune cell markers, indicating a potential role in modulating neoangiogenesis and inflammatory responses at the tumour site. 12-LO tumour epithelial and stromal expression showed positive correlations with VEGF and VEGFR2/KDR expression. A similar significant correlation between 12-LO metabolite 12(S)HETE serum levels with VEGF was also reported. Thus indicating a potential role of 12-LO in OAC tumour-associated angiogenesis.

Screening of novel LO inhibitors in angiogenic assays revealed NIH13, as a potent anti-angiogenic compound that could suppress proliferation and tubule formation of HUVEC human endothelial cells and induce apoptotic effects at higher doses. NIH13 downregulated the gene expression of VEGF receptor and co-receptor *KDR* and *NRP1*, *ANGPT1* and the ligand receptors *TIE1* and *TEK*, and the pro-angiogenic chemokine *CXCL1*, suggesting novel utility as an anti-angiogenic agent in OAC or indeed other cancers. The novel 5-LO inhibitor NIH4 and the novel 12-LO inhibitors NIH13 and GM5 were shown to suppress proliferation of OAC cells *in vitro* while causing alterations to the angiogenic secretion profile of *ex vivo* OAC tumours, including soluble bFGF, PlGF, Tie-2, Flt-1 and neuropilin-1. While further work is needed to fully elucidate the hypothesised role of 5-LO and 12-LO in the process of OAC development, this thesis has indicated novel anti-angiogenic potential of 5-LO and 12-LO inhibitors to treat OAC.

Acknowledgements

Firstly, I would like to express my gratitude to my supervisor Dr. Graham Pidgeon. Thank you for seeing potential in me over three years ago when I first met you as an undergrad student and thank you for encouraging me to use my initiative and to embrace independent thinking. Your approachability, invaluable guidance and positivity were greatly appreciated throughout this thesis and I've really enjoyed being part of the Bioactive Lipid research group.

Many thanks to Professor Reynolds for the opportunity to work in such a great department and for your dedication to translational research. To Jacintha and Joanne and all the post-docs: Mary-Clare, Sarah, Niamh, Margaret, Melissa, Mia and Susan, thank you individually for your help, expertise and support in many different ways over the past three years, and for being such great examples of hard-working women in science. It's been a pleasure learning from and working with you all, and I wish you all the best in the future. To Eamon in Flow, and Martin, Kathy and Steven in Thoracic Oncology thanks for all your advice and chats. To Lauren, thank you for all the late night lols in cell culture. To Paul and all the other guys in Pharmacology, thank you for all your advice and help, for allowing me to pretend to be a chemist for the day with my arachidonic acid, and for not kicking me out of your lab when I was in there distracting Mark! Mark, it was so nice having a friend like you during this time: from sharing science woes and wins to sharing a bag of chips from Tony's chipper. Thanks for all the laughs, many a scientific discussion and your constant willingness to lend a hand. You're honestly one of the best scientists I know.

To all the gang in the postgrad reading room, James, Róisín, Maria, Aoife; Ghia, Niamh G and Niamh C, and of course not forgetting our interim reading room members Nadia, Michelle and Eelke...thank you so much for your friendship over the past three years. Thank you for all the laughs, chats, moans and groans, the troubleshooting of experiments gone wrong and high-fiving of those that worked, the regular DailyMail and Journal discussions, fond memories of Dice Bar pizza nights, trips to IACR and of course Lahinch and Liverpool. Just like cake in the postgrad reading room... you guys were always there and I really couldn't have asked for a nicer bunch of people. I'll miss you all terribly! A special word for the troublesome twosome in my corner of the office: Niamhy G and Aoifs...you two are my kindred spirits in so many ways, thank you for everything.

To all my friends from home, particularly Leanne and Mandy, thank you for all your support, for always checking in with me and for still being my friends, despite my absence over the last few months. To Teresa, thank you for being such a good housemate and friend over the last two years and for always sharing your amazing Italian food when I was too busy or tired to cook! To Elaine, thank you for proofreading this thesis with your sharp eye and for reminding me how close the finish line was with each chapter completed (I'll happily return the favour when it's your turn!). To all in the Birch house, thank you for all the words of encouragement, for taking an interest, and for all the lovely dinners and odd glass of vino too!

To my family: Mam, Dad and Stephen, thank you all for your unwavering encouragement of everything that I do. Mam and Dad I don't know where to begin with the list of everything you've done and continue to do for me. Thank you so much for your constant support- emotional, financial and everything in between. I owe you both so very much and only hope that I can continue to make you proud.

Last, but by no means least, Ciarán, thank you so much for always being there for me and trying to understand the foreign language of science (you can have your own copy of my thesis now!). Thanks for all the taxi rides, always listening to my science ramblings and even filling my pipette boxes from time to time! For the late nights spent working together, for making me smile and laugh when I needed it the most and for just generally being lovely...thank you! I couldn't have done it without you.

Table of Contents

Declaration i

Summary ii

Acknowledgements iv

List of Figures xiv

List of Tables xxii

Abbreviations xxiv

Units xxvi

Research presentations and awards xxvii

Chapter 1 General Introduction 1

1.1 Oesophageal cancer 2

1.1.1 The clinical challenge and the requirement for targeted therapies 2

1.1.2 Pathology and epidemiology 4

1.1.3 Staging of oesophageal cancer 9

1.1.4 Current treatment strategies 12

1.2 Personalised medicine 14

1.2.1 The potential of targeted therapies 14

1.3 Challenges in personalised medicine 15

1.4 Potential targeted therapies in oesophageal cancer 18

1.5 Angiogenesis 19

1.5.1 Angiogenesis is a major hallmark of cancer 19

1.5.2 VEGF targeting in cancer: successes and failures 21

1.5.3 Alternative blocking of VEGF receptor with tyrosine kinase inhibitors 25

1.5.4 Resistance to anti-angiogenic molecular targeted therapies: The tumour microenvironment and alternate angiogenic pathways 26

1.6 Progress of anti-angiogenic therapy development to treat oesophageal cancer 29

1.6.1 VEGF inhibition 29

1.6.2 Cyclooxygenase-2: an alternative anti-inflammatory and anti-angiogenic target in cancer 35

1.7 Lipoxygenases and their implication in carcinogenesis and angiogenesis 38

1.7.1 Eicosanoids 38

1.7.2 The family of lipoxygenase enzymes: classification of its members and their associated metabolites 39

1.7.3 5-lipoxygenase and 12-lipoxygenase: potential role in driving cancer 40

1.7.4 Blocking 5-lipoxygenase and 12-lipoxygenase signalling in cancer 43

1.7.5 5-lipoxygenase interaction with immune cells 45

1.7.6 5-lipoxygenase and 12-lipoxygenase: role in tumour angiogenesis and VEGF signalling 46

1.7.7 The potential of 5-lipoxygenase and 12-lipoxygenase inhibitors as molecular targeted therapies in cancer 50

1.7.8 5-lipoxygenase and 12-lipoxygenase in oesophageal cancer: research to date 54

1.8 Aims and objectives 56

1.8.1 Specific objectives 56

Chapter 2 Materials and Methods **57**

2.1 Reagents and general lab equipment 58

2.2 Drugs, chemical reagents and other materials 58

2.3 Cell culture 58

2.3.1 Cell lines 59

2.3.2 Cell counting 60

2.3.3 Mycoplasma testing 60

2.4 Patient tissue samples 61
2.5 Anthropometry 61
2.6 Biological sample preparation 62
2.7 Isolation of RNA from epithelial tissue 63
2.8 Isolation of RNA from adipose tissue 63
2.9 RNA isolation for cells 64
2.10 RNA quantification 64
2.11 cDNA synthesis 65
2.12 Probe-based quantitative reverse transcription polymerase chain reaction 65
2.13 Human Angiogenesis Pathway Finder Array 66
2.14 SYBR-based quantitative reverse transcription polymerase chain reaction 68
2.15 Reverse transcription polymerase chain reaction (RT-PCR) 70
2.16 Immunohistochemistry 71
2.16.1 Staining procedure 71
2.16.2 Imaging and scoring stromal and epithelial staining 72
2.16.3 CD31 microvessel density counts 72
2.17 Cell and tissue lysate preparation 73
2.17.1 Cultured cells 73
2.17.2 Tissue 73
2.18 Protein quantification 73
2.19 Protein SDS-PAGE and Western blotting 74
2.19.1 Protein separation by SDS-PAGE 74
2.19.2 Protein transfer 75
2.19.3 Western blotting 75
2.20 Enzyme-linked Immunosorbent Assay 76
2.20.1 ELISA protein quantification from human serum 76
2.20.2 ELISA protein quantification from *ex vivo* cultured tumour explants 76

2.20.3 ELISA protein quantification from *in vitro* cultured cells 77
2.20.4 Competitive ELISA 78
2.20.5 DuoSet sandwich ELISA 79
2.20.6 Angiogenesis Multi-plex ELISA 80
2.21 Drug screening in *fli1:EGFP* zebrafish 81
2.21.1 Zebrafish husbandry 81
2.21.2 Intersegmental vessel assay 81
2.22 Cell proliferation by BrdU assay 82
2.23 Cell viability by MTT assay 82
2.24 AnnexinV-PI apoptosis assay 83
2.25 Endothelial cell tubule formation assay 84
2.26 12-lipoxygenase overexpression 84
2.26.1 *E.coli* transformation and plasmid amplification 84
2.26.2 Harvesting and purification of plasmid DNA 85
2.26.3 Transient transfection of plasmids in OE33 cells 85
2.27 xCELLigence RTCA for cell proliferation 86
2.28 Statistical analysis 87

Chapter 3 Investigation of 5-lipoxygenase expression in oesophageal cancer and its association with obesity 89

3.1 Introduction 90
3.2 Aims and Objectives 93
3.3 Results 94
3.3.1 Assessment of 5-LO and FLAP expression in OAC tumour and corresponding normal adjacent oesophageal tissue 94
3.3.2 VEGF expression in normal adjacent and OAC tumour biopsies 96
3.3.3 Association of 5-LO, FLAP and VEGF tumour expression with patient obesity status 99
3.3.4 Cytokeratin-8 is expressed in both OAC tumour and macroscopically normal biopsies 101

3.3.5 5-LO and FLAP expression are higher in normal adjacent tissue compared to tumour samples when normalised for columnar epithelium content by cytokeratin-8 103

3.3.6 OAC tumour gene expression and association with clinicopathological data 105

3.3.7 Oesophageal cancer tissue microarray demographics 106

3.3.8 Differential expression of 5-LO, cancer morphology and tissue type 109

3.3.9 OSCC 5-LO expression and clinical data 114

3.3.10 OAC 5-LO expression and clinical data 116

3.3.11 Association of tumour stromal derived 5-LO and obesity status 122

3.3.12 Association of 5-LO expression and angiogenic markers 123

3.3.13 5-LO stromal expression and association with immune markers 124

3.3.14 5-LO metabolite LTB4 levels in OAC patients and correlation with obesity and other clinicoparameters 125

3.3.15 Differential expression of lipoxygenases and VEGF in subcutaneous and omental adipose tissue from OAC patients 128

3.3.16 Association of omental derived lipoxygenase enzymes and VEGF gene expression and obesity status 130

3.4 Discussion 133

Chapter 4 Investigation of the expression of platelet-type 12-lipoxygenase in oesophageal cancer 141

4.1 Introduction 142

4.2 Aims and objectives 147

4.3 Results 148

4.3.1 Assessment of 12-LO and 15-LO-1 gene expression in OAC tumour and normal adjacent biopsies, and correlation with VEGF 148

4.3.2 Assessment of 12-LO protein expression in OAC tumour biopsies and matched normal adjacent tissue 150

4.3.3 12-LO expression in tissue microarray of oesophageal cancer patients 152
4.3.4 Differential 12-LO expression, cancer morphology and tissue type 155
4.3.5 OSCC 12-LO expression and patient clinical parameters 159
4.3.6 OAC 12-LO expression and patient clinical parameters 160
4.3.7 Association of oesophageal cancer 12-LO expression and angiogenic markers 165
4.3.8 Oesophageal cancer 12-LO stromal expression and association with immune markers 170
4.3.9 Oesophageal cancer VEGF and KDR expression and association with clinical parameters 170
4.3.10 12-LO metabolite 12(S)HETE in OAC serum 173
4.3.11 OAC 12(S)HETE levels and correlations with clinical parameters 175
4.3.12 Association of serum 12(S)HETE with VEGF levels in OAC patients 176
4.4 Discussion 177

Chapter 5 Assessment of the anti-angiogenic potential of novel 5-lipoxygenase and 12-lipoxygenase targeted inhibitors 183

5.1 Introduction 184
5.2 Aims and objectives 189
5.3 Results 190
5.3.1 Zebrafish screening 190
5.3.2 5-LO drug screen in the *fli1:EGFP* zebrafish angiogenesis model 192
5.3.3 12-LO drug screen in the *fli1:EGFP* zebrafish angiogenesis model 195
5.3.4 Investigation of the anti-angiogenic potential of 5-LO and 12-LO inhibitors using *in vitro* models 199

5.3.5 Confirmation of *ALOX12* expression in HUVECs 200

5.3.6 Endothelial cell proliferation following 5-LO inhibitor treatment 201

5.3.7 Endothelial cell proliferation following 12-LO inhibitor treatment 203

5.3.8 Investigation of the effect of lipoxygenase inhibitors on endothelial cell tube formation 207

5.3.9 Inhibitor blockage of OAC tissue conditioned medium-induced tubule formation 214

5.3.10 Effect of 12-LO inhibitors on endothelial cell apoptosis 216

5.3.11 Human Angiogenesis Pathway Finder Array: alterations in HUVEC gene expression following novel lipoxygenase inhibitor treatment 220

5.3.12 Validation of selected genes from Human Angiogenesis Pathway Finder array 224

5.3.13 Investigation of the effect of selected lipoxygenase inhibitors on angiogenic protein secretion by HUVECs 227

5.4 Discussion 229

Chapter 6 Assessment of the anti-cancer and anti-angiogenic potential of novel 5-lipoxygenase and 12-lipoxygenase targeted inhibitors in models of oesophageal adenocarcinoma 237

6.1 Introduction 238

6.2 Aims and objectives 241

6.3 Results 242

6.3.1 Confirmation of 5-LO and 12-LO expression in the OE33 cell line model 242

6.3.2 Assessing the effects of selected novel and commercial 5-LO and 12-LO inhibitors on the viability of OE33 cells 243

6.3.3 Assessment of the ability of selected 5-LO and 12-LO inhibitors to induce anti-proliferative effects on OE33 cells 245

6.3.4 Investigation of the ability of selected lipoxygenase inhibitors to induce cytotoxic effects on OE33 cells 248

6.3.5 Assessing 5-LO activity in OAC *in vitro* and *ex vivo* and the potency of 5-LO inhibitors to suppress this activity 253

6.3.6 Transient overexpression of 12-LO in OE33 cells 256

6.3.7 Assessing the potency of 12-LO inhibitors to suppress 12-LO enzyme activity *in vitro* and *ex vivo* 259

6.3.8 Assessment of 12-LO overexpressing OE33 cells using the xCELLigence RTCA 263

6.3.9 Human Angiogenesis Pathway Finder Array: alterations in OE33 gene expression following novel lipoxygenase inhibitor treatment 267

6.3.10 Assessment of VEGF and other angiogenic proteins in OE33 cells and the effect of novel lipoxygenase inhibitor treatment to these factors 272

6.3.11 Assessment of alterations to the OAC angiogenic secretory profile following lipoxygenase inhibitor treatment *ex vivo* 279

6.4 Discussion 285

Chapter 7 Concluding Discussion **295**

7.1 Concluding discussion 296

7.2 Future directions 304

References **309**

Appendices **339**

List of Figures

Figure 1.1 Estimated age-standardised incidence and mortality of oesophageal cancer, 2012 3

Figure 1.2 Oesophageal cancer incidence rate by sex and world area 5

Figure 1.3 Oesophageal cancer (C15) by subtype, European age-standardised incidence rates in females and males in Ireland between 1994 and 2009 6

Figure 1.4 Age-standardised prevalence of overweight and obesity or obesity alone, ages ≥20 years, by sex, 1980–2013 8

Figure 1.5 Association between BMI and cancer incidence: Summary risk estimates by cancer sites for men 9

Figure 1.6 AJCC 7th edition grading system and TNM classifications for oesophageal cancer 10

Figure 1.7 Staging system for OAC by TNM classification and histological grade 11

Figure 1.8 Staging system for OSCC by TNM classification and histological grade 11

Figure 1.9 Disease-specific survival has improved in oesophageal cancer patients treated with curative intent during the period of 2004-2008 vs. the preceding 15 years 13

Figure 1.10 Overall survival of CML patients treated with imatinib, interferon or chemotherapy 15

Figure 1.11 Heterogeneity in cancer occurs at many different levels 17

Figure 1.12 The updated hallmarks and enabling characteristics of cancer 20

Figure 1.13 Cancer specific survival of OAC patients according to high and low VEGF expression 22

Figure 1.14 Two modes of anti-angiogenic therapy resistance are hypothesised to exist in cancer 29

Figure 1.15 Cancer specific survival of OAC patients according to high and low COX-2 expression 36

Figure 1.16 Arachidonic acid metabolism produces bioactive lipid signalling molecules known as eicosanoids 39

Figure 1.17 Summary of cross talk between cancer cells and stromal cells of the tissue microenvironment through 5-LO signalling 41

Figure 1.18 Pharmacological inhibition of COX-2 signalling pathway results in a shunting of arachidonic acid to the 5-LO pathway and vice versa 51
Figure 3.1 5-LO expression is higher in normal adjacent tissue biopsies compared to OAC biopsies 95
Figure 3.2 FLAP OAC tumour biopsy gene expression is similar to the gene expression in normal adjacent tissue biopsies 96
Figure 3.3 VEGF gene expression is not statistically different between OAC tumour and normal adjacent biopsies 97
Figure 3.4 5-LO tumour or normal adjacent gene expression is correlated with FLAP and VEGF expression levels 98
Figure 3.5 VEGF and 5-LO gene expression are associated with visceral obesity in OAC 100
Figure 3.6 Cytokeratin-8 gene expression is higher in OAC tumour biopsies compared to normal adjacent tissue 102
Figure 3.7 5-LO and FLAP expression are higher in normal adjacent tissue compared to tumour biopsies following normalisation with cytokeratin-8 104
Figure 3.8 Tumour gene expression and 5-year disease free survival 105
Figure 3.9 Tissue microarray construction 106
Figure 3.10 5-LO antibody optimisation 108
Figure 3.11 Comparison of 5-LO expression in leading edge and non-leading edge oesophageal cancer 110
Figure 3.12 The majority of 5-LO expression is localised to the stromal compartment in oesophageal cancer 111
Figure 3.13 5-LO tumour epithelial staining was very low or absent from the majority of oesophageal cancer patients while stromal 5-LO was well expressed across the cohort 112
Figure 3.14 Tissue microarray 5-LO stromal staining in oesophageal cancer 113
Figure 3.15 Stromal 5-LO expression was associated with a less aggressive tumour phenotype in OSCC patients 115
Figure 3.16 OSCC patients with above median stromal 5-LO expression have an improved median survival time 116
Figure 3.17 OAC patients with the highest tumour epithelial 5-LO expression tended to have a more aggressive tumour phenotype 118

Figure 3.18 Stromal 5-LO in both leading edge and non-leading edge cores is preferentially expressed in OGJ type I tumours and patients with Barrett's morphology 119
Figure 3.19 Non-leading edge stromal 5-LO expression in neoadjuvant treatment naive patients is associated with Type I OGJ and Barrett's morphology and a lower T-stage 120
Figure 3.20 Leading edge stromal 5-LO trends towards an association with poor survival in neoadjuvant treatment naive OAC patients 121
Figure 3.21 Increased 5-LO stromal expression is associated with obesity measured by BMI in neoadjuvant treatment naive OAC patients 122
Figure 3.22 5-LO stromal positivity is associated with increased microvessel density within tumour cores of leading edge OAC patients 123
Figure 3.23 Average serum LTB4 levels in OAC serum samples are similar to age-matched non-cancer controls 126
Figure 3.24: LTB4 serum levels are associated with obesity measured by BMI in OAC patients 127
Figure 3.25 Differential lipoxygenase expression in adipose tissue from OAC patients 129
Figure 3.26 Omental adipose tissue 5-LO expression is associated with obesity status by multiple parameters in OAC patients 131
Figure 3.27 Differential expression of 15-LO isoforms in obese omental adipose tissue from OAC patients 132
Figure 3.28 Omental VEGF expression is higher in non-obese OAC patients compared to obese patients 133
Figure 4.1 Trends in intensity of lipoxygenase enzymes in normal kidney and RCC 145
Figure 4.2 Platelet-type 12-LO is significantly higher in normal adjacent tissue compared to OAC tumour biopsies 149
Figure 4.3 Normal adjacent OAC tissue 12-LO expression is correlated with corresponding VEGF levels 150
Figure 4.4 12-LO protein levels are higher in macroscopically normal adjacent tissue compared to matched OAC tumour 151
Figure 4.5 Platelet-type 12-LO antibody optimisation 153
Figure 4.6 Tissue microarray 12-LO staining pattern in oesophageal cancer 154
Figure 4.7 Stromal 12-LO expression is higher in OSCC compared to OAC 156

Figure 4.8 12-LO is strongly associated with the tumour epithelium in OAC but it is associated more strongly with the stromal compartment in OSCC 157
Figure 4.9 A variety of low and high expression of epithelial and stromal 12-LO is observed across the oesophageal cancer tissue microarray .. 158
Figure 4.10 OSCC stromal 12-LO at the invasive edge is associated with clinical parameters of a less aggressive tumour phenotype 159
Figure 4.11 Leading edge tumour epithelial 12-LO is associated with a poorer prognosis in OSCC 160
Figure 4.12 Leading edge OAC 12-LO epithelial expression is associated with an absence of dysplasia while stromal expression is associated with an absence of venous involvement 162
Figure 4.13 Non-leading edge OAC 12-LO expression is associated with a shorter tumour length and lower T-stage 163
Figure 4.14 12-LO epithelial expression at the invasive edge shows a non-significant association with increased survival time in OAC patients 164
Figure 4.15 Non-leading edge 12-LO stromal expression and association with survival in chemo-radiation therapy naive patients 165
Figure 4.16 Invasive edge 12-LO expression is correlated with VEGF levels in OSCC 167
Figure 4.17 12-LO epithelial expression at the invasive edge is correlated with corresponding VEGF and KDR levels of expression in OAC 168
Figure 4.18 12-LO epithelial and stromal expression in OAC non-leading edge cores are both associated with VEGF expression 169
Figure 4.19 Invasive edge VEGF expression is associated with a poorer prognosis in OSCC 171
Figure 4.20 Invasive edge KDR expression is associated with a lower T-stage and an improved patient prognosis in OAC 172
Figure 4.21 Serum 12(S)HETE levels are higher in OAC patients compared to non-cancer controls 174
Figure 4.22 Serum 12(S)HETE is associated with decreased recurrence-free survival in OAC 175
Figure 4.23 OAC serum levels of 12(S)HETE correlate with VEGF levels 176
Figure 5.1 *Fli:EGFP* zebrafish embryos were used as an angiogenic screening model 191

Figure 5.2 Novel 5-LO inhibitors do not affect angiogenesis in the zebrafish embryo however ketoconazole has both effects to vessel formation and larval development 193
Figure 5.3 Representative images of zebrafish embryos treated with 5-LO inhibitors 194
Figure 5.4 Novel 12-LO inhibitor NIH15 significantly reduces vessel formation by over thirty percent at a dose of 50 μM 196
Figure 5.5 50 μM NIH15 does not cause any curving of the dorsal axis of the zebrafish and does not have any other untoward morphological effects 197
Figure 5.6 Benzenesulfonamide based 12-LO inhibitors have no effect on angiogenesis or embryonic development in zebrafish 198
Figure 5.7 HUVEC endothelial cells are shown to express *ALOX12* 200
Figure 5.8 All 5-LO inhibitors tested except zileuton decrease HUVEC cell proliferation 202
Figure 5.9 NIH13 and NIH15 are the most potent inhibitors in the original panel with significant inhibition of HUVEC proliferation shown at 1 μM doses 204
Figure 5.10 Non-linear regression analysis using log transformed concentrations was used to calculate the IC_{50} for each 12-LO compound 205
Figure 5.11 12-LO inhibitors GM4, 5 and 6 inhibit HUVEC proliferation at a dose of 25 μM 206
Figure 5.12 Baicalein significantly decreases tubule formation of HUVECs 209
Figure 5.13 NIH6 and NIH13 significantly decrease tubule formation of HUVECs 210
Figure 5.14 NIH15 is the most potent inhibitor of tubule formation of the oxadiazol-2-yl -derived 12-LO inhibitors 211
Figure 5.15 GM4 and GM5 show modest inhibitory effects on tubule formation of HUVECs 212
Figure 5.16 Representative images of control-treated HUVECs versus HUVECs treated with potent 12-LO inhibitors 213
Figure 5.17 Pre-treatment of OAC tumour biopsies with NIH13 decreases the induction of HUVEC tubule formation by tissue conditioned medium 214

Figure 5.18 Images of HUVEC tubule formation induced by tissue conditioned media derived from untreated and NIH13 treated OAC tumour biopsies 215
Figure 5.19 12-LO inhibitors do not induce significant apoptosis in HUVECs by AnnexinV-PI staining, following 24 drug treatment 217
Figure 5.20 NIH13 treatment of HUVECs leads to significantly higher apoptosis at 48 hours compared to other 12-LO inhibitors and the untreated control 218
Figure 5.21 NIH13 treatment of HUVECs leads to significant apoptosis and necrosis at 72 hours compared to other novel 12-LO inhibitors and the untreated control 219
Figure 5.22 Eleven angiogenesis-related genes were chosen for validation which showed overlapping alterations in HUVECs treated with the four novel lipoxygenase inhibitors 223
Figure 5.23 Schematic of eleven angiogenic genes chosen for validation from the Angiogenic Pathway Finder array 223
Figure 5.24 NIH13 treatment significantly decreases *NRP1* and *KDR* gene expression in HUVECs 225
Figure 5.25 NIH13 treatment significantly decreases *ANGPT1, TIE1, TEK* and *CXCL1* gene expression in HUVECs 226
Figure 5.26 PDGF, IL-8, angiopoietin-2 and neuropilin-1 production are not altered in HUVECs following lipoxygenase inhibitor treatment 228
Figure 5.27 GRO-α levels produced by HUVECs are significantly decreased following NIH4, NIH13 and GM5 treatment 229
Figure 6.1 Confirmation of 5-LO and 12-LO expression in the OE33 cell line ... 242
Figure 6.2 Cell viability IC_{50} values of 5-LO inhibitors were established from MTT assay measurements by non-linear regression 243
Figure 6.3 Cell viability IC_{50} values of 12-LO inhibitors were established from MTT assay measurements by non-linear regression 244
Figure 6.4 NIH4 and REV 5901 significantly decrease OE33 cell proliferation at the highest tested dose of 25 μM 246
Figure 6.5 All 12-LO inhibitors significantly decrease cell proliferation at one or more doses tested 247
Figure 6.6 NIH4 does not induce significant apoptosis in OE33 cells up to 72 hours 249
Figure 6.7 Representative dot plots indicating proportion of AnnexinV/PI stained OE33 cells following 24 hour 12-LO inhibitor treatment 250

Figure 6.8 Representative dot plots indicating proportion of AnnexinV/PI stained OE33 cells following 48 and 72 hour treatment with NIH13 251
Figure 6.9 NIH13 induces significantly higher apoptosis at 24 hours and significantly higher necrosis at 72 hours compared to control at both 5 μM and 10 μM doses 252
Figure 6.10 LTB4 production by OE33 cells is decreased by 5-LO inhibitor treatment 254
Figure 6.11 OAC tumour LTB4 secretions are decreased by 5-LO inhibitor treatment 255
Figure 6.12: RT-PCR with nested primers verifies the overexpression of *ALOX12* in OE33 cells transfected with *ALOX12*-pcDNA(+3.1) plasmid 258
Figure 6.13: Probe-based qPCR verifies the overexpression of *ALOX12* in OE33 cells transfected with *ALOX12*-pcDNA(+3.1) plasmid 258
Figure 6.14: 12-LO enzyme activity is significantly higher in *ALOX12* overexpressing OE33 cells compared to wild-type or vector control transfected cells 259
Figure 6.15 12-LO inhibitor treatment of 12-LO overexpressing OE33 cells results in decreased 12(S)HETE production 261
Figure 6.16 12(S)HETE production of OAC tumour biopsies is not altered by 12-LO inhibitor treatment 262
Figure 6.17 Preliminary data suggests 12(S)HETE production is higher in normal adjacent tissue compared to OAC tumour 262
Figure 6.18 12-LO overexpressing OE33 cells demonstrate significantly increased cell adherence and cell spreading in comparison to vector control transfected cells 264
Figure 6.19 12-LO overexpressing OE33 cells demonstrate an increase in cell proliferation compared to vector control transfected cells 265
Figure 6.20 Preliminary results indicate the utility of the xCELLigence platform to investigate the functional effect of novel 12-LO inhibitor treatment on 12-LO overexpressing OE33 cells 266
Figure 6.21 NIH4 did not significantly alter angiogenic genes chosen for validation 270
Figure 6.22 NIH13 significantly downregulates *NRP1* in OE33 cells 271
Figure 6.23 *ALOX12* overexpression in OE33 cells does not alter VEGF gene expression and protein production levels 274

Figure 6.24 Assessment of VEGF production by OE33 cells following lipoxygenase inhibitor treatment 275
Figure 6.25 Assessment of neuropilin-1 production by OE33 cells following lipoxygenase inhibitor treatment 276
Figure 6.26 Assessment of GRO-α production by OE33 cells following lipoxygenase inhibitor treatment 277
Figure 6.27 Assessment of IL-8 production by OE33 cells following lipoxygenase inhibitor treatment 278
Figure 6.28 Assessment of non-VEGF pathway related angiogenic secretions by *ex vivo* cultured biopsies following 5-LO inhibitor treatment 281
Figure 6.29 Assessment of VEGF-related angiogenic secretions by *ex vivo* cultured biopsies following 5-LO inhibitor treatment 282
Figure 6.30 Assessment of non-VEGF related angiogenic secretions by *ex vivo* cultured biopsies following novel 12-LO inhibitor treatment 283
Figure 6.31 Assessment of VEGF-related angiogenic secretions by *ex vivo* cultured biopsies following novel 12-LO inhibitor treatment 284

List of Tables

Table 1.1 Potential therapeutic targets and biomarkers of oesophageal cancer 19

Table 1.2 Phase II and III clinical trials of targeted anti-angiogenic therapies in gastric and oesophageal cancer 32

Table 1.3 Commercially available 5-LO inhibitors in use in preclinical or clinical trials 53

Table 1.4 Natural non-selective 12-LO inhibitors currently available 54

Table 2.1 Reagents and volumes used in cDNA synthesis 65

Table 2.2 FAM-labelled primer probes and corresponding configuration numbers 66

Table 2.3 Primer sequences for SYBR-based PCR 68

Table 2.4 Sequences and amplicon length of primers used for nested RT-PCR 71

Table 2.5 List of antibodies and corresponding dilutions used in immunohistochemistry 72

Table 2.6 List of primary antibodies and corresponding dilutions used for western blotting 76

Table 2.7 LTB4 and 12(S)HETE ELISA kits used and corresponding standard concentration range 79

Table 2.8 DuoSet ELISA reagent standard and antibody specifications 80

Table 2.9 Seeding density, amount of plasmid DNA and volume of reagents used per well in the reverse transfection of OE33 cells 86

Table 3.1 Details of patient demographic used for tumour biopsy gene analysis study 95

Table 3.2 Summary of Spearman's correlation test results with cytokeratin-8 102

Table 3.3 Patient demographic for oesophageal cancer tissue microarray ... 107

Table 3.4 There is no association between 5-LO expression and oesophageal cancer morphology 110

Table 3.5 Summary of positive correlations between 5-LO stromal expression and stromal immune markers or cytokines in oesophageal cancer 124

Table 3.6 Details of OAC patient demographic used for LTB4 serum study 126

Table 4.1 Differential expression of 12-LO between normal adjacent and OAC tissue samples is shown to be consistent at both the gene and protein level..... 152
Table 4.2 Association of 12-LO expression with OAC clinical parameters: a comparison of p-values when patients who received neoadjuvant therapy are excluded..... 165
Table 4.3 Correlation of invasive edge stromal 12-LO expression with immune cell markers in OAC..... 170
Table 4.4 Details of patient demographic used for 12(S)HETE and VEGF serum study..... 173
Table 5.1 List indicating which lipoxygenase inhibitors from the original drug panel are no longer available due to flat structural activity relationship..... 199
Table 5.2 IC_{50} doses for HUVEC proliferation by 5-LO inhibitors determined by non-linear regression analysis..... 203
Table 5.3 IC_{50} doses for HUVEC proliferation by 12-LO inhibitors determined by non-linear regression analysis..... 207
Table 5.4 Fold change in total number of HUVEC tubule loops and tubule branch points formed with oxadiazol-2-yl -derived 12-LO inhibitor treatment compared to control..... 212
Table 5.5 List of HUVEC gene alterations following lipoxygenase inhibitor treatment..... 222
Table 6.1 IC_{50} doses for OE33 cell proliferation by 5-LO and 12-LO inhibitors determined by non-linear regression analysis..... 248
Table 6.2 12-LO overexpressing OE33 cells have an exponential increase in *ALOX12* relative gene expression compared to wild-type or vector control transfected OE33 cells..... 257
Table 6.3 List of gene alterations in OE33 cells following lipoxygenase inhibitor treatment..... 269
Table 6.4 OAC *ex vivo* angiogenic secretion study patient demographic.... 280

Abbreviations

12-LO	Platelet-type 12-lipoxygenase
15-LO-1	15-lipoxygenase
5-LO	5-lipoxygenase
8KRT	gene name for Cytokeratin-8
AA	Arachidonic acid
ACTB	β-actin
AJCC	American Joint Cancer Committee
ADME	Absorption, distribution, metabolism and excretion
ALDH	Aldehyde dehydrogenase
ALOX	Lipoxygenase gene family name
ANG	Angiogenin
ANGPT	Angiopoietin
ANOVA	Analysis of variance
APS	Ammonium persulfate
ATCC	American Tissue Culture Collection
ATP	Adenosine Triphosphate
BCA	Bicinchoninic acid assay
BSA	Bovine serum albumin
bFGF	Basic fibroblast growth factor
BHI	Brain Heart Infusion
BLT	Leukotriene B4 receptor
BMI	Body mass index
BO	Barrett's oesophagus
BSA	Bovine serum albumin
CAPOX	combined capecitabine and oxaliplatin therapy
CI	Cell index
CML	Chronic myeloid leukaemia
COX	Cyclooxygenase
CRT	Chemo-radiation therapy
Ct	Cycle threshold
CXCL	C-X-C chemokine ligand
CysLT	Cysteinyl leukotriene
DFS	Disease free survival
DMBA	7,12-dimethylbenz[a]anthracene
DMSO	Dimethylsulfoxide
DNA	Deoxyribonucleic acid
dNTP	nucleoside triphosphate
DSS	Disease specific survival
ECM	extracellular matrix
EDTA	Ethylenedaminetetraacetic acid
EET	Epoxyeicosatrienoic acid
EGFP	Enhanced green fluorescent protein
ELISA	Enzyme-linked immunosorbent assay
ERK1/2	Extracellular signal regulated kinases 1/2
EUS	Endoscopic ultrasound
F3	Coagulation factor III
FBS	Foetal bovine serum
FDA	Food and Drug Administration
FGF	Fibroblast growth factor
FLAP	5-lipoxygenase activating protein
Flt-1	VEGF receptor-1
FOLFOX4	Oxaliplatin, fluorouracil and leucovorin therapy
G	Tumour grade
GAPDH	Glyceraldehyde 3-phosphate dehydrogenase
GIST	Gastrointestinal stromal tumour
GORD	Gastric oesophageal reflux disease
HER-2	Human epidermal growth factor receptor 2
HETE	Hydroxylated eicosatetraenoic acid
HIF1α	Hypoxia induced factor alpha

HNSCC	Head and neck squamous cell carcinoma
HODE	hydroxyoctanoic acid
HPETE	Hydroperoxy-eicosatetraenoic acids
HRP	Horse radish peroxidase
HUVEC	Human umbilical vein endothelial cells
IL	Interleukin
ISV	Intersegmental vessels
KDR	VEGF receptor 2
LE	Leading edge
LT	Leukotriene
LVES	Large vessel endothelial supplement
MDSC	Myeloid derived suppressor cells
MMP	Matrix metalloproteinase
mRNA	messenger
MTT	3-(4,5-Dimethyl-2-thiazolyl)-2,5-diphenyl-2H-tetrazolium bromide
NCRI	National Cancer Registry Ireland
NDGA	Nor-dihydroguaiaretic acid
NK	Natural killer cell
NLE	Non-leading edge
NRP	Neuropilin-1
NSAID	Non-steroidal anti-inflammatory drug
NSB	Non specific binding
NSCLC	Non-small cell lung cancer
OAC	Oesophageal adenocarcinoma
OE33	Oesophageal adenocarcinoma cell line
OGJ	Oesophagogastric junction
OS	Overall survival
OSCC	Oesophageal squamous cell carcinoma
PBS	Phosphate buffered saline
PDGF	Platelet derived growth factor
PET-CT	Positron emission tomography- computed tomography
PFS	Progression free survival
PG	Prostaglandin
PI	Propidium Iodide
PI3K	Phosphoinositide 3-kinase
PlGF	Placental derived growth factor
PNET	Pancreatic neuroendocrine tumour
pRb	Retinoblastoma protein
PSA	Prostate specific antigen
PUFA	Polyunsaturated fatty acid
PVDF	Polyvinylidene fluoride
qHTS	Quantitative high-throughput screening
qPCR	Quantitative polymerase chain reaction
RCC	Renal cell carcinoma
RNA	Ribonucleic acid
RPMI	Rosa Parks Memorial Institute
RQ	Relative quantification
RTCA DP	Real Time Cell Analyser Dual Plate
RT-PCR	Reverse transcriptase polymerase chain reaction
SAR	Structural activity relationship
SCID	Severe combined immunodeficiency
SD	Standard deviation
SDS	Sodium dodecyl sulfate
SEM	Standard error of the mean
TA	Total activity
TAM	Tumour associated macrophage
TBS	Tris buffered saline
TCM	Tissue conditioned medium
TEK	Gene coding angiopoietin receptor tyrosine kinase 1

TF	Transfection regent only control
TIE	Gene coding angiopoietin receptor tyrosine kinase 2
TIMP	Tissue inhibitor of metalloproteinases
Tis	Carcinoma *in situ*
TKI	Tyrosine kinase inhibitor
TMA	Tissue microarray
TMB	3,3,',5,5'- Tetramethylbenzidine
TME	Tumour microenvironment
TNM	Tumour-Nodal-Metastasis
UT	Untreated
VC	Vector control
VEGF	Vascular endothelial growth factor
VFA	Visceral fat area
WC	Waist circumference

Units

°C	degrees Celsius
bp	base pairs
cfu	colony forming units
cm	centimetre
g	grams
Hz	Hertz
kD	kilodalton
kg	kilogram
M	molar
m	metre
mA	milliamp
mg	milligram
mL	millilitre
mm	millimetre
mM	millimolar
µg	microgram
µL	microlitre
µM	micromolar
ng	nanogram
nm	nanometre
nM	nanomolar
pg	picogram
px	pixel
rpm	revolutions per minute
U	units
V	volts
v/v	volume per volume
w/v	weight per volume
x g	acceleration due to gravity
X	magnification

Research Presentations and Awards

Oral presentations

- Institute of Molecular Medicine Lunch Time Research Seminars – April 2014

Poster presentations

- International Bioactive Lipids Conference, Puerto Rico – November 2013
- TCD School of Medicine Postgraduate Research Day, Dublin – November 2013
- Irish Association for Cancer Research Meeting, Galway – February 2014
- TCD Cancer Conference, Dublin – September 2014
- IMM Annual Meeting – Translational Medicine, Dublin – November 2014
- TCD School of Medicine Postgraduate Research Day, Dublin – December 2014
- Irish Association for Cancer Research Meeting, Limerick – February 2015
- International Bioactive Lipids Conference, Budapest – July 2015

Awards

- EMBARK Postgraduate Research Scholarship Award – September 2012
- Trinity Graduate Studies Travel Grant Award for poster presentation at the International Bioactive Lipids Conference, Puerto Rico – November 2013
- 2nd Place Poster Prize for poster presentation at the Irish Association for Cancer Research Meeting, Limerick – February 2015
- Trinity Graduate Studies Travel Grant Award for poster presentation at the International Bioactive Lipids Conference, Budapest – July 2015
- Cayman Biochemical Travel Award for poster presentation at the International Bioactive Lipids Conference, Budapest – July 2015

Courses attended

- Postgraduate Innovation Academy Creative Thinking and Innovation Module – December 2012
- TCD Ph.D. Skills Workshop – June 2013

Chapter 1 General Introduction

1.1 Oesophageal cancer

1.1.1 The clinical challenge and the requirement for targeted therapies

Oesophageal cancer is the eighth most common cause of cancer in the world with an estimated 456,000 cases confirmed in 2012 (Ferlay J , 2012). It is the sixth most common cause of cancer related deaths, accounting for an estimated 4.9% of all cancer mortalities worldwide, indicating the lethal nature of this disease (Ferlay J, 2012). In Europe, it is the 19th most common cancer with the UK, Ireland and Netherlands having the highest world age-matched incidence and mortality rates for this cancer (Ferlay J, 2012) (Figure 1.1). The incidence rate (cases per 100,000 per year) for oesophageal cancer in Ireland currently stands at 5.2 and 11.4 for females and males respectively, with a total of 386 cases diagnosed per year (National Cancer Registry, 2013). It is associated with a poor prognosis with fewer than 17% of all patients surviving 5 years after diagnosis (Howlader N, 2012). Surgery alone or in combination with neo-adjuvant chemotherapy and/or radiation therapy are the mainstay for treatment of localised disease, and although vast improvements have been made to curative treatment regimes in recent times, the 5 year survival rates remain poor. The 5 year survival rate of patients with non-metastatic disease undergoing treatment is only 36% -42%, with the best outcome observed where negative margins are achieved (Reynolds *et al.*, 2011). Therefore a large amount of patients that receive treatment do not gain any clinical benefit from it. Clearly there is a need to investigate the mechanisms of disease development and progression of this cancer in order to develop new diagnostic tools, and more effective and better tolerated treatment modalities, to supplement existing standards of care.

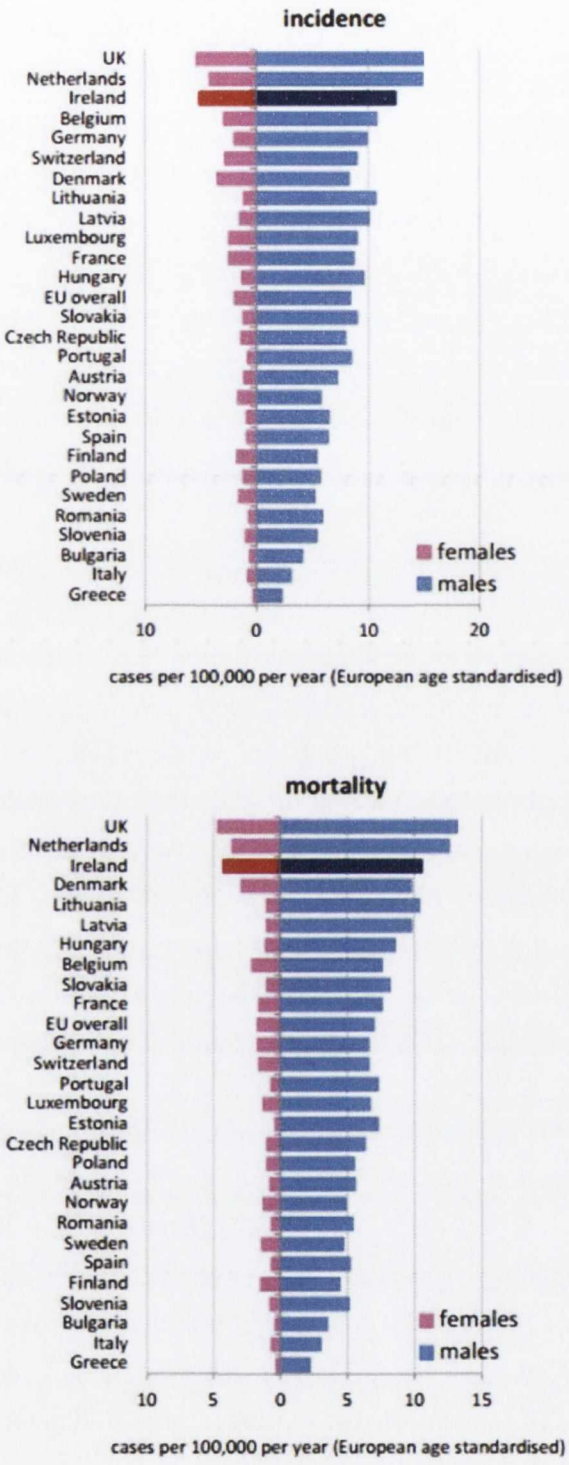

Figure 1.1 Estimated age-standardised incidence and mortality of oesophageal cancer, 2012. The UK, Netherlands and Ireland have the highest incidence rate of oesophageal cancer per 100,000. Reproduced from the National Cancer Registry (2013)

1.1.2 Pathology and epidemiology

There is a difference in oesophageal cancer incidence between genders, being up to 3 or 4 times more common in men than women in most parts of the world (Torre *et al.*, 2015) (Figure 1.2). Oesophageal cancer consists of two main histological subtypes: squamous cell carcinoma (OSCC) and oesophageal adenocarcinoma (OAC). OSCC can occur anywhere along the oesophagus in the squamous cells that line it but is most commonly found in the upper third or middle section. The main risk factors of this subtype include heavy alcohol intake and tobacco, with cancer risk reportedly increasing 3-7 fold in current smokers (Kamangar *et al.*, 2009). OSCC continues to be the major type of oesophageal cancer in South America and Asia with more than half of the global burden of OSCC occurring in China (Zhang *et al.*, 2012).In the highest risk areas known as the "Asian oesophageal cancer belt" extending from Turkey, through Iran and Central Asian republics into Northern China, 90% of oesophageal cancer cases are of the OSCC subtype compared to 26% in the US (Torre *et al.*, 2015). OSCC is the 8th most common cancer in the world due to the high incidence rates in places such as Northern China where it occurs at a frequency of 800 cases per 100,000 people (Chai and Jamal, 2012). Geographical variations and temporal trends of oesophageal cancer are larger than for any other cancer. Historically OSCC was the most common form of oesophageal cancer in the US and Western Europe, however in the last few decades these rates have been declining, mainly due to improved socio-economic standards, and decreased alcohol and tobacco use (Castro *et al.*, 2014). In stark contrast the incidence rate of OAC has been steadily rising in Westernised countries and now exceeds OSCC (Peters and Fitzgerald, 2007, Castro *et al.*, 2014).

In one of the most dramatic epidemiologic shifts ever seen OAC has gone from being a relatively non-existent disease until the 1950s to a current incidence rate that is rising more rapidly than any other malignancy in the US (Brown *et al.*, 2008). Indeed, the rising total number of oesophageal cancer cases seen in countries such as the UK and Ireland in recent decades is primarily due to this massive increase in OAC subtype cases. According to the National Cancer Registry, the incidence of oesophageal cancer has risen in Ireland by 27% in the last 15 years. This is accounted for by a 50% increase in the rate of OAC while the rate of OSCC has fallen by over 4% during the same time period (National Cancer Registry, 2013). In fact while the incidence rate of the squamous cell carcinoma (OSCC) subtype has fallen by 0.9% in females and 1.4% in males between 1994 and 2009, the incidence rate of OAC has increased by 2.2% and 3% per annum in Irish females and males respectively (National Cancer Registry, 2011) (Figure 1.3).

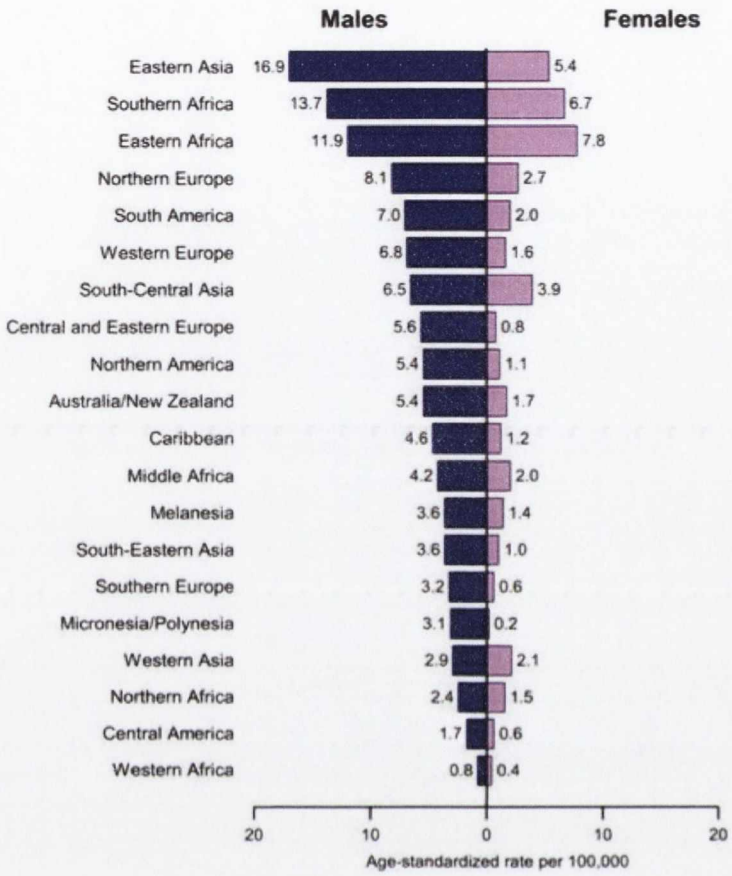

Figure 1.2 Oesophageal cancer incidence rate by sex and world area. Oesophageal cancer is three or four times more common in men than women in most parts of the world. Reproduced from Torre *et al.* (2015)

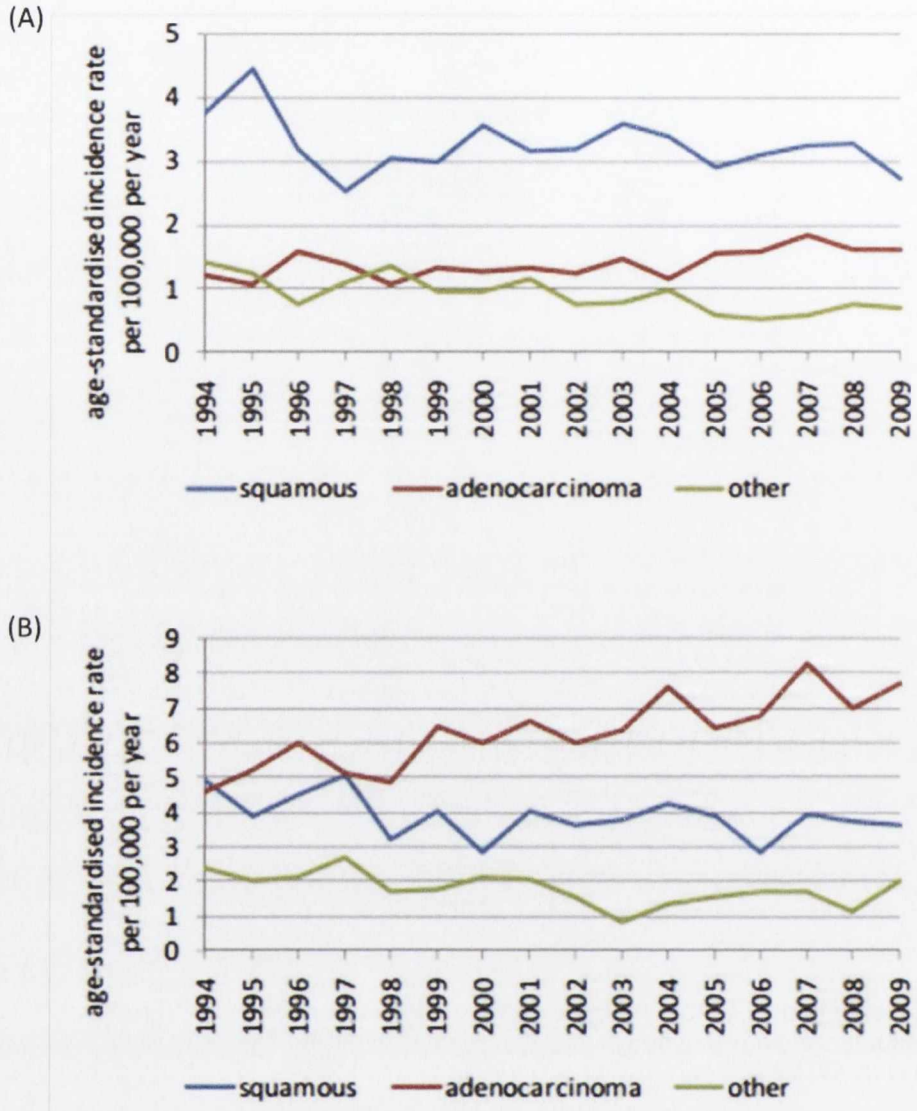

Figure 1.3 Oesophageal cancer (C15) by subtype, European age-standardised incidence rates in females and males in Ireland between 1994 and 2009. Oesophageal cancer incidence rates in (A) females and (B) males. The incidence rate for squamous carcinoma of the oesophagus fell by 0.9% annually for females and 1.4% for males between 1994 and 2009 while the incidence rate for adenocarcinoma increased by 2.2% annually for women and 3.0% for men. Reproduced from the National Cancer Registry (2011).

Most cases of OAC tend to arise in the lower third of the oesophagus where metaplastic glandular cells replace an area of squamous cells following damage, as a result of gastro-oesophageal reflux disease (GORD) or just chronic reflux oesophagitis (Fitzgerald *et al.*, 2014). Over time this cycle of inflammation/ injury may result in the transformation of squamous cells into those with an intestinal columnar phenotype. This is characteristic of the premalignant condition Barrett's oesophagus (BO) and may progress to dysplasia and subsequently OAC. Approximately 10-15% of patients with GORD develop BO (Sharma, 2009). Only a small percentage of BO patients go on to develop OAC. The annual risk for BO patients with and without dysplasia is approximately 6% and 0.25% respectively (Spechler, 2013).

The rise in prevalence of GORD is associated with a rapidly growing obese population (Pandolfino *et al.*, 2006). A recent study showed that rates of obesity and overweight on a global scale have risen by 28% in adults and 47% in children since 1980 due to poor diet and a more sedentary lifestyle (Ng *et al.*, 2014). This obesity epidemic is evident in high income countries such as the US, Australia, the UK and Ireland and is rising particularly in low and middle-income countries (which are home to 62% of the world's obese people) including China, India, Brazil, Mexico, Pakistan, Indonesia and Western Europe (Ng *et al.*, 2014) (Figure 1.4). A massive 66% and 50.9% of Irish men and women, respectively, over 20 years of age are considered overweight or obese according to the latest reports, percentages which are well in excess of the Western European average of 47.6% (Ng *et al.*, 2014). In this study obesity status was determined by body mass index (kg/m^2) (BMI) where a BMI of 25-29 was considered overweight and while $\geq$30 was classified as obese. The impact of obesity on cancer mortality has been described, implying a role in tumour progression (Calle *et al.*, 2003). Excess weight and obesity has been strongly implicated as a major risk factor in the progression of OAC (Calle *et al.*, 2003, Renehan *et al.*, 2008, Ryan *et al.*, 2006), in fact OAC is currently the leading paradigm of an obesity-driven malignancy (Figure 1.5). Despite convincing epidemiological data the underlying mechanisms involved in obesity-driven OAC are not clear. It is hypothesised that excess adipose tissue and excess adipose tissue secreted factors create a pro-tumourigenic environment that can aid in the acquisition of some of the hallmark properties of cancer as described by Hanahan and Weinberg (Hanahan and Weinberg, 2011).

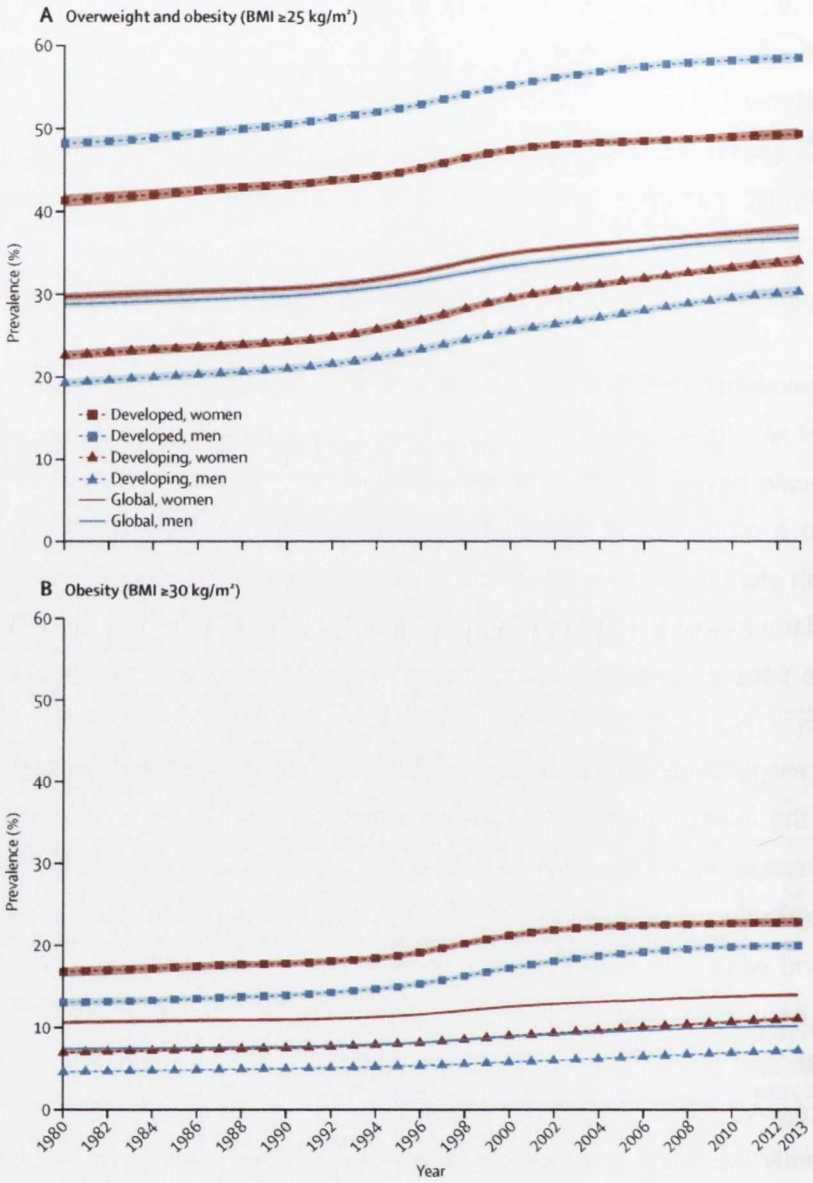

Figure 1.4 Age-standardised prevalence of overweight and obesity or obesity alone, ages ≥20 years, by sex, 1980–2013. Reproduced from Ng *et al.* (2014)

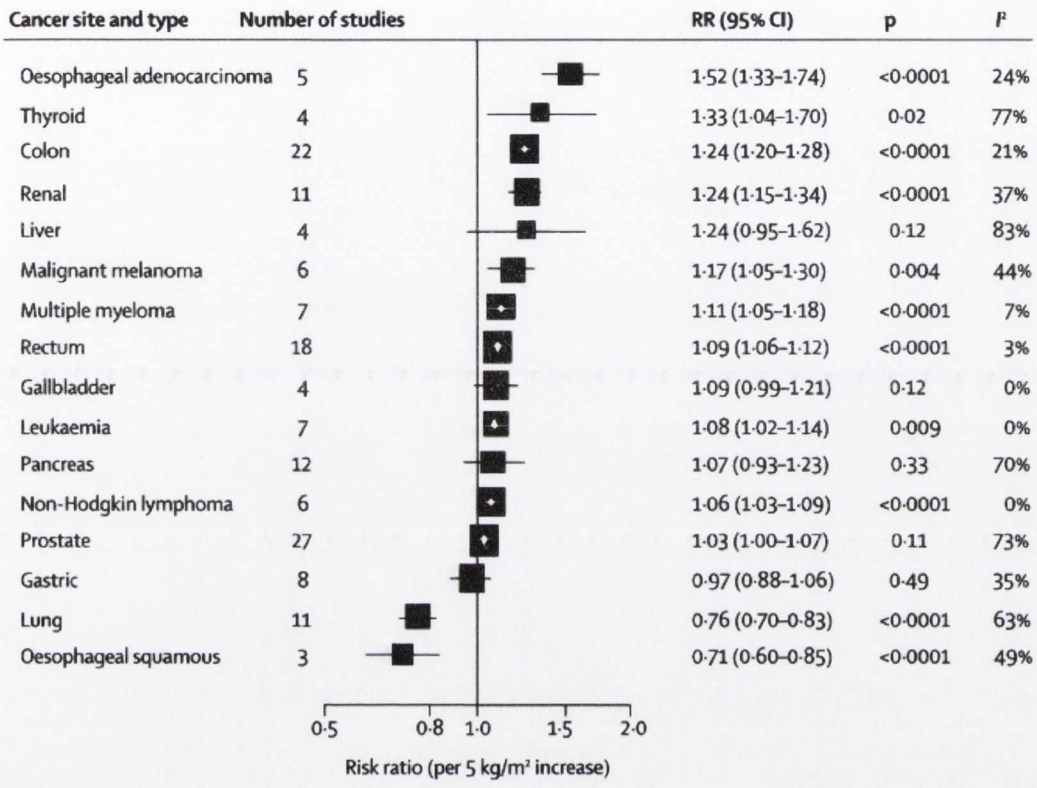

Figure 1.5 Association between BMI and cancer incidence: Summary risk estimates by cancer sites for men. Increased BMI was most strongly associated with OAC. In contrast increased BMI was negatively associated OSCC. Reproduced from Renehan *et al.* (2008)

1.1.3 Staging of oesophageal cancer

Accurate staging of oesophageal cancer is key to determining optimal treatment modalities. In Ireland staging of oesophageal cancer is routinely determined by a combination of positron emission tomography and computed tomography (i.e. PET-CT), endoscopic ultrasound (EUS) or laparoscopy in the case of locally advanced tumours below the diaphragm (Reynolds *et al.*, 2011). The American Joint Committee on Cancer (AJCC) tumour-node-metastasis (TNM) classification system (7th edition) is currently used for staging classification of oesophageal tumours (Rice, 2015). Tumours are classified based on three parameters: depth of invasion (T-stage), lymph node involvement (N-stage) and the presence or absence of distant metastases (M-stage) (Figure 1.6). Non-anatomic classifications including morphological type (squamous vs. adenocarcinoma), tumour location (upper and middle thoracic tumours vs. low thoracic tumours) and histological type (i.e. Grade 1 (G1), G2 or G3). Higher grade is

associated with incrementally decreasing survival in early stage cancers. In OAC G1 and G2 (well and moderately differentiated) are distinguished from G3 (undifferentiated) in early stage cancers (i.e. T1 and T2) (Figure 1.7). In contrast the distinction of G1 from both G2 and G3 is more important for squamous cell carcinoma and tumour location is important in the grouping of T2 and T3 primary tumours (i.e. T2-T3N0M0) (Figure 1.8).

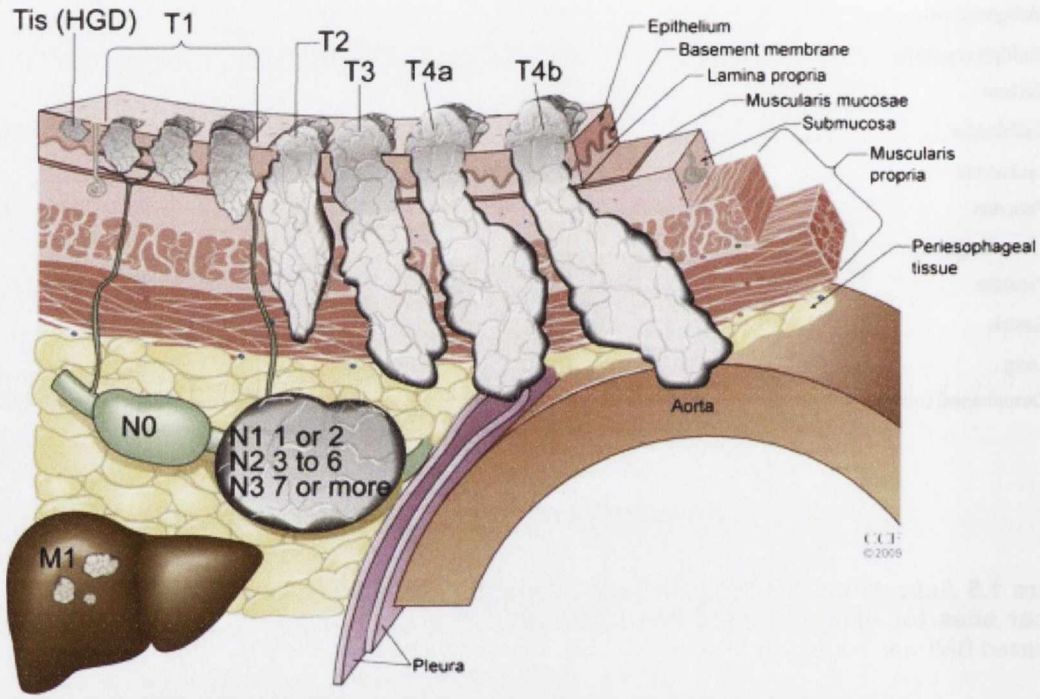

Figure 1.6 AJCC 7th edition grading system and TNM classifications for oesophageal cancer. Tumour (T) is classified as Tis, high grade dysplasia, T1, cancer invades lamina propria or muscularis mucosae (T1a) or submucosa (T1b); T2, invades muscularis propria; T3, invades adventitia, T4, resectable cancer invades adjacent structures, such as pleura, pericardium or diaphragm (T4a) or aorta, vertebral body or trachea (T4b). Lymph nodes (N) classifications are N0, no regional lymph node metastasis; N1, regional lymph node metastasis with 1-2 nodes involved; N2, metastasis involving 3-6 nodes and N3, metastasis with >7 nodes involved. Distant metastasis (M) is classified as M0, none or M1, distant metastasis. Reproduced from Rice (2015).

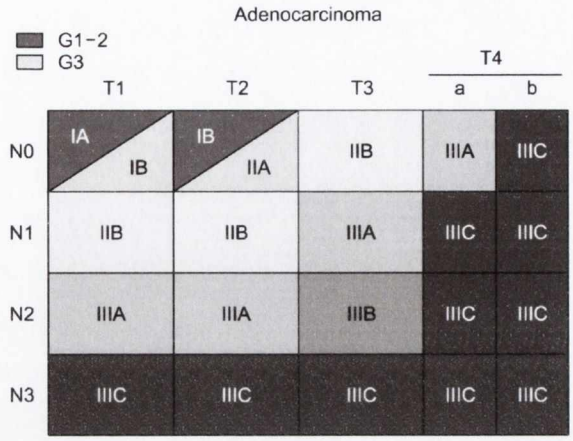

Figure 1.7 Staging system for OAC by TNM classification and histological grade. Reproduced from Rice (2015)

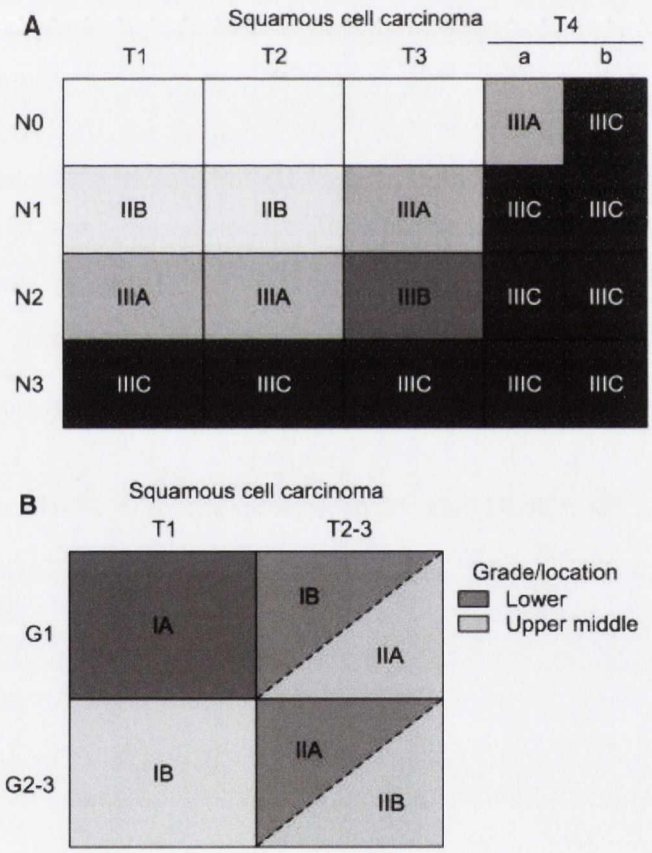

Figure 1.8 Staging system for OSCC by TNM classification and histological grade. Reproduced from Rice (2015)

1.1.4 Current treatment strategies

Despite improvements in early diagnosis of oesophageal cancer, particularly in the case of OAC where cancer can be detected through BO surveillance programmes (Olithselvan *et al.*, 2007, Picardo *et al.*, 2015) only 40-60% of oesophageal cancer patients will present with localised disease that can be treated with curative intent (Hwang *et al.*, 2014). Where patients have localised disease, and are of adequate physical health, they will be treated with curative intent. Surgery alone or in combination with chemotherapy or chemo-radiation therapy (CRT) is the mainstay of treatment for localised disease. Patients with distant metastasis may be suitable for palliative surgery or a combination of chemotherapy and radiation therapy. Palliative chemotherapy improves the quality of life and dysphagia in 60-80% of patients, with typical clinical responses lasting fewer than 4 months (Tew *et al.*, 2005). Tumour response to neoadjuvant CRT is used as a predictor of both disease-free survival (DFS) and overall survival (OS), with improved 5-year survival rates observed in 60% of patients displaying a complete response to CRT (Geh *et al.*, 2001, Reynolds *et al.*, 2007). At the same time however, only about 30% of patients achieve a complete pathological response (Reynolds *et al.*, 2007, van Hagen *et al.*, 2012). Results from the largest neoadjuvant CRT trial presented by van Hagen show an absolute OS benefit of only 7% at 5 years for patients receiving CRT before surgery versus surgery alone. Therefore a large number patients receiving this treatment do not gain any clinical benefit.

Advances in clinical procedures and patient care are demonstrated by a decreasing post-operative mortality rate of less than 2% (Reynolds *et al.*, 2011). Additionally, published data from our department have demonstrated a significantly improved disease-specific survival (DSS) in patients treated with curative intent during the period of 2004-2008 compared to data from the period of 1999-2003 and 1990-1998 (5 year DFS: 43% vs. 35% vs. 28%) (Reynolds *et al.*, 2012) (Figure 1.9). Despite this, prognosis is still poor and a large percentage of patients are not suitable for curative intent and those who are suitable have a high cancer-specific mortality rate. Clearly new treatment strategies, such as molecular targeted therapies, to boost patient responses to current regimes are necessary.

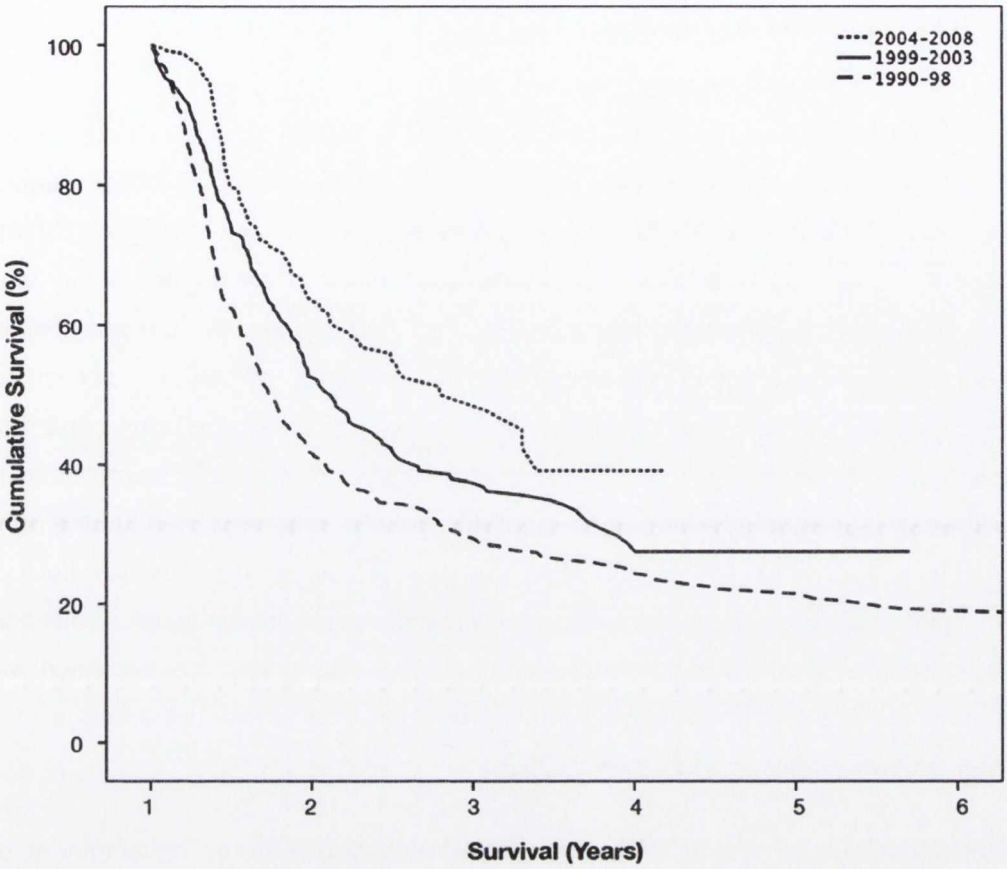

	1990-98		1999-2003		2004-08		p-value (log-rank)
	N	95% CI	n	95% CI	n	95% CI	
Median survival (months)	17.38	14.89-19.87	22.93	18.29-27.58	32.85	24.34-38.15	0.001

Survival	1990-98			1999-2003			2004-2008		
	No at risk	Deaths	% survival	No at risk	Deaths	% survival	No at risk	Deaths	% survival
0 years	471	0	100	254	0	100	342	0	100
1 year	462	151	65	208	51	75	253	65	80
3 years	241	103	36	144	60	43	144	60	55
5 years	151	27	27	99	13	35	84	13	44
10 years	102	15	19	63	8	28	n/a	n/a	n/a

Figure 1.9 Disease-specific survival has improved in oesophageal cancer patients treated with curative intent during the period of 2004-2008 vs. the preceding 15 years. Reproduced from Reynolds *et al.* (2012).

1.2 Personalised medicine

1.2.1 The potential of targeted therapies

The world cancer incidence currently stands at 14 million cases annually (Ferlay *et al.*, 2010). In 2012 there were 8.2 million cancer-related deaths and 32.6 million people living with cancer (within 5 years of diagnosis) (Ferlay *et al.*, 2012, Ferlay *et al.*, 2010). Advances in cancer research and a greater understanding of the heterogeneity and molecular evolution of different cancers has created new avenues for the therapeutic treatment and management of this disease. The importance of patient selection to maximise efficacy and minimise toxicities of treatments is now acknowledged and has necessitated novel biomarker and targeted therapy driven trials. The outcome of such trials will ideally allow the selection of the right drug for the right person and at the right treatment time point. The term personalised medicine first appeared in the literature in the late 1990s with the primary aim of linking established clinicopathological disease state with a cancer molecular profile or signature. It is hoped that this approach will create more detailed and effective diagnostic, prognostic and therapeutic strategies for individual patients (Jackson and Chester, 2015).

Acquired alterations to cellular DNA that are casually linked to the development of cancer are known as driver mutations (Stratton *et al.*, 2009). Unlike cytotoxic chemotherapeutic agents which indiscriminately kill all cells by affecting processes central to cell division, targeted therapies are in principle directed against cancer cell specific attributes and molecular pathways that are a consequence of driver mutations and thus essential to cancer cell survival. The BCR-ABL story is one of the most notable examples to date of exploiting the molecular biology of a particular cancer to successfully identify a therapeutic target and to develop an effective molecular targeted therapy (Wong and Witte, 2004). The majority of patients with chronic myeloid leukaemia (CML) harbour a driver mutation in the BCR-ABL gene resulting in a chromosomal translocation and imatinib, a monoclonal antibody, can effectively inhibit the BCR-ABL fusion protein leading to high response rates and improved patient survival (Wong and Witte, 2004). Drugs such as imatinib directed against the BCR-ABL mutation in CML or a mutant c-kit in gastrointestinal stromal tumour (GIST), erlotinib and gefitinib directed against mutant epithelial growth factor receptor (EGFR) in non-small cell lung cancer (NSCLC) and vemurafenib directed against mutant B-type Raf kinase (BRAF) for melanoma are now widely accepted as standard treatments (Saijo, 2012). This is due to high response rates, significantly prolonged DFS and OS. Despite these heralded success stories, many clinical trials of targeted therapies have produced disappointing results, highlighting a number of challenges to be addressed in

order to translate improved molecular knowledge of cancer initiation and progression into something that is of clinical use.

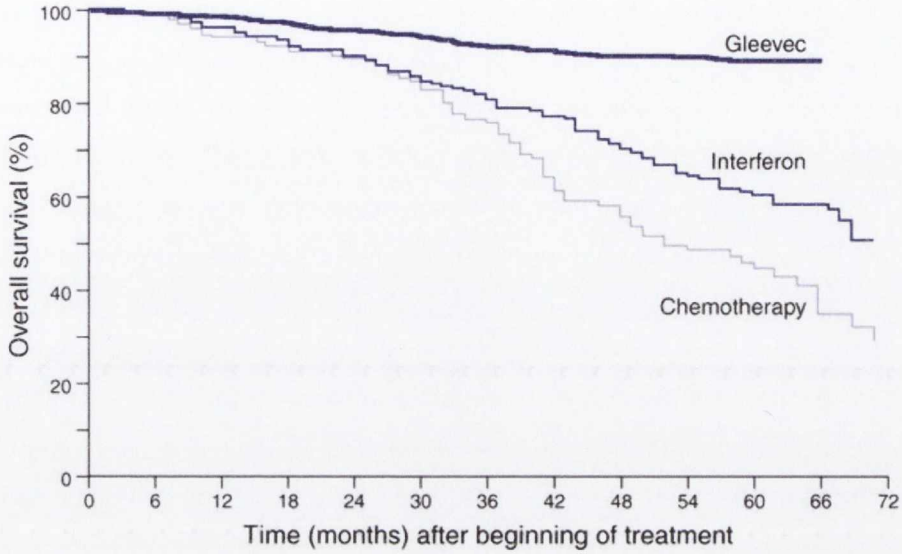

Figure 1.10 Overall survival of CML patients treated with imatinib, interferon or chemotherapy. Conventional chemotherapy delivered only a minimal effect on survival while treatment with interferon was associated with a 5 year survival <50%. In contrast treatment with imatinib (Gleevec) showed superior effects with a five year survival of 89%. Reproduced from Druker et al (2009)

1.3 Challenges in personalised medicine

The first major challenge of molecular targeted therapies is the inherent complexity and heterogeneity of cancer. Molecular sub-typing has demonstrated how radically different cancers from one primary site can be, having arisen from a different genetic background, despite a histologically similar appearance (Saijo, 2012). The frequency of driver mutations is considerably high in certain cancers, for example the BCR-ABL translocation and BRAF mutations occur at a frequency of >90% in CML or GIST patients and 40-60% in melanoma patients respectively, making treatment much more straightforward (Siehl and Thiel, 2007, Flaherty *et al.*, 2010). However, if a driver mutation is present in only a small fraction of patients, individualised drug discovery and selection of patients becomes more complicated. Adding another layer of complexity to the interpretation of data, we must also take into account the interplay between genetics and environmental factors that will determine clinical outcome (e.g. patient smoking status or obesity status) (Zhang *et al.*, 2015, Guiu *et al.*, 2010) to ensure that only patients with the correct signature and who are likely to benefit from a treatment are recruited for a particular clinical trial.

Secondly, heterogeneity is not just limited to differences between patients with the same histological tumour but also occurs within a single patient, i.e. intratumoural heterogeneity (Allison and Sledge, 2014) (Figure 1.11). Distinct dominant clones within a heterogeneous tumour in principle behave differently, for example having various responses to administered therapies or having different metastatic environment preferences (Figure 1.11). Some level of heterogeneity exists in all tumours, however identifying the most clinically relevant cell population within the mass can be difficult and leads to important questions such as identifying the percentage of cells that need to be positive for a particular biomarker of cancer to be considered positive and likely to respond to a particular therapy. For example estrogen receptor (ER) positive breast cancer patients with higher levels of biomarker expression had better responses to hormone therapy and improved DFS compared to those with <1% or negative ER expression (Harvey *et al.*, 1999). Therefore we need to define more clearly the clinical relevance of borderline threshold expressors to optimally predict patient outcomes.

Thirdly, the acquisition of resistance to therapy by a tumour is also a challenge for personalised medicine (Saijo, 2012). Just as the composition of a tumour is heterogeneous so too are responses to targeted therapies. In some cases patients do not respond at all to treatment or show only a partial response despite driver mutation presence and in principle being a good candidate for treatment selection. Unfortunately those who initially respond well to a targeted treatment may ultimately develop disease recurrence due to appearance of secondary mutations or the activation of other signalling pathways, presumably due to selection pressures on the heterogeneous cancer cell population. The cancer stem theory suggests that this varied functional response to therapy is due to cells in different states of differentiation. This theory suggests that the bulk of the tumour is composed of cancer cells with limited replicative ability and that amidst those there is a subpopulation of cells with stem-like characteristics that allow them to regenerate and sustain tumour growth (Tan *et al.*, 2006). A number of stem-cell specific markers have been identified in multiple tumour types in recent times including CD44, CD133 and aldehyde dehydrogenase (ALDH) and have shown promise as potential drug targets to combat drug resistance in maliganancies such breast, colon, ovarian and glioblastoma cancer (Robson and James, 2012, Du *et al.*, 2008, Landen *et al.*, 2010, Wang *et al.*, 2011b). Considering the impact of intertumoural and intratumoural heterogeneity, radical cure of cancer cannot be expected, even with sharp acting molecular targeted therapies, unless robust biomarkers for patient selection can be identified and resistance mechanisms can be circumvented. Therefore it is of utmost importance to design appropriate

combinations of molecular targeted drugs with standard cytotoxic chemotherapies or indeed combinations of multiple targeted therapies based on our understanding of interacting molecular pathways in a cancer, to boost patient responses and improve survival.

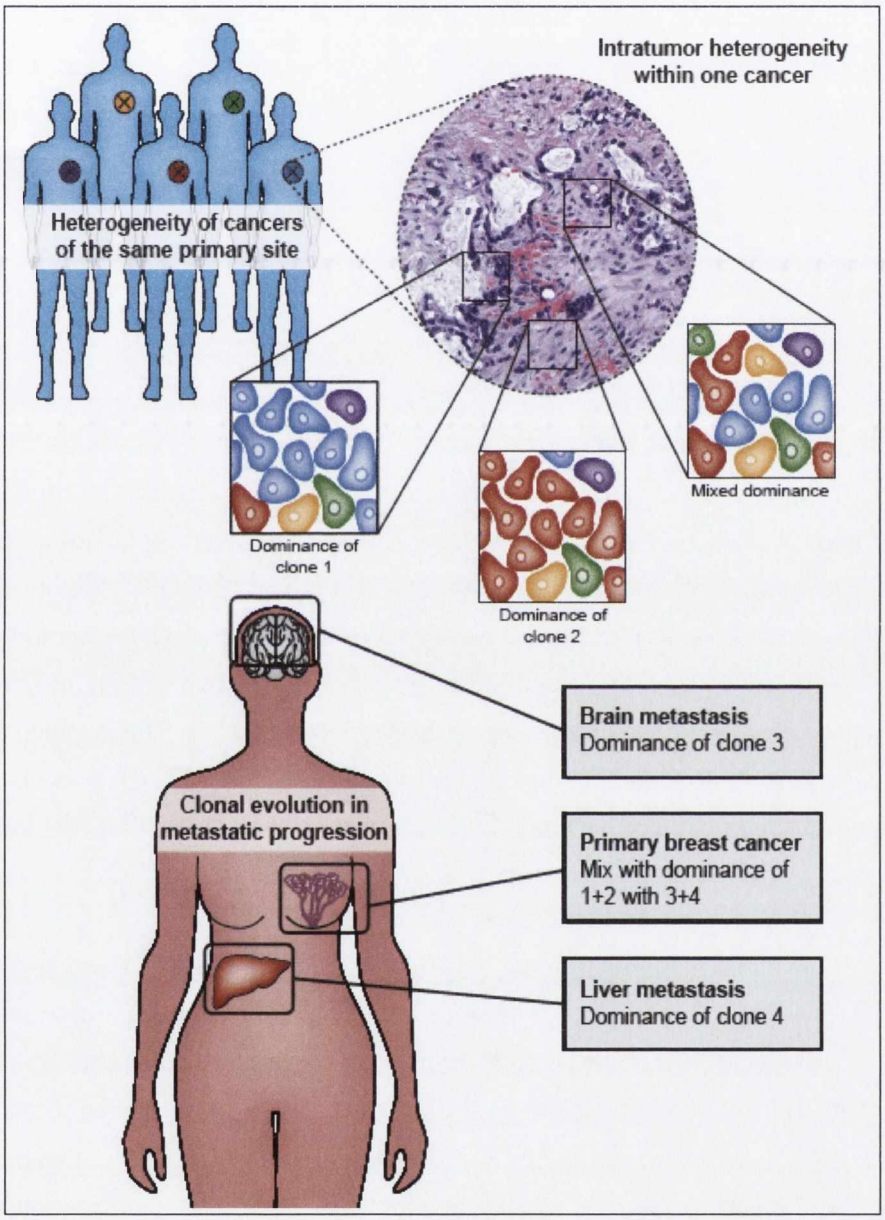

Figure 1.11 Heterogeneity in cancer occurs at many different levels. Cancers derived from the same primary site can have distinct and clinically relevant biological differences (i.e. different histology or different genetic or molecular signature) meaning two individuals may respond very differently to the same therapy. In addition, within one tumour there is intratumour heterogeneity where different clones respond differently to selective pressures i.e. different clones may respond to therapies differently, leading to partial responses and subsequent resistance or different clones may predominate in different metastatic niches (i.e. clone 3 preferentially metastasises to the brain). Reproduced from Allison and Sledge (2014)

1.4 Potential targeted therapies in oesophageal cancer

A major research focus in the past decade has been to understand the molecular evolution of oesophageal cancer. Most studies have concentrated on single mutations or proteins in the hope of uncovering relevant driver mutations or oncoproteins as therapeutic targets or clinical markers of disease. A number of potential targets/ markers of oesophageal cancer have been described in the literature that involve different cancer hallmarks such as tumour growth regulation, angiogenesis and inflammation (Table 1.1). Targeted therapies have been developed for a number of these proteins and are currently in various stages of clinical trials to treat oesophageal cancer.

The target closest to reaching the clinical setting is human epidermal growth factor receptor 2 (HER-2), a growth factor receptor from the same family as EGFR. HER-2 overexpression occurs in approximately 15% of OAC and 5% of OSCC cases (Reichelt *et al.*, 2007) however the prognostic value of HER-2 overexpression remains ambiguous (Uzunoglu *et al.*, 2014). The international TOGA Phase III randomised clinical trial demonstrated a significant increase in response rate and OS of metastatic HER-2 positive gastric cancer and oesophagogastric junction (OGJ) patients treated with the HER-2 monoclonal antibody trastuzumab in combination with chemotherapy. This led to its approval by the Food and Drug Administration (FDA) in 2010 for treatment naive HER-2 positive gastric cancers (Bang *et al.*, 2010). The ongoing RTOG 1010 is investigating neoadjuvant trastuzumab in combination with CRT in OAC and the publishing of these findings will help elucidate further the utility of HER-2 targeting in OAC (Safran, 2015).

Attempts to target EGFR in oesophageal cancer thus far have not been promising. While EGFR mutations do not occur frequently in oesophageal cancer, overexpression of EGFR in oesophageal cancer is common in approximately 30-70% of patients (Hanawa *et al.*, 2006, Kim *et al.*, 2008) and has been shown to be a prognostic factor of OSCC and OAC (Wilkinson *et al.*, 2004, Sunpaweravong *et al.*, 2005). Despite this, a number of Phase II studies using monoclonal antibodies (e.g. cetuximab, panitumumab) have shown little benefit to patients and do not increase OS of patients (Gold *et al.*, 2010, Waddell *et al.*, 2013). Latest results from a Phase III randomised trial of cetuximab in combination with chemotherapy failed to show improved OS (Suntharalingam *et al.*, 2014). Tyrosine kinase inhibitors (TKIs) erlotinib and gefitinib have both shown anti-tumour activity but no improvement to OS (Wainberg *et al.*, 2011, Dragovich *et al.*, 2006). A recent phase III multi-centre randomised study again showed

gefitinib was ineffective at improving OS however had significant palliative benefits (Dutton *et al.*, 2014). Given the limited effects to date, current EGFR therapies are not likely to become a component of standard care.

Another important area of interest for novel targeted treatments of oesophageal cancer that is at an earlier stage of development is anti-angiogenic therapies. Angiogenesis and current developments of anti-angiogenic targeted therapies in the treatment of cancer and specifically oesophageal cancer will be discussed in the following section.

Table 1.1 Potential therapeutic targets and biomarkers of oesophageal cancer. Proteins highlighted in red have been investigated as drug targets in clinical studies of oesophageal cancer.

Clincal Factor	Author(s) of clinical studies
Growth Regulation	
EGFR	(Sunpaweravong *et al.*,2005, Wilkinson *et al.*,2004, Dragovich, *et al.*,2006)
HER-2	(Reichelt *et al.*,2007, Bang *et al.*,2010)
Ki67	(Bianto *et al.*,2009)
Angiogenesis	
VEGF	(Chen *et al.*,2012, Peng *et al.*,2013, Fuchs *et al.*,2014)
COX-2	(Zhi *et al.*,2006, Prins *et al.*,2012, Dawson *et al.*,2007)
FGFR	(Murase *et al.*,2014, Sugiura *et al.*,2007)
c-MET	(Herrera *et al.*,2005, Ren *et al.*,2005, Jardim *et al.*,2014)
Inflammation	
COX-2	(Zhi *et al.*,2006, Prins *et al.*,2012, Dawson *et al.*,2007)
NFκB	(Abdel-Latif *et al.*,2004, Izzo *et al.*,2006, Nguyen *et al.*,2004)
Cell Cycle Control	
P16	(Sturm *et al.*,2001)
P21	(Shiozaki *et al.*,2013)
Cyclin D1	(Sunpaweravong *et al.*,2005)
mTOR	(Yu *et al.*,2009, Hirashima *et al.*,2010, Werner *et al.*,2013)
Apoptosis	
P53	(Shang *et al.*,2014)
Bax	(Ikeguchi *et al.*,2001, Sturm *et al.*,2001)
Bcl2	(Ohbu *et al.*,1997, Takikita *et al.*,2009)
IGFR	(Doyle *et al.*,2012, Adachi *et al.*,2014)
Metastasis	
TIMP	(Kozlowski *et al.*,2013, Salmela *et al.*,2001)
E-cadherin	(Xu *et al.*,2014b, Nair *et al.*,2005)

1.5 Angiogenesis

1.5.1 Angiogenesis is a major hallmark of cancer

Hanahan and Weinberg originally described six principle traits of cancer hallmarks which are essential for the transformation of a normal cell to a malignant cell: self-sufficiency in growth signals, evading apoptosis, insensitivity to anti-growth signals, sustained angiogenesis, tissue invasion and metastasis and limited replicative potential (Hanahan and Weinberg, 2000). Progress in our understanding of cancer has resulted

in the addition of two new hallmarks of cancer: reprogramming of energy metabolism and evading immune destruction. Two enabling characteristics are described which produce the environment where cancer can develop: genomic instability and tumour promoting inflammation driven by immune cells (Hanahan and Weinberg, 2011).

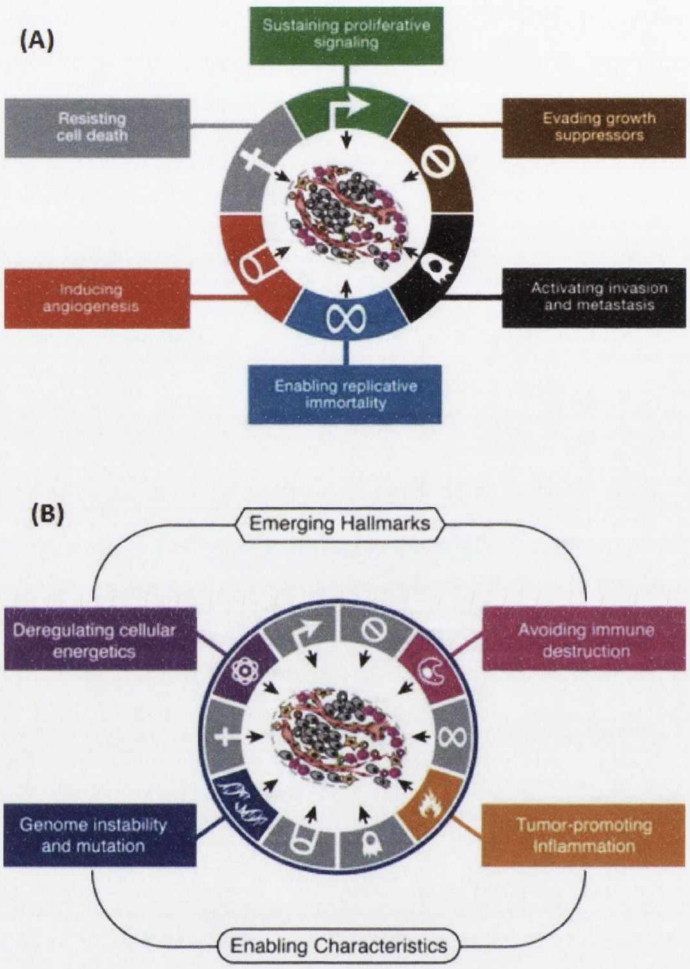

Figure 1.12 The updated hallmarks and enabling characteristics of cancer. (A) the original 6 hallmarks of cancer proposed by Hanahan and Weinberg and (B) the recently described additional hallmarks of cancer and the two enabling characteristics. Reproduced from (Hanahan and Weinberg, 2011)

In 1971 Judah Folkman hypothesised that the inhibition of angiogenesis could be an effective therapeutic strategy (Folkman, 1971). Angiogenesis is the formation of new blood vessels from pre-existing vasculature. Under normal physiological conditions which call for additional vasculature, angiogenesis is a tightly regulated process where new vessels mature and stabilise rapidly to restore homeostasis, forming a hierarchy of well-differentiated arteries, arterioles, capillaries, veins and venules. Tumour vessels on the other hand are described as "wounds that never heal" due to a failure to enter a quiescent state and a constant growth of new vessels (Dvorak, 1986). From a structural stand point they are often unevenly distributed with irregular branching and a lack of hierarchical organisation. They appear dilated and tortuous leading to a vascular network that is leaky. As mentioned, aberrant angiogenesis is considered an essential hallmark of cancer (Hanahan and Weinberg, 2011). During carcinogenesis an angiogenic switch is thought to occur in adaption to hypoxia and nutrient depletion in the tumour microenvironment, allowing the tumour to manipulate host vasculature to sustain growth. Without the concomitant neoangiogenesis and manipulation of existing capillary networks, tumours cannot expand beyond a minimal size or metastasise to distant sites (Folkman, 1995, Carmeliet and Jain, 2000).

1.5.2 VEGF targeting in cancer: successes and failures

Release of growth factors, in particular the key angiogenic mediator vascular endothelial growth factor (VEGF) from tumour cells themselves as well as endothelial cells, other stromal host cells and or tumour associated macrophages (TAMs) collectively stimulate angiogenesis (Riabov *et al.*, 2014). Production of these factors is associated with classical features of the tumour including hypoxic conditions and oncogene signalling (Carmeliet, 2005). Aside from its classical role of inducing angiogenesis in endothelial cells, it is now apparent that VEGF signalling has a role in tumour cells. VEGF is overexpressed in the majority of solid malignancies and has been shown to be associated with a poorer patient prognosis in a number of cancer types, including but not limited to, cancer of the bladder (Huang *et al.*, 2013), breast (Gasparini, 2000), colon or rectum (Takahashi *et al.*, 1997, Des Guetz *et al.*, 2006), lung (Zhan *et al.*, 2009) stomach (Chen *et al.*, 2013, Chen *et al.*, 2011) and oesophagus (Peng *et al.*, 2013). Two meta-analysis studies have reported a significant association between increased VEGF and poorer prognosis in OSCC patients however data was not sufficient to determine prognostic value of VEGF expression in OAC (Chen *et al.*, 2012, Peng *et al.*, 2013). This is due to the fact that the majority of studies with available survival data for inclusion in these two meta-analyses originated from Asian countries where squamous cell carcinoma is the main oesophageal cancer

subtype. Notably one recent immunohistochemical study that was not included in the aforementioned meta-analyses has reported an association of high VEGF expression with poor cancer specific survival in OAC (n=156) indicating its prognostic potential (Prins *et al.*, 2012) (Figure 1.13). Several lines of study have shown that cancer cells expressing VEGF can also express the VEGF-receptors, VEGFR-1 and VEGFR-2/KDR and that signalling through these receptors can promote cancer cell proliferation, migration, invasion and metastasis in addition to the activation of endothelial cells (Devery *et al.*, 2015, Fan *et al.*, 2005, Guo *et al.*, 2003). Therefore, VEGF blockade can either directly target the microvascular endothelial cells that have been recruited to the tumour mass or indirectly by targeting tumour cell VEGF signalling.

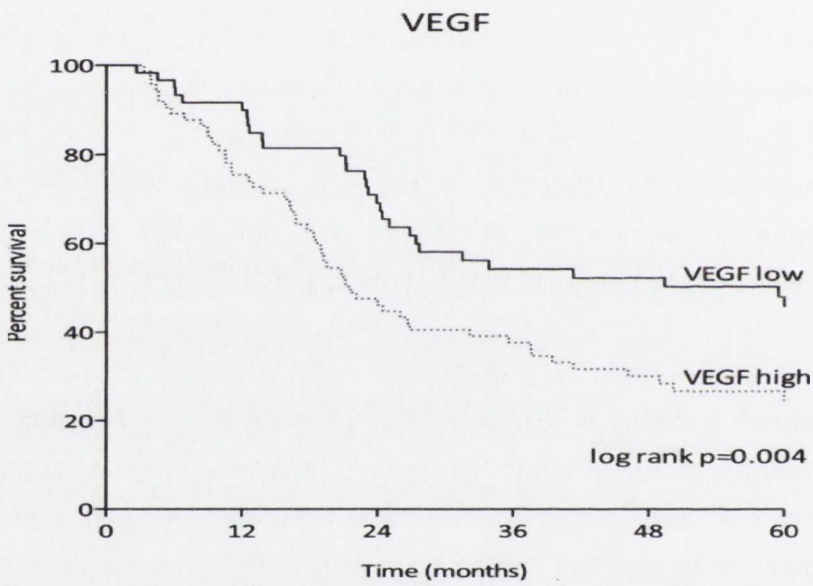

Figure 1.13 Cancer specific survival of OAC patients according to high and low VEGF expression. Patients with low VEGF had a median survival time of 59.5 months compared to patients with high VEGF expression who had a survival time of 21.6 months (n=156, p=0.004; log rank). Reproduced from (Prins *et al.*, 2012)

Given the tumour dependency on sustained angiogenesis, in addition to the lack of angiogenesis in normal tissues under physiological conditions (other than embryogenesis, female menstruation and wound healing) angiogenesis is a logical therapeutic target that would have minimal toxicity to the patient. Angiogenesis inhibitors have been evaluated in clinical studies in a number of different cancer types because in principle they are not organ-specific and exert their effects on the cancer milieu as opposed to cancer cells. Most research into anti-angiogenic therapies has focused on VEGF with three major classes of agents having been developed: monoclonal antibodies, VEGF decoy receptors and small tyrosine kinase inhibitors

(TKIs) (Al-Husein *et al.*, 2012). Some of these agents are in use clinically or are currently under investigation in clinical trials, either as monotherapy or more commonly in combination with cytotoxic chemotherapy or radiation.

Bevacizumab, a recombinant humanized monoclonal antibody that binds to all VEGF isoforms was FDA approved in 2004 for first line treatment of metastatic colorectal cancer in combination with standard chemotherapy drugs (irinotecan, 5-fluorouracil and leucovorin) due to an improved OS of 5 months compared to chemotherapy alone (Hurwitz *et al.*, 2004). Subsequently, labelling was extended to include approval for second line treatment of metastatic colorectal cancer that has progressed following treatment with fluoropyrimidine and irinotecan. In this case second line treatment of bevacizumab with FOLFOX4 (oxaliplatin, fluorouracil and leucovorin) was found to increase OS compared to FOLFOX4 alone (Giantonio *et al.*, 2007). Continuation of bevacizumab treatment has been approved in combination with fluoropyrimidine–irinotecan or fluoropyrimidine–oxaliplatin-based chemotherapy for patients whose treatment has progressed while on first line treatment with a bevacizumab-containing treatment (Giantonio *et al.*, 2007, Arnold *et al.*, 2012). Even more recently bevacizumab has been approved in combination therapy with either cisplatin or topotecan for the treatment of persistent, recurrent or metastatic cervical cancer as a result of a randomised trial where OS improved by 3.9 months compared to chemotherapy alone (Tewari *et al.*, 2014). Bevacizumab tends to show activity when used in combination with cytotoxic chemotherapy as opposed to a monotherapy. It has been hypothesised that an initial phase of vascular normalisation occurs following VEGF suppression leading to an increased delivery of the chemotherapy to the tumour site (Jain, 2005).

Despite some success stories of VEGF-targeted therapy, variable results have been obtained across different cancer types or even within the same cancer. For example in the treatment of metastatic colorectal cancer it has been found that visceral obesity is associated with poor outcomes in patients given first line bevacizumab treatment (Guiu *et al.*, 2010) suggesting that environmental factors such as obesity status may affect the efficacy of this drug. Although several clinical trials have generated data that have indicated an improved response and progression free survival (PFS), reaching an end point of improved OS has been more challenging, leading to somewhat conflicting results. Based on a randomized Phase III study, E4599, bevacizumab was approved for first line treatment of advanced NSCLC in combination with paclitaxel and carboplatin compared to chemotherapy alone due to an improved patient response,

PFS and increased median OS of two months (Sandler *et al.*, 2006). However a subsequent Phase III study reported a lack of improvement to OS (Reck *et al.*, 2010). Bevacizumab was approved for first line treatment of renal cell carcinoma (RCC) in combination with interferon-α compared to interferon-α alone due to a 5 month improved median PFS, but again failing to have any improvement to OS (Escudier *et al.*, 2007). While two single-arm Phase II trials were used to support the accelerated 2009 FDA approval of the drug as a single therapeutic agent for second line treatment of advanced glioblastoma in the US, this was not the case in Europe due to what was deemed insufficient evidence (Friedman *et al.*, 2009, Kreisl *et al.*, 2009, Chamberlain, 2011).

Results from bevacizumab trials in the treatment of HER-2-negative breast cancer have been controversial. It was approved for the first line treatment of metastatic breast cancer in combination with paclitaxel under the FDA's accelerated approval based on promising results from the landmark ECOG 2100 trial where improved PFS and a near 2-fold increase in response rate was observed. Notably, increased OS was not reported. Two additional seminal studies, the RIBBON trial and the AVADO trial, showed improved PFS but failed to confirm the magnitude of response initially seen in the ECOG 2100 study (Robert *et al.*, 2011, Miles *et al.*, 2010). In 2012 the FDA withdrew the approval of bevacizumab for the treatment of breast cancer due to the lack of OS from all three trials and because the available data on improved quality to life do not justify the risk of safety issues associated with the drug (Al-Husein *et al.*, 2012).

It was initially assumed that anti-angiogenic therapies would be non-toxic considering active angiogenesis is so rare in adults. However clinical experience has highlighted safety concerns associated with bevacizumab as a monotherapy including hypertension, proteinuria, impaired wound healing, gastric perforation, cardiac toxicity, endocrine dysfunction, bleeding and thromboembolic events (Genentech Inc., 2011, Vasudev and Reynolds, 2014). The reduction in VEGF-regulated molecules involved in controlling vasoconstriction (i.e. nitric oxide) and kidney function (i.e. nephrin) are thought to cause the common symptoms of VEGF inhibitor-induced hypertension and proteinuria (Robinson *et al.*, 2010, Izzedine *et al.*, 2010). Individualisation of VEGF treatment will be critical to overcoming these safety concerns. High risk patient groups (i.e. those with diabetes, high cholesterol or kidney disease) should be identified and patients should have controlled blood pressure before starting treatment (Robinson *et al.* 2010). The use of anti-hypertensive treatments during VEGF inhibitor treatment

may also help counteract these negative symptoms (Larochelle et al., 2012). As a result of the aforementioned safety concerns there has been efforts to identify other pro-angiogenic players that can be alternatively targeted, with the hope of providing effective anti-angiogenic therapies with less safety concerns.

1.5.3 Alternative blocking of VEGF receptor with tyrosine kinase inhibitors

The effect of VEGF targeted therapies is inevitably transient as tumours always develop resistance to treatment and this issue is likely to explain the diversity of treatment results between cancers. Due to the fact that angiogenesis encompasses multiple signalling pathways, the effect of anti-angiogenic agents targeting only one single pathway can be overcome by the expression of alternate pro-angiogenic signals. This has led to the development of multiple tyrosine kinase inhibitors as a targeted therapy. Following on from the success of imatinib to treat CML and GIST, inhibition of several tyrosine kinase receptors such as VEGF-R, fibroblast growth factor receptor (FGFR) and platelet derived growth factor receptor (PDGFR) that are involved in angiogenesis and multiple other signalling pathways has been investigated (Kim *et al.*, 2004). TKIs bind to the ATP binding site and inhibit activation of more than one receptor generally, making development of resistance less likely. Sorafenib targets VEGFR-2 and -3, PDGFR, fms-like tyrosine kinase 3 (Flt-3) and c-Kit and it was the first TKI to demonstrate activity in the treatment of metastatic RCC, showing improved PFS and OS, leading to its FDA approval in 2008 (Escudier *et al.*, 2007). Sunitinib malate, another pan TKI, targeting VEGFR-1-3, PDGFR, Flt-3 and c-Kit was originally approved in 2006 for the management of GIST following disease progression after or an intolerance to imatinib (Younus *et al.*, 2010). It was later approved for the treatment of metastatic RCC (Motzer *et al.*, 2007), pancreatic neuroendocrine tumours (PNET) and heptocellular carcinoma (Llovet *et al.*, 2008).

In contrast to these promising data, sorafenib showed minimal clinical activity in patients with prostate cancer and NSCLC (Hwang and Heath, 2010, Blumenschein *et al.*, 2009). Despite the striking response and improvement to survival of metastatic colorectal cancer patients treated with bevacizumab monoclonal therapy in combination with chemotherapy, efforts to combine TKIs with chemotherapy as an alternate therapeutic option have been disappointing in terms of improvements to OS (Hecht *et al.*, 2011, Van Cutsem *et al.*, 2011). Dual VEGF/VEGFR inhibition with bevacizumab and sunitinib in the treatment of advanced solid malignancies in a Phase I study has recently been investigated. However observed abnormal blood vessels

(microangiopathy) and significant toxicity has halted any further clinical development (Mittal *et al.*, 2014).

Although VEGF targeted therapies such as bevacizumab and the TKI sunitinib are now approved for the use in patients with advanced stage disease in a number of different malignancies, the identification of predictive biomarkers to help select patients that should -and more importantly- those who should not receive anti-angiogenic therapies remains elusive (Maru *et al.*, 2013). The utility of circulating VEGF as a predictive biomarker for bevacizumab was investigated retrospectively in pre-treatment serum samples of advanced gastric cancer patients in the aforementioned AVAGAST trial, using a new ELISA developed by Roche/Genetech that preferentially detects smaller VEGF isoforms (Van Cutsen *et al.*, 2012). Patients with low VEGF levels showed a trend towards an improved overall survival. This is in contrast to another study which did not identify predictive potential of pre-treatment VEGF levels across four Phase III trials evaluating bevacizumab in four different cancer types, using an ELISA detecting all major isoforms of VEGF (Hegde *et al.*, 2013). Intuitively it seems logical that increased VEGF serum levels would be predictive of VEGF treatment response, and perhaps all that is needed is the right robust and sensitive molecular tool to detect this biomarker. From this perspective there is a clear need for clinical trials that prospectively validate biomarkers for VEGF-targeted therapies to improve patient stratification.

1.5.4 Resistance to anti-angiogenic molecular targeted therapies: The tumour microenvironment and alternate angiogenic pathways

The contributory role of stromal cells to the acquisition of the hallmark traits of cancer cells has added another dimension to the complexity of tumour development. The stromal compartment surrounding a tumour which consists of mainly fibroblasts, extracellular matrix, immune cells and vasculature, was originally thought to just be an inactive bystander during tumour development (Balkwill *et al.*, 2012). Although most host stromal cells inherently possess tumour suppressing capabilities, alterations during cancer development result in a crosstalk between cancer cells and the stroma that has been reported to aid progression of tumourigenesis and metastasis by creating a tumour microenvironment (Balkwill *et al.*, 2012). There is a growing interest in the role of components of the tumour microenvironment, other than endothelial cells themselves, in the angiogenic process. Preclinical studies have demonstrated that a number of different cell types infiltrating the tumour mass including myeloid cells, fibroblasts and endothelial progenitor cells are all capable of mediating resistance to anti-VEGF therapies, through an upregulation of alternate angiogenic pathways (Chung *et al.*, 2013, di Tomaso *et al.*, 2009, Shaked *et al.*, 2006). Recently recurrent glioblastoma was shown to have increased TAMs following treatment with

bevacizumab. The levels of infiltrating TAMs was associated with poorer survival suggesting that these macrophages may participate in the anti-angiogenic resistance (Lu-Emerson *et al.*, 2013) and that the alternate targeting of angiogenic pathways used by stromal components, other than endothelial cells, in addition to tumour cells may have promise in the clinical setting.

While some clinical trials with anti-angiogenic drugs have achieved improvement by stalling tumour growth, decreasing tumour size or in some cases increasing patient survival, the effects are short lived, typically only lasting several months. Two modes of resistance have been hypothesised to account for the short comings of currently available anti-angiogenic therapies, particularly those targeting VEGF. Firstly there is intrinsic (pre-existing) non-responsiveness where, by virtue of the unique microenvironment in which the tumour developed and what selection pressures were present, the tumour has already adapted resistance mechanisms before the drug is even administered, rather than in response to the therapy itself (Figure 1.14) (Bergers and Hanahan, 2008). Some cancers are thought to be inherently resistant to anti-angiogenic therapies, for example breast cancer has had the poorest responses to any anti-angiogenic therapy to date (Al-Husein *et al.*, 2012).

Secondly acquired or evasive resistance despite VEGF blocking directly or via its receptor is thought to occur (Figure 1.14) (Bergers and Hanahan, 2008). Unlike traditional concepts of drug resistance involving mutations to the gene being targeted or alterations to drug uptake and efflux mechanisms, evasive resistance is thought to largely occur indirectly, upregulating alternate pathways and mechanisms to sustain tumour growth while the original therapeutic target remains blocked, This mode of resistance is thought to occur via a number of distinct mechanisms: first, the traditional upregulation of the angiogenic gene target, which will dilute the effect of the anti-angiogenic drug; second, upregulation of alternative pro-angiogenic signalling pathways, insensitive to the therapy; third, recruitment of bone marrow derived pro-angiogenic cells which can sustain angiogenesis in the tumour; fourth, recruitment of pro-angiogenic stromal cells of the tumour microenvironment e.g. increased pericyte recruitment and coverage of the vasculature, mitigating the need for VEGF survival signals; fifth, enhanced metastasis to well vascularised area of the host, circumventing the need for neovascularisation and lastly, adaptation of tumour cells to a hypoxic environment with decreased vasculature and blood flow (Bergers and Hanahan, 2008, Loges *et al.*, 2010).

Preclinical studies have identified alternative pro-angiogenic candidates including the angiopoietins (Hashizume *et al.*, 2010), FGF (Welti *et al.*, 2011), interleukin-8 (IL-8) (Huang *et al.*, 2010) and PDGF-C (di Tomaso *et al.*, 2009) where blocking of the candidate factor in addition to VEGF increases therapeutic response (Vasudev and Reynolds, 2014). VEGF receptors are known to interact with other cell surface co-receptors including neuropilin-1 (NRP1), NRP2 and CD146, providing another target to increase anti-angiogenic therapy responses (Raimondi and Ruhrberg, 2013, Olsson *et al.*, 2006, Lee *et al.*, 2015). For example, inhibition of neuropilin-1 with a monoclonal antibody in combination with VEGF blockage in an *in vivo* tumour model was shown to have an additive effect to tumour reduction (Pan *et al.*, 2007). Therefore therapies are being developed that attempt to inhibit angiogenesis through multiple pathways and receptor complexes under the rationale that this approach may be necessary to achieve efficient and durable suppression of tumour angiogenesis and growth, therapy resistance and ultimately improved patient survival.

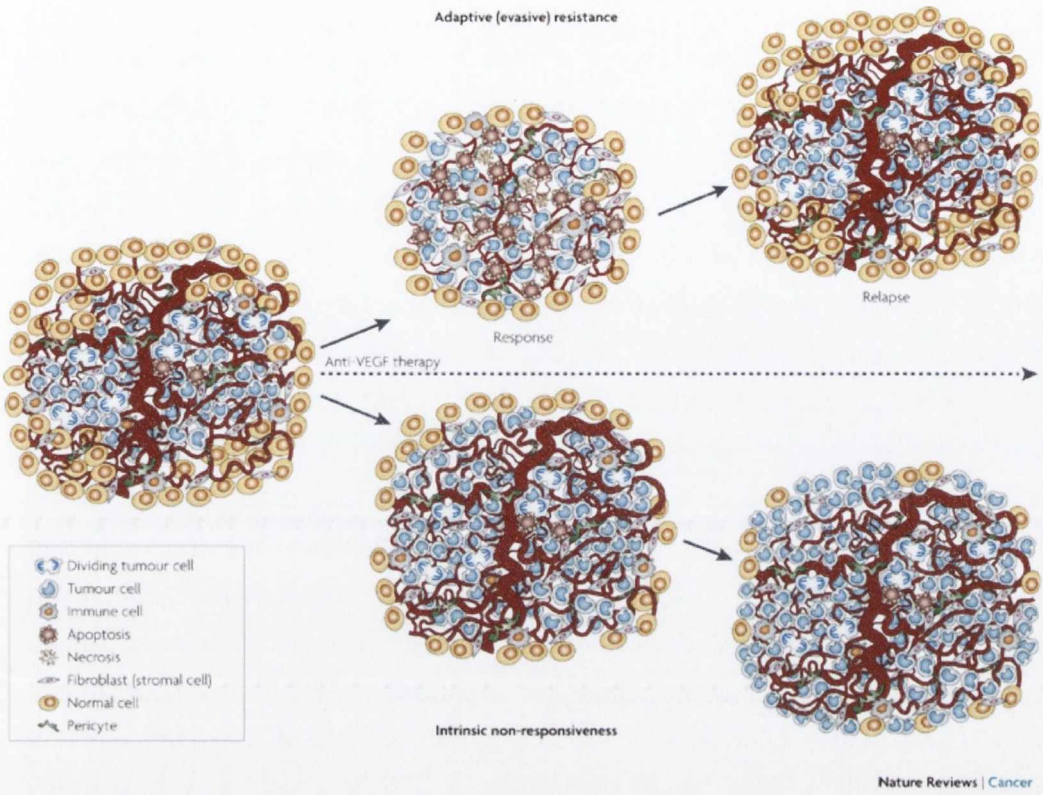

Figure 1.14 Two modes of anti-angiogenic therapy resistance are hypothesised to exist in cancer. First intrinsic non-responsiveness where treatment has no observed benefit to the patient and secondly adaptive (evasive) resistance where following a relatively short period of response, tumour growth and progression proceeds. In this scenario the tumour adapts alternative mechanisms to sustain tumour growth despite blockage of the therapeutic target (e.g. VEGF). Reproduced from Bergers and Hanahan (2008)

1.6 Progress of anti-angiogenic therapy development to treat oesophageal cancer

1.6.1 VEGF inhibition

VEGF is overexpressed in 30-60% of oesophageal cancer patients and expression levels correlate with advanced tumour stage and poor prognosis in patients undergoing oesophagectomy only, with curative intent (Shih *et al.*, 2000, Peng *et al.*, 2013, Prins *et al.*, 2012) (Figure 1.13). VEGF has also been found to be increasingly expressed across the sequence from Barrett's metaplasia to dysplasia to OAC (Vallbohmer *et al.*, 2006). The prognostic value of VEGF in oesophageal cancer patients who received neoadjuvant CRT is less clear. Some studies suggest VEGF still has prognostic value with pre-operative CRT (Imdahl *et al.*, 2002) however another study found no such association with the rationale that increased VEGF expression and thus angiogenic activity occurs in response to CRT (Kulke *et al.*, 2004).

To date, most studies of the monoclonal antibody bevacizumab have been limited to oesophagogastric cancers. A number of Phase II studies of bevacizumab in combination with different chemotherapy regimes in metastatic gastric and oesophagogastric adenocarcinoma have yielded promising results to date with regard to activity and safety (Shah *et al.*, 2005, El-Rayes *et al.*, 2010, Shah *et al.*, 2011) (Table 1.2). The AVAGAST Phase III randomised trial investigated the effect of bevacizumab in combination with chemotherapy on OS in patients with gastric cancer or oesophagogastric cancer (Ohtsu *et al.*, 2011). 774 patients were enrolled from over 17 countries, 50% were treated with bevacizumab or a placebo, both in combination with chemotherapy. While the end point of improved OS was not met, both median PFS and overall response were significantly improved in the bevacizumab arm of the trial (Kang Y, 2010, Ohtsu *et al.*, 2011). A recent Phase II trial has reported markedly improved response and survival for HER-2 positive gastric and OAC patients when bevacizumab was used in combination with capecitabine and oxaliplatin (CAPOX) and trastuzumab. Current reports for this ongoing trial indicate a median OS of 21 months and a response rate of 81% thus far (Enzinger *et al.*, 2015). This is a noteworthy improvement on previous results published for trastuzumab in combination with CAPOX (Bang *et al.*, 2010). Recent trials have investigated the combination of neoadjuvant CRT with promising targeted therapies such as bevacizumab or combination targeted therapies of bevacizumab and erlotinib (Enzinger *et al.*, 2008, Idelevich *et al.*, 2012) and so far these trials have not indicated any increased survival compared to CRT alone. A large multi-centre randomised phase II/III trial in the UK, recruiting 1000 patients, is investigating the safety and efficacy of bevacizumab in combination with neo-adjuvant chemotherapy in patients with gastric and OAC and should provide a better insight into the use of bevacizumab as a perioperative targeted therapy (Okines *et al.*, 2013). Ramucirumab is a fully humanised monoclonal antibody that binds to and selectively inhibits VEGFR-2. It has recently shown promising clinical efficacy as a single agent in a Phase III REGARD study for the second line treatment of advanced and metastatic chemotherapy pre-treated gastric and oesophagogastric cancer patients. Although modest, OS was significantly improved in patients treated with ramucirumab compared to placebo (5.2 months vs. 3.8 months) indicating its therapeutic potential in these difficult to treat patients (Fuchs *et al.*, 2014). Subsequently it was approved by the FDA for treatment of cases refractory to platinum or fluoropyrimidine containing treatment regimes (Casak *et al.*, 2015). The Phase III RAINBOW study is currently investigating ramucirumab and paclitaxel versus placebo and paclitaxel in the second line treatment of 665 gastric and oesophagogastric

adenocarcinoma patients refractory to first platinum or fluoropyrimidine (Table 1.2). Although full results are yet to be published, the trial reached the end point of an improved OS and PFS compared to the placebo group, which will likely lead to its FDA approval later in 2015 (Wilke *et al.*).

The TKI agents sunitinib and sorafenib (both discussed in section 1.5.3) are under early investigations in Phase II clinical trials for gastric and oesophageal cancer patients with mixed results to date (Bang *et al.*, 2011, Yi *et al.*, 2012, Schmitt *et al.*, 2012, Sun *et al.*, 2010) (Table 1.2). Phase II trials are currently recruiting to investigate the clinical efficacy of pazopanib (a TKI of VEGFR and PDGFR) in combination with chemotherapy as a first-line therapy for metastatic gastric and oesophagogastric adenocarcinoma patients (NCT01130805, 2014, NCT01503372). A full list of all the major angiogenic therapies in Phase II and Phase III clinical trials for the treatment of gastric and oesophageal cancer are detailed in Table 1.2 Further studies on biomarkers for therapeutic response to and patient selection for anti-angiogenic therapies in oesophageal cancer may increase the clinical benefits above those already demonstrated.

Table 1.2 Phase II and III clinical trials of targeted anti-angiogenic therapies in gastric and oesophageal cancer

Agent	Trial Type	Number of patients	Histology	Response Rate	Overall Survival (months)	Author
VEGF monoclonal antibodies						
Bevacizumab + irinotecan/ cisplatin	Multi-centre Phase II	47	Locally advanced gastric and OGJ AC	65%	12.3	(Shah *et al.*, 2005)
Bevacizumab + docetaxel/ oxaliplatin	Single-centre Phase II	38	Advanced gastric and OGJ adenocarcinoma	42%	11.1	(El-Rayes *et al.*, 2010)
Bevacizumab + cisplatin/ docetaxel/ 5-FU	Single-centre Phase II	44	Metastatic gastric, OGJ and OAC	85%	16.8	(Shah *et al.*, 2011)
Bevacizumab +capecitabine/ oxaliplatin	Multi-centre Phase II	37	Advanced gastric and OGJ adenocarcinoma	51.4%	10.8	(Uronis *et al.*, 2013)

Bevacizumab + cisplatin/ fluoropyrimidine	Multi- centre randomised double-blind, Phase III (AVAGAST)	774	Metastatic gastric and OGJ	46.0% (vs. 37.4% placebo)	12.1 (vs. 10.1)	(Ohtsu *et al.*, 2011)
Bevacizumab + trastuzumab + capecitabine/ oxaliplatin	Multi-centre Phase II	35	Metastatic gastric, OGJ and OAC	76.5%	26.92	(Enzinger *et al.*, 2015)
Bevacizumab + cisplatin/ 5-FU(neoadjuvant)	Multi-centre Phase II	22	Locally advanced resectable OAC and OSCC	30% (R0 resection rate=44%)	23	(Idelevich *et al.*, 2012)
Bevacizumab + erlotinib +paclitaxel/ carboplatin/ 5-FU (neoadjuvant)	Single-Centre Phase II	62	Locally advanced resectable gastric and OAC	29%	30.2	(Bendell *et al.*, 2012)
Bevacizumab + epirubicin/ cisplatin/ capecitabine	Multi-centre randomised Phase II/III	200 (Phase III to recruit 1000)	Locally advanced resectable gastric and OAC	To be published	To be published	(Okines *et al.*, 2013)

VEGFR2 monoclonal antibodies						
Ramucirumab mono-therapy	Multi-centre randomised, double-blinded, placebo controlled Phase III (REGARD)	355	Advanced gastric and OGJ adenocarcinoma	3% (vs. 3% of placebo)	5.2 (vs. 3.8)	(Fuchs *et al.*, 2014)
Ramucirumab monotherapy	Multi-centre randomised, double-blinded, placebo controlled Phase III (RAINBOW)	665	Advanced gastric, OGJ and OAC	28% (vs. 16% of placebo)	9.63 (vs. 7.26)	(Wilke *et al.*)
Multi- tyrosine kinase inhibitors						
Sunitinib monotherapy	Multi-centre Phase II	78	Advanced gastric and OGJ adenocarcinoma	2.6%	6.8	(Bang *et al.*, 2011)
Sorafenib + docetaxel/ cisplatin	Single-centre Phase II	44	Advanced gastric and OGJ adenocarcinoma	44%	13.6	(Sun *et al.*, 2010)

1.6.2 Cyclooxygenase-2: an alternative anti-inflammatory and anti-angiogenic target in cancer

As indicated in Table 1.1 there is ongoing research investigating multiple signalling pathways as potential drivers of oesophageal cancer and thus as biomarkers of disease and therapeutic targets. An interesting candidate is cyclooxygenase 2 (COX-2), an inducible enzyme that synthesises a group of bioactive lipid signalling molecules (i.e. eicosanoids, see section 1.7.1) known as the prostaglandins that are recognised to have anti-apoptotic and pro-angiogenic roles in cancer (Daniel *et al.*, 1999, Liu *et al.*, 2000, Sheng *et al.*, 1998, Klenke *et al.*, 2006).

Over the past decade there has been growing preclinical and clinical evidence linking the expression of COX-2 and aberrant prostaglandin activity with cancer, particularly gastrointestinal cancers (Eberhart *et al.*, 1994, Liu *et al.*, 2008, Mehta *et al.*, 2006), breast cancer (Kim *et al.*, 2012, Nassar *et al.*, 2007) and lung cancer (Brown and DuBois, 2004). A recent meta-analysis of nine epidemiological studies including 1831 patients showed a 43% lower rate of oesophageal cancer (both OAC and OSCC) in patients who were treated with aspirin or non-steroidal anti-inflammatory drugs, suggesting a role of COX-2 in this disease (Corley *et al.*, 2003). Indeed COX-2 has been shown to be increasingly expressed across the progressive sequence from normal squamous oesophagus or reflux oesophagitis to BO and finally to OAC (Shimizu *et al.*, 2006). *Ex vivo* BO culture models have also shown an increase in COX-2 following treatment with components of reflux such as acid bile salts, in addition to a suppression inflammatory effect by the addition of COX-2 selective inhibitors (Shirvani *et al.*, 2000). Selective and non-selective COX-2 inhibitors decrease proliferation of BO and oesophageal cancer cell lines (Buttar *et al.*, 2002a, Souza *et al.*, 2000). They have also been shown to suppress COX-2 activity, associated inflammation and progression to adenocarcinoma in an animal model of BO (Buttar *et al.*, 2002b). An ongoing randomised Phase III trial in the UK (AspECT) which has recruited more that 2500 BO patients is examining the use of aspirin in combination with esomeprazole (an acid suppressive agent to combat aspirin-induced ulcers) to prevent progression to oesophageal cancer (NCT00357682, 2006, Jankowski, 2012). In an immunohistochemical study COX-2 was found to be strongly expressed in both early dysplastic and invasive OSCC tissue compared to the weak-negative staining of normal squamous epithelium samples (Zhi *et al.*, 2006). A recent study reported high COX-2 expression in over a quarter of OAC cases and a significant association with poor prognosis (both cancer specific and OS), indicating its potential as a prognostic biomarker for OAC (Prins *et al.*, 2012) (Figure 1.15). High COX-2 expression in

oesophageal cancer patients treated with neoadjuvant CRT was associated with very poor prognosis, suggesting its utility as a biomarker for response to neoadjuvant therapy (Xi *et al.*, 2005).

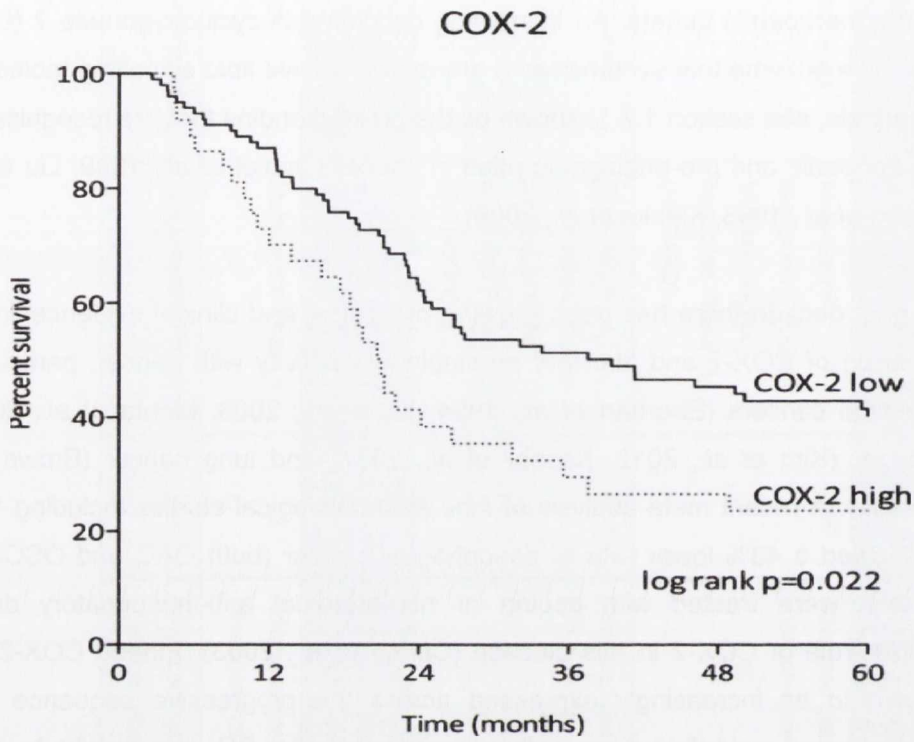

Figure 1.15 Cancer specific survival of OAC patients according to high and low COX-2 expression. Patients with low COX-2 had a median survival time of 39.5 months compared to patients with high COX-2 expression who had a survival time of 21 months (n=156, p=0.022; log rank). Reproduced from (Prins *et al.*, 2012)

Zhi *et al.* also noted that COX-2 was expressed in the angiogenic microvessels present within the oesophageal tumour suggesting it may have a function in angiogenesis (Zhi *et al.*, 2006). High COX-2 expression has been shown to be significantly associated with increased neovascularisation in Barrett's derived OAC (Mobius *et al.*, 2005). In contrast to this Prins *et al.* did not find a correlation between COX-2 and VEGF in a cohort of OAC patients (Prins *et al.*, 2012). COX-2 expression in colon cancer cells has been reported to induce neovascularisation by the increased production of VEGF and other pro-angiogenic factors (Tsujii *et al.*, 1998) while COX-2 inhibition blocked angiogenesis and suppressed tumour growth in a rat corneal model of angiogenesis and lung and colon mouse tumour models respectively (Masferrer *et al.*, 2000). Interestingly, other studies suggest COX-2 inhibition of tumour cell driven angiogenesis occurs via VEGF-independent pathways (Raut *et al.*, 2004, Xu *et al.*, 2014a). A recent

human colon cancer cell (HTC116) xenograft model with a VEGF knockout has shown restored tumour growth and angiogenesis when COX-2 was expressed suggesting COX-2 can actually induce pro-angiogenic effects independently of VEGF and may mediate resistance to VEGF-blocking therapies observed clinically (Xu *et al.*, 2014a). At the same time, dual inhibition of both COX-2 and VEGF with the selective inhibitors celecoxib and bevacizumab dramatically reduced tumour blood vessel densities compared to monotherapies, indicating that while these pathways can operate separately; COX-2 and VEGF can collaborate to enhance tumour angiogenesis (Xu *et al.*, 2014a). Thus pharmacological inhibition of COX-2 may prove to be an effective anti-cancer and anti-angiogenic strategy by firstly suppressing tumour growth and inducing apoptosis of cancer cells and secondly by blunting tumour cell production of angiogenic growth factors and by directly inhibiting the growth of the tumour neovasculature. The effects of COX-2 inhibition on angiogenesis in oesophageal cancer preclinically or clinically has not yet been described

A number of small Phase II trials have shown celecoxib in combination with neoadjuvant chemotherapy/ CRT to be active and well tolerated in patients with similar responses to other regimes (Govindan *et al.*, 2004, Dawson *et al.*, 2007) despite concerns over safety. In another Phase II trial an encouraging overall response rate of 35% was reported without increased toxicity (Enzinger *et al.*, 2004). The aforementioned safety concerns include evidence of increased cardiovascular toxicity and thrombosis risk with COX-2 inhibitors in clinical trials of other cancer types that have led to the early closure of trials by the FDA (e.g. Dawson *et al.*). These issues have deterred widespread clinical application and the initiation of randomised controlled trials in this research area at present. COX-2 inhibition has shown the greatest clinical benefits in colon cancer, significantly decreasing the sporadic formation of colorectal adenomas in patients with familial adenomatous polyposis (Bertagnolli *et al.*, 2006). Despite this, concerns over cardiovascular toxicities highlighted in the APPROVe (Adenomatous Polyp Prevention on Vioxx) trial have prevented its recommendation as a treatment to patients (Bresalier *et al.*, 2005). Efforts have now shifted to investigating other arachidonic acid derived eicosanoids such as lipoxygenase metabolites, in addition to COX-2 metabolites as drivers of gastrointestinal tumourigenesis and potential targets for dual therapies with celecoxib (Rao *et al.*, 2012). The lipoxygenase enzymes have been investigated in a number of different cancer types and their potential as clinical targets has been debated (Guo, 2012). Information on the role of these enzymes in oesophageal cancer is limited currently.

1.7 Lipoxygenases and their implication in carcinogenesis and angiogenesis

1.7.1 Eicosanoids

The eicosanoids are a family of membrane-derived lipid mediators which under normal physiological conditions play a role in the body's regulated response to infection and wound healing (Sivamani, 2014). However aberrant eicosanoid signalling is associated with pathological states including chronic inflammation and cancer (Khan *et al.*, 2015, Joshi and Pratico, 2014, Tersey *et al.*, 2015, Knab *et al.*, 2014). The n-6 twenty-carbon polyunsaturated fatty acid (PUFA) arachadonic acid (AA) is one of the most common PUFAs in our diet and it is the main source of eicosanoids. AA is stored in cell membrane phospholipids and can be mobilised by various phospholipase enzymes, such as phospholipase A2 in response to stimulation, and the released free fatty acid provides the substrate for the enzymes of the eicosanoid synthesis pathway. There are 3 classes of enzymes involved in the metabolism of AA: cyclooxygenases (COX) which metabolise AA to prostaglandins, prostacyclins and thromboxanes (collectively known as prostanoids), lipoxygenases (LO) which metabolise AA mainly to hydroxylated eicosatetraenoic acid (HETEs), leukotrienes and lipoxins, and finally cytochrome P450 which metabolises AA to dihydroxy acids and epoxyeicosatrienoic acids (EETs) (collectively known as epoxides) (Wang and DuBois, 2010) (Figure 1.16). Eicosanoids trigger signals for transcription of genes that modulate the immune system, haemostasis, apoptosis, cell proliferation as well as angiogenesis and many more processes which can result in an inflammatory environment that favours cancer development.

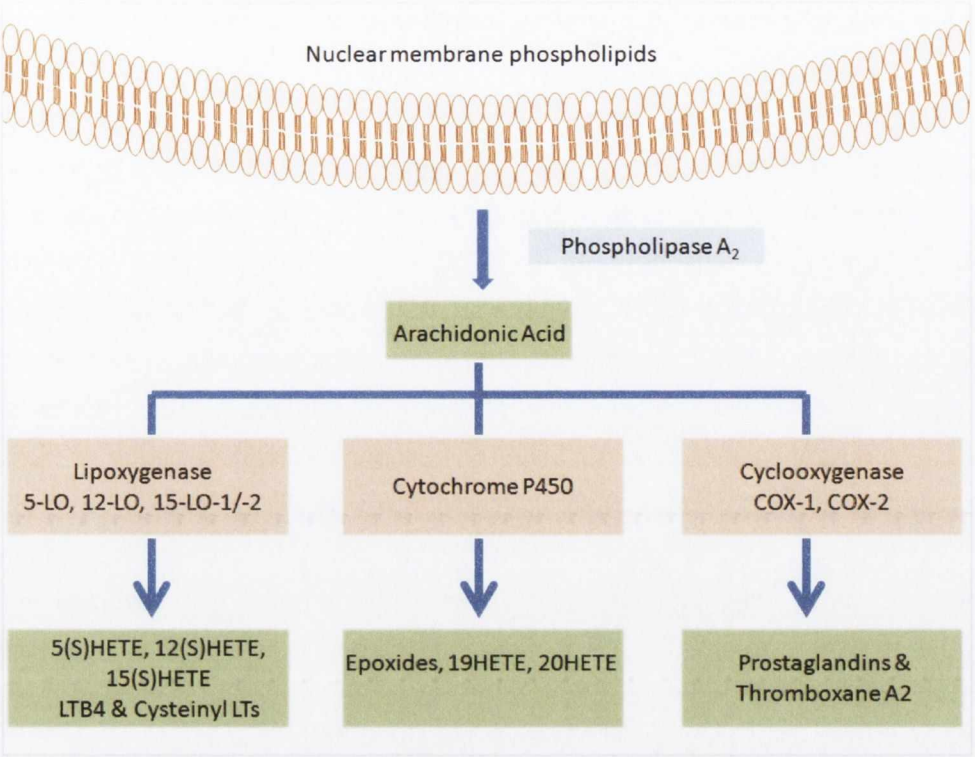

Figure 1.16 Arachidonic acid metabolism produces bioactive lipid signalling molecules known as eicosanoids. Upon cellular stimulation, phospholipase A2 induces the release of free fatty acids, mostly arachidonic acid (AA), from the lipid bilayer of the nucleus. The released AA is metabolised by one of three different enzymatic pathways into the bioactive lipid signalling molecules, known as eicosanoids. 5-LO metabolises AA to 5(S)HETE, LTB4 and the cysteinyl leukotrienes (LTC4, LTD4 and LTE4), 12-LO metabolises AA to 12(S)HETE. Both isoforms of 15-LO metabolise AA to 15(S)HETE and to a lesser extent 12(S)HETE. Cytochrome P450 metabolises AA to 19/20HETE but mostly epoxides. COX-1 and COX-2 metabolise AA to thromboxane A2 or a series of prostaglandins (PGD2, PGE2, PGF2, PGH2 and PGI2).

1.7.2 The family of lipoxygenase enzymes: classification of its members and their associated metabolites

Sequence homology studies have shown that all LO genes are derived from a single ancestral *ALOX* gene that through evolution has become duplicated several times to form the family of ALOX genes we study today (Guo and Nie, 2014). *ALOX5* is located on chromosome 5 while all other ALOX genes are located on chromosome 17. Members of the LO family are classified based on the position of a hydroperoxy group and include 3-, 5-, 8-, platelet type- 12(S)-, epidermal-type 12(R)- and 15-LO (Kuhn *et al.*, 2002). In humans 15-LO consists of two isoforms 15-LO-1 (gene name: *ALOX15*) and 15-LO-2 (*ALOX15B*) (Kuhn *et al.*, 2002). AA is metabolised to the biologically active metabolites hydroperoxy-eicosatetraenoic acids (HPETEs) which are then reduced to the corresponding HETEs, the major ones being 5(S)-, 8(S)-, 12(S)- and 15(S)HETE. Linoleic acid, as opposed to AA, is the preferred substrate of 15-LO-1 forming 13(S)- hydroxyoctanoic acid (HODE). To a lesser extent 15-LO-1 metabolises

AA to form 15(S)HETE and 12(S)-HETE. The murine form of 15-LO-1 is known as leukocyte-type 12-LO due to this formation of 12(S)HETE. On the other hand the only known metabolite of 15-LO-2 is solely 15(S)HETE. It is noteworthy that platelet type 12-LO (*ALOX12*) should not be confused with murine-derived leukocyte-type 12-LO. This terminology is outdated and it is now more correctly referred to as a 12-lipoxygenasing murine 15-LO (Kuhn *et al.*, 2015). Human *ALOX15* (15-LO-1) which is found in leukocyte subtypes such as eosinophils, stimulated monocytes and more recently some tumour cells shares 75% sequence homology with murine *Alox15.* (Mullin *et al.*, 2007). Human *ALOX15* preferentially produces 13(S)HODE and 15(S)HETE and to a lesser extend 12(S)HETE, hence it is often referred to as human 12/15-lipoxygenase in the literature. In comparison *ALOX12* shares only 57% sequence homology with murine *Alox15* (Mullin *et al.*, 2007). Despite the higher sequence homology with human *ALOX15* and the similar high expression in leukocytes, murine *Alox15* behaves more functionally like *ALOX12* producing 12(S)HETE mainly.

LOs, which are conceivably the least well studied of the three families of enzymes in the eicosanoid signalling pathway, have been indicated to have a role in cancer, both preclinically and clinically in a number of different cancer types. It is a complex relationship however, with both tumour suppressing and tumour promoting activities having been reported for various isoenzymes (Klil-Drori and Ariel, 2013). For example 15-LO-1 has been implicated as a tumour promoter of prostate cancer (Kelavkar and Cohen, 2004, Kelavkar *et al.*, 2001) but it was poorly expressed in breast and pancreatic cancer tissue compared to normal epithelium (Jiang *et al.*, 2006b, Hennig *et al.*, 2007a), and was reported to suppress CML and colorectal cancer (Middleton *et al.*, 2006, Nixon *et al.*, 2004, Shureiqi *et al.*, 1999). In contrast a largely anti-cancer role of 15-LO-2 has been reported, for example 15-LO-2 has been shown to be a tumour suppressor of prostate cancer (Suraneni *et al.*, 2014, Guo and Nie, 2014).

1.7.3 5-lipoxygenase and 12-lipoxygenase: potential role in driving cancer

The pronounced pro-inflammatory role of metabolites of the 5-LO pathway has been identified in a number of different pathological states including atherosclerosis, Alzheimer's disease, type 2 diabetes and cancer (Khan *et al.*, 2015, Joshi and Pratico, 2014, Neels, 2013). In resting cancer cells, 5-LO is located in the euchromatin region of the nucleus (Woods *et al.*, 1995), and upon activation 5-LO is translocated to the nuclear membrane where a vital interaction with FLAP (5-LO activating protein) allows

the metabolism of AA, released from the lipid bilayer by phospholipase A2 (Mancini *et al.*, 1993, Abramovitz *et al.*, 1993). AA is transformed to 5HPETE, which spontaneously reduces to 5(S)HETE. 5(S)HETE can be further metabolised to 5-oxo-ETE, a potent chemoattractant of eosinophils (Schwenk and Schroder, 1995), or to LTA4 (Samuelsson and Funk, 1989) (Figure 1.17). Subsequently LTA4 is oxidised by the enzyme leukotriene A4 hydrolase to LTB4, which is a potent chemo-attractant for monocytes, neutrophils and eosinophils, stimulating adhesion and extravasation through vascular endothelial barriers, migration to sites of inflammation, and their subsequent activation (Knab *et al.*, 2014). Alternatively LTA4 can be converted by LTC4 synthase to a number of other lipid mediators known collectively as the cysteinyl leukotrienes (LTC4, LTD4 and LTE4) which are known for their role in inflammatory cell recruitment, smooth muscle contraction, blood vessel dilation and permeability (Peters-Golden *et al.*, 2006) (Figure 1.17).

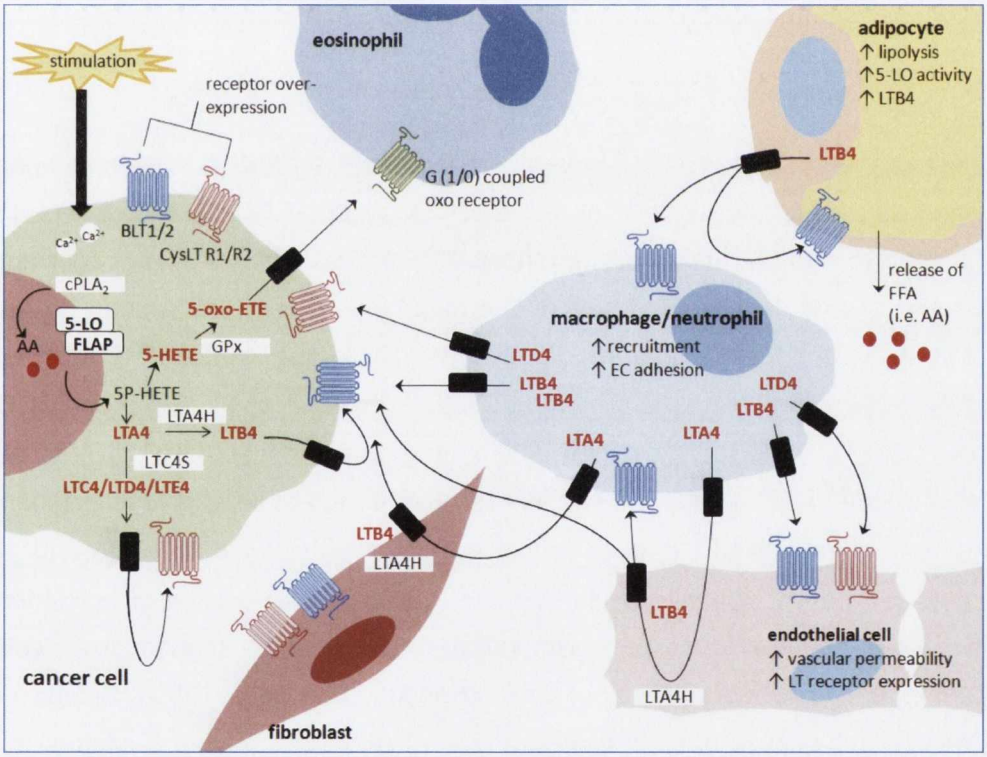

Figure 1.17 Summary of cross talk between cancer cells and stromal cells of the tissue microenvironment through 5-LO signalling. AA is transformed to 5PHETE, which spontaneously reduces to 5(S)HETE. 5(S)HETE can be further metabolised to 5-oxo-ETE, a potent chemoattractant of eosinophils or to LTA4. Subsequently LTA4 is oxidised by the enzyme leukotriene A4 hydrolase to LTB4, which is a potent chemo-attractant for monocytes, neutrophils and eosinophils. Alternatively LTA4 can be converted by LTC4 synthase to a number of other lipid mediators known collectively as the cysteinyl leukotrienes (LTC4, LTD4 and LTE4) which are known for their role in inflammatory cell recruitment, smooth muscle contraction, vessel dilation and permeability. Aside from cancer cells and immune cells, adipocytes are a major source of LTB4. Endothelial cells and fibroblasts in the tumour microenvironment have LTA4H activity and are capable of synthesising LTB4 by transcellular synthesis.

The involvement of the 5-LO pathway in the development and progression of tumours has led to its investigation as a potential biomarker in many cancers (Boger *et al.*, 2012, Shutt *et al.*, 2012). Reports indicate 5-LO activity was higher in a number of cancer tissues including prostate, renal, breast, colorectal and pancreatic tumours compared to normal tissue (Matsuyama *et al.*, 2004, Matsuyama *et al.*, 2007, Jiang *et al.*, 2006a, Hennig *et al.*, 2002, Barresi *et al.*, 2007). 5-LO gene and protein expression and 5(S)HETE production were significantly higher in malignant compared to benign tissue in a number of cancers including prostate, pancreatic and renal cell cancer (Gupta *et al.*, 2001, Hennig *et al.*, 2002,, Matsuyama *et al.*, 2005). 5-LO activity has been shown to correlate with clinical markers of disease progression (i.e. T-stage and lymph node metastasis) in prostate and colorectal cancer, suggesting its utility as a biomarker of disease progression (Matsuyama *et al.*, 2007, Barresi *et al.*, 2007). 5-LO expression has also been shown to be associated with early neoplastic changes during the development of pancreatic cancer (Hennig *et al.*, 2005a) and also with typical high risk factor for malignant transformation in benign colon polyps (Wasilewicz *et al.*, 2010) suggesting a role as an early biomarker of disease.

As mentioned previously, FLAP is a protein necessary for the activity and hence tumourigenicity of 5-LO by transferring AA to 5-LO (Figure 1.17). In a cohort of 154 breast samples (n=122) Jiang *et al.* showed that FLAP mRNA was aberrantly expressed in breast cancer compared to normal tissues and that expression was associated with prognosis (Jiang *et al.*, 2006a). There are 4 identified receptors involved in the 5-LO signalling pathway: The LTB4 receptors 1 and 2 (BLT1 and BLT2) and the LTC4, LTD4 and LTE4 cysteinyl leukotriene receptor 1 and 2 (CysLT-R1 and CysLT-R2) (Figure 1.17). BLT1 is a low affinity receptor for LTB4 expressed primarily by leukocytes whereas BLT2 is a more low affinity receptor for both LTB4 and 12-HETE expressed more ubiquitously (Tager and Luster, 2003). Cysteinyl leukotriene receptors have been reported in T-lymphocytes, eosinophils, mononuclear cells, macrophages and in certain cases neutrophils (Kanaoka and Boyce, 2004, Spinozzi *et al.*, 2004). Recent studies have indicated a role of these leukotriene receptors in a number of malignancies including urinary bladder, pancreatic, colon and breast cancer (Seo *et al.*, 2011, Hennig *et al.*, 2002, Magnusson *et al.*, 2010, Magnusson *et al.*, 2011).

Platelet 12-LO is thought to play a role in a number of chronically inflamed, pathological conditions including arthritis, atherosclerosis and cardiovascular disease, as well as an increasingly studied role in cancer (Liagre *et al.*, 1997, Poch, 2003, Catalano and

Procopio, 2005). Cellular stimulation results in the activation and translocation of 12-LO from the cytosol to the cell membrane in a Ca^{2+} dependant manner where it uses AA to form its only documented metabolite 12(S)HETE (Hagmann *et al.*, 1993). 12-LO is expressed in platelets, umbilical vein endothelial cells, megakaryocytes, and numerous cancer cells (Nie *et al.*, 2000, Sheppard *et al.*, 1992, Hussain *et al.*, 1994, Timar *et al.*, 1999, Yoshimura *et al.*, 2004).

As increased 12-LO activity has been documented in a number of cancers, its potential as a biomarker of disease has been investigated. Polymorphisms in the 12-LO gene are thought to affect susceptibility to certain cancer types. For example, 12-LO 261Gln/Gln is associated with heightened 12-LO activity and an increased risk of OSCC (Guo *et al.*, 2007) and colorectal cancer, and has also shown potential as a predictive biomarker of colorectal cancer (Li *et al.*, 2013b, Tan *et al.*, 2007). 12-LO was found to be higher in dysplastic and cancerous melanocytes compared to normal human skin melanocytes, indicating 12-LO as a potential biomarker of progression in melanoma cancer (Winer *et al.*, 2002). Overexpression of 12-LO has been reported in 38% of prostate cancers and high 12-LO transcript levels also associated with T-stage, high grade prostate cancer, suggesting its potential as a biomarker for progression and prognosis (Gao *et al.*, 1995). Although there has been limited success with patient serum and plasma (Rodriguez-Blanco *et al.*, 2014, Gondek *et al.*, 2014), urinary levels of 12(S)HETE were significantly elevated in cancer patients compared to normal controls, indicating its potential as a diagnostic marker (Nithipatikom *et al.*, 2006). In addition, removal of the prostate gland resulted in a normalisation of the urinary concentration of this eicosanoid (Nithipatikom *et al.*, 2006). 12-LO was also found to be more highly expressed in breast tumour tissue that normal tissue and there was a trend for 12-LO to be higher in patients who died of the disease, suggesting a potential prognostic role in breast cancer (Jiang *et al.*, 2003). Correlations of 12-LO expression with TNM staging in breast cancer have also been observed (Mohammad *et al.*, 2006).

1.7.4 Blocking 5-lipoxygenase and 12-lipoxygenase signalling in cancer

1.7.4.1 5-lipoxygenase

While research is still limited in this area, there have been efforts to elucidate the role that 5-LO and the leukotrienes play in cancer and the significance of their upregulation across a number of tumour types. Prostate cancer cells have been shown to constitutively produce 5(S)HETE in serum free/ unstimulated conditions *in vitro* (Ghosh and Myers, 1998). Treatment with MK886 (a FLAP inhibitor) and subsequent inhibition

of 5-LO signalling led to massive apoptosis (Ghosh and Myers, 1998). *In vivo,* 5(S)HETE production by metastatic prostate tumour mouse xenografts was significantly higher than that of *in situ* tumours while treatment with zileuton, a selective 5-LO inhibitor, resulted in fewer tumour masses (Meng *et al.*, 2013). Meng *et al.* also showed that treatment of prostate cancer cells with zileuton decreased their migratory ability in trans-well experiments. Furthermore Tong *et al.* documented similar results in an athymic mouse xenograft model of pancreatic cancer, where 5-LO inhibition was shown to decrease proliferation and cause apoptosis in the tumour mass (Tong *et al.*, 2002). A number of *in vitro* studies have reported an induction of apoptosis and/or decreased proliferation in cancer cells by 5-LO pathway inhibition that can be counteracted by the addition of exogenous 5(S)HETE (Matsuyama *et al.*, 2004, Sarveswaran *et al.*, 2011, Ding *et al.*, 1999). It has been established that 5-LO plays an important role in pancreatic cancer. Several pancreatic cancer cell lines, but not normal pancreatic ductal cells, have been shown to express 5-LO at both the gene and protein level (Hennig *et al.*, 2002). Inhibition of 5-LO (REV 5901) and FLAP (MK886) led to reduced pancreatic cell growth which could be reversed by the addition of 5(S)HETE, indicating a critical growth stimulatory role of 5-LO and its metabolite (Ding *et al.*, 1999). This pro-proliferative effect of 5(S)HETE, at least in pancreatic cancer cells, has been shown to occur via activation of the PI3 kinase/Akt pathway (Ding *et al.*, 2003). A number LO inhibitors including the specific 5-LO inhibitor REV 5901 altered pancreatic cancer cell proliferation through an induction of apoptosis with decreased Bcl2 and Mcl2 and increased Bax expression being reported (Tong *et al.*, 2002).

1.7.4.2 12-lipoxygenase

Similar to 5-LO, 12-LO and its bioactive metabolite 12(S)HETE have been reported to be involved in cancer development by modulating cell proliferation in a number of preclinical cancer models. Addition of 12(S)HETE to A431 epidermoid cell line cultures resulted in significant increase in cell proliferation while inhibition of 12-LO activity by 12-LO inhibitor baicalein led to apoptosis and a resulting decrease in the Bcl-2/Bax ratio and a downregulation of active ERK1/2 and PI3K-Akt pathways (Agarwal *et al.*, 2009). The effect of baicalein could be blocked by the addition of exogenous 12(S)HETE. Similar results were obtained in *in vitro* 12-LO inhibitory studies of heptocellular carcinoma cells (Xu *et al.*, 2012) and gastric cancer (Wong *et al.*, 2001, Chen *et al.*, 2008). Exogenous 12(S)HETE has been shown to enhance prostate cancer cell invasion (Liu *et al.*, 1994) and prostate cancer cells with higher metastatic potential (e.g. DU-145 vs. PC3) express significantly higher levels of 12-LO in

xenograft SCID mice studies (Timar *et al.*, 2000). In an *in vitro* breast cancer study, transient transfection of MCF-7 cells with 12-LO or addition of exogenous 12(S)HETE led to increased tumour cell proliferation and invasion (Liu *et al.*, 1996b, Liu *et al.*, 1996a). Inhibition of endogenous 12-LO expression in prostate cancer cell lines with baicalein was also shown to decrease cell survival through apoptosis (Matsuyama *et al.*, 2004). Furthermore, Pidgeon *et al.* found that this growth arrest was caused by a suppression of D cyclins (D1 and D3) and a decrease in phosphorylated retinoblastoma (pRB) while significant apoptosis was a result of decreased phosphorylated Akt, loss of survivin, upregulation of caspase-3 and decreased Bcl-2 (Pidgeon *et al.*, 2002). Interestingly, addition of 12(S)HETE blocked cell cycle inhibition and apoptotic effects of baicalein. Together these studies indicate a key regulatory role of 12-LO in cell proliferation and survival in cancer.

1.7.5 5-lipoxygenase interaction with immune cells

In addition to studies which focus on the role of LO in cancer cells, several studies have implicated LOs as regulators of the tumour microenvironment (TME) (Olkhanud *et al.*, 2011, Wejksza *et al.*, 2013). Given that both cancer cells and non-cancer stromal cells are potent producers of eicosanoids, tumour progression will likely involve an integrated response to eicosanoid signalling pathways. Apart from malignant cells, the TME consists of cells of the immune system, the tumour vasculature, lymphatics and extracellular matrix (ECM). Associated inflammation in the TME induces tumour development by providing fuels and growth factors to nurture epithelial cell growth and pro-angiogenic factors for vascularisation and angiogenesis.

There are a number of examples where 5-LO signalling cross-talk between tumour cells and innate myeloid cells (such as mast cells or tumour associated macrophages) or adaptive lymphocytes leads to increased tumourigenesis (Pace *et al.*, 2004 , Gounaris *et al.*, 2007, Wejksza *et al.*, 2013, Wen *et al.*, 2014). A recent murine study focusing on hematopoietic derived 5-LO, observed that specific deletion of this enzyme from bone marrow decreased polyp formation despite the presence of 5-LO proficient epithelial cells in these mice, indicating for the first time the importance of immune cell contribution to 5-LO activity (Cheon *et al.*, 2011). Mast cells, which have previously been shown to be critical for the formation of pre-neoplastic colon polyps (Gounaris *et al.*, 2007), were the most significantly reduced infiltrating myeloid cell type, losing their ability to produce 5-LO metabolites and capacity to stimulate intestinal epithelial proliferation and recruitment of myeloid-derived suppressor cells (MDSCs), a particular subset of immune cells capable of inhibiting protective anti-tumour cytotoxic T-cells.

They also lost their ability to modulate the immunosuppressive activity of arginase in MDSCs (Rodriguez *et al.*, 2004, Cheon *et al.*, 2011). Zileuton treated polyps were found to have significantly lower levels of infiltrating macrophages, mast cells, MDSCs (>50-60% lower) which Gounaris *et al.* suggest was responsible for the lower incidence of polyps in these mice. Therefore targeting myeloid 5-LO signalling may be an effective therapeutic strategy for polyposis and potentially colorectal cancer (Gounaris *et al.*, 2015). Reports have indicated that interactions between adipocytes and immune cells within adipose tissue may also be a major source of inflammatory 5-LO metabolites (Li *et al.*, 2015, Spite *et al.*, 2011) (Figure 1.17) and it is plausible that this interaction could increase inflammation in the TME and play a role in escalating obesity driven pathologies such as the pre-malignant condition BO and subsequent progression to OAC (Ryan *et al.*, 2011). In support of this, obese mice have been reported to have higher 5-LO and FLAP expression and enhanced LTB4 synthesis, in addition to increased levels of the leukocyte chemoattractants and activators TNF-α, IL-6 and MCP1 compared to lean mice (Horrillo *et al.*, 2010).

1.7.6 5-lipoxygenase and 12-lipoxygenase: role in tumour angiogenesis and VEGF signalling

1.7.6.1 5-lipoxyenase

There is some evidence of the expression of 5-LO in endothelial cells in the literature under different pathological conditions including pulmonary hypertension and highly angiogenic Kaposi sarcomas (Benard *et al.*, 2014, Walker *et al.*, 2002, Wright *et al.*, 1998, Sharma-Walia *et al.*, 2014). In general endothelial cells do not have the capacity to produce leukotrienes *de novo* due to low or negligible enzyme expression, however they do possess LTA4 hydrolase activity and therefore can convert the exogenous leukotriene intermediate LTA4, provided from another cellular source (e.g. macrophages, neutrophils, cancer cells) in the TME, to LTB4 and the cysteinyl leukotrienes LTC4, LTD4 and LTE4, in a process known as transcellular synthesis (Feinmark and Cannon, 1986, Folco and Murphy, 2006) (Figure 1.17). They also express both LTB4 receptors and CysLT receptors (Peters-Golden and Henderson, 2007), suggesting the probability of interactions between leukotriene synthesising cancer cells and non-cancer cells in the TME. In a number of studies LTB4 stimulation of endothelial cells in the presence of neutrophils led to increased vascular permeability both *in vitro* and *in vivo* (Bjork *et al.*, 1982, Rosengren *et al.*, 1991, Di Gennaro *et al.*, 2009). LTB4 has also been shown to induce endothelial cell migration, tubule formation and induce VEGF-mediated angiogenesis via BLT2 *in vivo* (Kim *et al.*, 2009). Glioma

tumour-derived microvascular cells have been shown to produce higher numbers of tubule structures in the presence or absence of VEGF compared to standard endothelial cell lines used such as the human umbilical vein endothelial cells (HUVEC) and ECV304. Recently a novel 5-LO inhibitor, synthetic dl-nordihydroguaiaretic acid (Nordy), has been shown to markedly reduce the tubule formation by glioma-derived endothelial cells, and also glioma xenograft induced neoangiogenesis *in vivo* suggesting that the previously described anti-tumour activity of this compound (Boado *et al.*, 1992) can be attributed at least in part to its ability to interfere with tumour angiogenesis (Bian *et al.*, 2006, Yang *et al.*, 2014).

Although one publication on oxygen-induced retinopathy has indicated an anti-angiogenic role of 5-LO (Sapieha *et al.*, 2011), the majority of evidence in a number of different pathological states, particularly cancer, indicate a pro-angiogenic role (Yang *et al.*, 2014, Chatterjee *et al.*, 2013, Ye *et al.*, 2004). For instance human malignant mesothelioma cells express catalytically active 5-LO, 5(S)HETE and LTA4, but not LTB4 and these metabolites were found to upregulate a major pro-angiogenic factor, VEGF, in human malignant mesothelioma model (Romano *et al.*, 2001). It can be hypothesised that 5-LO promotes tumour development by a dual mechanism, a direct proliferative stimulus on cancer cells, potentially through VEGF-suppressed apoptosis, and by driving a pro-angiogenic response by endothelial cells in the TME. Indeed Romano *et al.* observed that 5-LO products upregulate VEGF transcription HUVECs (Romano *et al.*, 2001). In cigarette smoke-induced inflammation of the colon in a mouse model 5-LO was found to be upregulated in adenomas. An accompanied increase in matrix metalloproteinase-9 (MMP-9) and VEGF, which could be blocked by pharmacologically inhibiting 5-LO, suggested that 5-LO expression in the inflamed colon may be involved in the angiogenic and inflammatory process of adenoma formation (Ye *et al.*, 2004). Furthermore in a study of 45 colorectal adenomas, 5-LO expression was found to correlate with microvessel density as indicated by CD105, suggesting tumour 5-LO activity may modulate the formation of blood vessels in this cancer (Barresi *et al.*, 2008). Phytochemicals in dietary black and brown rice bran have been shown to reduce tumour burden and tumour blood vessel formation in a mouse model of colon cancer and recent evidence suggests the mechanism of these natural chemicals is mediated through eicosanoid signalling pathways (Choi *et al.*, 2013). Transcript and protein expression of COX-2 and 5-LO as well as the production of their metabolites PGE2 and LTB4 were downregulated in addition to the major angiogenic factor VEGF. While definitive evidence was not provided, they suggest that the repression of VEGF and thus VEGF-induced tumour growth and neoangiogenesis is

mediated through a downregulation of these two eicosanoid enzymes, providing another example where 5-LO signalling is potentially involved in angiogenesis (Choi *et al.*, 2013). 7,12-Dimethylbenz[a]anthracene (DMBA)-induced mammary gland tumours in mouse models were shown to progressively express 5-LO (Chatterjee *et al.*, 2013). Treatment with zileuton not only reduced tumour burden but significantly reduced tumour-associated inflammation (indicated by immune infiltrate) and angiogenesis (indicated by microvessel density), implicating 5-LO as an important player in DMBA-induced mammary tumour development and angiogenesis. Similar to Ye *et al.*, 5-LO blocking by zileuton was shown to decrease VEGF and matrix metalloproteinase -2 (MMP-2) expression, indicating the crucial role of 5-LO in modulating the angiogenic process (Chatterjee M, 2013).

1.7.6.2 12-lipoxygenase

Overexpression of 12-LO in PC3 prostate cancer and A431 epidermoid cancer cells or addition of exogenous 12(S)HETE to cultures was found to increase surface integrin expression including αvβ5 as a method of increasing cancer cell survival (Pidgeon *et al.*, 2003). 12(S)HETE can also promote surface expression of integrin αvβ3 (a tumour-induced angiogenesis-related endothelial cell integrin) on endothelial cells (Tang *et al.*, 1994). 12-LO overexpressing prostate cancer cells injected into nude mice demonstrated increased tumourigenesis and vascularisation of the tumour, suggesting a growth advantage due to tumour-host interactions (Nie *et al.*, 1998). 12-LO overexpression in prostate cancer cells was also shown to increase adhesion properties towards certain collagens and vitronectin, increased invasiveness in matrigel and higher metastasis towards human bone in severe combined immunodeficiency (SCID) mice models compared to control (Nie *et al.*, 2003). Similarly, Connolly and Rose reported that 12-LO overexpressing breast cancer MCF-7 cells in nude mice xenografts demonstrated increased tumour growth and angiogenic activity in the tumour mass compared to control MCF-7 cells (Connolly and Rose, 1998).

Nie *et al.* showed that conditioned media from 12-LO overexpressing prostate cancer cells increased endothelial cell migration *in vitro* and vascularisation in matrigel implantation assay, confirming the angiogenicity of 12-LO transfectants (Nie *et al.* 2003). 12(S)HETE has effects on multiple processes associated with vessel growth and recent studies have tried to give some insight into how 12-LO executes its angiogenicity. Two separate studies revealed that overexpression of 12-LO in prostate cancer cells led to enhanced VEGF transcriptional activity and production while

blockage of 12-LO enzyme activity decreased VEGF, thus providing a mechanism through which 12-LO can stimulate angiogenicity in prostate cancer (McCabe *et al.*, 2006, Nie *et al.*, 2006). Increases in activated phosphorylated Erk1/2 and PI3 kinase in response to 12-LO overexpression were also noted in these two studies and inhibition of these two factors by specific inhibitors led to decreased VEGF. Thus suggesting Erk1/2 and PI3 kinase may be pathways linking 12-LO activity and VEGF transcription. A recent study investigated whether 12-LO regulates matrix metalloproteinase (MMP)-9, a key factor in invasion, metastasis and angiogenesis of prostate cancer, using 12-LO overexpressing prostate cancer cells (Dilly *et al.*, 2013). These cells were found to upregulate MMP-9 compared to controls. As previously discussed conditioned media from 12-LO overexpressing prostate cancer cells increased cell migration of HUVECs, indicating 12-LO angiogenicity. Dilly *et al.* indicated a specific involvement of upregulated MMP-9 in the angiogenicity of 12-LO by showing a downregulation of HUVEC migration in response to pre-treatment of the conditioned media with a neutralising antibody of MMP-9 (Dilly *et al.*, 2013).

Hypoxia induced factor 1 alpha (HIF1-α) is a transcription factor that is upregulated in response to hypoxic conditions and can activate key pathways involved in angiogenesis, including the VEGF pathway. In a recent publication it was shown that 12-LO overexpressing PC3 cells could upregulate HIF1-α expression and functional activity via the PI3K-Akt pathway (Krishnamoorthy *et al.*, 2010). siRNA knockdown of HIF1-α led to decreased 12-LO-induced VEGF expression in 12-LO overexpressing prostate cancer cells under hypoxic conditions, indicating that 12-LO mediates upregulation of VEGF through HIF1-α stimulation.

Nie *et al.*, showed that endothelial cells express a variety of eicosanoids including the 12-LO product 12(S)HETE and that endogenous 12-LO is involved in endothelial cell angiogenic responses (Nie *et al.*, 2000). They have also shown that 12-LO inhibitors reduce endothelial cell proliferation by downregulation of VEGF (Nie *et al.*, 2000). Furthermore 12-LO inhibitor baicalein and its analogue baicalin were shown to inhibit both proliferation and tubule formation of HUVEC endothelial cells in a dose dependant manner (Miocinovic *et al.*, 2005). Finally in another study natural curcuminoids, compounds that inhibit 12-LO, were shown to have the ability to reduce sprouting formation of endothelial cells (Jankun *et al.*, 2006). Clearly, 12-LO plays an important role in tumour cell and endothelial cell angiogenic responses and has potential as a therapeutic target.

1.7.7 The potential of 5-lipoxygenase and 12-lipoxygenase inhibitors as molecular targeted therapies in cancer

Despite the documented links between LO enzyme activity, and cancer development and progression in preclinical studies, the efficacy of lipoxygenase enzyme inhibitors as cancer chemotherapeutics clinically is a relatively under-researched area. The efficacy of targeting these pathways in the treatment of conditions of chronic inflammation is highlighted by the use of the 5-LO inhibitor zileuton, to improve pulmonary function in children and adults with mild-to-severe asthma (Kubavat *et al.*, 2013, Harris *et al.*, 1995). CysLT-R1 and CysLT-R2 antagonists such as montelukast and zafirlukast (Knorr *et al.*, 1998, Suissa *et al.*, 1997) are also available in some countries, however zileuton is the only FDA approved anti-leukotriene inhibitor.

Unlike the COX-2 story where epidemiological trials have linked non steroidal anti-inflammatory drug (NSAID) use to reduced cancer risk there are no published clinical trials involving LO inhibitors and there are no indications that patients who take zileuton or CysLT receptor antagonists such as montelukast and zafirlukast exhibit lower instances of cancer. An LTB4 receptor antagonist, LY293111, demonstrated promising activity and safety profiles in an initial Phase I study in patients with advanced solid tumours of various organs (Schwartz *et al.*, 2005). In an athymic mouse model of pancreatic cancer LY293111 was found to improve the efficacy of chemotherapy (Hennig *et al.*, 2005b). Unfortunately, LY293111 could not reproduce any beneficial effects for patients with metastatic pancreatic adenocarcinoma during Phase II (Saif *et al.*, 2009). New investigations and repurposing of current 5-LO pathway inhibitors may help to develop new therapies for cancer. For example zileuton is currently under investigation as an anti-cancer agent in a Phase I trial in a combination with imatinib to treat CML (NCT01130688).

5-LO has strong converging roles with another major eicosanoid COX-2, which has been strongly linked to tumourigenesis and angiogenesis, as discussed previously (Romano and Claria, 2003). Given that both enzymes utilise the same substrate of AA and have converging targets of VEGF expression and release, redundancy of these pathways has been suggested (Romano and Claria, 2003). Recent pharmacological inhibition studies have indicated a shunting mechanism between these two arms of the AA pathway where blocking of one enzymatic pathway leads to an upregulation of the other (Park *et al.*, 2012, Ye *et al.*, 2004) (Figure 1.18**).** Park *et al.* demonstrated that inhibition of COX-2 activity *in vitro* led to an increased LTB4 in head and neck squamous cell carcinoma (HNSCC). Knock-down of COX-2 showed only modest

effects to cell proliferation in several cell lines but combined knock-down of both COX-2 and 5-LO had superior inhibitory effects on tumour cell proliferation and VEGF production (Park *et al.*, 2012). Additionally, genetic disruption of 5-LO in a mouse model of ethanol-induced oral carcinoma resulted in activation of COX-2 and an increase in COX-2 metabolites thought to be produced mainly by inflammatory cells (Guo *et al.*, 2011, Romano and Claria, 2003). This evidence suggests dual inhibition of both these pathways may have a superior anti-cancer effect in the suppression of angiogenesis and highlights the question of whether other LO enzymes whose expression are often associated with cancer are also involved in this integrated system. A number of dual 5-LO/COX-2 inhibitors are currently under investigation however none have reached the market (Charlier and Michaux, 2003, Zhang *et al.*, 2008, Pommery *et al.*, 2004, Bitto *et al.*, 2012). Interestingly it has been recently shown that the selective COX-2 inhibitor celecoxib also has selectivity for 5-LO, indicating it's potential as a dual inhibitor (Sud'ina *et al.*, 2008, Maier *et al.*, 2008).

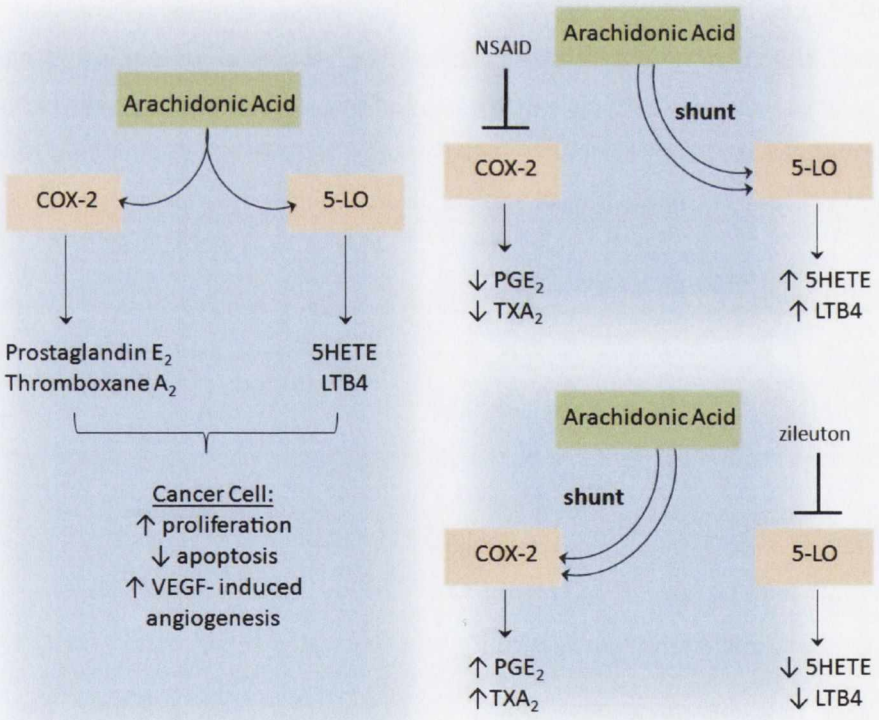

Figure 1.18 Pharmacological inhibition of COX-2 signalling pathway results in a shunting of arachidonic acid to the 5-LO pathway and vice versa

Some of the newest selective 5-LO inhibitors such as atreleuton (VIA Inc.), setileuton (Merck Inc.) and PF-419183 (Pfizer Inc.) and FLAP antagonists such as AM103 (Amira Pharmaceuticals and GlaxoSmith Kline) are currently undergoing clinical trials for non-cancer related pathologies such as cardiovascular disease, atherosclerosis, COPD and asthma. Thus indicating steady progress in the area of 5-LO drug development. (Steinhilber and Hofmann, 2014). A full list of different types of 5-LO pathway inhibitors currently in use in preclinical research or in clinical trials are listed in Table 1.3. In comparison to 5-LO, the discovery of selective and potent 12-LO inhibitors has had limited success, making it difficult to investigate thoroughly the effect of blocking this enzyme pathway in preclinical and subsequent clinical studies. Most drug discovery efforts in this area have isolated compounds from natural products that have later been shown to have poor selectivity for platelet-type 12-LO (see Table 1.4). For example baicalein is a commercially available flavonoid-based inhibitor of 12-LO originally shown to exert potent anti- 12-LO activity at nanomolar concentrations (Sekiya and Okuda, 1982) that has since been discovered to have equipotency for both 15-LO-1 and 12-LO (Deschamps *et al.*, 2006). In recent years alternative approaches such as quantitative high throughput screening (qHTS) of large libraries of compounds has yielded a number of new anti-12-LO structures with superior potency and specificity that may indicate a major turning point in research of 12-LO as therapeutic target in cancer (Kenyon *et al.*, 2011, Luci *et al.*, 2014). As of yet, no 12-LO inhibitors have been investigated in Phase I clinical trials.

Table 1.3 Commercially available 5-LO inhibitors in use in preclinical or clinical trials

5-LO Inhibitor type	Target	Reference
Iron chelating redox inhibitors		
Zileuton	selective 5-LO	(Harris *et al.*, 1995)
Nor-dihydroguaiaretic acid (NDGA) (creosote plant derivative)	non-selective LO	(Wang *et al.*, 2011a)
Competitive non-redox inhibitors		
Atreleuton-	selective 5-LO	(Tardif *et al.*, 2010)
Setileuton	selective 5-LO	(Ducharme *et al.*, 2010)
PF-4191834	selective 5-LO	(Masferrer *et al.*, 2010)
CJ-13610	selective 5-LO	(Cortes-Burgos *et al.*, 2009)
Other 5-LO pathway inhibitors		
Licofelone	Dual COX-2/FLAP	(Alvaro-Gracia, 2004, Fischer *et al.*, 2007)
Celecoxib	Dual COX-2/5-LO	(Sud'ina *et al.*, 2008)
Ketoconazole	Dual CYP51/5 LO/ TXS	(Nardone *et al.*, 1988)
AM103	FLAP antagonist	(Stock *et al.*, 2011)
REV 5901	Cysteinyl LT receptor antagonist	(Schroeder *et al.*, 2007)
Montelukast	Cysteinyl LT receptor antagonist	(Knorr *et al.*, 1998)
Zafirlukast	Cysteinyl LT receptor antagonist	(Suissa *et al.*, 1997)
LY293111	LTB4 receptor antagonist	(Saif *et al.*, 2009)

Table 1.4 Natural non-selective 12-LO inhibitors currently available

12-LO inhibitor Type	Target	Reference
NDGA (creosote bush extract)	Non-selective 12-LO	(Whitman *et al.*, 2002)
Caffeic acid	Non-selective 12-LO	(Cho *et al.*, 1991)
Baicalein (flavone)	Non-selective 12-LO and 15-LO	(Deschamps *et al.*, 2006)
Hinokitiol (Japanese cypress plant extract)	Moderate selective 12-LO	(Suzuki *et al.*, 2000)
Catechin (tea leaf extract)	Moderate selective 12-LO	(Yamamoto *et al.*, 2005)

1.7.8 5-lipoxygenase and 12-lipoxygenase in oesophageal cancer: research to date

There is currently limited research investigating the association of oesophageal cancer and LOs. In an immunohistochemical study of a mixed collection of oesophageal cancer cases (81 tissue samples from Anhui Medical University of China (all OSCC) and 80 from the MD Anderson Cancer Centre, USA (27 OSCC and 53 OAC)) 5-LO expression was present in 79% (127/161) of samples (Hoque *et al.*, 2005). Whereas only 13% (4/32) of distant normal oesophageal epithelium showed 5-LO expression. They correlated 5-LO with clinicopathological parameters available and 5-LO expression was associated with male cases (61/68) and moderate tumour differentiation and an absence of lymph node metastasis in OSCC cases only. Hoque *et al.*, also showed that inhibition of 5-LO with REV 5901 in a number of oesophageal cancer cell lines decreased cell viability and increased apoptosis suggesting its potential as a therapeutic target. Single inhibition of both COX-2 and 5-LO was found to decrease oesophageal tumour volume in an animal model of OSCC while dual inhibition showed increased effects (Shi *et al.*, 2011). Another immunohistochemical study examining a collection of human tissue samples from the University of Michigan (n=67) reported higher incidence of 5-LO tumour epithelial expression in OAC compared to normal oesophagus (53/56 cases showing at least weak positive (+) staining compared to 5/22 cases) (Chen *et al.*, 2004). A more recent study investigating 5-LO and other 5-LO pathway proteins expression in a mixed cohort of human BO metaplasia samples, OAC samples and proximal squamous oesophagus samples (UK cohort) (Boger *et al.*, 2012) only observed stromal staining of 5-LO. In contrast to the two previous studies discussed no epithelial staining was observed. The observed 5-LO stromal expression was increased in adenocarcinoma compared to normal

squamous tissue. Interestingly, LTC4 synthase, the enzyme that converts LTA4 to LTC4 was the only 5-LO signalling pathway protein where staining was found in both epithelial (BO and OAC) and stromal tissue in this study.

The role of platelet type 12-LO in the progression of oesophageal cancer is a relatively under-researched area. In one study, cDNA array analysis of OSCC patient samples (n=6 tumour and n=6 matched normal) was used to identify candidate genes involved in carcinogenesis. COX-2 and other genes involved with the AA pathway were identified to be upregulated, probing an investigation of the expression of other AA enzymes including 12-LO, 5-LO and COX-1 and COX-2. Although a small sample size group, marked increased expression of 12-LO was reported in the tumour OSCC samples by RT-PCR. Unfortunately despite this finding 12-LO was not included in a follow up immunohistochemical study in this publication (Zhi *et al.*, 2003). To our knowledge, other than the genotyping study previously mentioned (Guo *et al.*, 2007) there are no other studies in the literature linking 12-LO and oesophageal cancer. Additionally the angiogenic role of both 5-LO and 12-LO enzymes, previously documented in other cancer types (Section1.7.6) has not yet been investigated in oesophageal cancer specifically.

1.8 Aims and objectives

Due to the growing body of evidence implicating 5-LO and 12-LO signalling in tumourigenesis and tumour-associated inflammation and angiogenesis, it was hypothesised that these two enzymes play a role in the development and progression of oesophageal cancer, and angiogenic signalling in this cancer. Consequently the overall aim of this thesis was to investigate 5-LO and 12-LO expression in oesophageal cancer, with a main focus of the OAC subtype, and to assess the efficacy of inhibiting 5-LO and 12-LO with novel molecular targeted therapies. It was hoped that these novel inhibitors would show potential as an anti-cancer or anti-angiogenic treatment strategy for OAC.

1.8.1 Specific objectives

- Investigation of 5-LO expression in oesophageal cancer and its association with angiogenic and immune markers, obesity and patient clinical parameters

- Investigation of 12-LO expression and activity in oesophageal cancer and its association with angiogenic and immune markers, and clinical parameters

- Assessment of the anti-angiogenic effect of novel 5-LO and 12-LO inhibitors on *in vivo* and *in vitro* models of angiogenesis

- Assessment of the anti-cancer and anti-angiogenic effect of novel 5-LO and 12-LO inhibitors on *in vitro* and *ex vivo* models of OAC

Chapter 2 Materials and Methods

2.1 Reagents and general lab equipment

All laboratory chemicals and reagents were stored according to the manufacturer's instructions. All reagents were analytical grade and purchased from Sigma-Aldrich Chemical Company (Dublin, Ireland) unless otherwise stated. Solid chemicals were weighed out using a Radwag AS110.R2 analytic balance (Radwag, USA L.L.C.) and made up in sterile distilled water unless otherwise stated. The pH of solutions used was measured using a pH meter (Thermo Fisher Scientific, USA). Gilson pipettes (Gilson, PA, USA) were used for the transfer of volumes up to 1mL and were calibrated yearly. For volumes greater than 1 mL, an electronic pipette aid (Drummond Scientific Company, PA, USA) and disposable plastic 10 mL pipettes were used (Sarstedt, Ireland). All cell culture reagents were purchased from Lonza (Basel, Switzerland) unless otherwise stated. All plastic wear such as cell culture flasks and plates were purchased from Sarstedt (Wexford, Ireland) unless otherwise stated.

2.2 Drugs, chemical reagents and other materials

Ketoconazole, REV 5901, zileuton and SU11652 were purchased from Cayman Chemical (Ann Arbor, MI, USA). Novel 5-LO and 12-LO compounds were provided by Dr. David Maloney (NIH, Bethesda, MD, USA). The novel class of 5-LO inhibitors show nanomolar potency and more than 30-fold increased selectivity for 5-LO over other lipoxygenase paralogues (Hoobler *et al.*, 2013). The 12-LO synthetic inhibitors designed based on an 8-hydroxyquinoline or benzenesulfonamide scaffold have shown superior selectivity for 12-LO (IC_{50}~1 ±0.2 μM) compared to other lipoxygenase enzymes (Kenyon *et al.*, 2011, Luci *et al.*, 2014). All small molecule inhibitor compounds were in lyophilised form upon receipt and were reconstituted using dimethyl sulfoxide (DMSO). Arachidonic acid (AA) (Sigma Aldrich, Ireland) was in an oil form upon receipt, it was purged through a steady stream of liquid nitrogen, diluted with DMSO and dispensed into single use 250 μL plastic tubes. The tubes were briefly purged again with nitrogen before closing the lids and storing at -20°C. 12(S)HETE (Cayman Chemical, USA) were reconstituted in 100% ethanol. All drugs and metabolites were stored at 20°C. All experiments included a vehicle control of DMSO to ensure any effects observed were related to drug treatment specifically.

2.3 Cell culture

All cell culture work was carried out using aseptic technique within a grade II laminar air flow cabinet. The cabinet was allowed to run for at least 20 minutes prior to use. The

cabinet was sprayed down with 70% (v/v) ethanol to ensure sterility. All equipment and reagents used in cell culture were sanitised in a similar manner before putting in the cabinet. All liquid transfers in cell culture were performed using sterile 10 mL disposable pipettes and an automated pipette aid. A clean Howie lab coat with elasticated cuffs and sterile disposable gloves were worn at all times.

2.3.1 Cell lines

The OE33 cell line was used as an OAC cell model during this project. These cells were obtained from the American Collection of Cell Cultures (ATCC). They were maintained in Roswell Park Memorial Institute (RPMI) 1640 medium supplemented with 10% (v/v) foetal bovine serum (FBS) and penicillin streptomycin (50 U/mL penicillin, 50 U/mL streptomycin). HUVEC primary cells were used as a model of human macrovascular endothelial cells in the angiogenesis studies of this project. These cells were maintained in Gibco® Cascade Medium 200 supplemented with 10% (v/v) Gibco® Large Vessel Endothelial Supplement (LVES) and penicillin streptomycin (50 U/mL penicillin, 50 U/mL streptomycin).

All culture medias, phosphate buffered saline (PBS) and other reagents were heated to 37°C in a water bath before use in cell culture. Cells were examined daily using an inverted phase-contrast Nikon microscope (Nikon Corp., Tokyo, Japan). OE33 cells were incubated in 75 cm^2 vented flasks and HUVECs were incubated in 175 cm^2 vented flasks with Corning® CellBIND surface (to aid adherence). Both were kept in a humidified atmosphere with 5% CO_2 at 37°C. Sub-culturing was performed when cells reached 80-90% and 70% confluency for the OE33 cells and HUVECs respectively. For sub-culturing, growth medium was decanted from the flask and the cells were washed with 10 mL of PBS to remove residual serum. 1 mL (75 cm^2 flask) or 2.5 mL (175 cm^2 flask) of trypsin ethylene-diamine tetra-acetic acid (EDTA) (0.05% (w/v) trypsin, 0.02% (w/v) EDTA) was added to the flasks. Flasks were incubated at 37°C for approximately 5 minutes to allow cells to detach from the surface of the flask. 10 mL of complete medium (i.e. medium containing serum supplement) was then added to the flasks to inactivate the trypsin. Cells were transferred to a sterile 15 mL tube and pelleted by centrifugation at 180 x g for 2 minutes. This pellet was then resuspended in complete medium to the desired volume and was used to seed fresh flasks. In general confluent OE33 cells were sub-passaged using a 1:5- 1:6 ratio while HUVECs were sub-passaged using a 1:3-1:4 ratio. All culturing experiments with OE33 cells were carried out within 20 passages from the starting passage number. Primary HUVECs were only used between passage 2-8.

Cell stocks were stored under liquid nitrogen in a cryofreezer or at -80°C. Stocks were prepared from cells in the exponential phase of growth. To prepare frozen stocks, cells were washed with 10 mL PBS and trypsinised as described. The cell pellet from a 75 cm^2 flask of OE33 cells or a 175 cm^2 flask of HUVECs was resuspended in 4 mL of freezing medium (FBS and 10% (v/v) DMSO) and was divided into four 2 mL cryogenic vials and were placed at -80°C immediately. For long term storage, vials were transferred to liquid nitrogen. When breaking out fresh cells from frozen, the cryogenic vials were place at 37°C in the water bath to thaw rapidly. The thawed cell suspension was transferred to a 15 mL tube of complete culture medium and spun at 180 x g for 3 minutes to pellet the cells and remove as much of the DMSO as possible. The cell pellet was resuspended in 5 mL complete medium and transferred to a 25 cm^2 flask initially. After 24 hours media was replaced to remove any dead cells and residual DMSO. Once confluent, cells were transferred to larger culture flasks and were maintained as described previously.

2.3.2 Cell counting

For experiments requiring particular seeding densities, cell counting was carried out using a bright-line haemocytometer (Hausser Scientific, PA, USA). Pelleted cells were resuspended in 1 mL of medium. After brief pipetting up and down, 20 µL of cell suspension was added to 180 µL of 0.4% (v/v) trypan blue and mixed by pipetting. 20 µL of this suspension was added to the counter chamber of the slide. The number of viable cells (i.e. those unstained by the trypan blue) inside the four corners of the grid were counted under 40X magnification using a light microscope. Live cells that crossed the top and left hand side of the grid were also counted The average number of cells for the four corners was multiplied by the dilution factor (i.e. 10) and by $1x10^4$ to give an estimate of the cell density in cells/mL. This density could then be adjusted appropriately with cell culture medium to the required density for a particular experiment.

2.3.3 Mycoplasma testing

Cell lines were routinely tested for mycoplasma contamination using a MycoAlert® Mycoplasma detection kit (Lonza). This assay is a biochemical test that exploits the activity of certain mycoplasmal enzymes. These enzymes react with the MycoAlert® substrate, catalysing the conversion of ADP to ATP. A ratio of the level of ATP in a sample before and after addition of the substrate indicates the presence or absence of mycoplasma. If mycoplasmal enzymes are present, their reaction with the substrate

results in elevated ATP levels. Cells were maintained in antibiotic free medium for two passages before carrying out this assay. Briefly, 2 mL of culture medium was transferred into a centrifuge tube and spun at 200 x g for 3 minutes to pellet floating cells. 100 µL of the supernatant was transferred to a white-walled luminescence compatible 96-well plate. MycoAlert® reconstitution buffer was used as a negative control and supernatant from an in-house mycoplasma positive cell line provided a positive control. 100 µL of reconstituted MycoAlert® Reagent was then added to each sample and incubated for 5 minutes before a 1 second integrated reading was taken using the luminometer (reading A) (Victor™, Perkin ELmer, Columbus, OH, USA). 100 µL of the MycoAlert® substrate was then added to each sample for 10 minutes and a second reading was taken (reading B). The ratio of reading B to reading A was used to determine the presence of mycoplasma in the cell culture medium, with a ratio of greater that 1 indicating mycoplasma infected cells.

2.4 Patient tissue samples

All patients gave informed consent for use of their tissue in this project and samples were biobanked in accordance with the ethically approved standardised operating procedures of the department (Ennis *et al.*, 2010). All tissue samples used were collected from patients who underwent oesophagectomy for oesophageal cancer at St. James's hospital, Dublin. 196 oesophageal cancer patients from 1999-2009 with a minimum of 36 months of clinical follow up had paraffin embedded tumour sections arrayed on a tissue microarray (TMA). More recent frozen biobanked samples of tumour and matched normal adjacent tissue, adipose tissue and serum from oesophageal and junctional adenocarcinoma patients undergoing resection between 2007 and 2014 were used in other studies. Non-cancer serums (n=6) from patients undergoing hernia repair surgery during the same time frame were included in a serum study. Additionally, a small number of fresh OAC diagnostic tumour biopsies from September 2014 to July 2015 were used in an *ex vivo* study. Data pertaining to patient demographics, clinicopathological stage and outcomes were obtained for all patients included in these studies from a dedicated patient database.

2.5 Anthropometry

Accompanying anthropometric data was required for patient studies in Chapter 3. Patients were separated in to obese and non-obese categories based on waist circumference (WC), body mass index (BMI) and visceral fat area (VFA). Central

obesity indicated by waist circumference was defined by a cut of value of greater than 80 cm and 94 cm in female and male adults respectively (Alberti *et al.*, 2009). BMI was calculated by weight/height (kg/m^2) and a BMI of 25 and 30 were considered overweight and obese respectively. VFA was calculated by computed tomography staging scans. Obesity visceral adiposity was defined as VFA exceeding 163.8 cm^2 in males and 80.1 cm^2 in females (Doyle *et al.*, 2013).

2.6 Biological sample preparation

Blood samples were collected preoperatively for both cancer patients and the non-cancer control (i.e. hernia repair patients) following overnight fasting. Blood samples were allowed to clot in serum separator tubes at 4°C for 30 minutes and following centrifugation at 180 x *g* for 10 minutes the serum was decanted and frozen at -80°C. Both visceral and subcutaneous adipose tissue specimens were excised at an early stage in the oesophagectomy surgery procedure and immediately transferred to transport buffer (PBS, glucose (0.1% and gentamycin (0.05 mg/mL)) before fresh processing or snap freezing in liquid nitrogen and storage at -80°C. Multiple tumour tissue samples from the main resection specimen were taken by the designated upper GI biobank manager in the department shortly following surgery. Sampling of macroscopically normal tissue adjacent to the tumour (>10 cm from the tumour site) was also carried out. Normal adjacent and tumour tissue for RNA extraction were immediately submerged in Qiagen RNA*later* at 4°C overnight and the tissue was then snap frozen in liquid nitrogen and stored at -80°C until RNA preparation. Tissue samples for protein extraction were snap frozen immediately and stored at -80°C. The main resection specimen was formalin fixed and paraffin embedded for immunohistochemical staining. TMAs were created from the paraffin embedded resection specimens. Areas containing viable tumour cells, as indicated by haematoxylin and eosin staining, were marked by a qualified pathologist. Three 2 mm size sample cores were taken from tumour containing areas and were arrayed in a paraffin block. Each TMA was constructed to contain triplicates cores from fourteen tumour tissue blocks in addition to reference cores for correct slide orientation. The invasive edge of the tumour (i.e. the portion of tumour innervating into the surrounding muscle or fat) was marked by a pathologist if present and included in the TMA. Fresh OAC tumour biopsy tissue was also used in this project. This tissue was obtained from the endoscopy clinic where patients were undergoing diagnostic endoscopic examination and cancer was confirmed. The tissue was received in saline-soaked medical gauze and processed immediately as described in Section 2.20.2.

2.7 Isolation of RNA from epithelial tissue

Total RNA from tumour or normal adjacent tissue was extracted from approximately 20 mg of sample using a standardised protocol (RNAeasy® Mini Kit, Qiagen, Crawley, UK) and following the kit instructions. Tissue was disrupted and homogenised by rapid agitation in the presence of 7 mm metal beads and 600 µL lysis buffer.(buffer RLT with 10% β-mercaptoethanol) using a Qiagen TissueLyser (model RETSCH MM200) at 25 Hz for 30-40 seconds or until the lysate was uniformly homogenous. The lysate was centrifuged at 200 x g for 3 minutes and the supernatant was transferred to a microcentrifuge tube. 1 volume of 70% ethanol was added and the sample was mixed by pipetting. Up to 700 µL of the sample was transferred to an RNeasy spin column placed in a 2 mL collection tube and was centrifuged at 8000 x g for 15 seconds. The flow through was discarded and 700 µL of Buffer RW1 was added and the column was spun again for 15 seconds at 8000 x g. The flow through was discarded and 500 µL of RPE buffer was added and the column was centrifuged for 15 seconds at 8000 x g. The flow through was discarded and this step was repeated for a 2 minute spin. The column was then placed in a new 2 mL collection tube and spun at full speed for 2 minutes to remove any residual RPE flow-through. The column was placed in a 1.5 mL collection tube and 30-50 µL of RNase-free water was added directly to the column membrane. The sample was then centrifuged for 1 minute at 8000 x g to elute the RNA. The RNA was quantified and qualified as detailed in Section 2.10 and stored at -80°C.

2.8 Isolation of RNA from adipose tissue

Total RNA was isolated from fat tissue using the TRI reagent® method (MRC Inc., US). Approximately 100mg of tissue was homogenised in 1 mL of TRI reagent using the Qiagen TissueLyser for 2 minutes at 25 Hz. After incubation at room temperature for 5 minutes a centrifugation step at 12,000 x g and at 4°C for 10 minutes was performed. The resulting oily monolayer was carefully avoided while pipetting the rest of the sample into a 1.5 mL tube, 400 µL of 1-bromo-3-chloropropane was added and mixed by vortexing. After 3 minutes at room temperature the sample was centrifuged at 12,000 x g for 30 minutes. After centrifugation the sample has separated into three distinct layers, with the RNA in the upper phase. The RNA was carefully removed to a clean tube without disturbing the interface. 0.5 volumes of 2-propanol was added and the sample was gently inverted several times. After 5 minutes at room temperature the samples was centrifuged at 12,000 x g for 10 minutes. The 2-propanol was decanted off and the sample was washed twice with 1 mL of 100% molecular grade ethanol and

centrifugation at 12,000 x g for 5 minutes. After the second wash, the ethanol was decanted off and the pellet was air dried before resuspension in 30-40 µL RNase-free water. The RNA was quantified as detailed in Section 2.10 and stored at -80°C.

2.9 RNA isolation for cells

Cellular RNA used for Qiagen PCR profiler arrays was isolated using the RNeasy® Mini Kit. Cells grown in a monolayer in a 6-well plate were washed with PBS and cells membranes were disrupted and lysed by adding 350 µL of Buffer RLT to the well. Lysate was collected from the surface of the well, using a rubber policeman and was pipetted into a 1.5 mL microfuge tube. DNA in the sample was sheared by passing the lysate through a 20-gauge needle and syringe. The cell lysate was then processed in the same was as human tissue lysate in Section 2.7 to yield total cellular RNA.

All other cellular RNA was isolated using TRI reagent. Cells grown in monolayer were washed with PBS and then 1 mL of TRI reagent was added and the cell lysate was scraped into a microfuge tube and stored at -80°C for up to a month until the RNA extraction was carried out. On the day of extraction the lysate/TRI reagent sample was defrosted and kept at room temperature for 10 minutes. Following this 100 µL of bromo-3-chloro-propane was added to the sample per mL of TRI reagent. The sample was vortexed and then left to stand for 15 minutes. Next, the sample was centrifuged at 12,000 x g for 15 minutes at 4°C to allow phase separation. The clear layer overlying a pink layer separated by a white interface contains the RNA and was carefully removed, without disturbing the other layers. This was pipetted into a new microfuge tube and 500 µL of isopropanol was added, followed by thorough vortexing. A centrifugation step at 8000 x g was carried out for 8 minutes. The isopropanol was decanted and the remaining RNA pellet was washed with 75% ethanol by centrifugation at 12,000 x g for 2 minutes. The ethanol was decanted and the pellet was allowed to air dry before resuspension in 25-40 µL RNase free water. The RNA was quantified as detailed in Section 2.10 and stored at -80°C.

2.10 RNA quantification

The amount of RNA extracted was quantified by measuring the absorbance at 260 nm using the Nanodrop® ND-100 spectrophotometer (Nanodrop Technologies Inc., DE, USA). The A260/280 and 260/230 ratios were used to measure the purity of the sample, with a ratio of 1.8 or greater indicating low protein and low phenol

contamination. 1 µL of the isolated RNA sample was added to the pedestal of the instrument and the concentration was measured in ng/µL. Samples were kept on ice during this procedure to prevent degradation.

2.11 cDNA synthesis

All cDNA synthesis was carried out in a sterile hood environment using between 250 ng and 1 µg of RNA using the reagents and volumes listed in Table 2.1. The reverse transcriptase enzyme and 5x buffer were purchased from Bioline (Bioline, Kilkenny, Ireland) and all other reagents described were purchased from Invitrogen (invitrogen Corp, CA, USA). Initially the RNA, RNase-free water and 0.5 µg/µL random hexamer primers (40 ng/µl) were heated to 70°C for 10 minutes using a thermocycler (Applied Biosystems GeneAmp PCR system 9700) and then chilled on ice for 1 minute. Next, a master mix of RNaseOUT recombinant ribonuclease inhibitor (1 U/µL), deoxyribose nucleoside triphosphates (dNTPs) (10 mM: prepared as 1:1:1:1 ratio of dATP, dGTP, dTTP, dCTP) and Bioscript reverse transcriptase (200 U/µL) and 5x reaction buffer (Table 2.1) was added to the reaction and heated at 37°C for 1 hour, followed by 70°C for 10 minutes. The resulting cDNA was stored at -20°C until the qPCR run.

Table 2.1 Reagents and volumes used in cDNA synthesis

Step 1: Random primer annealing	
RNA + RNase-free water mix	11µl
Radom hexamer primers	1µl
Step 2: cDNA synthesis with master mix	
Bioscript reverse transcriptase	0.5µl
dNTP mix	1µl
RNaseOUT	0.5µl
5X Bioscript reaction buffer	4µl
RNase-free water	2µl
Total volume	**20µL**

2.12 Probe-based quantitative reverse transcription polymerase chain reaction

Probe-based quantitative polymerase chain reaction (qPCR) was used to quantify mRNA expression in samples relative to the *18S* ribosomal RNA endogenous control. In brief, sequence specific primers are designed with a fluorescent reporter molecule at the 5' end and a fluorescence quencher molecule at the 3' end. Upon transcription of the gene of interest, the Taq polymerase enzyme removes the quencher molecule from

the probe and allows fluorescence emission to be detected following laser excitation of the sample at a particular wavelength

A master mix containing 10 µl of Taqman® Gene Expression Master Mix (Applied Biosystems), 8 µL RNase-free water, 1 µL cDNA and 1 µL primer probe (Applied Biosystems) was added to each well of a MicroAmp™ Optical 96-well reaction plate (Applied Biosystems) in triplicate for each sample. A non-template control consisting of RNase-free water instead of cDNA was added to every plate that was run. Predesigned primer probes were sourced from either Applied Biosystems or Roche (Roche Diagnostics, Switzerland) (Table 2.2). Real time PCR detection was performed on the ABI Prism 7500 real time thermal cycler. The plate was heated to 95°C for 15 minutes, followed by 40 cycles of 95°C for 15 seconds and 60°C for 1 minute.

The relative quantification of target gene expression was performed using the comparative cycle threshold (Ct) method. A sample with median expression of the gene of interest is set at the calibrator (RQ value=1) which permits the quantification of all other samples relative to the calibrator. The relative target gene expression was given by the following formula:

2^(-ΔΔCt), where ΔΔCt= ΔCt sample - ΔCt sample calibrator sample,
with ΔCt=Ct target gene-Ct 18S.

Table 2.2 FAM-labelled primer probes and corresponding configuration numbers

Gene name of primer probe	Applied Biosystems	Roche
ALOX5	Hs01095330_m1	-
ALOX5AP	-	100052349
ALOX12	Hs00167524_m1	100053005
ALOX15	Hs00993765_g1	-
ALXO15B	Hs00153988_m1	-
8KRT	Hs01595539_g1	-
18S	Hs03928985_g1	-
VEGFA	Hs00900055_m1	100052376

2.13 Human Angiogenesis Pathway Finder Array

Changes in the expression profile of a panel of genes representative of molecular pathways of angiogenesis were examined using RT^2 profiler™ Human Angiogenesis Pathway Finder PCR Array technology (SABiosciences, MD, USA). This array is based

on a 96-well plate format, containing primer sets for 84 genes involved in angiogenesis including growth factors and receptors, cytokines, transcription factors and proteases and protease inhibitors (full list of gene is included in Appendix I). Five housekeeping genes were included to normalise the data and one genomic DNA contamination control, two reverse transcription controls and two positive controls were included to test the performance of the PCR system.

For this assay 3.0 x 10^5 cells (HUVECs or OE33 cells) were seeded per well of a 6-well plate. While HUVECs were allowed to adhere for approximately 24 hours, an additional 12-hour serum depletion step (0.5% FBS) for the OE33 cells was carried out at about 12 hours post seeding. At 24 hours the cells were treated with a specified drug or 0.1% DMSO as a vehicle control Drugs treatments and vehicle controls were made up in complete media for HUVECs and serum depleted media for the OE33 cells. 24 hours post treatment RNA was isolated using the RNAeasy® Mini Kit (Section 2.9). Using a First Strand cDNA synthesis kit (SABiosciences), 500 ng of each RNA sample was combined with 2 µL of Buffer GE in a sterile 500 µL PCR tube and made up to a final volume of 10 µL with RNase free water. The contents were vortexed briefly and centrifuged before being placed in a thermal cycler at 42°C for 5 minutes to eliminate genomic DNA. 10 µL of reverse transcriptase cocktail (4 µL 5x Buffer C3, 1 µL Control P2, 2 µL RE3 Reverse Transcriptase Mix and 3 µL of RNase free water) was added to each sample, briefly vortexed and centrifuged before incubating at 42°C for 15 minutes exactly, followed by 95°C for 5 minutes. 91 µL of RNase free water was added to each cDNA sample and samples were mixed.

Samples were prepared for the qPCR array by adding 1350 µL of 2x RT^2 SYBR Green master mix, 1248 µL RNase free water to 102 µL of the diluted cDNA sample in a 5mL tube to give a final reaction volume of 2700 µL. 25 µL of reaction mix was added to each well of the 96-well plate and the plate was sealed with optical adhesive film provided with the kit. Real time PCR detection was performed on an ABI Prism 7500 real time thermal cycler. The plate was heated to 95°C for 10 minutes, followed by 40 cycles of 95°C for 15 seconds and 60°C for 1 minute. The Ct value for each well was calculated using the instrument software and data analysis was carried out by uploading the data as an Excel file to a web-based PCR array data analysis software provided by SABiosciences. Data analysis was based on the ΔΔCt method with raw data normalised by the house keeping genes included in the plate. Gene changes were only reported if the transcript was amplified before 35 cycles.

2.14 SYBR-based quantitative reverse transcription polymerase chain reaction

A number of genes were selected from the array for validation by SYBR green dye based qPCR. cDNA from a minimum of three independent experiments was synthesised for the validation study. The cell culture set up and RNA isolation procedure was identical to that described in Section 2.13. cDNA was synthesised as described in Section 2.11 and a master mix containing 10 µL of GoTaq® qPCR master with BRYT Green® dye (Promega, WI, USA), 8 µL RNase-free water, 1 µL cDNA and 0.5 µL of 10 µM forward primer and 0.5 µL of 10 µM reverse primer (IDT, Integrated DNA Technologies, Iowa, USA) was added to each well of a 96-well qPCR reaction plate (Agilent Technologies, CA, USA) in triplicate for each sample. A non-template control consisting of RNase-free water instead of cDNA was added to every plate that was run. Predesigned primers sets were sourced using the online IDT PrimerQuest® design tool and the forward and reverse primer sequences are listed in Table 2.3. Real time PCR detection was performed on the Agilent MX3000P qPCR system (Agilent Technologies). The plate was heated to 95°C for 2 minutes, followed by 40 cycles of 95°C for 15 seconds and 61°C for 1 minute. Dissociation curve analysis was performed to ensure there were no primer-dimers and that all primers used in the same reaction plate had similar melting temperatures of 61-62°C. The relative quantification of target gene expression was performed using the comparative cycle threshold (Ct) method as described in section 2.12.

Table 2.3 Primer sequences for SYBR-based PCR

Gene	Primer Sequence
ALOX5	FWD: 5'- TCT TGG CAG TCA CAT TTC -3'
	REV: 5'- GAA TGG GTC CCT ATG GTG TTT A -3'
ALOX12	FWD: 5'- GAT CCG AGG AGA GAA GCA ATA C -3'
	REV: 5'- GGA GGC TGA ATC TGG ATG AC -3'
ANG	FWD: 5'- TGT TGG AAG AGA TGG TGA TGG -3'
	REV: 5'- GTG TGT GTA CCT GGA GTT ATC C -3'

ANGPT1	FWD: 5'- CCA AAG AGG CTG GAA GGA ATA -3'
	REV: 5'- GTA CTG CCT CTG ACT GGT AAT G -3'
ANGPT2	FWD: 5'- GAG GAA CAA AGG ACC GTG AA -3'
	REV: 5'- CTC TCC AGG CAT GCA GTA AA -3'
ACTB	FWD: 5'- GGA TCA GCA AGC ACC ACT ATG -3'
	REV: 5'- AGA AAG GGT GTA ACG CAA CTA A -3'
CXCL1	FWD: 5'- ACT CAA GAA TGG GCG GAA AG -3'
	REV:5'- CCC TTC TGG TCA GTT GGA TTT -3'
CXCL6	FWD: 5'- CCC TGG ACC CAG TAA GAA TAA G -3'
	REV: 5'- TAA ACT TCA GGG AGA AGC GTA G -3'
KDR	FWD: 5'- AGC AGG ATG GCA AAG ACT AC -3'
	REV: 5'- TAC TTC CTC CTC CTC CAT ACA G -3'
F3	FWD: 5'- CAC TAC CAC GCC AAG CTA AT -3'
	REV: 5'- GGT GGT TCA CGC CCA TAA TA -3'
GAPDH	FWD: 5'- CAA GAG CAC AAG AGG AAG AGA G -3'
	REV: 5'- CTA CAT GGC AAC TGT GAG GAG -3'
CXCL8	FWD: 5'- CTT GGC AGC CTT CCT GAT TT -3'
	REV: 5'- GGG TGG AAA GGT TTG GAG TAT G -3'
NRP1	FWD: 5'- GTC TGC CCT GGA GAA CTA TAA C -3'
	REV: 5'- GCC TTC ATG CCT CCG AAT AA -3'
TEK	FWD: 5'- TTT GCC CTC CTG GGT TTA TG -3'
	REV: 5'- CTT GTC CAC TGC ACC TTT CT -3'
TIE	FWD: 5'- CTA TCC TGG GCA TCC TTC TTT C -3'
	REV: 5'- GGC ATG TTA GTG GTG TGA GT -3'
TIMP1	FWD: 5'- GAT GGT GGG TGG ATG AGT AAT G-3'
	REV: 5'- CATTTATCCTCTAGCGCTCAGG-3'

VEGFA	FWD: 5'- CAG GAC ATT GCT GTG CTT TG -3'
	REV: 5'- CTC AGA AGC AGG TGA GAG TAA G -3'
VEGFB	FWD: 5'- GCT CTT CAC CAG GGT TCT TT -3'
	REV: 5'- GAC AAG CAA GGT CAC TCA GTA G -3'
VEGFC	FWD: 5'- TAC GGT CTG TGT CCA GTG TA -3'
	REV: 5'- TAT GTT GCC AGC CTC CTT TC -3'

2.15 Reverse transcription polymerase chain reaction (RT-PCR)

RT-PCR was used to confirm endogenous *ALOX12* expression of cell lines and to confirm overexpression of *ALOX12* following transient transfection. The following master mix was added to 1 µL of cDNA: 0.5 µL of 10 µM forward primer, 0.5 µL reverse primer (IDT, Integrated DNA Technologies, Iowa, USA), 10 µL of GoTaq® and 8 µL of RNase-free water. A non-template control with 1 µL RNase-free water instead of cDNA was included for each primer set used. For *ALOX12* expression the samples were denatured at 95°C for 5 minutes, followed by 30 cycles of 94°C for 30 seconds and 55°C for 1 minute and 72°C in a thermal cycler. For nested PCR 1 µL of product from the first round of PCR was then added to a master mix of 0.5 µL of 10 µM nested forward primer, 0.5 µL of 10 µM nested reverse primer (IDT), 10 µL of GoTaq® and 8 µL of RNase-free water and reamplified under the same conditions. β-actin (*ACTB*) was used as a housekeeping gene and was amplified in a thermal cycler under the optimised conditions described in section 2.14. 6x gel loading dye (Thermo Fisher Scientific) was added to PCR products and 15 µL of product was run on a 2% agarose gel (2% (w/v) agarose in 100 mL of tris acetate-EDTA (TAE) buffer (40mM Tris (pH 7.6, 20mM acetic acid, 1mM EDTA) and 0.005% GelRed™ (Biotium, Inc., CA, USA)) and imaged under UV light using the Fusion-FX7 Advance SUPER-BRIGHT imaging system.

Table 2.4 Sequences and amplicon length of primers used for nested RT-PCR

Gene	Primer Sequence	Amplicon length (bp)
ALOX12	FWD: 5'- CCT TCC CGT GCT ACC GCT GG -3	437
	REV: 5'- TGG GGT TGG CAC CAT TGA GG -3	
ALOX12 nested primers	FWD: 5'- CAG GAG ACA ATG CTT TGG AC -3	338
	REV: 5'- GAA CAA CTC ATC ATC CTG CC -3	
ACTB	FWD: 5'- GGA TCA GCA AGC ACC ACT ATG -3	99
	REV: 5'- AGA AAG GGT GTA ACG CAA CTA A -3'	

2.16 Immunohistochemistry

2.16.1 Staining procedure

TMA blocks containing 2 mm cores were made as described in section 2.6 and were cut into 4 µm sections that were mounted on to SuperFrost (Fisher Scientific) glass slides and baked overnight at 37°C. Pre-treatment of sections with Trilogy (Cell Marque) in an electric pressure cooker for 10 minutes at low pressure was sufficient for deparaffinisation, rehydration and antigen retrieval. After this the sections were left in fresh Trilogy at room temperature for 5 minutes followed by 5 minutes in distilled water. Next, the slides were treated with 3% H_2O_2 diluted in methanol for 30 minutes at room temperature in the dark to quench endogenous peroxidase activity. All primary antibodies used were rabbit anti-human and so accordingly the rabbit Vectastain Elite ABC kit (PK-6101, Vector Laboratories, CA, USA) was used. After 3x 5 minute PBS washes the sections were blocked using diluted goat serum (150 µL in 10 mL PBS) (Vectastain kit). Appropriate dilutions of 5-LO and 12-LO rabbit primary antibodies to be used were optimised on full face sections of tumour tissue. Diluted primary antibodies as described in Table 2.5 were added to the slides and incubated at room temperature for 1-2 hours. A negative control section incubated with PBS only was also included. Following 3x 5 minute PBS washes, diluted goat anti-rabbit secondary biotinylated antibody (50 µL secondary antibody, 150 µL goat serum in 10 mL PPBS) (Vectastain kit) was incubated on the sections. After 3x 5 minute PBS washes a diluted avidin-biotin complex reagent (150 µL reagent A and 150µL reagent B in 10 mL PSB) (Vectastain kit) was incubated on the sections at room temperature for 30 minutes. After 3x 5 minute PBS washes diaminobenzene (DAB) was added to the slides for

approximately 15 minutes or until sufficient colour development was observed. Slides were covered from direct light during this time. Next excess DAB was washed off the slides with distilled water and the sections were counterstained with haematoxylin and rinsed by a gentle stream of water for 5 minutes. The sections were dehydrated through methanol and xylene (Cell Path, UK) and mounted under coverslips (VWR International, PA, USA) using DPX (B.H.D. Prolabo Chemicals Ltd., UK). Immunohistochemical staining of VEGF, KDR and CD31 were carried out prior to this project and the dilution and incubation conditions are provided in Table 2.5. The staining procedure for VEGF and KDR was similar to that described above whereas CD31 staining was performed using a BondMax automated immunostainer (Vision BioSystems™), at the RCSI Research Centre, Beaumont Hospital, Dublin).

Table 2.5 List of antibodies and corresponding dilutions used in immunohistochemistry

Antibody	Isotype	Conditions (room temperature)	Supplier (cat#)
Anti-platelet 12LO	Rabbit polyclonal	1: 500, 1 hour	Abcam (ab125220)
Anti-5LO	Rabbit monoclonal	1:50 ; 1 hour	Cell Signalling (C49G1)
Anti-VEGF	Rabbit polyclonal	1: 200, 2 hours	Millipore (07-1420)
Anti-KDR	Goat polyclonal	1:20, overnight at 4°C	R&D Systems
Anti-CD31	Rabbit monoclonal	1:100, automated stainer	Dako

2.16.2 Imaging and scoring stromal and epithelial staining

Slides were digitally scanned and analysed using Philips Digital Pathology Ultra-Fast Scanner and software (Philips Digital Pathology Solutions, The Netherlands). Tumour epithelial and stromal staining was graded by 2-3 independent observers (at least 1 pathologist and 1 scientist). Staining was examined at high power for each core and quantified using a scoring system based upon the products of percentage positive cells (0-100%) and stain intensity (0 = negative, 1= weak, 2 = moderate, 3 = strong). to give an overall score for each core of 0-300. There were three 2 mm cores per patient and the mean score of these three cores was collated with clinicopathological and survival data from the prospective departmental database.

2.16.3 CD31 microvessel density counts

The same cohort of TMAs were previously stained for CD31, a vascular endothelial cell maker (Table 2.5). Full core microvessel density counts were carried out manually at 100X using a light microscope (Nikon Eclipse E200) by two independent observers. Vessels with strong membranous staining and a clearly defined lumen or well-defined

linear shape were counted, but not single endothelial cells. The mean number of vessels for the three cores of each patient was used for correlation studies.

2.17 Cell and tissue lysate preparation

2.17.1 Cultured cells

Culture medium was removed from cells grown in monolayer and added to a 1.5 mL microfuge tube and centrifuged at 180 x g for 3 minutes to pellet any floating cells. The monolayer of cells were then washed with ice cold PBS and then lysed directly in the culture vessel with ice cold lysis buffer (RIPA buffer (50mM Tris HCl, pH 7.4, 150 mM NaCl, 1 mM EDTA, 0.5% (w/v) sodium deoxycholate, 0.1% sodium dodecyl sulfate (SDS) and 1%Triton-X) and with added protease inhibitor cocktail (cOmplete™ protease inhibitor cocktail tablets, Roche)). 10 µL of lysis buffer was added per cm^2. If higher concentration protein was required the lysis buffer volume was reduced accordingly. The lysed cells were scraped up using a rubber police man and added to the pellet of floating cells collected from the culture medium. The sample was vortexed thoroughly and left on ice for 30 minutes with occasional brief vortexing. Then the lysate was passed through a 20-gauge needle and syringe to shear DNA. Isolated protein lysates were stored at -80°C.

2.17.2 Tissue

10-20 mg of tissue was disrupted and homogenised by rapid agitation in the presence of 7 mm metal beads and 50 µL lysis buffer (RIPA buffer and protease inhibitor cocktail) using a Qiagen TissueLyser at 25 Hz for 30-40 seconds or until it was uniformly homogenous. The sample was then left on ice for 30 minutes, briefly vortexing occasionally. The lysate was then centrifuged at 10,000 x g for 20 minutes at 4°C to pellet any debris and the clear lysate was transferred to new 1.5 mL microfuge tube. After passing through a 20-gauge needle and syringe to shear DNA, the sample was stored at -80°C.

2.18 Protein quantification

The Pierce bicinchoninic acid (BCA) protein assay (Thermo Scientific, IL, USA) was used to determine protein concentration of cell and tissue lysate samples. The principle behind the technique is as follows: in the presence of protein, Cu^{2+} is oxidised to Cu^{+} which reacts with the BCA reagent under alkaline conditions, yielding a coloured (purple) product. A seven point standard curve of bovine serum albumin (BSA) from 0 to 2,000 µg/mL with a working range of 20 -2,000 µg/mL was used to determine the

protein concentration of unknown samples (see representative standard curve in Appendix II). 25 µL of each standard and unknown sample were pipetted in duplicate into a 96-well microplate. 200 µL of BCA working reagent (1 part BCA reagent A and 50 parts BCA reagent B) was added to each well. Depending on the origin of the protein lysate, the unknown sample may have been pre-diluted to fit in the range of the standard curve. The plate was shaken briefly and incubated at 37°C for 30 minutes. Then the absorbance of all wells was read a 562 nm on a Versamax microplate reader and the concentration of samples was determined by extrapolation of the curve, multiplying the determined concentration by dilution factors if necessary to give the final concentration.

2.19 Protein SDS-PAGE and Western blotting

2.19.1 Protein separation by SDS-PAGE

Polyacrylamide gel electrophoresis of protein samples was carried out using the Mini-PROTEAN Tetra Cell (Bio-Rad, CA, USA) hand cast gel apparatus and electrophoresis tank. A 12% (w/v) SDS-PAGE gel separation gel was made using 9.2 mL 30% (w/v) acrylamide:bisacrylamide, 4.5 mL 1.875 M Tris HCl (pH 8.8), 8.3 mL distilled water, 176 µL 10%(w/v) sodium dodecyl sulfate (SDS), 120 µL 10% (w/v) fresh ammonium persulfate (APS) and 10 µL N,N,N',N'-tetramethylethane-1,2-diamine (TEMED). This solution was sufficient volume for two gels. The solution was gently mixed and the gels were cast between upright glass plates. Isopropanol was layered onto the gels to exclude air and aid polymerisation. After polymerisation the isopropanol was removed and the surface of the gel was rinsed with water. A 5% (w/v) stacking gel was prepared containing 1.7 mL 30% (w/v) acrylamide:bisacrylamide, 2 mL 0.6 M Tris-HCl (pH 6.8), 6 mL distilled water, 100 µL 10% (w/v) SDS, 150 µL 10% (w/v) APS and 10 µL TEMED. After gentle mixing the stacking gel was added to the top of the polymerised gel and a 15-well comb was inserted before allowing the gel to set. Protein samples were diluted in 4x Laemmli buffer (for 10 mL stock: 2 mL 1 M Tris-HCl, pH 6.8, 0.8 g SDS, 4 mL 100% glycerol, 0.4 mL 14.7 M β-mercaptoethanol, 1 mL 0.5 M EDTA, 8 mg bromophenol blue, 2.6 mL distilled water) and denatured by heating at 95°C for 10 minutes. 40 µg of protein was loaded into the gel for cell or tissue lysate samples. In the case of recombinant 12-LO protein 100 ng was loaded as recommended by the manufacturer (ab112250, Abcam). Additionally 9 µL of prestained Spectra™ Multicolour Broad Range Protein Ladder (Thermo Fisher Scientific, USA) was also loaded into the gel. Samples were separated by electrophoresis at a constant voltage

of 200V for 2 gels in electrode buffer (50 mM Base Trizma, 384 mM glycine, 0.1% (w/v) SDS) for approximately 60 minutes or until the dye front reached the end of the gel.

2.19.2 Protein transfer

Separated proteins were transferred onto polyvinylidene fluoride (PVDF) membrane (Pall corp., FL, USA) using the Mini Trans Blot® (Bio-Rad) wet transfer apparatus. The PVDF membrane was pre-activated in 100% methanol for 1 minute and then soaked alongside Whatman filter paper (Whatman Laboratory Division, Kent, UK) in cold transfer buffer prior to transfer. The gel and PVDF membrane were sandwiched between two layers of filter paper in the transfer cassette and placed in the buffer tank with the PVDF membrane orientated towards the positive electrode. An ice pack was added to the buffer tank and the tank was filled with ice cold transfer buffer (0.15 M glycine, 20 mM Trizma base, 0.1% (w/v) SDS, 20% (v/v) methanol). Proteins were transferred for 1 hour at 100V constant (~350mA).

2.19.3 Western blotting

Following the transfer of proteins, the PVDF membrane was blocked with 5% (w/v) BSA in Tris-buffered saline (25 mM Tris HCl (pH 7.6), 150 mM NaCl) containing 0.1% Tween-20 (TBST) on a shaker for 1 hour at room temperature. The membrane was then incubated in a 50 mL conical tube with 5 mL of rabbit primary antibody (see Table 2.6) diluted in 5% (w/v) BSA in TBST on an electrical roller overnight at 4°C. After 3x 5 minute washes with TBST, the membrane was incubated in a 50 mL conical tube with 5 mL horse-radish peroxidase (HRP) conjugated goat anti-rabbit secondary antibody (1:5000 dilution in 5% (w/v) BSA in TBST) (sc-2030, Santa Cruz, TX, USA) on an electrical roller for 1 hour at room temperature. Following 3x 5 minute washes in TBST, Supersignal® West Pico Chemiluminescent Substrate kit (Thermo Scientific, IL, USA) was added to the membrane to detect bound antibody complexes. Working solution was prepared by mixing .equal parts of the stable peroxidase solution and the luminol/enhancer solution and incubated with membrane for 5 minutes. The blot was removed from the working solution, excess reagent was drained off and the blot was placed between acetate for exposure and imaging using an automated chemiluminescent imager (Fusion-FX7 Advance SUPER-BRIGHT). Densitometric analysis was carried out using ImageJ software (NIH, MD, USA). β-actin protein levels were used as a house keeping protein loading control. Values were represented as a ratio of sample band intensity to that of corresponding β-actin.

Table 2.6 List of primary antibodies and corresponding dilutions used for western blotting

Antibody	Isotype	Dilution	Supplier (Cat#)
Anti-5-LO	Rabbit monoclonal	1:1000 in 5% BSA/ TBST, overnight 4°C	Cell Signalling (C49G1)
Anti-12-LO	Rabbit monoclonal	1:1000 in 5% BSA/ TBST overnight 4°C	Abcam (ab16834)
Anti-β-actin	Rabbit monoclonal	1:1000 in 5% BSA/ TBST 1 hour room temperature	Cell Signalling (4970S)

2.20 Enzyme-linked Immunosorbent Assay

2.20.1 ELISA protein quantification from human serum

Enzyme linked immunosorbent assay (ELISA) was used to detect LTB4 (Enzo, NY, USA), 12(S)HETE (ENZO) and VEGF (R&D systems, Inc., MN, USA) levels in human serum samples. Serum samples obtained from the biobank were vortexed thoroughly once defrosted and they were kept on ice while in use. Serum was diluted 1:4 and 1:100 with reagent diluents for LTB4 and 12(S)HETE detection respectively while serum samples were undiluted for VEGF detection.

2.20.2 ELISA protein quantification from *ex vivo* cultured tumour explants

Fresh pre-treatment diagnostic OAC biopsies were obtained from the day clinic at St. James's hospital and processed immediately. Biopsies were cut into several similar sized pieces where possible and each tumour piece was added to a well in a 12-well plate containing 1 mL *ex vivo* medium (Medium-199, 10% FBS, 1 µg/mL insulin, 50 U/mL penicillin) plus a drug or vehicle control (i.e. DMSO). The plate was sealed with parafilm and incubated for 24 hours at 37°C with 5% CO_2. After 24 hours the piece of tumour was transferred to a 1.5 mL screw cap microfuge tube and the conditioned media was pipetted into another microfuge tube. Both were snap frozen in liquid nitrogen and stored at -80°C until further processing. LTB4 and 12(S)HETE were measured by competitive ELISA (Section 2.20.4), neuropilin-1 and GRO-α were measured by DuoSet sandwich ELISA (Section 2.20.5) and a panel of angiogenic factors were measured using a multiplex ELISA (Meso Scale Discovery, MD, USA) (Section 2.20.6) using undiluted conditioned medium samples following drug treatment. The snap frozen tumour tissue was homogenised and lysed and total protein was quantified as described in Section 2.17.2 and Section 2.18 to normalise detected analyte concentrations to total protein content.

2.20.3 ELISA protein quantification from *in vitro* cultured cells

LTB4 and 12(S)HETE ELISAs and a number of angiogenic protein Duoset® ELISAs (R&D systems) were used to determine the analyte concentrations in cell culture supernatants following treatment. In order to assess LO metabolite and angiogenic protein levels in cell culture supernatants, 5.0 x 10^4 cells (either HUVECs or wild-type OE33 cells) were seeded into a 24-well plate and incubated at 37°C in 5% CO_2. HUVECs were allowed to adhere and grow for 24 hours, while in the case of the OE33 cells, a extra 12 hour serum depletion step (0.5% FBS) was carried out at about 12 hours post seeding. At 24 hours post-seeding the cell culture media was removed and the cells were treated for 24 hours with either a drug or vehicle control in combination with 10 µM AA, dissolved in 1 mL of complete medium/well for the HUVECs or 1 mL of serum depleted media/well for the OE33 cells. While wild-type OE33 cells were used for the assessment of 5-LO inhibitor effects on secreted proteins, 12-LO overexpressing OE33 cells were used for the assessment of 12-LO inhibitor effects. The protocol for reverse transfection of OE33 cells in a 24-well plate is described in Section 2.26.3. Similar to wild-type OE33 cells, a 12 hour serum depletion step, 12 hours post seeding and a 24 hour drug treatment were carried out.

After 24 hour treatment the cell supernatants were harvested and stored at -20°C. If a large number of non-adherent cells were observed in the culture medium, the plates was centrifuged at 180 x g for 3 minutes before removing the supernatant. The monolayer of cells was washed with PBS and then lysed with lysis buffer as described in section 2.17.1 and protein was quantified by BCA assay (section 2.18). Lipoxygenase metabolite and angiogenic protein levels were measured in undiluted cell supernatant and concentrations were normalised by total protein content of the cells to account for treatment induced apoptosis or cellular senescence.

2.20.4 Competitive ELISA

LTB4 and 12(S)HETE levels were measured by competitive ELISA. Competitive ELISAs use a polyclonal antibody to bind competitively to antigen in the sample or conjugated-antigen. recombinant antigen conjugated to a alkaline phosphatase molecule or antigen present in the test sample. The more antigen present in the sample the less recombinant analyte is bound to the antibody and the less signal is produced when substrate is added. Thus the amount of signal produced is inversely proportional to the amount of antigen in the sample.

The 96-well assay plate was pre-coated with goat antibody specific to rabbit IgG upon arrival. 100 µL of Assay Buffer diluent was pipetted into the non-specific binding (NSB) and the Bo wells (0 pg/mL standard). The stock of supplied antigen standard was diluted with Assay Buffer to the appropriate concentration of the highest standard (see Table 2.7) and this was subsequently serially diluted 1:2 to create a 5 point standard curve. 100 µL of Standards were added in duplicate to the appropriate wells. 100 µL of samples (neat or pre-diluted depending on sample type) were added to the appropriate wells. 50 µL of blue conjugate was added to all wells except the blank and total activity (TA) wells. 50 µL of yellow polyclonal antibody was added to each well except the Blank, TA and NSB wells. At this point the Blank and TA wells should be empty, the NSB wells should be blue and all other wells should be green). The plate was sealed with a plastic seal provided and incubated for 2 hours at room temperature on a plate shaker at 500 rpm. The contents of the wells were then emptied and 3x 400 µL washes with Wash Buffer were carried out. The final Wash Buffer step was completely aspirated and the plate was firmed tapped on tissue paper to remove are residual Wash Buffer. At this point 5 µL of Blue Conjugate was added to the TA wells (in the 12(S)HETE kit only, the Blue Conjugate was diluted 1:10 with Assay Buffer for the TA wells). 200 µL of pNpp Substrate solution was added to all 96-wells. The plate was resealed and incubated at 37°C for 2 and 3 hours without shaking for the LTB4 and 12(S)HETE kit respectively. 50 µL of Stop Solution was added to each well. The plate was read at 450 nm using the microplate reader. The optical density (OD) of the blank wells was subtracted from all the readings. Metabolite concentrations were determined using 4 parameter non-linear regression (curve fitting).

Table 2.7 LTB4 and 12(S)HETE ELISA kits used and corresponding standard concentration range

ELISA kit	Highest Standard	Lowest Standard	Company (Cat. #)
12(S)HETE	50,000 pg/mL	195 pg/mL	ENZO ADI-900-050
LTB4	3,000 pg/mL	11.7 pg/mL	ENZO ADI-900-068

2.20.5 DuoSet sandwich ELISA

A number of angiogenic proteins were measured in cell culture supernatants using DuoSet® sandwich ELISAs and the assay was carried out as per manufacturer's protocol. In principle a capture antibody pre-coated on the surface of the plate binds any antigen present in the sample. Any bound antigen is then also bound by a detection antibody which is subsequently bound by an enzyme-linked secondary antibody to emit a signal that is proportional to the amount of bound antigen. A high binding 96-well ELISA plate (Greiner-Bio, Frickenhausen, Germany) was coated with 100 µL of diluted capture antibody overnight at room temperature. The next day the capture antibody was aspirated and 3x 400 µL washes with Wash Buffer (0.05% Tween-20 in PBS) were carried out. Residual Wash Buffer was removed by tapping on tissue paper. The plate was then blocked with Reagent Diluent (1% BSA in PBS) for 1 hour at room temperature to prevent non-specific binding. The stock of supplied antigen standard was diluted with Reagent Diluent to the appropriate concentration of the highest standard (see Table 2.8 for kit specifications) and this was subsequently serially diluted 1:2 with Reagent Diluent to create a 7 point standard. 100 µL of Standards were added in duplicate to the appropriate wells, in addition to Diluent Reagent only wells and cell culture medium only wells. Neat samples were added to the appropriate wells and the plate was sealed and incubated for 2 hours at room temperature. After 3x 400 µL washes with Wash Buffer 100 µL of Detection antibody, diluted in Reagent Diluent, was added to each well and incubated for 2 hours at room temperature. After another 3x 400 µL washes with Wash Buffer, 100 µL of a working solution of Streptavidin-HRP (1:200 dilution with Reagent Diluent) was added to each well and the plate was covered with tinfoil and incubated for 20 minutes at room temperature. 100 µL of substrate solution tetramethylbenzidine (TMB) was added to each well and the plate was covered with tinfoil and incubated for 20 minutes at room temperature to allow for colour development. Next 50 µL of stop solution (2N H_2SO_4) was added to each well and the plate was shaken gently to ensure thorough mixing. The OD value of each well was read immediately at 450 nm using the Versamax

microplate reader. All OD values for duplicate wells were averaged. Background OD values of the no standard wells were subtracted from the averaged standards and unknown sample OD values. A standard curve of average absorbance for each standard was plotted against concentration (in pg/mL) and the concentration of the unknown supernatants samples was determined by non-linear regression (curve fitting).

Table 2.8 DuoSet ELISA reagent standard and antibody specifications

ELISA kit	Top Standard	Capture Antibody	Detection Antibody	R&D Systems Cat#
VEGF	2000 pg/mL	1 µg/mL	100 ng/mL	DY293B
PlGF	2000 pg/mL	1 µg/mL	100 ng/mL	DY220
bFGF	1000 pg/mL	2 µg/mL	100 ng/mL	DY233
GRO-α	2000 pg/mL	4 µg/mL	75 ng/mL	DY275
IL-8	2000 pg/mL	4 µg/mL	20 ng/mL	DY208
Angiopoietin-2	6000 pg/mL	1 µg/mL	2000 ng/mL	DY623
Neuropilin-1	2000 pg/mL	4 µg/mL	200 ng/mL	DY3870

2.20.6 Angiogenesis Multi-plex ELISA

MSD® Angiogenesis Panel 1 v-plex ELISA (Meso Scale Diagnostics, Rockville, MA, USA) was used to assess levels of 7 major angiogenic markers (VEGF, VEGF-C, VEGF-D, Tie-2 (angiopoietin receptor), Flt-1(VEGF receptor 1), PlGF (placental growth factor) and bFGF (basic fibroblast growth factor) in TCM collected from OAC biopsies following drug treatments as described in Section 2.20.2. This 7-plex ELISA allows simultaneous detection of multiple markers in the one biological sample. 150 µl Blocker A was added to each well. The plate was sealed with parafilm and incubated for 1 hour at room temperature with vigorous shaking (500-600 rpm) on an electrical plate shaker. The plate was washed three times with 200 µL PBS-T (0.05%). 20 µL of 20x stock calibrator blend was diluted in 380 µL Diluent 7 to provide the highest standard for each analyte: VEGF (39,400 pg/mL), VEGF-C (46,700 pg/mL), VEGF-D (43,8200 pg/mL), Tie-2 (1,546,400 pg/mL), Flt-1 (163,400 pg/mL), PlGF (69,200 pg/mL) and bFGF (35,600 pg/mL). A 4-fold serial dilution of the calibrator blend in Diluent 7 was carried out to generate the other 6 standards. An 8^{th} standard of Diluent 7 alone was used as the zero calibrator control. 50 µL of the serially diluted calibrators were added in duplicate. 25 µL of Diluent 7 was added to each sample well sample followed by 25 µL of undiluted TCM. The plate was resealed and incubated with vigorous shaking for 2 hours at room temperature. The plate was washed as before and 25 µL/well 1x Detection Antibody Solution (60 µL of each 50x SULFO-TAG Detection Antibody to a final volume of 3 mL in Diluent 11, prepared just before use) was added and the plate

was incubated with vigorous shaking for 2 hours at room temperature. The plate was washed as before and 150 µL/well 2X MSD® Read Butter T (4x diluted in deionised water) was added and the plate was read on the SECTOR™ Imager. A standard curve was generated and sample values were interpolated. Values were normalised to protein content (protein was isolated as described in Section 2.17.2 and quantified as described in Section 2.18).

2.21 Drug screening in *fli1:EGFP* zebrafish

2.21.1 Zebrafish husbandry

All experiments were carried out under the ethical approval granted by UCD animal research ethics committee. Zebrafish (*Danio rerio*) were maintained according to standard procedures at 28.5°C on a 14 hour light/ 10 hour dark cycle. Embryos were obtained by natural spawning and developmental stages were established by time and morphological criteria. Transgenic zebrafish Tg[*Fli1:EGFP*] were used for all experiments in which all endothelial cells (including blood vessels) are labelled with EGFP (enhanced green fluorescent protein).

2.21.2 Intersegmental vessel assay

Drug treatments were carried out in duplicate wells of a 48-well plate with each well containing 5 embryos at 6 hours post fertilisation. Embryos were treated with drugs or vehicle control (1% DMSO) diluted in embryonic medium (Holtfreter's solution: 60 mM NaCl, 2.4 mM sodium bicarbonate, 0.8 mM $CaCl_2$, 0.67 mM KCl and 10 mM HEPES). 10 µM SU11652 was used as a positive control as indicated by 100% inhibition of intersegmental vessel (ISV) formation. 2 days post fertilisation the embryos were observed in their chorions and any signs of morphological defects or toxicity were noted. The embryos were then euthanised, dechorionated and fixed in 4% paraformaldehyde for 2 hours. Following 3x 5 minute PBS washes the embryos were stored in PBS at 4°C until analysis and imaging using a fluorescent microscope (Nikon Eclipse 90i). A healthy zebrafish embryo has between 28 and 30 ISVs on the dorsal side. Changes to the number of fully formed ISVs were visualised under the microscope at 4X and 10X magnification and recorded following drug treatments as a measure of anti-angiogenic potential. The distance from the head to the tail of the embryo was also measured in pixels using a line drawing tool as an indication of axis curvature and embryo deformation.

2.22 Cell proliferation by BrdU assay

Cell proliferation in culture was quantified using the BrdU cell proliferation ELISA (Roche) whereby the amount of BrdU incorporation in cells correlates with the amount of DNA synthesis and thus active proliferation. $3.5x10^3$ HUVECs were seeded in a 96-well plate and left to adhere for 24 hours. In the case of OE33 cells $5.0x10^3$ cells were seeded in a 96-well plate and allowed to adhere overnight and the cells were then serum depleted (0.5% FBS) for approximately 12 hours. At this point media was removed and replace with fresh media containing drug treatments or vehicle control (i.e. DMSO). Drugs treatments and vehicle controls were made up in complete media for HUVECs and serum depleted media for the OE33 cells. Cells were incubated for a further 24 hours. At the 24 hour time point 10 µL of working BrdU-labelling reagent (100 µM) was added directly to the culture media of each well and the plate was returned to the incubator for 4 hours at 37°C, 5% CO_2 to allow incorporation of BrdU into synthesised cellular DNA. No cell wells (blanks) were included to account for non-specific binding of BrdU or anti-BrdU conjugate to the tissue culture plate. Then the labelling medium was removed and any residual drops were tapped off in tissue paper. 200 µL of FixDenat was added per well and incubated at room temperature for 30 minutes. The FixDenat solution was removed fully and 100 µL of working solution of anti-BrdU-POD antibody conjugate was added per well and incubated at room temperature for 1 hour and 30 minutes. Then the antibody conjugate was removed and the wells were washed with 3x300 µL of diluted washing buffer. After removing the wash buffer, 100 µL of substrate solution was added per well and the plate was covered in tinfoil and incubated at room temperature for 10 minutes or until sufficient colour development was observed. 25 µL of stop solution (2N H_2SO_4) was added directly to the substrate solution and the plate was briefly shaken on an electrical shaker before measuring the absorbance values at 450 nm using the Versamax microplate reader. The blank well absorbance (i.e. no cells) was subtracted from all other absorbance values on the plate to give the final absorbance measurement for data analysis.

2.23 Cell viability by MTT assay

OE33 cells were seeded in a 96-well plate at $5x10^3$ cells/well. Cells were left to adhere overnight. A serum depletion step (0.5% FBS) was carried out for at least 12 hours for the OE33 cells only. 24 hours post seeding the media was changed and vehicle control or drug treatments dissolved in fresh media were added to the cells for a total treatment time of 24 hours. 2.5 mg of MTT reagent (3-(4,5-Dimethylthiazol-2-yl)-2,5-Diphenyltetrazolium Bromide) dissolved per 1 mL of PBS) was added directly to cell

culture medium in wells at a final concentration of 0.5 mg/mL. After 2 hours incubation at 37°C, or until sufficient purple crystal formation in the cells, the media was removed gently by pipetting. 100 µL of DMSO was added to each well to lyse the cells. The plate was shaken briefly to dissolve the purple crystals and was read immediately at 595 nm on a Versamax microplate reader.

2.24 AnnexinV-PI apoptosis assay

AnnexinV and Propidium Iodide (PI) are widely used to determine if cells are viable, apoptotic, or necrotic through differences in plasma membrane integrity and permeability. The ability of PI to enter a cell is dependent upon the permeability of the membrane; PI does not stain live or early apoptotic cells due to the presence of an intact plasma membrane. As the cell undergoes apoptosis, phosphatidylserine residues, which normally reside in the plasma membrane, appear on the surface of cells. AnnexinV has a strong affinity for phosphatidylserine residues and will bind to them in a Ca^{2+} dependent manner. Thus early stage apoptosis is quantified as $AnnexinV^{+}$ only cells and late stage apoptosis and necrosis as dual $AnnexinV^{+}PI^{+}$ staining cells. Cells were seeded at a density of 3.0×10^{5} cells/well of a 6-well plate. After adherence over night OE33 cells were serum depleted for 12 hours while HUVECs were allowed to grow for 24 hours in complete medium. At 24 hours cells were treated with drugs or controls for 24, 48 and 72 hours. Drugs treatments and vehicle controls were made up in complete media for HUVECs and serum depleted media for the OE33 cells. At each time point cell supernatants were collected and spun at 180 x g for 3 minutes to pellet non-adhered and apoptosed cells. Following trypsinisation of the monolayer of cells, cells were centrifuged at 180 x g for 3 minutes and this pellet was combined with the non-adhered cell pellet and re-centrifuged at 180 x g for 3 minutes. The supernatant was discarded and the cell pellet was re-suspended in 1mL Annexin Binding Buffer (10 mM Hepes/NaOH, 140 mM NaCl, and 2.5 mM $CaCl_2$). Cells were centrifuged at 180 x g for 3 minutes and the supernatant discarded. 3 µL of AnnexinV antibody (IQ Products, The Netherlands) was added to each sample and left to incubate at 4°C for 30 minutes. Following incubation, 1 mL of Binding Buffer was added to each sample and samples were centrifuged as before. After centrifugation, supernatants were discarded. Immediately before acquiring on the flow cytometer, 500 µL of 0.25 µg/mL PI was added to each tube. Samples were acquired on a Beckman Coulter Cyan ADP Analyzer flow cytometer. All flow cytometry analysis was conducted using FlowJo® version 7.6.5.

2.25 Endothelial cell tubule formation assay

96-well tubule assay plates, µ-Plate Angiogenesis (Ibidi GmbH, Germany) were used. Growth factor reduced Matrigel (BD Sciences) was thawed on ice overnight at 4°C. 10 µL of gel was added to the inner wells of the µ-Plate and allowed to polymerase at 37°C for 60 minutes. 80% confluent HUVECs between passage two to eight were trypsinised and a cell suspension of $1.0x10^4$ cells/35 µL complete growth medium was gently added to the surface of the polymerised gel of each well. Drugs were added to the wells to give a final well volume of 70 µL. Each treatment was carried out in three experimental wells. Tubule networks were fully formed after 10-14 hours. At this point the wells were fixed with 4% paraformaldehyde for 30 minutes, followed by 3x PBS washes, permeabilisation with 0.01% Triton-X-100 for 10 minutes and another 3x PBS washes. Next the tubules were stained with Phalloidin (Alexa Fluor® 488 Phalloidin, Thermo Fisher Scientific) (1:200 dilution) for 30 minutes, followed by 3x PBS washes. Finally the wells were filled with 70 µL of PBS and fluorescent images were taken using the Cellavista imaging system (Roche). Images were analysed with ImageJ software and effects on angiogenesis were determined by manually measuring a number of different parameters: number of lumen/loops, number of branch points and the average length of the tubules formed. A subset of images was quantified by a blinded observer to ensure consistency. Representative images of parameters measured are shown in Appendix III.

2.26 12-lipoxygenase overexpression

2.26.1 *E.coli* transformation and plasmid amplification

Plasmid pcDNA3.1(+)-*ALOX12* and empty pcDNA3.1(+) vector (see Appendix IV) were kindly provided by Prof. Kenneth Honn (Wayne State University, MI). Chemically competent TOP10 *E.coli* (transformation efficiency of $1.6x10^7$ cfu/µg DNA) were transformed with 30 ng of DNA by heat shock (42°C for exactly 30 seconds) and immediately placed on ice for 5 minutes. A negative control (no DNA) was also included. Transformed cells were then allowed to recover for 1 hour in 250 µL of BHI (brain heart infusion) medium, in a microcentrifuge rack in a 37°C rotary- shaker, at 200 rpm. 250 µL of the transformed bacteria were plated onto solid LB agar (20 g/L LB medium, 20 g/L agar, 100 µg/mL ampicillin in distilled water) overnight at 37°C in a shaking incubator. Single colonies were lifted and plated one more time to ensure transformation efficiency and antibiotic resistance. Finally, a single colony was chosen and used to inoculate 50 µL of LB-medium (20 g/L LB medium, 100 µg/ml ampicillin) in a 200 mL glass conical flask, overnight at 37°C at 200 rpm. The LB broth containing

the transformed *E.coli* was split into multiple 50 mL centrifuge tubes and was centrifuged at 6000 x g for 15 minutes at 4°C. The resulting pellets were combined and plasmid extraction and purification was carried out using a Qiagen® Plasmid Midi Kit.

2.26.2 Harvesting and purification of plasmid DNA

Plasmid DNA was harvested using the Qiagen® Plasmid Midi Kit. The transformed bacterial pellets were resuspended in 4 mL of Resuspension Buffer. 4 mL of Buffer P2 (with LyseBlue® reagent added at a ratio of 1:1000) was added and mixed thoroughly by inverting 4-6 times to lyse the cells. The solution turns blue and was incubated for 5 minutes at room temperature. 4 mL of pre-chilled Buffer P3. was added to neutralise the solution, which again was inverted 4-6 times until the blue colour disappeared. The lysate was then transferred to the barrel of a QIAfilter™ Midi Cartridge 25 and incubated at room temperature for 10 minutes to allow white precipitate to float to the top. The plunger was inserted into the cartridge and the clear lysate containing plasmid DNA was expelled into a clean 50 mL. The Qiagen-tip 100 was equilibrated with 10 mL Buffer QBT. After allowing the buffer to empty by gravity, the supernatant containing the plasmid DNA was applied to the Qiagen-tip and allowed to enter the resin by gravity. The Qiagen-tip was then washed with 2x10 mL of Buffer QC and the flow through discarded. The DNA was eluted into a clean 15 mL tube using 5 mL of Elution Buffer QF. The DNA was then precipitated by adding 3.5 mL of room temperature isopropanol. The sample was mixed thoroughly by vortexing and centrifuged at ≥15,000 x g for 30 minutes at room temperature. The supernatant was decanted and the DNA pellet was washed with 2 mL of 70% ethanol and centrifuged at ≥15,000 x g for 10 minutes. The supernatant was carefully decanted and the pellet was allowed to air-dry for 5-10 minutes before resuspending in an appropriate volume of TE buffer, pH 8.0. DNA concentration and purity were measured using the Nanodrop® ND-100 spectrophotometer.

2.26.3 Transient transfection of plasmids in OE33 cells

Transient overexpression of 12-LO in OE33 cells was achieved by transient reverse transfection of purified plasmid DNA with Turbofect™ transfection reagent (Thermo Fisher Scientific). Reverse transfections were carried out in 2 cm^2 well (24-well plate) for the assessment of supernatant by ELISA and in 0.3 cm^2 wells (E-plate 16) for xCELLigence real time proliferation measurements. For a 2 cm^2 well, 1 ug of pcDNA3.1+*ALOX12* plasmid DNA was diluted in 100 µL serum free RPMI. Turbofect reagent was briefly vortex and 2 µL was added to the diluted DNA and incubated for

15-20 minutes at room temperature. 100 µL of this solution was evenly distributed drop-wise across the surface of the well. OE33 cells in the log phase of growth were trypsinised, centrifuged at 180 x g and resuspended in normal complete medium with FBS and antibiotics to a density of $1x10^5$ cells/mL. 1 mL of the cell suspension was gently added on top of the transfection reagent/ DNA mix. Cells were incubated at 37°C, after 16-18 hours the medium was gently removed and replaced with 1 mL of serum-depleted medium overnight. The next day drug treatments were added in serum depleted medium for the appropriate length of time (i.e. 24 hours for assessment of secretions by ELISA and 24-72 hours for RT measurements by xCELLigence). The appropriate amount of DNA, volume of reagents and seeding density for the 0.3 cm^2 well size are detailed in Table 2.9. Simultaneous to the experimental wells cells were reverse transfected with vector control (empty pcDNA3.1), pcDNA3.1+*ALOX12* or treated with transfection reagent only (2 µL) and RNA was isolated at 24, 48 and 72 hours to confirm overexpression *ALOX12*.

Table 2.9 Seeding density, amount of plasmid DNA and volume of reagents used per well in the reverse transfection of OE33 cells

Plate type	Growth area	Seeding density	Amount of DNA	Volume of Turbofect	Volume of growth medium
24-well plate	2 cm^2/well	$1x10^5$cells/well	0.2 µg	0.4 µL	0.2 mL
xCELLigence plate	0.3 cm^2/well	$1.25x10^4$ cells/well	1 µg	2 µL	1 mL

2.27 xCELLigence RTCA for cell proliferation

Cell proliferation were monitored using the xCELLigence™ RTCA DP (Real Time Cell Analyser Dual Plate) (ACEA Biosciences, San Diego, CA, USA). The specialist 16-well E-plate was used to measure proliferation. The bottom of the E-plate well has been designed with a surface of microelectrode sensors. When cells adhere and proliferate on the surface of the E-plate or impedance signals are recorded by the xCELLigence software. Thus the platform offers a label-free, real time cellular assay to measures changes in cell behaviour in response to stimuli or inhibitors. 100 µL of culture media was added to each well of the plate and the surface of the plate was allowed to equilibrate for 30-60 minutes at room temperature. The plate was then inserted into the machine to perform Step 1 which records the background impedance signal of each well. Freshly split OE33 cells at 75-85% confluence were reverse transfected as described in Section 2.26.3 directly into each well of the E-plate at a density of $1.5x\ 10^4$ cells/100 µL giving a total volume of 200 µL in each well. The plate was left in the cell

culture hood for 30 minutes to allow the cells to settle in an evenly distributed pattern. The plate was inserted and the machine was set to record the impedance signals of the plate every 30 minutes for a total of 200 recordings (i.e. 100 hours). In the case of a drug treatment experiment, transfected OE33 cells were serum depleted (0.5% FBS) at about 16-18 hours post seeding. The machine was paused and the plate was carefully removed and the media was gently pipetted off and replaced with media containing drug without touching the bottom of the well. The plate was returned to the machine and impedance signals were recorded for the required length of time. At this point appropriate treatments were added to the wells in serum depleted medium (0.5% FBS) and the impedance signals were continually monitored over the next 48-72 hours.

2.28 Statistical analysis

All statistical analysis was performed using GraphPad Prism software version 5.01. (GraphPad software Inc., La Jolla, CA, USA). All data presented are expressed as mean ± the standard error of the mean (S.E.M.), unless otherwise stated. The S.E.M. is the standard deviation (S.D.) of the distribution of the mean. The normality of the data was assessed and non-parametric analysis was used as appropriate. Differences between continuous variables of matched patient groups were measured by Wilcoxon signed-rank test while unmatched groups were measured by Mann-Whitney. In the case where parametric data was paired (i.e. untreated versus treated) a paired student t-test was used. For statistical analysis involving three or more group the one-way ANOVA was used. Tukey multiple comparisons *post-hoc* analysis was to determine significance between groups, while Dunnett's multiple comparisons *post-hoc* test was used to compare multiple groups to a single group (i.e. a control group). In the case of multiple comparisons between non-parametric data the Kruskal-Wallis test with Dunn's *post-hoc* test was used. For patient data correlations between variables were assessed by Spearman correlation coefficients. Survival statistics were calculated using Kaplan Meier method and the log rank test (Mantel-Cox test) was used to assess differences in survival between the two groups. Gehan-Breslow-Wilcoxon test was also reported if necessary. In comparison the Mantel-Cox test gives equal weight to all deaths while Gehan-Breslow-Wilcoxon test gives more weight to earlier deaths. In most cases disease-specific survival was assessed, with survival time measured from the date of diagnosis to the date of disease-specific death or last follow up. In the case were recurrence-free survival was assessed; survival time was measured from the date of surgery to the date at which cancer recurrence was reported or last follow-up. A probability of $p<0.05$ was considered to be a significant finding for all analyses and all p-values reported are two-tailed.

Chapter 3 Investigation of 5-lipoxygenase expression in oesophageal cancer and its association with obesity

3.1 Introduction

Chronic inflammation has been well established as a contributory risk factor in the development of cancers, particularly gastrointestinal malignancies such as colon cancer and OAC (Coussens and Werb, 2002, Abdel-Latif *et al.*, 2009). It is now appreciated that cancer cells co-opt signalling pathways and receptors that have been primarily known for roles in immune cell regulation, in order to enhance their migration, invasion and metastasis (Coussens and Werb, 2002). Eicosanoid signalling molecules produced by COX and LO enzymes are thought to have a major contribution to cancer-promoting inflammation (Greene *et al.*, 2011). 5-LO is expressed by a wide variety of cancer cell types such as colon, lung, breast, prostate and mesothelium (Romano and Claria, 2003). The role of this enzyme in cancer has been reported in a growing number of *in vitro* and murine studies (Ding *et al.*, 1999, Matsuyama *et al.*, 2004, Wen *et al.*, 2014) which has led to further interest in the evaluation of the 5-LO signalling pathway as a potential cancer biomarker. For example in a small study of 22-matched benign and malignant prostate tissues 5-LO gene and protein expression and 5(S)HETE production were significantly higher in malignant compared to benign tissue (Gupta *et al.*, 2001). Another study of 55 patients with sporadic colorectal adenocarcinoma found a positive correlation of 5-LO protein expression with tumour stage and lymph node metastasis (Barresi *et al.*, 2007). Notably other proteins involved in the 5-LO pathway, besides 5-LO itself have also been implicated in cancer. In a study of 211 prostate samples (151 prostate cancer cases), 5-LO LTD4 receptor expression was shown to be higher in prostate cancer tissue compared to benign or normal prostate tissue and expression correlated with tumour grade, indicating a role of 5-LO pathway in prostate cancer progression (Matsuyama *et al.*, 2007). In a colorectal cancer study LTD4 receptor was found to correlate with both 5-LO and the closely related enzyme COX-2 and patients with elevated LTD4 receptor expression showed markedly poorer survival (Ohd *et al.*, 2003). In a cohort of 154 breast samples (breast cancer, n=122) FLAP mRNA was aberrantly expressed in breast cancer compared to normal tissue and this expression was associated with prognosis (Jiang *et al.*, 2006a).

There are several studies in the literature that have investigated 5-LO expression in oesophageal cancer, however results have been conflicting to date. One immunohistochemical study reported high incidence of 5-LO tumour epithelial expression in OAC compared to normal oesophagus (53/56 cases showing at least weak positive (+) staining compared to 5/22 cases) (Chen *et al.*, 2004). Overexpression (++ or +++) was found in 50% of tumours (28/56). It was not clear if

clinical parameters were available for the patients in this study but no associations with such parameters were reported. Notably in this study a higher incidence of 5-LO expression was found in early stage adenocarcinoma, in both columnar lined oesophagus and dysplastic tissue (7/7 and 7/9 cases) indicating a potential role in tumour initiation. Interestingly, 5-LO is reportedly expressed during early neoplastic changes of pancreatic cancer and malignant transformation of adenomas providing further support of a role of 5-LO early in cancer development (Hennig *et al.*, 2005a, Wasilewicz *et al.*, 2010).

In another immunohistochemical study of a mixed collection of oesophageal cancer cases (both OSCC and OAC) from both China and the US (108 OSCC and 53 OAC) 5-LO expression was present in 79% of samples overall (69% for OAC cases only compared to 96% in the previous study by Chen *et al.*) (Hoque *et al.*, 2005). Only 13% (4/32) of distant normal oesophageal epithelium showed 5-LO expression. The tissue was scored as positive if >10% staining was observed and in contrast to the previous study by Chen *et al.*, no staining intensity score was assigned. They correlated 5-LO with available clinicopathological parameters but again this was only done correlating with positive and negative scores. Significant associations with male cases and moderate tumour differentiation and an absence of lymph node metastasis were reported with the Chinese OSCC cohort only and not the OAC cohort.

A more recent study investigated the expression of 5-LO and other 5-LO pathway proteins in a cohort of 16 human Barrett's metaplasia samples, 7 OAC samples and 5 proximal squamous oesophagus samples (UK cohort). Interestingly they reported no observed 5-LO epithelial staining in this cohort and instead documented 5-LO specific staining that was confined to the stromal compartment only (Boger *et al.*, 2012). Significantly increased 5-LO and FLAP stromal expression in adenocarcinoma compared to normal squamous tissue was observed. LTC4 synthase, the enzyme that converts LTA4 to LTC4 was the only marker where staining was found in both epithelial (normal squamous, BO and OAC) and stromal tissue in this study. Taking these three studies together it is clear that additional studies involving a larger patient cohort, in particular OAC patients and access to full clinical parameters are needed to address the role of 5-LO in oesophageal cancer.

An upregulation of stromal 5-LO in the progression from normal squamous epithelium to BO and subsequently to OAC was reported by Boger *et al.* and points towards a potential role of 5-LO immune cell activity in the development of this disease.

Associated inflammation in the tumour microenvironment induces tumour development by providing fuels to nurture epithelial cell growth and pro-angiogenic factors for vascularisation and angiogenesis. It is thought that immune populations such as neutrophils and macrophages may contribute to this process through 5-LO signalling (Boger *et al.*, 2012). A recent murine study focusing on hematopoietic-derived 5-LO, observed that specific deletion of this enzyme from bone marrow decreased polyp formation despite the presence of 5-LO proficient epithelial cells in these mice, indicating for the first time the importance of immune cell contribution to 5-LO activity (Cheon *et al.*, 2011). Aside from a role in immune cell-mediated inflammation, 5-LO has also been linked to the process of angiogenesis (see Section 1.7.6.1), reportedly upregulating the key pro-angiogenic factor, VEGF, in models of colon adenoma, mammary carcinoma and mesothelioma (Ye *et al.*, 2004, Romano *et al.*, 2001).

Obesity, a state of chronic of low grade inflammation, is a risk factor in the development of the pre-malignant condition BO and subsequent progression to OAC (Ryan *et al.*, 2011). 5-LO is emerging as a potential target for obesity-driven disorders, insulin resistance, metabolic dysfunction and steatohepatitis (non-alcoholic fatty liver disease) (Sharma-Walia *et al.*, 2014). In a recent study high fat diet fed obese mice were found to have higher secreted levels of LTB4 in the liver, skeletal muscle and adipose tissue compared to lean mice (Li *et al.*, 2015). 5-LO and FLAP have been shown to be expressed in human adipocytes, albeit at a lower level than cells of the stromal vascular compartment and adipose tissue and FLAP was shown to be significantly higher in obese and insulin resistant patients (Kaaman *et al.*, 2006). This report investigated FLAP expression in subcutaneous fat from obese patients only and not omental fat. Considering omentum (i.e. central adipose tissue) is the more metabolically active of the two it would be interesting to perform a comparison of the two adipose tissue compartments (Wajchenberg, 2000). While other LO forms, such as 15-LO-1, have been investigated in human omentum, no study has investigated 5-LO. Additionally no study has investigated the association of 5-LO activity in the context of cancer.

With this in mind, the main aim of this chapter was to assess 5-LO expression and activity in OAC and to determine its clinical relevance as a biomarker of disease, and to discover whether it is associated with obesity-driven-disease specifically. A secondary aim of this chapter also investigated 5-LO association with angiogenesis and inflammation in oesophageal cancer patients.

3.2 Aims and Objectives

The aim of this chapter was to study the clinical relevance of the 5-LO signalling pathway in oesophageal cancer and more specifically the OAC sub-type, using a number of different biological sample types including biopsy RNA, tumour tissue microarrays and serum. 5-LO has been previously linked to obesity, angiogenesis and inflammation in the literature and thus another aim of this study was to explore whether 5-LO is associated with these pathways in the specific clinical context of OAC.

Specific Objectives:

- Investigate the gene and protein expression of 5-LO in resected oesophageal tumour tissue and determine whether 5-LO expression is associated with clinical parameters including stage, grade and disease specific survival

- Investigate if expression of 5-LO and it's metabolite LTB4 are associated with patient obesity status in OAC

- Investigate expression of 5-LO in OAC patient derived adipose tissue in comparison to the other main LO enzymes and determine whether there is an association with obesity

- Correlate 5-LO expression with markers of angiogenesis and immune cell markers to provide insight into the potential role of 5-LO in OAC

3.3 Results

3.3.1 Assessment of 5-LO and FLAP expression in OAC tumour and corresponding normal adjacent oesophageal tissue

5-LO expression has been found to be elevated in some cancer types relative to normal tissue. Consequently to address this in the context of OAC, 5-LO mRNA levels were assessed in OAC tumour and macroscopically normal adjacent biopsies. Biopsy samples were collected from the main specimen post-surgical resection from OAC patients as described in Section 2.6. The patient demographic is detailed in Table 3.1. RNA was isolated and 5-LO expression was measured by qPCR as described in Section 2.7 and Section 2.12. The RQ value for one patient sample was arbitrarily set as the calibrator to allow normalisation of the data set. The calibrator sample was chosen based on detectable and close to median expression of all genes targets investigated in this cohort of samples and this same calibrator sample was used across all genes investigated. 5-LO expression of matched tumour and normal adjacent tissue samples (n=26) was compared and although a trend for higher expression in the normal adjacent samples was noted no significant difference was observed (0.54 ±0.48 versus 0.43 ±0.73, p=0.0645) (Figure 3.1).

As a surrogate marker of 5-LO activity, 5-lipoxygenase activating protein (FLAP), a protein critical for 5-LO enzyme activity was investigated in tumour and corresponding normal adjacent tissue (n=26). Appreciable (i.e. Ct≤35) FLAP mRNA expression was found in 17/26 normal adjacent samples and 9/26 tumour samples. There was no significant difference in expression levels observed between matched tumour and normal adjacent tissue samples (p=0.250, n=26) (Figure 3.2).

Table 3.1 Details of patient demographic used for tumour biopsy gene analysis study

	Mean (S.D.) or n(%) as appropriate	
Male: Female	31:3 (91.18%: 8.82%)	
Age (years)	67.7(10.3)	
Neoadjuvant therapy	0	
Non-obese: obese	18:16 (52.9%: 47.1%)	
Non-obese visceral fat area (cm^2)	90.3 (51.2)	
Obese visceral fat area (cm^2)	237.3 (54.7)	
T-stage	T1	13 (38.2%)
	T2	5 (14.7%)
	T3	16 (47.1%)
N-stage	Negative (N0)	16 (47.1%)
	Positive (≥N1)	17 (50%)
	Not specified	1 (2.9%)
Tumour grade (differentiation)	Moderate-well	20 (58.8%)
	Poorly	13 (38.2%)
	Not specified	1 (2.(%)

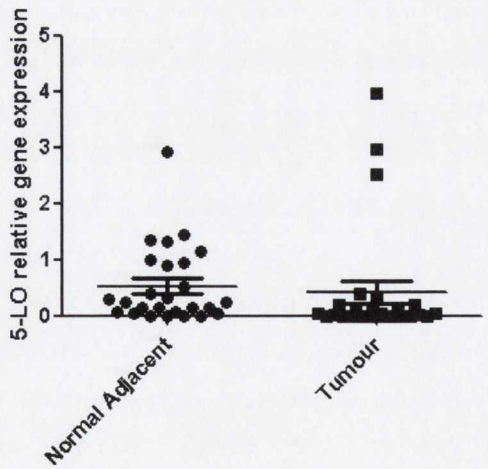

Figure 3.1 5-LO expression is higher in normal adjacent tissue biopsies compared to OAC biopsies. 5-LO mRNA expression was quantified by qPCR using cDNA synthesised from isolated RNA of matched tumour and normal adjacent biopsy tissue. There was a trend for higher 5-LO expression in normal adjacent tissue compared to tumour samples, although this was not significant (p=0.0614, n=26). Statistic test used was Wilcoxon signed rank test. Error bar denotes mean ± S.E.M.

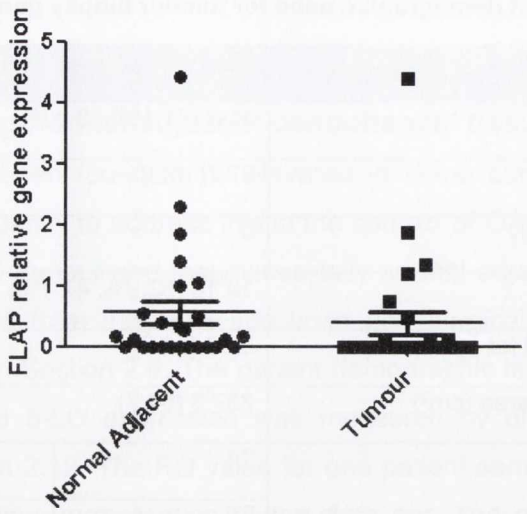

Figure 3.2 FLAP OAC tumour biopsy gene expression is similar to the gene expression in normal adjacent tissue biopsies. FLAP mRNA expression was quantified by qPCR using cDNA synthesised from isolated RNA of tumour and normal adjacent biopsy tissue. There was no difference between FLAP normal adjacent tissue and tumour expression (p=0.250, n=26). Statistical test used was Wilcoxon signed rank test. Error bar denotes mean ± S.E.M.

3.3.2 VEGF expression in normal adjacent and OAC tumour biopsies

It has been shown previously that 5-LO signalling is associated with angiogenesis and VEGF in cancer (Romano *et al.*, 2001, Ye *et al.*, 2004). Consequently VEGF mRNA levels was assessed in the tumour biopsy and correlations with 5-LO and FLAP expression were explored. Due to limited biopsy RNA, VEGF expression was assessed in a subset of the matched tumour and normal adjacent tissue samples (n=18). Although examination of the scatter plots revealed that the highest VEGF expression tended to be in tumour biopsy samples, this did not reach statistical significance (0.45 ±0.08 versus 0.85 ±0.30, n=18, p=0.384) (Figure 3.3). Notably, Spearman's correlation test revealed that tumour 5-LO mRNA expression positively correlated with FLAP expression levels (n=34, r=0.7797, p<0.0001) and VEGF expression levels (n=32, r=0.8948, p<0.0001) (Figure 3.4a and Figure 3.4b). In a similar manner tumour FLAP levels also showed a positive correlation with VEGF (n=32, r=0.8041, p<0.0001) (Figure 3.4c). Additionally normal adjacent 5-LO mRNA expression positively correlated with FLAP expression levels (n=29, r=0.6619, p<0.0001) and VEGF expression levels (n=18, r=0.6350, p<0.01) (Figure 3.4d and Figure 3.4e).

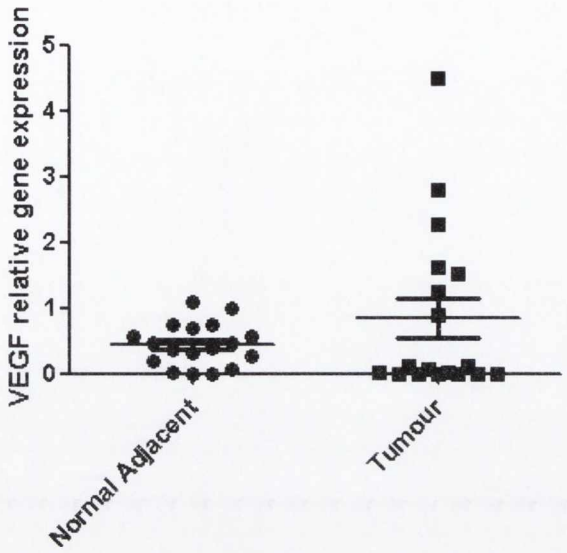

Figure 3.3 VEGF gene expression is not statistically different between OAC tumour and normal adjacent biopsies. VEGF mRNA expression was quantified by qPCR using cDNA synthesised from isolated RNA of tumour and normal adjacent biopsy tissue. There was no significant difference between VEGF normal adjacent tissue and tumour expression (p=0.384, n=18). Statistical test used was Wilcoxon signed rank test for paired analysis. Error bar denotes mean ± S.E.M.

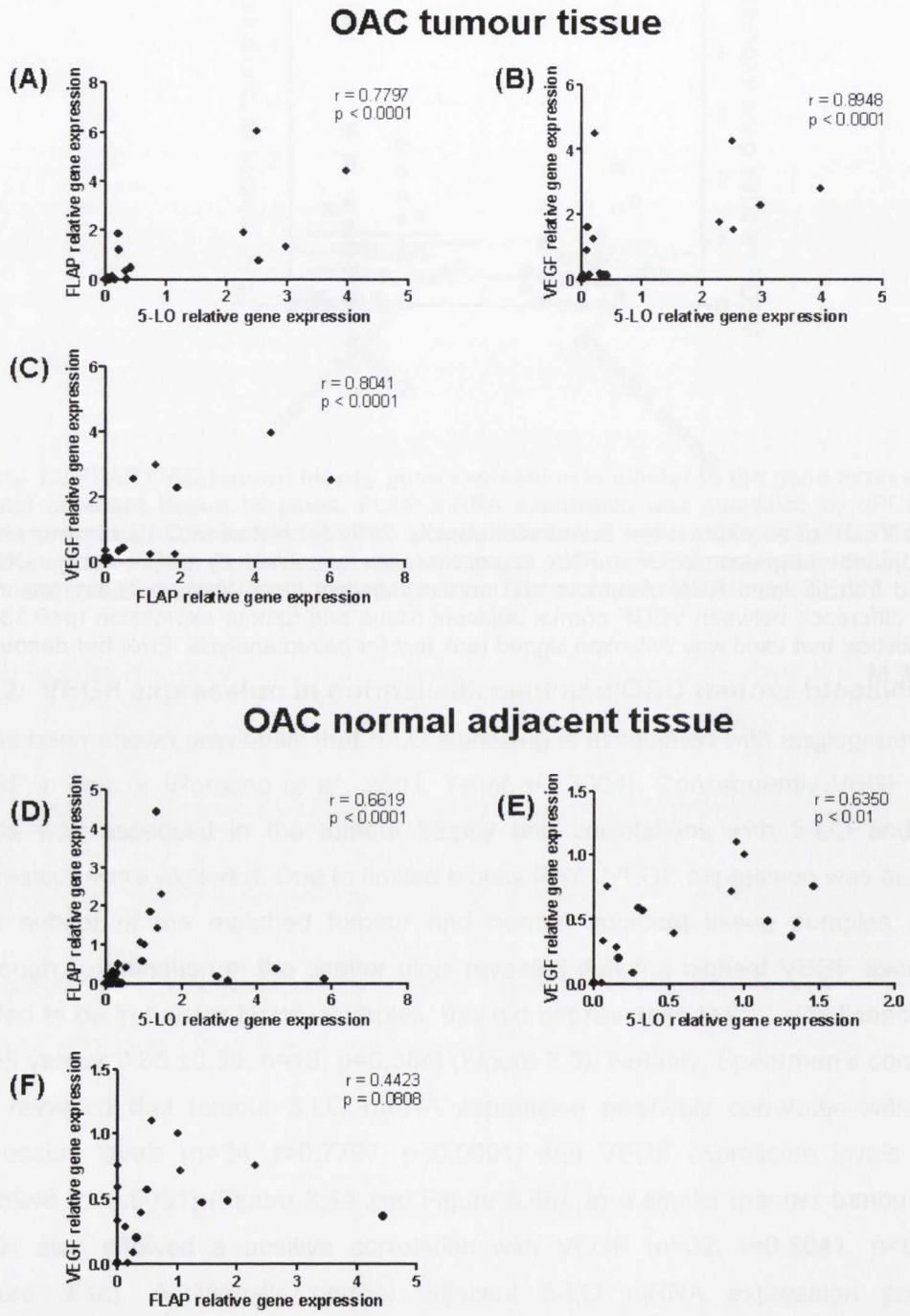

Figure 3.4 5-LO tumour or normal adjacent gene expression is correlated with FLAP and VEGF expression levels. (A) Relative gene expression of tumour 5-LO was found to be correlated with FLAP (n=34, r=0.7797, p<0.0001) and (B) VEGF. (n=32, r=0.8948, p<0.0001). (C) Higher FLAP expression was associated with increasing VEGF levels (n=32, r=0.8041, p<0.0001). (D) Normal adjacent 5-LO mRNA expression positively correlated with FLAP expression levels (n=29, r=0.6619, p<0.0001) and (E) VEGF expression levels (n=18, r=0.6350, p<0.01). (F) There was no significant correlation between normal adjacent FLAP and VEGF expression. Statistical test used was Spearman's correlation test.

3.3.3 Association of 5-LO, FLAP and VEGF tumour expression with patient obesity status

There is emerging evidence of an involvement of 5-LO signalling in obesity-associated inflammation (Neels, 2013). Additionally data from our research group (Allott *et al.*, unpublished) has shown an upregulation of 5-LO expression following co-culture of OAC cells with obese omental adipose tissue fragments, suggesting that this pathway may be upregulated in obesity-driven OAC. The same OAC patient cohort (i.e. Table 3) were grouped into obese (n=17) and non-obese (n=17) based on VFA measurements (Section 2.5) and the association between 5-LO expression and obesity status was explored in tumour biopsies. Patients classified as viscerally obese had significantly higher 5-LO mRNA expression in their tumours (mean RQ value: 0.20 ±0.15 versus. 0.76 ±0.31, $p<0.05$) (Figure 3.5a). VEGF mRNA expression was also significantly higher in viscerally obese patient tumour samples compared to non-obese (mean RQ value: 0.29 ±0.15 versus 0.78 ±0.31, $p<0.05$) (Figure 3.5b). There was not a significant association between FLAP expression and obesity status, indicated by VFA (0.15 ±0.08 versus 0.94 ±0.43, $p=0.2752$) (Figure 3.5c).

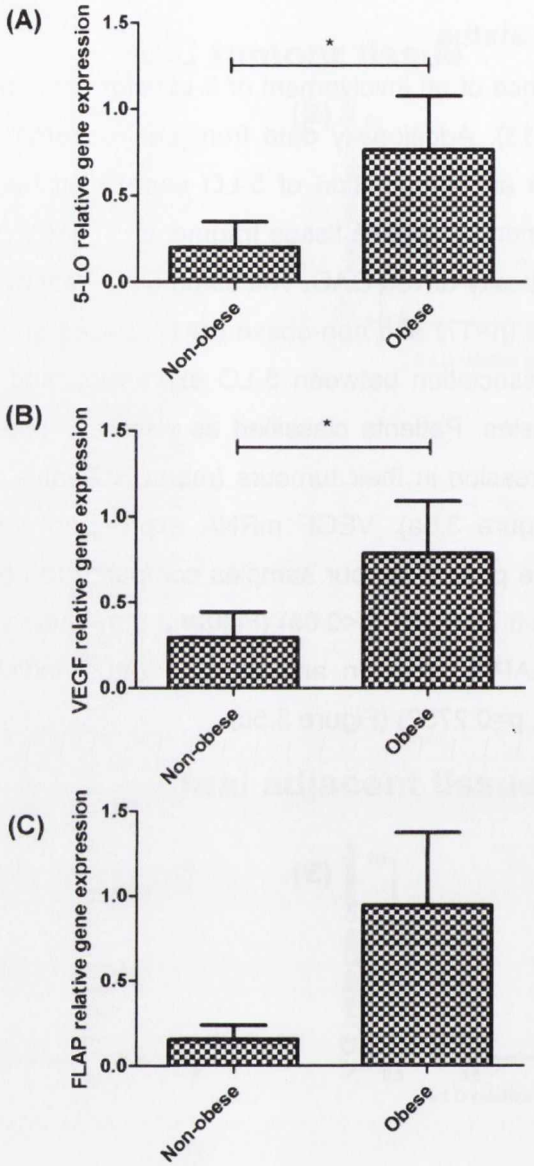

Figure 3.5 VEGF and 5-LO gene expression are associated with visceral obesity in OAC. Relative gene expression of 5-LO, FLAP and VEGF was analysed in tumour tissue derived from obese and non-obese patients segregated based on an obese VFA cut off value 163.8 cm^2 in males and 80.1 cm^2 in females. (A) Viscerally obese patients had significantly higher tumour 5-LO ($n=34$, $p<0.05$). (B) Viscerally obese patients had significantly higher VEGF expression ($n=32$, $p<0.05$). There was not a significant association between FLAP expression and obesity status determined by VFA ($n=34$, $p=0.2752$). Statistical test used was Mann Whitney U test: $p<0.05$(*). Error bar denotes mean ± S.E.M.

3.3.4 Cytokeratin-8 is expressed in both OAC tumour and macroscopically normal biopsies

Cytokeratin-8 (*8KRT*) is a marker of simple columnar epithelium and as such it is not expressed in squamous epithelium. Considering the higher levels of 5-LO in normal adjacent squamous epithelium compared to tumour tissue observed previously, the levels of cytokeratin 8 were measured to explore whether differences in glandular epithelial content was a contributing factor. Cytokeratin-8 was investigated in both normal adjacent and tumour biopsies and found to be expressed in the majority of both tissue types. Samples with Ct values of less than 30 were considered high expressors, while samples with Ct values 35-40 were deemed to have low to negligible expression. 92.31% (24/26) of normal adjacent samples expressed cytokeratin-8 and 42.31% (11/26) were considered high expressors. 92.31% (24/26) tumour samples expressed *8KRT* while 61.54% (16/26) were considered high expressors. Following normalisation by *18S* and relative quantification, as was expected cytokeratin-8 was found to be significantly higher in tumour samples compared to matched normal adjacent samples (0.31 ±0.13 versus 4.07 ±2.52, n=26, $p<0.01$) (Figure 3.6). The unexpected expression of cytokeratin-8, in the majority of normal adjacent biopsies sampled from the normal oesophagus (and not the cardia) may be indicative of metaplasia. These cytokeratin-8 levels were found to positively correlate with 5-LO and FLAP mRNA levels in both normal adjacent ($r=0.66$, $p<0.0001$ and $r=0.80$, $p<0.0001$) and tumour samples ($r=0.79$, $p<0.0001$ and $r=0.70$, $p<0.0001$) (Table 3.2). VEGF mRNA tumour levels positively correlated with tumour KRT8 ($r=0.78$, $p<0.0001$) but this association was not found with the normal adjacent samples (Table 3.2).

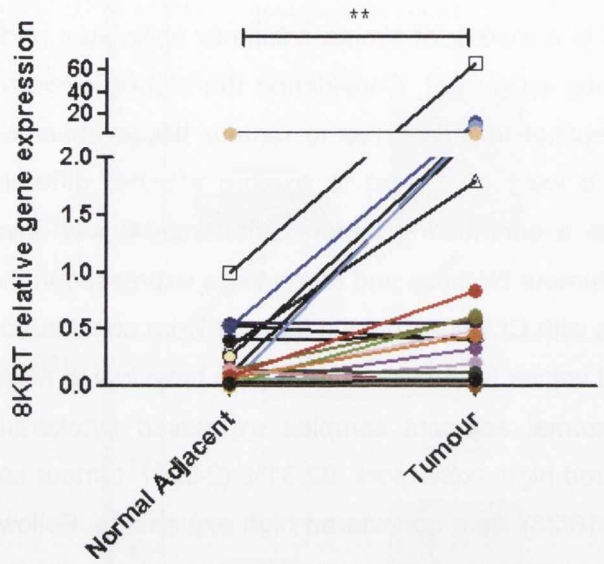

Figure 3.6 Cytokeratin-8 gene expression is higher in OAC tumour biopsies compared to normal adjacent tissue. *8KRT* mRNA expression was quantified by qPCR using cDNA synthesised from isolated RNA of OAC tumour and normal adjacent biopsy tissue. Tumour biopsies expressed higher levels of *8KRT* compared to matched normal adjacent tissue (n=26, $p<0.01$) as indicated by different coloured dots or different shapes joined by a line. Statistical test used were Wilcoxon signed rank test: $p<0.01$(**). Error bar denotes mean ± S.E.M.

Table 3.2 Summary of Spearman's correlation test results with cytokeratin-8

Biopsy tissue type	Gene	n	Spearman r	p-value
Tumour	5-LO	34	0.7879	<0.0001
	FLAP	34	0.6988	<0.0001
	VEGF	32	0.7753	<0.0001
Normal adjacent	5-LO	28	0.6564	<0.0001
	FLAP	28	0.7993	<0.0001
	VEGF	18	0.2921	0.2896

3.3.5 5-LO and FLAP expression are higher in normal adjacent tissue compared to tumour samples when normalised for columnar epithelium content by cytokeratin-8

Since RNA was isolated from whole tumour biopsies for cDNA synthesis and qPCR analysis 5-LO or FLAP gene expression may be due to a combination both the epithelial and stromal compartment. Given that both normal adjacent and tumour biopsies had moderate to high cytokeratin-8 expression, this epithelial marker was used to normalise 5-LO and FLAP for differences in columnar epithelial content in the samples and thus to indicate the contribution of other non-columnar epithelial sources in the biopsies to observed expression levels of 5-LO and FLAP (i.e. stromal cells or squamous epithelial contribution). The 5-LO and FLAP RQ values for each sample were divided by the corresponding *8KRT* RQ values, to normalise for columnar epithelium and glands. 5-LO expression, corrected for columnar epithelial content was higher in normal adjacent compared to matched tumour samples ($p<0.0001$, both $n=26$) (Figure 3.7a). FLAP expression was significantly higher in normal adjacent tissue samples compared to matched tumour samples following normalisation for columnar epithelial content ($p<0.01$, both $n=26$) (Figure 3.7b). Considering the strong participation of the 5-LO signalling pathway in immune cell activation and inflammatory response (Back *et al.*, 2007, Peters-Golden and Henderson, 2007, Evans *et al.*, 2008) it is likely that increased 5-LO pathway expression in normal adjacent following normalisation for epithelial content is due a contribution for immune cells.

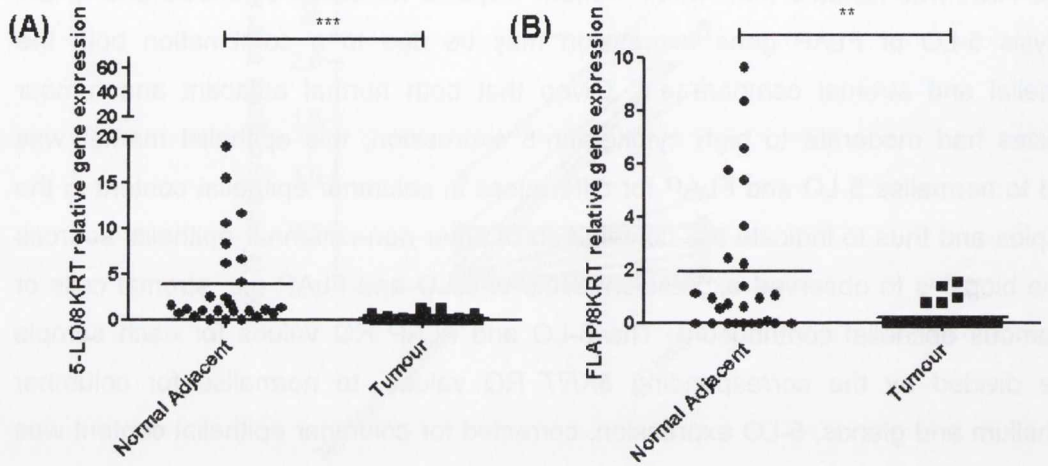

Figure 3.7 5-LO and FLAP expression are higher in normal adjacent tissue compared to tumour biopsies following normalisation with cytokeratin-8. 5-LO and FLAP RQ values were divided by their corresponding cytokeratin-8 RQ value to normalise for columnar epithelial content in the samples. (A) 5-LO expression was highest in normal adjacent samples compared to tumour ($p<0.0001$, both $n=26$). (B) FLAP expression was highest in normal adjacent samples also ($p<0.01$, both $n=26$). Statistical test used was Wilcoxon signed rank test: $p<0.01$(**) and $p<0.001$(***). Error bar denotes mean ± S.E.M.

3.3.6 OAC tumour gene expression and association with clinicopathological data

The role of 5-LO, FLAP, VEGF and cytokeratin-8 as prognostic markers of 5-year disease specific survival were assessed from initial diagnosis. Deaths from post-operative complications were omitted from the analysis. Patients were divided into two groups based on gene expression: either below/equal to median expression or above the median expression. 5-LO, FLAP and VEGF tumour gene expression did not show a significant association with 5-year disease specific survival (Figure 3.8**).** Interestingly, a trend towards worse survival with increasing cytokeratin-8 expression was noted (p=0.0712, n=34) (Figure 3.8). There was no significant association between tumour expression of any of the genes and other clinical parameters investigated including tumour stage (T and N stage) and tumour grade.

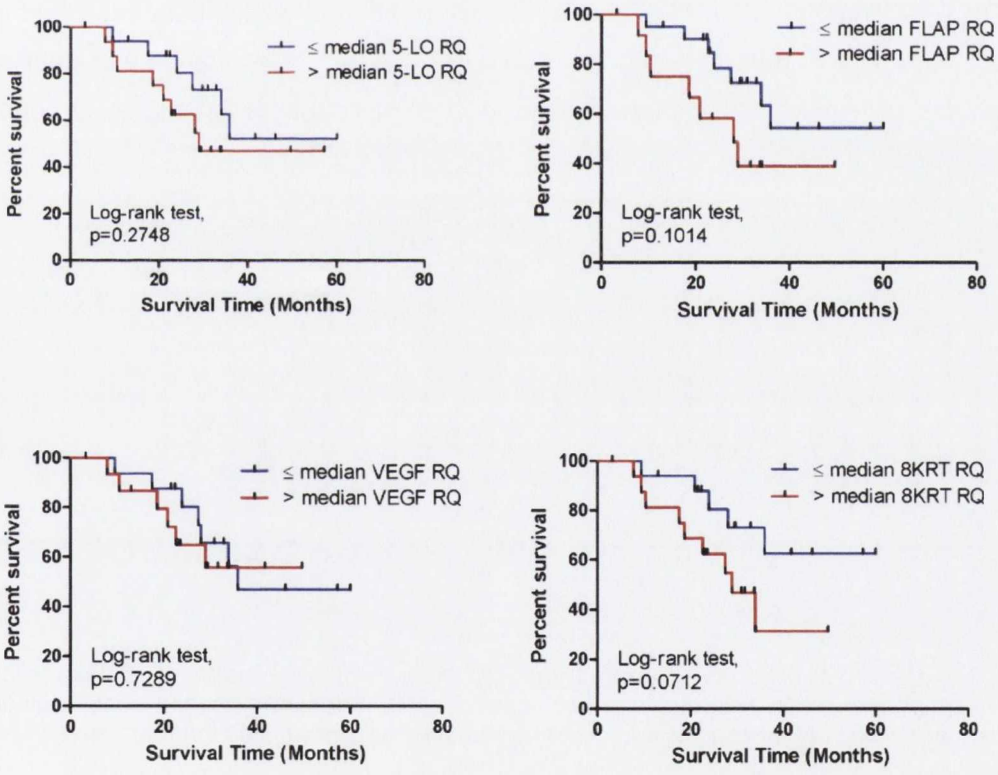

Figure 3.8 Tumour gene expression and 5-year disease free survival. Patients were divided into two groups based on gene expression of 5-LO (n=34), FLAP (n=34), VEGF (n=32) and 8KRT (n=34): below and/or equal to or above the median expression. A trend towards worse survival with increasing *8KRT* expression was noted (p=0.0712, n=34). Statistical test used was Kaplan Meier survival curve with Log-rank (Mantel-Cox) test.

3.3.7 Oesophageal cancer tissue microarray demographics

Paraffin-embedded tumour sections from 196 oesophageal cancer patients with a minimum of 36 months of clinical follow up were arrayed on a tissue microarray (TMA) (Figure 3.9a) as described in Section 2.6. Matched tumour leading edge (Figure 3.9b), where available was also included (136/196). As illustrated in Table 3.3 this patient cohort consisted of approximately four-fifths OAC patients and one-fifth OSCC patients.

The TMA was stained for 5-LO as described in section 2.16.1 and immunohistochemical scoring was carried out as described in section 2.16.2. Staining of VEGF, KDR (VEGFR-2), CD31 and a number of immune cell markers (see Appendix V for list of immune cell markers and cytokines) were completed prior to this project and used for correlations with 5-LO protein levels. The specificity of the 5-LO primary antibody was confirmed by the presence of a single band of protein in cell lysates at approximately 78 kDa (Figure 3.10a). Optimisation of primary antibody was carried out on full face sections of tumour tissue at a number of different dilutions as described in (Figure 3.10b) prior to staining the TMAs. There was only a subtle difference in staining between the dilutions tested, with the chosen dilution of 1:50 showing slightly stronger staining overall.

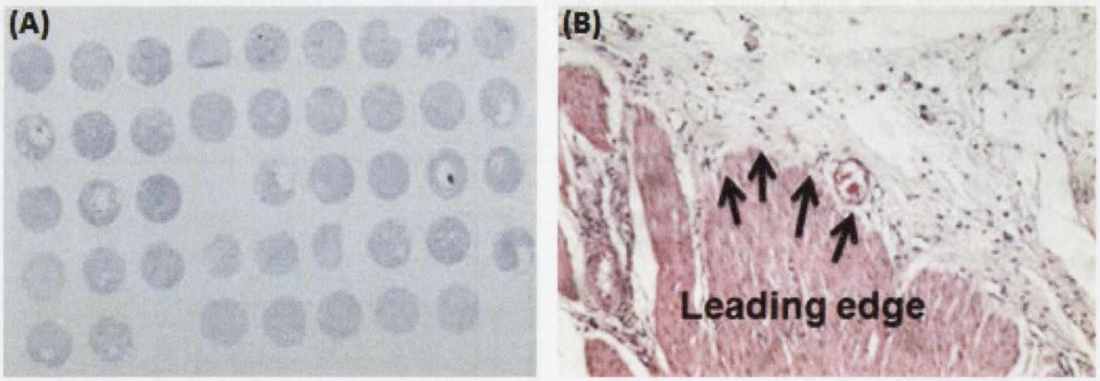

Figure 3.9 Tissue microarray construction. (A) Representative image of a TMA slide containing triplicate 2 mm tissue cores for 14 patients (B) Haematoxylin and eosin stained tissue indicating the leading edge of a tumour invading into the surrounding stromal tissue.

Table 3.3 Patient demographic for oesophageal cancer tissue microarray

n=196	Mean (S.D.) or n (%) as appropriate	
Morphology (OAC:OSCC)	155:44 (79.1%: 20.9%)	
Male: female	135: 61 (68.9%: 31.3%)	
Age	64.66 (11.1)	
Pathological T-stage	T1	24 (12.2%)
	T2	41 (20.9%)
	T3	120 (61.2%)
	T4	6 (3.1%)
	Missing	5 (2.6%)
Pathological N-stage	N0	68 (34.7%)
	N1	106 (54.1%)
	N2	11 (5.6%)
	N3	6 (3.1%)
	Missing	5 (2.6%)
Neoadjuvant treatment	48 (24.5%)	

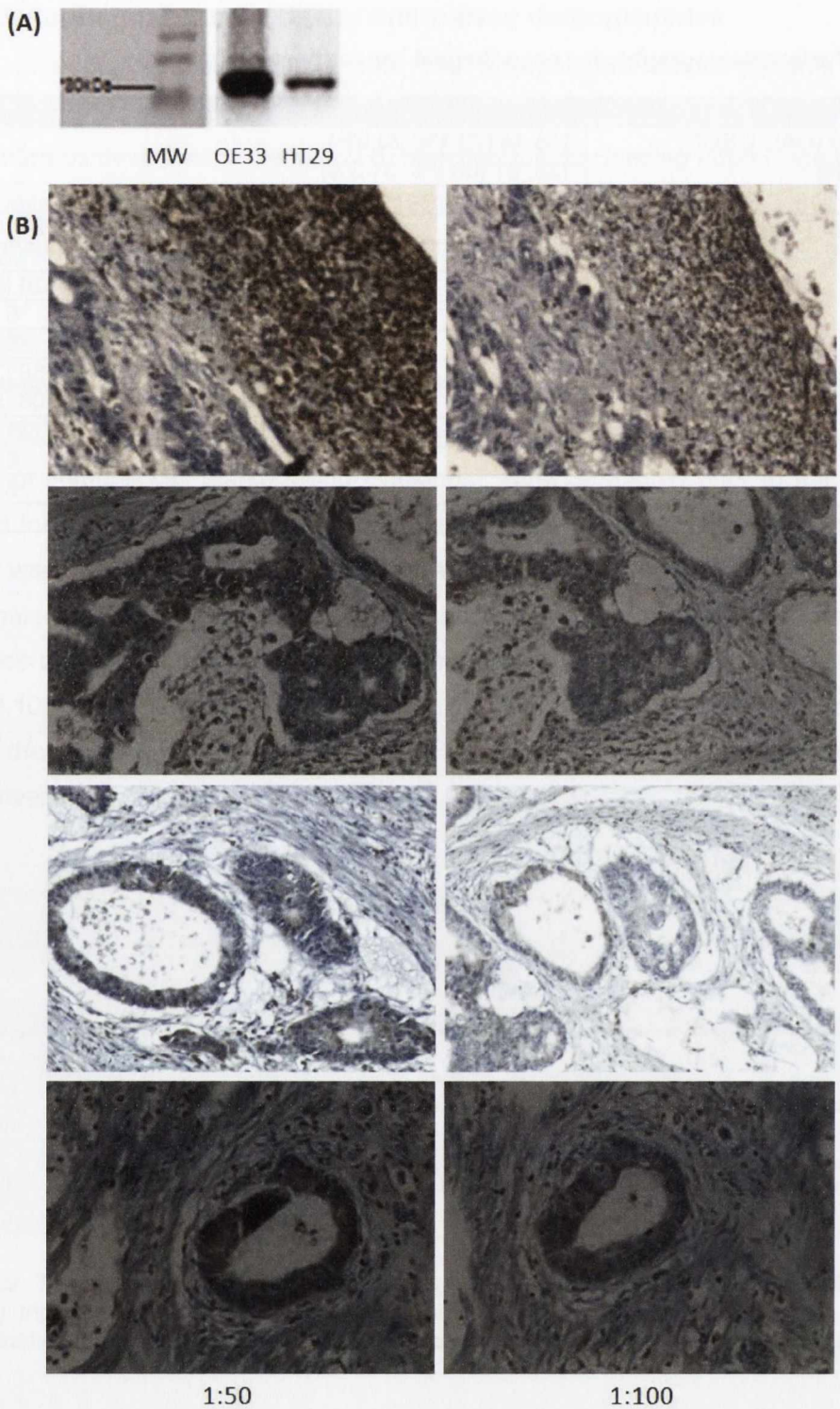

Figure 3.10 5-LO antibody optimisation. (A) The 5-LO antibody specificity was tested for by western blot. A single band of protein at approximately 78kDa was obtained for OAC (OE33) and colorectal cancer (HT29) cell line lysate. (B) Full-face sections of tumour tissue were used for IHC optimisation of the 5-LO antibody at 3 different dilutions: 1:50, 1:100 and 1:200. Representative images of 1:50 and 1:100 staining in matched tissue sections are shown. 20X magnification.

3.3.8 Differential expression of 5-LO, cancer morphology and tissue type

An average tumour epithelial and stromal score was assigned to each patient, except in cases where tissue cores had become damaged and impossible to score. There was no association between 5-LO staining and cancer morphology (i.e. OSCC versus OAC) in either the stromal or epithelial compartment, in both invasive/ leading edge (LE) or non-leading edge (NLE) cores (Table 3.4)

A subset of OAC or OSCC patients with intact matched NLE and LE tissue (OAC: 110/126 cases and OSCC: 24/26 cases) were analysed for 5-LO stromal and epithelial expression. There were similar levels of stromal 5-LO expression observed in NLE and LE OAC patients samples (Figure 3.11a and Figure 3.11b). While not statistically significant there was a trend for higher stromal 5-LO expression in the LE of the tumour in OSCC patients compared to NLE (73.35 ±9.69 versus 51.74 ±7.42, n=24, p=0.0789) (Figure 3.11c and Figure 3.11d). There was no difference in 5-LO tumour epithelial staining between LE and NLE regardless of cancer type (Figure 3.11e and Figure 3.11f).

5-LO expression was found to be significantly higher in the stroma of tissue samples compared to the tumour epithelium (LE: 58.74 ±4.01 versus 3.93 ±1.56, $p<0.001$ and NLE: 50.55 ±2.98 versus 6.82 ±1.57, $p<0.001$) (Figure 3.12). In fact less than 10% of the patients displayed appreciable 5-LO epithelial expression and these were a mixture of OSCC and OAC. The largest areas of epithelial staining identified were in benign gastric mucosa or glands with high grade dysplasia on a background of intestinal metaplasia (Figure 3.13c and Figure 3.13e). There were several cases of invasive carcinoma (i.e. glands in the muscle or fat in the TMA core) that stained positively for 5-LO. In these infrequent cases, staining tended to be restricted to the nucleus (Figure 3.13b and Figure 3.13d) in low grade invasive tumours. Greater than 85% of patients had appreciable 5-LO stromal staining (Figure 3.13g and Figure 3.13h). Polymorphonuclear cells such as neutrophils and plasmacytoid cells were used as an internal positive control for staining. Representative images of rare epithelial staining and the frequently observed stromal staining are indicated in Figure 3.13. The majority of the scoring for 5-LO was concerned with the stromal compartment and representative images of the scoring system used are detailed in Figure 3.14.

Table 3.4 There is no association between 5-LO expression and oesophageal cancer morphology

		Mean Score (S.E.M.)		p-value
		OAC	OSCC	
Non-leading edge (NLE)	5-LO epithelium	9.05 (2.64)	1.43 (3.29)	0.455
	5-LO stroma	46.58 (3.74)	50.23 (7.28)	0.526
Leading edge (LE)	5-LO epithelium	4.12 (2.05)	1.71 (0.51)	0.155
	5-LO stroma	57.35 (4.73)	71.43 (9.23)	0.086

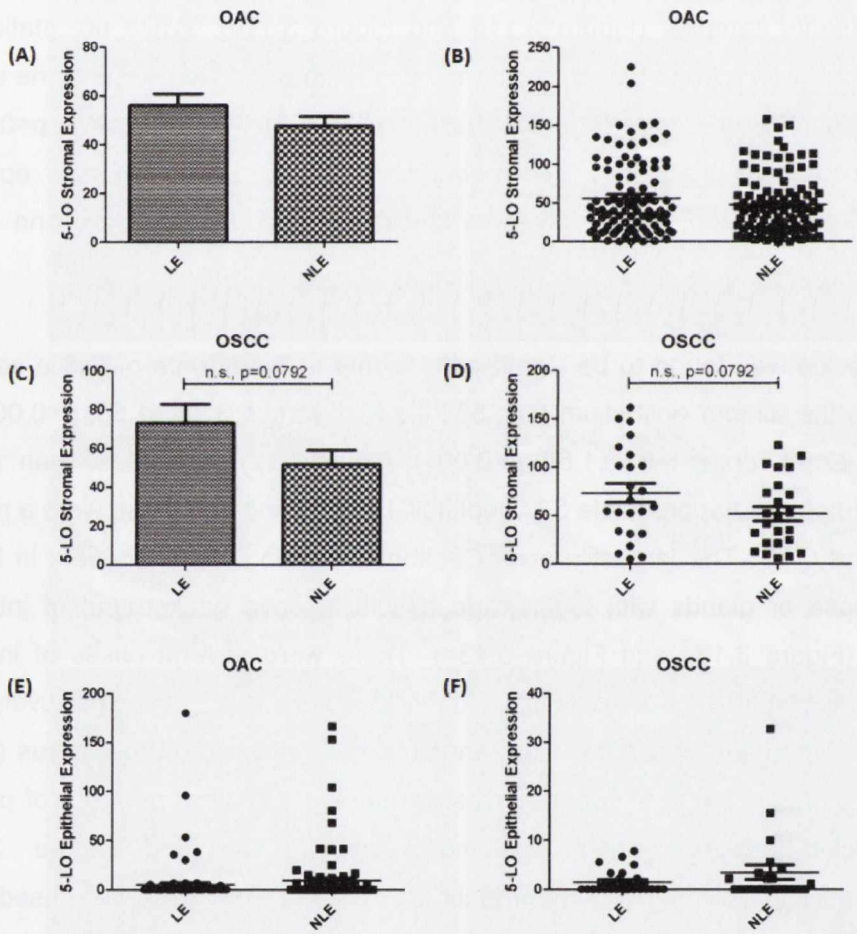

Figure 3.11 Comparison of 5-LO expression in leading edge and non-leading edge oesophageal cancer. (A) There was no difference in OAC 5-LO stromal expression between LE and NLE tissue. (B) The distribution of the 5-LO expression across OAC patient cores is shown by scatter plot. (C) Although there was a trend for higher OSCC 5-LO stromal expression in LE compared to NLE samples, this was not significant (p=0.0792, n=24). (D) The distribution of 5-LO expression across OSCC patient cores is shown by scatter plot. There was no preferential expression of 5-LO in tumour epithelium of either LE or NLE samples in OAC (E) or OSCC (F). Statistical test used was Wilcoxon signed rank test. Error bar denotes mean ± S.E.M.

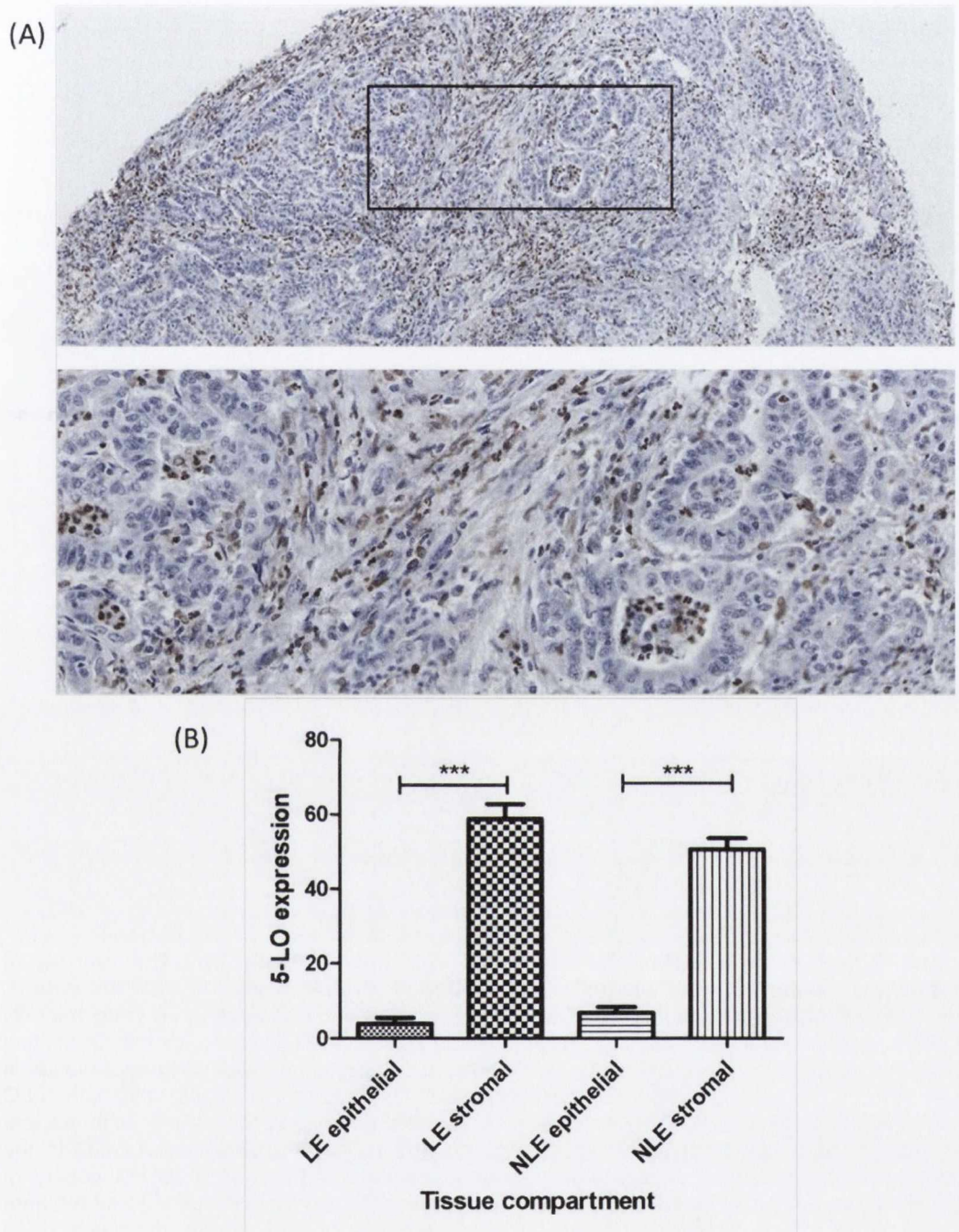

Figure 3.12 -The majority of 5-LO expression is localised to the stromal compartment in oesophageal cancer. (A) Representative image of high OAC stromal staining and absent tumour staining (top image is 4X image and boxed region is 20X). (B) Grouping all oesophageal cancer patients together 5-LO staining was significantly higher in the stromal compartment compared to the tumour epithelium ($p<0.001$), regardless of invasiveness (i.e. NLE or LE). LE epithelial cores, n= 142 and LE stromal cores, n= 141. NLE epithelial and stromal cores, both n= 148. Statistical test used was Mann Whitney U test: $p<0.001$(***). Error bar denotes mean ± S.E.M.

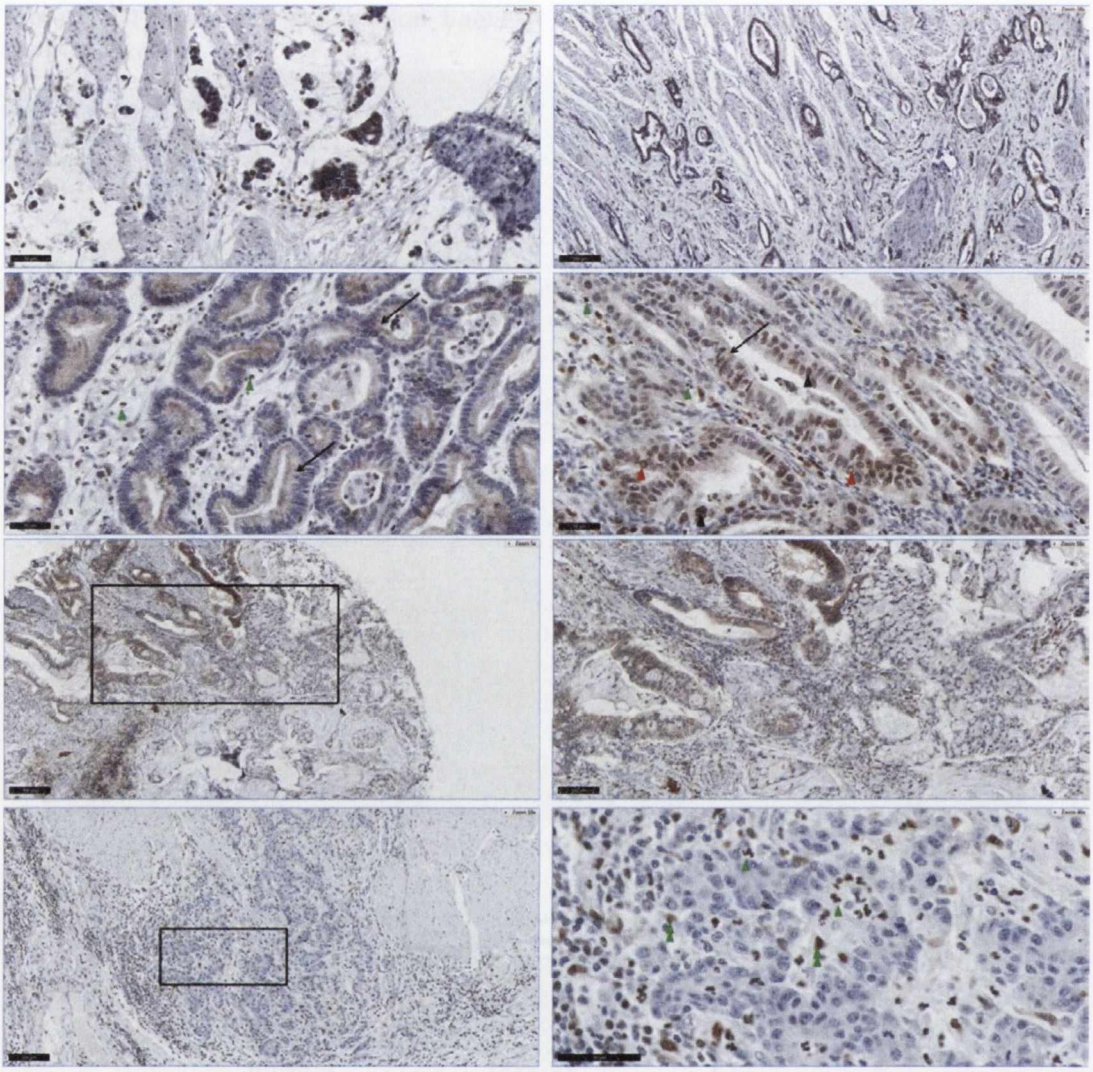

Figure 3.13 5-LO tumour epithelial staining was very low or absent from the majority of oesophageal cancer patients while stromal 5-LO was well expressed across the cohort. (A) and (B) are representative images of strong epithelial staining observed in a small minority of patient tumour tissue. (A) depicts invasive single cancer cells in mucin pools, dissecting through muscle bundles while (B) shows 5-LO stained differentiated invasive tumour glands in the muscle. (C) indicates dilated non-dysplastic and non-cancerous glands with high 5-LO cytosolic staining (black arrow). (D) indicates differentiated invasive carcinoma with nuclear (black arrow head) and cytoplasmic staining (black arrow). The translocation of 5-LO to the nuclear envelope was also observed in tumour epithelium (red arrows in D). A variety of epithelial staining even within the same core was observed, for example image (E) and a higher magnification version (F) depicts highly stained glands with high grade dysplasia on a background of intestinal metaplasia, adjacent to negative staining signet ring-form carcinoma and mucin pools (bottom right). Image (G) and a higher magnification version (H) show undifferentiated invasive carcinoma with no 5-LO epithelial staining but high immune cell staining in the stroma. Polymorphonuclear cells, such as neutrophils (green arrow head in C, D and H) and plasmacytoid leukocytes (green double-headed arrow in H) were used as positive controls for 5-LO expression. Magnification of the images and scale bar are indicated in top right and bottom left hand corner of images.

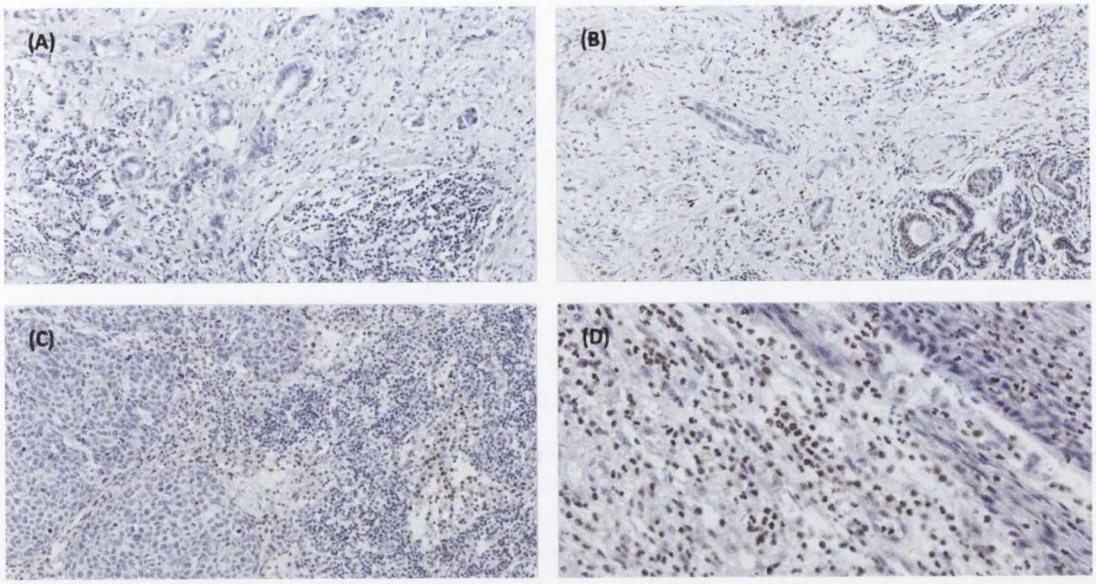

Figure 3.14 Tissue microarray 5-LO stromal staining in oesophageal cancer. TMAs were stained using immunohistochemistry for 5-LO. Stromal staining was scored based on a combination of intensity and percentage of cells staining within the core. Representative images (A-D) indicate negative, low, moderate and high stromal expression respectively. Images A-C are 10X magnification while image D is 20X magnification.

3.3.9 OSCC 5-LO expression and clinical data

OSCC 5-LO expression was correlated with available clinical parameters including sex, age, tumour and nodal stage, grade, lymph node involvement, venous involvement, perineural involvement and disease specific survival. No significant association between 5-LO tumour epithelial expression and clinical parameters was found, presumably due to the infrequent presence of epithelial staining. NLE OSCC 5-LO stromal expression was higher in patients with absence of lymph involvement compared to lymph node positive patients (68.04 ±10.37 versus 43.45 ±6.96, n=15 versus n=22 $p<0.05$) and a similar trend was observed for N0 patients (61.54 ±8.97 versus 46.84 ±7.50, n=13 versus n=24, p=0.1477) (Figure 3.15a and Figure 3.15b). A significant association between higher 5-LO stromal expression and absence of lymph node invasion (79.54 ±12.32 versus 44.51 ±7.21, n=11 versus n=21, $p<0.05$) and N0 patients (74.34 ±11.53 versus 48.42 ±9.63, n=11 versus n=22, $p<0.05$) was found when analysing CRT-naive patients only (Figure 3.15c and Figure 3.15d). In LE tumour cores (note: none of these patients had neoadjuvant CRT), a significantly greater proportion of patients with higher 5-LO stromal expression showed absence of venous involvement (84.29 ±11.90 versus 44.49 ±13.38, n=17 versus n=8, $p<0.05$) and presence of dysplasia (87.81 ±9.65 versus 56.71 ±14.12, n=12 versus n=14, $p<0.05$) (Figure 3.15e and Figure 3.15f). No significant association between 5-LO stromal expression and 5-year disease free survival was observed however there was a tendency for CRT-naive patients with above median NLE 5-LO stromal expression to survive longer (median survival: 39.9 months versus 11.7 months, both n=16, log-ranks test, p=0.202) (Figure 3.16).

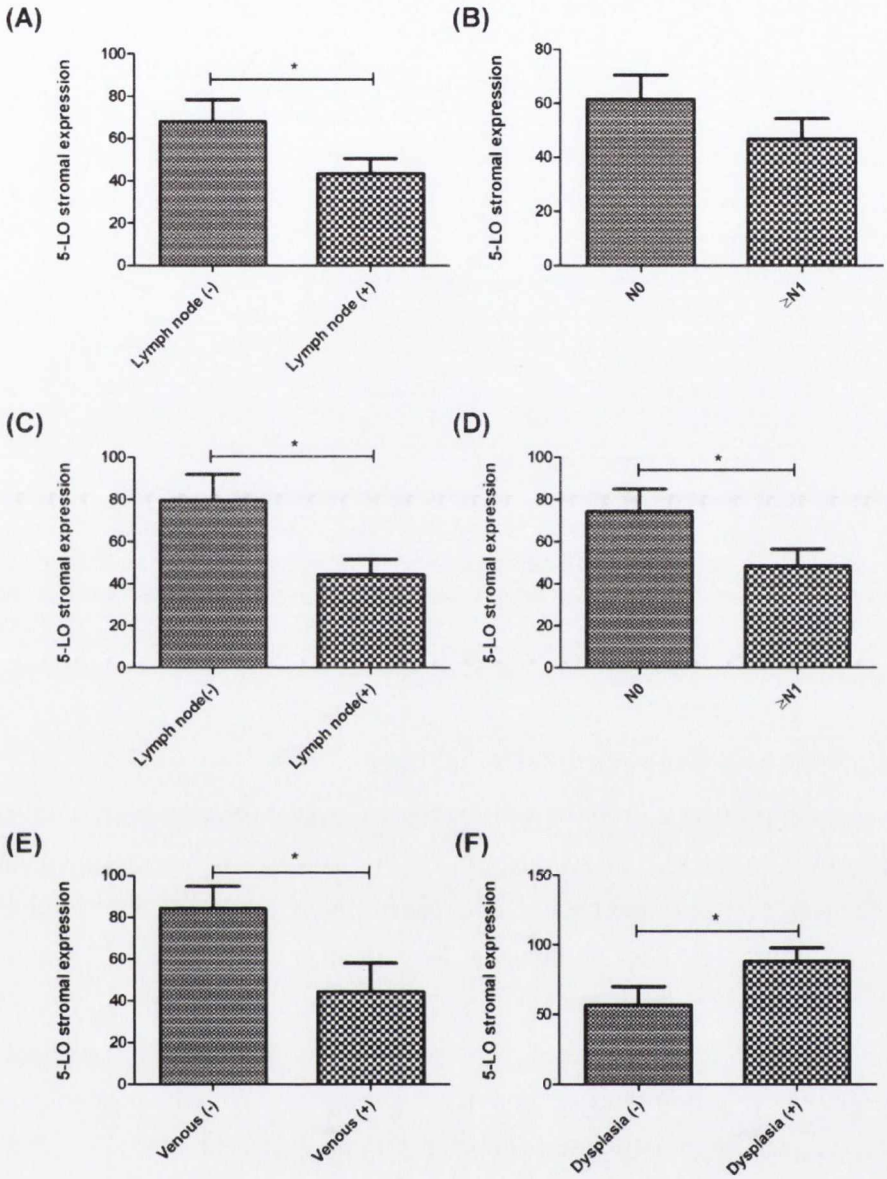

Figure 3.15 Stromal 5-LO expression was associated with a less aggressive tumour phenotype in OSCC patients. (A) Higher NLE OSCC 5-LO stromal expression was associated with absence of lymph involvement ($p<0.05$, n=15 versus n=22). (B) a similar non significant trend was observed for N0 patients ($p=0.1477$, n=13 versus n=24). (C) Sub-analysis of OSCC patients excluding those with CRT prior to surgery revealed a significant association between higher 5-LO stromal expression and negative lymph node invasion ($p<0.05$, n=11 versus n=21) and (D) N0 patients ($p<0.05$, n=11 versus n=22). In LE OSCC tumour cores a significantly greater proportion of patients with higher 5-LO stromal expression showed (E) absence of venous involvement (n=17 versus n=8, $p<0.05$) and (F) presence of dysplasia ($p<0.05$, n=12 versus n=14). Statistic test used was Mann Whitney U test $p<0.05$(*). Error bar denotes mean ± S.E.M.

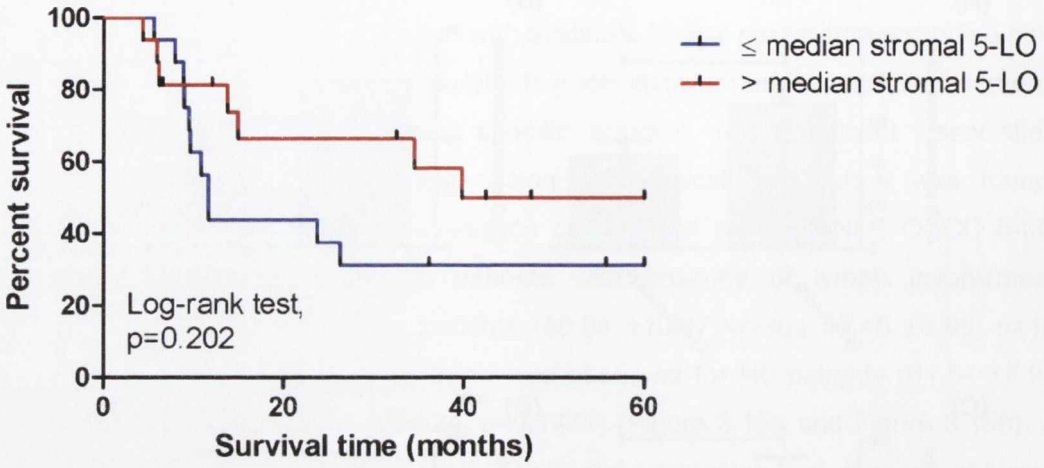

Figure 3.16 OSCC patients with above median stromal 5-LO expression have an improved median survival time. CRT-naive patients with above median NLE 5-LO stromal expression tended to survive longer (median survival: 39.9 months versus 11.7 months) however this observation was not significant, log-ranks test, p=0.202, both n=16). Statistical test used was Kaplan Meier survival curve with Log-rank (Mantel-Cox) test.

3.3.10 OAC 5-LO expression and clinical data

OAC 5-LO expression was correlated with available clinical parameters including sex, age, tumour and nodal stage, grade, lymph node involvement, venous involvement, perineural involvement, BO metaplasia, OGJ (oesophagogastric junction) tumour type (if applicable) and disease-specific survival. No significant association between 5-LO tumour epithelial expression and clinical parameters was found, presumably due to the infrequent presence of epithelial staining. However it was noted that the highest 5-LO epithelial scores in the cohort tended to have a more aggressive tumour phenotype (i.e. positive N-stage and lymph node and venous involvement) (Figure 3.17).

LE OAC 5-LO stromal expression were associated with OGJ type I tumour compared to the pathologically distinct gastric cardia/ proximal gastric derived OGJ type II and III (66.90 ±5.65 versus 44.28 ±7.41, n=61 versus n=47, $p<0.001$) (Figure 3.18a) and also the presence of the premalignant inflammatory disease, BO (61.70 ±6.51 versus 49.18 ±6.90, n=60 versus n= 42, $p<0.05$) (Figure 3.18c). A similar non-significant trend between NLE stromal 5-LO and OGJ type I morphology (52.1 ±5.20 versus 42.63 ±3.94, n=59 versus n=79, p=0.1376) and a significant association between NLE stromal 5-LO and BO morphology was noted (56.02 ±5.07 versus 40.04 ±4.03, n=64 versus n=73, $p<0.05$). There was no association with T-stage or any other parameter.

71% (110/145) of OAC patients in the TMA study did not receive any CRT prior to surgery. Sub-analysis of this population in isolation results in several associations with clinical parameters. Similar to analysis of all OAC regardless of treatment status, high LE 5-LO stromal expression showed an association with OGJ type I morphology (68.45 ±6.85 versus 35.05 ±6.36, n=57 versus n=22, $p<0.01$) and BO (72.64 ±8.88 versus 45.31 ±6.41, n=37 versus n=39, $p<0.01$) upon sub-analysis of OAC patients excluding those who had received pre-operative CRT (Figure 3.19a and Figure 3.19b). Analysis of NLE cores excluding neoadjuvant CRT patients, revealed additional significant results. Higher 5-LO stromal expression in NLE cores of CRT-naive patients was associated with a lower T-stage (55.63 ±7.02 versus 38.73 ±4.28, n=36 versus n=71, $p<0.05$) (Figure 3.19e) in addition to a stronger association with OGJ type I tumours (59.13 ±7.76 versus 39.39 ±4.49, n=34 versus n=63, $p<0.05$) and BO (63.03 ±6.72 versus 34.27 ±4.23, n=45 versus n=57, $p<0.001$) (Figure 3.19c and Figure 3.19d). There was a non significant trend towards lower N-stage with increased 5-LO stromal expression in this sub-cohort of CRT-naive NLE tumour cores however it was not significant (55.54 ±7.87 versus 38.79 ±3.89, n=46 versus n=71, $p=0.1793$) (Figure 3.19f).

There was no association between NLE 5-LO expression (both epithelial and stromal) and 5-year disease specific survival regardless of neoadjuvant treatment (data not shown). Higher LE 5-LO stromal expression did not show any association with survival upon analysis of the entire OAC (n=110, median survival 49.57 versus 36.37 months, $p=0.4456$) (Figure 3.20a). However there was a trend towards a lower chance of survival with above-median LE stromal 5-LO expression in CRT-naive patients (n=83, $p=0.0835$) (Figure 3.20b).

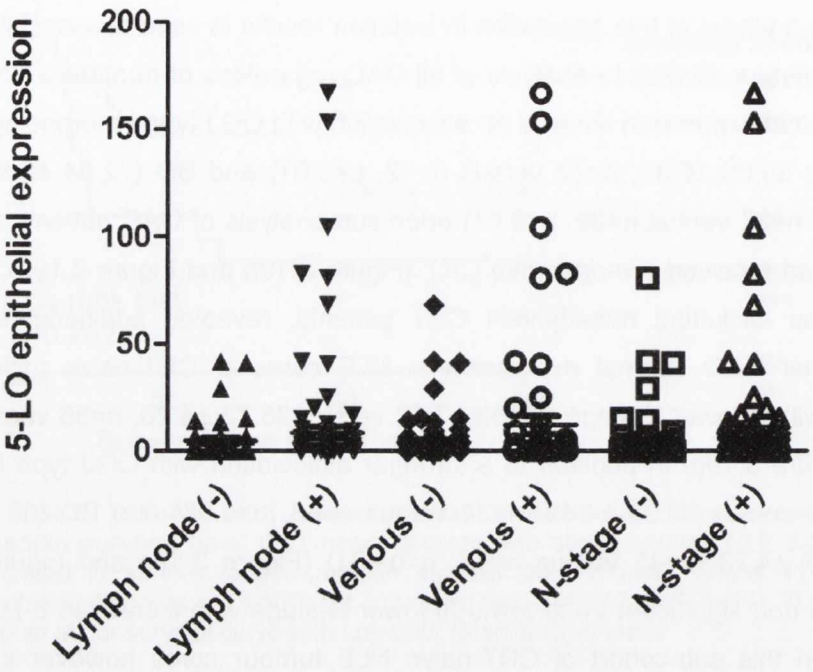

Figure 3.17 OAC patients with the highest tumour epithelial 5-LO expression tended to have a more aggressive tumour phenotype. Less than 10% of patients were positive for 5-LO epithelial expression. NLE epithelial 5-LO expression level was compared in lymph node negative versus lymph node positive; venous negative versus venous positive and N0 versus N1 CRT-naive OAC patients. The highest 5-LO epithelial expression scores tended to cluster with lymph node involvement, venous involvement and positive N-stage. No statistical significance was observed between positive and negative groupings by Mann Whitney U test.

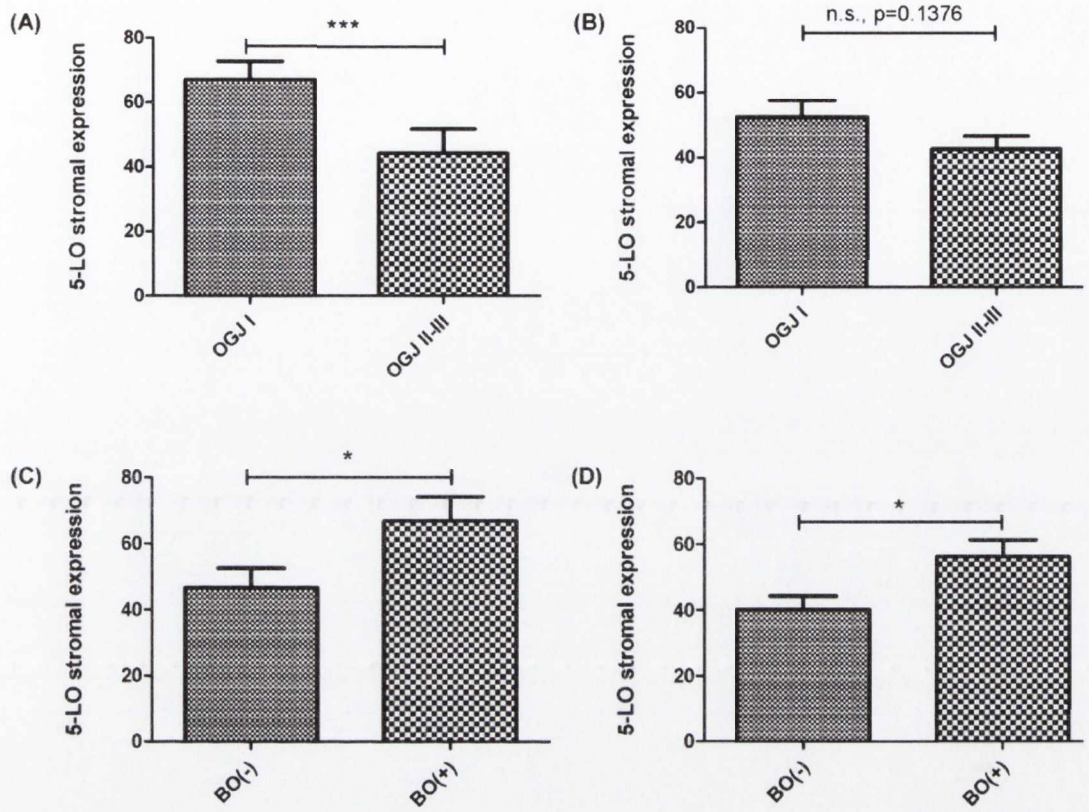

Figure 3.18 Stromal 5-LO in both leading edge and non-leading edge cores is preferentially expressed in OGJ type I tumours and patients with Barrett's morphology. OAC patients with OGJ tumours were subdivided into OGJ type I (i.e. cancer derived from the oesophagus) or OGJ type II and III (i.e. cancer derived from the stomach). (A) 5-LO stromal expression was significantly associated with type I tumour morphology in LE cores ($p<0.001$, n=61 versus n=47) and (B) a similar non-significant trend was observed with the NLE cores ($p=0.1376$, n=59 versus n=79). All OAC patients were subdivided based on the presence or absence of BO morphology. (C) 5-LO stromal expression was significantly higher in BO positive LE cores ($p<0.05$, n=59 versus n=79) and (D) BO positive NLE cores ($p<0.05$, n=64 versus n=73). Statistical test used was Mann Whitney U test. $p<0.05$(*) and $p<0.001$(***) Error bar denotes mean ± S.E.M.

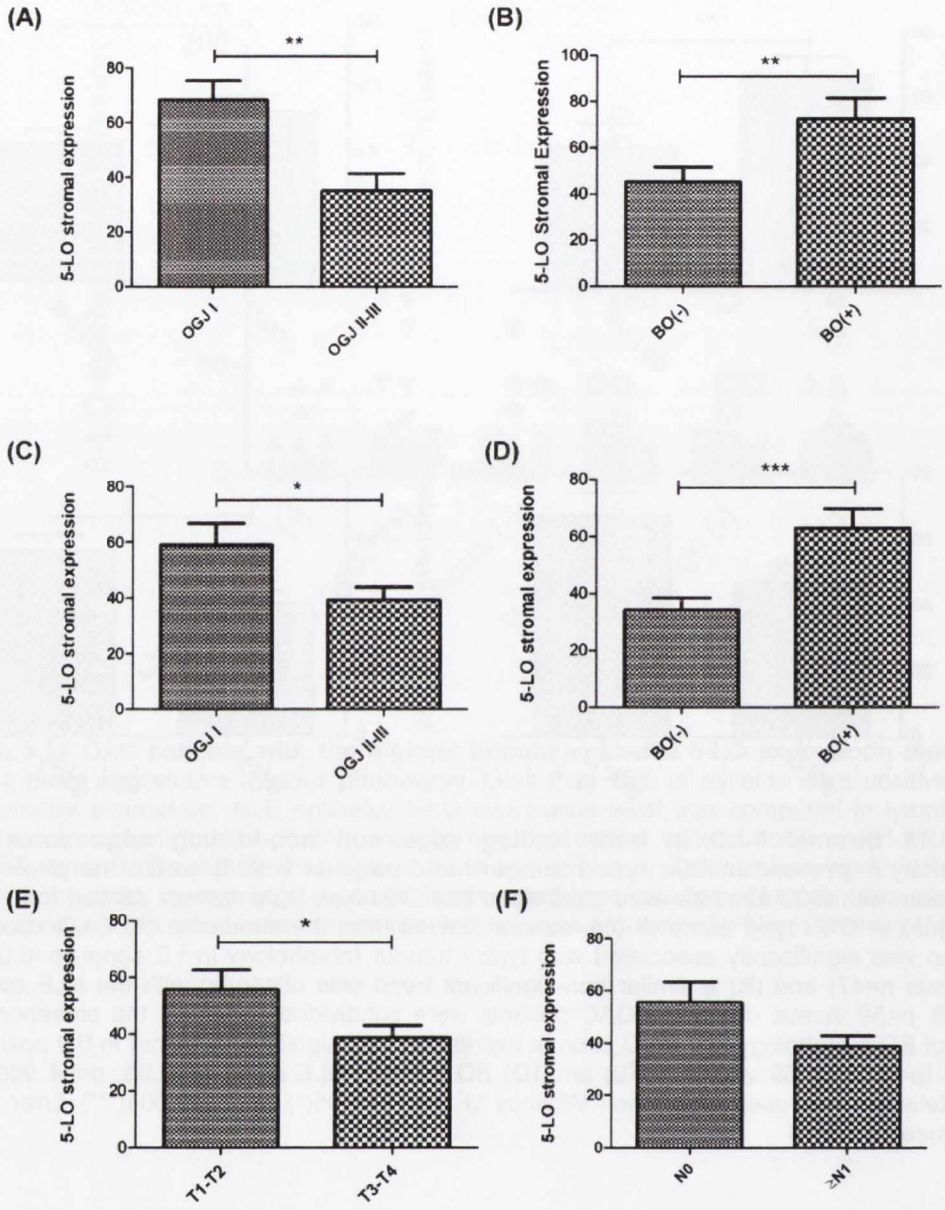

Figure 3.19 Non-leading edge stromal 5-LO expression in neoadjuvant treatment naive patients is associated with Type I OGJ and Barrett's morphology and a lower T-stage. Sub-analysis of OAC patients excluding those who had received pre-operative CRT was carried out. (A-B) Increased 5-LO stromal expression was associated with LE cores from CRT-naive OGJ type I tumours ($p<0.01$, n=57 versus n=22) and CRT-naive OAC tumours with BO ($p<0.01$, n=37 versus n=39). (C) 5-LO stromal expression was significantly associated with OGJ type I morphology in NLE cores derived from CRT-naive patients ($p<0.05$, n=34 versus n=63,). (D) Similarly 5-LO stromal expression was significantly higher in BO positive NLE cores ($p<0.001$, n=45 versus n=57). (E) Higher stromal 5-LO was associated with lower T-stage (i.e. T1-T2) in NLE cores ($p<0.05$, n=36 versus n=71). (F) 5-LO stromal expression was higher in nodal negative patients however this was not significant ($p=0.1793$, n=46 versus n=71). Statistical test used was Mann Whitney U test. $p<0.05$(*), $p<0.01$(**) and $p<0.001$(***) Error bar denotes mean ± S.E.M.

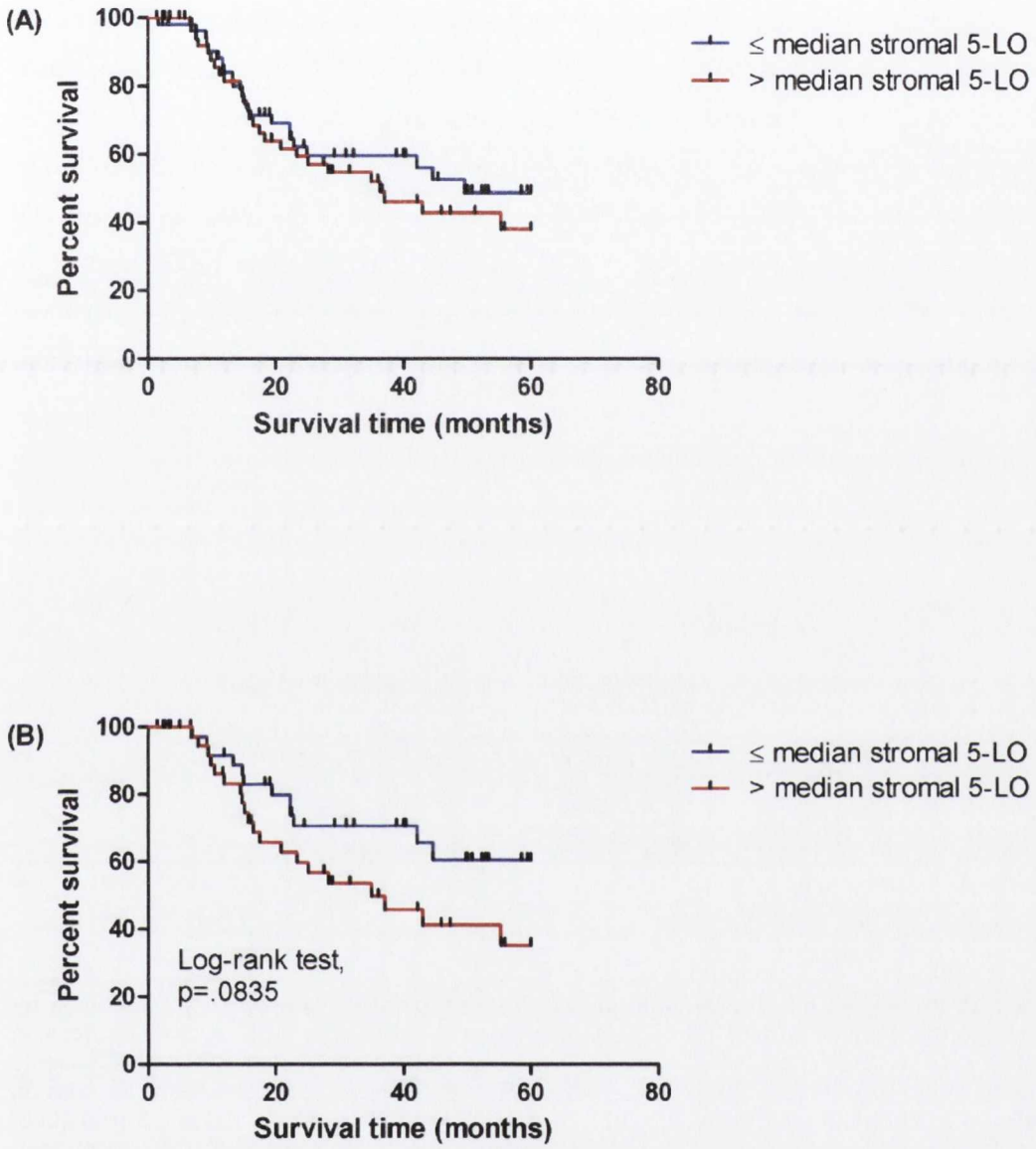

Figure 3.20 Leading edge stromal 5-LO trends towards an association with poor survival in neoadjuvant treatment naive OAC patients. (A) Above-median LE 5-LO stromal expression was associated with a decreased median survival time (n=110, median survival 49.57 versus 36.37 months) however this association was not significant (p=0.4456). (B) In a sub-analysis of LE 5-LO stromal expression in CRT-naive patients only (n=83) while significance was not shown, a definite trend towards a poorer patient survival with increasing 5-LO stromal expression was observed (p=0.0835). Statistical test used was Kaplan Meier survival curve with Log-rank (Mantel-Cox) test.

3.3.11 Association of tumour stromal derived 5-LO and obesity status

In section 3.3.3 an association between 5-LO mRNA expression levels and visceral obesity measured by VFA in neoadjuvant CRT naive patients (n=34, $p<0.05$) was shown. BMI was the only anthropomorphic measurement available for patients in the TMA study. This measurement was available for 78% of neoadjuvant CRT naive patients (86/110). Patients were grouped based on their obesity status by BMI (i.e. ≥ 30 kg/m^2). While there was a bias towards non-obese BMI measurements in this cohort of patients (non-obese versus obese: 86% versus 14%) there was a statistically significant association between higher 5-LO stromal expression in NLE cores from CRT-naive patients and an obese BMI compared to non-obese (72.52 ±14.21 versus 42.19 ±4.68, n=11 versus n=70, $p<0.05$) (Figure 3.21a). Analysis of all over-weight and obese patients only (i.e. BMI>25) indicated a moderate correlation between 5-LO stromal expression and BMI ($r=0.4005$, n=43, $p<0.01$) (Figure 3.21b).

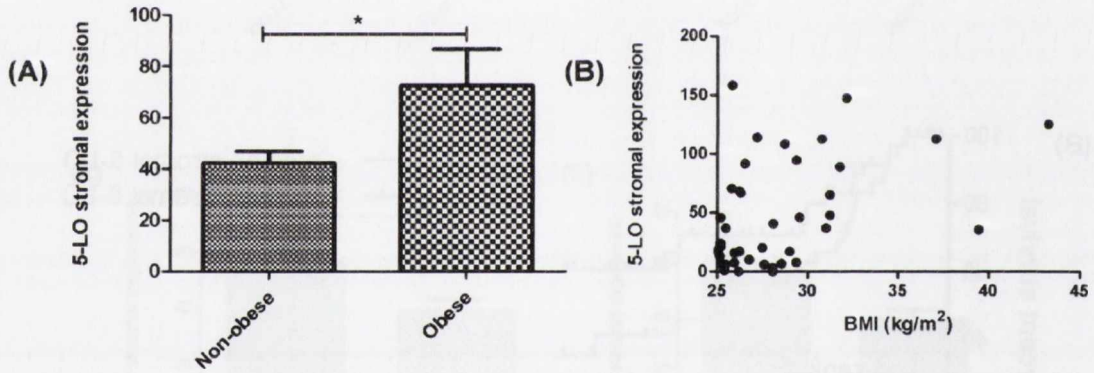

Figure 3.21 Increased 5-LO stromal expression is associated with obesity measured by BMI in neoadjuvant treatment naive OAC patients. (A) Levels of 5-LO stromal expression were found to be significantly higher in NLE tumour cores from obese CRT-naive patients compared to non-obese ($p<0.05$, n=11 versus n=70). (B) Increasing 5-LO stromal expression was shown to correlate with increasing BMI in patients with BMI values above 25 ($r=0.4005$, $p<0.01$, n=43). Statistical test used was Mann Whitney U test and Spearman's correlation test: $p<0.05$(*). Error bar denotes mean ± S.E.M.

3.3.12 Association of 5-LO expression and angiogenic markers

In section 3.3.2 a positive correlation between tumour biopsy 5-LO expression and VEGF levels was shown. NLE tumour cores from the TMA cohort were stained and graded for VEGF and CD31, a marker of microvessel density while LE tumour cores were stained for VEGF and KDR (VEGFR-2). Spearman's correlation test showed no association between 5-LO stromal expression and VEGF or KDR expression (data not shown), regardless of cancer morphology (i.e. OSCC or OAC).

The microvessel density of LE TMA cores, as indicated by CD31 was quantified as described in Section 2.16.3. No correlation between 5-LO stromal expression and microvessel density was found in the OSCC cohort (data not shown). However a weak but significant correlation between 5-LO stromal expression and microvessel density counts was observed ($r=0.3067$, $n=125$, $p<0.01$) (Figure 3.22).

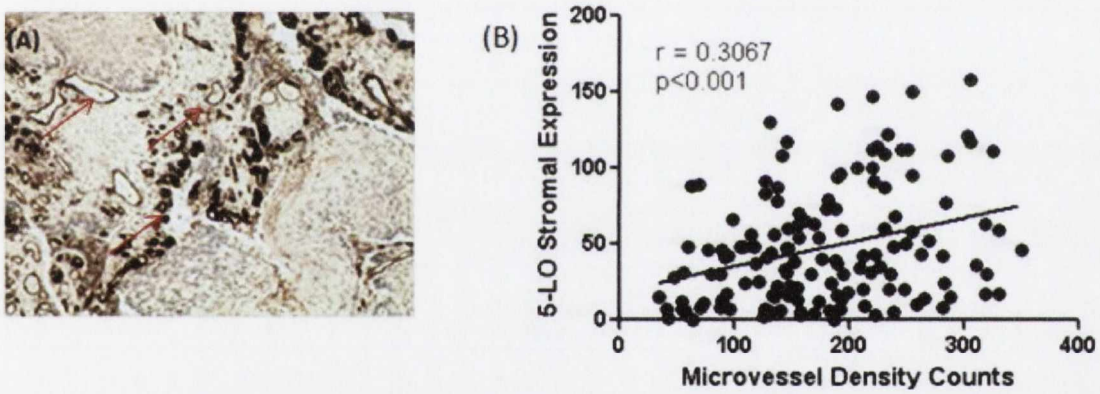

Figure 3.22 5-LO stromal positivity is associated with increased microvessel density within tumour cores of leading edge OAC patients. LE cores were stained for CD31 and the average microvessel density per patient was quantified. (A) example of CD31 staining in an OAC TMA core with circular blood vessels indicated by red arrow. (B) Increased 5-LO stromal expression was shown to correlate with dense regions of microvessel density ($r=0.3067$, $p<0.01$, $n=125$). Spearman's correlation test was used for statistical analysis.

3.3.13 5-LO stromal expression and association with immune markers

The LE TMA cores were stained and graded for a number of immune cell markers prior to this project (see Appendix V for full panel of immune markers and cytokines stained). Spearman's correlation test was used to investigate the association of stromal 5-LO and levels of these immune markers in the stroma. OSCC 5-LO stromal expression was shown to correlate with stromal CD107A ($r=0.4664$, $P<0.05$) (Table 3.5). A number of correlations with OAC 5-LO stromal expression and stromal immune markers were also noted and are listed in Table 3.5.

Table 3.5 Summary of positive correlations between 5-LO stromal expression and stromal immune markers or cytokines in oesophageal cancer

Cancer Type	Immune marker or cytokine	Function	N	Spearman r	p-value
OSCC	CD107A	Degranulation marker of CD8 and NK cells	24	0.4664	0.0216
OAC	CD45RO	Regulation of B- and T-cell antigen receptor signalling	70	0.3174	0.0074
	CD8	T-cell marker	71	0.2917	0.0136
	FOXP3	Immuno-suppression against cancer cells	58	0.3553	0.0062
	IFN-γ	Macrophage activation	61	0.3284	0.0098
	IL-4	Differentiation of Th2 memory cells	69	0.2485	0.0395

3.3.14 5-LO metabolite LTB4 levels in OAC patients and correlation with obesity and other clinicoparameters

Increased LTB4 levels have been linked to both cancer and obesity derived inflammation (Ye *et al.*, 2005a, Chakrabarti *et al.*, 2011, Guriec *et al.*, 2014). Consequently the serum levels of the major 5-LO metabolite LTB4 in OAC patients was investigated by ELISA as described in Section 2.20.4 to explore the association of this marker with both disease status and obesity status. Serum samples were handled as detailed in section 2.20.1. Serum selected for this study was from male CRT-naive OAC patients (n=60) with available VFA, BMI and WC measurements (BMI measurement was missing for 1 patient). 27/60 patients had non-obese VFA while 33/60 had obese VFA. VFA values and other clinical parameters of the cohort are detailed in Table 3.6. Six age-matched non-cancer control males were also included in this study (mean age± S.D= 67.91 ±8.84). These six patients were admitted for hernia repair surgery and did not have a history of cancer.

There was no difference in the mean level of LTB4 between cancer serum samples and non-cancer controls (668.77 ±74.24 pg/mL versus 593.60 ±140.55 pg/mL) (Figure 3.23). However notably 35% (21/60) of the cancer serums had LTB4 concentrations that were above the average of the non-cancer control group.

Previously 5-LO gene expression was found to associate with obesity status by VFA and 5-LO protein expression correlated with obesity status by BMI (Section 3.3.3 and Section 3.3.11). Consequently the association between 5-LO metabolite LTB4 in OAC serum and obesity status indicated by VFA, BMI and WC were investigated. There was not a significant association between LTB4 expression and VFA or WC ($p=0.1022$ and $p=0.1038$ respectively) (Figure 3.24a and Figure 3.24c). Nevertheless it was noted that the highest LTB4 serum levels detected were found in obese patients. Sub-analysis of the patient cohort comparing patients with obese BMI (i.e. ≥ 30, n=24) and normal weight BMI (i.e. <25, n=18) revealed a significant association between LTB4 levels and obesity (761.90 ±146.06 pg/mL versus 403.61 ±56.02 pg/mL, $p<0.05$) (Figure 3.24e).

Table 3.6 Details of OAC patient demographic used for LTB4 serum study

Male OAC (n=60)	Mean (S.D.) or n (%) as appropriate	
Age	65.26 (11.85)	
Non obese: Obese by VFA	27: 33 (45%:55%)	
Non-obese VFA (cm^2)	104.75 (45.5)	
Obese VFA (cm^2)	228.65 (54.92)	
T-stage	T0	6 (10%)
	T1	19 (31.67%)
	T2	15 (25%)
	T3	17 (28.33%)
	Not specified	3 (5%)
N-stage	N0	33 (55%)
	≥N1	24 (40%)
	Not specified	3 (5%)
Tumour grade	Moderate-well	39 (65.1%)
	Poorly	16 (26.7%)
	Not specified	5 (8.3%)
Neoadjuvant treatment	0 (0%)	

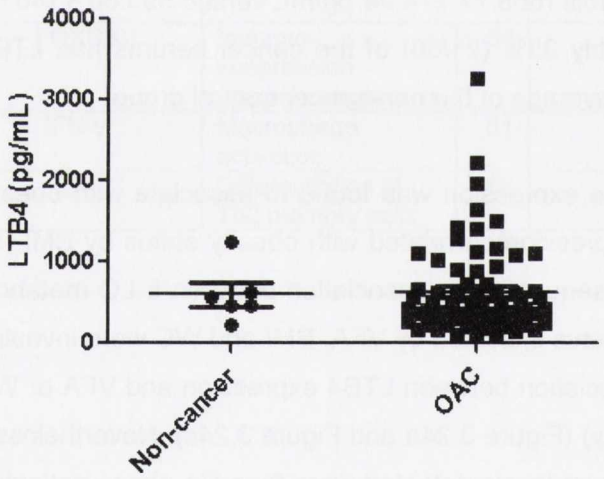

Figure 3.23 Average serum LTB4 levels in OAC serum samples are similar to age-matched non-cancer controls. LTB4 levels were measured by competitive ELISA in OAC serums samples (n=60) and non-cancer control controls (n=6). There was no significant difference between cancer serum LTB4 levels (668.77 ±74.24 pg/mL) and non-cancer control levels (593.60 ±140.55 pg/mL) (p=0.8148). Statistical test used was Mann-Whitney U test. Error bar denotes mean ± S.E.M.

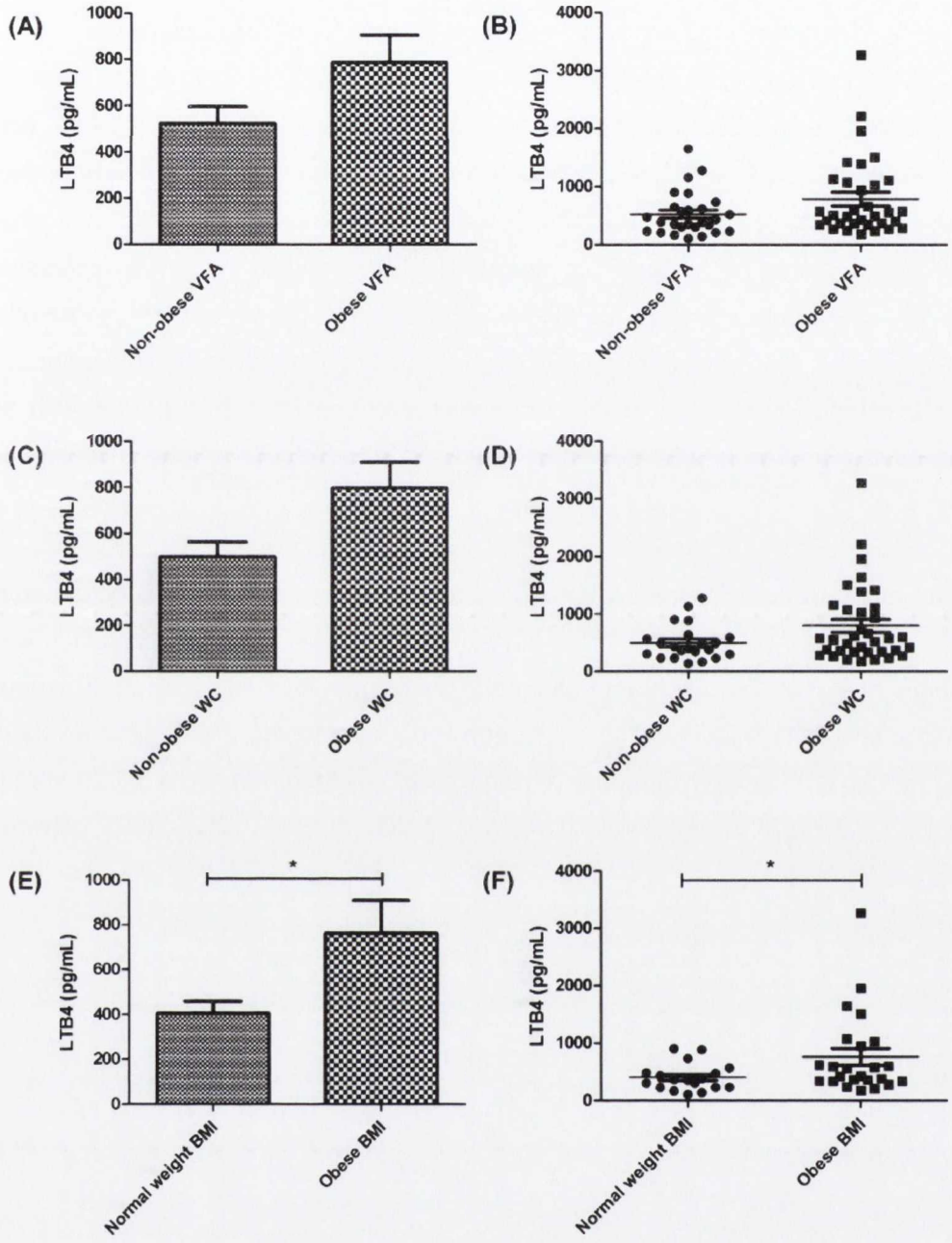

Figure 3.24: LTB4 serum levels are associated with obesity measured by BMI in OAC patients. LTB4 levels were measured by competitive ELISA in male treatment-naive OAC serums (n=60). Patients were grouped into obese and non-obese by VFA, WC and BMI with cut-off points of 163.8 cm^2, 94 cm and 30 kg/m^2 respectively. (A) The highest LTB4 levels were detected in serums from obese patients indicated by VFA however this was not significant ($p=0.1022$, n=33 versus n=27) (distribution of data points indicated in (B)). (C) A similar but non-significant trend was also found for obesity indicated by WC ($p=0.1038$, n=36 versus n=22) (distribution of data points indicated in (D)). (E) Comparison of normal weight BMI patient serum LTB4 levels and obese BMI serum levels showed a significant association with obesity status ($p<0.05$, n=18 versus n=24,) (distribution of data points indicated in (F)). Statistical test used was Mann-Whitney U test: $p<0.05$ (*). Error bar denotes mean ± S.E.M.

3.3.15 Differential expression of lipoxygenases and VEGF in subcutaneous and omental adipose tissue from OAC patients

Matched subcutaneous and omental adipose tissue biopsies were obtained from 12 male OAC patients at the beginning of the oesophagectomy procedure. RNA was isolated as described in Section 2.8 and expression of the four main lipoxygenase enzymes (5-LO, platelet-type 12-LO, 15-LO-1 and 15-LO-2) and VEGF were measured by qPCR as described in Section 2.12. 5-LO and VEGF showed moderate expression in both fat types with average Ct values of 28-30. 15-LO-1 showed preferential expression in the omental samples (average Ct of 26) compared to subcutaneous samples (average Ct of 33) .15-LO-2 was lowly expressed in both fat types with an average Ct of 35. 12-LO was undetermined (i.e. Ct >40) for all samples investigated (data not shown).

5-LO was found to be significantly higher in the omentum compared to subcutaneous fat (2.79 ±0.56 versus 1.35 ±0.31, $p<0.01$) (Figure 3.25a). Similarly 15-LO-1 was significantly higher in the omentum compared to subcutaneous fat (1.36 ±0.26 versus 0.12 ±0.10, $p<0.001$) (Figure 3.25b). Although lowly expressed, the highest levels of 15-LO-2 were found in subcutaneous fat compared to omentum (9.24 ±3.79 versus 1.40 ±0.56, $p<0.05$) (Figure 3.25c). There was no difference in VEGF levels between fat depots in this cohort (2.08 ±0.54 versus 1.49 ±0.39) (Figure 3.25d).

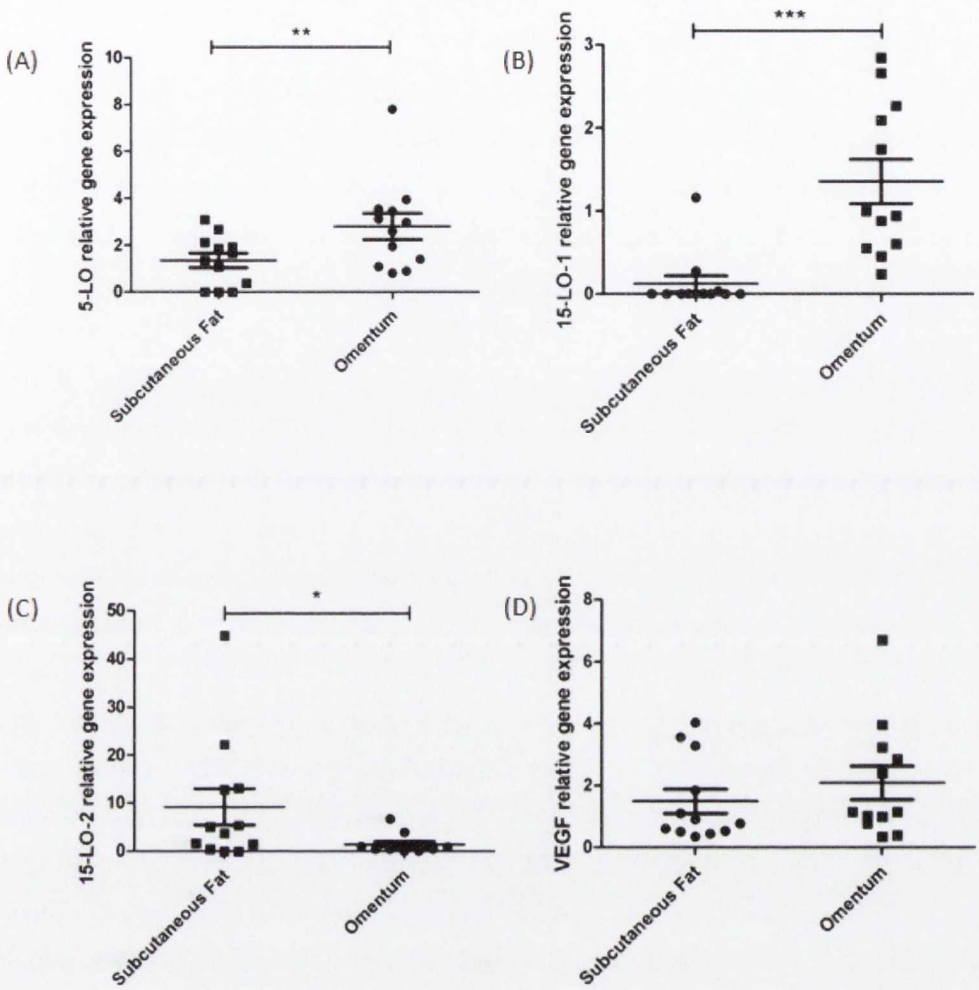

Figure 3.25 Differential lipoxygenase expression in adipose tissue from OAC patients. 5-LO, 15LO-1 and 15LO-2 and VEGF mRNA expression was quantified by qPCR using cDNA synthesised from isolated RNA of matched subcutaneous and omental adipose tissue collected from OAC patients undergoing an oesophagectomy (n=12). (A) Significantly greater 5-LO expression was found in omental adipose tissue compared to subcutaneous ($p<0.01$). (B) 15-LO-1 expression was strongly associated with omental adipose tissue ($p<0.001$). (C) In contrast, 15-LO-2 expression was higher in subcutaneous fat compared to omental fat ($p<0.05$). (D) There was no significant difference between omental and subcutaneous VEGF expression. Statistical test used was Wilcoxon signed rank test for paired analysis $p<0.05$(*), $p<0.01$(**) and $p<0.001$(***).Error bar denotes mean ± S.E.M.

3.3.16 Association of omental derived lipoxygenase enzymes and VEGF gene expression and obesity status

The twelve male patient omental adipose tissue samples were divided into two groups (n=6 each) based on anthropomorphic measurements as described in Section 2.5. The average non-obese and obese VFA, BMI and WC measurements for the two groups were as follows: 65.65 ±67.41 cm^2 versus 294.45 ±112.37 cm^2; 24.91 ±3.12 kg/m^2 versus 32.99 ±4.01 kg/m^2 and 86.20 ±7.13 cm versus 112.14 ±14.84 cm.

Omental 5-LO expression was significantly higher in obese patients compared to non-obese indicated by VFA (0.29 ±0.07 versus 0.13 ±0.03, $p<0.05$), WC (same graph as VFA) and BMI (0.33 ±0.08 versus 0.12 ±0.02, $p<0.01$) (Figure 3.26a and Figure 3.26b). Positive correlations between 5-LO RQ values and WC, BMI and VFA were also noted ($r=0.61$, $p<0.05$; $r=0.78$, $p<0.01$; $r=0.54$, $p=0.058$ respectively) (Figure 3.26c-Figure 3.26e). There was no association between 15-LO-1 expression and obesity status when patients were separated into obese and non-obese patients (Figure 3.27a). A negative correlation between 15-LO-1 RQ values and corresponding patient VFA measurements was observed ($r= -0.6014$, $p<0.05$) (Figure 3.27b). There was a significant association between omental 15-LO-2 expression and patients with obese VFA (2.36 ±0.99 versus 0.44 ±0.16, $p<0.05$) WC (same graph as VFA) and BMI (3.19 ±1.34 versus 0.50 ±0.14, $p<0.05$) (Figure 3.27c and Figure 3.27d). Positive correlations between 15-LO-2 RQ values and VFA, BMI and WC were also found ($r=0.78$, $p<0.01$; $r=0.78$, $p<0.01$; $r=0.82$, $p<0.01$ respectively) (Figure 3.27e-Figure 3.27g). Finally, VEGF levels were found to be higher in the omental samples of non-obese patients compared to obese by both VFA (3.07 ±1.05 versus 1.08 ±0.37, $p<0.05$) and WC (same graph as VFA) (Figure 3.28a). There was no significant difference between obese and non-obese by BMI (data not shown). A significant inverse relationship between VEGF RQ values and WC measurements was observed ($r= -0.70$, $p<0.05$) (Figure 3.28b). A similar trend was observed with both VFA and BMI, however they were not significant ($r= -0.52$, $p=0.08$ and $r= - 0.56$, $p=0.06$, data not shown).

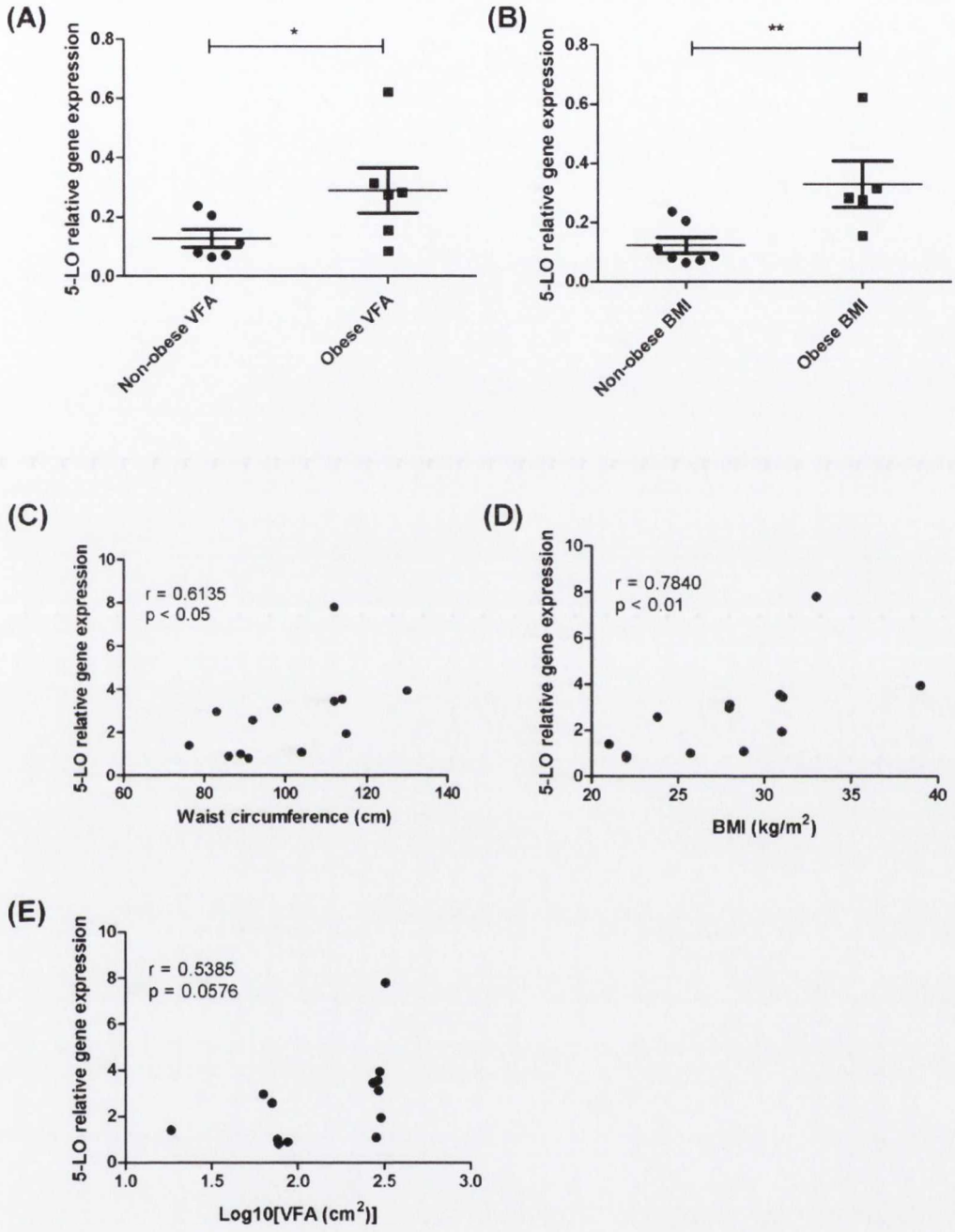

Figure 3.26 Omental adipose tissue 5-LO expression is associated with obesity status by multiple parameters in OAC patients. Omental adipose tissue samples (n=12) were divided into obese and non-obese based on VFA, WC or BMI measurements. Average 5-LO RQ values were compared between the two groups. (A) 5-LO expression was significantly associated with obese VFA (same graph is generated using WC measurements). (B) 5-LO expression was also associated with an obese BMI. (C) Increasing levels of 5-LO expression were associated with increasing WC and (D) BMI and (E) a trend towards a positive correlation was observed for log10[VFA]. Statistical test used was Mann Whitney U test for comparison of obese and non obese adipose tissue and Spearman's test was used for correlations with anthropomorphic measurements. $p<0.05$(*) and $p<0.01$(**).Error bar denotes mean ± S.E.M.

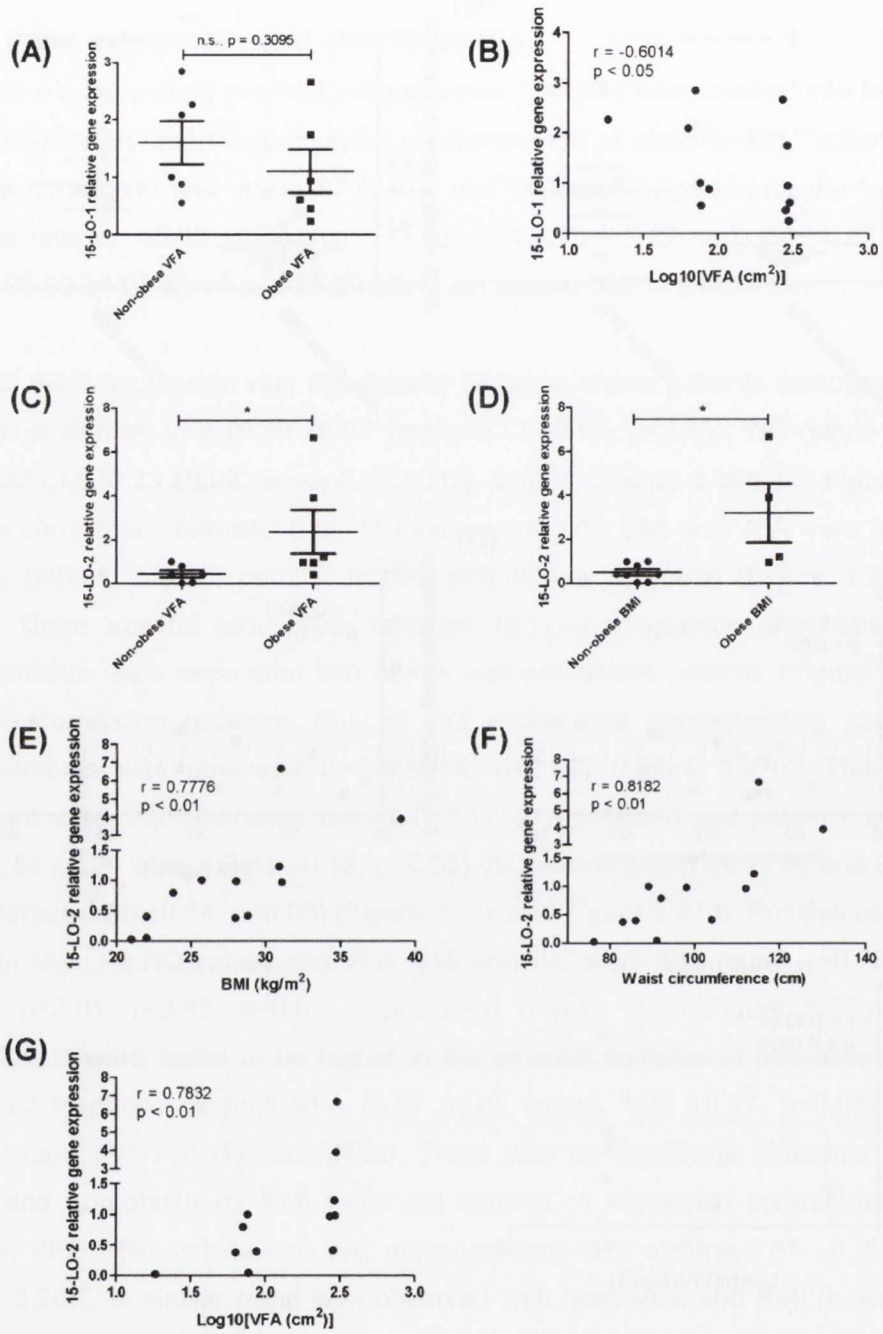

Figure 3.27 Differential expression of 15-LO isoforms in obese omental adipose tissue from OAC patients. (A) 15-LO-1 expression was not preferentially expressed in obese omental tissue. (B) 15-LO-1 was inversely correlated with increasing VFA (graphed as log10[VFA]) ($p<0.05$). (C) Obese omental 15-LO-2 was significantly higher compared to non-obese omentum by VFA (same graph is generated using WC measurements) ($p<0.05$) and (D) BMI ($p<0.05$). (E-G) Positive correlations between 15-LO-2 RQ values and VFA, BMI and WC (all $p<0.01$) were found. Statistical test used was Mann Whitney U for comparison of obese and non obese adipose tissue and Spearman's test was used for correlations with anthropomorphic measurements: $p<0.05$(*). Error bar denotes mean ± S.E.M.

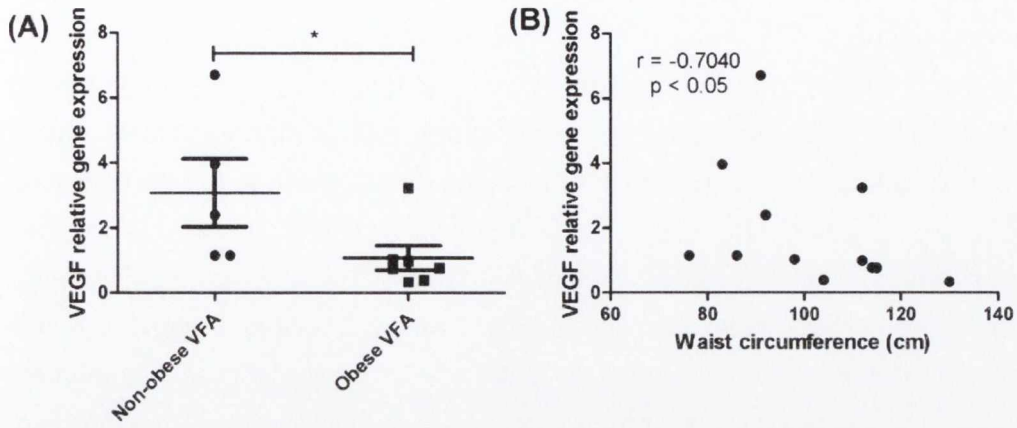

Figure 3.28 Omental VEGF expression is higher in non-obese OAC patients compared to obese patients. (A) VEGF expression was significantly higher in omental adipose tissue from non-obese patients compared to obese ($p<0.05$) (the same graph was generated with WC measurements). (B) VEGF expression was inversely correlated with WC ($p<0.05$). Statistical test used was Mann Whitney U test for comparison of non obese and obese adipose tissue and Spearman's test was used for correlations with anthropomorphic measurements: $p<0.05$(*). Error bar denotes mean ± S.E.M.

3.4 Discussion

The elucidation of biomarkers or potential molecular targets of oesophageal cancer is critical to our evolving knowledge of this malignancy. Given its association with cancer development and progression evidenced in the literature (Ghosh and Myers, 1998, Tong *et al.*, 2002, Ye *et al.*, 2004), the 5-LO pathway is an interesting route of investigation for OAC. Additionally, its emerging role in obesity (Spite *et al.*, 2011, Neels, 2013) and the well-established link between obesity and OAC (Pandolfino *et al.*, 2006, Ryan *et al.*, 2011) make it an interesting target for investigation in OAC.

Investigation of 5-LO in oesophageal cancer biopsies revealed a trend for higher expression in macroscopically normal adjacent tissue. This is in contrast to data from other studies using matched benign and cancer tissue reporting the opposite trend (Gupta *et al.*, 2001, Jiang *et al.*, 2006a). To investigate this finding further we investigated the levels of cytokeratin-8, a cytokeratin known to be expressed in columnar epithelium or glands but not normal squamous epithelium. Cytokeratin-8 expression was significantly higher in the tumour samples as expected due to the replacement of normal squamous epithelium with glandular-like carcinoma. However the majority of normal adjacent tissue samples also showed moderate cytokeratin-8. Cytokeratin-8 is reportedly not expressed in normal squamous epithelium but is known to be expressed in OAC, normal gastric cardia and also regions of BO (van Baal *et al.*,

2008). A number of the patients had confirmed BO which may partially explain the higher cytokeratin-8 mRNA levels in the normal adjacent samples, however it seems likely that the majority of apparently normal adjacent samples may contain abnormal or pre-malignant cells. This highlights the likelihood that macroscopically normal tissue adjacent to a tumour is not truly normal at all as has been discussed in the literature (Braakhuis *et al.*, 2004). Normalising 5-LO and its associated protein, FLAP gene expression levels for differences in columnar epithelial content revealed significantly higher expression in the normal adjacent samples. Stromal 5-LO expression as a result of high immune infiltration and inflammation in normal tissue adjacent tissue compared to the tumour may be responsible for the difference in expression between the matched tissue samples following columnar epithelial normalisation. This would need to be confirmed in an immunohistochemical study, investigating the levels of 5-LO in the stromal compartment of tumour samples compared to matched proximal normal adjacent tissue. 5-LO is known to be highly expressed in pancreatic cancer (Hennig *et al.*, 2002). Interestingly, 5-LO is also found to be expressed in the majority of pancreatic tissue taken from the resection margins of the tumour in contrast to truly normal pancreatic tissue from multi-organ donors which tend to be negative for 5-LO. As hypothesised for pancreatic cancer, 5-LO may play a role in the development of OAC.

Although not directly linked to this study, it was inadvertently observed that increased levels of tumour cytokeratin-8 in OAC patients showed a definite trend towards poorer 5-year survival ($p=0.0710$). Results from other studies have reported cytokeratin-8 and cytokeratin-18 as poor prognosis marker in oral squamous cell carcinoma and OSCC (Fillies *et al.*, 2006, Makino *et al.*, 2009). This is the first study to investigate cytokeratin 8 levels as a prognostic marker in OAC and this finding, while not significant, warrants further analysis with a large gene study or preferentially a TMA study.

As detailed in Section 3.1, 5-LO expression has been investigated in oesophageal cancer in a number of published studies (Chen *et al.*, 2004, Hoque *et al.*, 2005, Boger *et al.*, 2012). Two of the studies report 5-LO epithelial staining in the majority of tumour samples. However similarly to the third study by Boger *et al.* we only observed 5-LO stromal staining in the majority of cases with less than 10% of the patients showing appreciable 5-LO staining in tumour epithelium. The reason for this diversity amongst studies is unknown, however it may suggest a different etiology between the study populations or differences in antibody specificities. In this study 5-LO stromal expression in OSCC was associated with a less aggressive or early-stage tumour

phenotype showing significant correlation with absent lymph node and venous involvement and negative N-stage. Similarly, in the aforementioned Chinese-American TMA study (Hoque *et al.*, 2005), 5-LO positivity was associated with a lack of lymph node metastasis. We also observed that 5-LO stromal expression was associated with the presence of dysplasia which may be indicative of carcinoma *in situ*. It is possible that inflammation in OSCC via the 5-LO pathway is associated with the initiation of cancer as has been indicated for 5-LO activity expressed in precancerous lesions (Cheon *et al.*, 2012). Although not significant there was an improvement in disease-specific median survival time in OSCC patients with higher 5-LO stromal expression (39.9 months versus 11.7 months) providing an alternative explanation for the association of 5-LO stromal expression with a less aggressive tumour phenotype, indicating a potential protective role of 5-LO expression by immune cells in this cancer setting.

This study has shown that the immune component of oesophageal cancer, may have an important role in mediating the pro-inflammatory and pro-tumourigenic effects of 5-LO, in the case of OAC. 5-LO stromal expression in OAC was associated with increased vascularisation (indicated by CD31 staining) in the vicinity of the tumour suggesting 5-LO stromal activity may modulate the formation of blood vessels in this cancer. A similar association has been observed in colorectal adenomas (Barresi *et al.*, 2008). 5-LO stromal staining was significantly associated with OGJ cancer derived from the oesophagus (type I) as opposed to cancer derived from gastric tissue (type II-III). 5-LO stromal staining in OAC was also associated with patients who had BO before developing cancer, suggesting an association with this background of chronic inflammation. An association of 5-LO stromal staining with lower T-stage in CRT-naive patients was also reported and may be indicative of a role in an early tumour phenotype or tumour initiation. A recent murine study focusing on hematopoietic-derived 5-LO, observed that specific deletion of this enzyme from bone marrow decreases polyp formation despite the presence of 5-LO proficient epithelial cells in these mice, indicating for the first time the importance of immune cell contribution to 5-LO activity (Cheon *et al.*, 2011). Although not significant CRT-naive patients with higher stromal 5-LO expression tended to have a poorer disease specific survival indicating its potential as a prognostic marker of disease. Further analysis in a larger patient cohort may be required to validate this observed trend and its potential as an independent prognostic marker.

A major metabolite of the 5-LO pathway, LTB4 was measured by ELISA in OAC and non cancer control serum to investigate whether systemic levels of LTB4 could be used as a biomarker of disease or whether within the cancer cohort of serum LTB4 levels were associated with any clinical parameters. Certain 5-LO inhibitors have been shown to elicit anti-cancer effects against 5-LO overexpressing tumour types and cell culture models (Ghosh and Myers, 1998, Ding *et al.*, 1999), thus targeting this pathway is considered a novel treatment strategy for cancer prevention and therapy. Given that 5-LO metabolites, such as LTB4, are circulating in the blood they may have biomarker potential for selecting patients suitable for a 5-LO inhibitor treatment. *Ex vivo* LTB4 has been shown to be increased in oesophagitis and BO biopsies compared to normal control (Triadafilopoulos *et al.*, 1996). Similarly another 5-LO metabolite, 5(S)HETE, has been shown to be associated with prostate cancer biopsies *ex vivo* compared to matched normal adjacent tissue (Gupta *et al.*, 2001). LTB4 levels in OAC serum have not been investigated until now. We observed no significant difference in the mean level of LTB4 between cancer serum samples and non-cancer controls. However, it was noted that 35% (21/60) of the cancer serum samples had LTB4 concentrations that were above the average of the non-cancer control group. A limitation of this study was the small size of the non-cancer control group to accommodate the experimental design. There were no significant associations between serum LTB4 levels and clinical parameters. Investigation of LTB4 levels locally in tumour explants as opposed to systemically, may indicate differences between normal oesophagus and cancer in this setting and provide some insight into the role of 5-LO activity in the tumour microenvironment.

5-LO is expressed in a number of leukocytes including neutrophils, monocytes, macrophages, mast cells, basophils, eosinophils and B-cells and under certain stimuli they can synthesise leukotrienes that can induce inflammation by attracting and activating more leukocytes (Brock, 2005). In a recent study, 5-LO positivity of infiltrating immune cells in OAC was shown to correlate with $CD68^+$ macrophages and $EG2^+$ eosinophils (Boger *et al.*, 2012). In this study 5-LO stromal expression was correlated with a panel of thirteen immune markers/ cytokines. OSCC 5-LO stromal expression was found to correlate with $CD107A^+$ the granulocyte marker (i.e. cells such as cytotoxic T-cells, NK cells and basophils) while OAC 5-LO stromal expression correlated with immunosuppressive marker FOXP3 and T-cell marker CD8. memory/activation T-cell marker CD45RO and the proinflammatory cytokines IL-4 and IFN-γ. $CD8^+FOXP3^+$ cells are a relatively new class of immunosuppressive T-cells with strong immunosuppressive properties having been observed in colorectal cancer

(Sobhani and Le Gouvello, 2009, Chaput *et al.*, 2009) however some contrasting studies have also emerged that support a role of $FOXP3^+$ regulatory T-cells in increased survival in colorectal cancer (Salama *et al.*, 2009) and a less aggressive tumour type (i.e. lower t-stage and lower n-stage) (Loddenkemper *et al.*, 2006, Salama *et al.*, 2009). On the other hand IFN-γ producing-$CD8^+CD45RO^+$ memory T-cells known have been shown to play a role in preventing tumour progression and recurrence and to have prognostic significance in gastric cancer (Wakatsuki *et al.*, 2013). Clearly the role of these immune subsets is complex, with both pro-cancer and anti-cancer roles possible. It would be interesting to see if 5-LO signalling is involved in the activity of these immune subsets.

The gene expression study investigated the association of 5-LO and its associated protein FLAP with the major angiogenic factor VEGF. A significantly positive correlation was found, indicating the potential link between 5-LO signalling pathway and angiogenesis in OAC, as previously reported for other cancers (Chatterjee *et al.*, 2013, Ye *et al.*, 2005a). The TMA cohort used in this study were previously stained and graded for VEGF tumour epithelial expression. No correlation between this VEGF epithelial staining and stromal 5-LO staining was observed. A limitation of the TMA study was the lack of VEGF stromal scores available for correlation with the stromal 5-LO scores. In the case of the gene study however, a comparison of total 5-LO and total VEGF expression in the tumour tissue was carried out as opposed to a particular tissue compartment. In the comparison of protein levels of 5-LO and VEGF there may be slight variation in tissue core composition between cuts of the paraffin embedded block in the construction of the multiple TMAs for different stains. And staining depends on the antibody specificity. The validity of the gene study is strengthened by the fact that qPCR analysis was carried out for all genes using RNA isolated from the same gene and the primer probes used had a pre-optimised design. Laser capture microdissection of TMAs would provide a method to investigate stromal-derived 5-LO and VEGF and whether they are associated.

Finally this study investigated the association of 5-LO expression with obesity driven OAC. Data from our research group (Allott *et al.*, unpublished) has shown an upregulation of 5-LO expression following co-culture of OAC cells with obese omental adipose tissue fragments, suggesting that this pathway may be upregulated in obesity-driven OAC. Increased 5-LO tumour biopsy expression was found to be associated with obesity status measured by VFA. Protein levels of 5-LO stromal expression were found to be significantly higher in NLE tumour cores from obese CRT-naive patients

compared to non-obese by BMI. Analysis of all over-weight and obese patients only (i.e. BMI>25) indicated a moderate correlation between 5-LO stromal expression and BMI. Association between 5-LO metabolite LTB4 in serum and obesity status, indicated by VFA, BMI and WC was investigated. Sub-analysis of the patient cohort comparing patients with obese BMI (i.e. ≥30) and normal weight BMI (i.e. <25) revealed a significant association between LTB4 levels and obesity ($p<0.05$). These data indicate that 5-LO may be involved in obesity driven OAC.

As discussed previously 5-LO signalling is emerging as an important target for obesity driven disorders. Much of this work has been carried out in animal models (Horrillo *et al.*, 2010, Sharma-Walia *et al.*, 2014). While it is known the 5-LO is expressed by human adipocytes in culture, it has not been measured in adipose tissue. One previous study has investigated the differential distribution of lipoxygenase enzymes (12-LO, 15-LO-1 and 15-LO-2) (Dobrian *et al.*, 2010) excluding 5-LO in adipose tissue depots in obese bariatric patients. In another study FLAP was shown to be higher in obese subcutaneous fat compared to non-obese fat and was associated with insulin resistance (Kaaman *et al.*, 2006). No study has looked at 5-LO expression in human adipose tissue. Additionally no study has looked at adipose tissue derived lipoxygenase expression in the context of cancer. 5-LO and 15-LO-1 were shown to be preferentially expressed in omental adipose tissue whereas high 15-LO-2 showed a greater association with subcutaneous fat. Investigating lipoxygenase expression in omental fat samples, it was found that 5-LO expression and 15-LO-2 were positively associated obesity status. Positive correlations with increasing obesity measurements by VFA, BMI and WC were found for both 5-LO and 15-LO-2. There was no significant association between 15-LO-1 and obesity status, in fact an inverse correlation with VFA was noted. Admittedly the number of biological samples used in this adipose tissue study was small (n=12) and these results will need to be validated in a larger cohort.

In summary 5-LO is present in adipose tissue and is higher in the most metabolically active fat depot, the omentum. Expression in the omentum is associated with obesity status and increasing 5-LO shows a correlation with increasing weight measurement by VFA, BMI and WC. 5-LO expression was increased in OAC cells following co-culture with omentum fat pieces. Subsequently 5-LO tumour biopsy gene expression and TMA expression was shown to be associated with VFA and BMI respectively, in addition to a positive association between serum levels of 5-LO metabolite LTB4 and BMI. Given that 5-LO expression is present in adipose tissue and tumour tissue (mostly stromal

expression) of OAC patients this pathway may provide a link between obesity, inflammation and cancer.

Chapter 4 Investigation of the expression of platelet-type 12-lipoxygenase in oesophageal cancer

4.1 Introduction

The role of lipoxygenases in the development and progression of cancer is complicated due to the variety of lipoxygenase isoforms that have been identified in humans. The observation of different expression and activity profiles of these enzymes between cancer types also adds another layer of complexity to the story. The majority of studies have indicated a pro-tumourigenic role of 12-LO in a number of cancers including melanoma, breast and prostate cancer (Winer *et al.*, 2002, Mohammad *et al.*, 2006, Wen *et al.*, Gondek *et al.*, 2014). It was previously shown that exogenous 12(S)HETE can lead to enhanced invasive capacity and metastatic potential of prostate cancer cells (Liu *et al.*, 1994). This finding led to the exploration of whether 12-LO enzyme expression had utility as a clinical marker of aggressiveness. *In situ* hybridisation of 20 prostate cancer tissue samples revealed focal activity of 12-LO transcript in the basal cells of normal prostate gland, with weak to absent presence in the secretory cells. 12-LO mRNA reactivity tended to be heterogeneous within a given patient sample, showing a spectrum of activity from negative to intensely positive (Gao *et al.*, 1995). In a larger cohort of 122 patients mRNA expression levels of 12-LO were measured by RT-PCR and correlations were analysed with TNM staging, tumour differentiation (Gleason score), age, race, lymph node metastasis and pre-surgical levels of the diagnostic marker prostate specific antigen (PSA) (Gao *et al.*, 1995). Over a third of samples (46/122, 38%) samples were found to have at least 25% more mRNA 12-LO expression than normal adjacent tissue. Among T3 patients 54% had elevated 12-LO whereas 13% of T2 cancers confined to the prostate had elevated 12-LO. 12-LO was elevated in 66% of poorly differentiated tumours (Gleason score >8) versus 21% in well-differentiated tumours (Gleason score <6). In addition, pre-surgical PSA levels were also found to correlate with 12-LO mRNA levels. Therefore this study indicated that 12-LO may predict aggressiveness of disease in this subset of patients (Gao *et al.*, 1995). Further studies examining 12-LO protein expression or metabolite levels as a diagnostic marker of disease have had mixed results to date. Ideally, the concentration of a tumour biomarker in blood, plasma, serum or urine of patients should vary considerably from the normal population, thus providing a quick and easy diagnostic tool. A study involving 88 men, 54 of which had diagnosed prostate cancer, investigated the prognostic potential of 12-LO failed to report any difference in the concentration of plasma 12-LO between prostate cancer patients and healthy men (Piotrowska *et al.*, 2013). This result was surprising considering previous studies had indicated elevated levels of 12-LO expression and activity in prostate cancer (Tan *et al.*, 2007). Another study involving a larger cohort of 149 men including 118 prostate

cancer patients found a similar conclusion, with 12-LO concentrations in platelet-rich serum significantly higher in benign prostate hyperplasia samples as opposed to prostate cancer (Gondek *et al.*, 2014). A recent study investigated AA and HETE serum levels by a liquid chromatography technique in a cohort of 222 patients ranging from low PSA levels and no prostate cancer to invasive prostate carcinoma (Rodriguez-Blanco *et al.*, 2014). Looking at AA and five different HETE levels (i.e. 5-HETE, 8-HETE, 11-HETE, 12-HETE and 15-HETE) they observed a trend for increased HETE levels and decreased AA levels in advanced prostate cancer serum samples (30% of advanced prostate cancer patients had increased HETE levels compared to control). 5-HETE, 8- HETE, 11-HETE, and 15-HETE were high in a selected group of patients having an advanced stage of prostate cancer, however contrary to the study by Gao *et al.*, no difference in serum levels of 12-LO metabolite 12-HETE was observed between cancer and control groups (Rodriguez-Blanco *et al.*, 2014). The authors suggested that differentiation of 12-HETE levels between normal and tumour samples in this study may be confounded by the fact that the technique used could not differentiate between the platelet-type 12(S)HETE and the non-platelet type stereoisomer metabolite 12(R)HETE. In contrast to the blood sample related studies, urinary levels of 12-HETE were significantly elevated in cancer patients (n=10) and benign prostatic hypertrophy patients (n=10) compared to normal controls (n=10). There was no detectable difference in 12(S)HETE levels between cancer and benign samples indicating an involvement in pre-cancerous disease as well as invasive carcinoma. Although the study was based on a small number of samples and 12(S)HETE was not shown to correlate with clinical parameters of disease such as stage and grade, it does provide preliminary evidence in corroboration with other preclinical and gene expression studies for the potential of 12-LO activity as a diagnostic marker of prostate cancer (Nithipatikom *et al.*, 2006). Interestingly, tests of pre- and post-surgery prostate cancer serum levels demonstrated that removal of the prostate gland resulted in a normalisation of the urinary concentration of 12-HETE to levels similar to that of the non-cancer controls (Nithipatikom *et al.*, 2006). Clearly 12-LO is involved in prostate cancer and these conflicting studies show its use as a biomarker of disease is in need of further clarification.

12-LO is expressed in melanoma cell lines (Timar *et al.*, 1999) and its expression has been shown to be higher in dysplastic and cancerous melanocytes compared to normal human skin melanocytes (Winer *et al.*, 2002) and to be increased in spontaneously metastasising skin xenografts (Raso *et al.*, 2004) indicating 12-LO as a potential biomarker of progression in melanoma cancer. Overexpression of 12-LO in breast

cancer cells has also been shown to lead to reduced apoptosis and enhanced tumour-forming capabilities in xenografts (Natarajan *et al.*, 1997, Connolly and Rose, 1998). This has led others to investigate the role of the 12-LO pathway in breast cancer progression and as a biomarker of disease. A study involving 64 breast cancer biopsies and matched normal adjacent tissue revealed elevated mRNA levels in 62.5% of the carcinoma samples compared to normal tissue and additionally 12-LO levels were found to correlate with TNM staging (Mohammad *et al.*, 2006). In a case-controlled study of 86 diagnosed breast cancer serums and 40 healthy serums, 12-LO levels detected by both surface plasma resonance and standard ELISA were 3-fold higher in the cancer patients (Singh *et al.*, 2011). Cancer serum 12-LO expression was also found to correlate with lymph node metastasis indicating for the first time an association between breast cancer serum 12-LO level and disease progression (Singh *et al.*, 2011).

In contrast to the previous findings there are a number of isolated studies indicating an anti-cancer role of 12-LO (Nigam *et al.*, 1999, Gohara *et al.*, 2012). For example, recent methylation studies have revealed that suppression of *ALOX12* in leukocyte DNA was negatively associated with prognosis in AML patients (Ohgami *et al.*, 2012). 12-LO has also been suggested to have an anti-tumourigenic role in cervical cancer (Nigam *et al.*, 1999). Additionally while 12-LO mRNA is present in normal nasal epithelium it is lost in pre-cancerous nasal polyps (Ergin *et al.*, 2012). In another study the lipoxygenase metabolite profile of colorectal tumourigenesis across normal, polyp and cancer biopsies was investigated to delineate the relevance of this family of enzymes (Shureiqi *et al.*, 2010). While 15-LO-1 metabolite 13(S)HODE was significantly downregulated and indicated to be anti-tumourigenic, there was no difference in 12-LO activity or that of other LO enzyme metabolites, questioning the role of these LO isoenzymes in colorectal cancer (Shureiqi *et al.*, 2010). Another pathology study evaluated the presence of the three major lipoxygenase enzymes (5-LO, 12-LO and 15-LO-1) in the kidney tissue of both RCC patients and healthy people (13 normal kidney, 17 normal tissue adjacent to cancer , 31 renal clear cell carcinoma, and 23 renal papillary carcinoma, (Gohara *et al.*, 2012). Using intensity scores, 12-LO was found to consistently dominate over 5-LO and 15-LO-1 levels in both tumour and normal tissue. 5-LO and 12-LO were found to be higher in normal tissue than at the onset of disease (i.e. low stage and grade samples) and this reversed with the progression of disease (i.e. higher stage samples) (Figure 4.1). It was only samples from a more advanced stage of cancer that approached or exceeded the presence of 5-LO or 12-LO in the normal tissue (Gohara *et al.*, 2012).

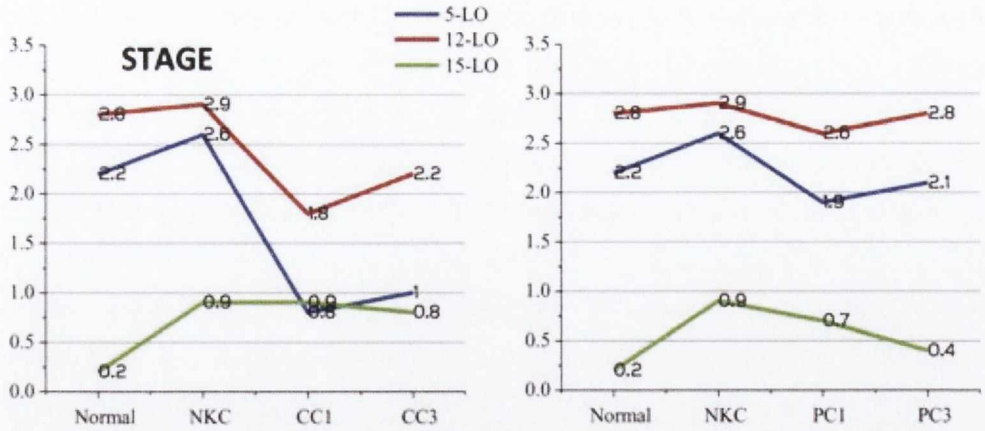

Figure 4.1 Trends in intensity of lipoxygenase enzymes in normal kidney and RCC. 12-LO expression was found to be highest in healthy normal kidney tissue and normal tissue adjacent to cancer (NKC) compared to both renal cell clear carcinoma and papillary carcinoma types (CC and PC). Only advanced stage tumour samples (CC3 and PC3) showed staining intensity which approached or exceeded that of the normal tissue. Similar trends were observed for 5-LO, while 15-LO-1 intensity peaked in NKC samples and decreased during progression to cancer. Reproduced from (Gohara *et al.*, 2012).

Reviewing the literature available it is obvious that the level of 12-LO in cancer is likely conditional on the organ or tissue type and may fluctuate based on tumour characteristics and the stage of disease. Currently there is a lack of wide clinical data on levels of lipoxygenase isoforms in the process of tumourigenesis. Of specific interest to this project, the role of platelet-type 12-LO in oesophageal cancer is a relatively under-researched area. Other than a genotyping study which has indicated for the first time polymorphisms in the 12-LO gene that are linked to OSCC risk (Guo *et al.*, 2007), there are currently no other studies in the literature investigating the link between 12-LO and oesophageal cancer, making it an interesting and novel line of investigation.

As discussed in the general introduction angiogenesis is currently under investigation as a therapeutic target in the treatment of oesophageal cancer (see Table 1.2 list of anti-angiogenic therapies in clinical trials). To date, the relationship between AA metabolism and tumour-associated angiogenesis and cancer progression has been addressed from a number of aspects. For example COX-2 and its associated prostaglandins have been shown to have anti-apoptotic and pro-angiogenic roles in cancer (Daniel *et al.*, 1999, Liu *et al.*, 2000, Sheng *et al.*, 1998, Klenke *et al.*, 2006). 12-LO has been shown to be involved in tumour angiogenesis in models of prostate cancer (Nie *et al.* 2003) and has also been shown to directly stimulate VEGF activity (McCabe *et al.*, 2006, Nie *et al.*, 2006) and other angiogenic proteins such as MMPs

(Dilly *et al.*, 2013). Similarly, 12-LO overexpression in breast cancer cells was found to enhance tumour growth and angiogenicity in mouse xenografts compared to control (Connolly and Rose, 1998) indicating a role of 12-LO in angiogenesis. In the case of oesophageal cancer there is mounting evidence of a link between COX-2 and VEGF signalling and angiogenesis (von Rahden *et al.*, 2005) while in contrast there are currently no studies investigating a link between 12-LO and angiogenesis in this malignancy. Furthermore, evidence in other cancer types that support a link between 12-LO and VEGF has only been explored *in vitro* or in murine models with no published clinical finding in support of this relationship. Bearing this in mind, we therefore wanted to explore the expression of 12-LO in oesophageal cancer patient tissue and whether there was any evidence to suggest a link with VEGF.

4.2 Aims and objectives

The aim of this chapter was to study the clinical relevance of the 12-LO signalling pathway in oesophageal cancer, with a greater emphasis on OAC specifically, using a number of different biological sample types including biopsy RNA, tumour TMAs and serum. Bearing in mind the current lack of clinical evidence in the literature establishing the link between 12-LO and angiogenesis, this potential association was investigated in the context of oesophageal cancer.

Specific Objectives:

- Investigate the gene and protein expression of 12-LO in resected oesophageal tumour tissue and determine whether 12-LO expression is associated with clinical parameters including stage, grade and disease specific survival

- Investigate the association of 12-LO and angiogenesis through correlation studies with angiogenic markers

- Investigate the association of angiogenic markers VEGF and KDR with clinical parameters in oesophageal cancer

- Investigate the correlation between 12-LO stromal expression and immune cell markers

4.3 Results

4.3.1 Assessment of 12-LO and 15-LO-1 gene expression in OAC tumour and normal adjacent biopsies, and correlation with VEGF

12-LO has been found to be overexpressed in tumour tissue of some cancers compared to normal tissue (Gao *et al.*, 1995, Natarajan *et al.*, 1997) consequently 12-LO mRNA expression was assessed in OAC. 15-LO-1 was also measured in the samples. Tumour (n=34) and macroscopically normal adjacent (n=28) biopsies were collected from the main specimen following surgical resection from OAC patients as described in Section 2.6. The patient demographic was the same as that used in the 5-LO gene study in Section 3.3.1 (Table 3.1). RNA was isolated as described in Section 2.7 and 12-LO and 15-LO-1 gene expression was measured in both tumour and normal adjacent samples by qPCR as described in Section 2.16.1. The RQ value for one patient sample was set as the calibrator to allow normalisation of the data set. Samples with Ct values of less than 30 were considered high expressors, while samples with Ct values between 35 and 40 were deemed to have negligible expression.

15-LO-1 expression was found to be negligibly expressed in both OAC tumour and normal adjacent tissue with the majority of samples having undetermined Ct values (i.e. Ct>40). Appreciable 12-LO expression was found in 22/28 normal adjacent samples with Cts ranging from 26 to 34 (average Ct=30.3), 4/28 samples had Ct values between 35 and 40 and the remaining 2 samples had undetermined Ct values. In contrast, the majority of the tumour biopsies did not have detectable levels of 12-LO. 13/34 samples had Ct values between 35 and 40, 20/34 samples had undetermined Ct values and only one sample showed moderate Ct values of 29.8. 12-LO was found to be significantly higher in normal adjacent tissue compared to tumour in pair-matched samples (65.35 ±14.09 versus 5.78 ±4.98, n=26 per group, $p<0.001$) (Figure 4.2). Analysis including extra non-matched samples showed the same association (75.44 ±15.32 versus 4.42 ±3.90, n=28 vs. n=34, $p<0.0001$) (data not shown). The quality of the RNA was confirmed as explained in Section 2.10 and the average *18S* Ct value for all biopsies (n=62) was 11.89 ±0.18, indicating a consistent cDNA synthesis procedure across all samples. This same cohort of patient biopsies were analysed for VEGF expression. Correlation between 12-LO and VEGF in tumour biopsies was not possible due to lack of 12-LO detection in the tumour biopsies however analysis of normal adjacent tissue VEGF expression (n=16) with the corresponding 12-LO levels revealed a positive correlation ($r=0.6463$, $p<0.01$) (Figure 4.3).

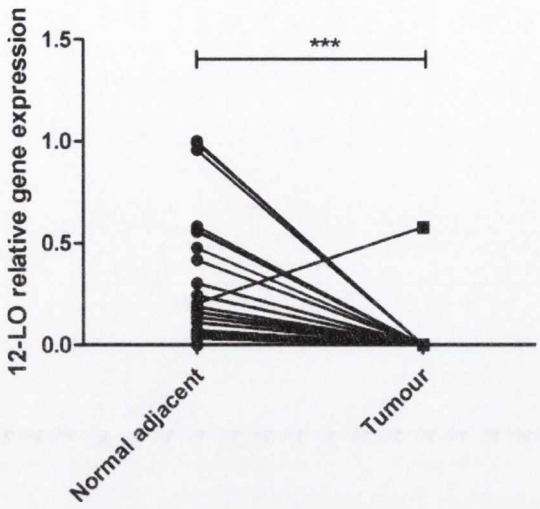

Figure 4.2 Platelet-type 12-LO is significantly higher in normal adjacent tissue compared to OAC tumour biopsies. Normal adjacent tissue had higher 12-LO expression whereas the majority of matched tumour tissue samples were 12-LO negative (n=26 per group, $p<0.001$). Statistical test used was Wilcoxon signed rank test for paired analysis: $p<0.001$(***). Error bar denotes mean ± S.E.M.

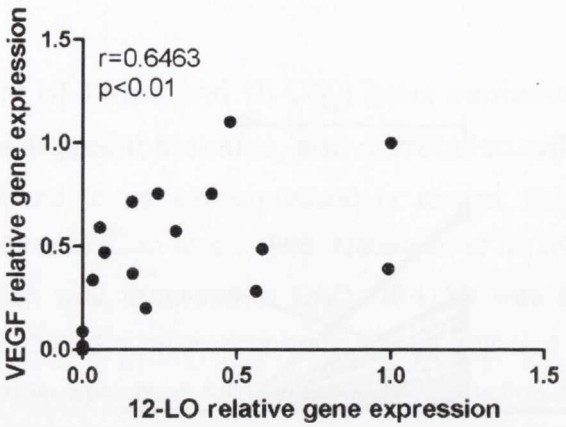

Figure 4.3 Normal adjacent OAC tissue 12-LO expression is correlated with corresponding VEGF levels. 12-LO and VEGF gene expression in normal tissue adjacent to OAC tumour site was measured and there was a significant correlation between both genes ($n=16$, $p<0.01$). Statistical test use was Spearman correlation test.

4.3.2 Assessment of 12-LO protein expression in OAC tumour biopsies and matched normal adjacent tissue

To further investigate the results of the gene analysis study, the level of 12-LO protein expression was measured in a number of tumour and matching macroscopically normal adjacent oesophageal tissue samples. Protein was isolated from 8 tumour biopsies as discussed in Section 2.17.2 and total protein concentration was measured by the BCA assay (Section 2.18). There was enough biobanked tumour and matched normal tissue available to include a maximum of 4 patients from the original gene study (labelled 2-5 in Figure 4.4 and Table 4.1). The other 4 patients were OAC samples with matched normal adjacent tissue that had not been used in the gene study. 40 µg of protein was loaded per sample and platelet lysate was used as a positive control for 12-LO. The western blot procedure was performed as described in Section 2.19. Single bands of 12-LO at the expected molecular weight of 78 kDa were observed. β-actin was used to normalise for total protein content and was observed at a molecular weight of approximately 42 kDa. An image of the western blot containing the first 5 matched samples is shown in Figure 4.4a. Following protein band densitometry, normalisation of the data to β-actin, and fold change relative to a chosen sample it was found that 12-LO expression in normal adjacent tissue was higher than matched tumour tissue (0.58 ±0.17 versus 0.07 ±0.05, $n=8$ for both $p<0.01$) (Figure 4.4b). As indicated in Table 4.1 12-LO expression levels in the normal adjacent and tumour samples from the four overlapping patients showed consistency across both gene and protein expression analysis.

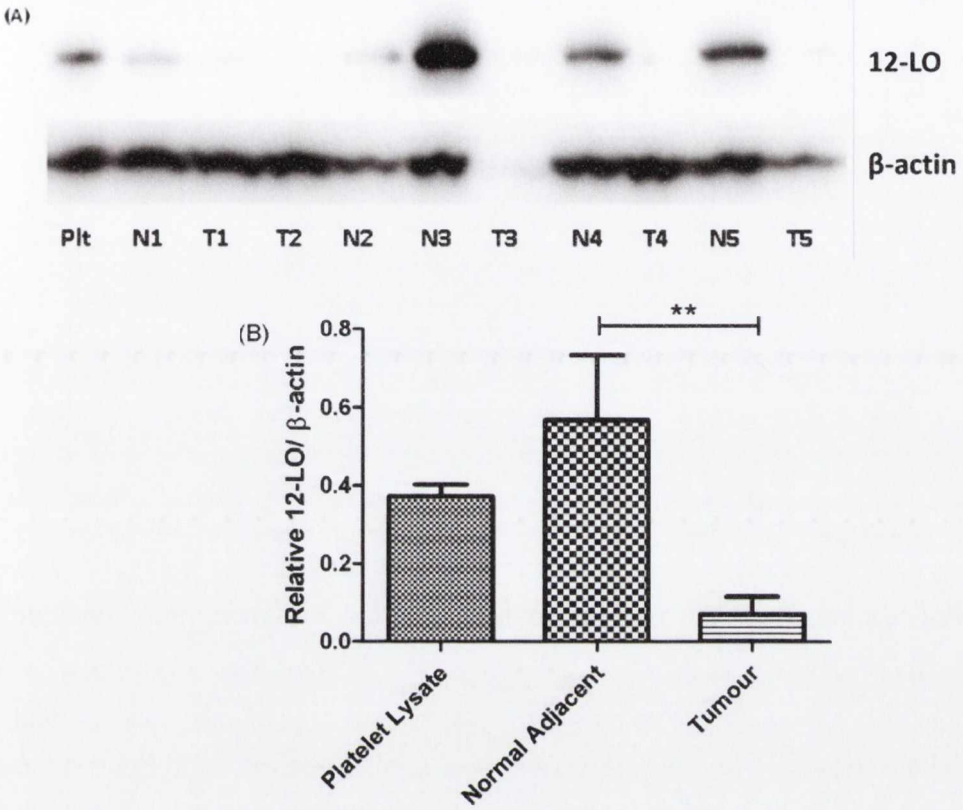

Figure 4.4 12-LO protein levels are higher in macroscopically normal adjacent tissue compared to matched OAC tumour. (A) OAC normal adjacent (N) and tumour protein (T) (n=8) were extracted and analysed by western blot for 12-LO expression. 40 µg of protein was loaded per sample and a sample of platelet lysate (Plt) was used as a positive control. (B) Relative 12-LO protein expression following normalisation with β-actin was found to be significantly higher in normal adjacent tissue compared to matched OAC tumour (0.57 versus 0.07, $p<0.01$). Protein loading for sample T3 was inaccurate compared to other samples, (see faint β-actin band) however normalisation of 12-LO to β-actin was still possible. Statistical test used was Wilcoxon signed rank test for paired analysis, $p<0.01$(**). Error bar denotes mean ± S.E.M.

Table 4.1 Differential expression of 12-LO between normal adjacent and OAC tissue samples is shown to be consistent at both the gene and protein level

Sample I.D.	Average Ct	Δ Ct ($Ct_{12\text{-}LO}$ - Ct_{18s})	RQ value (gene)	Relative 12-LO/β-actin (protein)
2 N	30.07	20.22	1	1
2T	Undetermined	28.51	0	0
3N	31.07	18.76	2.74	6.23
3T	39.76	25.28	0	1.69
4N	28.97	19.46	1.70	2.04
4T	Undetermined	27.56	0	0.15
5N	32.14	19.68	1.46	2.90
5T	36.29	22.56	0	0.20

4.3.3 12-LO expression in tissue microarray of oesophageal cancer patients

Paraffin-embedded tumour sections from one hundred and ninety-six oesophageal cancer patients were arrayed on a TMA (See Figure 3.9a) as described in Section 2.6 and where available matched tumour LE (Figure 3.9b) was also included (136/196). This patient cohort consisted of approximately four-fifths OAC patients and one-fifth OSCC patients and clinical parameters are as detailed previously in Section 3.3.7 (Table 3.1).

The TMA was stained for 12-LO and immunohistochemical scoring was carried out as described in Section 2.16. Staining of VEGF, KDR, CD31 and a number of immune cell markers (see Appendix V for full list of immune markers and cytokines) were completed prior to this project and used for correlations with 12-LO protein levels. The antibody was tested by western blot using a purified full length platelet-type 12-LO recombinant protein and a single band of protein at the expected weight of approximately 100 kDa (including extra weight for the attached His-tag) was observed (Figure 4.5a). Optimisation of primary antibody was carried out on full-face sections of tumour tissue at a number of different dilutions as described in (Figure 4.5b) prior to staining the TMAs. Representative images of low-moderate-high 12-LO tissue expression used for TMA scoring are indicated in Figure 4.6.

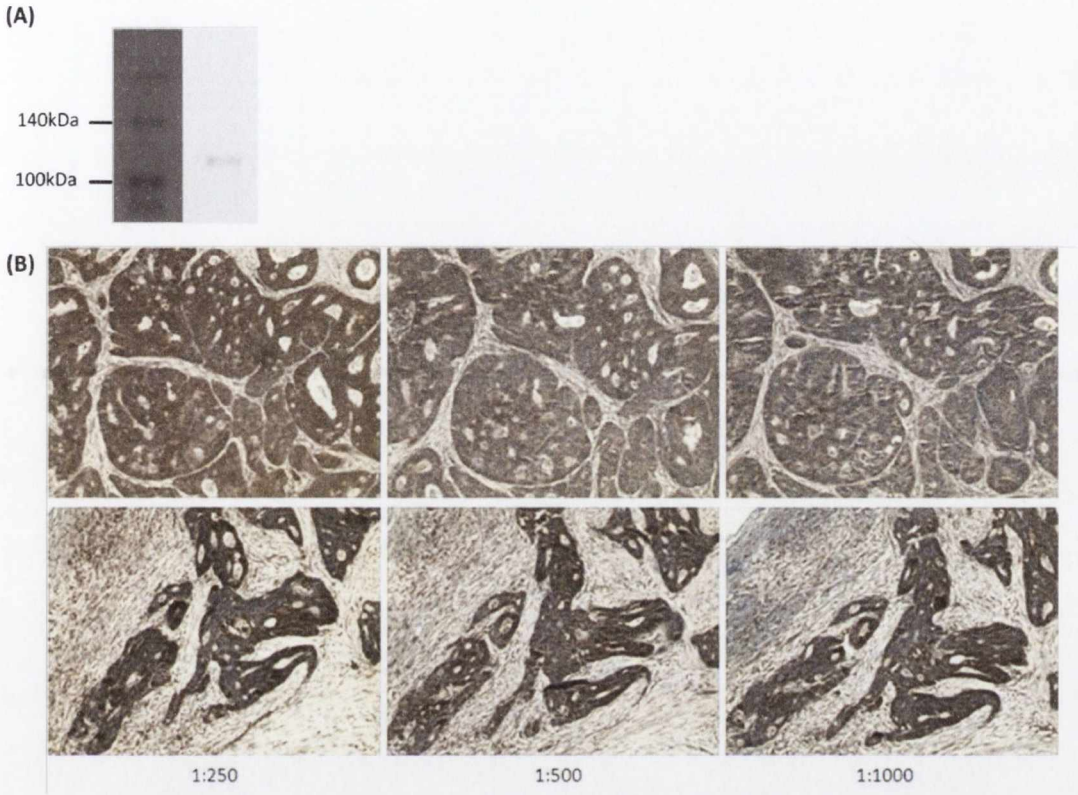

Figure 4.5 Platelet-type 12-LO antibody optimisation. (A) The specificity of the 12-LO antibody was tested with recombinant full length platelet-type 12-LO protein (100 ng) and a single band was observed at approximately 100 kDa. (B) Full face sections of tumour tissue were used for immunohistochemical optimisation of the 12-LO antibody at 3 different dilutions: 1:250, 1:500 and 1:1000. Images are 10X magnification.

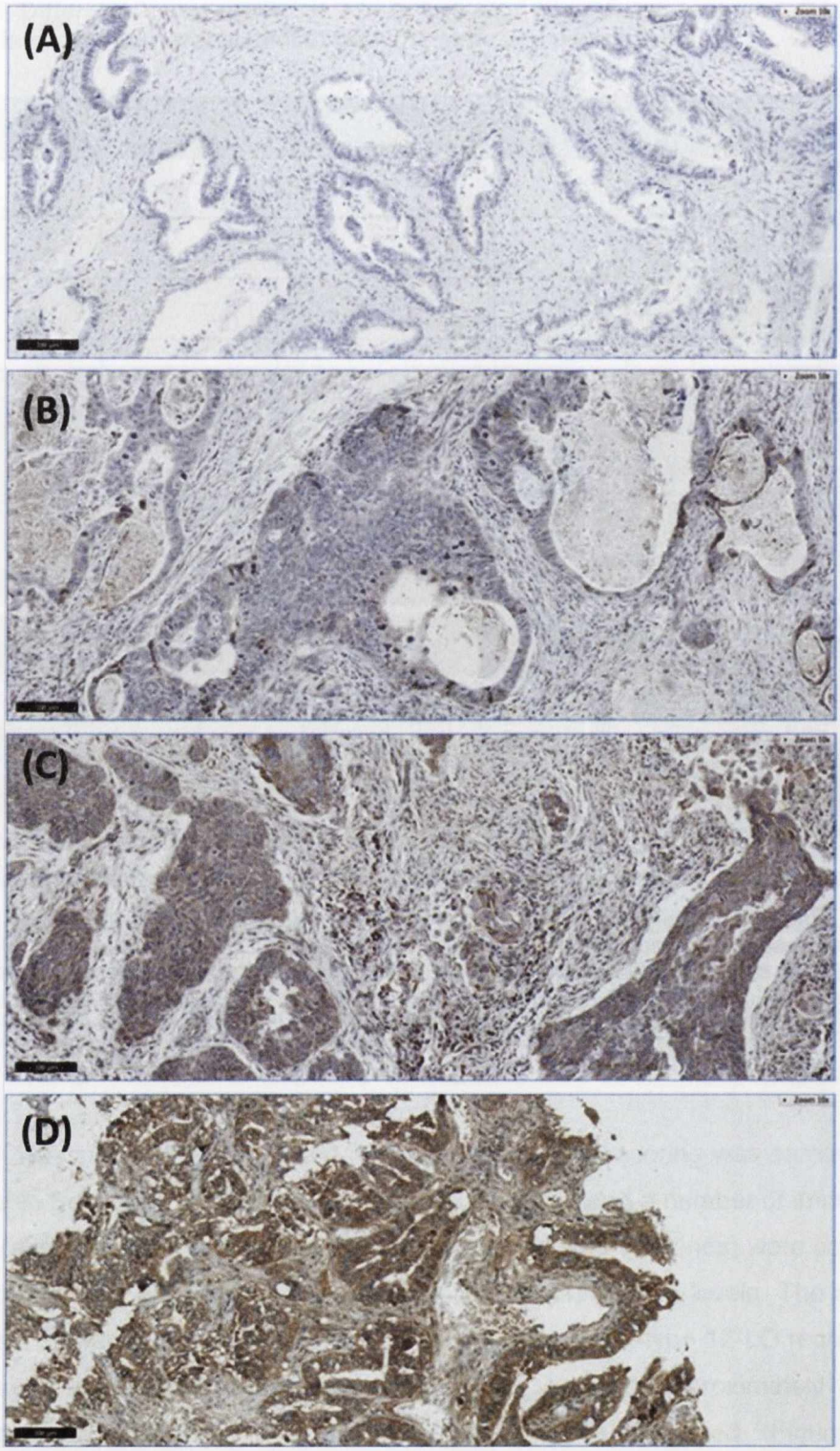

Figure 4.6 Tissue microarray 12-LO staining pattern in oesophageal cancer. Following immunohistochemical staining for 12-LO a grade scoring system was devised on the basis of a combination of intensity and percentage of cell staining within the core. Representative image (A) indicates negative control staining (i.e. no primary antibody), (B) low tumour epithelial and stromal staining, (C) moderate epithelial and moderate-high stromal staining and (D) high epithelial staining. Images are 10X magnification.

4.3.4 Differential 12-LO expression, cancer morphology and tissue type

Following 12-LO staining and grading, an average tumour epithelial and stromal score was assigned to each patient, except in cases where tissue cores had become damaged and impossible to score. There was no association between 12-LO tumour epithelial staining and cancer morphology (i.e. OAC versus OSCC in both LE and NLE samples ($p=0.4397$ and $p=0.2680$ respectively), data not shown). 12-LO stromal expression was significantly higher in OSCC samples compared to OAC, both at the invasive LE (111.12 ±14.77 versus 53.52 ±5.45, $n=25$ and $n=111$, $p<0.001$) and NLE (120.48 ±10.82 versus 69.33 ±5.21, $n=36$ and 147, $p<0.0001$) (Figure 4.7a and Figure 4.7b).

A subset of OAC or OSCC patients with intact matched NLE and LE tissue (OAC: 110/126 cases and OSCC: 24/26 cases) were analysed for 12-LO epithelial and stromal expression. 12-LO expression was found to be more strongly associated with the tumour epithelium compared to stroma in both LE OAC samples (102.47 ±9.04 versus 55.04 ±5.90, $n=107$ each, $p<0.001$) and NLE OAC samples (107.33 ±9.18 versus 71.53 ±6.25, $n=106$ each, $p<0.001$) (Figure 4.8a). There was a trend for stromal 12-LO expression to be higher in the tumour core (NLE) compared to LE in OAC however this was not significant ($p=0.0610$) (Figure 4.8a). No difference in epithelial 12-LO expression was observed between LE and NLE OAC cores. In OSCC 12-LO expression was more strongly associated with tumour stroma compared to epithelium in NLE samples (123.77 ±14.11 versus 78.90 ±17.54, $n=23$ each, $p<0.01$) and a similar non-significant trend was observed in the LE samples (111.12 ±14.77 versus 87.58 ±17.52, $n=25$ each, $p=0.08$) (Figure 4.8b).

12-LO staining was confined to the cytosol of cells in both epithelial cells of the tumour mass and circulating immune cells in the surrounding stroma (Figure 4.9f). In the stroma it was noted that endothelial cells of tumour associated blood vessels also expressed 12-LO as previously published (Nie *et al.*, 2000) and were used as an internal positive control for 12-LO staining (Figure 4.9e). Representative images of the variety of stromal and epithelial staining observed across the TMA cohort are shown in Figure 4.9. Additionally, smooth muscle was positive for 12-LO, as previously published (Preston *et al.*, 2006). Figure 4.9g indicates positive smooth muscle staining and normal squamous epithelial staining of basal cells and negative staining for islands of tumour all in the same TMA core.

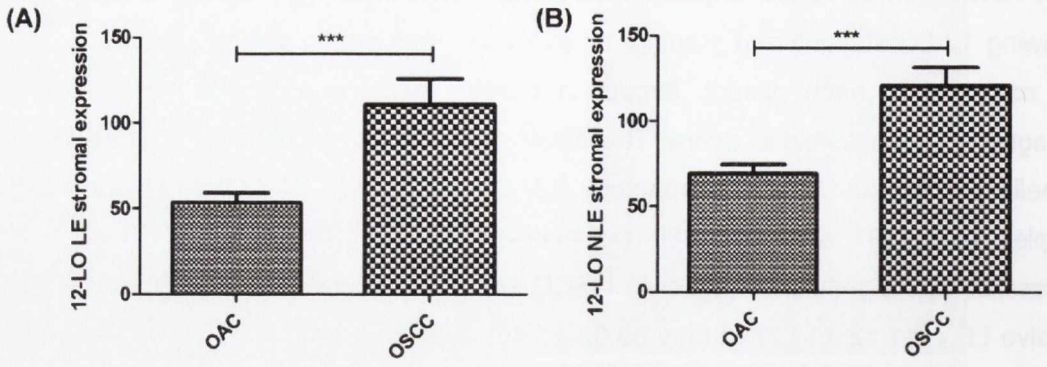

Figure 4.7 Stromal 12-LO expression is higher in OSCC compared to OAC. Following TMA staining for 12-LO patients were grouped on the basis of morphology (OAC versus OSCC) and it was found that in both (A) LE tissue core 12-LO staining in the stromal compartment was significantly higher in OSCC samples compared to OAC ($p<0.001$, n=25 and n=111) and (B) NLE tissue core 12-LO staining in the stromal compartment was significantly higher in OSCC samples compared to OAC ($p<0.0001$, n=36 and 147). Statistical test used was Mann-Whitney U test. $p<0.001$(***).Error bar denotes mean ± S.E.M.

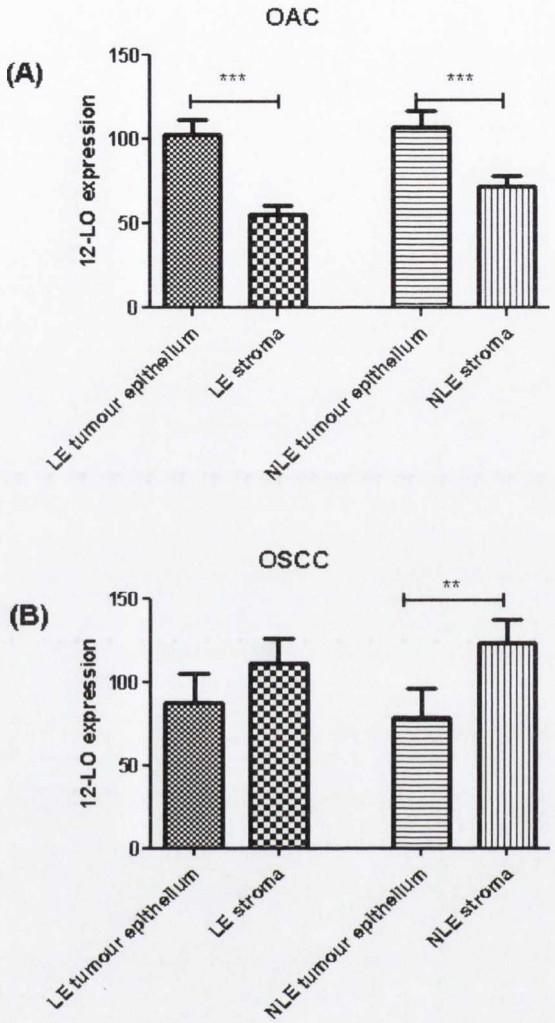

Figure 4.8 12-LO is strongly associated with the tumour epithelium in OAC but it is associated more strongly with the stromal compartment in OSCC. (A) LE tumour epithelial expression was higher than stromal expression in OAC ($p<0.001$, both n=107) and NLE tumour epithelial expression was higher than stromal expression in OAC ($p<0.001$, both n=106). There was also a trend for higher stromal 12-LO expression in NLE OAC compared to matched LE samples ($p=0.0610$). (B) There was a significantly stronger association between 12-LO expression and NLE stroma compared to tumour epithelium in the OSCC cohort ($p<0.01$,both n=23). Statistical test used was Wilcoxon paired t-test: $p<0.001$(***). Error bar denotes mean ± S.E.M.

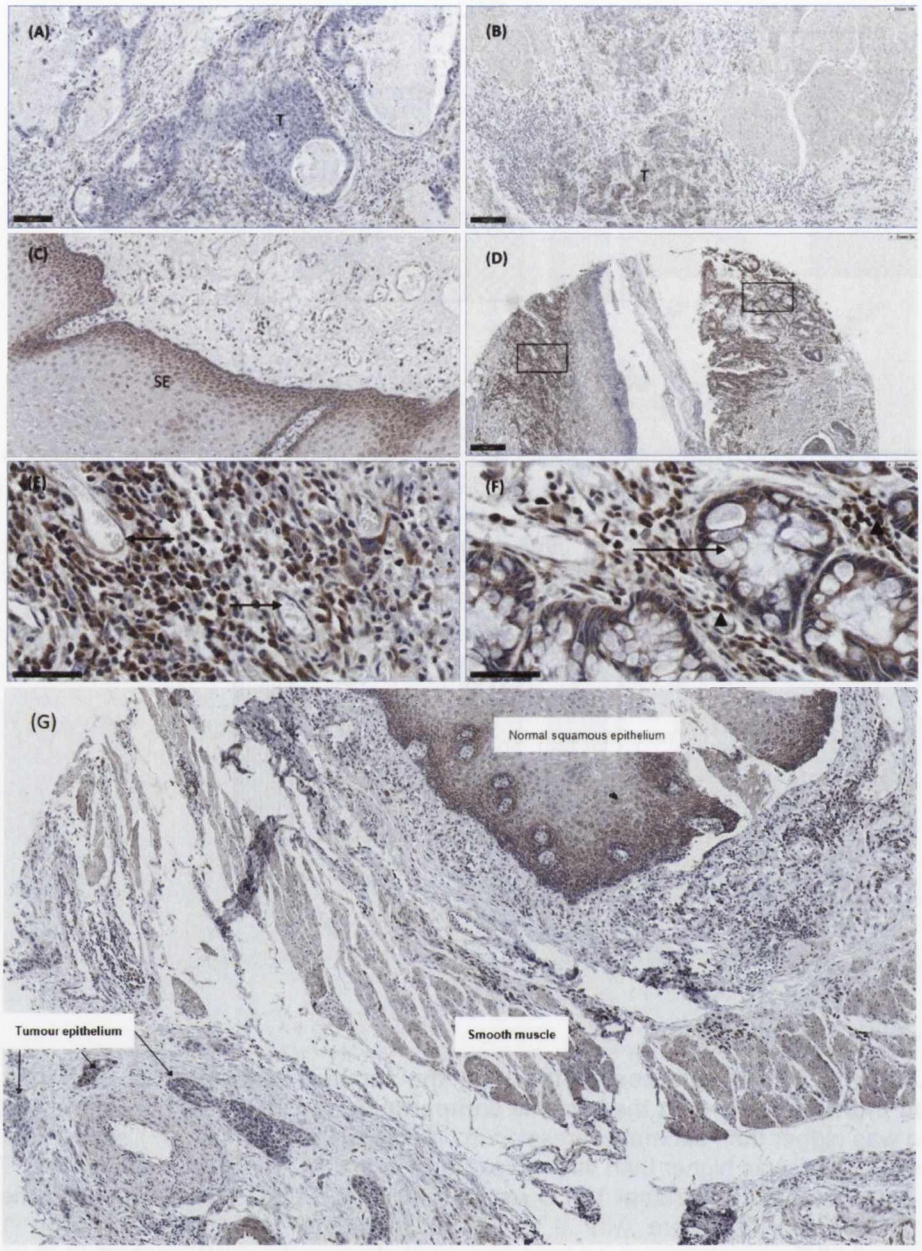

Figure 4.9 A variety of low and high expression of epithelial and stromal 12-LO is observed across the oesophageal cancer tissue microarray. (A) indicates moderate 12-LO stromal staining and no epithelial staining in islands of tumour. (B) indicates weak-moderate 12-LO tumour epithelial and stromal staining. (C) indicates 12-LO basal cell staining of normal stratified squamous epithelium (SE). (D) indicates strong 12-LO staining in both tumour epithelium and stroma. (E) High magnification image of boxed region on the left of image (D) shows 12-LO staining of dense plasma cell infiltrates and endothelial cells (black arrow). (F) High magnification image of boxed region on the right of image (D) shows strong epithelial staining of mucinous carcinoma (black arrow) surrounded by stained infiltrating plasma cells. 12-LO is confined to the cytosol of positively stained cells (arrow head). (G) TMA core showing 12-LO smooth muscle and normal squamous epithelial staining and negative tumour epithelium in the same field. Images (A-C) and (G) are 10X, (D) is 4X and (E-F) are 20X magnification.

4.3.5 OSCC 12-LO expression and patient clinical parameters

OSCC 12-LO expression (LE samples, n=26 and NLE samples, n=36) was assessed for correlations with available clinical parameters including sex, age, tumour and nodal stage, grade, lymph node involvement, venous involvement, perineural involvement and disease specific survival. LE stromal 12-LO was found to associate with shorter tumour length (138.72 ±19.76 versus 85.64 ±19.90, p=0.0556) and absence of venous involvement (133.97 ±17.36 versus 70.77 ±20.01, p<0.05) (Figure 4.10a and Figure 4.10b). There were no associations with NLE 12-LO expression and clinical parameters.

OSCC LE epithelial 12-LO expression showed a significant association with 5-year survival. Patients with above-median 12-LO expression had a poorer prognosis than those with lower 12-LO expression (n=25, p<0.05) (Figure 4.11a). There was no association between LE 12-LO stromal expression and survival (n=25, p=0.6643) (Figure 4.11b). Similarly, there was no association observed between NLE 12-LO and survival (data not shown).

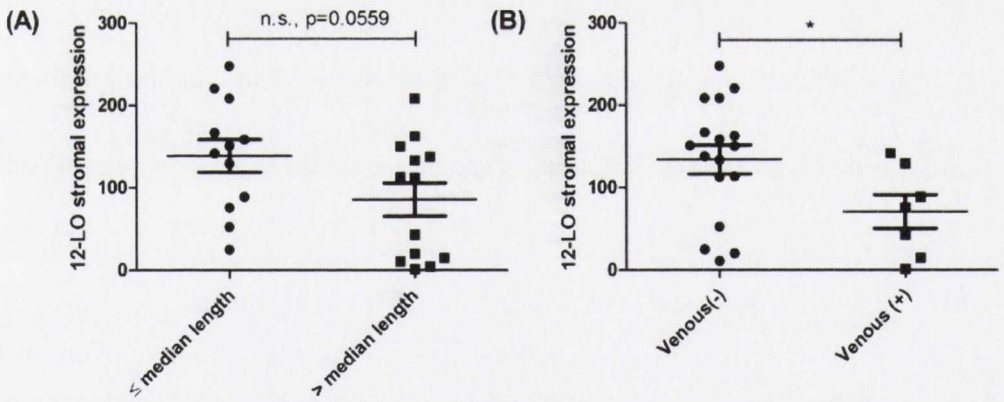

Figure 4.10 OSCC stromal 12-LO at the invasive edge is associated with clinical parameters of a less aggressive tumour phenotype. (A) LE stromal 12-LO trended toward an association with smaller tumour size (p=0.0559). (B) LE stromal 12-LO was associated with patients who have no venous invasion. Statistical test used was Mann-Whitney U test: p<0.05(*). Error bar denotes mean ± S.E.M.

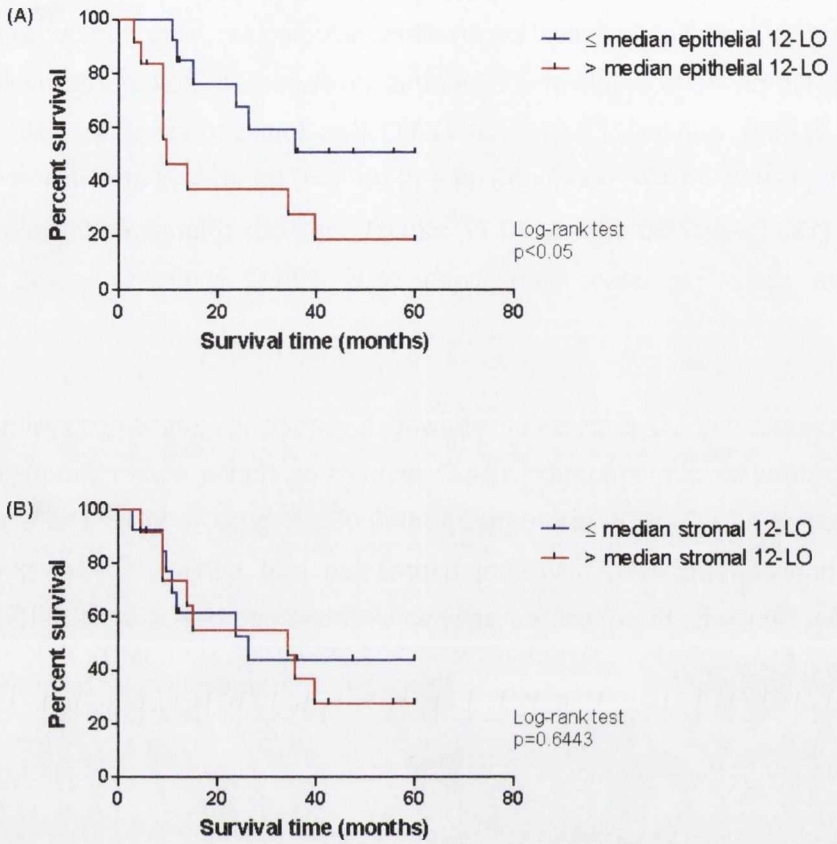

Figure 4.11 Leading edge tumour epithelial 12-LO is associated with a poorer prognosis in OSCC. (A) OSCC patients with above-median LE 12-LO epithelial expression had significantly decreased survival (n=25, $p<0.05$). (B) No association was found with LE stromal 12-LO expression (n=25, p=0.6643). Statistical test used was Kaplan Meier survival curve with Log-rank (Mantel-Cox) test.

4.3.6 OAC 12-LO expression and patient clinical parameters

12-LO LE (n=116) and NLE (n=154) expression in the OAC patient cohort was investigated for potential associations with available clinical parameters including sex, age, tumour and nodal stage, grade, tumour length, lymph node involvement, venous involvement, perineural involvement and disease specific survival.

LE tumour epithelial 12-LO expression was higher in patients with no evident dysplasia (118.10 ±11.62 versus 83.72 ±13.75, n=66 and n=41, $p<0.05$) and a similar trend was observed for LE stromal 12-LO (61.64 ±7.82 versus 43.79 ±8.76, n=66 and n=41, p=0.107) (Figure 4.12a). Significant associations or observed non-significant trends with clinical parameters indicated that higher LE 12-LO expression in the stromal compartment was associated with an earlier or less aggressive tumour phenotype i.e. a

lack of venous invasion (69.51 ±9.01 versus 32.30 ±5.53, n=58 and n=51, $p<0.01$) and a moderate to well differentiated tumour (61.18 ±7.93 versus 41.74 ±8.02, n=68 and n=41, p=0.123) (Figure 4.12b and Figure 4.12c). Analysis of the NLE cores indicated that OAC epithelial 12-LO expression was associated with a less aggressive phenotype showing associations with both shorter tumour length (112.47 ±10.90 versus 86.96 ±10.77, n=71 and n=68, p=0.0631) and a lower pathological T-stage (127.62 ±14.02 versus 89.21 ±8.80, n=47 and n=97, $p<0.05$) (Figure 4.13a and Figure 4.13b). Similar associations with shorter tumour length (78.57 ±7.73 versus 56.32 ±6.72, n=73 and n=69, $p<0.05$) and lower T-stage (85.95 ±10.32 versus 61.52 ±5.80, n=47 and n=100, $p<0.05$) were observed for NLE 12-LO stromal expression levels in OAC (Figure 4.13a and Figure 4.13b).

While not significant, LE 12-LO epithelial expression tended to be associated with an improved prognosis in OAC patients (n=111, $p<0.1220$) (Figure 4.14a). Patients with below-median 12-LO epithelial levels have a shorter median survival time of 39.43 months. Patients with above-median 12-LO levels did not reach the 50% survival point within the 5-year period and therefore the median survival time could not yet be calculated but it is at least 60 months or more. There was no association between LE 12-LO stromal expression and survival (n=111, p=5722) (Figure 4.14b).

Analysis of the entire cohort of NLE samples did not reveal a significant association between 12-LO epithelial or stromal expression and survival (p=0.2952 and p=0.2136, data not shown). Sub-analysis of only CRT naive patients (111/154 patients) showed an increased trend for an association of 12-LO stromal expression with improved survival, similar to that seen with epithelial staining of LE cores, but again it was not significant (p=0.1232) (Figure 4.15). An increased association with clinical parameters, such as lower T-stage, was also noted (see comparison of p-values in Table 4.2). Sub-analysis of CRT-naive patient LE cores did not reveal any stronger associations with clinical parameters and it did not change survival status (data not shown).

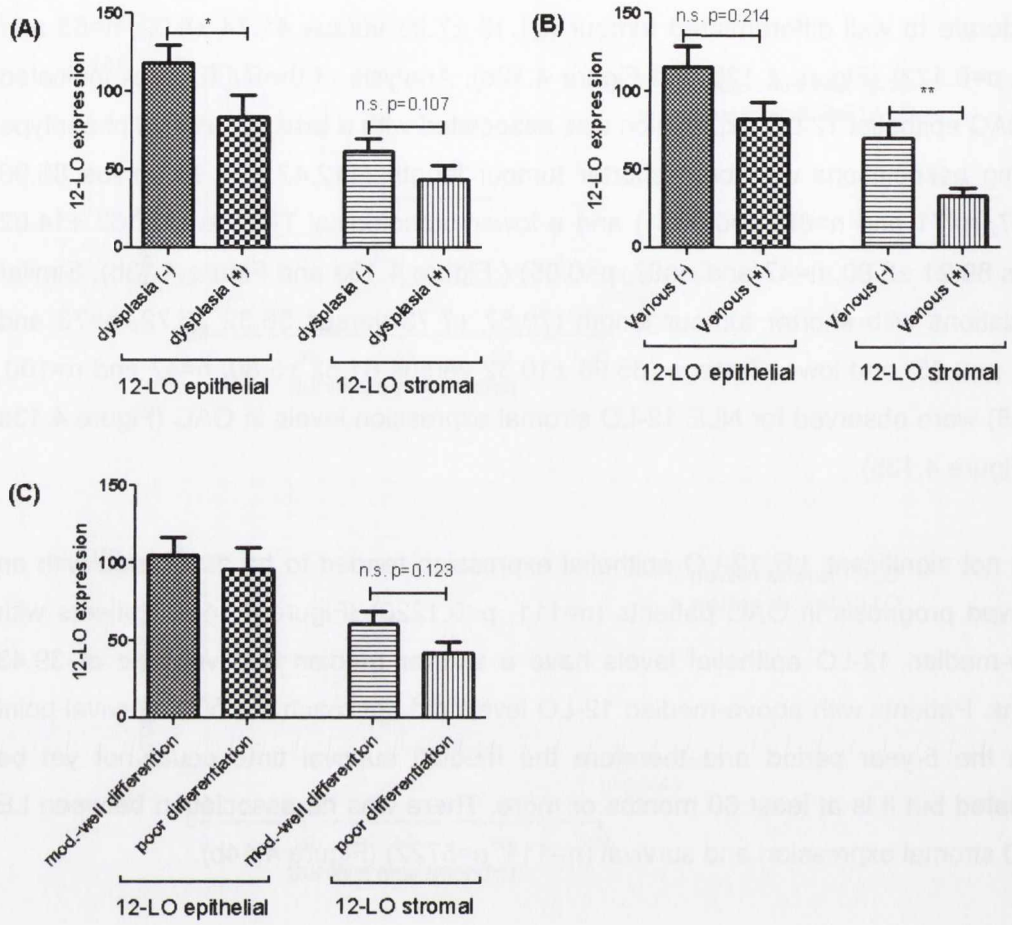

Figure 4.12 Leading edge OAC 12-LO epithelial expression is associated with an absence of dysplasia while stromal expression is associated with an absence of venous involvement. LE OAC patient (n=116) 12-LO expression was correlated with available clinical parameters. Only two statistically significant associations were found: (A) 12-LO epithelial expression was higher in patients without dysplasia ($p<0.05$, n=66 versus n=41) while (B) 12-LO stromal expression was higher in those without venous involvement ($p<0.01$, n=58 versus n=51). A similar but statistically non-significant association was seen between (A) stromal 12-LO and absent dysplasia (p=0.107) and (B) epithelial 12-LO and absent venous involvement (p=0.214). (C) There was also a trend for 12-LO stromal expression to be higher in the stromal compartment of lower grade tumours (p=0.123). Statistical test used was Mann-Whitney U test: $p<0.05$(*), $p<0.01$(**). Error bar denotes mean ± S.E.M.

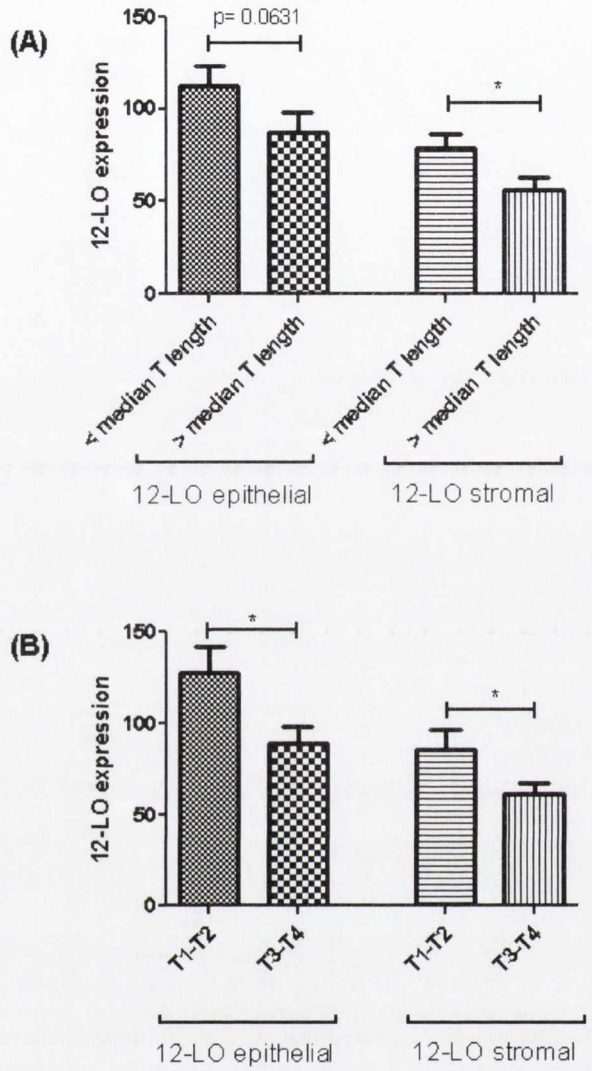

Figure 4.13 Non-leading edge OAC 12-LO expression is associated with a shorter tumour length and lower T-stage. NLE OAC patient (n=154) 12-LO expression was correlated with available clinical parameters. (A) Increased 12-LO epithelial and stromal expression was associated with a shorter tumour length in OAC patients ($p=0.0631$ and $p<0.05$ respectively). (B) Increased 12-LO epithelial and stromal expression was also associated with lower T-stage patients ($p<0.05$ for both) Statistical test used was Mann-Whitney U test: $p<0.05$(*). Error bar denotes mean ± S.E.M.

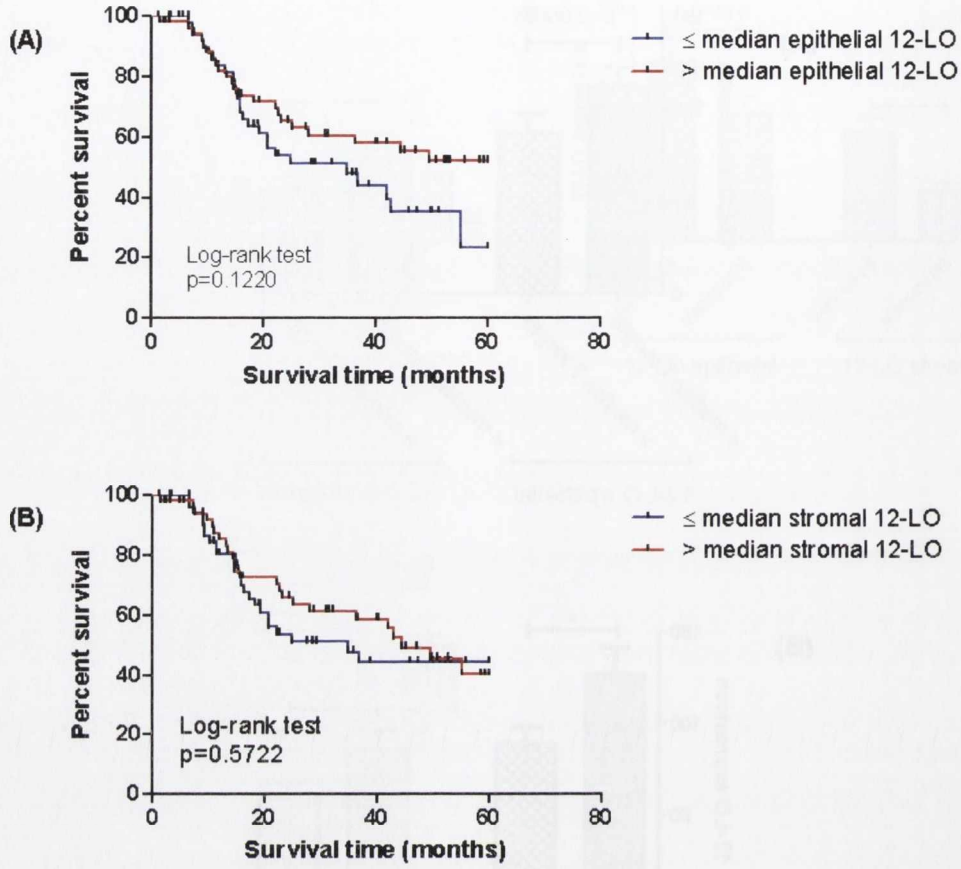

Figure 4.14 12-LO epithelial expression at the invasive edge shows a non-significant association with increased survival time in OAC patients. The association of LE 12-LO expression and 5-year survival was investigated in OAC patients. (A) OAC LE patients expressing above-median epithelial 12-LO levels tended to have a better prognosis than lower expressors, however this was not significant (p=0.1220, n=111). (B) There was no observed association between stromal 12-LO expression and 5-year survival (p=0.5722, n=111). Statistical test used was Kaplan Meier survival curve with Log-rank (Mantel-Cox) test.

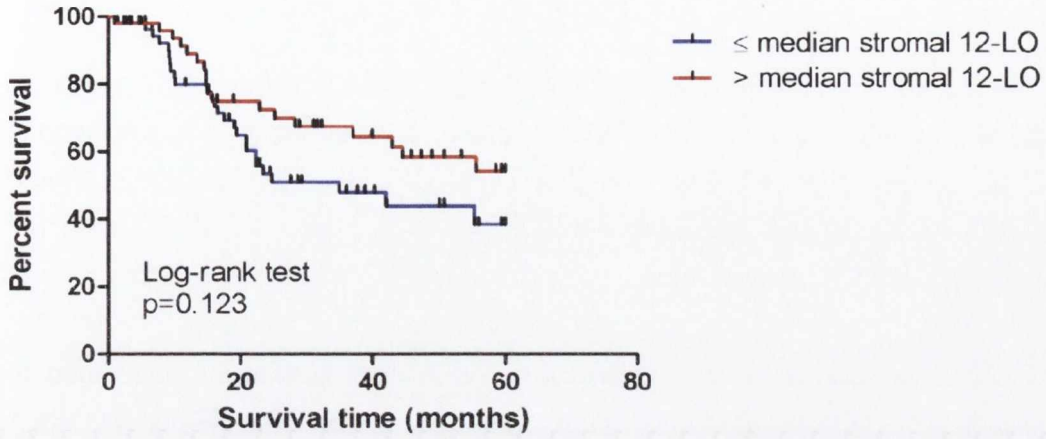

Figure 4.15 Non-leading edge 12-LO stromal expression and association with survival in chemo-radiation therapy naive patients. Patients who received neoadjuvant CRT were excluded from the cohort for this analysis. Above median NLE 12-LO stromal expression showed an increased trend towards an improved prognosis compared to low expressors when neoadjuvant patients were excluded (n=111, p=0.123). Statistical test used was Kaplan Meier survival curve with Log-rank (Mantel-Cox) test.

Table 4.2 Association of 12-LO expression with OAC clinical parameters: a comparison of p-values when patients who received neoadjuvant therapy are excluded

Clinical parameter	OAC NLE (n=154)		OAC NLE CRT naive (n=111)	
	12-LO epithelial p-value	12-LO stromal p-value	12-LO epithelial p-value	12-LO stromal p-value
< Median tumour length	0.0631	**0.0285**	0.0589	**0.0309**
Low T-stage	**0.0157**	**0.0333**	**0.0087**	**0.0351**
Low N-stage	0.2274	0.1115	0.2910	0.0706
Venous involvement (-)	0.1683	0.2435	0.0685	0.0853

4.3.7 Association of oesophageal cancer 12-LO expression and angiogenic markers

It has previously been shown *in vitro* in prostate cancer that 12-LO regulates VEGF activity (Nie *et al.*, 2006) and that xenografts of 12-LO overexpressing breast cancer cells produces larger and more angiogenic tumours thus indicating a role of 12-LO in tumour angiogenesis (Connolly and Rose, 1998). Consequently, this study explored the potential link between 12-LO and angiogenesis in oesophageal cancer. Previously a positive association was found between OAC normal adjacent tissue 12-LO mRNA expression and VEGF expression ($p<0.01$) (Figure 4.3). Prior to this project

oesophageal cancer TMA LE tumour cores were stained for VEGF and the VEGF receptor- 2/KDR, while NLE cores were stained for VEGF only.

A positive correlation between 12-LO epithelial staining of tumour masses or surrounding stromal compartment and VEGF tumour epithelial expression was found in LE OSCC cores (n=24; r=0.5889, p<0.01 and r=0.5042, p<0.05 respectively) (Figure 4.16). No correlation was observed with NLE OSCC 12-LO and VEGF (data not shown).

OAC 12-LO expression at the invasive edge of tumour epithelium was found to correlate with VEGF epithelial expression (n=100, r=0.3929, p<0.001) (Figure 4.17a). A similar positive association was also found with the VEGF receptor, KDR epithelial staining (n=96, r=0.2458, p<0.05) (Figure 4.17b). NLE OAC 12-LO expression, both in the tumour epithelium and stromal compartment showed a significant positive correlation with VEGF epithelial expression (n=141, r=0.3060, p=0.0002 and n=145, r=0.2552, p<0.01 respectively) (Figure 4.18).

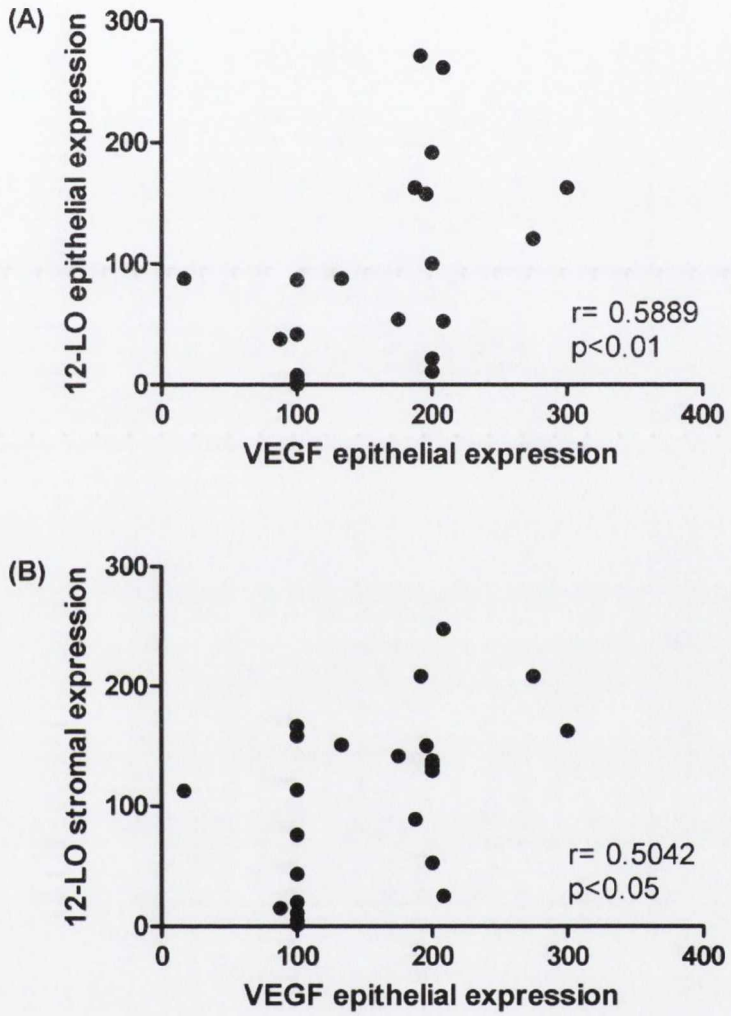

Figure 4.16 Invasive edge 12-LO expression is correlated with VEGF levels in OSCC. (A) Following immunohistochemical staining of LE OSCC TMA cores for 12-LO and VEGF (n=24), a positive correlation was found between 12-LO epithelial staining and VEGF epithelial expression (r=0.5889, p<0.01). (B) A similar association was found between 12-LO expression of the stromal compartment and VEGF epithelial staining (r=0.5042, p<0.05). Statistical test used was a Spearman correlation.

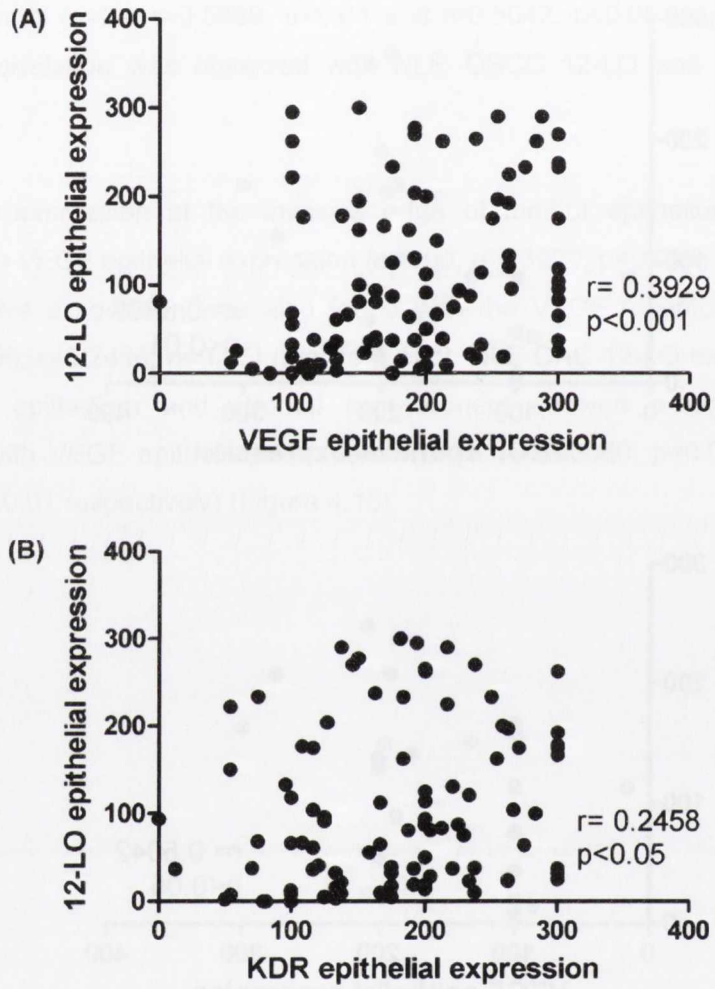

Figure 4.17 12-LO epithelial expression at the invasive edge is correlated with corresponding VEGF and KDR levels of expression in OAC. (A) Following immunohistochemical staining of LE TMA cores for 12-LO, VEGF and VEGFR-2/KDR, a positive correlation was found between 12-LO epithelial staining and VEGF epithelial expression ($r=0.3929$, $p<0.001$). (B) A positive association was also found between 12-LO epithelial staining and KDR staining ($r=0.2458$, $p<0.05$). Statistical test used was a Spearman correlation.

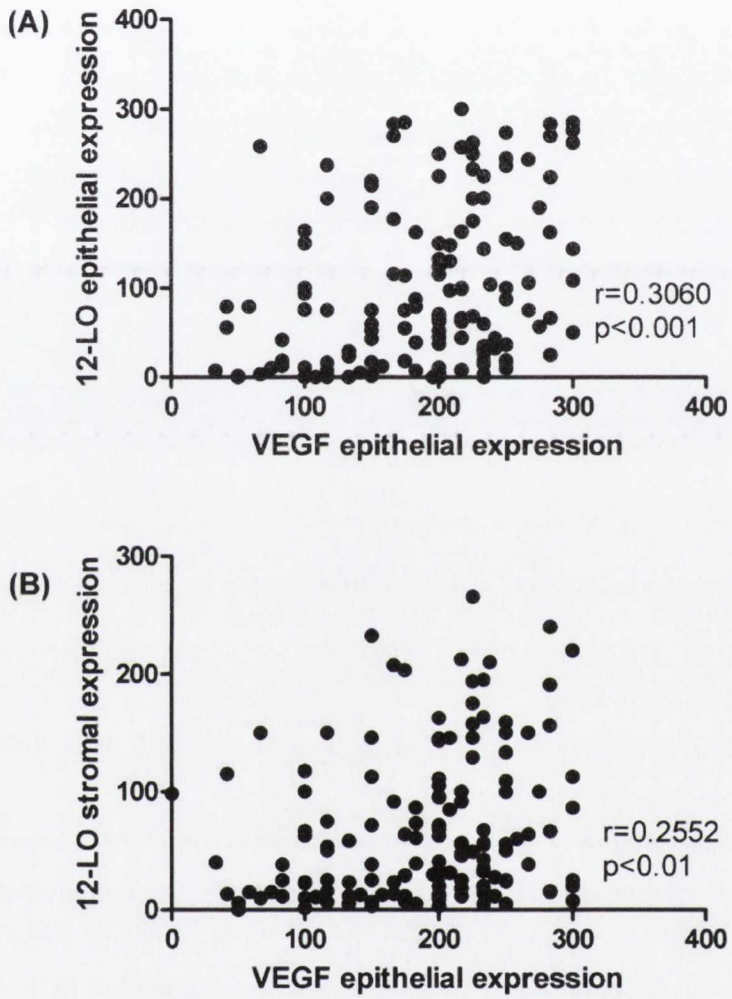

Figure 4.18 12-LO epithelial and stromal expression in OAC non-leading edge cores are both associated with VEGF expression. (A) A positive correlation was found between 12-LO NLE OAC epithelial staining and VEGF epithelial expression (r=0.3060, p=0.0002). (B) A positive correlation was also found between 12-LO stromal staining and VEGF (r=0.2552, p<0.01). Statistical test used was a Spearman correlation.

4.3.8 Oesophageal cancer 12-LO stromal expression and association with immune markers

Prior to this project the LE TMA cores were stained and graded for a panel of 13 common immune cell markers and cytokines (A full list can be found in Appendix V). Substantial and variable stromal-specific 12-LO staining was observed in the TMA and thus potential associations of 12-LO stromal expression with immune markers and cytokines was explored by Spearman correlation tests. No association between LE OSCC cores and stromal immune marker staining was observed (data not shown). However a positive correlation between 12-LO expression and the immune marker CD45RO and the two cytokines IFN-γ, and IL-4 was observed (Table 4.3).

Table 4.3 Correlation of invasive edge stromal 12-LO expression with immune cell markers in OAC

Immune marker or cytokine	Function	n	Spearman r	p-value
CD45RO	Regulation of B- and T-cell antigen receptor signalling	70	0.2401	0.043
IFN-γ	Macrophage activation	61	0.3335	0.0083
IL-4	Differentiation of Th2 memory cells	69	0.2454	0.0421

4.3.9 Oesophageal cancer VEGF and KDR expression and association with clinical parameters

The primary aim of this chapter was to explore the association of 12-LO expression in oesophageal cancer with clinical parameters. However an additional study investigating the association of VEGF and the major VEGF receptor, KDR, epithelial expression with clinical parameters in oesophageal cancer was also of interest. VEGF and KDR expression in LE and NLE OSCC did not show an association with clinical parameters such as stage, grade, lymph node involvement etc. However it was observed that patients with high VEGF expression at the LE tended to have a shortened survival time (median survival time: 13.83 months versus 39.87 months). (n=25, Log rank p=0.0576; Gehan-Breslow-Wilcoxon test, $p<0.05$) (Figure 4.19).

Unexpectedly, KDR LE OAC epithelial expression was found to correlate with a better prognosis and a less aggressive tumour phenotype. Higher LE KDR expression levels were significantly associated with lower T-stage (i.e. T1-T2) (199.64 ±12.61 versus 165.65 ±8.51, n=35 and n=68, $p<0.05$) and improved 5-year disease specific survival (log-rank test, $p<0.01$) (Figure 4.20a and Figure 4.20c). VEGF LE OAC expression did

not show an association with any of the investigated clinical parameters including survival (Figure 4.20d). Similarly VEGF NLE OAC expression was not associated with survival (data not shown). A near significant association between VEGF NLE expression and absent venous involvement was noted (200.30 ±7.26 versus 179.42 ±8.37, n=82 and n=64, p=0.0601, graph not shown). No other associations were found.

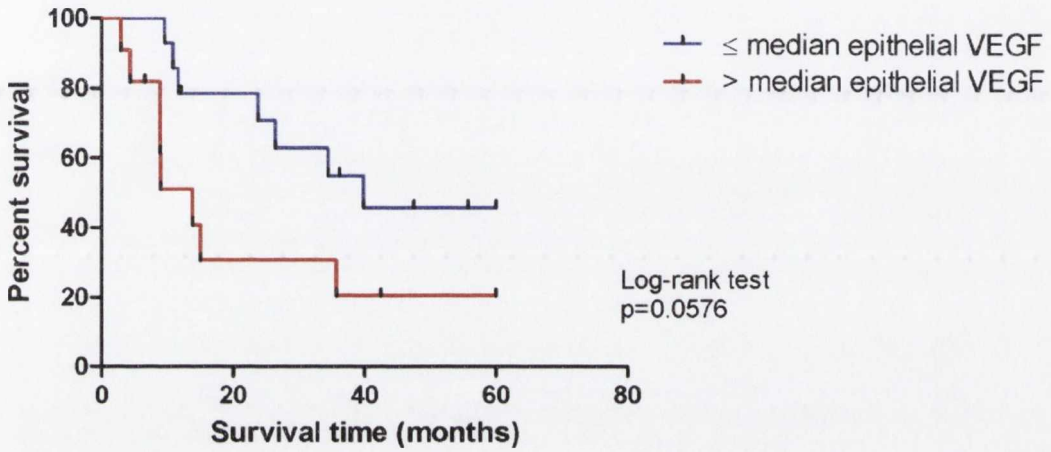

Figure 4.19 Invasive edge VEGF expression is associated with a poorer prognosis in OSCC. LE VEGF expression in OSCC (n=25) had a shorter survival time (log rank p=0.0576; Gehan -Breslow-Wilcoxon test, $p<0.05$). No association was observed in NLE OSCC samples (data not shown). Statistical test used was Kaplan Meier survival curve with Log-rank (Mantel-Cox) test and Gehan-Breslow-Wilcoxon test.

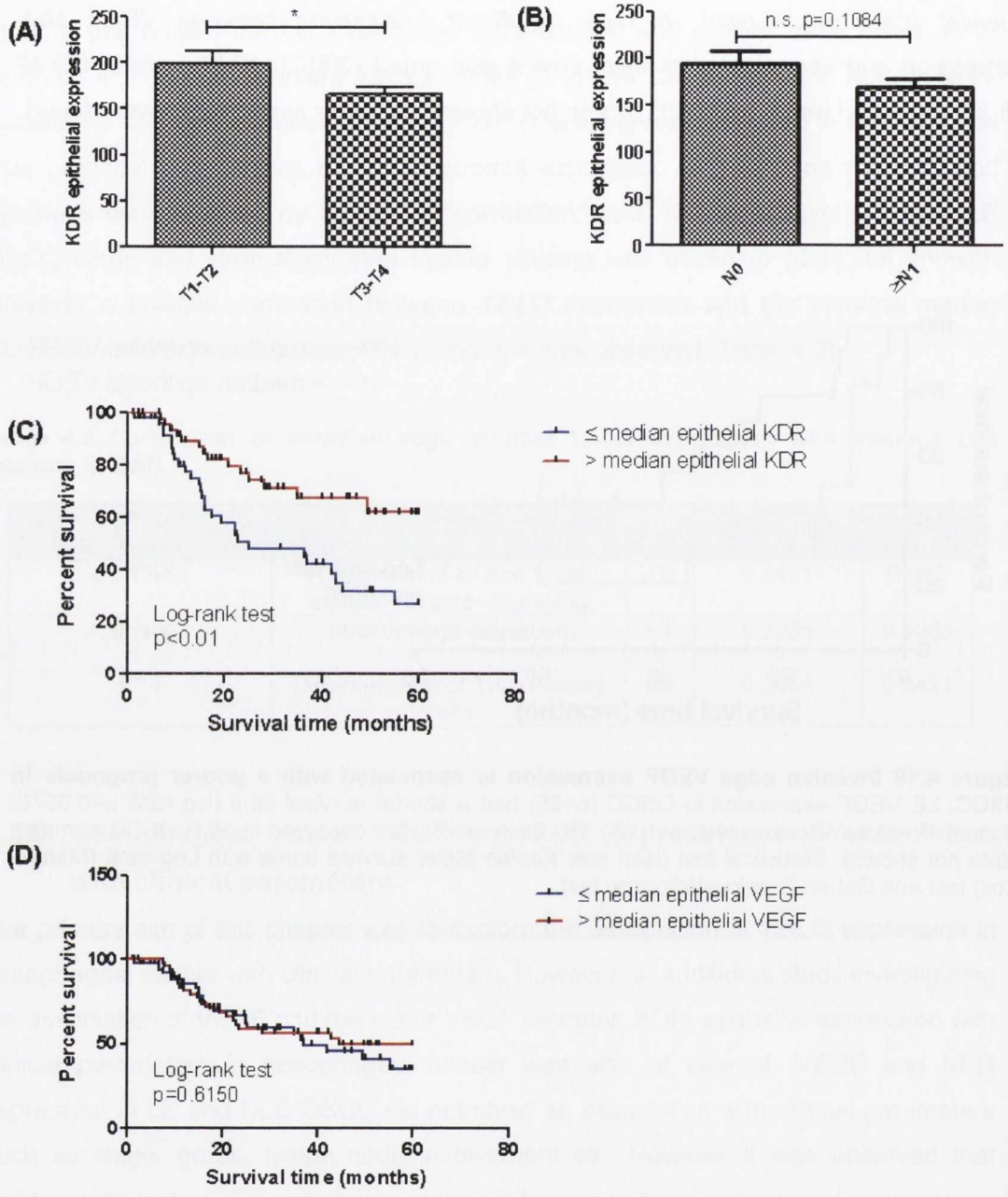

Figure 4.20 Invasive edge KDR expression is associated with a lower T-stage and an improved patient prognosis in OAC. (A) LE KDR expression was associated with a lower T-stage (T1-T2) compared to high T-stage ($p<0.05$, n=35 versus n=68). (B) There was a trend towards an association between KDR and negative N-stage ($p=0.1064$, n=33 versus n=71). (C) Higher LE KDR expression was associated with an increased 5-year survival (n=101, $p<0.01$) whereas (D) LE VEGF expression did not show any association with survival (n=109, $p=0.6150$). Statistical test used was Kaplan Meier survival curve with Log-rank (Mantel-Cox) test. $p<0.05$(*).Error bar denotes mean ± S.E.M.

4.3.10 12-LO metabolite 12(S)HETE in OAC serum

Circulating levels of 12-LO or its metabolite 12(S)HETE have been investigated as a biomarker of disease in several cancers (Singh *et al.*, 2011, Piotrowska *et al.*, 2013, Rodriguez-Blanco *et al.*, 2014). Consequently the serum level of the 12-LO metabolite 12(S)HETE in OAC patients was investigated to determine its biomarker potential. Serum samples were handled and diluted as detailed in Section 2.20.1. Serum selected for this study was from male CRT-naive OAC patients (n=68). Clinical parameters of the serum cohort are detailed in Table 4.4. Six age-matched non-cancer control males (mean age± S.D. = 67.91 ±8.85) were also included in this study to give an indication of baseline level 12(S)HETE. These six patients were admitted for hernia repair surgery and did not have a history of cancer. 12(S)HETE levels were measured by ELISA as described in Section 2.20.4. 12(S)HETE was found to be significantly higher in OAC patient serum compared to the non-cancer controls (209.89 ±54.84 ng/mL versus 12.40 ±2.14 ng/mL). The majority (72%) of OAC serum had a 12(S)HETE concentration above the mean of the baseline concentration indicated by the non-cancer control serums.

Table 4.4 Details of patient demographic used for 12(S)HETE and VEGF serum study

Male OAC (n=68)	Mean (S.D.) or n (%) as appropriate	
Age	64.98 (14.23)	
T-stage	T0	6 (8.84%)
	T1	23 (33.82%)
	T2	16 (23.53%)
	T3	20 (29.41%)
	Not specified	3 (4.41%)
N-stage	N0	38 (55%)
	≥N1	27 (40%)
	Not specified	3 (5%)
Tumour grade	Moderate-well	44 (64.71%)
	Poorly	19 (27.94%)
	Not specified	5 (7.35%)
Neoadjuvant treatment	0 (0%)	

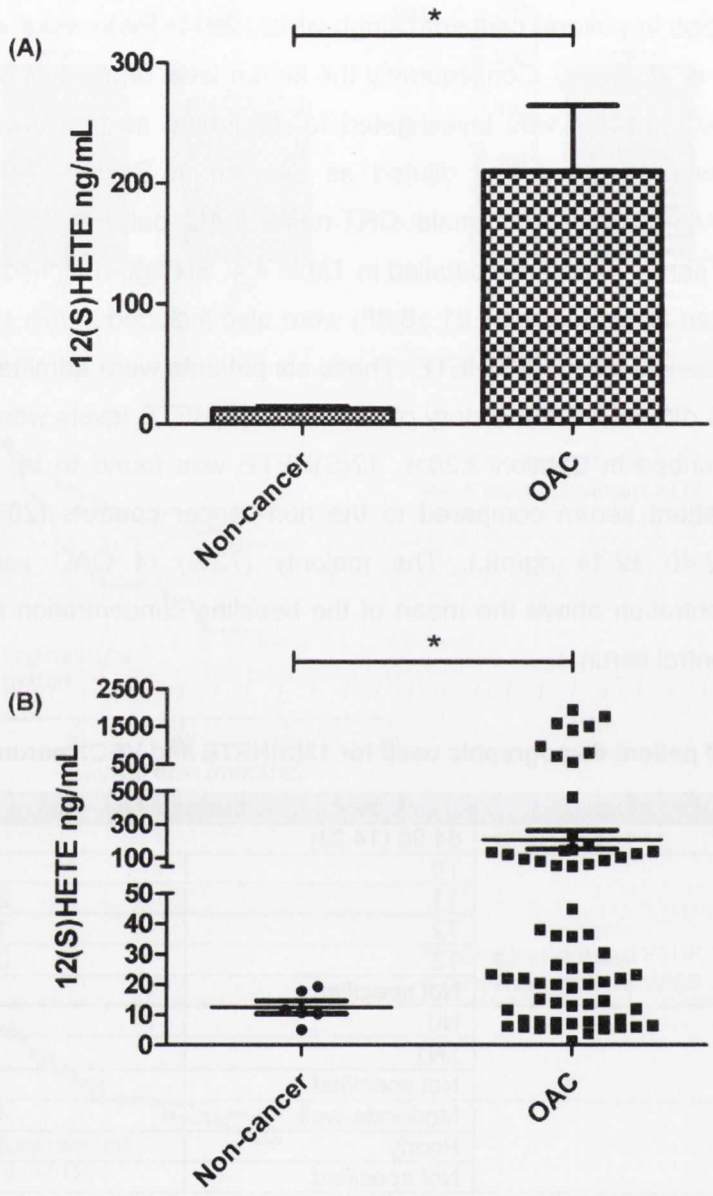

Figure 4.21 Serum 12(S)HETE levels are higher in OAC patients compared to non-cancer controls. Serum 12(S)HETE was measured in OAC patient serum samples (n=68) and non-cancer control serum samples (n=6). (A) The average 12(S)HETE level in OAC serum was significantly higher compared to non-cancer control serum (209.15 ±54.84 ng/mL versus 12.40 ±2.14 ng/mL , $p<0.05$). (B) Distribution of the data is shown in the scatter plot. Statistical test used was Mann-Whitney U test: $p<0.05$(*). Error bar denotes mean ± S.E.M.

4.3.11 OAC 12(S)HETE levels and correlations with clinical parameters

12(S)HETE levels in OAC patient serum (n=68) was compared to clinical parameters. Serum levels of 12(S)HETE did not show an association with any of the clinical parameters including T-stage, N-stage, tumour grade, absence/presence of dysplasia, lymph node or venous metastasis. There was not a statistically significant relationship between OAC serum 12(S)HETE and 5-year disease specific survival, however a lower percentage of patients with above-median 12(S)HETE were still alive at 5 years (<62.31% versus 79.88%, p=0.1521) (Figure 4.22a). Median survival was not available as both curves did not reach 50% survival with currently available patient data. A significant association between OAC serum 12(S)HETE and recurrence free survival was observed (p<0.05). Patients with above-median 12(S)HETE levels had a shorter interval of time from surgery to progression of disease compared to those with lower 12(S)HETE levels (Figure 4.22b).

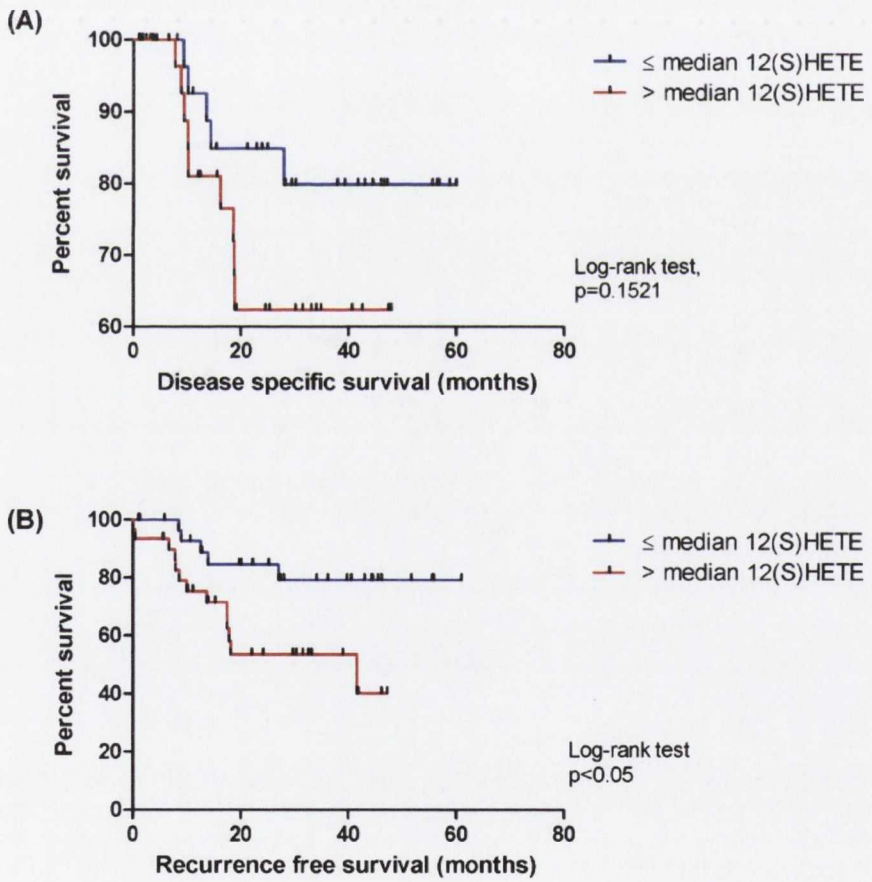

Figure 4.22 Serum 12(S)HETE is associated with decreased recurrence-free survival in OAC. Patients were divided into two groups on the basis of 12(S)HETE serum concentrations below or equal to median expression or above the median expression (n=68). (A) 12(S)HETE was not significantly associated with disease specific 5-year survival (p=0.1521). (B) Higher 12(S)HETE levels were associated with decreased recurrence-free survival following surgery (p<0.05). Statistical test used was Kaplan Meier survival curve with Log-rank (Mantel-Cox) test.

4.3.12 Association of serum 12(S)HETE with VEGF levels in OAC patients

Overexpression of 12-LO expression in prostate cancer has been shown to be associated with an increase in VEGF, suggesting a regulatory role of 12-LO (Nie *et al.*, 2006, McCabe *et al.*, 2006). Additionally, a correlation between serum 12-LO metabolite levels and VEGF levels in lung cancer has also been reported, suggesting that 12-LO and VEGF signalling pathways are linked (Cathcart *et al.*, 2011a). Consequently we investigated the potential link between circulating levels of 12(S)HETE and VEGF in OAC serum (n=68). In Section 4.3.7 a significant association between 12-LO tumour epithelial and stromal expression and VEGF levels was noted. A correlation between OAC normal adjacent tissue 12-LO mRNA expression and VEGF levels was also observed (section 4.3.1). VEGF was measured by ELISA as described in Section 2.20.5 using the same serum sample aliquot used for 12(S)HETE measurement. A weak but positive correlation was found between 12(S)HETE and corresponding VEGF levels ($r=0.2970$, $p<0.05$). The mean VEGF OAC serum concentration was 236.72 ±29.86 pg/mL and no association was found between VEGF levels and available clinical parameters in this patient cohort.

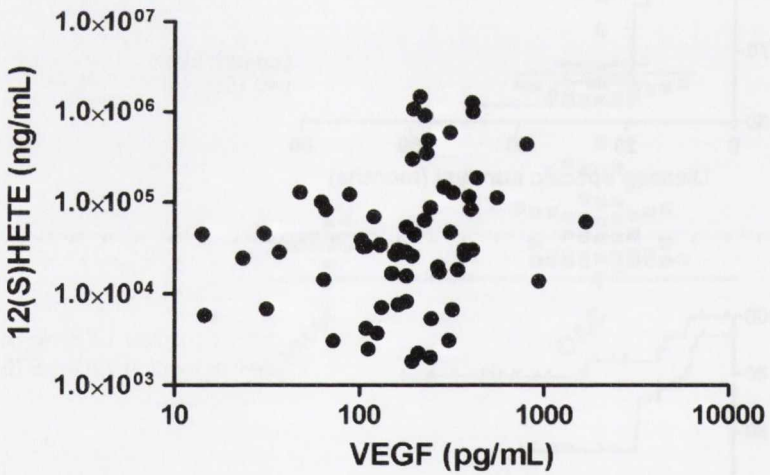

Figure 4.23 OAC serum levels of 12(S)HETE correlate with VEGF levels. Circulating 12(S)HETE and VEGF levels were measured in 68 OAC patients and a weak correlation was found between the two proteins ($r=0.297$, $p=0.0139$). A Spearman's correlation test was performed on actual concentration values while the axis of the graph were stretched to a log scale.

4.4 Discussion

A major aim of this study was to elucidate the role of 12-LO in OAC and to a lesser extent OSCC. Despite evidence in malignancies such as prostate cancer (Gao *et al.*, 1995), there has been little or no insight to date on the role of 12-LO in oesophageal cancer and considering the evidenced role of other eicosanoid signalling pathways such as COX-2 in this cancer (Hashimoto *et al.*, 2007), this line of investigation was warranted.

Contrary to expectations 12-LO mRNA expression was found to be significantly higher in macroscopically normal adjacent tissue and was practically undetected in the majority of the matched tumour samples indicating it is potentially downregulated in OAC. *ALOX12* is known to have approximately 60% sequence homology with *ALOX15* in humans. The specificity of the FAM-labelled primer probes for *ALOX12* used in this study was confirmed by the fact that nearly all OAC tissue samples (both normal adjacent and tumour) did not express detectable mRNA expression of 15-LO (i.e. Ct>40) when using *ALOX15*-specific FAM-labelled primer probes. These OAC samples were also analysed for cytokeratin-8 (*8KRT)* expression (Section 3.3.4), a surface marker of columnar epithelium that is known to be absent from normal squamous epithelium but expressed in normal gastric tissue and in the pathological states of BO metaplasia and OAC where normal squamous epithelial cells have transformed into gland-like cells (van Baal *et al.*, 2008). While OAC tumour samples showed higher *8KRT* compared to the normal adjacent, moderate expression was still observed in normal adjacent samples of the oesophagus suggesting that this tissue may not be normal, but is likely metaplastic and/or dysplastic and inflamed. Truly normal non-cancerous and non-inflamed oesophageal squamous epithelial tissue samples were not available for this project but would be a valuable resource to determine whether the observed expression levels of 12-LO in the "normal" tumour adjacent tissue are abnormally high and actually an early pre-cancerous high-risk biomarker of disease. In the alternate scenario 12-LO upregulation in the normal adjacent squamous epithelium may suggest anti- proliferative and anti-cancerous effects, as seen for the ambiguous LO enzyme, 15-LO-1 in certain cancers (Hennig *et al.*, 2007b, Jiang *et al.*, 2006b).

To verify the findings of this qPCR study, 4 patient samples from the original gene study along with 4 other OAC tumour samples with matched normal adjacent tissue were investigated for 12-LO expression using a rabbit monoclonal antibody for 12-LO, suitable for western blot. The specificity of the antibody was confirmed by a single band

of protein in the platelet cell lysate positive control. While faint bands of 12-LO were observed in most tumour samples indicating some level of tumour 12-LO translation, the corresponding normal adjacent protein bands were much stronger, supporting the validity of the gene expression results. As discussed in Section 4.1, certain polymorphisms in the *ALOX12* gene are associated with increased oesophageal cancer risk (Guo *et al.*, 2007) and may provide a rationale for this finding. If such polymorphisms are present in the tumour biopsies the gene sequence may not be amplifiable due to inadequate primer design and the monoclonal antibody used for protein analysis that binds to only one epitope may be too specific.

The TMA study was carried out using a different 12-LO antibody that was suitable for IHC. The qPCR and western blot study examined 12-LO expression in crude RNA and protein samples of tumour and normal adjacent tissue and it should be noted that varying amounts of connective tissue in these samples may account for the differences observed. In contrast, immunohistochemistry offers the opportunity to investigate the tissue compartment specific expression of 12-LO in oesophageal cancer. The first observation of note was that 12-LO protein was readily detected in oesophageal cancer tissue at a variety of levels with approximately 20% of patients having epithelial 12-LO scores of more than 200 and approximately another 20% of patients with 12-LO scores of less than 10. Smooth muscle, known to express platelet-type 12-LO stained positively in the TMAs (Preston *et al.*, 2006). Some TMA cores were found to contain normal squamous epithelium and similar to the previous qPCR and western blot study, 12-LO expression was observed, specifically in the basal cells of the stratified epithelium. The antibody used was a polyclonal antibody which would therefore usually be better at amplifying signal from target protein with low expression or tolerating small changes to antigen (e.g. polymorphisms) because multiple epitopes are bound. While the specify of the antibody was verified by western blot using purified full length recombinant platelet-type 12-LO, the potential for cross-reactivity with other proteins, particularly LO isoenzymes such as 15-LO-1, cannot be disregarded.

The TMA study provided a number of novel findings. All observed significant associations (and non-significant trends) between 12-LO expression and clinical parameters were associated with a less aggressive form of OAC. NLE tumour epithelial and stromal expression was associated with lower T-stage and decreased tumour length. Invasive edge (LE) 12-LO epithelial expression was associated with an absence of dysplasia and a trend toward absent venous involvement while stromal expression was significantly associated with absent venous involvement and a trend towards an

association with low grade and absence of dysplasia. While not significant, tumour 12-LO epithelial expression tended to be associated with an improved prognosis in OAC patients, with patients showing an increased survival time of at least 20 months. These results indicate that 12-LO expression may play a role in the early stages of development of OAC tumours and thus may have potential as an early biomarker of disease. Alternatively 12-LO may be potentially protective in disease, despite the majority of research to date in other tumour types which contradicts this idea (Winer *et al.*, 2002, Natarajan *et al.*, 1997). Verification of observed survival trends in a larger cohort would be necessary before any full conclusions could be made.

Analysis of the small OSCC cohort 12-LO stromal expression also revealed an association with a less aggressive tumour phenotype (reduced tumour length and absence of venous involvement). In contrast, analysis of 5-year survival revealed a significant association between 12-LO tumour epithelial expression and decreased patient prognosis, suggesting that 12-LO expression in the epithelial component specifically may be pro-carcinogenic. While the cohort of 25 patients is too small to draw major conclusions, it is an observation worthy of further follow up in a larger patient cohort of OSCC patients.

Previously the biomarker potential of 12(S)HETE was discussed in the context of prostate cancer where urinary levels of the protein were shown to correlate with prostate cancer compared to normal or benign tumour urine samples (Nithipatikom *et al.*, 2006). In this study increased levels of 12(S)HETE serum levels were significantly associated with OAC, indicating its potential as a biomarker of disease. It was also shown that OAC patients with high 12(S)HETE tended to have a shorter progress-free survival following surgery. There are a number of limitations to this study that must be noted. Firstly, only a small non-cancer control population (n=6) could be accommodated due to experiment design and increasing this number may provide a better insight into the significance of the observed association between 12(S)HETE and patients with OAC. Secondly, clinical follow up time was relatively short for many of the censored patients in the Kaplan Meier's survival curve (i.e. those still alive or those with no cancer present). Clinical follow-up of less than one year was all that was available for 50% of the cohort which may skew the results. The survival data presented here will need be analysed with caution and updated as and when further patient follow up information becomes available. Finally it must also be pointed out that serum samples are likely to be contaminated by the highly active production of 12(S)HETE from

platelets. Analysis of 12(S)HETE in plasma or locally in OAC tumour explant tissue would provide a better strategy to measure tumour relevant levels of 12(S)HETE.

As discussed previously Section 1.7.6.2 12-LO has been shown to play a role in tumour angiogenesis in a number of experimental models, however clinical evidence is lacking and the potential of 12-LO as a pro-angiogenic player in oesophageal cancer has not yet been explored. In this study a positive association was found between OAC normal adjacent tissue, 12-LO mRNA expression and VEGF mRNA expression. A positive correlation between 12-LO epithelial staining of tumour masses or surrounding stromal compartment and VEGF tumour epithelial expression was found in LE OSCC. Furthermore, OAC 12-LO expression at the invasive edge of tumour epithelium was found to correlate with VEGF and KDR epithelial expression. NLE OAC 12-LO expression, both in the tumour epithelium and stromal compartment showed a significant positive correlation with VEGF epithelial expression. A weak but significant correlation of 12(S)HETE with VEGF circulating levels in serum was also observed. This link has not been shown in patient data to date and may be applicable beyond OAC, to a variety of angiogenic tumours with 12-LO expression. Further studies blocking 12-LO activity are necessary to investigate whether a causative relationship between 12-LO and angiogenesis exists. This idea was explored in Chapter 6.

Varying 12-LO stromal staining was observed in oesophageal cancer TMA however to date unlike 5-LO and 15-LO-1 whose immune expression is well documented (Wen *et al.*, 2014, Wejksza *et al.*, 2013, Kusmartsev, 2012), human platelet 12-LO expression has not been detailed for any immune cell subtypes. Correlation studies with a panel of 13 immune markers (see Appendix V for full list) revealed some weak but significant associations with stromal IFN-γ, IL-4 and CD45RO. CD45RO is indicative of the presence of memory T-cells (Michie *et al.*, 1992). Recently, increased tumour infiltration of $CD45RO^+$ immune cells has been shown to play a role in preventing tumour progression and recurrence and to have prognostic significance in gastric cancer (Wakatsuki *et al.*, 2013). IFN-γ was found to be significantly higher in high $CD45RO^+$ gastric tumours compared to low $CD45RO^+$ tumours, indicating a role in the activation of anti-tumour immune responses. Bearing in mind that in this study stromal 12-LO expression in OAC tended to be associated with a less advanced cancer, it would be interesting to investigate the expression of platelet 12-LO in $CD45RO^+$ cells to elucidate whether this pathway is relevant to tumour immunity.

Finally, the association of VEGF and KDR with clinical parameters in oesophageal cancer was investigated. It has previously been shown that increased VEGF expression is associated with poorer prognosis in other cancers including oesophageal cancer. However there are also clinical studies published which did not find an association, indicating the ambiguity of immunohistochemical studies considering factors such as population etiology, in addition to antibody source variations. In this study VEGF showed a close to significant association with poorer prognosis in the small cohort of OSCC patients ($p<0.056$) which agrees well with current literature on OSCC (Shih *et al.*, 2000, Peng *et al.*, 2013). However these other studies have only found significance with survival in Asian populations. In a meta-analysis of nearly 1500 patients across 19 studies, it was reported that no significant correlation with survival in oesophageal cancer patients (both OAC and OSCC) from non-Asian countries was observed. In one study VEGF was not shown to have prognostic significance in OAC patients who received pre-operative CRT (Kulke *et al.*, 2004) however another more recent immunohistochemical study has reported an association of high VEGF expression with poor cancer specific survival in CRT naive OAC indicating its prognostic potential (Prins *et al.*, 2012). In this study no significant association between VEGF expression and clinical parameters or survival was found in the OAC cohort, including a sub-analysis of CRT naive patients and therefore we were not able to reproduce findings from other studies.

Recent evidence in hepatocellular carcinoma and breast cancer suggests VEGFR-1 is indicative of prognosis (Li *et al.*, 2012, Dhakal *et al.*, 2012). VEGFR-2, or KDR, has also been investigated for its prognostic potential in gastric cancer and breast cancer, however no survival significance was observed (Ozdemir *et al.*, 2006, Meunier-Carpentier *et al.*, 2005). However it was associated with the early stage of tumour development in ovarian cancer (Klasa-Mazurkiewicz *et al.*, 2011). Interestingly in this study tumour epithelial KDR expression in OAC was shown to be significantly associated with lower T-stage and with an improved patient survival. These results are in corroboration with data published concerning urinary cancer and an association with improved survival (Gakiopoulou-Givalou *et al.*, 2003, Shah *et al.*, 2014). It is unclear currently why patients with increased KDR have improved disease free survival and overall survival rates and this association warrants further investigation.

In summary, this the first study of its kind to explore the association of 12-LO and oesophageal cancer. In this study we evaluated 12-LO levels by 4 different parameters: mRNA expression was assessed by qPCR, protein expression was evaluated in a

small cohort by western blot and a larger cohort by immunohistochemical TMA examination and finally 12-LO enzyme activity via it's circulating metabolite product 12(S)HETE was measured in serum by ELISA. Contrary to studies in other cancer types 12-LO was found to be higher in normal adjacent tissue while very low to negligible 12-LO gene expression was found in corresponding tumour samples. This was further supported by western blot data, suggesting 12-LO is either protective or involved in early pre-cancerous processes in the development of OAC. On the other hand the immunohistochemical study revealed strong and variable 12-LO across almost 200 TMA tumour tissue samples, suggesting that there are discrepancies in the methods used to measure 12-LO. Other than an association between invasive edge 12-LO epithelial staining and poorer survival in the small OSCC cohort, all other strong trends or significant associations with 12-LO expression in both OAC and OSCC were in favour of a less aggressive tumour phenotype. While these results are somewhat confounding in relation to previously published data in other cancers they would suggest that 12-LO is either protective or involved in an early stage of cancer development and subsequently downregulated as the cancer progresses. Finally 12-LO expression and enzyme activity were found to correlate with VEGF and its receptor KDR, suggest 12-LO may be linked to angiogenesis in oesophageal cancer.

Chapter 5 Assessment of the anti-angiogenic potential of novel 5-lipoxygenase and 12-lipoxygenase targeted inhibitors

5.1 Introduction

The sprouting of new capillaries from pre-existing vessels is driven by pro-angiogenic factors such as VEGF, bFGF, placenta growth factor (PlGF) and the angiopoietin family (Ferrara *et al.*, 2003, Presta *et al.*, 2005, De Falco, 2012, Augustin *et al.*, 2009). Together with numerous anti-angiogenic factors such as thrombospondin, angiostatin, the FK506 binding-like protein and other proteolytic enzymes and surface integrins (Bluff *et al.*, 2008, Tarui *et al.*, 2002, Robson and James, 2012, Yakkundi *et al.*, 2015, Rundhaug, 2005, Avraamides *et al.*, 2008), these pro and anti-angiogenic mediators tightly regulate the intricate process of angiogenesis. An imbalance in these mediators can result in excessive and dysregulated vessel growth, subsequently contributing to the initiation, progression of a number of pathological states including arthritis, cardiovascular disease and cancer (Mapp and Walsh, 2012, Khurana *et al.*, 2005, Weis and Cheresh, 2011). Of all known angiogenic signalling molecules, VEGF is a key mediator of this pathological process exerting its effects by binding to one of its major receptors KDR/VEGF receptor-2. Both of these proteins have been recognised as two of the most important targets in terms of angiogenic pathology with anti-angiogenic cancer therapies targeting these proteins in use clinically (Vasudev and Reynolds, 2014). The use of currently available anti-angiogenic therapies has been met with attrition however due sub-optimal efficacy, narrow therapeutic windows and issues with organ-specific toxicities and secondary metastases in patients (Faivre *et al.*, 2006, Verheul and Pinedo, 2007), leading to a shift in emphasis to the targeting of other angiogenic growth factors such as PlGF (Snuderl *et al.*, 2013) or inflammatory mediators such as vasoactive amines (Medina and Rivera, 2010), plasma proteases (Cathcart *et al.*, 2015), cytokines (Matsuo *et al.*, 2012) and bioactive lipid eicosanoids (Gately and Li, 2004, Wang and DuBois, 2010).

High fat, n-6 fatty-acid rich diets, have been shown to be associated with relatively poor prognosis in breast cancer patients and an enhanced cancer progression in mouse models, thus suggesting a role of n-6 fatty-acid-derived bioactive lipid eicosanoid signalling molecules in angiogenesis and tumourigenesis (Rose and Connolly, 2000). 5-LO and 12-LO and their metabolites have been indicated to enhance angiogenesis. For instance 5-LO products actively produced by mesothelioma cells upregulate VEGF transcription in these cells and in HUVECs (Romano *et al.*, 2001). 5-LO metabolite LTB4 has also been shown to induce endothelial cell migration, tubule formation and to induce VEGF-mediated angiogenesis (Kim *et al.*, 2009). There is also evidence to suggest 5-LO is expressed in endothelial cells in different pathological states (Benard

et al., 2014, Walker *et al.*, 2002, Wright *et al.*, 1998, Sharma-Walia *et al.*, 2014). In a mouse model of cigarette smoke -induced inflammation of the colon, 5-LO expression was found to be upregulated in addition to increased MMP-2 and MMP-9, and VEGF (Ye *et al.*, 2004). Interestingly, pharmacologically inhibiting 5-LO downregulated these angiogenic mediators suggesting 5-LO is involved in the angiogenic process of cigarette smoke-enhanced adenoma formation (Ye *et al.*, 2004). In another study treatment of 5-LO-expressing DMBA-induced mouse mammary gland tumours with zileuton was able to significantly reduce tumour-derived inflammation and angiogenesis, and associated VEGF and MMP-2 levels, implicating 5-LO signalling in tumourigenesis and angiogenesis (Chatterjee *et al.*, 2013).

12-LO is also reported to have angiogenic effects and to date this enzyme has been most widely studied in the setting of prostate cancer (Pidgeon *et al.*, 2007). It has been reported that 12-LO overexpression in prostate cancer cells stimulated tumour growth in nude mice by enhancing tumour-associated angiogenesis and producing a larger tumour with denser volume of blood vessels (Nie *et al.*, 1998). Similarly 12-overexpressing breast cancer cells had increased tumourigenesis and angiogenesis in mouse xenograft models (Connolly and Rose, 1998). Additionally, conditioned media from 12-LO overexpressing prostate cancer cells or exogenous 12-LO metabolite 12(S)HETE enhanced endothelial cell migration *in vitro* (Nie *et al.*, 1998). Several studies have been carried out to investigate what angiogenic pathways 12-LO is interacting with to elicit the observed pro-angiogenic effects. Firstly, two independent studies reported that overexpression of 12-LO in prostate cancer cells led to enhanced VEGF transcriptional activity and enhanced VEGF promoter activity via activated extracellular-signal-related kinase 1/2 (ERK1/2) and PI3 kinase (McCabe *et al.*, 2006, Nie *et al.*, 2006). Secondly 12(S)HETE has been shown to upregulate integrin αvβ3 expression, a surface integrin know for its role in angiogenesis on the surface of prostate cancer cells, thus potentially modulating tumour and endothelial cell interactions (Tang *et al.*, 1993). Thirdly, HIF1-α, a key transcription factor in the activation of the VEGF pathway, has been shown to be upregulated in 12-LO overexpressing prostate cancer cells under hypoxic conditions, via the PI3K-Akt pathway (Krishnamoorthy *et al.*, 2010) providing another mechanism of action for 12-LO pro-angiogenic activity in the tumour microenvironment. Lastly, a recent study indicated a specific involvement of upregulated MMP-9, a key factor in invasion and metastasis, in the angiogenicity of 12-LO in prostate cancer *in vitro* by showing a downregulation of HUVEC migration in response to pre-treatment of the conditioned media with a neutralising antibody of MMP-9 (Dilly *et al.*, 2013). Endothelial cells such

as HUVECs are known to express platelet-type 12-LO (Funk *et al.*, 1992, Nie *et al.*, 2000).In one study 12-LO inhibitors have been shown to reduce endothelial cell proliferation by downregulation of VEGF (Nie *et al.*, 2000) while in another study the non-specific 12-LO inhibitor baicalein was shown to inhibit both proliferation and tubule formation of HUVEC endothelial cells in a dose-dependent manner (Miocinovic *et al.*, 2005).

Given that angiogenesis is one of the major routes of invasion and metastasis exploited by tumours, it represents a rational drug target and has been a focus of cancer drug discovery over the last decade. There have been vast developments in angiogenic assay design over this time. Aside from the functional 2-D *in vitro* assays that are often used in drug discovery such as proliferation, survival, migration/invasion and degradation zymography assays, the most widely used *in vitro* tool for novel anti-angiogenic screens is the tubule formation assay which mimics endothelial cell morphogenesis (Goodwin, 2007). A limitation of this model is the lack of complexity of an *in vivo* microenvironment. Other commonly used animal models such as the matrigel plug assay, chick chorioallantoic membrane assay or the corneal angiogenesis assay maintain complexity but have certain limitations such as being low through-put and semi-quantitative (Chimote *et al.*, 2014). The *fli1:EGFP* zebrafish developmental angiogenesis model has emerged in recent times as a valuable model to evaluate the efficacy and toxicity of novel anti-angiogenic compounds. This model expresses enhanced green fluorescent protein (EGFP) in the entire vasculature under the control of the fli1 promoter and thus enables the visualisation of effects to vessel formation by anti-angiogenic therapies and offers an easy-to-maintain, high-throughput and easily quantifiable screening tool. It has proven efficacy as an angiogenesis model for the investigation of the main classes of anti-angiogenic therapies used pre-clinically and clinically such as VEGF/VEGFR inhibitors or multi tyrosine kinase inhibitors such as sunitinib and sorafenib (Chimote *et al.*, 2014). In this model the sprouting of intersegmental vessels (ISV) from the dorsal aorta is monitored. It is not known if migrating angioblasts differentiate into endothelial cells before the sprouting process or whether this is a later event as there is no known marker to differentiate the two cell types (Staton *et al.*, 2004). This is a limitation of the model because if angioblasts remain during sprouting, the process is actually vasculogenesis and not angiogenesis (Staton *et al.*, 2004). Therefore the importance of *in vitro* models such as the 2-D tubule formation assay, which use differentiated human endothelial cells such as HUVECs, cannot be disregarded. *In vitro* models still have utility in determining anti-angiogenic effects, particularly in combination with more complex screening tools.

There are some examples in the literature of the pre-clinical use of novel lipoxygenase inhibitors as anti-angiogenic therapies. For example a synthetic dl-nordihydroguaiaretic acid (Nordy) compound that inhibits 5-LO activity and was previously shown to have anti-tumour activity in glioblastoma (Boado *et al.*, 1992) has been shown recently to markedly reduce tubule formation by tumour-derived endothelial cells, and also glioma xenograft -induced neoangiogenesis in a zebrafish model, (Bian *et al.*, 2006, Yang *et al.*, 2014). In another study a class of novel compounds derived from natural curcuminoids, which have been shown to have 12-LO inhibitory potential, were shown to reduce sprouting formation of endothelial cells (Jankun *et al.*, 2006). A number of 5-LO inhibitors are currently in clinical trial for different inflammatory diseases, including the FDA approved potent and selective 5-LO inhibitor Zileuton (Harris *et al.*, 1995, Berger *et al.*, 2007) and some of the newer industry developed inhibitors such as atreleuton (VIA Inc.), setileuton (Merck Inc.) and PF-419183 (Pfizer Inc.) (see Table 1.3). A novel class of 5-LO inhibitors based on a phenylenediamine scaffold have been developed which show nanomolar potency and more than 30-fold increased selectivity for 5-LO over other lipoxygenase paralogues (Hoobler *et al.*, 2013). In comparison to the continued interest in 5-LO inhibitor development, the discovery of selective and potent 12-LO inhibitors has had limited success, making it difficult to investigate thoroughly the anti-angiogenic effects of blocking this enzyme pathway. For example baicalein, one of the only commercially available inhibitors of the 12-LO pathway originally shown to exert potent anti- 12-LO activity at nanomolar concentrations (Sekiya and Okuda, 1982) has since been discovered to have equipotency for both 15-LO-1 and 12-LO (Deschamps *et al.*, 2006). Therefore the anti-angiogenic effects of this compound described previously (Miocinovic *et al.*, 2005) may be due to alternate/dual pathway inhibition. The same chemists who created the novel 5-LO inhibitors discussed (Hoobler *et al.*, 2013) have used qHTS of large libraries of compounds to yield a number of new anti-12-LO structures with superior potency and specificity over previous natural compounds (Kenyon *et al.*, 2011, Luci *et al.*, 2014). A new generation of 12-LO synthetic inhibitors designed based on an 8-hydroxyquinoline scaffold have shown superior selectivity for 12-LO, (IC_{50}~1 ±0.2 μM) compared to 15-LO (IC_{50} > 150 μM) and COX-1/COX-2 (IC_{50} >100 μM) purified enzymes (Kenyon *et al.*, 2011). Primary investigations using an *in vitro* human platelet assay revealed an IC_{50} value of 13 ±5 μM and an inhibition of 12(S)HETE production of 70-74% in donor beta islets cells. Re-analysis of the original qHTS has uncovered a second generation of 12-LO inhibitors based on a benzenesulfonamide scaffold (Luci *et al.*, 2014). This new class of 12-LO inhibitor have 12-LO IC_{50} values of less than 250 nM and similar inhibition of

12(S)HETE production as reported for the first generation compounds however they appear to be more drug-like and amenable to modification. The generation of new lipoxygenase inhibitors with greater specificity and potency, such as these may potentiate research on the role of these enzymes in different pathophysiologies and validate their potential as therapeutic targets.

Bearing in mind the evidenced role of 5 and 12-LO in tumourigenesis and angiogenesis and the unexplored effect of the aforementioned novel compounds in the context of angiogenesis, a panel of these compounds were assessed using *in vitro* and *in vivo* angiogenic models.

5.2 Aims and objectives

The aim of this chapter was to investigate the anti-angiogenic effect of novel 5-LO and 12-LO inhibitors. A panel of drugs including published phenylenediamine-based 5-LO inhibitors and 8-hydroxyquinoline-based 12-LO inhibitors and a second panel of the published benzenesulfonamide-based compounds were provided by our collaborator Dr. David Maloney (NIH Chemical Genomics Centre, National Centre for Advancing Translational Sciences, Bethesda, Maryland, USA) for this purpose. In addition a number of unpublished oxadiazol-2-yl benzamide-based structures with 12-LO inhibitory potential were also included. Through investigations with a number of molecular techniques, namely a zebrafish developmental model and HUVEC *in vitro* assays, we aimed to identify compounds from the panel with novel anti-angiogenic effects

Specific Objectives:

- Investigate the anti-angiogenic potential of novel 5-LO and 12-LO inhibitors using an *in vivo fli1:EGFP* zebrafish model

- Investigate the functional effects of novel compounds on endothelial cell proliferation and apoptosis and their anti-angiogenic potential using the tubule formation assay

- Investigate whether these compounds affect angiogenesis-related gene expression and protein production

5.3 Results

5.3.1 Zebrafish screening

As discussed in Section 5.1, the *fli1:EGFP* zebrafish has become an important screening tool for anti-angiogenic compounds. The suitability of this model to test the anti-angiogenic potential of commercial and novel small molecule 5-LO and 12-LO inhibitors was investigated through a collaboration with Dr. Breadan Kennedy (Conway Institute of Biomolecular and Biomedical Research, University College, Dublin). A panel of 5-LO inhibitors (named NIH1-4) with a phenylenediamine-based scaffold and a mixed panel of 12-LO inhibitors based on either an oxadiazol-2-yl benzamide or an 8-hydroxyquinoline backbone were initially tested (named NIH5-15). An additional panel of 12-LO inhibitors based on a benzenesulfonamide structure were subsequently tested (named GM1-7). The full structure of all novel compounds can be found in Appendix VI). DMSO (0.25%-1.0%), which does not affect zebrafish embryonic development was used as the vehicle/negative control (Figure 5.1a) and 10 μM SU11652, multi-kinase inhibitor with similar efficacy to sunitinib, was used as a positive control in every screen due to its potent anti-angiogenic effects (Figure 5.1b). As discussed in Section 2.21.2, the number of intersegmental vessels (ISVs) were counted (indicates anti-angiogenic specific effects of drugs) and the length of the embryo from head to tail was measured (indicates developmental or toxic effects of drugs) (Figure 5.1c). Examination of the literature indicated that a minimum of 30-40% decrease in ISV formation was observed in this model with known anti-angiogenic compounds (Chimote *et al.*, 2014) and therefore 30% was used as a cut-off value for potential anti-angiogenic drug hits.

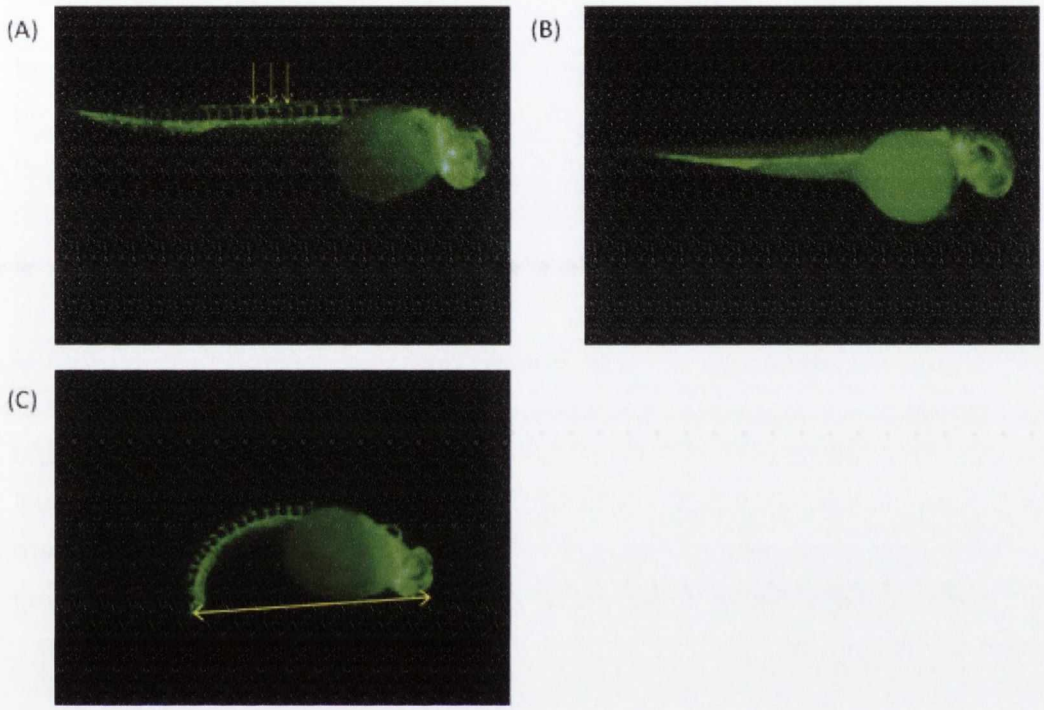

Figure 5.1 *Fli:EGFP* zebrafish embryos were used as an angiogenic screening model. Embryos at 6 hours post-fertilization were treated with drugs for 48 hours. After fixation the embryos were examined and imaged at 4X magnification using a fluorescent microscope. (A) a normal healthy control contains a full set of ISVs (yellow arrows). (B) SU11652 was used as a positive control and resulted in 100% blockage of ISV formation at treatment dose of 10 μM. (C) A measurement of the length between the head and tail of the embryo was used as an indication of toxicity-induced dorsal axis curvature. Images are 4X magnification.

5.3.2 5-LO drug screen in the *fli1:EGFP* zebrafish angiogenesis model

An initial screen of all novel 5-LO inhibitors (NIH1-4) and commercially available inhibitors (zileuton, REV 5901 and dual thromboxane synthase/5-LO inhibitor ketoconazole), at 10 μM, showed no effects on ISV formation or on the overall development of the zebrafish embryos (data not shown). No effect on ISV was noted at the higher dose of 25 μM in any of the novel 5-LO inhibitors but developmental effects to zebrafish were noted by measuring the length of the zebrafish as an indication of axis curvature (Figure 5.2a and Figure 5.2b). A decrease of >50% in ISVs was noted with ketoconazole treatment, however this was accompanied by undesired larval malformations in most embryos (Figure 5.2b). Representative images of zebrafish treated with 5-LO inhibitors at higher doses of 25 μM, 50 μM and 100 μM are depicted in Figure 5.3. The type and severity of the malformations varied but were consistently present across all experiments at these higher doses. For example NIH4 at 50 μM resulted in mild effects on curvature and no apparent effect on ISVs whereas NIH2 at 50 μM treatment led to a more severe corkscrew tail morphology (Figure 5.2 and Figure 5.3). In contrast, specific 5-LO inhibitor zileuton had no effect on ISV or larval development up to the highest test dose of 100 μM (Figure 5.3). All drug screens were carried out on three separate experimental days (n=3), with 10 embryos per drug treatment per experiment.

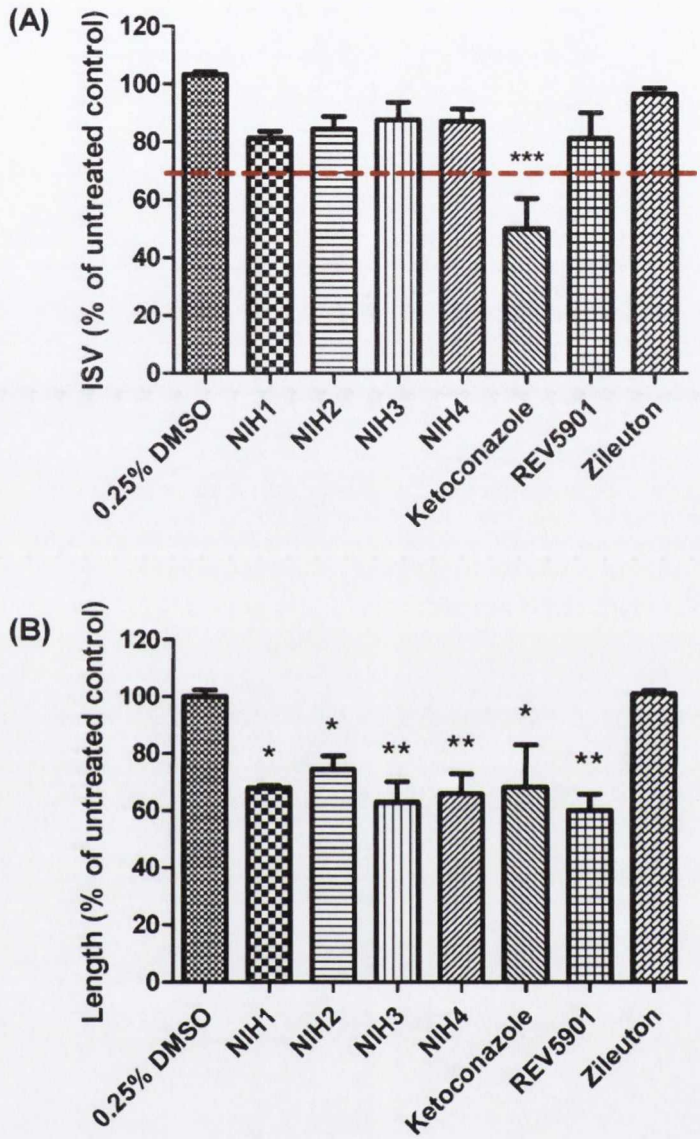

Figure 5.2 Novel 5-LO inhibitors do not affect angiogenesis in the zebrafish embryo however ketoconazole has both effects to vessel formation and larval development. (A) 25 μM NIH-4 REV 5901 and zileuton treatment did not affect ISV formation (n=3) however 25 μM ketoconazole caused a significant decrease in ISV numbers (103.37 ±0.87% versus 59.33 ± 7.08%, $p<0.001$) that was greater than the 30% decrease cut-off set for this study (see red dotted line). (B) 25 μM Ketoconazole and all other 5-LO inhibitors caused significant decreases to embryo length compared to the vehicle control indicating toxicity or developmental effects. Statistical test used was one-way ANOVA with Tukey's Multiple Comparison Test: n=3, $p<0.05$(*), $p<0.01$(**) and $p<0.001$(***). Error bar denotes mean ± S.E.M.

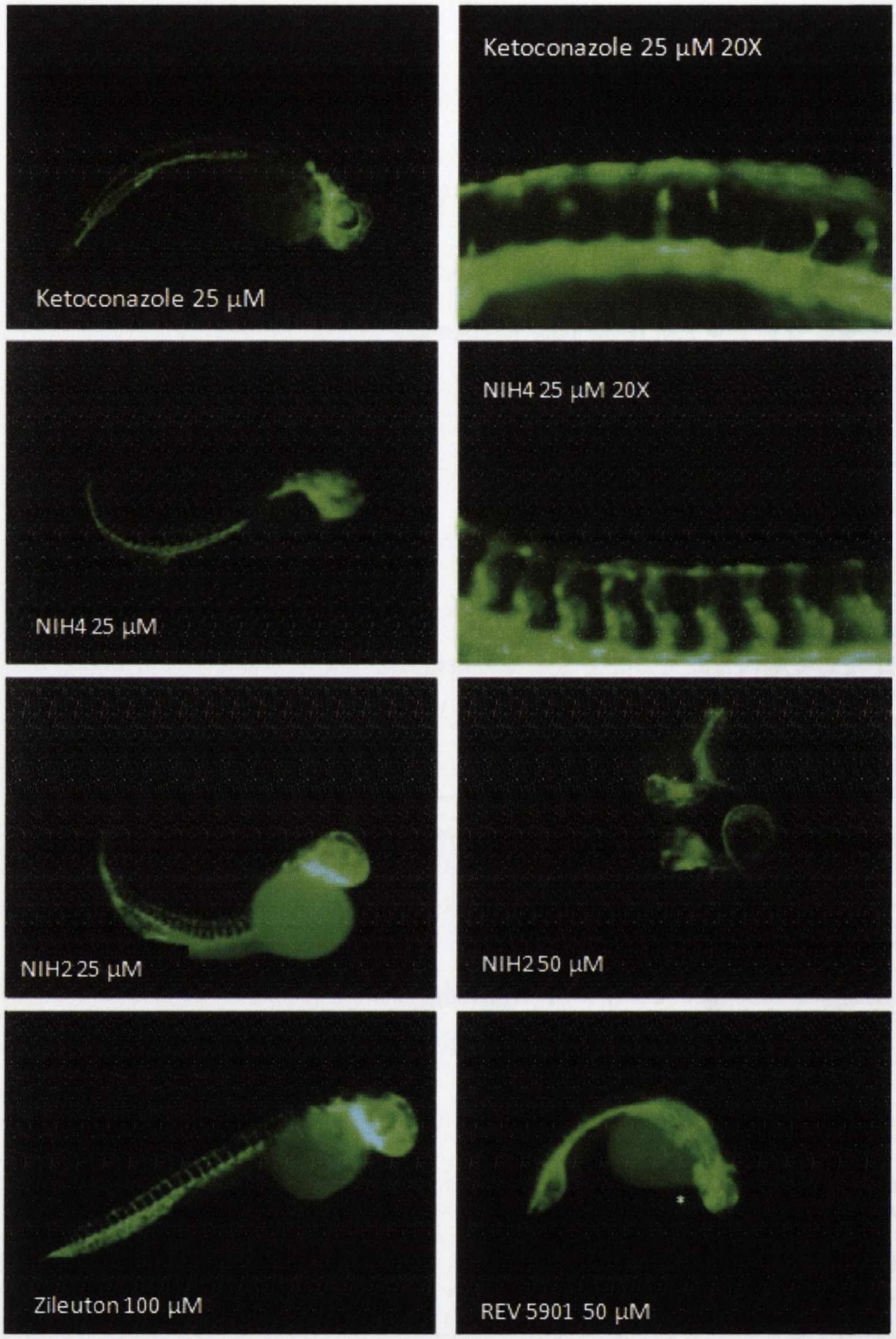

Figure 5.3 Representative images of zebrafish embryos treated with 5-LO inhibitors. 25 µM ketoconazole treatment led to missing or sprouting ISVs. 50 µM NIH4 resulted in mild effects to axial curvature but no effect to ISV number. 50 µM NIH2 resulted in a more severe corkscrew tail morphology. 50 µM REV 5901 caused severe axial curving and pericardial oedema (indicated by *) while a maximum tested concentration of 100 µM zileuton had no effect on ISV number or larval development. Images are 4X and 20X magnification.

5.3.3 12-LO drug screen in the *fli1:EGFP* zebrafish angiogenesis model

At the recommended starting dose of 10 μM the novel 12-LO inhibitors (NIH5-15) and the commercial 12-LO inhibitor baicalein did not show any effect on ISV number or any toxic effect (n=3, data not shown). Similarly there was no effect at 25 μM (n=2, data not shown). A dose 50 μM NIH15 was the only drug at this higher screening dose to significantly decrease ISV number compared to control (99.30 ±0.58% versus 64.73 ±8.27%, n=2, ANOVA with Tukey post-test; $p<0.001$) (Figure 5.4a). This was not without an accompanying decreased larval length (99.39 ±0.41% versus 74.67 ±9.82%, n=2, ANOVA with Tukey post-test $p<0.001$) (Figure 5.4a). This decrease was found to be due to an overall minor reduction in the size of the fish rather than dorsal axis curvature defects (see Figure 5.5). In a dose escalation study of NIH15 the maximal tested dose of 100 μM NIH15 was very toxic to normal embryonic development and led to almost a 50% decrease in larval length (Figure 5.4c and Figure 5.5). Although not significant it was noted that NIH13 decreased ISV number by approximately one-fifth with no change to larval length indicating a minor anti-angiogenic effect in this model (99.30 ±0.58% versus 82.28 ±1.27%) (Figure 5.4a).

As discussed in Section 5.3.1 an additional panel of second generation 12-LO inhibitors based on a benzenesulfonamide scaffold were provided. Screening of these new compounds (GM1-7) in the *fli1:EGFP* zebrafish model failed to reveal any anti-angiogenic potential at 10 μM (n=3, data not shown). The compounds were screened up to a maximum dose of 100 μM (n=2) and did not show any effect to ISVs or normal larval development (Figure 5.6).

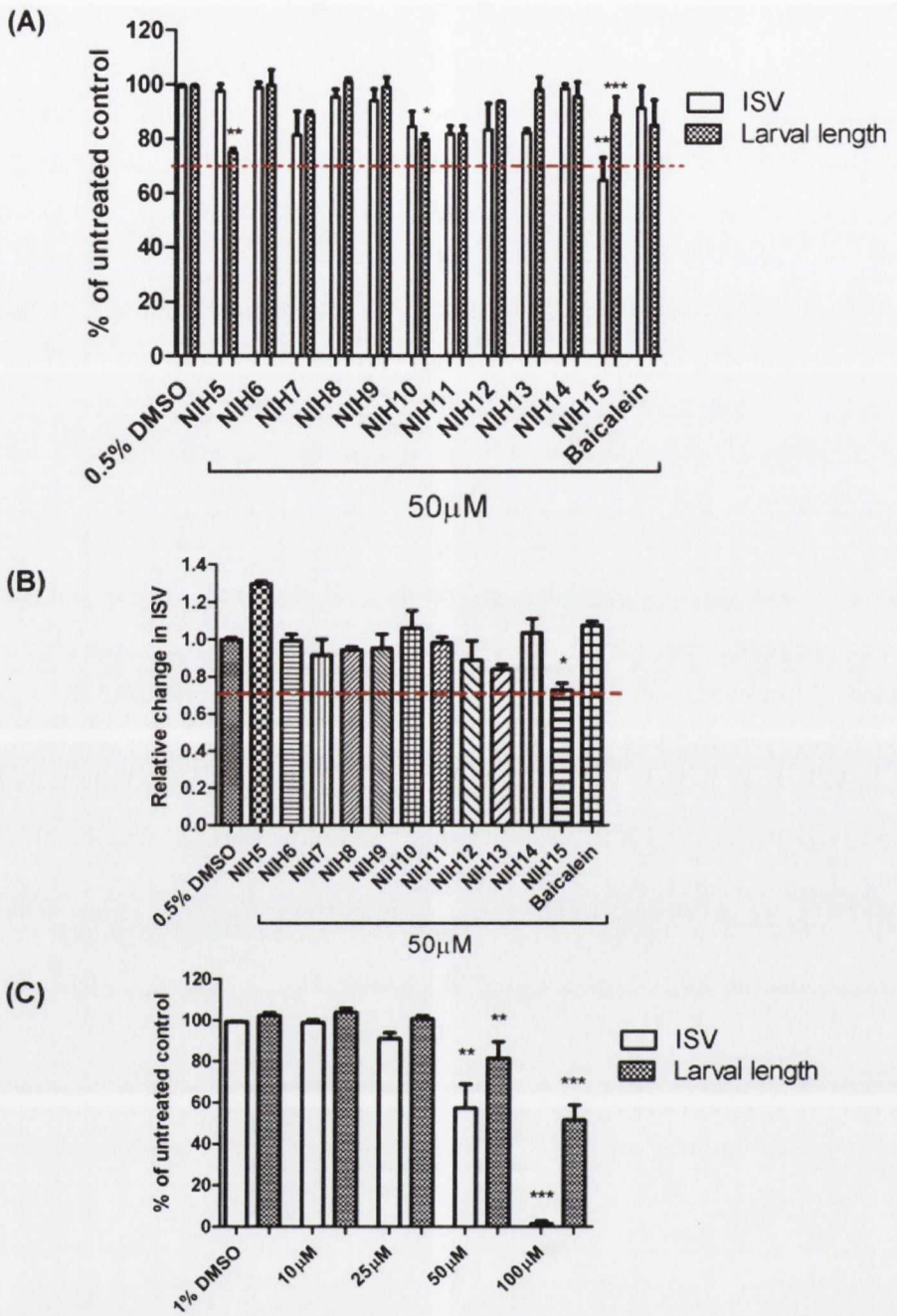

Figure 5.4 Novel 12-LO inhibitor NIH15 significantly reduces vessel formation by over thirty percent at a dose of 50 μM. (A) In a 50 μM screen of 12-LO inhibitors (n=2, 10 embryos per treatment and per experiment) baicalein and novel 12-LO compounds NIH5-14 did not significantly affect ISV formation. 50 μM NIH15 caused a significant decrease to ISV that was greater than the 30% decrease cut-off set for this study (see red dotted line) ($p<0.01$). Although not significant it was noted that NIH13 decreased ISV formation by about one-fifth (99.30 ±0.58% versus 82.28 ±1.27%). Undesired significant decreases in larval length compared to control for NIH5, NIH10 and NIH15 were noted. (B) Alternate graphical representation showing % change in ISV relative to % change in larval length. (C) In a dose escalation study of NIH15 (n=3) the maximal tested dose of 100 μM was toxic to normal embryonic development and led to almost a 50% decrease in larval length, indicating drug toxicity. Statistical test used was one-way ANOVA with Tukey's Multiple Comparison Test. $p<0.05$(*), $p<0.01$(**) and $p<0.001$(***). Error bar denotes mean ± S.E.M.

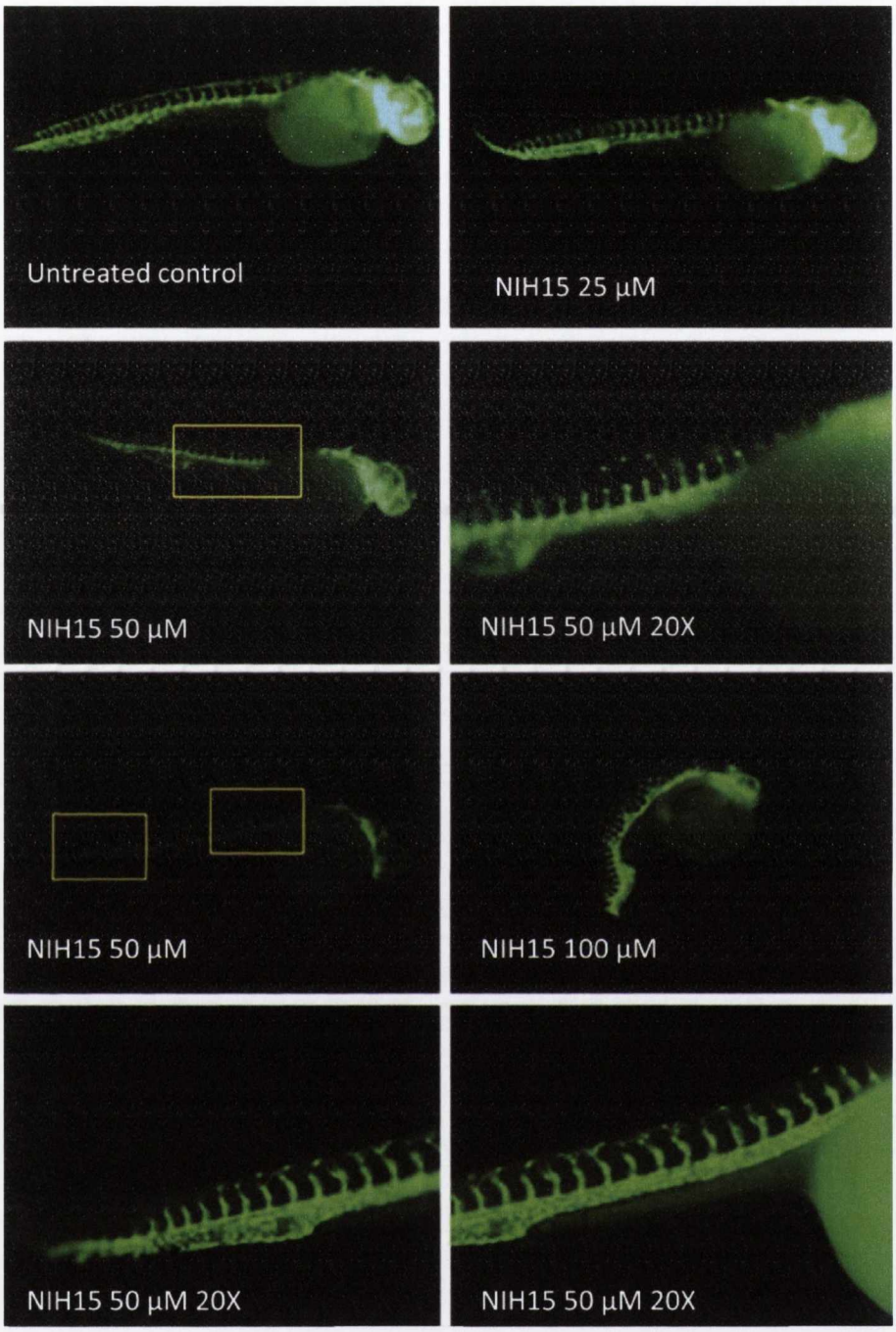

Figure 5.5 50 µM NIH15 does cause any curving of the dorsal axis of the zebrafish and does not have any other untoward morphological effects. Images show embryos from the same experimental day: untreated (i.e. DMSO vehicle control), 25 µM, 50 µM and 100 µM NIH15 treatment. Zebrafish treated with 25 µM NIH15 were unaffected and look similar to untreated control. Zebrafish treated with 50 µM NIH15 also tend to look similar to the untreated control, i.e. there is no axial curving and no obvious yolk sac oedema. Only a minor reduction in the overall size of the embryo compared to control was noted. Abnormally thin / fragile ISVs can be seen following 50 µM NIH15 treatment (see 20X images). At the highest dose of 100 µM axis-curving of the larvae and yolk sac oedema can be seen. Images are 4X and 20X magnification.

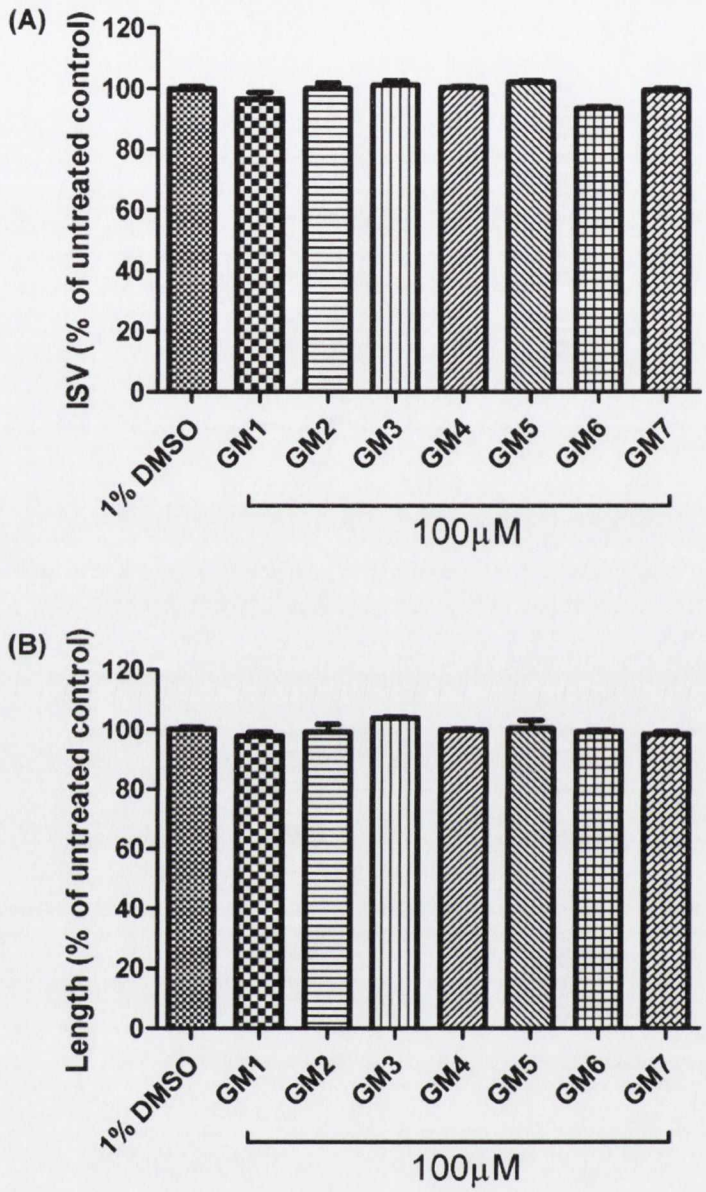

Figure 5.6 Benzenesulfonamide based 12-LO inhibitors have no effect on angiogenesis or embryonic development in zebrafish. (A) 100 μM GM1-7 did not affect ISV formation and (B) larval length compared to control (1% DMSO). Statistical test used was one-way ANOVA (n=2).

5.3.4 Investigation of the anti-angiogenic potential of 5-LO and 12-LO inhibitors using *in vitro* models

The process of angiogenesis requires a number of steps including endothelial cell proliferation, migration and differentiation. As an alternative strategy to study the anti-angiogenic potential of novel 5-LO and 12-LO inhibitors, the effect of the compounds on endothelial cell (HUVECs) proliferation at a number of concentrations was studied by BrdU proliferation assay (Section 2.22). Additionally, *in vitro* tubule formation (i.e. endothelial cell migration and differentiation) was used as a model to test the anti-angiogenic effects of the compounds (Section 2.25).

A number of compounds in the initial panel (i.e. NIH1-15) were no longer available for further study after the zebrafish screen due to the discovery of a flat structural activity relationship (SAR, i.e. the compound is not amenable to structural modification to increase potency) and subsequent cessation of synthesis by our collaborators (Maloney *et al.*) (see Table 5.1). Fortunately the drugs in the panel that were no longer available had not shown any effect in the initial zebrafish screens and the two compounds of interest NIH15 and NIH13 were both still available. 6 compounds were still available: one 5-LO inhibitor NIH4, four 12-LO inhibitors based on a oxadiazol-2-yl backbone, including the only zebrafish screen hit, NIH15, and 2 compounds with an 8-hydroxyquinoline backbone, including NIH13 which had minor anti-angiogenic effects).The second panel of seven benzenesulfonamide-derived structures (GM1-7) which are the most recently developed and best in class 12-LO inhibitors developed by our collaborators, were all available for *in vitro* work.

Table 5.1 List indicating which lipoxygenase inhibitors from the original drug panel are no longer available due to flat structural activity relationship

Drug	Target	Backbone	Availability (Y/N)
NIH1	5-LO	Phenylenediamine	N
NIH2	5-LO	Phenylenediamine	N
NIH3	5-LO	Phenylenediamine	N
NIH4	5-LO	Phenylenediamine	Y
NIH5	12-LO	8- hydroxyquinoline	N
NIH6	12-LO	8-hydroxyquinoline	Y
NIH7	12-LO	Oxadiazol-2-yl benzamide	Y
NIH8	12-LO	Oxadiazol-2-yl benzamide	Y
NIH9	12-LO	Oxadiazol-2-yl benzamide	Y
NIH10	12-LO	8-hydroxyquinoline	N
NIH11	12-LO	8-hydroxyquinoline	N
NIH12	12-LO	Oxadiazol-2-yl benzamide	N
NIH13	12-LO	8-hydroxyquinoline	Y
NIH14	12-LO	Oxadiazol-2-yl benzamide	N
NIH15	12-LO	Oxadiazol-2-yl benzamide	Y

5.3.5 Confirmation of *ALOX12* expression in HUVECs

While 5-LO is not normally expressed in HUVECs except under pathological circumstances (Benard *et al.*, 2014), endogenous 12-LO expression has been established (Funk *et al.*, 1992, Nie *et al.*, 2000). To confirm 12-LO expression in the HUVECs used for the duration of this study 1 µg of RNA from three different passages of HUVECs was analysed by RT-PCR using nested primers specific for *ALOX12* as previously described (Gao *et al.*, 1995, Nie *et al.*, 2000). PCR was conducted as described in Section 2.15 using primers located in different exons of the human platelet-type 12-LO to increase the sensitivity and/or specificity of the PCR reaction. A loading control of β-actin (*ACTB*) was used and a no template control was also included. First round PCR and second round nested PCR revealed single band products of approximately 450 base pairs (bp) and 345 bp respectively, as previously reported, indicating 12-LO expression (Figure 5.7).

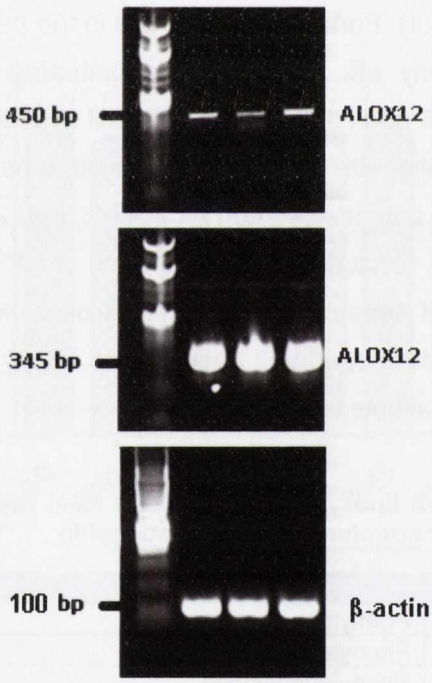

Figure 5.7 HUVEC endothelial cells are shown to express *ALOX12*. The sample lanes adjacent to the DNA ladder indicate three HUVEC cDNA samples derived from three different passages of cells and *ALOX12* was detected by nested PCR. The first round of PCR revealed a single band of approximately 450 bp and the second round PCR revealed a band size of approximately 345 bp. β-actin (*ACTB*) was used as a housekeeping gene/loading control.

5.3.6 Endothelial cell proliferation following 5-LO inhibitor treatment

HUVECs were treated with four doses (0.1 μM, 1 μM, 10 μM and 25 μM) of commercial 5-LO inhibitors and the novel 5-LO inhibitor NIH4 for 24 hours. Cell proliferation was assessed by BrdU incorporation as described in Section 2.22. Ketoconazole and NIH4 were found to significantly inhibit cell proliferation compared to vehicle control (0.25% DMSO) at 10 μM and 25 μM doses (Figure 5.8a and Figure 5.8d) while REV 5901 significantly inhibited proliferation at a dose of 25 μM (Figure 5.8b). Zileuton did not show any effect on HUVEC cell proliferation after 24 hour treatment (Figure 5.8d). Non-linear regression analysis was used to determine the inhibitory concentration required to reduce the proliferative capacity of the cells by 50% of the observed range of response for each compound (i.e. IC_{50} dose) and NIH4 was found to have the lowest IC_{50} dose (Table 5.2).

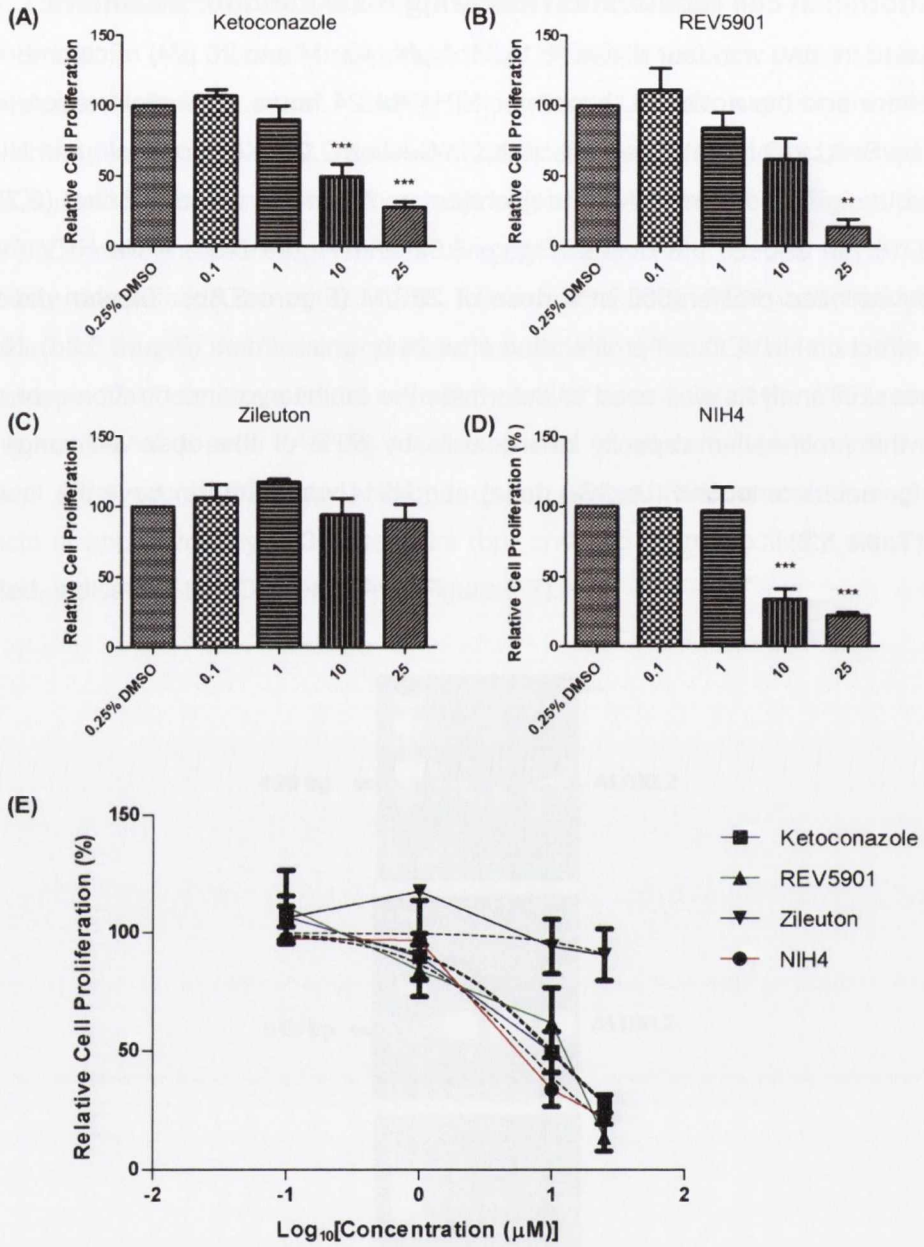

Figure 5.8 All 5-LO inhibitors tested except zileuton decrease HUVEC cell proliferation. Following drug treatment for 24 hours HUVEC relative cell proliferation (%) compared to vehicle control (0.25% DMSO) was measured by BrdU incorporation. (A) Ketoconazole decreased cell proliferation at 10 μM and (100% versus 49.53% ±8.76, $p<0.001$) and 25 μM (100% versus 27.80 ±3.77%, $p<0.001$). (B) 25 μM REV 5901 significantly decreased proliferation (100% versus 13.50 ±5.69%, $p<0.01$). (C) Zileuton did not affect HUVEC proliferation at any of the tested doses. (D) NIH4 significantly decreased cell proliferation at 10 μM (100% versus 33.85% ±7.23, $p<0.001$) and 25 μM (100% versus 22.09 ±2.11%, $p<0.001$). Statistical test used was one-way ANOVA with Tukey's Multiple Comparison Test: n=4, $p<0.01$(**) and $p<0.001$(***). Error bar denotes mean ± S.E.M. (E) Non-linear regression analysis using log transformed concentrations was used to calculate the IC_{50} for each compound.

Table 5.2 IC_{50} doses for HUVEC proliferation by 5-LO inhibitors determined by non-linear regression analysis

Drug	IC_{50} (μM)
Ketoconazole	9.73 ±0.09
REV 5901	10.17 ±0.16
NIH4	6.55 ±0.13

5.3.7 Endothelial cell proliferation following 12-LO inhibitor treatment

HUVECs were treated with four doses (0.1 μM, 1 μM, 10 μM and 25 μM) of the first panel of 12-LO inhibitors and three doses of baicalein (1 μM, 10 μM and 25 μM) for 24 hours and cell proliferation was assessed by BrdU incorporation. All of the compounds were found to significantly inhibit proliferation at 10 μM (Figure 5.9) while NIH13 and NIH15 were found to be the most potent with significant levels of suppression of cellular proliferation at doses as low as 1 μM (Figure 5.9e and Figure 5.9f). Notably, NIH13 and NIH15 were the only two compounds to show anti-angiogenic potential in the zebrafish model.

HUVECs were treated with three doses (1 μM, 10 μM and 25 μM) of the second panel of 12-LO inhibitors (GM1-7). The only significant effects on proliferation observed were at the higher dose of 25 μM in compound GM4, GM5 and GM6 (Figure 5.11). Non-linear regression analysis was used to determine the IC_{50} dose for all 12-LO compounds (Figure 5.10 and Figure 5.11h) where possible and the doses are listed in Table 5.3. NIH13, NIH15 and GM5 had the lowest IC_{50} doses for their respective structural groups and had lower IC_{50} doses than the commercially available 12-LO inhibitor baicalein.

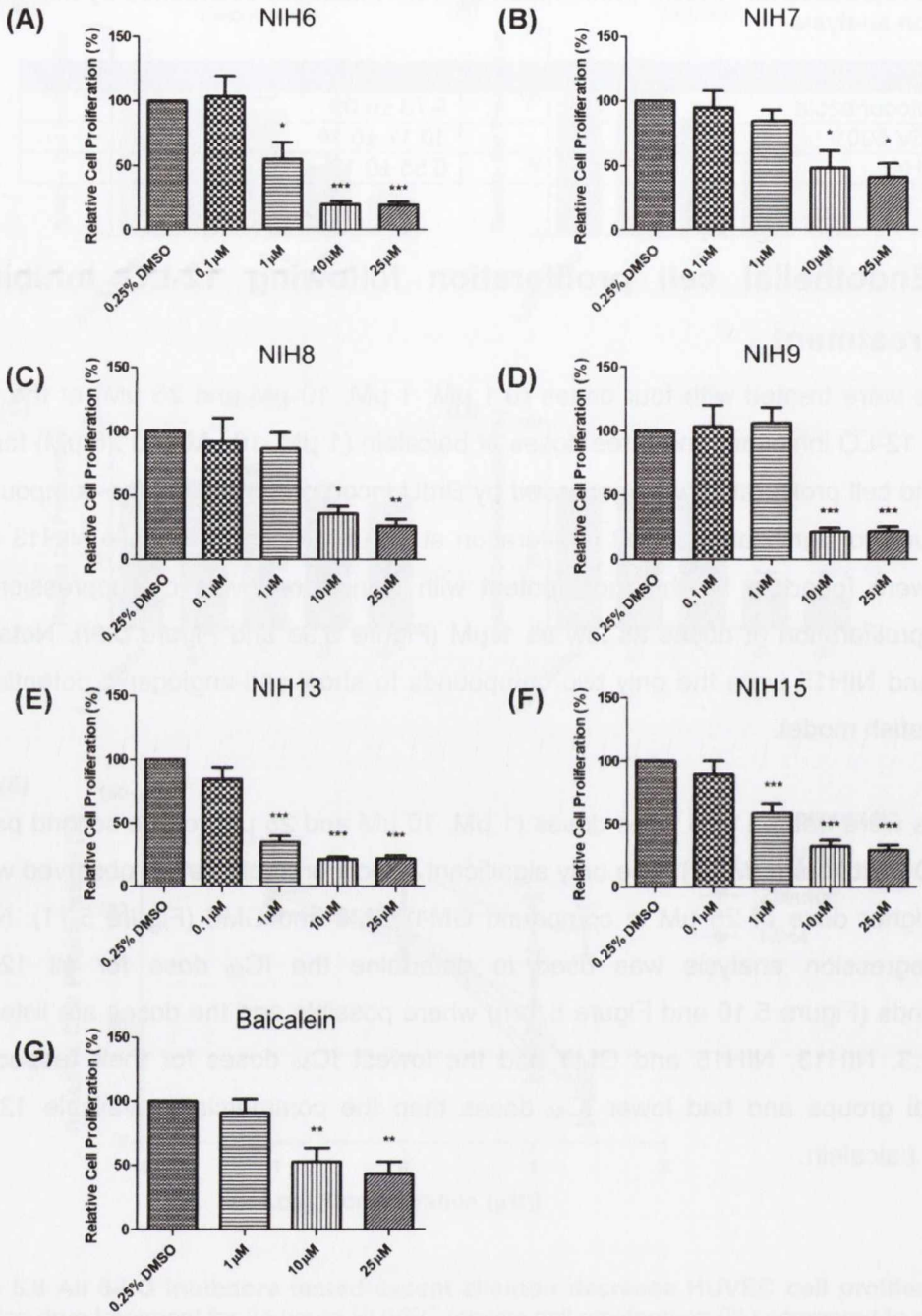

Figure 5.9 NIH13 and NIH15 are the most potent inhibitors in the original panel with significant inhibition of HUVEC proliferation shown at 1 μM doses. Following drug treatment for 24 hours HUVEC relative cell proliferation (%) compared to vehicle control (0.25% DMSO) was measured by BrdU incorporation. (A) NIH6, (B) NIH7 (C) NIH8 (D) NIH9, (E) NIH13, (F) NIH15 and (G) baicalein. NIH13 and NIH15 were shown to be the most potent drugs in the panel of novel drugs significantly decreasing proliferation at the lower dose of 1 μM (100% versus 34.76 ±4.76%, $p<0.001$ and 100% versus 58.44 ±8.17% respectively). In comparison, baicalein did not show any effect on proliferation at the 1 μM dose. Statistical test used was one-way ANOVA with Tukey's Multiple Comparison Test: n=4, $p<0.05$(*), $p<0.01$(**) and $p<0.001$(***). Error bar denotes mean ± S.E.M.

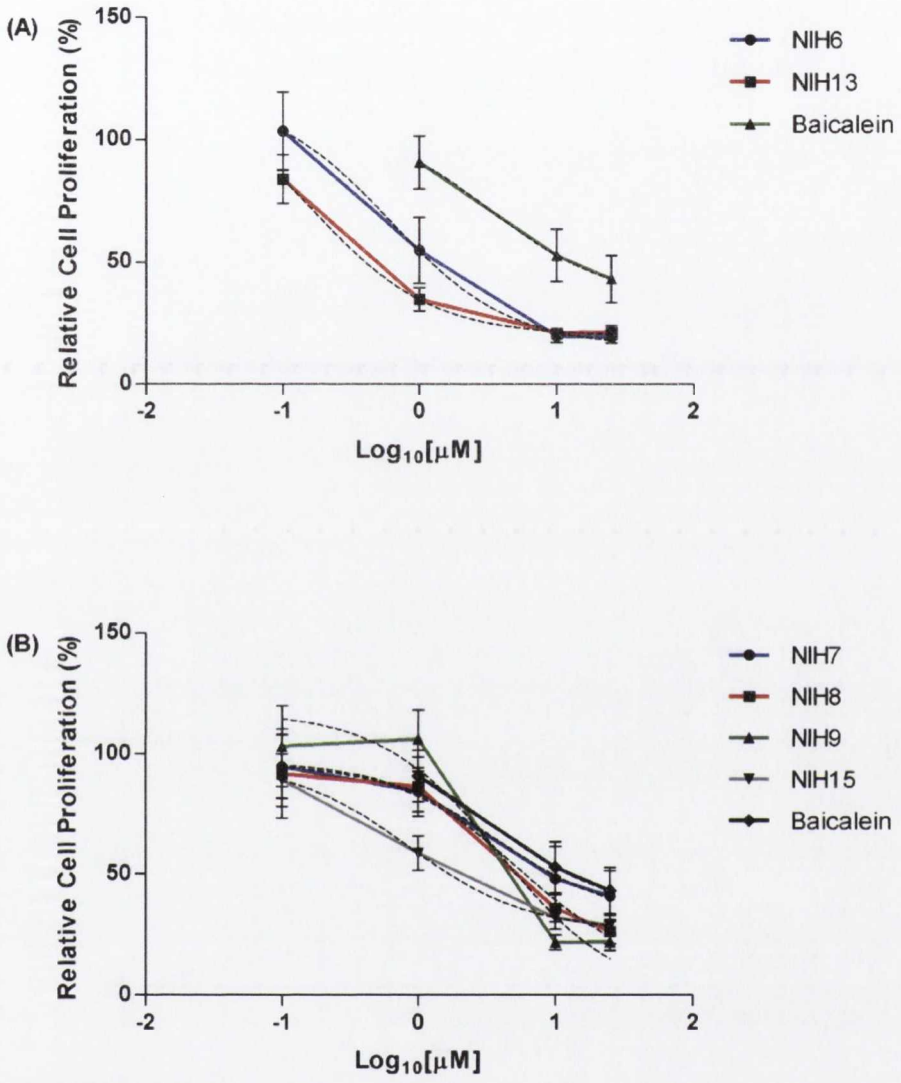

Figure 5.10 Non-linear regression analysis using log transformed concentrations was used to calculate the IC_{50} for each 12-LO compound. For this analysis the 8-hydroxyquinoline -derived compounds and baicalein were compared (A) or the oxadiazol-2-yl derived compounds and baicalein were compared (B). NIH13 and NIH15 had the lowest calculated IC_{50} doses.

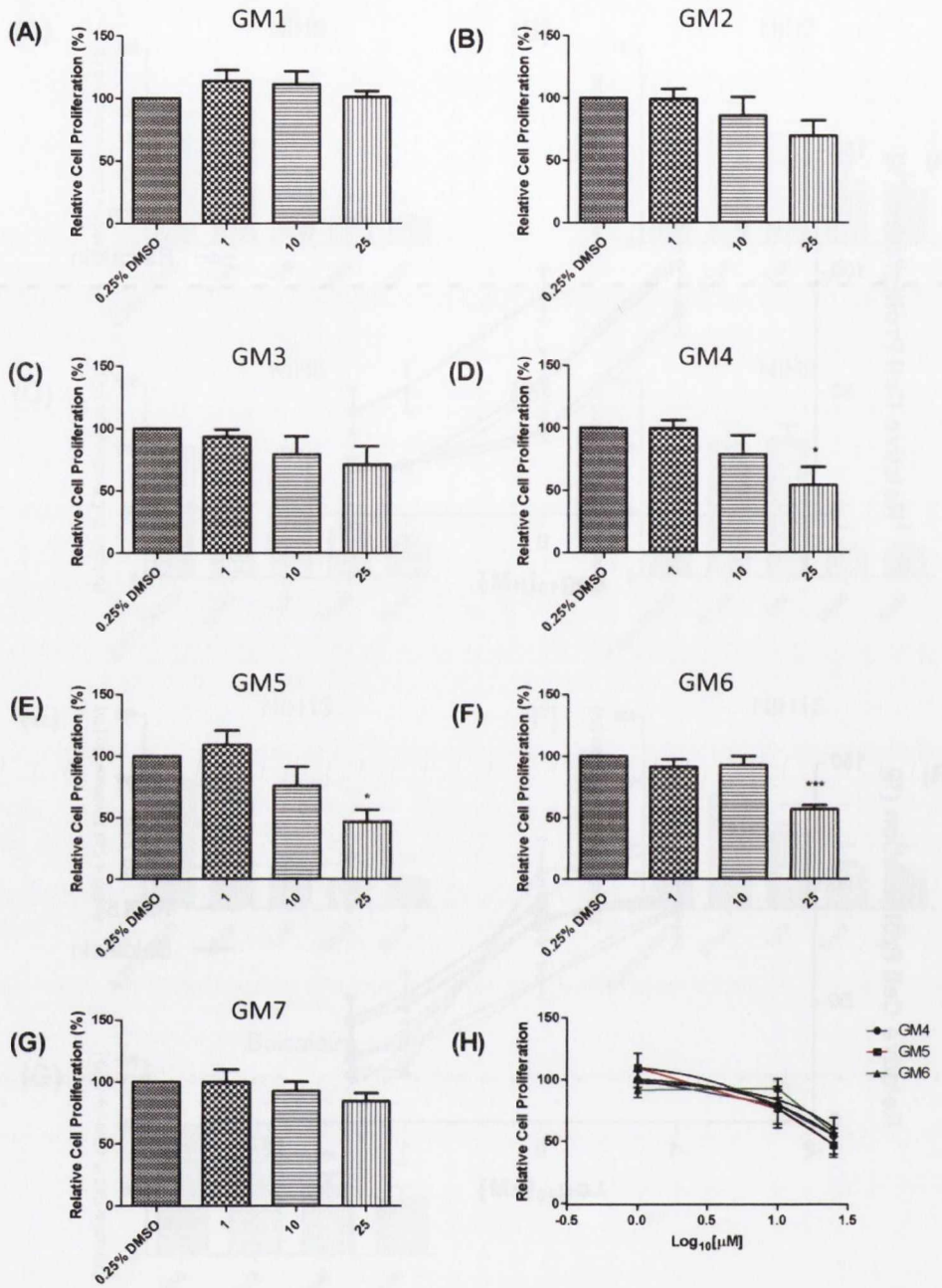

Figure 5.11 12-LO inhibitors GM4, 5 and 6 inhibit HUVEC proliferation at a dose of 25 μM. Following drug treatment for 24 hours HUVEC relative cell proliferation (%) compared to vehicle control (0.25% DMSO) was measured by BrdU incorporation. (A) GM1, (B) GM2, (C) GM3, and (G) GM7 showed no effect on cell proliferation. (D) GM4 inhibited cell proliferation at 25 μM. (E) GM5 inhibited cell proliferation at 25μM. (F) GM6 also inhibited cell proliferation at 25μM. Statistical test used was one-way ANOVA with Tukey's Multiple Comparison Test: n=4, $p<0.05$(*), and $p<0.001$(***). Error bar denotes mean ± S.E.M. (H) Non-linear regression analysis using log transformed concentrations was used to calculate the IC_{50} for each compound.

Table 5.3 IC_{50} doses for HUVEC proliferation by 12-LO inhibitors determined by non-linear regression analysis

Structure	Drug	IC_{50} dose (μM)
5,6,7-trihydroxyflavone	Baicalein	11.78
8-hydroxylquinoline	NIH 6	1.67
	NIH13	0.64
Oxadiazol-2-yl	NIH7	11.59
	NIH8	6.45
	NIH9	5.27
	NIH15	3.69
Benzenesulfonamide	GM4	>25*
	GM5	25.88
	GM6	>25*

*cannot determine IC_{50} accurately as dose escalation study did not reach 50% inhibition of proliferation

5.3.8 Investigation of the effect of lipoxygenase inhibitors on endothelial cell tube formation

Endothelial cells have the inherent ability to form capillary-like structures (tubules) when seeded on a growth factor-reduced collagen gel matrix. This early re-organisation stage of angiogenesis is characterised by multiple cellular-activated processes such as cell-cell adhesion, migration, survival and apoptosis and has been used extensively to screen the ability of potential anti-angiogenic compounds to inhibit tubule formation (Staton *et al.*, 2004). In this study the tubule formation assay was employed to investigate the anti-angiogenic potential of novel lipoxygenase inhibitors. Sub-confluent HUVECs were seeded onto collagen gel matrix coated wells and were incubated with compounds at concentrations of 10 μM and 25 μM as described in Section 2.25. DMSO (0.25%) was used as a vehicle control and 10 μM SU11652 was used as a positive control for tubule inhibition for each assay performed. Following fixation and imaging, the ability of a compound to inhibit tubule formation was assessed by measuring three parameters: the total tubule cord length in a well, the number of branch points (i.e. an intersection of two or more cords) and the number of loops (i.e. cord-enclosed regions). Appendix V displays representative images of these measurements in a HUVEC tubule formation assay image.

Ketoconazole, zileuton, REV 5901 and NIH4 did not show any significant inhibition of tubule formation compared to control at either 10 μM or 25 μM (n=3, data not shown). The commercial 12-LO inhibitor baicalein was shown to significantly inhibit tubule formation at a dose of both 10 and 25 μM (Figure 5.12). Structurally similar 8-hydroxyquinoline-derived compounds NIH6 and NIH13 showed consistent and significant inhibition of tubule formation in four to five independent experiments (Figure

5.13). Given that significant inhibition of tubule formation was observed at 10 μM for NIH13 (e.g. tubule length: 0.34 ±0.13, n=5, $p<0.01$), a 1 μM dose was also included in subsequent tubule assay plates however no effect was observed (n=3) (Figure 5.13d to Figure 5.13f). Comparison of the oxadiazol-2-yl-derived 12-LO inhibitors revealed that NIH15 was the most potent, showing increased inhibition of tubule formation indicated by total number of loops and total number of branch points (see Table 5.4) and the only significant decrease in total tubule length for this group of compounds (Figure 5.14). Investigation of inhibitory effects on HUVEC tubule formation by the panel of benzenesulfonamide-derived compounds revealed a modest but significant inhibition of tubule length by GM4 and GM5 at the 25 μM dose ($p<0.05$, n=4) (Figure 5.15). None of the other derivatives had any obvious effect to tubule length. The other 2 parameters quantified, i.e. total number of loops and total number of branch points were not significantly altered by GM1-GM7 compared to the vehicle control (n=3 or 4, data not shown). This would suggest that benzenesulfonamide class are not as effective at suppressing tubule formation as the other two 12-LO inhibitor structural groups. Additionally, this data suggests that measurement of total tubule length is the most sensitive of the three parameters for the detection of anti-angiogenic effects.

Of the compounds tested 10 μM NIH13 had the most potent effect in this assay decreasing total number of loops, total tubule length and total number of branch points by over 50% compared to untreated control (0.42 ±0.13, 0.43 ±0.13 and 0.36 ±0.13 respectively, where n=5 and $p<0.01$) (Figure 5.12d-f). Figure 5.16 shows representative images of the most potent 12-LO inhibitors from each different structural group (i.e. NIH13, NIH15 and GM5) with a corresponding vehicle control well from the same experimental set. Effects of baicalein and SU11652 (positive control) to tubule formation are also shown (Figure 5.16). The 12-LO inhibitors NIH13, NIH15 and GM5 were selected going forward for subsequent assays, in addition to the novel 5-LO inhibitor NIH4.

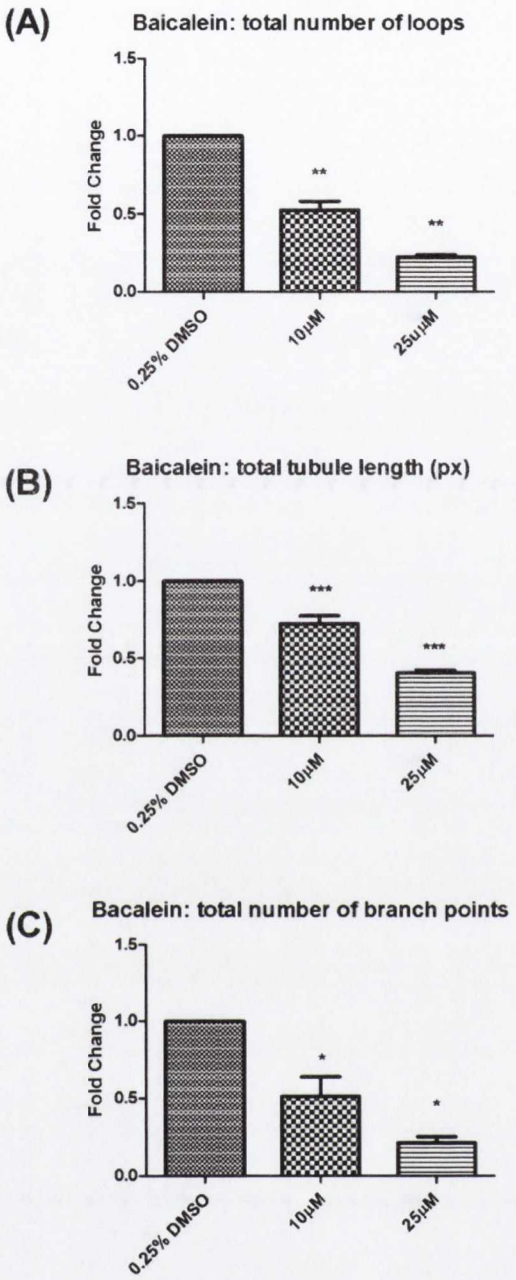

Figure 5.12 Baicalein significantly decreases tubule formation of HUVECs. HUVECs were seeded onto a collagen gel matrix suspended in 10 μM and 25 μM concentrations of baicalein. Tubule formation was examined after 10-12 hours incubation time. 10 μM baicalein showed significant inhibitory effects to tubule formation across all three parameters measured: (A) number of loop regions, (B) total tubule length and (C) number of branch points. This inhibitory effect was enhanced at the 25 μM dose. Statistical test used was one-way ANOVA with Tukey's Multiple Comparison Test. n=5 for 10 μM doses and n=4 for 25 μM doses, $p<0.05$(*), $p<0.1$(**), $p<0.001$(***). Error bar denotes mean ± S.E.M.

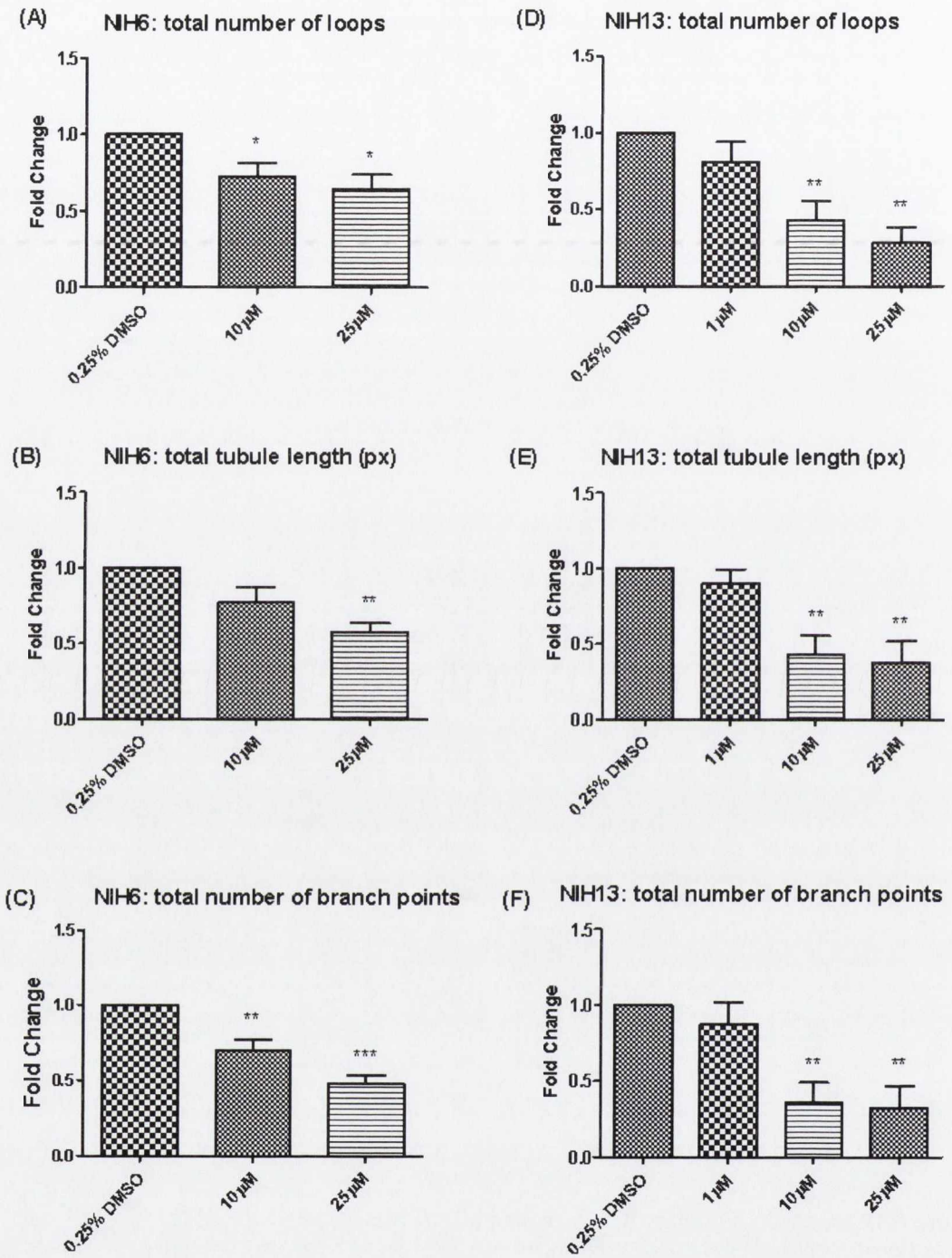

Figure 5.13 NIH6 and NIH13 significantly decrease tubule formation of HUVECs. HUVECs were seeded onto a collagen gel matrix suspended in 10 μM and 25 μM concentrations of baicalein, NIH6 and NIH13. A 1 μM dose was included for NIH13 too. NIH6 (A-C) and NIH13 (D-F) demonstrate significant inhibitory effects on all three parameters measured at both doses tested. NIH13 was shown to be the most potent decreasing number loops, total tubule length and number of branch points by more than 50% at the 10 μM dose (0.42 ±0.13, 0.43 ±0.13 and 0.36 ±0.13 respectively, where $n=5$ and $p<0.01$). Statistical test used was one-way ANOVA with Tukey's Multiple Comparison Test. $n=3$ for 1 μM dose, $n=5$ for 10 μM doses and $n=4$ for 25 μM doses, $p<0.05$(*), $p<0.1$(**), $p<0.001$(***). Error bar denotes mean ± S.E.M.

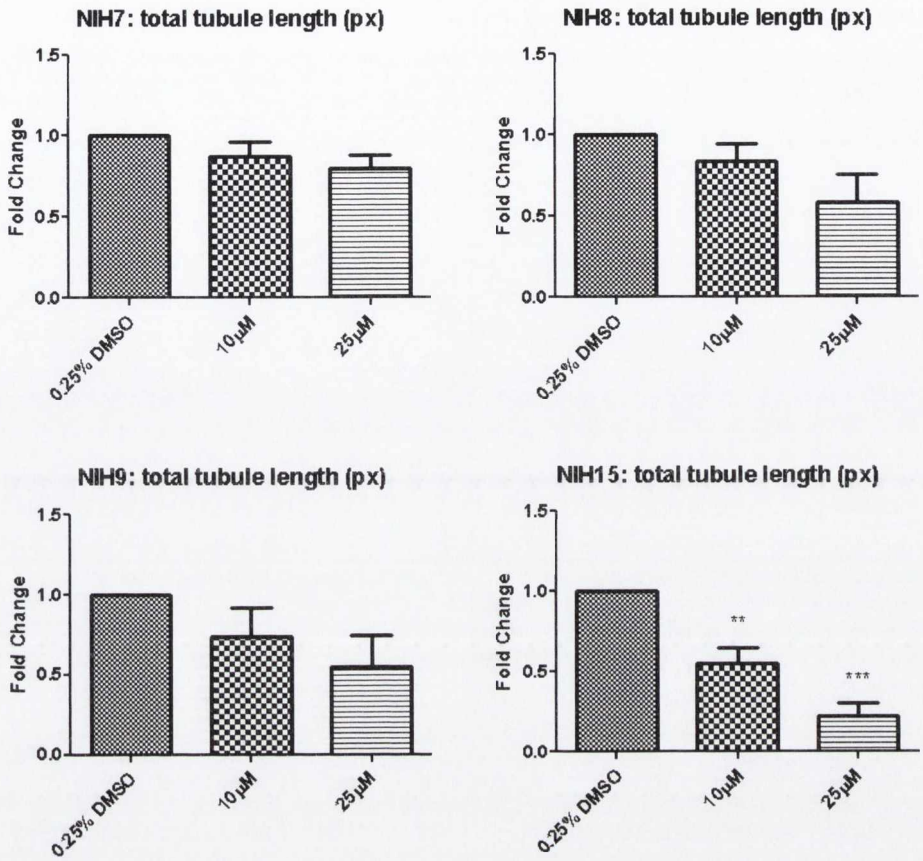

Figure 5.14 NIH15 is the most potent inhibitor of tubule formation of the oxadiazol-2-yl - derived 12-LO inhibitors. HUVECs were seeded onto a collagen gel matrix suspended in 10 μM and 25 μM of NIH7, NIH8, NIH9 and NIH15. NIH15 was only compound in the group to significantly decrease tubule length compared to control at both the 10 μM (0.55 ±0.10, n=4, $p<0.01$) and 25 μM dose (0.22 ±0.09, n=3, $p<0.001$). Statistical test used was one-way ANOVA with Tukey's Multiple Comparison Test. n=4 for 10 μM doses and n=3 for 25 μM doses, $p<0.1$(**), $p<0.001$(***). Error bar denotes mean ± S.E.M.

Table 5.4 Fold change in total number of HUVEC tubule loops and tubule branch points formed with oxadiazol-2-yl -derived 12-LO inhibitor treatment compared to control

Total number of tubule loops			
Drug Concentration	**Drug**	**Fold Change**	**p-value**
10 μM (n=4)	NIH7	0.98 ±0.03	N.S.
	NIH8	0.86 ±0.10	N.S.
	NIH9	0.76 ±0.15	N.S.
	NIH15	0.53 ±0.12	p<0.05
25 μM (n=3)	NIH7	0.90 ±0.06	N.S.
	NIH8	0.58 ±0.12	p<0.05
	NIH9	0.45 ±0.11	p<0.05
	NIH15	0.27 ±0.14	p<0.01
Total number of branch points			
Drug Concentration	**Drug**	**Fold Change**	**p-value**
10 μM (n=4)	NIH7	0.84 ±0.09	N.S.
	NIH8	0.79 ±0.09	N.S.
	NIH9	0.72 ±0.19	N.S.
	NIH15	0.41 ±0.11	p<0.01
25 μM (n=3)	NIH7	0.77 ±0.09	N.S.
	NIH8	0.57 ±0.16	p<0.05
	NIH9	0.32 ±0.14	p<0.05
	NIH15	0.16 ±0.10	p<0.01

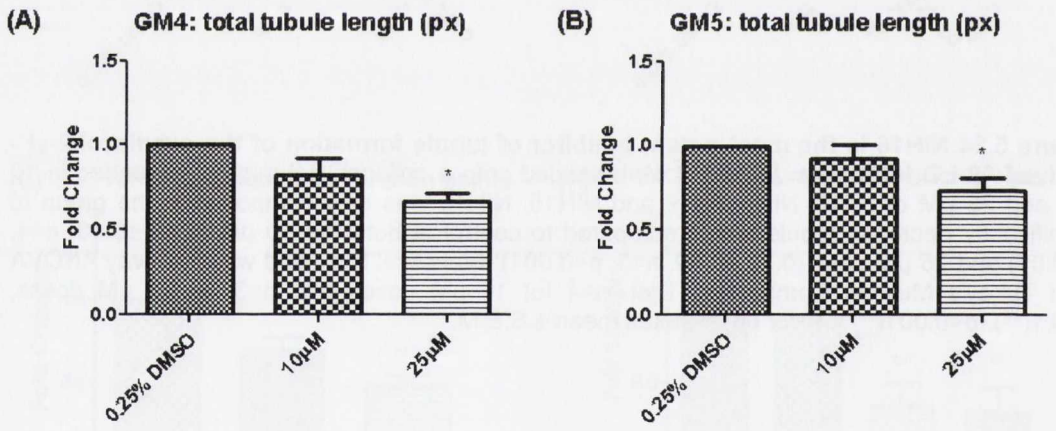

Figure 5.15 GM4 and GM5 show modest inhibitory effects on tubule formation of HUVECs. HUVECs were seeded onto a collagen gel matrix suspended in 10 μM and 25 μM concentrations of the benzenesulfonamide-derived panel of compounds (i.e. GM1-GM7). GM4 and GM5 were the only drugs to show modest but significant inhibitory effects on tubule formation, indicated by total tubule length, relative to untreated control (0.67 ±0.05,n=4, p<0.05 and 0.73 ±0.08, n=4, p<0.05 respectively). Statistical test used was one-way ANOVA with Tukey's Multiple Comparisons test. p<0.05(*).Error bar denotes mean ± S.E.M.

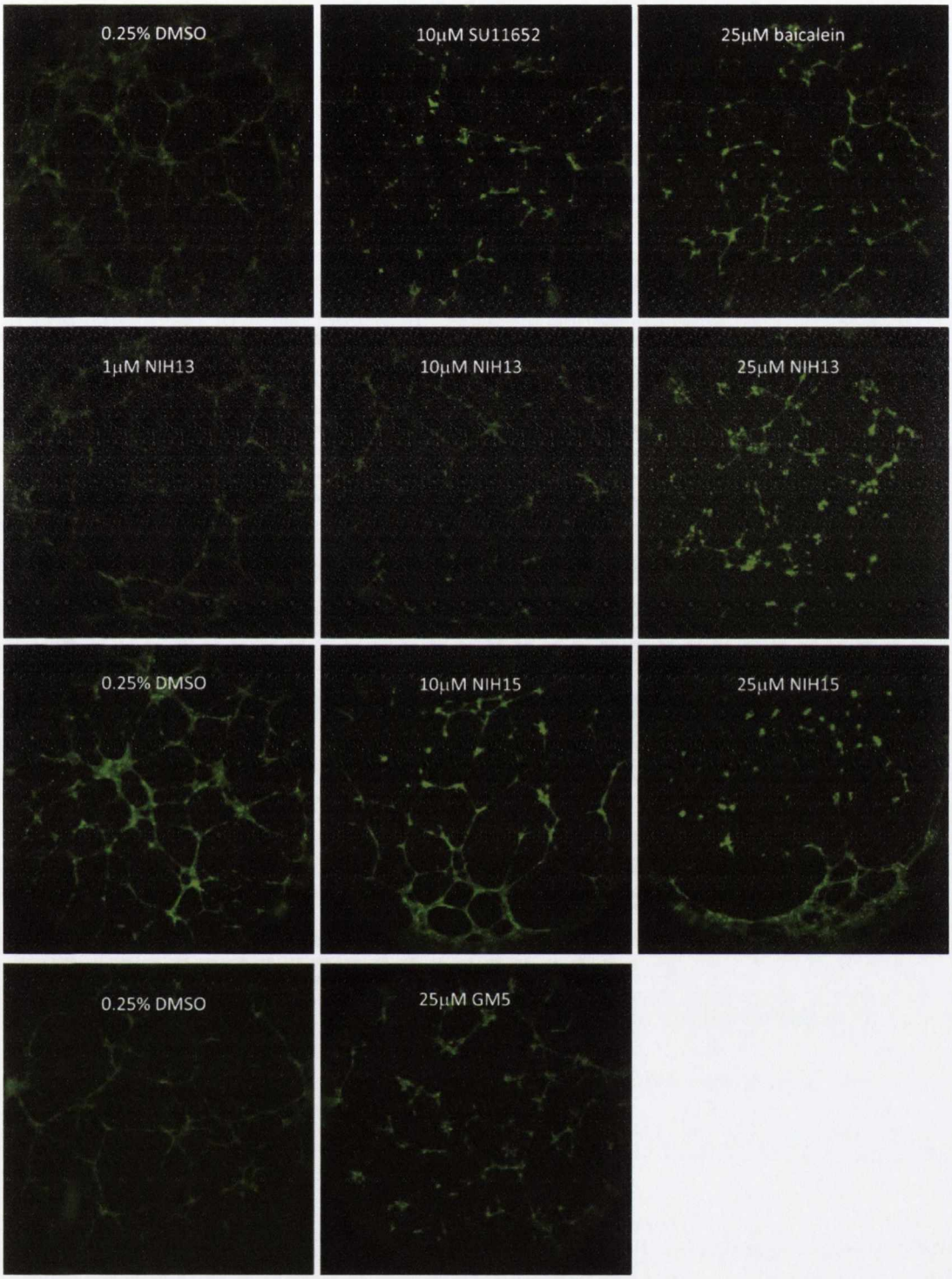

Figure 5.16 Representative images of control-treated HUVECs versus HUVECs treated with potent 12-LO inhibitors. Treatment with 10 μM SU11652 resulted in almost complete suppression of tubule formation and was used as a positive control in all assays. All fluorescent images are 4X magnification. The first 0.25% DMSO image is a representative control for images of 10 μM SU11652, 25 μM baicalein and 1 μM-25 μM NIH13 taken from the same experiment. The second 0.25% DMSO image is a representative control for images of 10 μM and 25 μM NIH15 taken from the same experiment while the third 0.25% DMSO image is a representative control for the image of 25 μM GM5 from the same experiment.

5.3.9 Inhibitor blockage of OAC tissue conditioned medium-induced tubule formation

Fresh OAC tumour biopsies were cultured *ex vivo* with selected lipoxygenase inhibitors as discussed in Section 2.20.2 for 24 hours. Tissue conditioned medium (TCM) from these treatments were investigated for the ability to induce tubule formation of HUVECs. Required cell numbers of freshly split HUVECs were pelleted and re-suspended in TCM and pipetted onto matrigel in order to have $1x10^4$ cells/well in 70 µL of TCM. Each TCM was tested in duplicate wells. All tested TCM samples derived from untreated (0.1% DMSO) tumour biopsies were able to induce high tubule formation of HUVECs (see Figure 5.18). Total tubule length induced by the untreated TCM samples was compared to that of TCM derived from drug treated matching tumour biopsies (n=8). Drug treatments were 10 µM NIH4, 5 µM NIH13, 10 µM NIH15 and 10 µM GM5. All TCMs were tested in the same plate with the same passage of HUVECs. There was no observed significant difference in tubule formation between the NIH4, NIH15 and GM5 treated TCM and untreated TCM (data not shown). However a significant decrease in tubule formation was observed in wells with NIH13-treated TCM (0.97 ±0.04 versus 0.56 ±0.11, n=8, $p<0.05$) (Figure 5.17and Figure 5.18).

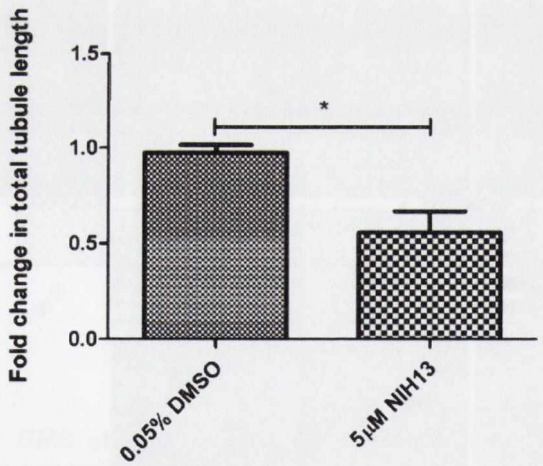

Figure 5.17 Pre-treatment of OAC tumour biopsies with NIH13 decreases the induction of HUVEC tubule formation by tissue conditioned medium. Untreated biopsy TCM (0.1% DMSO) and matched 5 µM NIH13 biopsy treated TCM were collected following 24 hour culture of the tumour biopsies (n=8) and induction of tubule formation was investigated. TCM derived from NIH13 treated biopsies had a reduced capacity to induce tubule formation compared to untreated control (0.97 ±0.04 versus 0.56 ±0.11, $p<0.05$). Statistical test used was paired student *t*-test. $p<0.05$(*).Error bar denotes mean ± S.E.M.

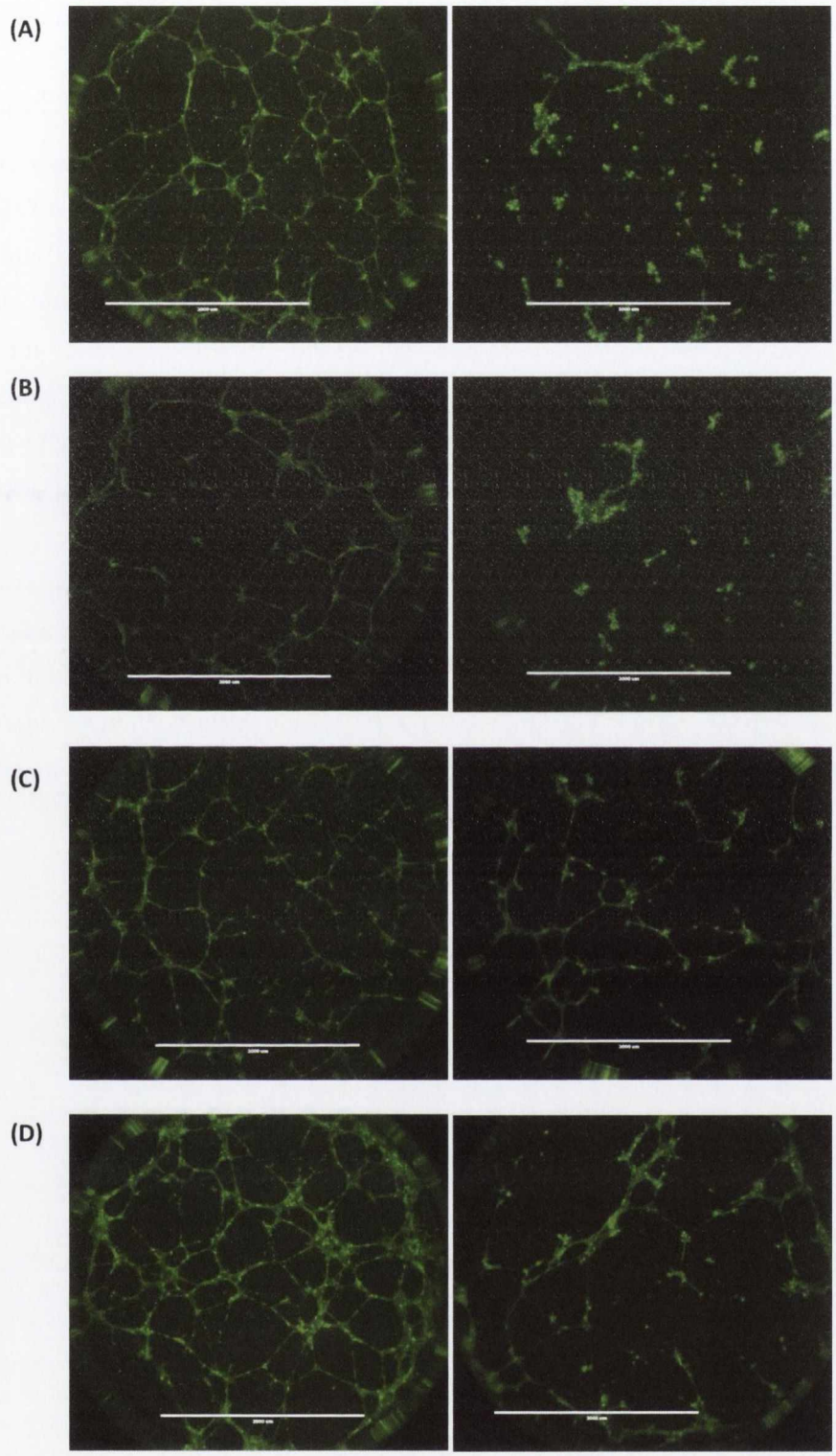

Figure 5.18 Images of HUVEC tubule formation induced by tissue conditioned media derived from untreated and NIH13 treated OAC tumour biopsies. After tubule formation, assay wells were fixed and stained with Phalloidin for fluorescent imaging. The extent of inhibition of TCM-induced tubule formation by NIH13 varied across samples as can be seen in panel A-D. (A) patient 1 untreated-TCM versus NIH13 treated TCM, (B) patient 2 untreated-TCM versus NIH13 treated (C) patient 3 untreated-TCM versus NIH13 treated and (D) patient 4 untreated-TCM versus NIH13 treated. Images shown are at 4X magnification.

5.3.10 Effect of 12-LO inhibitors on endothelial cell apoptosis

The observed inhibition of proliferation and tubule formation by the selected 12-LO inhibitors raised the question of whether the observed effects were occurring through an apoptotic mechanism. This was investigated by staining cells with AnnexinV-FITC and PI and the proportion of stained cells was assessed by flow cytometry (Section 2.24). Early stage apoptosis was quantified as AnnexinV$^+$ only cells and late stage apoptosis and necrosis as dual AnnexinV$^+$PI$^+$ staining cells. Low to negligible levels of apoptosis (<8% of total cells stained for Annexin V and / or PI) were noted for 10 μM doses of NIH13, NIH15 and GM5 following 24 hour drug treatment (n=3) (Figure 5.19). Given that the proliferation data and tubule formation data were for a 24 hour and 10-14 hour drug treatment time point respectively, this indicated that effects of decreased proliferation and tubule formation were not a result of apoptosis or non-specific necrotic death. Notably, the 10μM dose of NIH13 significantly increased early apoptosis compared to control after 48 hour drug treatment ($p<0.015$, n=3) (Figure 5.20) while prolonged exposure to the drug up to 72 hours led to significantly higher early apoptosis at both doses ($p<0.05$ and n=3 for both) and an induction of necrosis at 10μM ($p<0.05$, n=3) compared to the untreated control (Figure 5.21). In contrast, NIH15 and GM5 did not induce apoptosis up to the 72 hours.

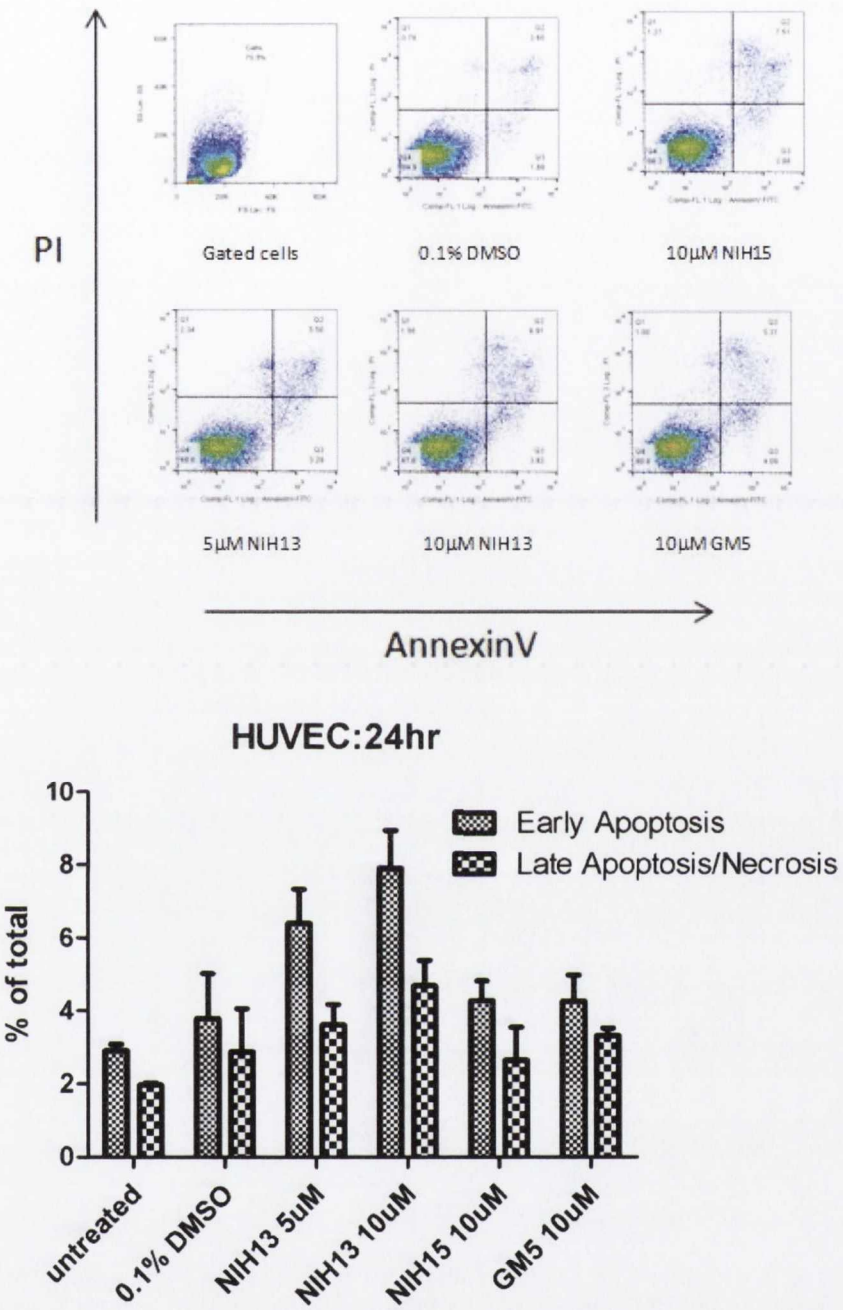

Figure 5.19 12-LO inhibitors do not induce significant apoptosis in HUVECs by AnnexinV-PI staining, following 24 drug treatment. HUVECs were treated with compounds at the indicated doses for 24 hours and were subsequently stained for AnnexinV and PI. Representative dot plots of Annexin and/or PI positive cells are shown for each compound tested. Graph indicates no significant difference in early apoptosis ($Annexin^{+}$) or late apoptosis ($AnnexinV^{+}/PI^{+}$) between drug treated and vehicle control cells (n=3). Statistical test used was one-way ANOVA with Tukey's Multiple Comparison Test. Error bar denotes mean ± S.E.M.

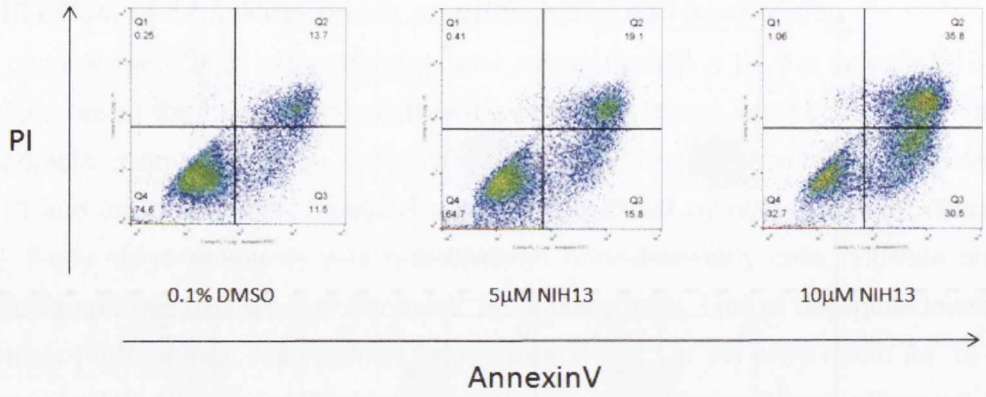

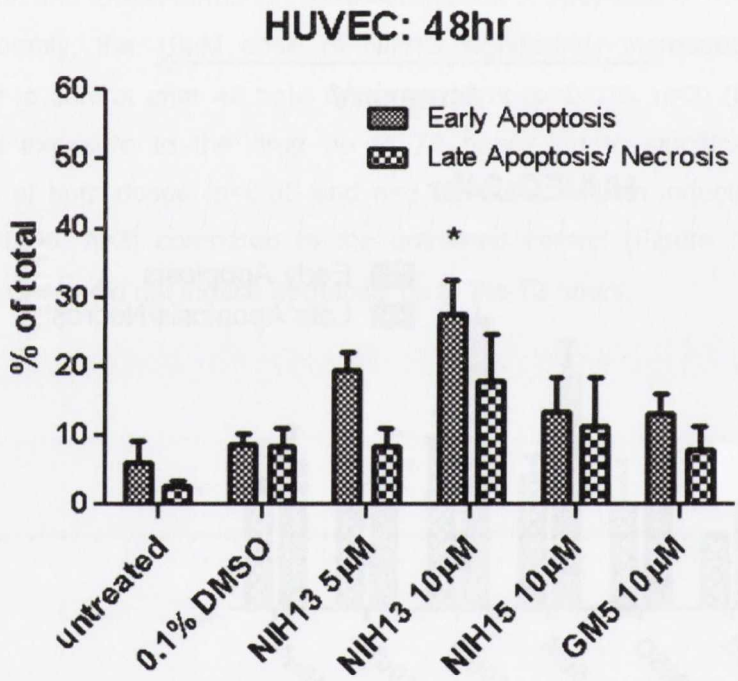

Figure 5.20 NIH13 treatment of HUVECs leads to significantly higher apoptosis at 48 hours compared to other 12-LO inhibitors and the untreated control. HUVECs were treated with compounds at the indicated doses for 48 hours and were subsequently stained for AnnexinV and PI. Representative dot plots of Annexin and/or PI positive cells are shown for NIH13 at 48 hours. 10 μM NIH13 treatment had increased early apoptosis compared to control at 48 hours ($p<0.05$, $n=3$). Statistical test used was one-way ANOVA with Tukey's Multiple Comparison Test. Error bar denotes mean ± S.E.M.

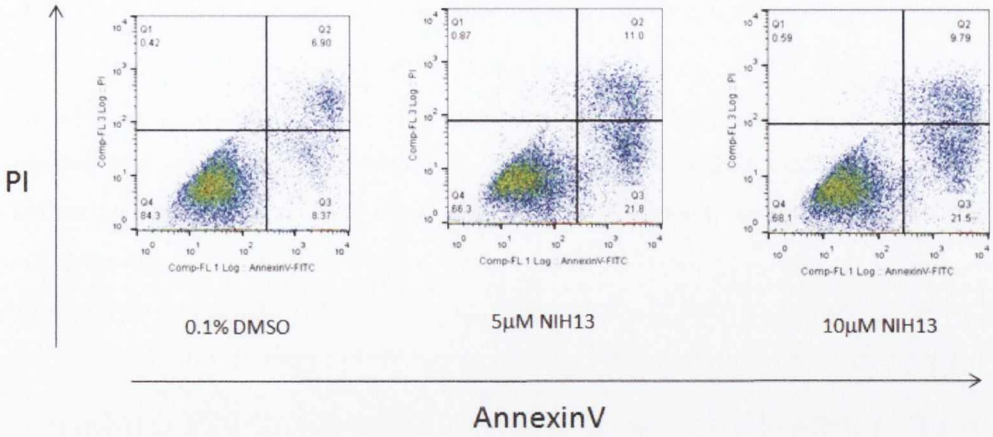

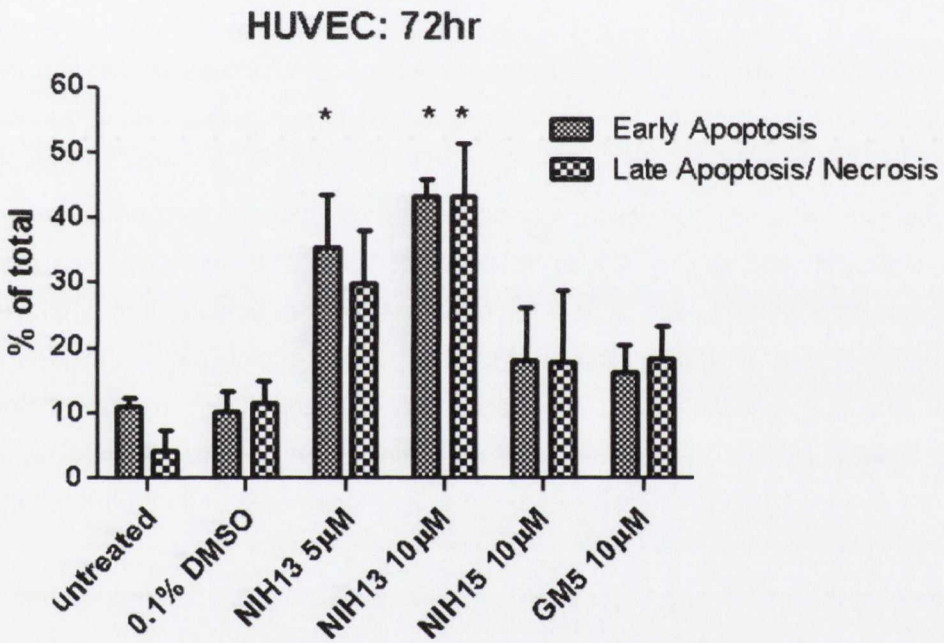

Figure 5.21 NIH13 treatment of HUVECs leads to significant apoptosis and necrosis at 72 hours compared to other novel 12-LO inhibitors and the untreated control. HUVECs were treated with compounds at the indicated doses for 72 hours and were subsequently stained for AnnexinV and PI. Representative dot plots of Annexin and/or PI positive cells are shown for NIH13 at 72 hours. 5 µM and 10 µM doses of NIH13 had significantly higher early apoptosis ($p<0.05$, n=3) at 72 hours compared to untreated control. NIH13 10 µM treatment also caused increased late apoptosis/ necrosis at 72 hours ($p<0.05$, n=3). Statistical test used was one-way ANOVA with Tukey's Multiple Comparison Test. Error bar denotes mean ± S.E.M.

5.3.11 Human Angiogenesis Pathway Finder Array: alterations in HUVEC gene expression following novel lipoxygenase inhibitor treatment

Having demonstrated that novel lipoxygenase inhibitors had functional effects on HUVEC proliferation and tubule formation, in particular NIH13, the mechanisms regulating these effects were investigated. The Human Angiogenesis Pathway profiler array was used to investigate whether compound treatment of HUVECs affected the transcript levels of genes involved in key processes of angiogenesis and to indentify which of the selected compounds being screened had the most potent effect.

HUVEC cells were prepared as described in Section 2.13 and were treated for 24 hours with 0.1% DMSO as a vehicle control or with one of the selected compounds (i.e. 5-LO: NIH4 and 12-LO: NIH13, NIH15 and GM5). NIH4, NIH15 and GM5 were used at a dose of 10 μM because this was a concentration at which biological activity was observed *in vitro*. In the case of NIH13 it was decided that the dose would be reduced to 5 μM considering its highly potent effects to proliferation and tubule formation, and apoptosis at 48 and 72 hours. RNA was isolated as described in Section 2.9 and cDNA was synthesised and run on the array as described in Section 2.13. Analysis was performed using a web-based PCR array data tool (SABiosciences) that employed the ΔΔCt method with raw data normalised by the house-keeping genes included in the plate. Gene changes were only reported if the transcript was amplified before 35 cycles. Values were displayed as fold regulation where a threshold fold regulation value of 2 indicated differential expression of a gene compared to the untreated control.

Alterations of 22 genes were reported in NIH4-treated HUVECs compared to untreated. It was noted that half (11/22) of the alterations were growth factors and receptor genes. All three 12-LO inhibitors NIH13, NIH15 and GM5 showed alterations in 39/84, 38/84 and 31/84 genes respectively. It was noted that the growth factor and receptor gene category accounted for approximately half of the gene alteration by these compounds; NIH13: 18/39 (46.2%), NIH15: 15/38 (39.5%) and GM5: 15/31 (48.4%). A list of all the genes altered by at least one the four compounds compound is shown in Table 5.5. A full list of the 84 genes featured on the array can be found in Appendix I. This array screen was only carried out for n=1 for each compound and was used to indicate potential gene targets for follow up validations (n=3). The greatest overlap in gene alterations between all 4 compounds was in the growth factor and receptor category followed by the cytokines and chemokines functional category. Consequently genes for validation were chosen from these two categories. Eleven genes were chosen for validation by qPCR. The overlap of alterations in these genes between the four

compounds is illustrated in Figure 5.22. A large number of the positive hits on the array were in the lower expression region with Ct values of 31-35. Consequently genes for validation were picked based on a moderate-high expression in untreated HUVECs (Ct<30) while less reliable gene alterations with values in the low expression range were avoided. The genes selected had clustering biological functions, for example the putative angiogenic growth factor VEGF (*VEGFA*), two other VEGF isoforms (*VEGFB* and *VEGFC*), the major VEGF receptor VEGFR-2 (*KDR*), to which VEGF and VEGFC bind, and the essential VEGF co-receptor neuropilin-1 (*NRP1*) were chosen. Two other angiogenesis stimulating growth factors angiogenin (*ANG*) and angiopoietin-1 (*ANGPT1*) were included in addition to the endothelial cell specific angiopoietin binding receptor tyrosine kinase heterodimer which consists of Tie-1 (*TIE1)* and Tie-2 (*TEK)*. Two pro-angiogenic chemokines GRO-α (*CXCL1*) and CXCL6 (*CXCL6*) were also included. A schematic of the interactions between the eleven genes is shown in Figure 5.23.

Table 5.5 List of HUVEC gene alterations following lipoxygenase inhibitor treatment

Functional group	Gene	NIH4	NIH13	NIH15	GM5
Adhesion molecules	COL18A1				
	COL4A3				
	ENG				
	IL8				
	S1PR1				
Cytokines and chemokines	CCL2				
	CXCL1				
	CXCL5				
	CXCL6				
	IL6				
Growth factors and receptors	ANG				
	ANGPT1				
	ANPEP				
	EDN1				
	ERBB2				
	F3				
	FGF1				
	FGF2				
	FIGF				
	KDR				
	NRP1				
	NRP2				
	PDGFA				
	PGF				
	TEK				
	TGFB2				
	TGFBR1				
	THBS1				
	THBS2				
	TIE1				
	TYMP				
	VEGFA				
	VEGFB				
	VEGFC				
Proteases and inhibitors	ANGPTL4				
	MMP2				
	PECAM1				
	PLAU				
	PLG				
	SERPINF				
	TIMP1				
	TIMP2				
	TIMP3				
Transcription factors and other	AKT1				
	HIF1A				
	HPSE				
	ID1				
	NOS3				
	NOTCH4				
	PTGS1				
	SPHK1				

Red = upregulation >2 fold, green = downregulation of <-2 and grey = no alteration to gene expression

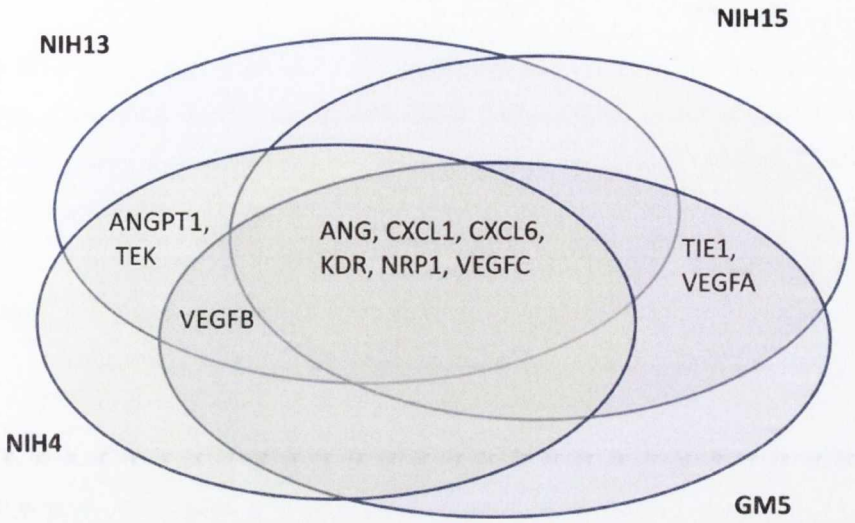

Figure 5.22 Eleven angiogenesis-related genes were chosen for validation which showed overlapping alterations in HUVECs treated with the four novel lipoxygenase inhibitors.

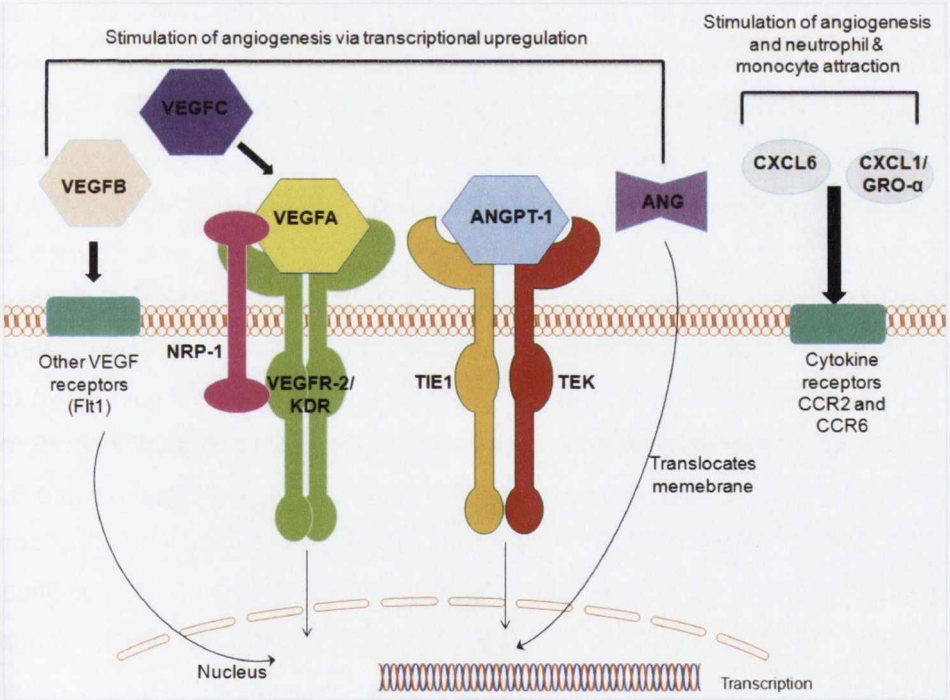

Figure 5.23 Schematic of eleven angiogenic genes chosen for validation from the Angiogenic Pathway Finder array. 5 growth factors (*VEGFA, VEGFB, VEGFC, ANGPT1* and *ANG*), 3 associated receptors (VEGF receptor *KDR* and the angiopoietin receptor monomers *TIE1* and *TEK*) and 2 pro-angiogenic and pro-inflammatory cytokines (*CXCL1*/GRO-α and *CXCL6*) were chosen for validation by qPCR.

5.3.12 Validation of selected genes from Human Angiogenesis Pathway Finder array

HUVECs were treated with 0.1% DMSO, 10 μM NIH4, 5 μM NIH13, 10 μM NIH15 or 10 μM GM5 for 24 hours in three independent experiments with three different passages of cells. The expression of the panel of angiogenic genes chosen from the array were investigated by SYBR-based qPCR, and using the primer sets detailed in Section 2.14. *GAPDH*, a house-keeping gene that featured in the initial array set, was used to normalise gene expression. Gene expression was determined using the ΔΔCt method as described previously and values were graphed relative to control expression.

In contrast to results suggested from the initial array the treatment of HUVECs with NIH4, NIH15 and GM5 did not appear to significantly alter the expression of any of the genes investigated and thus failed to validate. On the other hand repeat NIH13 treatments for the validation set were shown to reproduce the initial array results for several of the genes of interest and showed clear but not significant trends of decreased expression for several other genes. Compared to control 5μM NIH13 decreased *KDR* (1.52 ±0.35 versus 0.59 ±0.16, n=4) and *NRP1* (1.42 ±0.51 versus 0.39 ±0.18, n=4) expression significantly ($p<0.05$ and $p<0.01$ respectively) suggesting a blocking of VEGF signalling (Figure 5.24a and Figure 5.24b). There was a significant downregulation of *ANGPT1* (2.48 ±0.66 versus 0.59 ±0.15, n=4, $p<0.01$) and its dimer receptor components *TEK* and *TIE1* (0.77 ±0.16 versus 0.13 ±0.06, n=3, $p<0.05$ and 0.75 ±0.37 versus 0.17 ±0.04, n=3, $p<0.05$) observed (Figure 5.25b and Figure 5.25c). In the initial angiogenic profiler array screen *VEGFA* was not reported as an altered gene following NIH13 treatment while *VEGFB* and *VEGFC* were downregulated. In contrast in the validation set *VEGFA* and *VEGFB* were both unexpectedly shown to be increased (0.77±0.20 versus 2.38 ±0.43, n=3 and 1.57 ±0.40 versus 3.79 ±1.15, n=3) significantly ($p<0.01$ and $p<0.05$ respectively) following NIH13 treatment. (Figure 5.24c and Figure 5.24d). *VEGFC* did not show altered regulation compared to the control (Figure 5.24e). Similarly to *VEGFA* and *VEGFB, ANG* expression was significantly increased (0.83 ±0.1 versus 1.75 ±0.38, n=3, $p<0.05$) following NIH13 treatment (Figure 5.24f). In comparison to the control, *CXCL1* was found to be significantly decreased over four-fold following NIH13 treatment (0.91 ±0.24 versus 0.18 ±0.09, n=3, $p<0.01$) (Figure 5.25d). *CXCL6* decreased over two-fold, similar to the array, however it was not significant (0.78 ±0.14 versus 0.30 ±0.19, n=3, $p=0.14$) (Figure 5.25e). From this study it was shown that of the four lipoxygenase inhibitors tested, consistent with previous *in vitro* data in this chapter, NIH13 had the most potency as an

anti-angiogenic compound, at least for the growth factor and chemokine gene set investigated in this study.

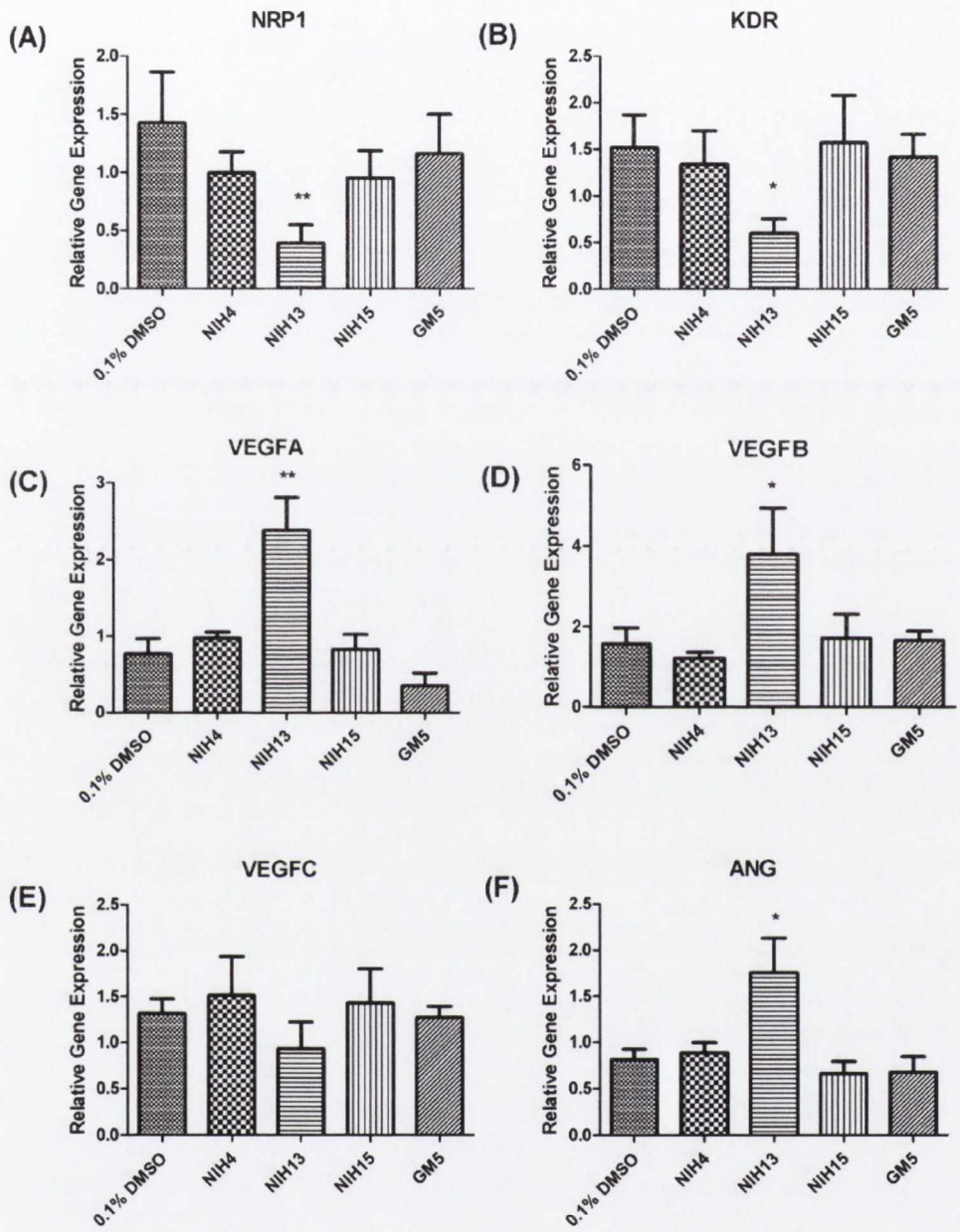

Figure 5.24 NIH13 treatment significantly decreases *NRP1* and *KDR* gene expression in HUVECs. HUVECs were treated with selected lipoxygenase inhibitors and cDNA was analysed by SYBR-based qPCR to determine alterations in a panel of angiogenesis related genes. There was no significant up or downregulation of gene expression observed for NIH4, NIH15 and GM5 treatment. However NIH13 treatment resulted in statistically significant downregulation of (A) *NRP1* and (B) *KDR* ($p<0.01$ and $p<0.05$, $n=4$). A significant increase in (C) *VEGFA* ($p<0.01$, $n=3$), (D) *VEGFB* ($p<0.05$, $n=3$) and (F) *ANG* ($p<0.05$, $n=3$) gene expression was noted following NIH13 treatment. No alteration in (E) *VEGFC* was observed with any of the drug treatments. Statistical test used was one-way ANOVA with Dunnett's Multiple Comparison Test comparing untreated (0.1% DMSO) and drug treatments: $p<0.05$(*), $p<0.01$(**). Error bar denotes mean ± S.E.M.

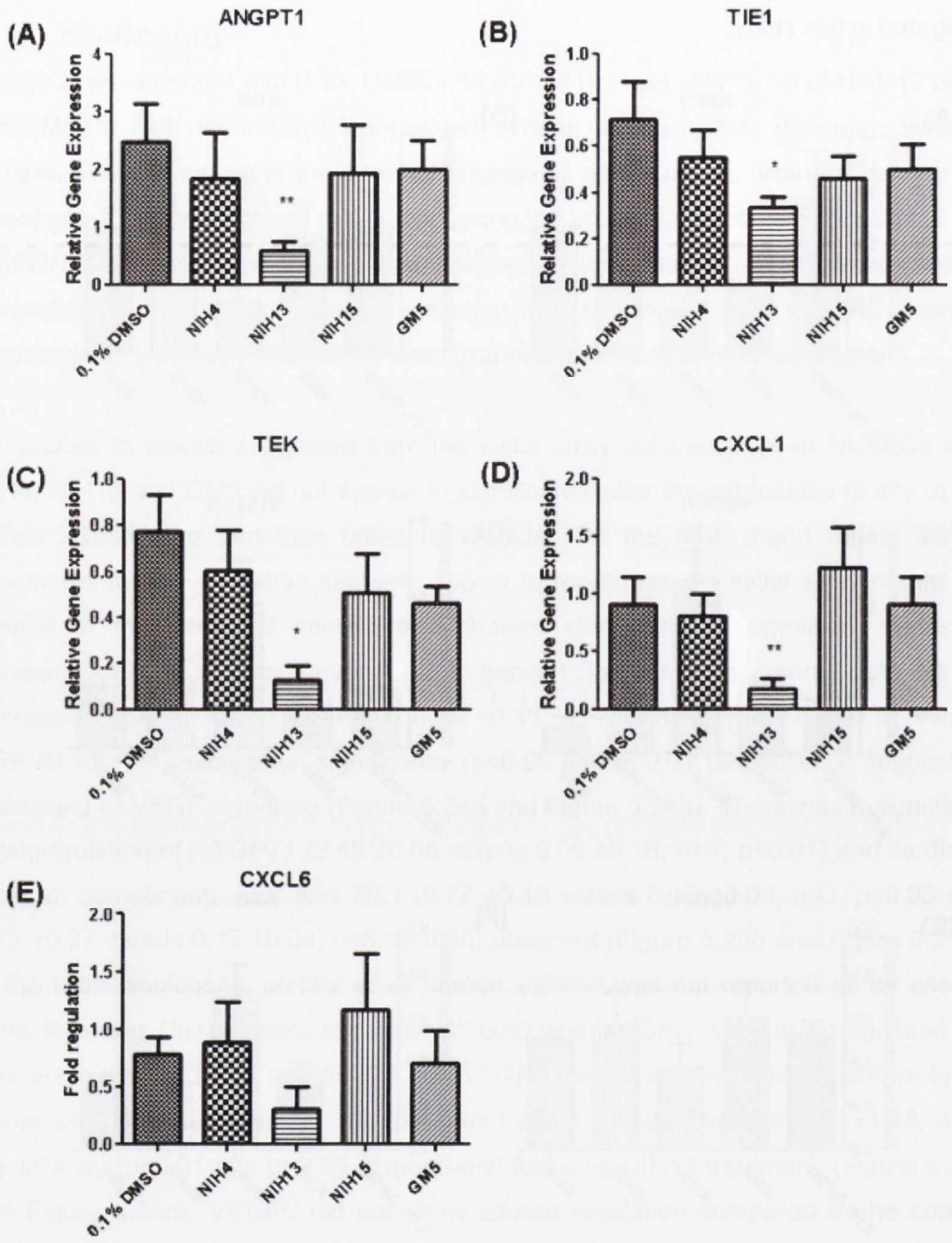

Figure 5.25 NIH13 treatment significantly decreases *ANGPT1, TIE1, TEK* and *CXCL1* gene expression in HUVECs. HUVECs were treated with selected lipoxygenase inhibitors and cDNA was analysed by SYBR-based qPCR to determine angiogenic gene alterations. There were no significant up or downregulations of gene expression observed for NIH4, NIH15 and GM5 treatment. NIH13 treatment resulted in downregulation of (A) *ANGPT1* ($p<0.01$). (B) *TIE1* and (C) *TEK* expression were also downregulated by NIH13 ($p<0.05$). (D) *CXCL1* was significantly downregulated ($p<0.01$). A non-significant decrease in *CXCL6* was noted following NIH13 treatment ($p=0.14$). Statistical test used was one-way ANOVA with Dunnett's Multiple Comparison Test comparing untreated (0.1% DMSO) and drug treatments: $p<0.05$(*) $p<0.01$(**). Error bar denotes mean ± S.E.M.

5.3.13 Investigation of the effect of selected lipoxygenase inhibitors on angiogenic protein secretion by HUVECs

In this section the effect of novel and commercial lipoxygenase inhibitor treatment on angiogenic protein secretions by HUVECs was investigated. Cells were prepared as described in Section 2.20.3 and treated for 24 hours with a particular drug or vehicle control (0.1% DMSO). Of the 5-LO inhibitors HUVECs were treated with 10 μM of novel 5-LO inhibitor NIH4 or 10 μM zileuton. Of the 12-LO inhibitors HUVECs were treated with 1, 5 and 10 μM of NIH13, 10 μM and 20 μM of GM5 and 10 μM and 20 μM baicalein. Angiogenic protein production in cellular supernatants was measured by DuoSet® ELISA as described in Section 2.20.5. A panel of common angiogenic markers covering a number of pathways (VEGF, PDGF, neuropilin-1, GRO-α/CXCL1, IL-8 and angiopoietin-2 were investigated. As described in Section 2.20.3 after removing the cellular supernatant from the cells, the monolayer of cells were lysed with RIPA buffer and the total cellular protein concentration of each experimental well was measured by BCA assay (Section 2.18). This was used to normalise the secretion levels determined by ELISA to total cellular protein. Each treatment was carried out in three independent biological replicates and the average normalised protein levels in pg/mL were reported.

Secreted VEGF was not detected in HUVECs in this experimental set up as previously described by (Nanobashvili *et al.*, 2003) and therefore could not be analysed. Low levels of PDGF were detected (untreated control = 32.83 ±2.27 pg/mL) however there was no difference in secreted levels compared to the drug treatments (Figure 5.26a). Similarly, while IL-8, angiopoietin-2 and neuropilin-1 were all detected by ELISA (control= 181.17 ±11.88 pg/mL; 1703.40 ±156.56 pg/mL; 685.18 ±44.93 pg/mL) there was no observed difference in exogenous protein levels between the control group and the treatment groups (Figure 5.26b-d). In contrast, compared to the control, secreted GRO-α was found to be significantly decreased following 1 μM (987.22 ±72.08 pg/mL versus 669.88 ±85.12 pg/mL, $p<0.05$), 5 μM (987.22 ±72.0 pg/mL versus 540.08 ±44.01 pg/mL, $p<0.01$) and 10 μM (987.22 ±72.08 pg/mL versus 430.92 ±55.49 pg/mL, $p<0.001$) NIH13 treatment (Figure 5.27). Additionally 10 μM NIH4 and 20 μM GM5 reduced GRO-α secretion (672.83 ±33.76 pg/mL, $p<0.05$ and 566.53 ±60.76 pg/mL, $p<0.01$) (Figure 5.27).

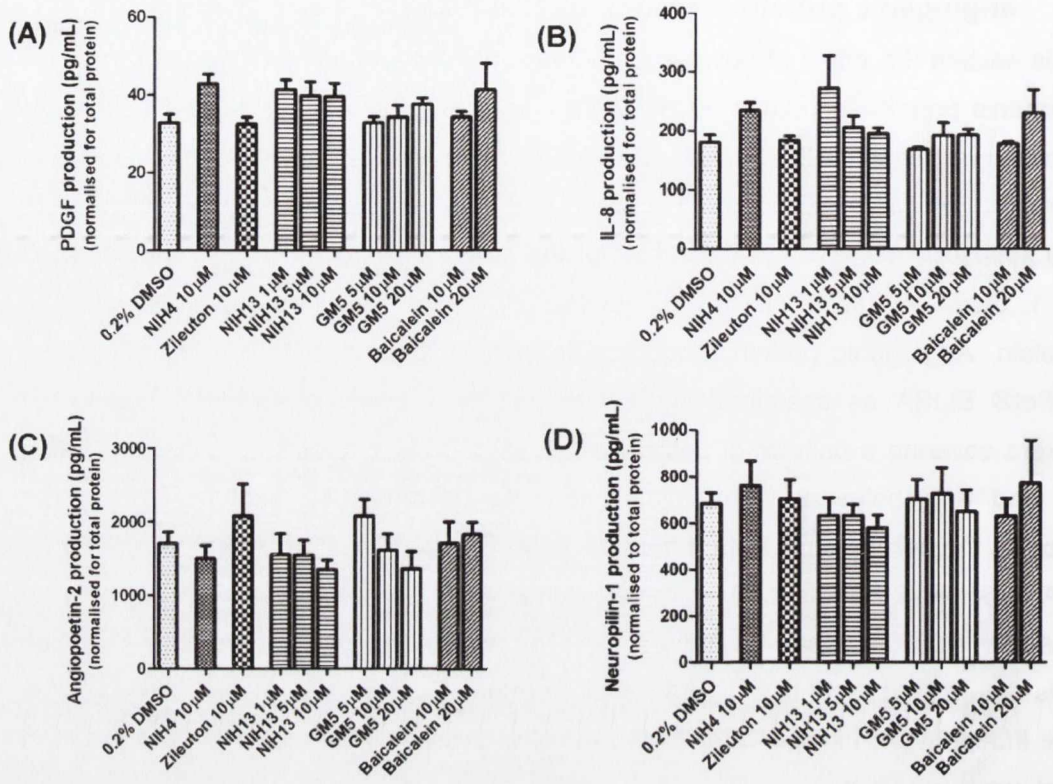

Figure 5.26 PDGF, IL-8, angiopoietin-2 and neuropilin-1 production are not altered in HUVECs following lipoxygenase inhibitor treatment. HUVECs were treated with selected novel and commercially available 5-LO and 12-LO inhibitors for 24 hours. The cell culture supernatant was investigated for changes to common angiogenic proteins by ELISA. Detected levels of (A) PDGF, (B) IL-8, (C) angiopoietin-2 and (D) neuropilin-1 were not altered by any of the drug treatments tested. Statistical test used was one-way ANOVA with Dunnett's Multiple Comparison Test comparing untreated (0.1% DMSO) and drug treatments. n=3, $p<0.05$(*), $p<0.01$(**), $p<0.001$(***). Error bar denotes mean ± S.E.M.

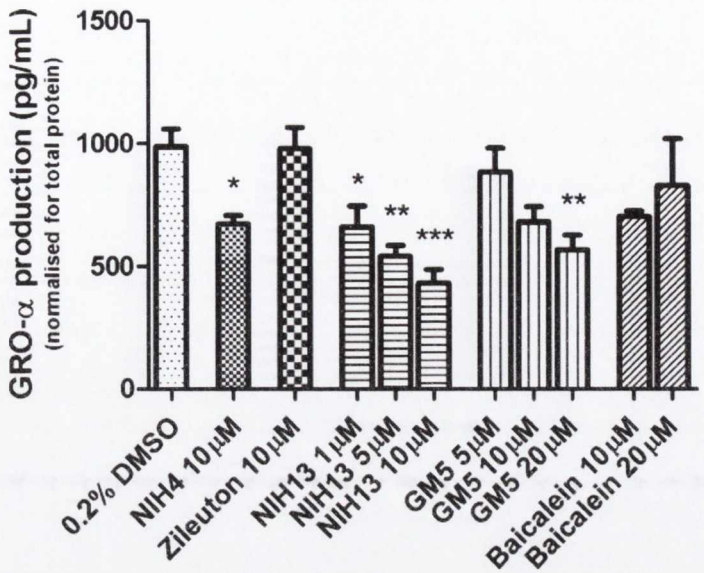

Figure 5.27 GRO-α levels produced by HUVECs are significantly decreased following NIH4, NIH13 and GM5 treatment. HUVECs were treated with selected novel and commercially available 5-LO and 12-LO inhibitors for 24 hours. GRO-α was significantly decreased following NIH13 treatment at 1 μM ($p<0.05$), 5 μM ($p<0.01$) and 10 μM ($p<0.001$) doses. There was also significant decreases observed for NIH4 treatment at 10 μM and GM5 treatment at 20 μM compared to control ($p<0.05$ and $p<0.01$ respectively). Statistical test used was one-way ANOVA with Dunnett's Multiple Comparison Test comparing untreated (0.1% DMSO) and drug treatments. n=3, $p<0.05$(*), $p<0.01$(**), $p<0.001$(***). Error bar denotes mean ± S.E.M.

5.4 Discussion

The discovery and development of small molecule drugs has been revolutionised over the last decade (Hoelder *et al.*, 2012) especially with the advent of HTS techniques to find drug target hits, as evidenced by the success story of the VEGFR and tyrosine kinase inhibitor sorafenib (Macarron *et al.*, 2011). As is the case of this study, preclinical models are imperative in the lead optimisation phase of drug development, because they provide critical information on how the chemical compound in question is behaving and any novel effects it is having. In this study we investigated the anti-angiogenic potential of novel 5-LO and 12-LO inhibitors using a number of assays.

Firstly the efficacy of these compounds as anti-angiogenics was investigated using the popular *fli1:EGFP* zebrafish developmental angiogenesis model. The FDA approved potent and selective 5-LO inhibitor zileuton failed to showed any anti-angiogenic effect to ISV formation and also no toxic effects up to the highest test dose of 100 μM, indicating the good safety profile of this compound *in vivo,* as expected and potentially indicating that 5-LO is not involved in this model of developmental angiogenesis. The

novel 5-LO inhibitors based on a phenylenediamine scaffold similarly failed to show an effect on vessel sprouting, with subsequent dose escalation studies leading to larval deformation starting at a dose of 50 µM and non-viable embryos at 100 µM which most likely indicates off-target non-selective toxicity. In the case of ketoconazole, while inhibition of vessel formation was observed at a dose of 25 µM it was accompanied by undesired morphologic effects. A synthetic dl-nordihydroguaiaretic acid compound (Nordy), which has previously been shown to inhibit 5-LO in glioblastoma (Boado *et al.*, 1992) has recently been shown to markedly reduce neoangiogenesis induced by xenograft glioblastoma cancer cells (Bian *et al.*, 2006, Yang *et al.*, 2014). It was interesting to note in this study that Nordy had no reported effects on developmental angiogenesis in dose escalation studies suggesting that the 5-LO pathway is only involved in pathological *de novo* angiogenesis post-development. Although the technical expertise to perform this assay was not available during this study it would very interesting to see what effect these novel and commercial 5-LO inhibitors have to *de novo* angiogenesis in a zebrafish xenograft model.

Our collaborators previously investigated the *in vitro* ADME (absorption, distribution, metabolism and excretion) properties of the 8-hydroxyquinoline-based compounds and showed good cell permeability and stability. The predicted *in vivo* PK (pharmacokinetics) showed a short half-life of 10 minutes in mouse liver microsomes but a more stable half-life of 3.5 hours in mouse serum, indicating a possibility for use *in vivo* (Kenyon *et al.*, 2011). No such data was available for the other compound classes and to our knowledge none of the novel 12-LO inhibitors from the published 8-hydroxyquinoline and benzenesulfonamide-based structures or the unpublished oxadiazol-2-yl benzamide structure have been tested *in vivo*. The *fli1:EGFP* zebrafish model has proven efficacy as an angiogenesis model for the testing of major classes of anti-angiogenic therapies that are used clinically. For example the VEGF receptor and multi-tyrosine kinase inhibitors such as sunitinib and sorafenib cause complete regression of ISVs at doses of <250 nM and 1 µM respectively (Chimote *et al.*, 2014). In contrast, in our study, the 12-LO novel inhibitors did not exhibit anti-angiogenic effects at the lowest test dose of 10 µM. At 50 µM NIH15 showed a 35% decrease in vessel formation and a noted decrease to overall the size of the embryo without any obvious toxicity effect. NIH13 had a 20% decrease in ISV formation at 50 µM with no observed toxicity. These effects are similar to the more modest effects of known anti-angiogenic therapies in this same model, which do not target the VEGF/VEGFR pathway directly, such as the anti-fibroblast growth factor inhibitor suramin. Suramin demonstrated a 30% vessel decrease at a max dose 250 µM in the *fli1:EGFP* model

(Chimote *et al.*, 2014). Therefore the compounds tested may still have anti-angiogenic effects in other models, particularly NIH13 and NIH15.

The second generation of 12-LO compounds GM1-GM7 exhibited no effect to zebrafish morphology up to a maximal dose of 100 μM indicating a good safety profile. Considering they have similar potency for 12-LO as the 8-hydroxylquinoline based compounds, modest effects to ISV formation may have been expected however this was not this case and the drug treated embryos were indistinguishable from the negative controls. This may indicate issues with solubility in the embryo medium or with uptake into the chorion (i.e. the membranous sac surrounding the embryo). To rule out potential issues with drug uptake affecting activity, the drugs should be injected directly into the zebrafsh embryo. While platelet-type 12-LO has been implicated in human angiogenesis with expression and activity found in endothelial cells (Nie *et al.*, 2000, McCabe *et al.*, 2006) the modest or negative results indicated from our inhibitor screen show that this role may not be conserved in zebrafish. Human and zebrafish *ALOX12* genes show only a 43% sequence homology, in comparison to *ALOX5* which has 75% sequence homology (source: BLAST®). It has been reported that zebrafish possess a single atypical 12(S)LO gene that, unlike humans, is predominantly expressed in the dermis of the fish and knockdown leads to severe phenotypes with yolk sac oedema, and abnormal development of the tail and notochord (Haas *et al.*, 2011) indicating it may not function in the vasculature.

As an alternative strategy the novel lipoxygenase compounds were screened in the commonly used human primary endothelial cell HUVEC model. Due to the number of compounds to be screened and limited BrdU reagent a single treatment time point of 24 hours was chosen. The identification of anti-proliferative effects as early as 24 hours is indicative of a more potent compound than at the later time point of 48 or 72 hours. Admittedly choosing this 24 hour time point comes at the expense of missing potential anti-proliferative effects that may occur at longer treatment times in the compounds that had low activity across all doses following 24 hour treatment. While the novel 5-LO compound, NIH4, ketoconazole and REV 5901 showed inhibitory effects on cell proliferation, HUVECs and most endothelial cells do not express 5-LO and therefore compound effects to proliferation were presumably due to alternate 5-LO independent mechanisms. It must be noted that NIH4, ketoconazole and REV 5901 treatment did not affect the functional migration or tubule formation of the endothelial cells on a collagen gel matrix, therefore effects on proliferation over 24 hours were not considered to be due to cytotoxicity but some other unknown mechanism.

In the case of the 12-LO inhibitors NIH13, NIH15 and GM5 were the most potent compounds of the three classes tested in proliferation and tubule formation assays. Of these top compounds, NIH13 showed superior effects in both assays. GM5 showed more modest but still significant effects on tubule formation at a dose of 25 μM. Effects on HUVEC tubule formation may have been due to cytotoxic effects of the compounds. Therefore we tested the compounds at the effective tubule inhibitory dose of 10 μM in the AnnexinV/PI assay to assess whether the observed effects on tube formation were due to drug-induced apoptosis or non-specific cytotoxicity-induced necrosis. AnnexinV/PI staining of HUVECs was negligible for all drugs following 24 hours treatment for both apoptosis and necrosis, indicating the observed effects are not due to an induction of cell death but potentially suppression of an angiogenic mechanism. Significant effects on early apoptosis by NIH13-treated HUVECs were noted at 48 and 72 hours while significant spontaneous cell death occurred at 72 hours at a dose of 10 μM, indicating toxic effects of the drug following prolonged exposure. The rationale for choosing a 24 hour proliferation assay time point has been discussed previously. Having identified NIH13 as a compound with dramatic anti-proliferative effects at a 1 μM dose as early as 24 hours, future work should include extended treatment time points for proliferation assays (i.e. 48 and 72 hour) and also a clonagenic cell survival assay.

To investigate the effect of the selected compounds on tumour-induced tubule formation of HUVECs, fresh OAC tissue was treated with the novel compounds for 24 hours and the TCM was frozen until the tubule assay was performed. In this study TCM derived from tumour biopsies treated with 5 μM NIH13 had decreased capacity to induce tubule formation compared to control TCM. The effect of NIH13 on the angiogenic stimulatory ability of the tumour tissue (i.e. alterations to the secreted milieu of pro-angiogenic growth factors available in the TCM) versus the effect of NIH13 on endothelial cell response to the TCM could not be distinguished in this assay. However it is likely a combination of both effects. Subsequently in Chapter 6 we investigated if NIH13 treatment alters the secretory profile of TCMs in order to elucidate this further.

Previously it had been shown that inhibition of 12-LO results in a downregulation of VEGF in endothelial cells (Nie *et al.*, 2000). Knockdown of 12-LO was shown to suppress the migratory and tubule forming capability of HUVECs, while addition of 12-LO metabolite 12(S)HETE restored angiogenic potential (Kim *et al.*, 2009) (Lu and

Bergers, 2013). The novel 12-LO inhibitors in the study have shown effects in functional assays including the characteristic tubule formation of HUVECs. The effects of novel compounds on the angiogenic gene expression profile of HUVECs was subsequently investigated to elucidate novel gene pathways and mechanisms through which these inhibitors potentially elicit observed functional effects. While the novel 5-LO and three selected 12-LO inhibitors were included in the gene study, interestingly only one of the compounds had validated gene targets. NIH13, which was revealed to be the most potent inhibitor in the functional assays tested showed validated alterations in a number of pathway-related angiogenic genes. The putative VEGFR-2 (*KDR*) and the co-receptor neuropilin-1 (*NRP1*) were both significantly downregulated. VEGFR-2/KDR is one of the most researched anti-angiogenic targets today, with a number of small molecule inhibitors currently in use clinically (Chimote *et al.*, 2014). Neuropilin-1 is a receptor for VEGF and the neuronal guidance protein semaphorin 3A with key roles in vascular and neuronal development (Plein *et al.*, 2014). When expressed with VEGFR-2, neuropilin-1 enhances the binding of VEGF to VEGFR2 and VEGF-mediated chemotaxis (Soker *et al.*, 1998). Neuropilin-1 has also been implicated in having a role in tumour growth and associated angiogenesis. Antibody blocking of VEGF binding to neuropilin-1 has been shown to enhance the anti-tumour effects of the VEGF monoclonal antibody, bevacizumab in mouse tumour xenograft models (Pan *et al.*, 2007). There is evidence to suggest the 12-LO metabolite, 12(S)HETE, binds to neuropilin-1. In neuronal cells, 12(S)HETE has been shown to mimic the actions of semaphorin 3A, by binding to neuropilin-1, while inhibition with a 12-LO inhibitor cinnamyl-3,4-dihydroxy-α-cyanocinnamate suppressed semaphorin 3As actions in certain neural processes (Mikule *et al.*, 2002). Bearing this in mind 12(S)HETE may act in combination with VEGF to regulate neuropilin-1 or indeed VEGFR-2 in HUVECs. Thus blocking of 12-LO activity by NIH13 may elicit the observed anti-angiogenic effects such as reduced tubule formation through a downregulation of NRP1 and VEGFR 2 genes.

In concert with VEGF, the angiopoietin-Tie1 system is another endothelial specific growth factor receptor system with an established role in vascular remodelling and maturation during vessel development (Saharinen *et al.*, 2011). NIH13 treatment significantly downregulated angiopoietin-1 (*ANGPT1*), a pro-angiogenic factor which is involved in vessel stabilization and maintenance, in addition to its receptor monomers Tie-1 (*TIE1*) and Tie-2 (*TEK*). This was a novel finding and there is currently no link between angiopoietins and the eicosanoid signalling pathway in the literature. In the context of cancer, angiopoietin-1 may actually stabilize leaky vessels in the presence of

VEGF thus potentially inhibiting tumour growth. Nevertheless several reports indicate that angiopoietin-1 in combination with angiopoietin-2 are both upregulated during therapeutic VEGF blocking, leading to resistance and enhanced progression (Huang *et al.*, 2009). The dual-blocking of VEGF and angiopoietins with a novel chimeric decoy receptor has shown effectiveness at suppressing tumour angiogenesis and metastasis *in vivo* (Koh *et al.*, 2010) indicating the therapeutic potential of blocking this alternate angiogenic growth factor system.

Autocrine production of the pro-inflammatory chemokine GRO-α by endothelial cells has been shown to be a potent mitogen, needed for HUVEC growth (Fujisawa *et al.*, 1999). It has also been shown to be a potent mediator of tumour associated angiogenesis in Kaposi sarcoma, NSCLC and colorectal cancer (Lane *et al.*, 2002, Arenberg *et al.*, 1997, Wang *et al.*, 2006). In this study 12-LO inhibition in HUVECs by NIH13 was found to significantly downregulate *CXCL1* gene expression and to decrease the corresponding secreted protein, GRO-α, in a dose-dependent manner. While other eicosanoids such as COX-2-derived PGE2 have been shown to induce *CXCL1* expression by cancer cells, leading to endothelial cell migration *in vitro* and more highly vascularised tumour *in vivo,* this is the first study to link lipoxygenase signalling to the pro-angiogenic chemokine GRO-α.

It was interesting to note that at the 24 hour treatment time-point, HUVECs treated with NIH13 showed an upregulation in gene expression of the growth factors VEGF (*VEGFA*), VEGFB (*VEGFB*) and angiogenin (*ANG*). Given the critical importance of available VEGFR2 and neuropilin-1, in the VEGF signal transduction it is not surprising downregulation of these receptors leads to a compensatory upregulation in VEGF and other related growth factors. For example glioma cancer stem cells were shown to upregulate a number of pro-angiogenic factors such as angiogenin and bFGF following bevacizumab treatment (Lucio-Eterovic *et al.*, 2009). While further validation of the significantly downregulated gene targets is required using assays measuring protein levels, it was interesting to note how effectively NIH13 can alter multiple angiogenic-related genes.

In summary, in this study we have demonstrated novel *in vitro* inhibitory activities elicited by a panel of 12-LO compounds with mixed structural scaffolds. We have also validated the utility of compound NIH13 and its associated structural properties (i.e. an 8-hydroxyquinoline scaffold) as a class of 12-LO inhibitor with novel anti-angiogenic properties *in vitro*. In addition a reasonable safety profile *in vivo* (i.e. in the zebrafish)

indicates its potential as a candidate for other alternative *in vivo* models of angiogenesis. While previous studies have indicated that blocking 12-LO in endothelial cells decreases angiogenic tubule formation and VEGF expression, this is the first study to screen the effect of 12-LO inhibitors on multiple angiogenic gene expression pathways. Given that we observed downregulations of the angiopoietin-Tie system and the pro-angiogenic and pro-inflammatory chemokine GRO-α, in addition to the VEGF receptor and co-receptor KDR and neuropilin we suggest that inhibition of 12-LO activity in HUVECs is having anti-angiogenic effects beyond VEGF signalling itself that require further investigation.

Chapter 6 Assessment of the anti-cancer and anti-angiogenic potential of novel 5-lipoxygenase and 12-lipoxygenase targeted inhibitors in models of oesophageal adenocarcinoma

6.1 Introduction

Oesophageal cancer is currently the eighth most common cause of cancer-related death worldwide (Ferlay *et al.*, 2012). The Irish population has one of the highest rates of oesophageal cancer in Europe with approximately 400 cases (of which 68% are OAC subtype) diagnosed per year (Reynolds *et al.*, 2011). The incidence of oesophageal cancer has risen in Ireland by 27% in the last 15 years and is primarily due to a 50% increase in the rate of OAC during this time period (National Cancer Registry, 2013), thus rising OAC rates are a major challenge for both clinicians and scientists. While major improvements to treatment regimes have been implemented over the last decade, particularly in the case of neoadjuvant CRT, there are still many patients who do not derive any benefits from such treatment modalities (Reynolds *et al.*, 2007). In recent times an increasing proportion of cancer research has therefore focused on the development of molecular therapies that target tumour-dependent processes such as growth regulation and angiogenesis (Shah *et al.*, 2005, El-Rayes *et al.*, 2010) to complement standard treatment regimes in the future.

Eicosanoid signalling pathways including the cyclooxygenases and lipoxygenases have been strongly implicated in inflammation and cancer development for malignancies such as breast, prostate and colorectal cancer (Rao *et al.*, 2012). Cyclooxygenases, or more specifically COX-2, have shown promising results as therapeutic biomarkers and targets in oesophageal and gastric cancer to date (Zhi *et al.*, 2006, Prins *et al.*, 2012, Dawson *et al.*, 2007). In contrast there has been very little focus on the other arm of the eicosanoid pathway, i.e. the lipoxygenase enzyme family, particularly 12-LO, as a therapeutic route for oesophageal cancer.

The involvement of 5-LO and 12-LO in cancer progression is supported by a growing body of literature. Increased 5-LO activity is associated with a number of cancer types including prostate, renal, breast, colorectal and pancreatic cancer (Matsuyama *et al.*, 2004, Matsuyama *et al.*, 2007, Jiang *et al.*, 2006a, Hennig *et al.*, 2002, Barresi *et al.*, 2007). Similarly an association between increased 12-LO activity and several malignancies including melanoma, prostate and breast cancer have been reported (Winer *et al.*, 2002, Gao *et al.*, 1995, Jiang *et al.*, 2003). This wealth of evidence clearly indicates the potential of targeting the lipoxygenase pathway as an anti-cancer treatment strategy (Pidgeon *et al.*, 2007).

Numerous studies have investigated the use of 5-LO and 12-LO small molecule inhibitors in human cancer *in vitro* models and murine *in vivo* models, providing novels insights into the role of these enzymes in cancer development and progression. 5-LO inhibition has been shown to decrease cell proliferation and to induce apoptosis in prostate, renal cell and pancreatic cancer (Ghosh and Myers, 1998, Matsuyama *et al.*, 2004, Sarveswaran *et al.*, 2011, Ding *et al.*, 1999). Similar results have been obtained through *in vitro* studies blocking 12-LO activities in a number of cancer models including epidermoid, prostate, hepatocellular and breast cancer (Agarwal *et al.*, 2009, Matsuyama *et al.*, 2004, Xu *et al.*, 2012, Wong *et al.*, 2001). Evidence suggests that both 5-LO and 12-LO inhibitors, such as REV 5901 and baicalein respectively, induce apoptosis via a downregulation of anti-apoptotic Bcl-2 and Mcl-1 and an elevation of pro-apoptotic Bax and a downregulation of active ERK1/2 and PI3K-Akt pathways (Tong *et al.*, 2002, Pidgeon *et al.*, 2002, Agarwal *et al.*, 2009). More recently it has been shown that 5-LO inhibition-induced apoptosis in prostate cancer cells occurs via mechanisms independent of the pro-survival signals Akt and ERK, instead involving the alternate suppression of protein kinase C-epsilon (Sarveswaran *et al.*, 2011). Regardless of the specific mechanisms involved, the induction of apoptosis across different cancer cell types, highlights the applicability of 5-LO and 12-LO inhibitors as anti-cancer agents. 5-LO and 12-LO activity has been shown to regulate adhesive and invasive capacities of cancer cells. For example 5-LO-specific inhibition in prostate cancer cells decreased migration *in vitro* (Meng *et al.*, 2013) while overexpression of 12-LO resulted in increased surface integrin adhesion molecules and cell survival (Pidgeon *et al.*, 2003). Additionally it has also been reported that 5-LO inhibition decreased prostate derived tumour masses in murine models, leading to a less aggressive tumour (Meng *et al.*, 2013). Thus 5-LO and 12-LO inhibition has the potential to target multiple tumour-dependent processes.

It has been mentioned at numerous points throughout this thesis, that lipoxygenases have been linked to angiogenesis both in cells of the vasculature itself (see Chapter 5 introduction) and in cancer cells (Ye *et al.*, 2005b, Chatterjee *et al.*, 2013, Connolly and Rose, 1998, Nie *et al.*, 2003). Thus pharmacological blockage of lipoxygenases may elicit anti-cancer effects, at least partially through a blockage of vessel formation in growing tumours. For instance, a study by Ye *et al.*, has shown that 5-LO inhibition in pre-cancerous colon adenomas decreased angiogenesis in the vicinity of the polyp and that this effect coincided with decreased expression of the pro-angiogenic factors VEGF and MMP-9 (Ye *et al.*, 2004). Similarly overexpression of 12-LO has been shown to be associated with increased VEGF activity in models of prostate cancer and

this activity can be suppressed by 12-LO inhibitor treatment (McCabe *et al.*, 2006, Nie *et al.*, 2006).

Taken together these results provide evidence in support of the multiple routes by which lipoxygenase inhibition can elicit anti-cancer effects i.e. via a downregulation of growth regulation, invasiveness and/or tumour-associated angiogenesis. In regard to oesophageal cancer, only one published study has investigated the effect of 5-LO inhibition *in vitro* (Hoque *et al.*, 2005). To date no study has investigated the role of 12-LO in oesophageal cancer or what effect 12-LO inhibition has in models of this cancer. To our knowledge no study has examined the association of 5-LO and 12-LO signalling and angiogenesis in a model of oesophageal cancer. Consequently in this chapter we addressed these questions utilising novel compounds targeting 5-LO and 12-LO.

6.2 Aims and objectives

The aim of this chapter was to investigate the anti-cancer and anti-angiogenic effects of novel 5-LO and 12-LO inhibitors in models of OAC. A number of novel lipoxygenase inhibitors selected from Chapter 5, including the 5-LO inhibitor NIH4 and three 12-LO inhibitors NIH13, NIH15 and GM5, were tested *in vitro* and *ex vivo*. It was hoped that this work would provide insight into the relevance of targeting these two enzymatic pathways as therapeutic approaches for OAC.

Specific Objectives:

- To investigate the anti-cancer efficacy of 5-LO and 12-LO inhibitors in the OE33 cell model, through measurement of effects to cell viability, proliferation and apoptosis

- To assess the ability of novel and commercial 5-LO and 12-LO inhibitors to specifically suppress 5-LO or 12-LO activity in wild-type OE33 cells or 12-LO overexpressing OE33 cells respectively

- To investigate the effect of novel inhibitors to 5-LO and 12-LO metabolite production in *ex vivo* cultured OAC biopsies

- To investigate whether overexpression of 12-LO in OE33 cells alters VEGF gene expression and VEGF production

- To investigate the effect of novel 5-LO and 12-LO inhibitors on angiogenic gene expression and protein production by OE33 cells

- To assess the effect of 5-LO and 12-LO inhibitor treatment on the angiogenic secretory profile of OAC patient biopsies cultured *ex vivo*

6.3 Results

6.3.1 Confirmation of 5-LO and 12-LO expression in the OE33 cell line model

For this portion of the project an established OAC cell line, OE33, was used (Boonstra *et al.*, 2010). OE33 cells are derived from non-metastatic stage IIa, poorly differentiated adenocarcinoma of the lower oesophagus with a history of BO metaplasia. 5-LO expression in OE33 cells was confirmed by both western blot and qPCR using protein lysate and RNA isolated from untreated OE33 cells (Figure 6.1a and Figure 6.1b). Similarly, 12-LO expression was confirmed by nested RT-PCR while qPCR indicated a low basal level of expression (Figure 6.1a and Figure 6.1c).

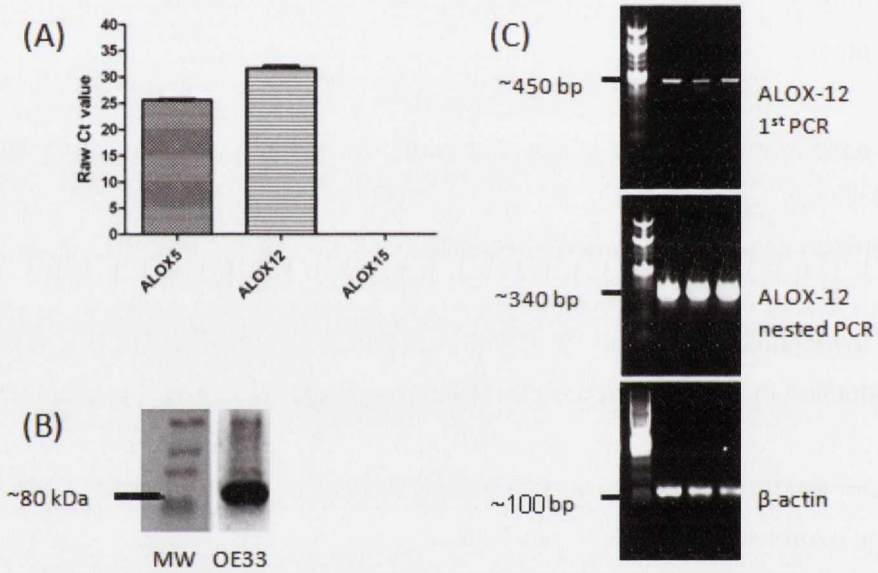

Figure 6.1 Confirmation of 5-LO and 12-LO expression in the OE33 cell line. (A) High endogenous levels of *ALOX5* were detected in OE33 cells (Ct<25), while a lower level of *ALOX12* were found (Ct=32-34) by qPCR. In comparison, *ALOX15*, another lipoxygenase enzyme was undetermined in OE33 cells up to a cycle number of 45. Error bars indicate mean ± S.E.M. of three technical replicates. (B) 40 µg of OE33 protein lysate was used to confirm 5-LO expression by western blot, indicated by a single band at ~80 kDa. (C) *ALOX12* was confirmed using a second set of primers specific for *ALOX12*, by nested RT-PCR. The product from the first round of PCR was ~450 base pairs (bp) while re-amplification of this product with the nested primers resulted in single product band of ~340 bp. β-actin (*ACTB*) was used as a loading control.

6.3.2 Assessing the effects of selected novel and commercial 5-LO and 12-LO inhibitors on the viability of OE33 cells

Overall viability of OE33 cells was assessed by measuring metabolic activity by the MTT assay as described in Section 2.23. OE33 cells were treated with increasing concentrations of the novel 5-LO inhibitor NIH4, ketoconazole, REV 5901 and zileuton for 24 hours. Doses used were 0.1 μM, 1 μM, 10 μM, 25 μM, 50 μM, 100 μM and 150 μM in order to establish IC_{50} values as determined by non-linear regression. Similar to ketoconazole and REV 5901, the novel 5-LO inhibitor NIH4 showed a dose-dependent decrease in cell viability (Figure 6.2). In contrast the potent 5-LO inhibitor, zileuton showed little effect on viability up to 100 μM dose (Figure 6.2). The same experiment was carried out for all selected 12-LO inhibitors (NIH13, NIH15 and GM5) and baicalein. They all had a dose response effect with NIH13 displaying the most potent effects to cell viability with an estimated IC_{50} value of 18.24 μM.

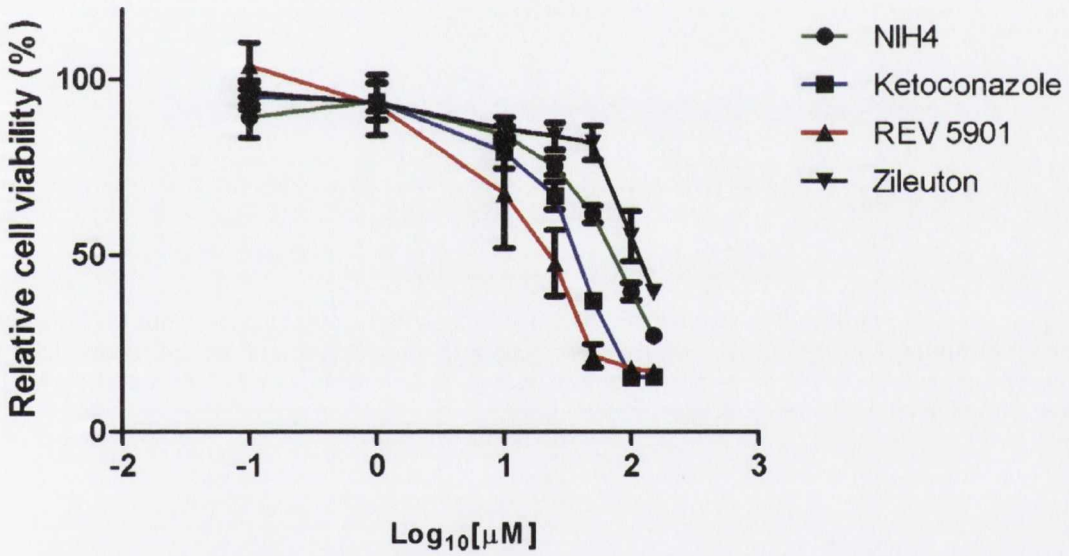

Compound	IC_{50} (μM)
NIH4	67.85
Ketoconazole	37.35
REV 5901	20.59
Zileuton	123.0

Figure 6.2 Cell viability IC_{50} values of 5-LO inhibitors were established from MTT assay measurements by non-linear regression. Following drug treatment for 24 hours OE33 cell relative viability (%) compared to vehicle control (0.25%) was measured by MTT assay for at least 3 independent experimental sets.

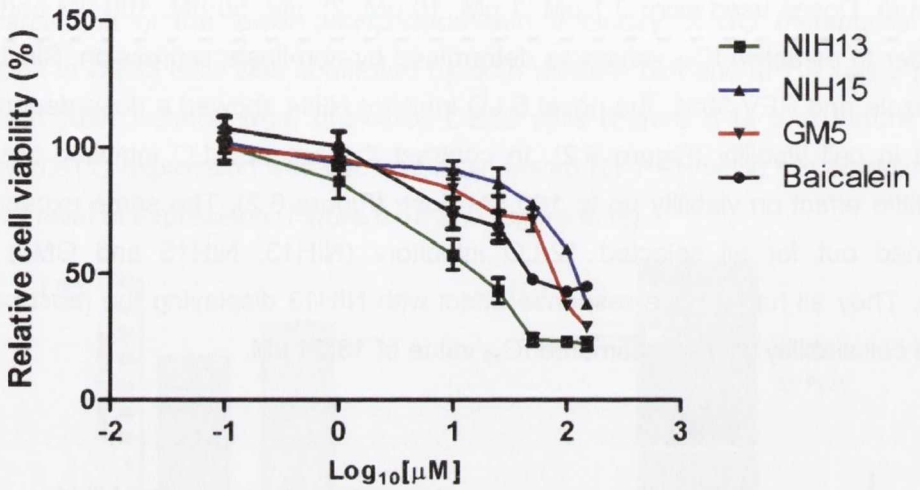

Compound	IC_{50} (μM)
NIH13	17.12
NIH15	131.0
GM5	71.63
Baicalein	59.42

Figure 6.3 Cell viability IC_{50} values of 12-LO inhibitors were established from MTT assay measurements by non-linear regression. Following drug treatment for 24 hours OE33 relative cell viability (%) compared to vehicle control (0.25% DMSO) was measured by MTT assay for at least 3 independent experimental sets.

6.3.3 Assessment of the ability of selected 5-LO and 12-LO inhibitors to induce anti-proliferative effects on OE33 cells

To evaluate whether anti-proliferative effects contribute to a reduction in overall cell viability observed by the MTT assay, active DNA synthesis was measured by the incorporation of BrdU. Cell were prepared as described in Section 2.22 and then treated with novel or commercial lipoxygenase inhibitors at doses of 1 μM, 10 μM and 25 μM. 25 μM was chosen as the upper dose to test based on the activity of the drugs at this concentration in the MTT assay and due to limited BrdU reagent and novel compounds. For each experimental biological replicate performed, the vehicle control was set to 100% cell proliferation. All experiments were carried out three to four times. Ketoconazole and NIH4 both showed an incremental decrease in cell proliferation with increasing concentration, however only the dose of 25 μM NIH4 caused cell proliferation to be significantly decreased in comparison to the vehicle control (100% versus 22.3 ±11.0%, $p<0.01$) (Figure 6.4). REV 5901 was shown to significantly decrease DNA synthesis at a dose of 25 μM (11.06 ±0.29% $p<0.001$) (Figure 6.4c) however considering the IC_{50} for cell viability was 20.59 μM, it is possible that the observed effect is a combination of anti-proliferative and cytotoxic effects. Notably, BrdU incorporation was not affected by zileuton (Figure 6.4d). Assessment of the anti-proliferative effect of 12-LO inhibitors indicated that NIH13 was the most potent of all the drugs tested significantly decreasing OE33 cell proliferation across all doses tested (Figure 6.5) (1 μM: 97.85 ±4.68% ($p<0.05$), 10 μM: 13.09 ±8.15% ($p<0.001$), 25 μM: 8.77 ±4.51% ($p<0.001$)). The IC_{50} for all lipoxygenase inhibitors, if available, can be found in Table 6.1.

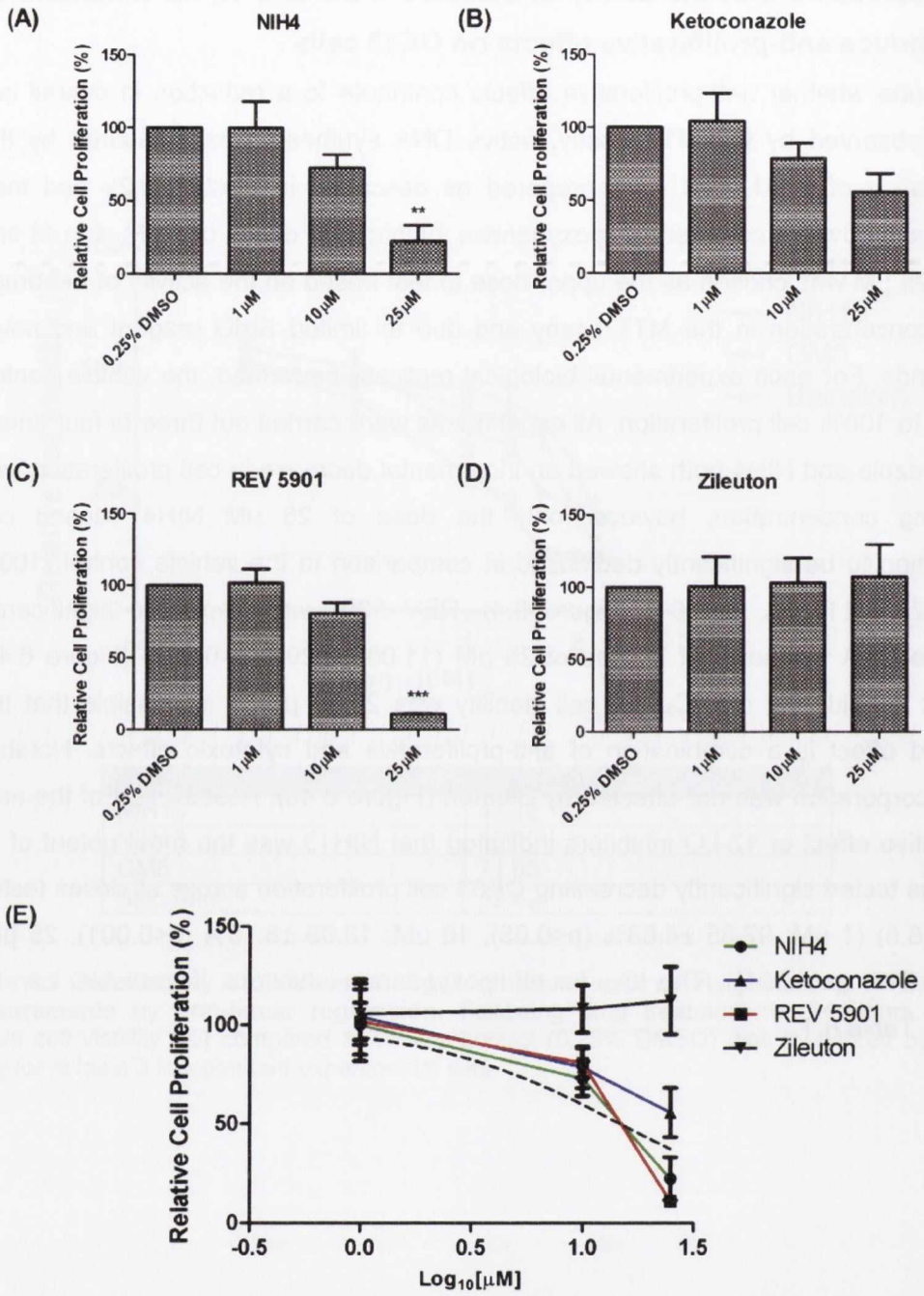

Figure 6.4 NIH4 and REV 5901 significantly decrease OE33 cell proliferation at the highest tested dose of 25 μM. Following drug treatment for 24 hours OE33 relative cell proliferation (%) compared to vehicle control (0.25% DMSO) was measured by BrdU incorporation. (A) NIH4 significantly decreased proliferation at 25 μM (100% versus 22.3 ±11.0%, $p<0.01$) (B) Ketoconazole showed a decreasing at 10 μM and 25 μM, although not significant. (C) REV 5901 showed a significant decrease at 25 μM (100% versus 11.06 ±0.29% , $p<0.001$). (D) zileuton had no effect. (E) IC_{50} values were determined by non-linear regression. Statistical test used was one-way ANOVA with Tukey's Multiple Comparison Test: n=3-4 $p<0.01$(**) and $p<0.001$(***). Error bar denotes mean ± S.E.M.

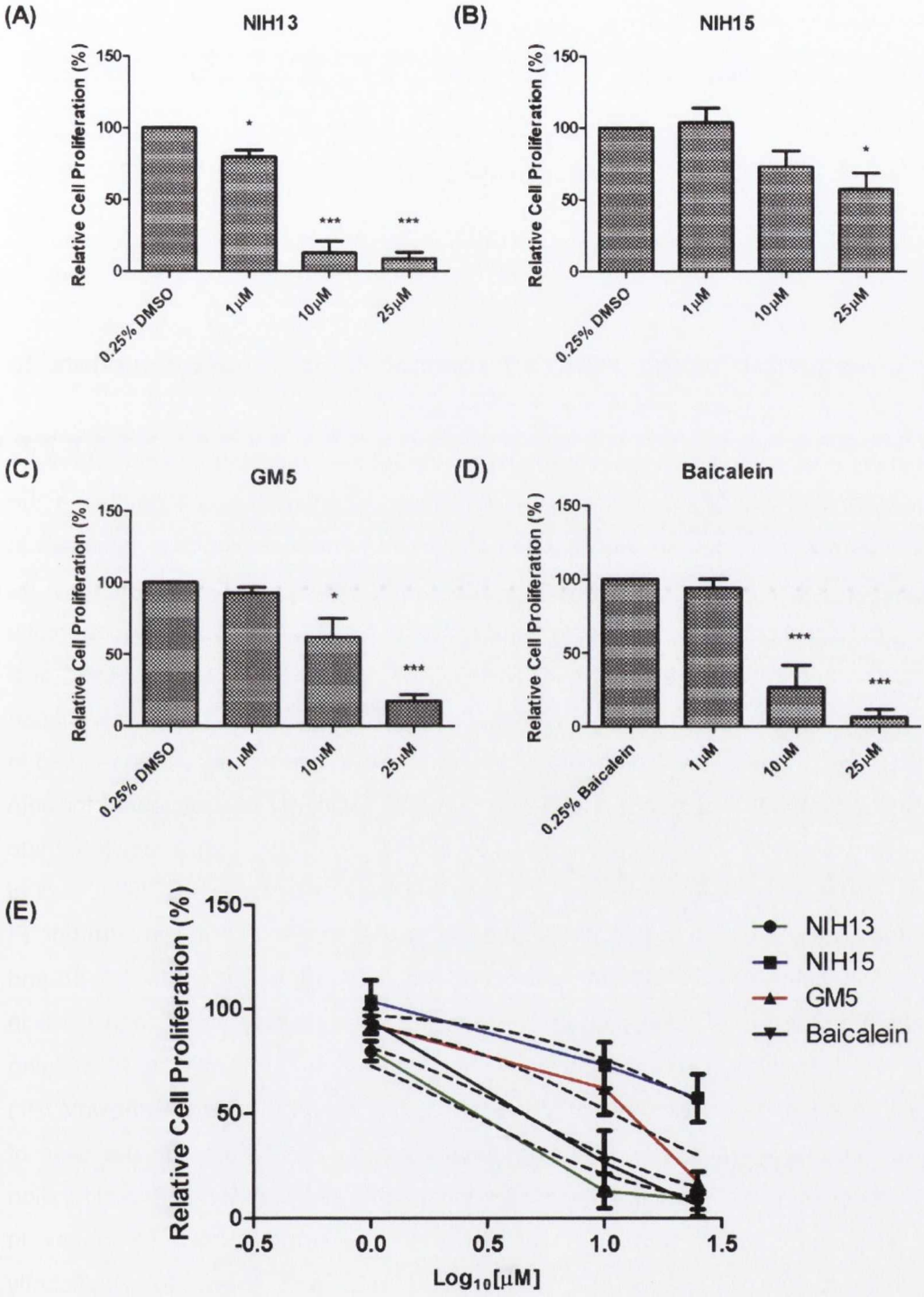

Figure 6.5 All 12-LO inhibitors significantly decrease cell proliferation at one or more doses tested. Following drug treatment for 24 hours OE33 relative cell proliferation (%) compared to vehicle control (0.25% DMSO) was measured by BrdU incorporation. (A) NIH13 significantly decreased proliferation across all doses. (B) NIH15 significantly decreased cell proliferation at 25 μM. (C) GM5 and (D) baicalein both significantly decreased cell proliferation at 10 μM and 25 μM. (E) IC_{50} values were determined by non-linear regression. Statistical test used was one-way ANOVA with Dunnett's Multiple Comparison Test: n=3 for NIH15 treatments while n=4 for others. $p<0.05$(*) and $p<0.001$(***).Error bar denotes mean ± S.E.M.

Table 6.1 IC_{50} doses for OE33 cell proliferation by 5-LO and 12-LO inhibitors determined by non-linear regression analysis

Compound	IC_{50} (μM)
NIH4	14.87
Ketoconazole	>25, did not reach IC50
REV 5901	14.24
Zileuton	>25, did not reach IC50
NIH13	2.67
NIH15	>25 did not reach IC50
GM5	10.81
Baicalein	4.38

6.3.4 Investigation of the ability of selected lipoxygenase inhibitors to induce cytotoxic effects on OE33 cells

The reduction of tumour cell viability mediated by the lipoxygenase inhibitors may be attributed to their ability to induce cytotoxic effects by triggering cell death via the intrinsic pathway of apoptosis as has been shown for some lipoxygenase inhibitors in other cancer cells (Ghosh and Myers, 1998). Alternatively the inhibitors may be inducing cytotoxic effects by triggering passive cell death (i.e. necrosis). The apoptotic effect of the novel inhibitors (i.e. NIH4, NIH13, NIH15 and GM5) was assessed at a single inhibitor dose of 10 μM by AnnexinV/PI (Section 2.24). This dose was chosen because it was a dose at which some level of anti-proliferative activity was observed in all compounds and it was also a dose where anti-12-LO activity was observed for both the 8-hydroxyquinole compound class (i.e. NIH13) and the benzenesulfonamide compound class (i.e. GM5) in assays with beta islet cells (Kenyon *et al.*, 2011, Luci *et al.*, 2014). There was no significant difference in the levels of AnnexinV and/or PI staining cells between NIH4 and the vehicle control following treatment for 24, 48 and 72 hours (Figure 6.6). Similarly analysis of the 12-LO inhibitors NIH15 and GM5 in comparison to control, indicated no significant increase in AnnexinV or PI staining following 24, 48 or 72 hour treatment. It was noted that early apoptosis ($AnnexinV^+/PI^-$) increased across all conditions including vehicle control at 72 hours. In the case of NIH13, considering its particular high potency in the cell viability and proliferation assay, a second lower dose of 5 μM was also assessed in the AnnexinV/PI assay. In comparison to vehicle control (12.10% ±1.77) NIH13 was shown to significantly increase early apoptosis at the 5 μM (25.58 ±4.16%, n=5, $p<0.05$) and 10 μM dose (27.42 ±4.17%, n=5, $p<0.01$) 24 hours post treatment. The same trend was seen at 48 hours and a rise in early apoptosis in the vehicle-treated cells was also observed. By 72 hours a similar level of early apoptosis was seen across all treatments, including the vehicle control and therefore was not a drug-specific effect. Compared to mean control levels (9.25 ±1.60%) NIH13 showed significantly increased necrosis at 5 μM (19.68

±3.70%, n=5, $p<0.05$) and 10 μM doses (25.38 ±3.66%, n=4, $p<0.05$) indicating that prolonged exposure to NIH13 induces a higher level of passive cell death or necrosis.

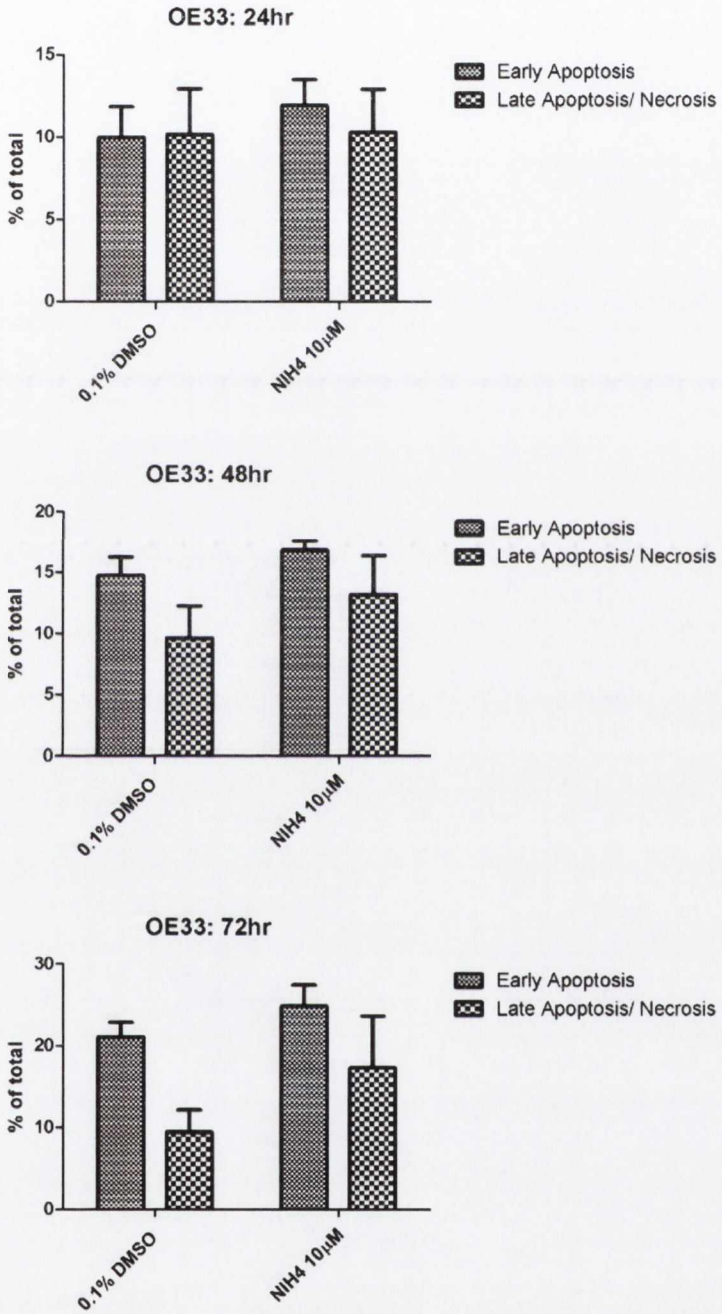

Figure 6.6 NIH4 does not induce significant apoptosis in OE33 cells up to 72 hours. OE33 cells were treated with NIH4 at 10 μM for 24, 48 and 72 hours and were subsequently stained for AnnexinV and PI. Representative dot plots of Annexin and/or PI positive cells are shown for each compound tested. Graph indicates no significant difference in early apoptosis ($AnnexinV^+$) or late apoptosis ($AnnexinV^+/PI^+$) between drug-treated and vehicle control cells (n=3). Statistical test used was one-way ANOVA with Tukey's Multiple Comparison Test. Error bar denotes mean ± S.E.M.

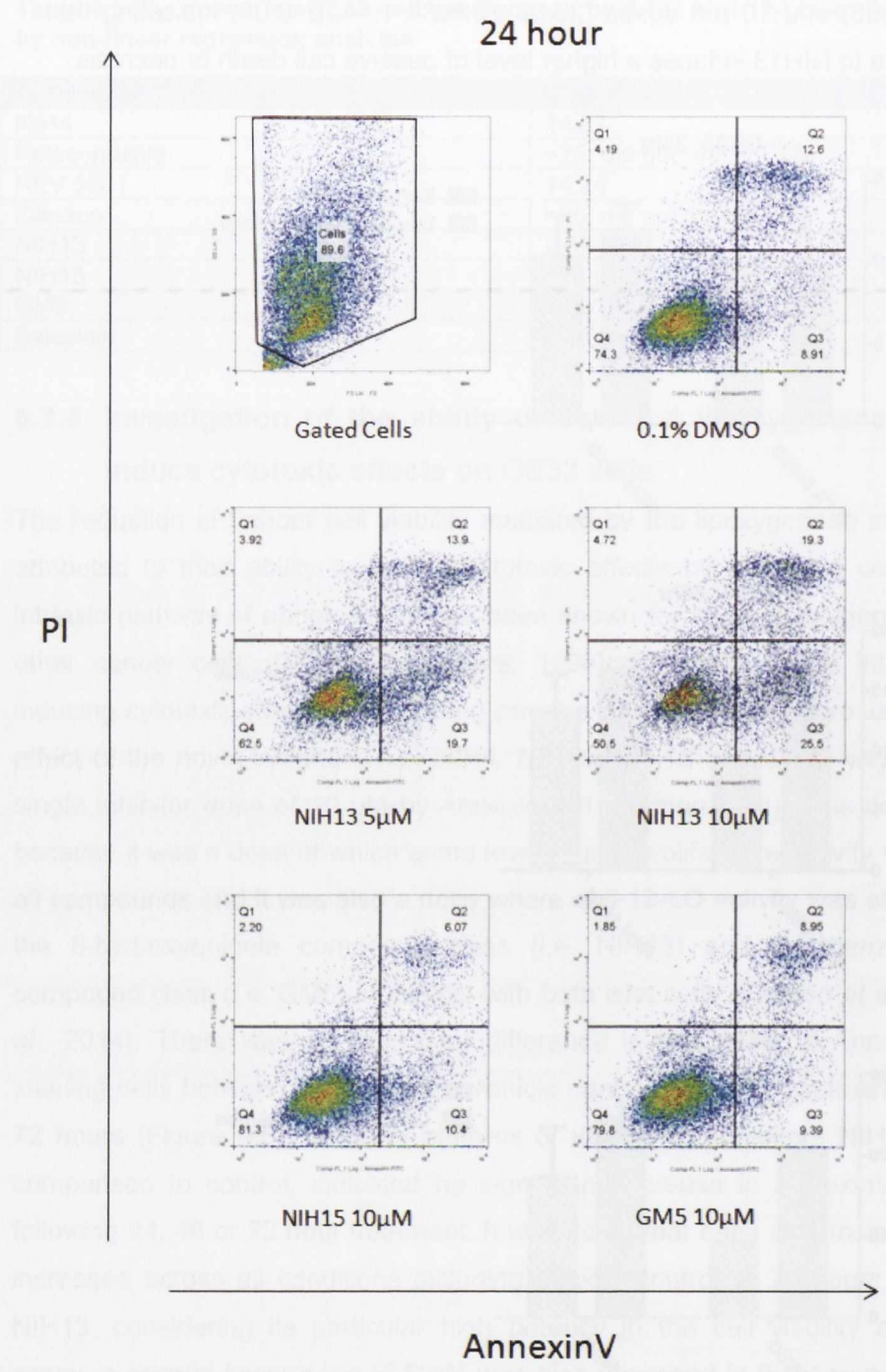

Figure 6.7 Representative dot plots indicating proportion of AnnexinV/PI stained OE33 cells following 24 hour 12-LO inhibitor treatment. There was an increased proportion of early apoptotic ($AnnexinV^+/PI^-$) cells following 24 hour NIH13 treatment at both 5 μM and 10 μM compared to vehicle control.

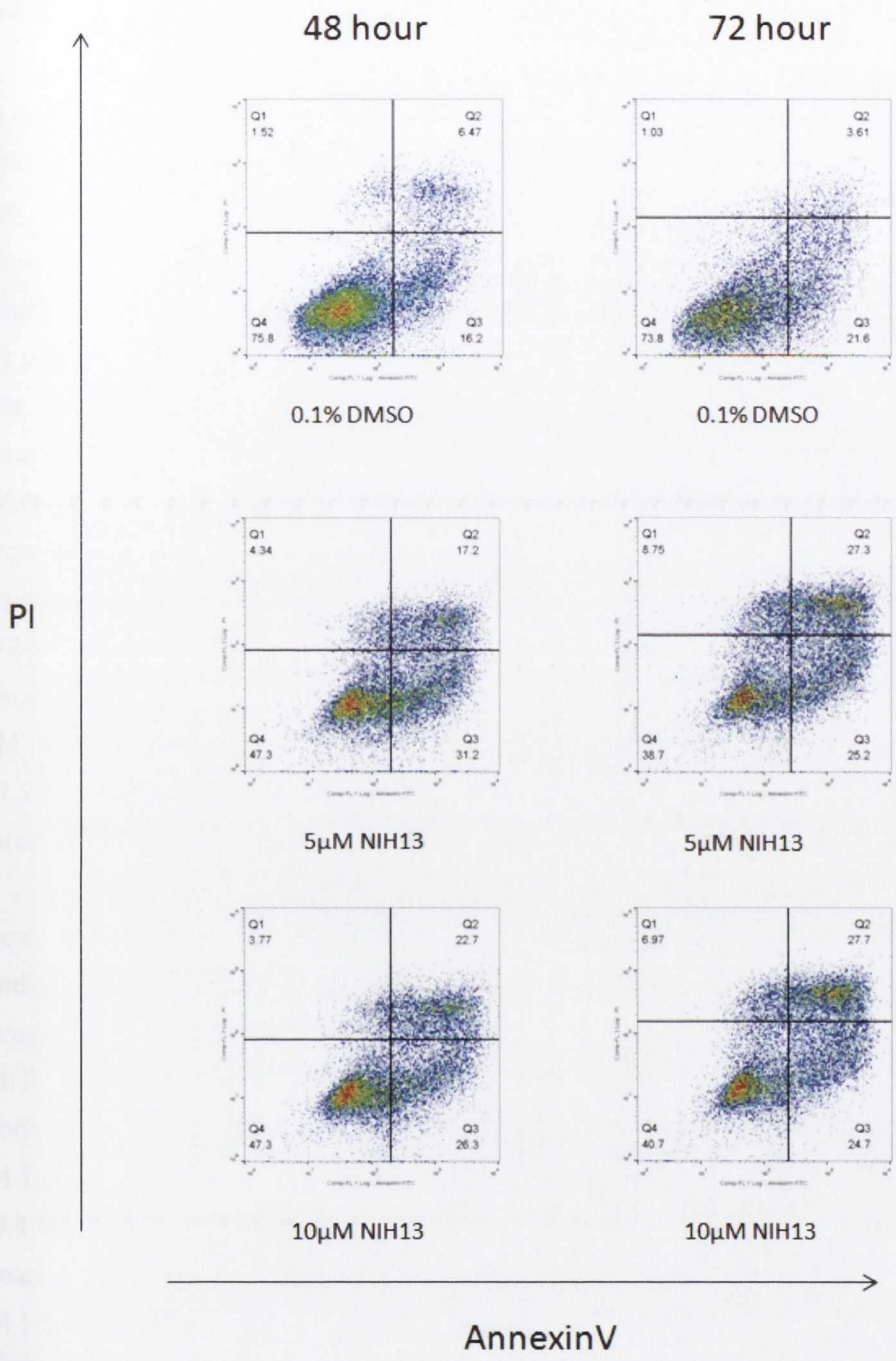

Figure 6.8 Representative dot plots indicating proportion of AnnexinV/PI stained OE33 cells following 48 and 72 hour treatment with NIH13. There was a higher proportion of stained cells for early and late apoptosis following 48 hour NIH13 treatment although this was not significant (see Figure 6.9). At 72 hours post NIH13 treatment there was a significantly higher amount of late apoptotic/necrotic cells compared to the vehicle control (see Figure 6.9).

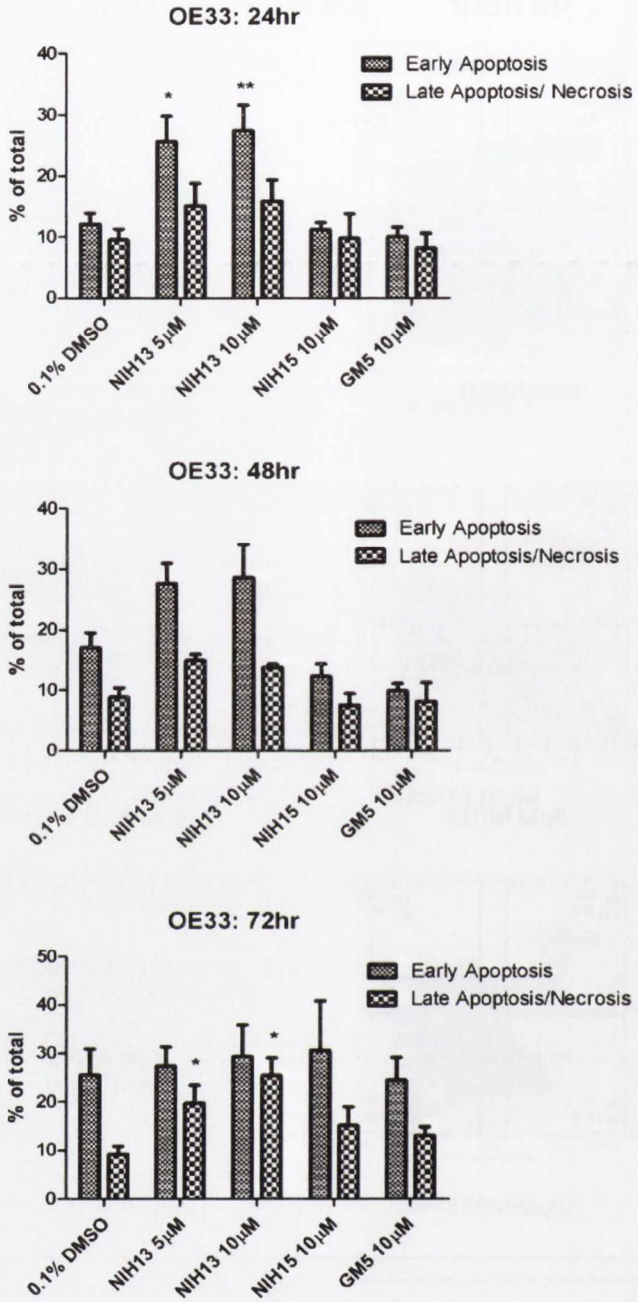

Figure 6.9 NIH13 induces significantly higher apoptosis at 24 hours and significantly higher necrosis at 72 hours compared to control at both 5 μM and 10 μM doses . OE33 cells were treated with NIH13, NIH15 and GM5. An extra dose of 5 μM was included in the assessment of NIH13 apoptotic effects. Graph indicates no significant difference in early apoptosis ($AnnexinV^+PI^-$) or late apoptosis ($AnnexinV^+/PI^+$) between drug treated and vehicle control cells for NIH15 and GM5 over all time points (24 hour: n=4, 48 and 72 hour: n=3-5). In the case of NIH13 a significant increase in early apoptosis at both the 5 μM ($n=5, p<0.5$) and 10 μM ($n=4$, $p<0.01$) dose was noted at 24 hours. There was a significant induction of late apoptosis/ necrosis by NIH13 at 5 μM ($n=5$, $p<0.05$) and 10 μM ($n=4$, $p<0.05$) at 72 hours. Statistical test used was one-way ANOVA with Tukey's Multiple Comparison Test. $p<0.05$(*) and $p<0.01$(**). Error bar denotes mean ± S.E.M.

6.3.5 Assessing 5-LO activity in OAC *in vitro* and *ex vivo* and the potency of 5-LO inhibitors to suppress this activity

In order to assess whether the novel 5-LO inhibitor NIH4 and the other 5-LO inhibitors ketoconazole, REV 5901 and zileuton could inhibit 5-LO enzyme activity of OE33 cells, the level of LTB4 was measured by ELISA. Cells were treated with 10 μM AA as a source of substrate in combination with a drug or vehicle control (0.1% DMSO) for 24 hours. Cells were treated with 5 μM and 10 μM NIH4, 10 μM ketoconazole, 5 μM and 10 μM REV 5901 and 5 μM and 10 μM zileuton. Three independent experiments with this setup were performed. The conditioned media collected after the 24 hour treatments was then assessed by ELISA for the levels of LTB4 as described in Section 2.20.4. The concentration of total cellular protein was determined by BCA assay and used to normalise the ELISA data. This ELISA has a minimum detection limit of 5.62 pg/mL. The vehicle control treated cells demonstrated a high level of LTB4 production (124.13 ±8.88 pg/mL). All inhibitors at all concentrations were found to significantly decrease LTB4 levels ($p<0.001$) in the range of 58-85%. NIH4 10 μM and Zileuton 10 μM doses were found to have the most potent effects reducing OE33 LTB4 levels to 31.21 ±2.22 pg/mL and 18.34 ±2.38 pg/mL respectively. Due to limited reagent the three biological replicates for each treatment were only run singly on the ELISA plate.

Next, the endogenous production of LTB4 by OAC tumour biopsies cultured *ex vivo* and the effect of selected 5-LO inhibitors was also investigated. Due to limited biopsy availability, it was only possible to test two chosen compounds: the novel 5-LO inhibitor NIH4 and the FDA-approved 5-LO inhibitor zileuton. Fresh biopsies were collected from the clinic and cut into equally sized pieces. Each piece of tissue was cultured for 24 hours in *ex vivo* medium as described in Section 2.20.2 with either vehicle control (0.1% DMSO), 10 μM NIH4 or 10 μM Zileuton. Biopsies from 11 OAC patients were treated with NIH4 and a smaller subset of these were treated with zileuton (n=4). After 24 hour treatment the TCM was collected to run on the LTB4 ELISA plate. The biopsy tissue pieces were homogenised and total protein concentration was determined by BCA assay to normalise protein secretions detected to the size of the biopsy pieces. Only 6/11 biopsies produced detectable levels of LTB4 (i.e. >5.62 pg/mL). The mean level detected in the TCM was 45.61 ±17.37 pg/mL with a range of 14.02-120.07 pg/mL. Two of the patient biopsies had particularly high levels of detected LTB4 (indicated as green and red dots in Figure 6.11a). In all biopsy sets the level of LTB4 was approximately 50% less in the TCM from biopsies treated with NIH4 or zileuton compared to vehicle control. This biological effect was masked by the two data sets which higher mean LTB4 levels (i.e. green and red dots) and therefore the data was

better represented as fold change. Represented as fold change LTB4 secretion by tumour biopsies was found to be significantly decreased following treatment with NIH4 or zileuton ($p<0.001$) (Figure 6.11b).

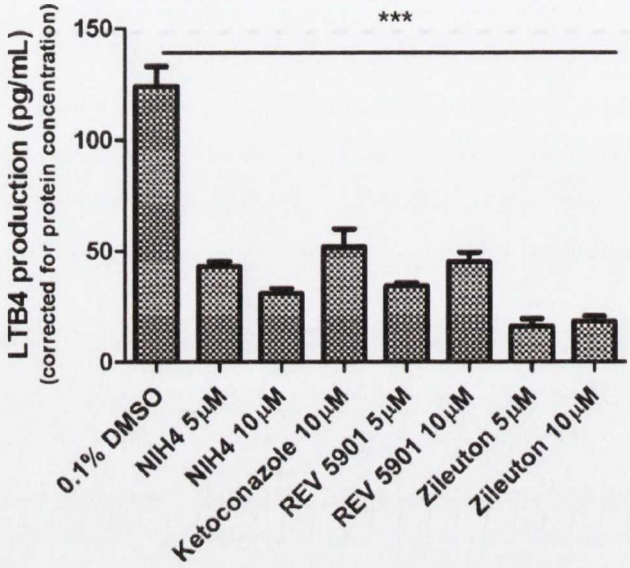

Figure 6.10 LTB4 production by OE33 cells is decreased by 5-LO inhibitor treatment . OE33 cells were treated with 5-LO inhibitors for 24 hours in combination with 10 μM AA. The supernatant from the cells was assessed for LTB4 production by ELISA and data was normalised to total cellular protein. LTB4 levels were decreased by all treatments by at least 58% and zileuton was shown to have the greatest potency decreasing LTB4 levels by over 85%.*** indicates significance between vehicle control and all treatment group. Statistical test used was one-way ANOVA with Dunnett's Multiple Comparison Test: $p<0.001$(***). Error bar denotes mean ± S.E.M.

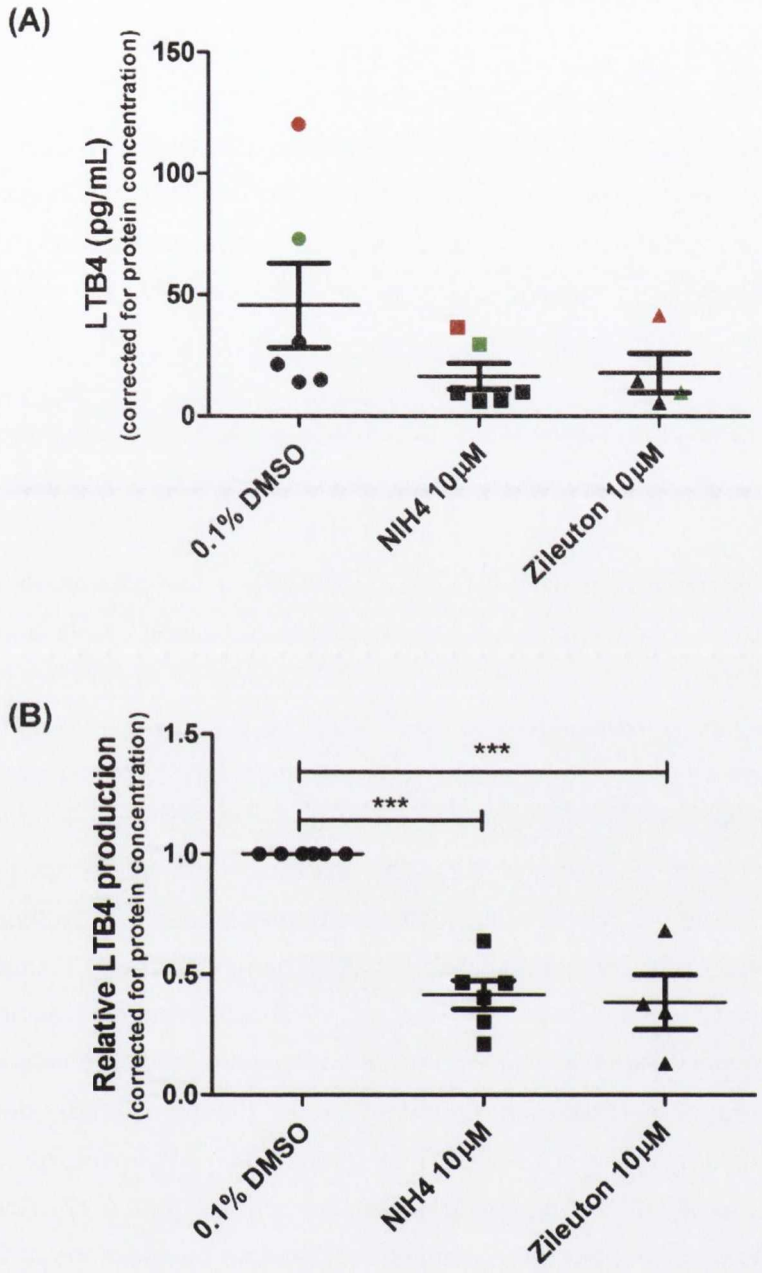

Figure 6.11 OAC tumour LTB4 secretions are decreased by 5-LO inhibitor treatment. Fresh tumour biopsies were cultured *ex vivo* for 24 hours in combination with either vehicle control (0.1% DMSO) or, 10 µM NIH4 (n=11) or 10 µM zileuton (n=4) and TCM was assessed by ELISA for endogenous LTB4 production and normalised to total biopsy protein. Only 6/11 biopsy sets had detectable levels of LTB4.(A) 2 sets of biopsies had particularly high levels of LTB4 (green and red dots) and skewed the data however they did show the same pattern as other biopsy sets i.e. a decrease in LTB4 following drug treatment. (B) The data is represented as fold change relative to control and reveals a similar biological effect of NIH4 and zileuton in which LTB4 is decreased ($p<0.001$). Statistical test used was Kruskal-Wallis test with Dunn's Comparison Test: $p<0.001$(***). Error bar denotes mean ± S.E.M.

6.3.6 Transient overexpression of 12-LO in OE33 cells

Transient overexpression of 12-LO in cancer cells has been used in previous studies as a model to test the specificity of 12-LO inhibitors (Bednar *et al.*, 2007). In previous sections it was shown that 12-LO inhibitors decrease cell viability of OE33 cells and that this effect involved, at least partially, an inhibitory effect to the process of cell proliferation. In this part of the project OE33 cells transiently transfected to overexpress 12-LO were utilised to assess the ability of selected novel 12-LO compounds to specifically inhibit 12-LO enzyme activity *in vitro*.

Overexpression of 12-LO in OE33 cells was achieved through the transient transfection of cells with a 12-LO overexpression vector, *ALOX12*-pcDNA(+3.1). OE33 cells that were 70-80% confluent were reverse transfected as described in Section 2.26.3. In order to verify the overexpression of 12-LO transcript in comparison to the vector control and wild type OE33 cells, RNA was isolated from cells at 24, 48 and 72 hours post transfection and cDNA was assessed by qPCR using an *ALOX12* primer probe. *18S* was utilised as a house-keeping gene. Due to the low expression levels of *ALOX12* detected in both untransfected (UT) wild-type OE33 cells and the vector control (VC) transfected cells, overexpression of 12-LO led to an exponential increase in the RQ values determined (Table 6.2). This effect was maintained up until the 72 hour time point tested. As an alternate method of verification cDNA synthesised from OE33 cells 72 hours post transfection was amplified by nested RT-PCR using primers specific for *ALOX12*. The product was run on an agarose gel and an increase in *ALOX12* in overexpressing cells was visible in comparison to wild-type cells and vector control transfected cells. Following normalisation to β-actin (*ACTB*), densitometry revealed a 2.71-fold increase in *ALOX12* PCR product in 12-LO overexpressing cells following the first round of PCR compared to vector control (Figure 6.12). RNA isolated 48 hours post transfection from three independent reverse transfections of OE33 cells with *ALOX12*-pcDNA(+3.1), verified the significance of this overexpression by qPCR ($p<0.0001$) (Figure 6.13).

To further validate the overexpression of 12-LO in *ALOX12*-pcDNA(+3.1) transfected cells, the production of the 12-LO metabolite, 12(S)HETE was measured. After 24 hours incubation with 10 μM AA, the cell supernatant of transfected cells was assessed for 12(S)HETE levels using a 12(S)HETE competitive ELISA as described in Section 2.20.2. While there was some level of variability between the biological replicates (range 21043.45-13283.14 pg/mL), mean 12(S)HETE concentration of the 12-LO overexpressing cells (19799.68 ±3458.67 pg/mL) was significantly higher ($p<0.001$,

n=3) compared to cells transfected with the empty pcDNA(+3.1) vector (3144.20 ±432.74 pg/mL). The increased production of 12(S)HETE is indicative of increased 12-LO protein, thus verifying the 12-LO overexpression transfection procedure. It was also noted that untransfected wild-type OE33 cells were capable of 12(S)HETE synthesis, albeit at a lower level than the 12-LO overexpressing cells. (1702.26 ±668.01 pg/mL).

Table 6.2 12-LO overexpressing OE33 cells have an exponential increase in *ALOX12* relative gene expression compared to wild-type or vector control transfected OE33 cells

Transfection treatment	Gene	Average Ct	ΔCt	RQ (relative to UT)
UT 24 hour	*ALOX12*	32.28	18.78	1
	18S	13.5		
VC 24 hour	*ALOX12*	33.4	17.44	2.52
	18S	15.96		
ALOX12 24 hour	*ALOX12*	10.63	-4.82	$1.27x10^7$
	18S	15.46		
UT 48 hour	*ALOX12*	34.7	21.95	1
	18S	12.75		
VC 48 hour	*ALOX12*	32.08	19.62	5.01
	18S	12.46		
ALOX12 48 hour	*ALOX12*	14.19	1.45	$1.49X10^6$
	18S	12.74		
UT 72 hour	*ALOX12*	34.92	19.78	1
	18S	15.14		
VC 72 hour	*ALOX12*	33.55	18.31	2.76
	18S	15.24		
ALOX12 72 hour	*ALOX12*	17.84	2.57	$1.52x10^5$
	18S	15.27		

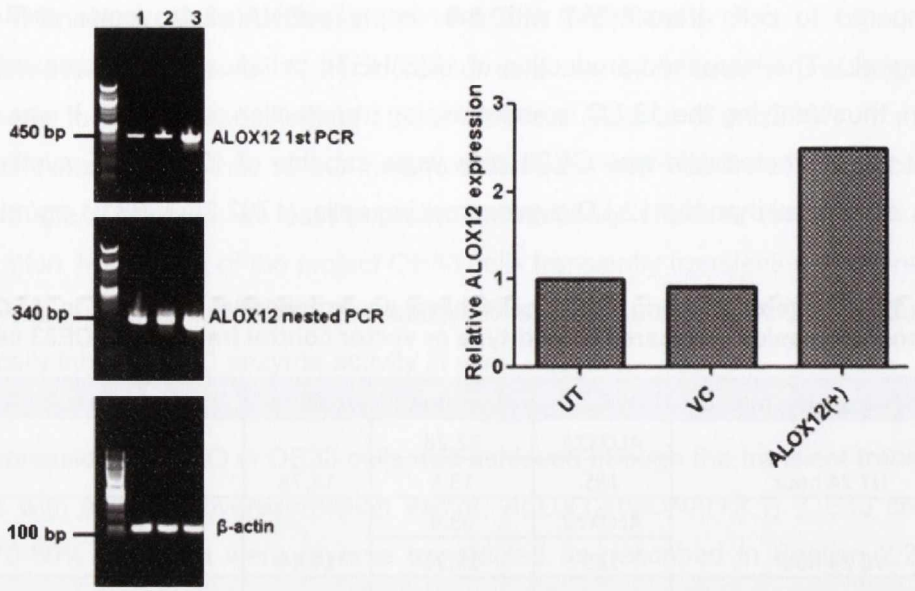

Figure 6.12: RT-PCR with nested primers verifies the overexpression of *ALOX12* in OE33 cells transfected with *ALOX12*-pcDNA(+3.1) plasmid . OE33 cells were reverse transfected with *ALOX12*-pcDNA(+3.1) or an empty pcDNA(+3.1) vector (VC). RNA was isolated 72 hours post-transfection and cDNA was analysed by gel PCR using nested primers in the *ALOX12* sequence. *ALOX12* was higher in the overexpressing OE33 (well 3) compared to untransfected (UT) (well 1) and VC (well 2). Analysis by densitometry revealed a 2.71-fold increase in *ALOX12* compared to VC following the first round of PCR, as indicated in the bar chart (n=1). Densitometric *ALOX12* measures were normalised to β-actin (*ACTB*) measures.

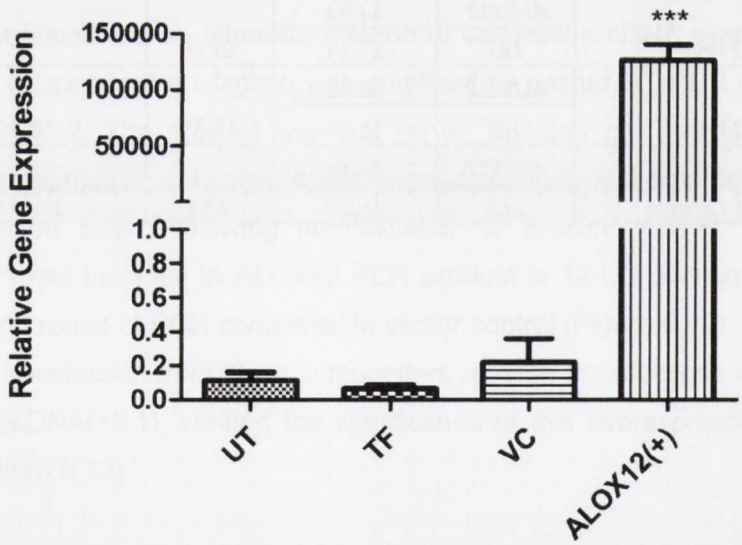

Figure 6.13: Probe-based qPCR verifies the overexpression of *ALOX12* in OE33 cells transfected with *ALOX12*-pcDNA(+3.1) plasmid DNA. 48 hours post transfection, *ALOX12*(+) overexpressing OE33 cells had significantly higher RQ values than vector control transfected cells, in addition to untransfected (UT) OE33 cells and OE33 cells treated with transfection reagent only (TF) ($p<0.001$, n=3). Statistical test used was one-way ANOVA with Dunnett's Multiple Comparison Test: $p<0.001$(***). Error bar denotes mean ± S.E.M.

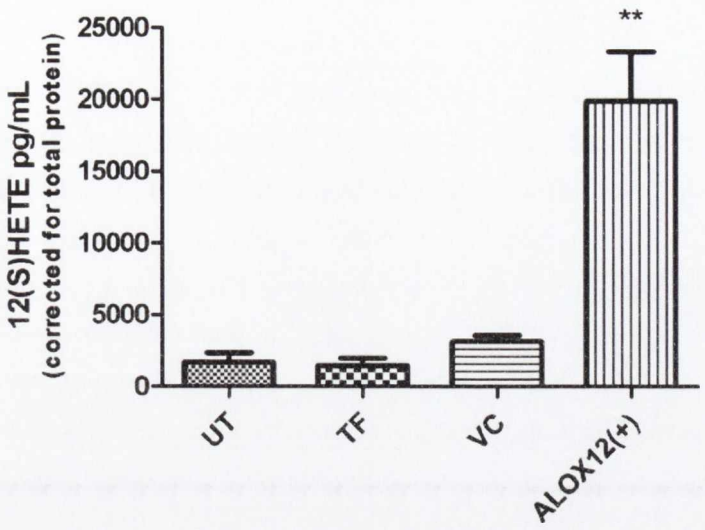

Figure 6.14: 12-LO enzyme activity is significantly higher in *ALOX12* overexpressing OE33 cells compared to wild-type or vector control transfected cells. Transfected cells were serum-depleted for 12 hours before treatment with 10 μM AA. 24 hours later cell supernatants were collected and 12(S)HETE levels were assessed by ELISA (n=3). *ALOX12*(+) overexpressing cells had significantly higher 12(S)HETE levels compared to the vector control treated cells, or wild type cells alone (UT) or treated with transfection reagent (TF) ($p<0.01$, n=3). Statistical test used was one-way ANOVA with Dunnett's Multiple Comparison Test: $p<0.01$(**). Error bar denotes mean ± S.E.M.

6.3.7 Assessing the potency of 12-LO inhibitors to suppress 12-LO enzyme activity *in vitro* and *ex vivo*

In order to assess whether the novel 12-LO inhibitor could inhibit enzyme activity of 12-LO overexpressing OE33 cells, the levels of 12(S)HETE was measured by ELISA. Cells were reverse transfected as described and treated with a combination of 10 μM AA and a drug or vehicle control (0.1% DMSO) for 24 hours. Due to limited ELISA kit, testing of NIH13, the most potent compound identified from Chapter 5, and GM5, the most drug-like new class of 12-LO inhibitor were prioritised. NIH13 and GM5 inhibition of 12(S)HETE was compared to the commercially available 12-LO inhibitor baicalein which has previously been shown to inhibit 12-LO activity (Bednar *et al.*, 2007). Cells were treated with 1 μM and 5 μM baicalein as this was in the range of previously published *in vitro* data (Klampfl *et al.*, 2012). GM5 was tested at 1 μM, 5 μM and 10 μM doses while NIH13 was only tested at 1 μM and 5 μM, due to its potent effects to cell viability at higher doses. The conditioned media collected after 24 hour drug treatment from three independent experiments were assessed by ELISA for the levels of 12(S)HETE and the concentration of total cellular protein was determined by BCA assay and used to normalise the ELISA data. The vehicle control treated *ALOX12*(+) cells demonstrated a high level of 12(S)HETE production (19799.68 ±3458.67 pg/mL).

12(S)HETE levels following baicalein treatment at both the 1 μM (5327.16 ±1982.782 pg/mL) and 5 μM (5005.13 ±103.99 pg/mL) dose significantly decreased 12(S)HETE levels ($p<0.001$) (Figure 6.15). In the case of NIH13 and GM5 there was a non-significant decrease at 1 μM (17556.52 ±2115.61 pg/mL and 16544.56 ±2537.22 pg/mL respectively) and also increasingly significant effects at higher concentrations, indicating a dose response effect. 5μM doses of both NIH13 and GM5 significantly decreased 12(S)HETE to similar concentrations (9463.02 ±1547.30 pg/mL and 9376.34 ±1564.11 pg/mL) ($p<0.01$) (Figure 6.15). In this assay doses were used that were below the IC_{50} for cell viability to limit this effect to the cells. NIH13 caused a 42.40 ±6.04% decrease in OE33 viability at 10 μM. In contrast GM5 only decreased cell viability by 16.43 ±7.38% at 10 μM and therefore was included in the ELISA. 10 μM GM5 was found to significantly decrease 12(S)HETE to a similar concentration as that observed with baicalein treatment at the 5 μM dose (5246.33 ±919.82 pg/mL) ($p<0.001$) (Figure 6.15).

Next, the endogenous production of 12(S)HETE by OAC tumour biopsies cultured *ex vivo* and the effect of selected 12-LO inhibitors was also investigated. Treatments with novel 12-LO inhibitors with the biopsy tissue available were prioritised in the following order: NIH13 5 μM, GM5 10 μM and NIH15 10 μM. Fresh biopsies were treated with either vehicle control (0.1% DMSO) or the aforementioned 12-LO inhibitor treatments. Biopsies from 8 OAC patients were treated with NIH13 and smaller subsets of 6 and 4 of these patients were treated with GM5 and NIH15 respectively. Levels of 12(S)HETE detected were normalised to total protein content of the biopsy. The mean level of 12(S)HETE detected in TCM derived from untreated biopsies was 6990.10 ±1491.738 pg/mL with a range of 3986.31-15071.66 pg/mL. Due to variability between patients data was represented as fold change relative to control. In contrast to the *in vitro* data there was no observed difference in 12(S)HETE following any of the three drug treatments in comparison to the vehicle control treated biopsy (Figure 6.16).

In Chapter 4 contrary to expectation, it was shown than 12-LO gene and protein expression were higher in normal adjacent patient tissue compared to matched OAC tumour. Normal adjacent tissue biopsies in addition to tumour biopsy tissue were available for 3/8 patients in the biopsy group. A comparison of the levels of 12(S)HETE production between these matched samples was carried out. Although very preliminary results (n=3) and requiring further validation, this data suggests that 12(S)HETE production was higher in the tissue adjacent to the tumour than the tumour tissue itself ($p<0.05$).

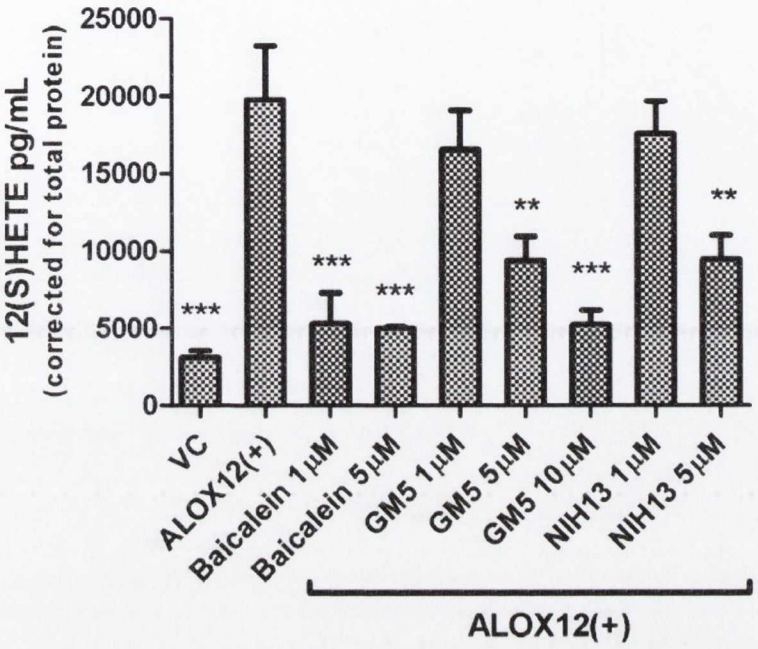

Figure 6.15 12-LO inhibitor treatment of 12-LO overexpressing OE33 cells results in decreased 12(S)HETE production. Supernatant from *ALOX12* overexpressing OE33 cells following 24 hour drug treatment in combination with 10 μM AA was assessed by ELISA for the levels of 12(S)HETE (n=3). *ALOX12* overexpressing cells were shown to produce significantly more 12(S)HETE than vector control (VC) cells ($p<0.001$). Treatment with GM5 and NIH13 at a 5 μM dose resulted in a significant decrease in 12(S)HETE ($p<0.01$). Treatment with baicalein at 1 μM and 5 μM and GM5 at 10 μM reduced 12(S)HETE production of *ALOX12* overexpressing cells to a level similar to the VC ($p<0.001$). Statistical test used was one-way ANOVA with Dunnett's Multiple Comparison Test: $p<0.01$(**) and $p<0.001$(***). Error bar denotes mean ± S.E.M.

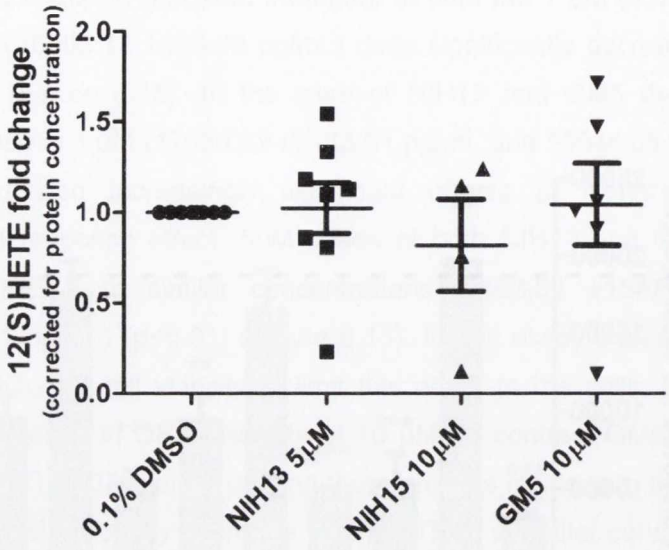

Figure 6.16 12(S)HETE production of OAC tumour biopsies is not altered by 12-LO inhibitor treatment. Biopsy tumour tissue samples were cultured *ex vivo* with either vehicle control or 5 μM NIH13 (n=8), 10 μM NIH15 (n=4) or 10 μM GM5 (n=6) for 24 hours and TCM was assessed for 12(S)HETE levels by ELISA and the data was normalised to tumour biopsy total protein content. In this small data set there was no difference in 12(S)HETE levels observed between control and any the treatment groups. 12(S)HETE levels are represented as fold change relative to vehicle control. Statistical test used was Kruskal-Wallis test with Dunn's comparison test. Error bar denotes mean ± S.E.M.

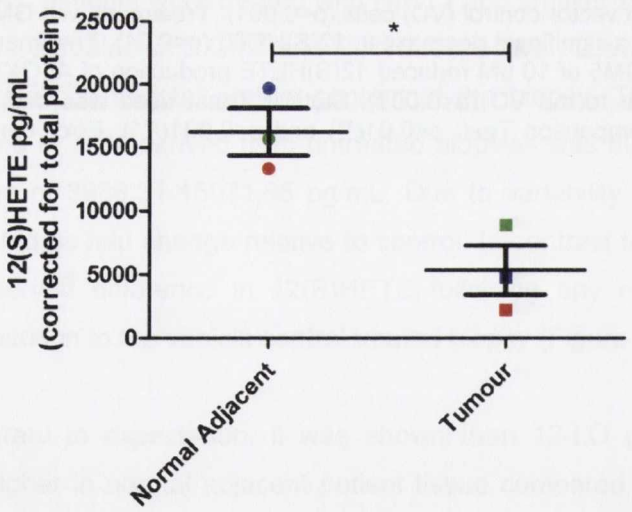

Figure 6.17 Preliminary data suggests 12(S)HETE production is higher in normal adjacent tissue compared to OAC tumour. 12(S)HETE levels were measured in TCM collected from matched tumour and normal adjacent biopsy tissue cultured *ex vivo* for 24 hours (n=3). 12(S)HETE was found to be significantly higher in normal adjacent tissue compared to the matched tumour. Statistical test was paired t-test: $p<0.05$(*). Error bar denotes mean ± S.E.M.

6.3.8 Assessment of 12-LO overexpressing OE33 cells using the xCELLigence RTCA

The xCELLigence™ RTCA DP (Real Time Cell Analyser Dual Plate) uses a specialist 16-well E-plate to measure proliferation. The well surface of the E-plate is covered by a layer of microelectrode sensors. When cells adhere and proliferate on the surface of the E-plate impedance signals are recorded by the xCELLigence software. Thus the platform offers a label-free, real time cellular assay to measure changes in cell behaviour in response to stimuli or inhibitors. We explored the use of this technology to assess the effect of 12-LO overexpression on adherence and proliferative capacity of OE33 cells. We also tested 12-LO overexpressing cells in combination with NIH13, the best anti-proliferative compound we identified previously from BrdU assays with wild-type OE33 cells. 12-LO overexpressing OE33 cells were also treated with 100 nM 12-LO metabolite 12(S)HETE or a combination of NIH13 and 12(S)HETE.

OE33 cells were reverse transfected with either the empty vector or the 12-LO overexpression vector directly into the 16-well E-plate and the xCELLigence machine was set to record the impedance signals of the plate every 30 minutes. The rate of cell adherence and cell growth were determined by calculating the slope between two time points. It was found that 12-LO overexpressing OE33 cells had increased cell adherence and cell spreading over the first 12-14 hours upon seeding i.e. before cell doubling begins ($n=5$, $p<0.05$) (Figure 6.18). Cell index (CI) values were variable in the two transfection groups in experiments beyond this time point however it was noted that there was a trend towards a increase in proliferation for cells overexpressing 12-LO ($n=5$, $p<0.1373$) (Figure 6.19). There were issues optimising this protocol for the assessment of inhibitor anti-proliferative effects on 12-LO overexpressing OE33 cells, resulting in only one trustworthy experimental plate that could be examined. For this experimental setup cells were serum depleted 16-18 hours post-transfection and about 30 hours the cells were treated with 5 μM NIH13 alone and/or 100 nM 12(S)HETE as indicated in Figure 6.20. Although very preliminary, ($n=1$) the slope values calculated by the xCELLigence software as shown in Figure 6.20 indicate that exogenous 12(S)HETE was mitogenic and NIH13 could decrease the growth of 12-LO overexpressing cells, while the addition of 12(S)HETE could reverse these effects.

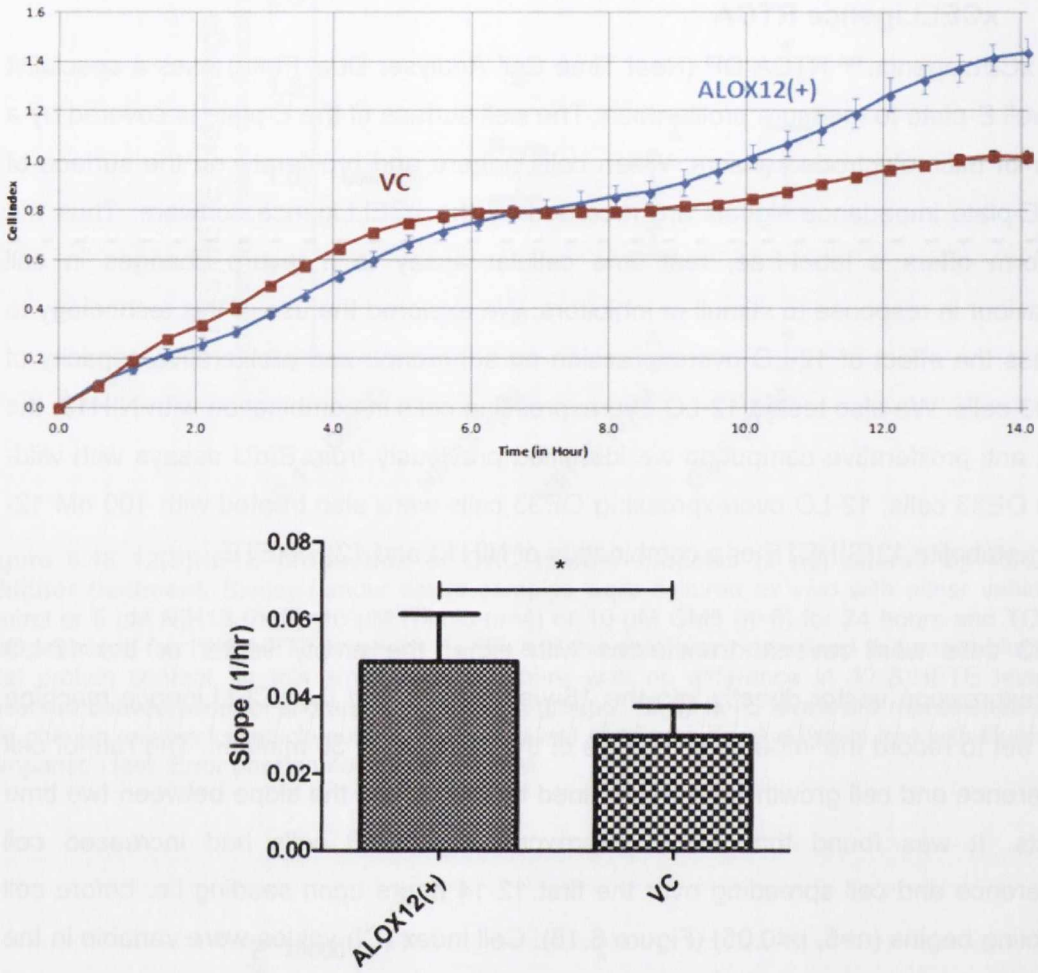

Figure 6.18 12-LO overexpressing OE33 cells demonstrate significantly increased cell adherence and cell spreading in comparison to vector control transfected cells. OE33 cells were reverse transfected with 12-LO overexpressing plasmid (*ALOX12*(+)) or the empty vector (VC) and CI values were monitored between 0-14 hours. CI values of the *ALOX12*(+) cells were higher than the VC over this time frame as indicated by the blue and red line in the representative xCELLigence graph. Slope values calculated by the xCELLigence software indicate a significantly enhanced adherence and cell spreading capacity of the *ALOX12*(+) OE33 cells compared to the VC ($n=5$, $p<0.05$). Statistical test used was a paired t-test. $p<0.05$(*).Error bar denotes mean ± S.E.M.

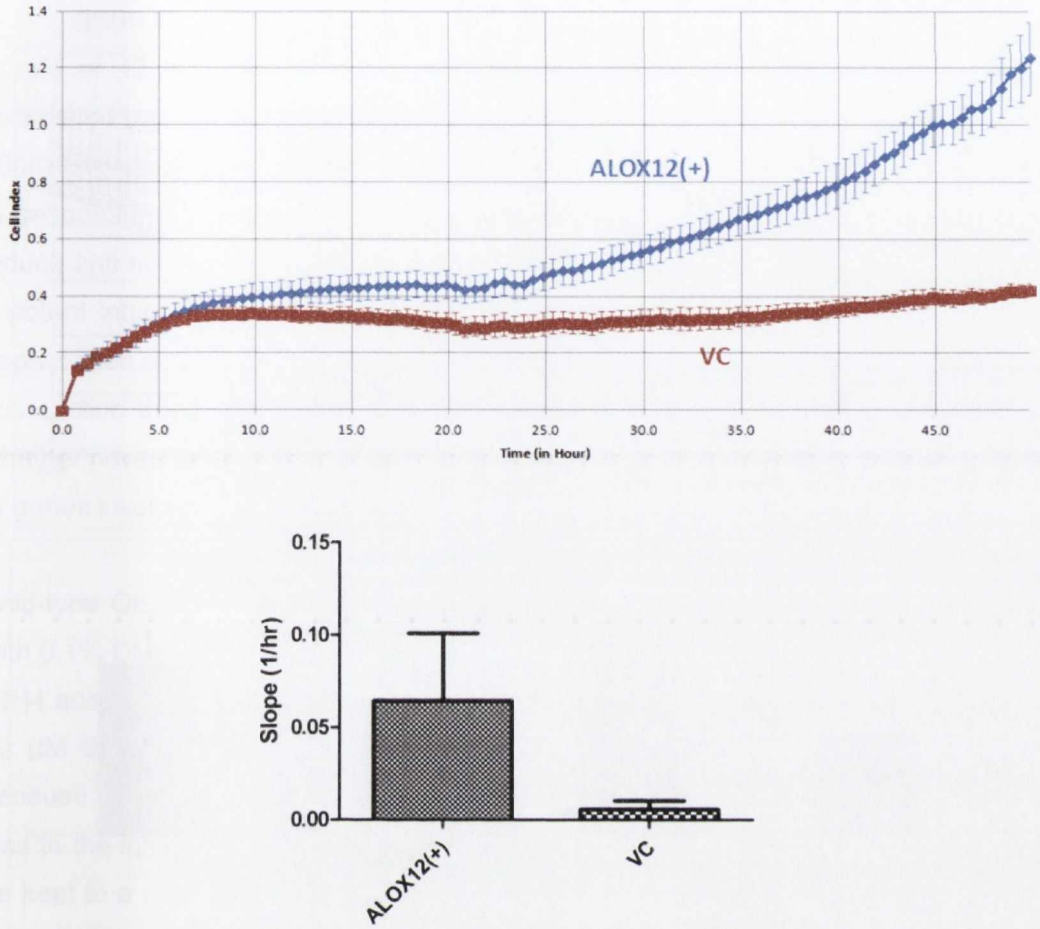

Figure 6.19 12-LO overexpressing OE33 cells demonstrate an increase in cell proliferation compared to vector control transfected cells. OE33 cells were reverse transfected with 12-LO overexpressing plasmid (*ALOX12*(+)) or the empty vector (VC) and CI values were monitored between 0-48 hours. CI values of the *ALOX12*(+) cells were higher than the VC over this time frame as indicated by the blue and red line in the representative xCELLigence graph. Although not significant due to variation in CI values between experiments, slope values calculated by the xCELLigence software indicate that 12-LO overexpression in OE33 cells increases their growth (n=5, $p<0.1373$). Statistical test used was a paired t-test. Error bar denotes mean ± S.E.M.

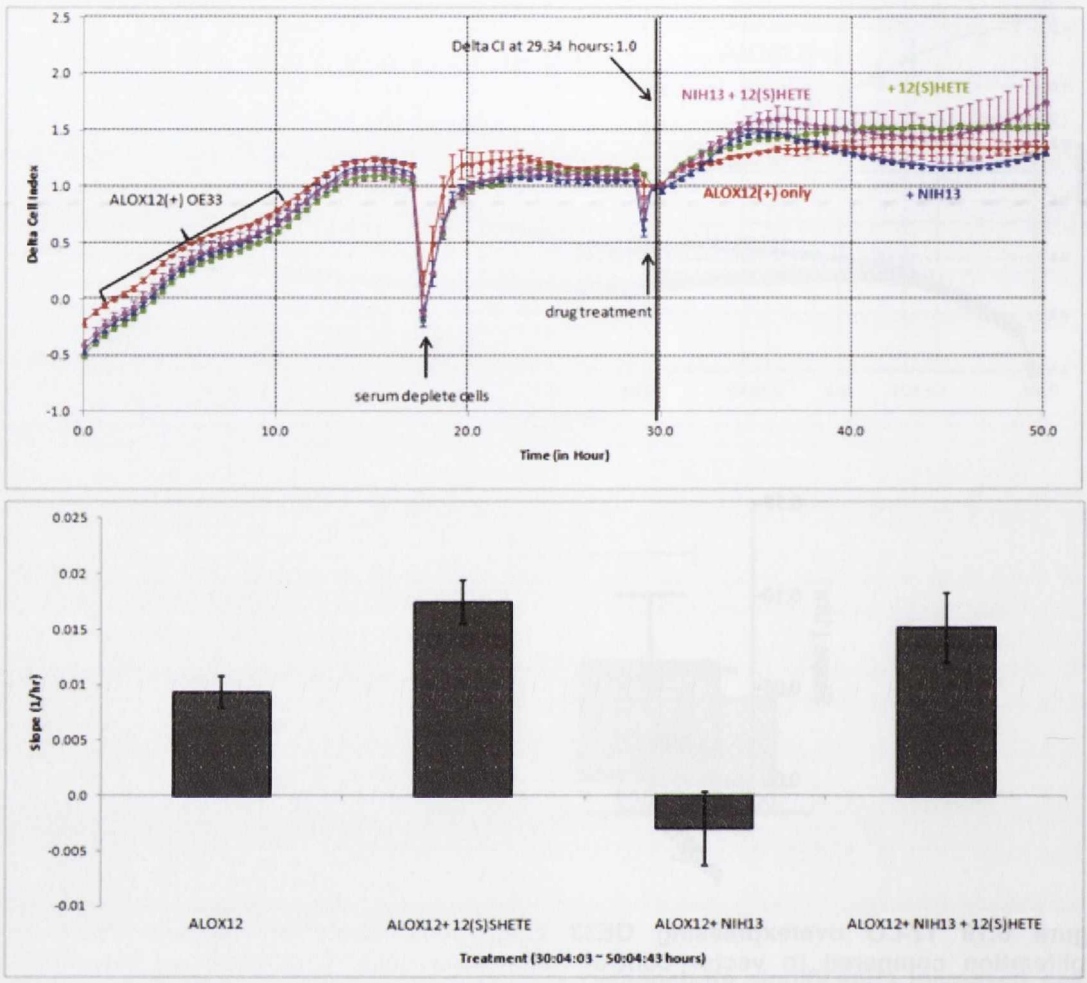

Figure 6.20 Preliminary results indicate the utility of the xCELLigence platform to investigate the functional effect of novel 12-LO inhibitor treatment on 12-LO overexpressing OE33 cells. *ALOX12* overexpressing OE33 cells were serum depleted at 18 hours after transfection and treatments were added before 30 hours as indicated in the xCELLigence raw data line graph. *ALOX12*(+) OE33 cells were treated with 5 μM NIH13 or 100 nM 12(S)HETE or combination of the two. The data was normalised just after the drug treatment (i.e. Delta CI=1 for all treatment groups) and the rate of cell growth (i.e. slope) was calculated between 30-50 hours. These slope values indicated an increase in *ALOX12*(+) OE33 cell growth with the addition of 12(S)HETE. NIH13 decreased cell growth as indicated by the negative slope between 30-50 hours while the addition of 12(S)HETE in combination with NIH13 reversed the anti-proliferative effect of NIH13. Error bars indicate S.D. of technical replicates for this one experiment. No statistical analysis was performed.

6.3.9 Human Angiogenesis Pathway Finder Array: alterations in OE33 gene expression following novel lipoxygenase inhibitor treatment

A role of 12-LO, and to a lesser extent 5-LO, in the regulation of angiogenesis-associated pathways in cancer cells has been established for some cancers (Nie *et al.*, 2006, McCabe *et al.*, 2006, Romano *et al.*, 2001), however this has not been explored in oesophageal cancer. In Chapter 5 it was shown that novel 12-LO inhibitors could induce anti-angiogenic effects on endothelial cell tubule formation and that NIH13 was a potent inhibitor of a number of key angiogenic gene pathways. Given the growing appreciation of the role cancer cells play in the regulation of the angiogenic process, in this section the Human Angiogenesis Pathway profiler array was used to investigate whether novel 5-LO and 12-LO compound treatment could affect OE33 transcript levels of genes involved in key processes of angiogenesis.

Wild-type OE33 cells were prepared as described in Section 2.13 and were treated with 0.1% DMSO as a vehicle control or with one of the selected compounds (i.e. 5-LO: NIH4 and 12-LO: NIH13, NIH15 or GM5). A 5 μM dose was selected for NIH13 while a 10 μM dose was selected for NIH4, NIH15 and GM5. These doses were chosen because they were below the IC_{50} for OE33 cell viability and thus contribution of cell loss to the inhibition of enzyme activity and potential angiogenic gene alterations could be kept to a minimum. Following 24 hour drug treatment RNA was isolated and cDNA was synthesised and run on the Angiogenesis Pathway Finder profiler array. Analysis was performed using a web-based PCR array data tool (SABiosciences) that employed the ΔΔCt method with raw data normalised by the house-keeping genes included in the plate. Gene changes were only reported if the transcript was amplified before 35 cycles. Values were displayed as fold regulation where a threshold fold regulation value of 2 indicated differential expression of a gene compared to the untreated control.

In comparison to the HUVECs which had detectable expression of over 90% of the genes featured on the array OE33 cells only showed expression of 50/84 genes (59.5%) (See Appendix I for basal expression status of all genes in both cell lines). Similar to the HUVEC angiogenic gene array study, the growth factor and receptor functional group showed that greatest number of gene alterations. Validations of the genes from the OE33 array were limited to the panel of angiogenic growth factor and cytokine genes investigated in the HUVECs and the addition of 3 extra genes: the protease inhibitor (*TIMP1*), coagulation factor III (*F3*) and the pro-angiogenic cytokine IL-8 (*CXCL8*). Due to limited resources and the fact that NIH13 was the only 12-LO inhibitor of the three classes of compounds to show significant gene changes in the

follow-up validations with the HUVECs, it was decided to only validate NIH13 and the 5-LO inhibitor NIH4 in the OE33 cell model. There was no significant difference between untreated and NIH4 treated cells for the panel of genes investigated: *NRP1, VEGFB, ANGPT2 and CXCL1* (n=3) (Figure 6.21). Although not identified from the array, *VEGFA* expression was also included in the validation set and similarly showed no significant alteration (Figure 6.21).

Five genes were chosen for validation from the array set for OE33 cells treated with 12-LO inhibitor NIH13. Tissue inhibitor of metalloprotease-1 (*TIMP1*) and coagulation factor III (*F3*) were downregulated by more than 2-fold for all 12-LO inhibitor treatments and were chosen for validation with NIH13 treatment. *NRP1* which was a validated gene target for NIH13 in HUVECs, also showed a downregulation in OE33 cells and thus was included for validation. Although an alteration of less than 2-fold was observed for *CXCL1* expression (1.92 fold regulation), this gene was included in the OE33 validation gene set because NIH13 was shown to significantly decrease expression in HUVECs. In contrast, *CXCL8* expression was shown to be up-regulated by more than 2-fold in the array screen and was chosen for validation. Although not identified from the array set *VEGFA* was included because of the previously referenced link with 12-LO activity and VEGFA signalling. These 6 genes assessed in OE33 cells following 5 μM NIH13 treatment demonstrated mixed results (n=3). *TIMP1, F3* and *CXCL1* showed no alteration in gene expression. *CXCL8* showed a strong trend towards an increase in expression although not significant ($p=0.073$, n=3). *NRP1* was shown to be significantly decreased with NIH13 treatment ($p<0.05$, n=5) while in contrast *VEGFA* was upregulated ($p=0.056$, n=4).

Table 6.3 List of gene alterations in OE33 cells following lipoxygenase inhibitor treatment

Functional group	Gene	NIH4	NH13	NIH15	GM5
Adhesion molecules	COL18A1		-2.2244	-2.3152	
	ENG		-2.9727		
Cytokines and chemokines	CXCL1	-2.3935	-1.9155	-2.9162	-5.8494
	CXCL6			-2.5246	-4.8126
	IL8	-4.6932	2.6135		-2.4197
Growth factors and receptors	NRP1	-2.7105	-2.4391		
	TIMP1		-2.426	-2.8585	-2.5127
	TYMP			-2.1906	
	VEGFB	-7.1346			
	JAG1	-5.8553			
	ANGPT2	-2.0135			
	CTGF		3.8194		3.7636
	EPHB4		-2.3702		
	F3		-2.7972	-4.7756	-7.3627
	FGFR3		-2.5758	-2.6258	
	SERPINF1	-2.482		-3.0464	-5.8029
	TGFB2		-2.3234		
	TGFBR1			-2.8055	-2.1304
Proteases and inhibitors	ANGPTL4	-2.1549			-2.4287
	PLG			-63.1366	-13.0493
	FN1		-2.11		
	MDK				-3.4298
	PLAU		2.3082		3.0999
	THBS2		-2.6461		-2.4792
Transcription factors and other	HPSE		-2.002		
	ID1	-2.4452	-2.904		-2.1246
	MMP14			-2.7292	
	NOS3			-2.1035	2.3395
	NOTCH4	-7.2888			

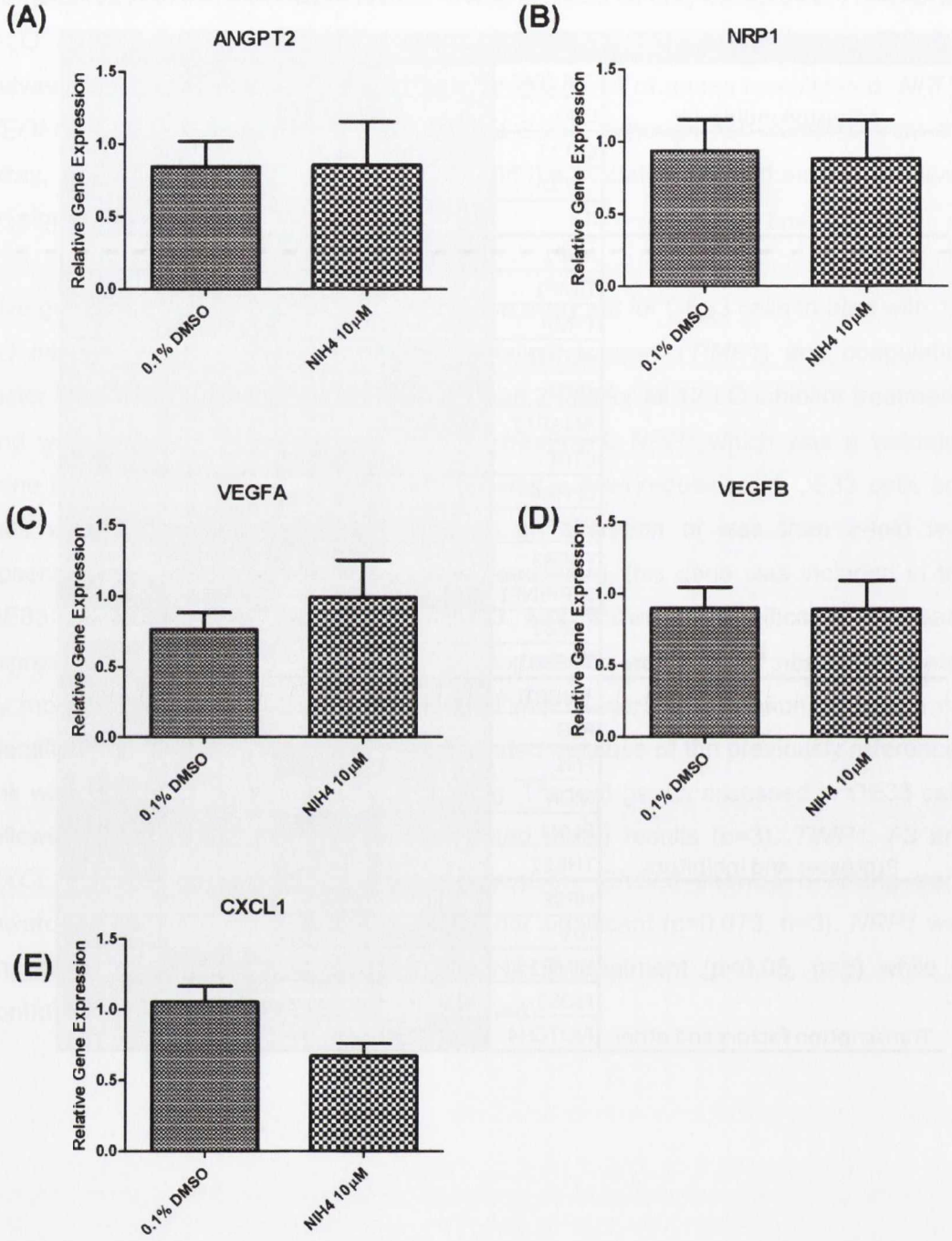

Figure 6.21 NIH4 did not significantly alter angiogenic genes chosen for validation. Selected altered angiogenic genes from the initial array screen (n=1) were assessed by SYBR-based qPCR in three independent experiments. (A-D): None of the genes investigated were found to be significantly altered following 24 hour 10 µM NIH4 treatment. (E) *CXCL1* showed a trend towards decrease in fold change compared to control (0.68 ±0.09 versus 1.05 ±0.1096) however it was not significant (p=0.1205, n=3). Statistical test used was paired student t-est. Error bar denotes mean ± S.E.M.

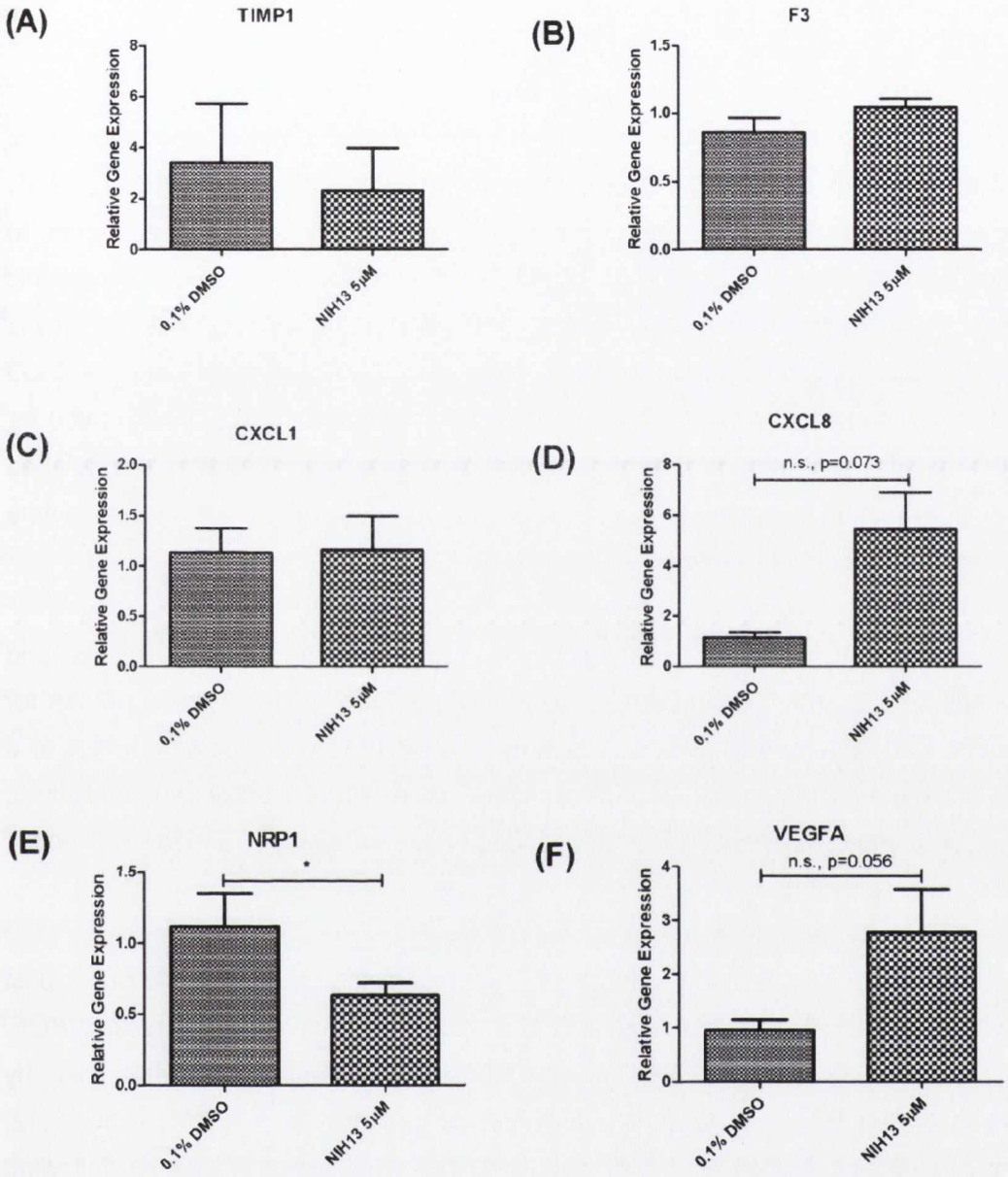

Figure 6.22 NIH13 significantly downregulates *NRP1* in OE33 cells. Selected altered angiogenic genes from the initial array screen (n=1) were assessed by SYBR-based qPCR in three independent experiments. *TIMP1, F3* and *CXCL1* were not altered in the validation set following 24 hour 5 µM NIH13 treatment. (D) *CXCL8* showed a trend towards an increase although it was not significant (p=0.073, n=3). (E) *NRP1* was significantly downregulated ($p<0.05$) while (F) *VEGFA* showed a trend towards an increase (p=0.058, n=5), following NIH13 treatment. Statistical test used was paired student t-est. $p<0.05$(*). Error bar denotes mean ± S.E.M.

6.3.10 Assessment of VEGF and other angiogenic proteins in OE33 cells and the effect of novel lipoxygenase inhibitor treatment to these factors

12-LO and 5-LO inhibition has been shown to decrease VEGF and angiogenic signalling in several models of cancer (Nie *et al.*, 2006, McCabe *et al.*, 2006, Ye *et al.*, 2005b), however this has not been investigated in a model of oesophageal cancer. In this section the effect of 5-LO and 12-LO inhibitor treatment on OE33 cell angiogenic secretions was investigated to provide insight into whether the lipoxygenase pathway is a relevant anti-angiogenic target in OAC. Wild-type OE33 cells were used for 5-LO inhibitor treatments while OE33 cells transiently overexpressing 12-LO were used for 12-LO inhibitor treatments. In addition, the 12-LO overexpressing OE33 cells provided a model to simultaneously assess endogenous production of angiogenic factors relative to vector control or wild-type OE33 cells.

In this study wild-type or 12-LO overexpressing OE33 cells were treated with novel and commercial 5-LO and 12-LO inhibitors respectively in combination with 10 μM AA for 24 hours. Cell supernatant was assessed by DuoSet ELISA for secreted levels of a panel of common angiogenic factors including VEGF, PDGF, bFGF, angiopoietin-2, GRO-α, IL-8 and soluble neuropilin-1 (n=3). Secretions were normalised to total cellular protein, determined by BCA.

Additionally, RNA was isolated from 12-LO overexpressing OE33 cells 48 hours post transfection to assess transcript levels of the major angiogenic growth factor VEGF. *ALOX12* overexpression was verified and VEGF gene levels were determined by probe-based qPCR, using *18S* as a house-keeping gene as described in Section 2.12. Notably there was no significant difference in OE33 VEGF gene expression following overexpression of 12-LO, (n=3) (Figure 6.23a). Similarly assessment of exogenous VEGF levels in the cell supernatant of cells 48 hours post transfection revealed no difference in VEGF secretion between 12-LO overexpressing OE33 cells and vector control transfected or wild type cells (n=3) (Figure 6.23b).

Of the panel of angiogenic proteins assessed in this study, only 4/7 were detectable in the supernatant of OE33 cells. PDGF, bFGF and angiopoietin-2 levels were all found to be below the lowest level of detection when assessed in undiluted cell supernatant by ELISA. Of the remaining 4 angiogenic analytes mean detected levels in wild type OE33 cells for VEGF, neuropilin-1, GRO-α and IL-8 were 56.44 ±4.83 pg/mL, 201.87 ±11.74

pg/mL, 256.11 ±16.75 pg/mL and 128.69 ±8.41 pg/mL respectively. Similar to VEGF levels, there was no difference in the secretion levels of neuropilin-1, GRO-α or IL-8 observed between 12-LO overexpressing OE33 cells and vector control treated cells (Figure 6.24b - Figure 6.27b).

5-LO inhibitors NIH4, ketoconazole, REV 5901 and zileuton were assessed for the ability to alter angiogenic secretions by OE33 cells at a single dose of 10 μM following 24 hour treatment (n=3). Notably, a significant increase in VEGF production was observed following NIH4 (123.21 ±7.10 pg/mL) and REV 5901 (112.49 ±0.81 pg/mL) treatment compared to untreated control (56.44 ±4.83 pg/mL) ($p<0.001$ for both) while no effect was observed for zileuton or ketoconazole (Figure 6.24a). Soluble neuropilin-1 showed a non-significant decrease following ketoconazole treatment compared to control (143.56 ±0.82 pg/mL versus 201.87 ±11.74 pg/mL) while the other three drug treatments showed levels similar to that of the untreated control (Figure 6.25a). Angiogenic cytokine levels of IL-8 were unaltered by 5-LO inhibitor, however GRO-α was significantly downregulated by ketoconazole (171.96 ±21.80 pg/mL) and REV 5901 (166.93 ±11.39 pg/mL) ($p<0.05$ for both). NIH4 reduced GRO-α levels by 21.5% compared to the control (201.04 ±15.98pg/mL versus 256.11 ±16.75pg/mL) however this change was not significant by Dunnett's Multiple Comparison Test.

Novel 12-LO inhibitors NIH13 and GM5 and the commercial 12-LO inhibitor baicalein were assessed for the ability to alter angiogenic secretions by 12-LO overexpressing OE33 cells following 24 hour treatment at a 10 μM dose (n=3). Given the potent effect of NIH13 to OE33 cell viability (>40% inhibition) a lower dose of 5 μM was also included for all biological replicates. No significant alteration to VEGF, neuropilin-1 or IL-8 secretion was observed for any of the 12-LO treatments (Figure 6.24b, Figure 6.25b and Figure 6.27b). Notably, GM5 treatment significantly decreased GRO-α levels by 44.5% compared to the untreated 12-LO overexpressing cells (197.21 ±6.40 pg/mL versus 355.50 ±37.78 pg/mL, $p<0.05$) (Figure 6.26b). Although not statistically significant, a 29.1% decrease in GRO-α cytokine levels was observed following NIH13 treatment at the 5 μM dose compared to untreated 12-LO overexpressing OE33 cells (271.92 ±41.24 pg/mL versus 383.58 ±43.59 pg/mL). A similar trend was found for NIH13 10 μM treatment (Figure 6.26b).

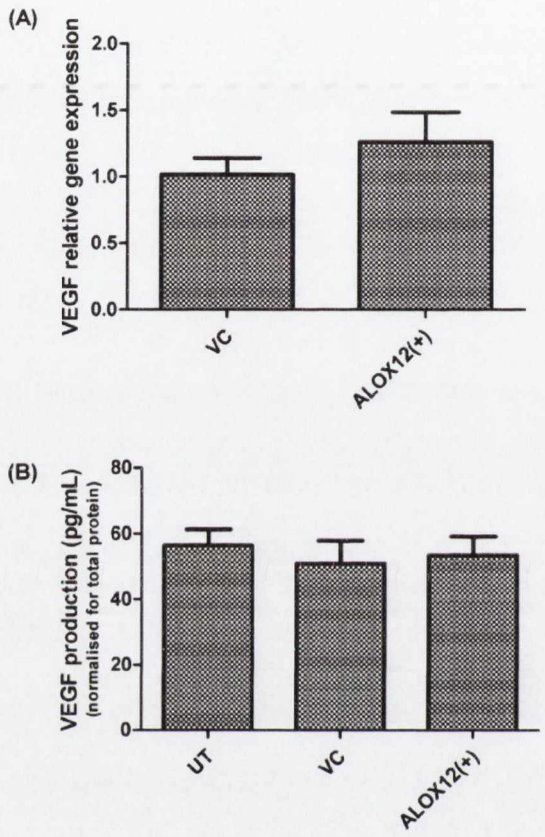

Figure 6.23 *ALOX12* overexpression in OE33 cells does not alter VEGF gene expression and protein production levels. RNA was isolated from OE33 cells 48 hours post transfection and analysed by qPCR for alteration in VEGF gene expression. (A) Cell supernatant was assessed by ELISA for exogenous levels of VEGF. *ALOX12*(+) overexpressing cells did not show increased VEGF expression compared to vector control cells (n=3). (B) Similarly, secreted VEGF levels were similar between *ALOX12*(+) overexpressing cells and vector control (VC) or untransfected wild-type OE33 (UT) (n=3). Statistical test used was paired student t-test and one-way ANOVA with Dunnett's Multiple Comparison.

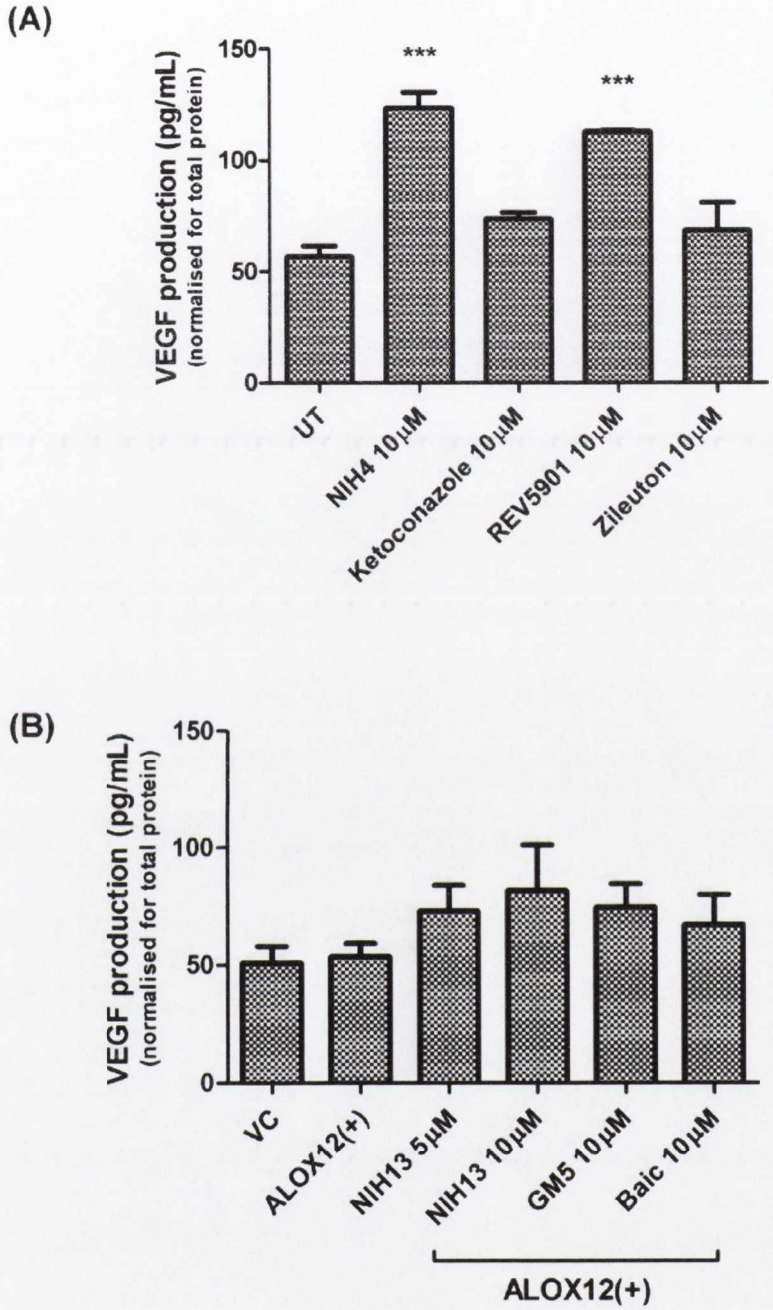

Figure 6.24 Assessment of VEGF production by OE33 cells following lipoxygenase inhibitor treatment. Wild-type OE33 cells were treated with 5-LO inhibitors and 12-LO overexpressing cells were treated with 12-LO inhibitors. Following 24 hour drug treatment VEGF secretions were measured by ELISA and were normalised to total protein content. (A) NIH4 and REV 5901 significantly increased VEGF production in OE33 cells compared to control ($p<0.001$, n=3). (B) There was no change to VEGF production by *ALOX12*(+) cells following treatment with 12-LO inhibitors (n=3). Statistical test used was one-way ANOVA with Dunnett's Multiple Comparison Test: $p<0.001$(***). Error bar denotes mean ± S.E.M.

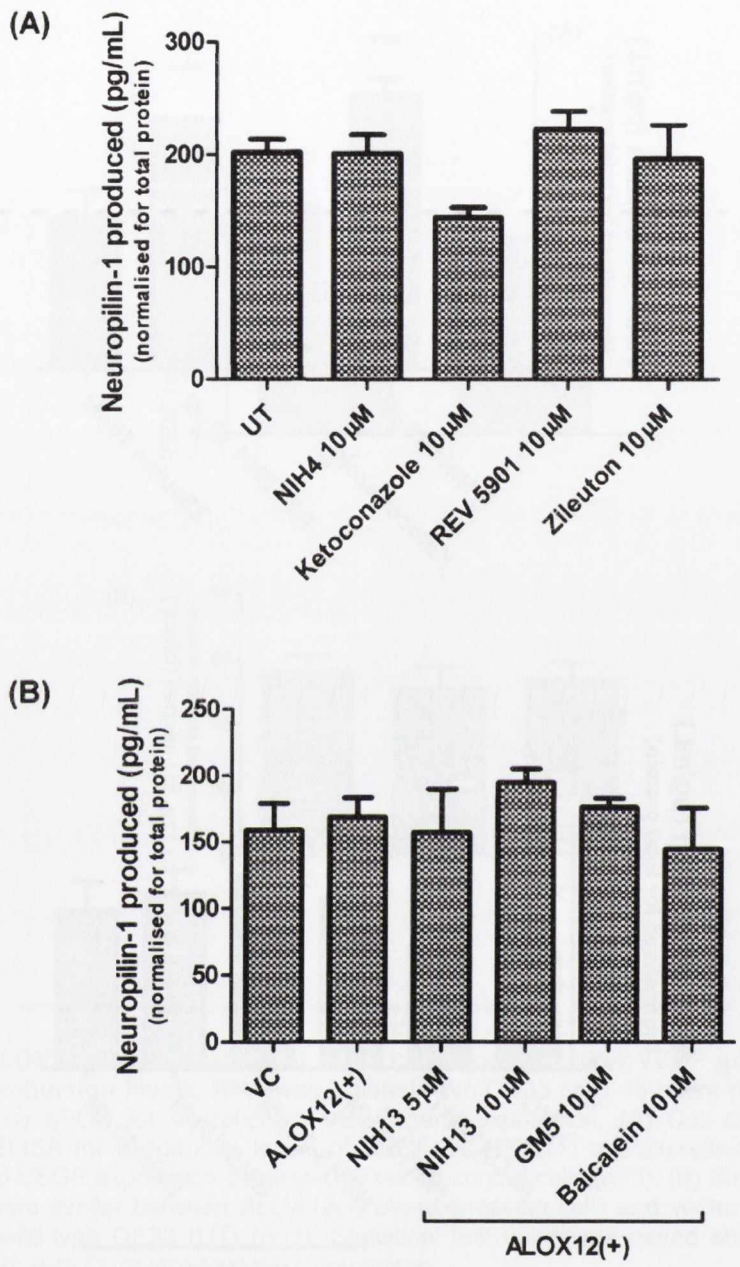

Figure 6.25 Assessment of neuropilin-1 production by OE33 cells following lipoxygenase inhibitor treatment. Wild-type OE33 cells were treated with 5-LO inhibitors and 12-LO overexpressing cells were treated with 12-LO inhibitors. Following 24 hour drug treatment soluble neuropilin-1 levels were measured by ELISA and normalised to total cellular protein content. (A) Ketoconazole was the only 5-LO inhibitor to alter neuropilin-1 levels ($p<0.05$ in comparison to REV 5901, n=3). (B) There was no change to neuropilin-1 secretion by *ALOX12*(+) OE33 cells following treatment with 12-LO inhibitors (n=3). Statistical test used was one-way ANOVA with Dunnett's Multiple Comparison Test: $p<0.05$(*). Error bar denotes mean ± S.E.M.

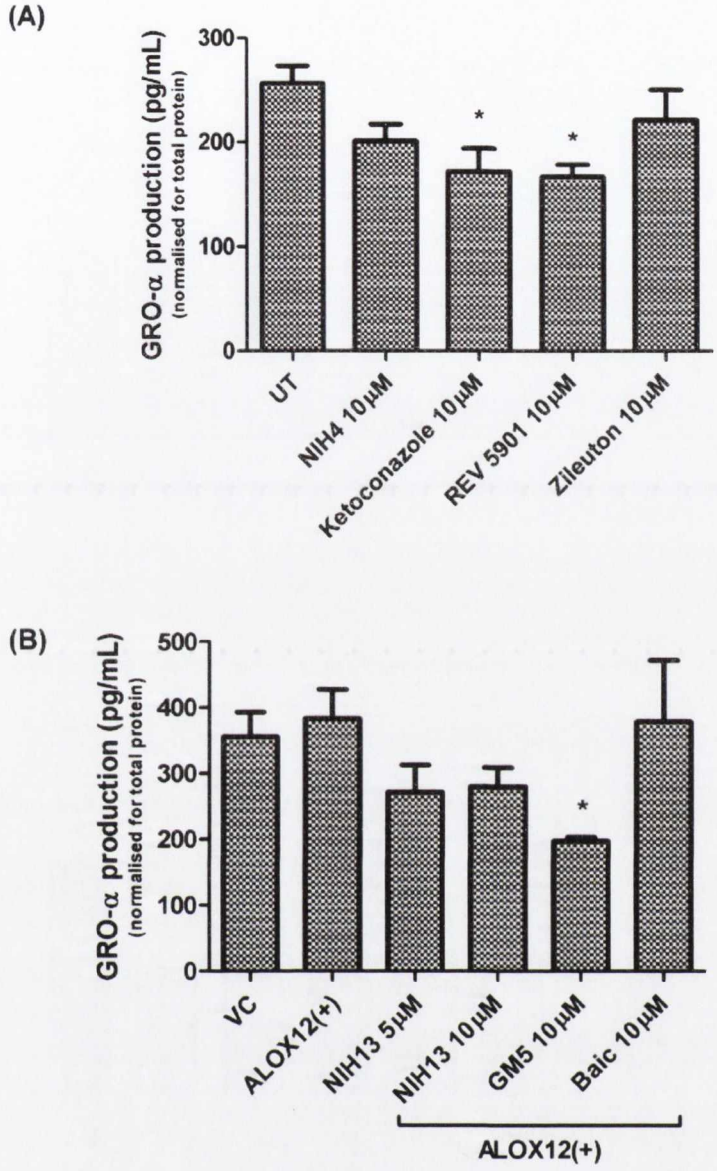

Figure 6.26 Assessment of GRO-α production by OE33 cells following lipoxygenase inhibitor treatment. Wild-type OE33 cells were treated with 5-LO inhibitors and 12-LO overexpressing cells were treated with 12-LO inhibitors. Following 24 hour drug treatment GRO-α levels were measured by ELISA and normalised to total cellular protein content. (A) Ketoconazole and REV 5901 significantly decreased GRO-α ($p<0.05$, n=3) while NIH4 treatment showed a non-significant decrease of 21.5% compared to untreated cells (n=3). (B) GRO-α was significantly decreased by GM5 treatment ($p<0.05$,n=3) compared to untreated *ALOX12*(+) OE33 cells. A similar, but non-significant decreasing trend was observed for NIH13. Statistical test used was one-way ANOVA with Dunnett's Multiple Comparison Test: $p<0.05$(*). Error bar denotes mean ± S.E.M.

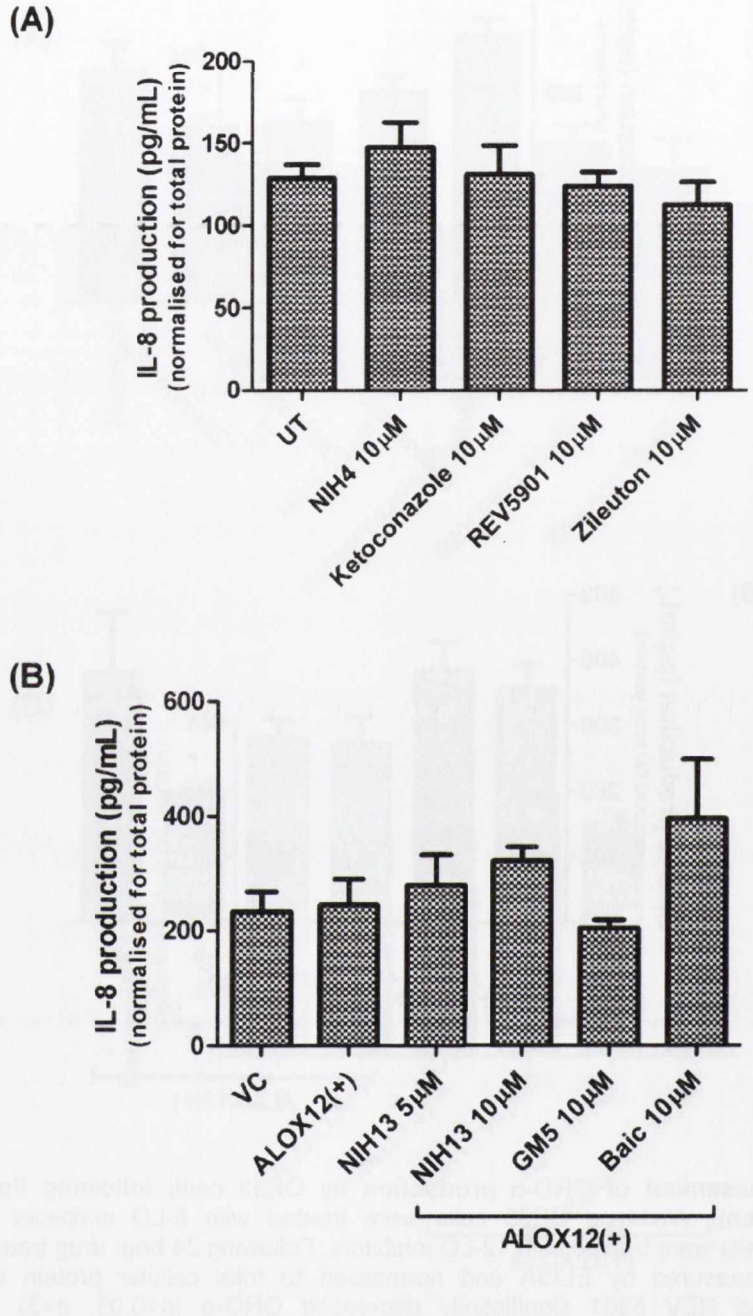

Figure 6.27 Assessment of IL-8 production by OE33 cells following lipoxygenase inhibitor treatment. Wild-type OE33 cells were treated with 5-LO inhibitors and 12-LO overexpressing cells were treated with 12-LO inhibitors. Following 24 hour drug treatment IL-8 cytokine levels were measured by ELISA and normalised to total cellular protein content. (A) There was no significant alteration in IL-8 compared to untreated control following 5-LO inhibitor treatment. (B) Similarly there was significant alteration of IL-8 levels following 12-LO inhibitor treatment of *ALOX12*(+) OE33 cells. Statistical test used was one-way ANOVA with Dunnett's Multiple Comparison Test. Error bar denotes mean ± S.E.M.

6.3.11 Assessment of alterations to the OAC angiogenic secretory profile following lipoxygenase inhibitor treatment *ex vivo*

While *in vitro* models are critical to pre-clinical drug testing, they are not truly representative of the heterogeneity of an *in vivo* tumour. Therefore as an alternate strategy, the ability of 5-LO and 12-LO inhibitors to alter the angiogenic secretory profile of OAC tumour biopsies in an *ex vivo* culture system was investigated. This model offers a unique opportunity to study the effect of lipoxygenase inhibitor treatment to tumour cells and associated peri-tumoural stroma.

Fresh OAC tumour biopsies obtained from the patient clinic at St. James's Hospital were cultured *ex vivo* for 24 hours in combination with lipoxygenase inhibitor treatments as described in Section 2.20.2. Fourteen patient biopsy samples were collected during this study and depending on the size of the biopsy it was cut into smaller pieces to carry out multiple drugs treatments prioritising NIH13, NIH4 or GM5 treatments, followed by NIH15 and zileuton where possible. The demographic for the patient cohort is detailed in Table 6.4. TCM collected following *ex vivo* culture for 24 hours was assessed for levels of angiogenic secretions using an MSD® Angiogenic Panel 1 V-PLEX™ ELISA as described in 2.20.6. This multiplex ELISA contains 7 analytes: VEGF, VEGFC, VEGFD, Tie-2, Flt-1, bFGF and PlGF. Due to observed alterations in neuropilin-1 gene expression by NIH13 and GRO-α secretions by GM5 *in vitro*, the levels of these two angiogenic proteins were also assessed in TCM by DuoSet ELISA. Due to inherent variability of the biopsies from patient to patient all data are represented as fold change relative to untreated control.

Firstly, VEGFC and VEGFD levels in TCM were found to be below the level of detection of the MSD V-PLEX, preventing further analysis of these angiogenic factors. NIH4 treatment was found to significantly decrease bFGF relative to control ($p<0.01$, $n=10$) (Figure 6.28a). Tie-2 levels were detected in eight patients biopsies and levels were found to be lower in TCM derived from biopsies treated with NIH4 ($p<0.05$, $n=8$) (Figure 6.28b). Over two-thirds of the biopsies had reduced PlGF levels following NIH4 treatment however this did not reach significance (Kruskal-Wallis test, $p=0.0938$, $n=10$). However, alternative sub-analysis of NIH4 treated biopsies versus vehicle control treated biopsies by paired Wilcoxon signed rank test revealed a significant relationship between NIH4 treatment and decreased PlGF ($p<0.05$, $n=10$). GRO-α and the VEGF pathway-related proteins i.e. VEGF, Flt-1 and neuropilin-1 levels following NIH4 treatment indicated non-significant and variable results in the data set (Figure 6.28 and Figure 6.29). However similarly to PlGF, alternative sub-analysis of NIH4

treated biopsies versus vehicle control treated biopsies by paired Wilcoxon signed rank test revealed a significant relationship between NIH4 treatment and decreased Flt-1 ($p<0.05$, $n=10$). The smaller zileuton treatment subset ($n=5$) did not show any significant protein alterations. In the case of the novel 12-LO inhibitors treatment with GM5 showed the most compelling effects, significantly decreasing bFGF($p<0.05$), Tie-2 ($p<0.001$), PlGF ($p<0.05$) (Figure 6.30) and the VEGF signalling protein Flt-1 ($p<0.05$) and neuropilin-1 (<0.01) (Figure 6.31). In addition NIH13 treatment showed a significant decrease in both Tie-2 and neuropilin-1 ($p<0.01$ and $p<0.05$) (Figure 6.30and Figure 6.31). There was no significant alteration of VEGF or GRO-α across all 12-LO inhibitor treatment groups (Figure 6.30and Figure 6.31).

Table 6.4 OAC *ex vivo* angiogenic secretion study patient demographic

OAC (n=14)	**Mean (S.D.) or n(%) as appropriate**	
Male: Female	14:0 (100%: 0%)	
Age (years)	63.57 (±8.06)	
T-stage	T1	1 (7.2%)
	T2	3 (21.4%)
	T3	10 (71.4%)
N-stage	Negative (N0)	6 (42.9%)
	Positive (≥N1)	8 (57.1%)
Tumour grade (differentiation)	Moderate	4 (28.6%)
	Poor	10 (71.4%)

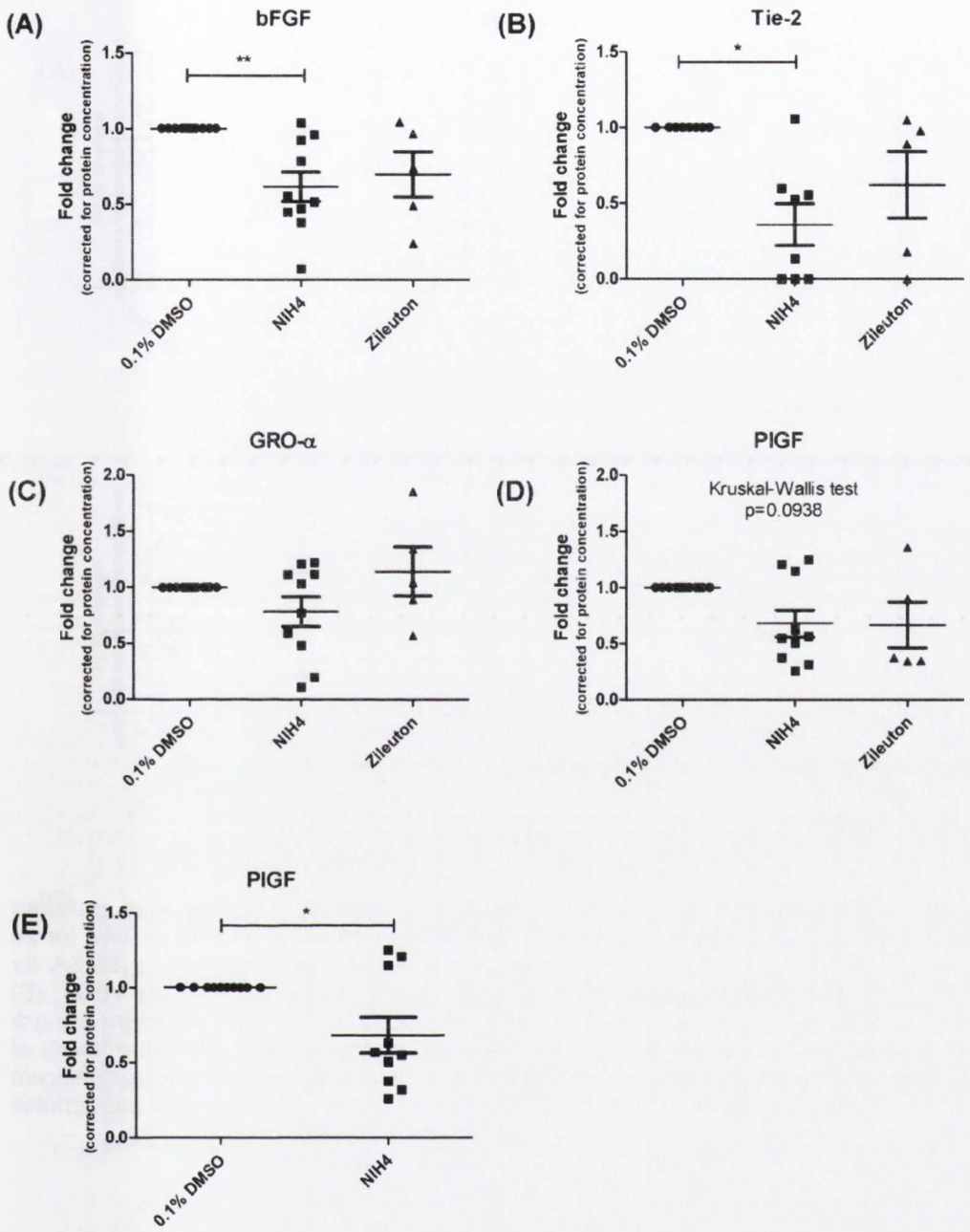

Figure 6.28 Assessment of non-VEGF pathway related angiogenic secretions by *ex vivo* cultured biopsies following 5-LO inhibitor treatment. Tumour biopsies were cultured *ex vivo* for 24 hours with 10 μM NIH4 or 10 μM zileuton treatment and TCM was analysed by ELISA for alterations to a panel of major angiogenic factors. Significant decreases in (A) bFGF (n=10, $p<0.05$) and (B) Tie-2 (n=8, $p<0.05$,). (C) Drug treatment did not alter GRO-α levels ($p=0.6140$). (D) There was a decreasing trend in PIGF secretion with NIH4 treatment relative to control (n=10, $p=0.0938$). The smaller zileuton treatment subset (n=5) did not show any significant alterations to angiogenic secretions. Statistical test used was Kruskal-Wallis non-parametric test with Dunn's multiple comparisons test. Sub-analysis of the NIH4 treatments versus control by paired Wilcoxon signed rank test revealed a significant relationship between NIH4 treatment and PIGF secretion (n=10, $p<0.05$). The statistical significance of bFGF or Tie-2 suppression was not altered by paired analysis. $p<0.05$(*) and $p<0.01$(**). Error bar denotes mean ± S.E.M.

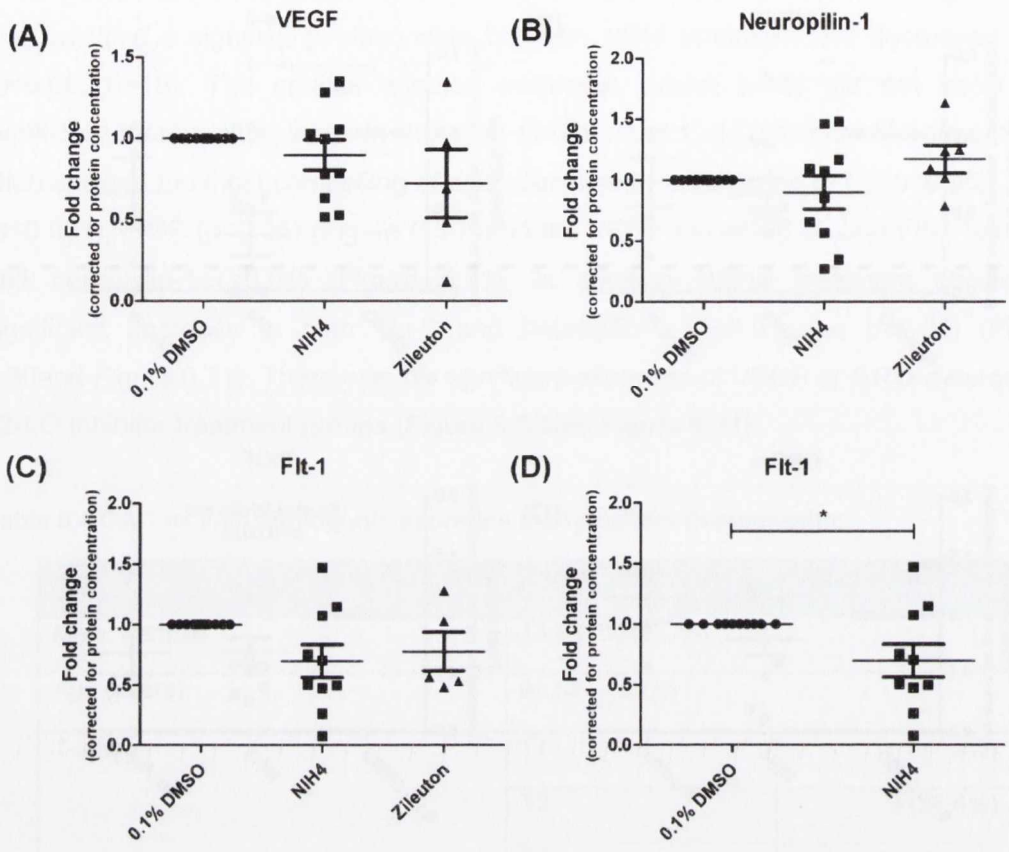

Figure 6.29 Assessment of VEGF-related angiogenic secretions by *ex vivo* cultured biopsies following 5-LO inhibitor treatment. Tumour biopsies were cultured *ex vivo* for 24 hours with 10 μM NIH4 or 10 μM zileuton treatment and TCM was analysed by ELISA for alterations to a panel of major angiogenic factors. No significant alteration to (A) VEGF, (B) neuropilin-1 or (C) Flt-1 was noted following NIH4 (n=10) or zileuton (n=5) treatment using a Kruskal-Wallis non-parametric test with Dunn's multiple comparisons test. (D) Sub-analysis of the NIH4 treatment versus control by paired Wilcoxon signed rank test revealed a significant relationship between NIH4 treatment and Flt-1 secretion ($p<0.05$). $p<0.05$(*). Error bar denotes mean ± S.E.M.

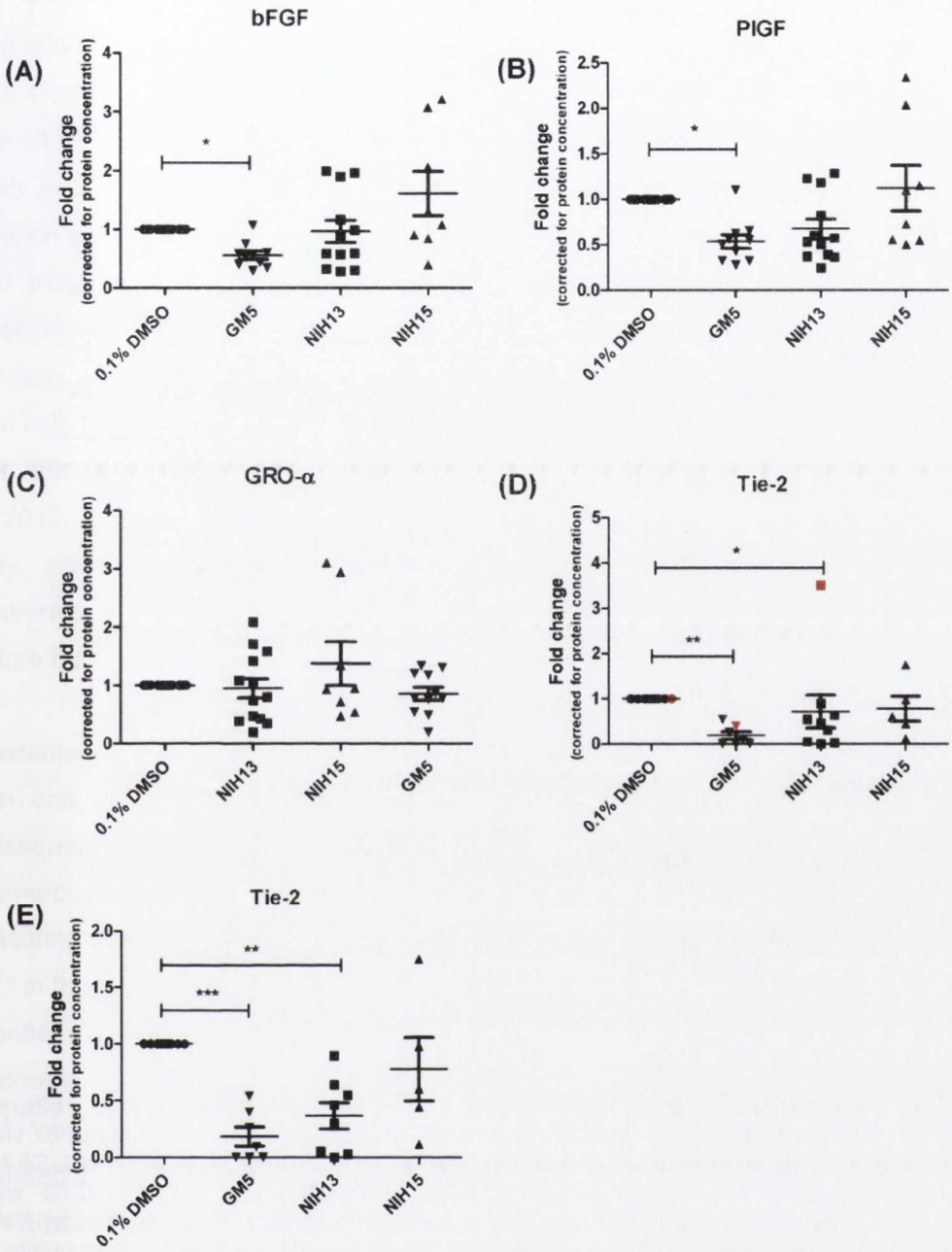

Figure 6.30 Assessment of non-VEGF related angiogenic secretions by *ex vivo* cultured biopsies following novel 12-LO inhibitor treatment. Tumour biopsies were cultured *ex vivo* for 24 hours with 12-LO inhibitors. TCM was analysed by ELISA. (A) bFGF and (B) PIGF were significantly decreased following GM5 treatment (n=10, $p<0.05$ for both) while (C) GRO-α secretion was not significantly altered by any of the 12-LO inhibitors. (D) Tie-2 secretion was significantly reduced following GM5 and NIH13 treatment (n=8, $p<0.01$ and n=9, $p<0.05$ respectively). (E) Sub-analysis removing the NIH13 outlier point from the biopsy data set highlighted in red led to an increased statistical significance of alterations to Tie-2 by both GM5 and NIH13 treatment (n=8, $p<0.001$ and n=8, $p<0.01$ respectively). Statistical test used was Kruskal-Wallis non-parametric test with Dunn's multiple comparisons test: $p<0.05$(*), $p<0.01$(**) and $p<0.001$(***). Error bar denotes mean ± S.E.M.

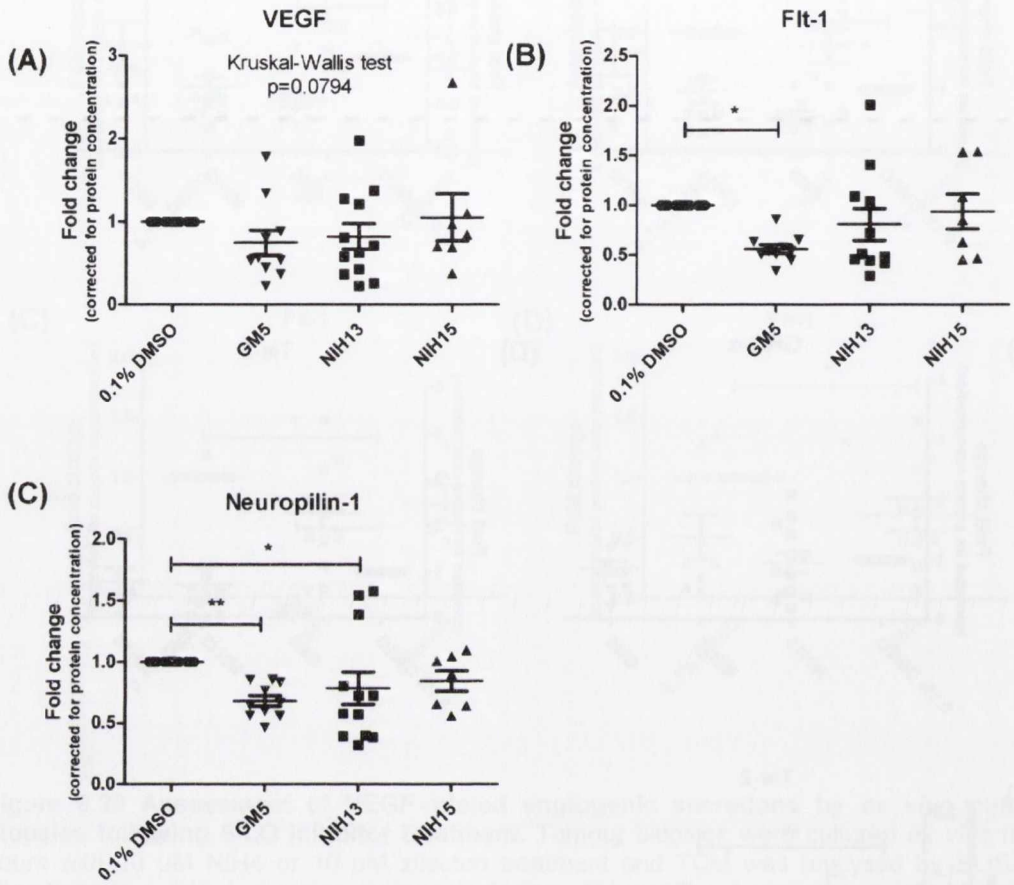

Figure 6.31 Assessment of VEGF-related angiogenic secretions by *ex vivo* cultured biopsies following novel 12-LO inhibitor treatment. Tumour biopsies were cultured *ex vivo* for 24 hours with 10 μM GM5, 5 μM NIH13 and 10 μM NIH15. TCM was analysed by ELISA for alterations to a panel of major angiogenic factors. No significant alteration to (A) VEGF was observed (p=0.0794). (B) Flt-1 and (C) neuropilin-1 were both significantly decreased by GM5 treatment (n=10, $p<0.05$ and $p<0.01$ respectively). (C) Despite a dichotomy of the data points in the NIH13 treatment group there was significant decrease in neuropilin-1 found following NIH13 treatment (n=12, $p<0.05$). Statistical test used was Kruskal-Wallis non-parametric test with Dunn's multiple comparison's test. Error bar denotes mean ± S.E.M.

6.4 Discussion

In an effort to combat the rising rates of OAC in Ireland and other parts of the western world (National Cancer Registry, 2013), a large proportion of research efforts have focused on identifying novel molecular targets involved in pro-tumourigenic pathways (Shah *et al.*, 2005, El-Rayes *et al.*, 2010) with the rationale that pharmacological inhibition of these processes will weaken the cancer and boost responses to currently used treatment strategies. The role of the 5-LO and 12-LO pathways and their metabolite products in carcinogenesis has been reported and inhibition of these pathways as a potential anti-cancer therapy has been explored in lung, prostate, colon, renal cell, hepatocellular, gastric and pancreatic cancer (Schroeder *et al.*, 2007, Meng *et al.*, 2013, Sarveswaran *et al.*, 2011, Ye *et al.*, 2005a, Yoshimura *et al.*, 2004, Xu *et al.*, 2012, Wong *et al.*, 2001, Pidgeon *et al.*, 2002, Ding *et al.*, 1999). In this novel study, new structural classes of 5-LO and 12-LO inhibitors identified by our collaborators (Dr. Maloney, NIH, Bethesda, MI) using qHTS methods were used to explore the inhibition of lipoxygenase pathways in OAC.

Assessment of effects on cell viability and cell proliferation of cancer cells *in vitro* is often one of the first stages of preclinical investigation with novel therapeutics. Consequently, in this study we compared the effect of the novel 5-LO inhibitor NIH4, to commercially available 5-LO inhibitors, REV 5901, ketoconazole and zileuton, measuring cell viability and cell proliferation of the OE33 cells. The high expression of 5-LO in this cell line was confirmed at both the mRNA and protein level indicating their potential susceptibility to such targeted therapies. Similar to other *in vitro* studies in pancreatic cancer cell lines (Tong *et al.*, 2002, Fischer *et al.*, 2010), in this study REV 5901 was shown to potently inhibit both OE33 cell viability and specifically cell proliferation with IC_{50} values of 20.59 μM and 14.24 μM respectively. Research findings from other studies suggest that such observed effects of REV 5901 on cancer cell proliferation occur by triggering cell cycle arrest and cell death via the intrinsic apoptotic pathway (Tong *et al.*, 2002). Ketoconazole and zileuton were much less potent at decreasing cell viability with IC_{50} values of 37.35 μM and 123 μM respectively. Notably other studies have also reported a lack of activity of the only FDA-approved 5-LO inhibitor zileuton in functional assays *in vitro* (Fischer *et al.*, 2010). Interestingly, the novel 5-LO inhibitor NIH4 did not show a potent effect on cell viability (IC_{50} 67.85 μM), however it proved very effective at blocking BrdU incorporation with an IC_{50} value of 14.87 μM. This result indicates the superior sensitivity of the BrdU assay to detect changes in cell number in comparison to MTT assay. NIH4 did not induce appreciable

apoptosis or necrosis in OE33 cells compared to control up to the 72 hour time point. This indicates that the suppression of DNA synthesis caused by NIH4, as indicated by the BrdU assay results occurred independently of cytotoxicity induced apoptosis or necrosis. It is interesting to note that NIH4, ketoconazole and REV 5901 all inhibited cell proliferation in HUVECs, a non-cancer model that reportedly does not express 5-LO. In contrast zileuton failed to induce anti-proliferative or cytotoxic responses in HUVECs (Section 5.3.4). Taking into consideration that zileuton failed to show activity in the discussed *in vitro* assays with OE33 cell model, this may suggest that other direct 5-LO enzyme inhibitors such as the novel NIH4 compound and REV 5901 are having anti-proliferative and cytotoxic effects respectively, independent of their 5-LO inhibition.

Similar comparisons were carried out with the three novel and structurally different 12-LO inhibitors selected from screening assays in Chapter 5 and the non-selective but best available commercial 12-LO inhibitor baicalein. While a low 12-LO gene copy number was detected by qPCR (Ct values ≥32), a basal level of 12-LO was confirmed by nested RT-PCR in the OE33 cells as previously described (Gao *et al.*, 1995, Chen *et al.*, 1994), indicating their potential susceptibility to 12-LO-specific inhibition. Assessment of cell viability revealed NIH13 as the most potent inducer of cell death compared to all other compounds tested with an IC_{50} value of 17.12 μM versus the next lowest IC_{50} value of 59.42 μM following baicalein treatment. NIH13 was found to completely block BrdU incorporation at low doses with an IC_{50} value of 2.67 μM indicating its potential as a potent anti-cancer agent. In contrast NIH15 was not shown to have significant cytotoxic or anti-proliferative effects on OE33 cells at any doses tested. While baicalein and GM5 only affected cell number by MTT at high doses (IC_{50} of 59.42 μM and 71.63 μM respectively) they did show specific anti-proliferative effects measured by BrdU incorporation at lower doses of 4.38 μM and 10.81 μM. Upon reviewing the literature the cell viability and cell proliferation IC_{50} values following baicalein treatment in OE33 cells are lower than those previously reported for epidermoid, gastric and prostate cancer (Wong *et al.*, 2001, Pidgeon *et al.*, 2002, Agarwal *et al.*, 2009), suggesting that OAC cell lines may be more susceptible to this treatment.

Only the novel compounds were tested by AnnexinV/PI staining for apoptotic activity. Novel 12-LO inhibitors NIH15 and GM5 did not show significant effects on apoptosis following 24-72 hour drug treatment. In contrast, NIH13 showed significant apoptosis at the higher test dose of 10 μM at 48 hours and an induction of necrosis at both 5 μM

and 10 μM doses by 72 hours. These results indicate that the potent effects of NIH13 on cell viability are at least in part, due to an induction of cell death. Although not investigated in our study, reports in other cancers suggest that 12-LO inhibitor-induced apoptosis occurs via a downregulation of anti-apoptotic Bcl-2 and Mcl-1 and an elevation of pro-apoptotic Bax and a downregulation of active ERK1/2 and PI3K-Akt pathways (Pidgeon *et al.*, 2002, Agarwal *et al.*, 2009). Therefore, it would be interesting to measure the levels of these markers of apoptosis following NIH13 treatment of OE33 cells. It would also be interesting to investigate whether the effects of the 5-LO inhibitor, NIH4, and the 12-LO inhibitor, GM5, on cell proliferation are through a mechanism involving cell cycle arrest as has been reported previously for lipoxygenase inhibitors (Schroeder *et al.*, 2007, Pidgeon *et al.*, 2002).

The effect of increased 12-LO expression and activity on cancer cell phenotype has been investigated in some cancer types with some contrasting results reported. For example, the overexpression of 12-LO in primary tumour-derived colorectal cancer cells or metastatic colorectal cancer cells has been shown to enhance cell growth and migration *in vitro* however tumour growth was not affected *in vivo* (Klampfl *et al.*, 2012). In the case of 12-LO overexpression in prostate cancer cells there was no detectable effect on cell growth *in vitro* however 12-LO overexpression stimulated tumour growth *in vivo* (Nie *et al.*, 1998), indicating that the growth advantage to 12-LO overexpressing cells was dependent on interactions with the host and tumour microenvironment. We attempted to address this question with the 12-LO overexpressing OE33 cells using the xCELLigence RTCA. It was found that 12-LO overexpression significantly enhanced the ability of OE33 cells to adhere to the cell surface of the well as previously reported for prostate cancer cells (Nie *et al.*, 2003). A similar convincing trend for increased proliferation was observed, thus indicating that 12-LO overexpression in OE33 cells produced a cancer cell with a more aggressive growth phenotype, at least *in vitro*. NIH13 was identified previously as the novel 12-LO inhibitor with the most potent anti-proliferative effects to wild-type OE33 cells. We attempted to verify the effect of NIH13 on OE33 cells overexpressing 12-LO using xCELLigence and to investigate whether addition of the 12-LO metabolite 12(S)HETE gave cells a growth advantage. We experienced technical issues when running xCELLigence experiments with drug and metabolite additions, whereby the CI values fell dramatically (to negative CI values in some cases) after removal of the E-plate to add treatments and failed to recover to the expected CI value when the plate was returned to the machine. Out of three test plates run only one had positive CI values after treatment addition and showed a continued increase in CI for the untreated control well as expected. Thus the other two plates

could not be analysed. While we cannot place too much emphasis on the result obtained from this single plate it was encouraging to see the NIH13 decreased the rate of proliferation of *ALOX12*(+) OE33 cells, supporting previous BrdU data. Exogenous 12(S)HETE appeared to increase proliferation and counteracted the inhibitory effect of the 12-LO inhibitor NIH13, as has been shown in other studies with 12-LO inhibitors (Klampfl *et al.*, 2012). This preliminary data indicates the need to optimise this experiment further to see if we can reproduce this result. Although very preliminary this n=1 experiment demonstrates the potential utility of the xCELLigence real-time platform to investigate functional effects of the novel lipoxygenase inhibitors, if optimised sufficiently.

The efficacy of the class of 5-LO inhibitors from which NIH4 is derived has been tested measuring inhibition of LTB4 synthesis by whole blood from human donors (Hoobler *et al.*, 2013) however to our knowledge they have not been investigated *in vitro* using cancer cells. Firstly, OE33 cells were shown to produce substantial levels of LTB4 in cell supernatant (124.13 ±8.88 pg/mL) indicating the suitability of the model to assess inhibition of 5-LO activity. All 5-LO inhibitors at all test concentrations were found to significantly decrease LTB4 levels in the range of 58-85%. NIH4 10 μM and zileuton 10 μM doses were found to have the most potent effects. Translating this to a more clinically relevant model we investigated the effect of NIH4 and zileuton on LTB4 production by OAC tumour biopsies. Upon studying the literature no study was found which explored the secretion of LTB4 by OAC tumour tissue or indeed any other tissue type *ex vivo* and therefore this represented a novel experiment. LTB4 production was very low or undectable in some patients, however investigating a subset of patient biopsies with LTB4 levels in the range of the assay, it was found that NIH4 and zileuton could significantly decrease LTB4 secretion. Thus indicating the potential of these drugs to block the 5-LO signalling pathway in OAC. This finding was particularly interesting in the case of NIH4 because we have previously shown *in vitro* that NIH4 can inhibit cell proliferation specifically at concentrations in the range of 10 μM and therefore in OE33 cells the anti-proliferative effect appears to be a result of blocking LTB4 production.

In the case of the novel 12-LO inhibitors both the 8-hydroxyquinoline (i.e. NIH13) and benzenesulfonamide (i.e. GM5) drugs have been tested by our collaborators in assays with beta islet cells from human donors, where they showed efficacy at doses of 10 μM (Kenyon *et al.*, 2011, Luci *et al.*, 2014). However there are no published studies investigating their efficacy in cancer cell models. The most common approach to test

the specificity of a lipoxygenase inhibitor is to monitor lipoxygenase enzymatic activity via the synthesis of it metabolite product. Despite high expression of 12-LO in human tumour tissue of certain cancer types, cancer cell line models often have a low basal level of 12-LO expression and activity i.e. 12(S)HETE production, as in the case of the commonly used prostate, colorectal and breast cancer cell lines (Nie *et al.*, 1998, Klampfl *et al.*, 2012, Connolly and Rose, 1998). Thus, transient or stable overexpression of 12-LO in cancer cells has been previously used to provide a suitable model to investigate the specificity of 12-LO inhibitors (Bednar *et al.*, 2007). Consequently, in this study 12-LO overexpressing OE33 cells were constructed to provide an OAC model of sustained 12(S)HETE production to test the specificity of the novel 12-LO inhibitors. All three of the novel compounds tested could substantially inhibit 12(S)HETE secretion by 12-LO overexpressing OE33 cells, however baicalein was found to be the most potent, significantly decreasing 12(S)HETE by over 75% to levels in the range of wild-type OE33 cells at a 1 μM dose. In contrast NIH13 and GM5 did not significantly decrease 12(S)HETE at 1 μM doses. At 5 μM doses both compounds decreased 12(S)HETE by nearly 50% while the 10 μM test dose of GM5 decreased 12(S)HETE by nearly 75%. Endogenous 12(S)HETE production from OAC tumour biopsy tissue was observed (6990.10 ±1491.738 pg/mL). Unlike the observed decrease in LTB4 secreted by OAC biopsies following 5-LO inhibitor treatment, unfortunately there was no observed alteration to 12(S)HETE levels following 12-LO inhibitor treatment. This suggests that the complex and heterogeneous microenvironment of the tumour biopsy may be somehow impacting the effect of the inhibitors in comparison to the simplified OE33 single cell line model. It may be the case that higher doses of the compounds are needed to have efficacy *in vivo*, however limited biopsies during the project did not allow scope to test multiple doses. Similarly each treatment group only consisted of 4-8 biopsy samples and due to this small number and the variability associated with patient material, these factors may have an impact on the conclusiveness of the results.

We discussed previously that a role of 5-LO and 12-LO in angiogenesis has emerged from several cancer studies, for example colon cancer and breast cancer in the case of 5-LO (Ye *et al.*, 2004, Chatterjee *et al.*, 2013) and prostate cancer in the case of 12-LO (Nie *et al.*, 2006, McCabe *et al.*, 2006). The angiogenic role of these two enzymes in oesophageal cancer or OAC specifically is not yet known. Consequently, we investigated the anti-angiogenic potential of the novel 5-LO and 12-LO inhibitors in models of OAC. An assessment of the effect of selected 5-LO and 12-LO inhibitors on the expression of major angiogenic factors was conducted, at the gene level *in vitro*

and at the secreted protein level both *in vitro* and *ex vivo*. For all experiments doses of drugs were used at which inhibitory effects on 5-LO and 12-LO enzymatic activity had been observed.

An initial, single angiogenic gene array screen highlighted a number of genes in the growth factor and receptor and cytokine/chemokine functional groups that were altered by NIH4 treatment of OE33 cells. However, upon validation, none of the selected genes (*NRP1, VEGFB, CXCL1, ANGPT2*) were found to be significantly altered by NIH4 treatment. Given that a number of significant changes to angiogenic secretions were observed following *ex vivo* NIH4 treatment of OAC biopsies, we question the reliability of a single angiogenic array screen to accurately identify gene changes and suggest that increasing the array screen to an n=2 or n=3 would highlight more reproducible and relevant angiogenic gene changes. The putative angiogenic growth factor VEGF was unaltered by NIH4 treatment in OE33 cells in the angiogenic pathway array screen. Regardless of this, it was included in the validation cohort due to its reported association with 5-LO signalling in mouse studies (Ye *et al.*, 2004, Chatterjee *et al.*, 2013). Similarly, to the other angiogenic genes, no downregulation of VEGF was observed. In the *ex vivo* study, no significant alteration to VEGF was observed by NIH4 treatment or zileuton too. Interestingly VEGF secretion was found to be significantly upregulated in OE33 cell conditioned media by both NIH4 and REV 5901 treatment, suggesting that 5-LO or other pathways induced by 5-LO are regulated by VEGF signalling hence the counteracting increase in VEGF production. The regulation of 5-LO signalling by VEGF has not been reported previously however other studies have indicated that VEGF regulates similar enzymes such as COX-1 and COX-2 in certain pathologies (Bryant *et al.*, 1998, Akarasereenont *et al.*, 2002). Our findings are in contrast to the two publications to date which have shown that inhibition of 5-LO decreases VEGF (Ye *et al.*, 2004, Chatterjee *et al.*, 2013). It must be noted that in the mouse study by Ye *et al.*, the decrease in VEGF by 5-LO inhibition was dependant on cigarette smoke exposure. Thus a regulation of VEGF by 5-LO signalling may not only be tumour-type specific but also dependant on environmental factors. The affect of NIH4 and other 5-LO inhibitors (REV 5901, ketoconazole and zileuton) to the secretion of angiogenic protein by OE33 cells was assessed by ELISA. Of the panel of angiogenic proteins available, only 4/7 analytes were detectable in OE33 cell supernatant: VEGF, neuropilin-1, GRO-α and IL-8. Similarly to VEGF, there was no significant alteration to neuropilin-1, GRO-α and IL-8.

We investigated the effect of novel 12-LO inhibitors on the angiogenic gene profile of wild-type OE33 cells, previously shown to have a basal level of 12-LO expression. Given that NIH13 was the only compound to show significant effects on angiogenic gene expression in HUVECs (see Chapter 5) it was decided, due to limited resources, that we would validate a number of genes following treatment with NIH13 only. From the six genes chosen for validation (*TIMP1, F3, CXCL1, IL-8, VEGF* and *NRP1*) only one was found to be significantly altered following NIH13 inhibition and that was neuropilin-1. Neuropilin-1 is a receptor for VEGF and the neuronal guidance protein semaphorin 3A with key roles in vascular and neuronal development (Plein *et al.*, 2014) and is believed to have a role in tumour growth and associated angiogenesis (Pan *et al.*, 2007). Neuropilin-1 expression with VEGFR has been shown to enhance VEGF signalling (Soker *et al.*, 1998) and has been shown more recently to act independently of the VEGFR (Ellis, 2006, Plein *et al.*, 2014). There is evidence to suggest 12(S)HETE binds to neuropilin-1 in neuronal cells mimicking the actions of semaphorin 3A, while inhibition with a 12-LO inhibitor suppressed semaphorin 3As actions in certain neural processes (Mikule *et al.*, 2002). Thus in cancer cells blocking 12-LO may be preventing the pro-angiogenic regulation of neuropilin-1 by 12(S)HETE. At this 24 hour drug treatment time point VEGF gene expression showed a trend towards an upregulation following NIH13 treatment, which may be a compensatory effect in response to decreased availability of neuropilin-1 to transduce VEGF signalling. Similarly an apparent trend towards an upregulation in IL-8 in the validation cohort suggests that this pro-angiogenic cytokine is upregulated following 12-LO inhibition. Previous reports have suggested that IL-8 angiogenic signalling functionally compensates for an inhibition of VEGF/neuropilin-1/VEGFR-mediated signalling as is potentially the case in OE33 cells if 12-LO inhibition is downregulating neuropilin-1 (Mizukami *et al.*, 2005, Huang *et al.*, 2010).

The effect of the novel 12-LO inhibitors and baicalein to angiogenic secretions was assessed in 12-LO overexpressing OE33 cells, an OAC model with demonstrated high 12-LO enzyme activity. Of the 7 angiogenic proteins assessed (bFGF, PDGF, angiopoietin-2, IL-8, neuropilin-1, VEGF and GRO-α) only IL-8, Neuropilin-1, VEGF and GRO-α were detectable in the undiluted supernatant of wild-type OE33 cells and those transfected with the empty vector or 12-LO expression vector. No alteration to IL-8, neuropilin-1 or VEGF secreted levels were noted following 12-LO inhibitor treatment of 12-LO overexpressing OE33 cells. Additionally the overexpression 12-LO in OE33 cells did not alter VEGF mRNA levels or VEGF protein production. This was in contrast to findings in prostate cancer where overexpression of 12-LO *in vitro* resulted in an

upregulation of VEGF protein levels (Nie *et al.*, 2003). Notably a recent study overexpressing 12-LO in two colorectal cell lines, similarly to our study, did not find an association with increased VEGF expression (Klampfl *et al.*, 2012). Thus this phenomenon may be specific to the prostate cancer cell line model. Interestingly, it was noted that GM5 treatment of 12-LO overexpressing OE33 cells significantly decreased GRO-α by nearly 50%. While this is the first study to link any lipoxygenase signalling to the pro-angiogenic chemokine GRO-α, it has been previously documented that other eicosanoid signalling molecules such as COX-2 derived PGE2 can induce GRO-α expression by cancer cells (Wang *et al.*, 2006). PGE2 induced GRO-α in colorectal cancer cells enhanced endothelial cell migration *in vitro* and also led to a highly vascularised tumour *in vivo* (Wang *et al.*, 2006). Thus it would be interesting to see if 12(S)HETE could induce GRO-α in the OAC cell line model.

As a final route of investigation, we explored the effect of 5-LO and 12-LO inhibitor treatments on angiogenic secretions by OAC tumour biopsies cultured *ex vivo*. While *in vitro* models such as the OE33 cell line, are critical to pre-clinical drug testing, they are not representative of the heterogeneity of an *in vivo* tumour. In contrast, the *ex vivo* tumour biopsy culture model we used offered a unique opportunity to study the effect of 5-LO and 12-LO inhibitor treatments on tumour cells and intact associated peri-tumoural stroma. Although this study consisted of a relatively small number of biopsies (a maximum of n=12 for any treatment group), a number of significant associations were observed, providing some insight into the molecular pathways being affected by novel lipoxygenase inhibitor treatment in OAC. Notably NIH4 and zileuton did not appear to alter VEGF *ex vivo,* unlike the two *in vivo* murine studies previously mentioned and similarly 12-LO inhibitors did not alter VEGF secretion. These findings are consistent our OAC *in vitro* results discussed previously. Interestingly, NIH4 treatment was found to significantly decrease bFGF, the angiopoietin receptor Tie-2, PlGF and the VEGF-receptor Flt-1. In comparison ,none of the angiogenic secretions investigated were altered by zileuton treatment, however this may have been on account of the small treatment group size (n=5). Of the three investigated 12-LO inhibitors, GM5 was the most potent *ex vivo,* showing significant decreases in bFGF, PlGF and Tie-2, in addition to the VEGF receptor Flt-1 and co-receptor neuropilin-1. While the data points were more variable in the NIH13 treatment group, the compound was shown to significantly decrease neuropilin-1 and Tie-2. Interestingly the gene expression of both of these receptors components were significantly downregulated by NIH13 treatment of HUVECs in Chapter 5, suggesting that anti-angiogenic effects of the novel lipoxygenase inhibitors ex vivo is a combination of effects to both cancer cells

and the surrounding tumour microenvironment. bFGF has shown prognostic value in oesophageal cancer previously (Barclay *et al.*, 2005). Specific inhibition of the related eicosanoid synthesising enzyme COX-2, and associated suppression of cell growth and induction of apoptosis, were shown to be mediated through bFGF (Baguma-Nibasheka *et al.*, 2007). Thus targeting bFGF through 5-LO or 12-LO inhibition may be an interesting therapeutic route in the treatment of OAC. Flt-1 is often overexpressed in cancer and its prognostic value has been investigated in a number of cancers including metastatic oesophageal cancer, with mixed results (Rades *et al.*, 2008, Rades *et al.*, 2010, Ghanem *et al.*, 2003). Interestingly, while no lipoxygenase specific studies are available in the literature, silencing of COX-2 in gastric cancer cells was shown to decrease Flt-1 suggesting COX-2 regulation is involved (Yao *et al.*, 2011). Tie-2 has not been investigated in OAC specifically, however reports in other cancer types such as breast cancer indicate its association with prognosis and metastasis (Meunier-Carpentier *et al.*, 2005). Similarly, cancer cell specific PlGF, a relatively newly investigated anti-cancer target has also been associated with increased metastasis in oesophageal, mouth and lung cancer (Chen *et al.*, 2014, Bu *et al.*, 2015, Li *et al.*, 2013a).

In conclusion in this study we have shown that the novel 5-LO inhibitor NIH4 can induce specific anti-proliferative effects on OE33 cells, unlike zileuton. Additionally anti-proliferative effects at 10 μM occurred independently of the intrinsic apoptosis pathway. NIH4 was shown to reduce 5-LO activity in OE33 cells and OAC biopsies by a reduction in LTB4, indicating the efficacy of NIH4 in targeting 5-LO in OAC. A significant upregulation of VEGF production was observed following NIH4 treatment of OE33 cells. This may suggest that 5-LO or other pathways stimulated by 5-LO are regulated by VEGF signalling, hence the counteracting increase in VEGF production. Through *in vitro* and *ex vivo* assessments NIH4 was found to elicit potential anti-cancer or anti-angiogenic effects through mechanisms involving bFGF, PlGF,Flt-1 and the angiopoietin-Tie-2 signalling pathway *ex vivo*. In the case of the 12-LO inhibitors, discrete differences in the effects of the three novel classes of compound were observed, despite their common target. NIH15 did not to show activity *in vitro* in cell viability, proliferation and apoptosis assays. In contrast NIH13 had potent anti-proliferative and/or cytotoxic effects in the nanomolar range and could induce significant apoptosis and necrosis at 24 and 72 hours respectively. GM5, a less active compound from initial tests in HUVECs, was shown to elicit specific anti-proliferative effects without an induction of apoptosis or apparent cytotoxic effects in OE33 cells. Although NIH15 was not assessed, NIH13 and GM5 were shown to have potent

inhibitory effects on 12(S)HETE production *in vitro* indicating their specificity as anti-12-LO therapeutics. Based on initial results in Chapter 5, it was expected that NIH13 would have the greatest anti-angiogenic effects. However in the context of a cancer model, it was GM5 that had the greatest effect. Nevertheless NIH13 treatment *ex vivo* was shown to significantly downregulate Tie-2 and neuropilin-1, two targets also downregulated at the mRNA level in HUVECs following NIH13 treatment *in vitro*. Neuropilin-1 mRNA levels were also downregulated in OE33 cells with NIH13 treatment. Thus indicating potential effects of NIH13 on both tumour cells and stromal components *ex vivo*. GM5 anti-cancer and anti-angiogenic effects were found to be mediated through mechanisms involving bFGF, PlGF, the angiopoietin-Tie-2 pathway and the VEGF-Flt1-neuropilin-1 pathway, but not VEGF specifically. Thus novel 5-LO and 12-LO inhibitor treatments of an *ex vivo* OAC model has highlighted a number of interesting anti-cancer and anti-angiogenic targets other that may involve not only effects to cancer cells but also to the surrounding tumour microenvironment.

Chapter 7 Concluding Discussion

7.1 Concluding discussion

Over the past decade there has been a dramatic increase in the incidence of oesophageal cancer, particularly OAC, in Europe and the US (Ferlay *et al.*, 2012). This is especially true in Ireland, where we have the second and third highest European incidence rates in females and males respectively (National Cancer Registry, 2013). Despite major improvements to patient outcomes through more advanced CRT regimes and the implementation of BO surveillance programs in Irish hospitals (Picardo *et al.*, 2015), the fact remains that fewer than 20% of oesophageal cancer patients remain alive 5 years after their diagnosis (Howlader N, 2012). Clearly, this cancer represents a palpable burden to the Irish health system and a challenge to clinicians and scientists alike. Thus an increased understanding of the molecular mechanisms underlying this cancer is invaluable and will advance the development of novel biomarkers, for both the earlier detection and molecular therapeutic targeting of this disease. The eicosanoid signalling pathway and its associated enzymes, namely the cyclooxygenases, lipoxygenases and cytochrome P450, are an area of interest in cancer research due to the evidenced involvement of aberrant eicosanoid signalling in chronic inflammation, enhanced tumour growth and angiogenesis (Wang and DuBois, 2010, Cathcart *et al.*, 2011b). In gastrointestinal malignancies such as colorectal cancer, inhibition of COX-2 derived eicosanoid signalling has been shown to reduce the progression of pre-malignant adenomas to full-blown carcinoma indicating the therapeutic potential of targeting these pathways (Bertagnolli *et al.*, 2006). COX-2 has also been investigated in oesophageal cancer to a lesser extent (Zhi *et al.*, 2006, Cui *et al.*, 2015). Although complicated by the variety of lipoxygenase isoforms, research is accumulating on the role of these enzymes in colorectal cancer and dual targeting approaches with COX-2 inhibitors have been investigated (Rao *et al.*, 2012). Given the fact that oesophageal cancer, similar to colorectal cancer, arises on a background of chronic inflammation (Abdel-Latif *et al.*, 2009) the lipoxygenase family of enzymes are interesting biomarker candidates for investigation. Currently available research on the role lipoxygenase isoforms in the context of oesophageal cancer is both limited and conflicting as in the case of 5-LO (Hoque *et al.*, 2005, Boger *et al.*, 2012) or effectively unaddressed as in the case of 12-LO. Thus, it represents a gap in the literature, requiring investigation.

In Chapter 3 and Chapter 4 we provide for the first time clinical data on the comparative gene expression levels of the three main lipoxygenase isoforms: 5-LO, 12-LO and 15-LO-1 in the same cohort of OAC biopsies and matched normal adjacent

tissue. 15-LO has been shown to have opposing roles in cancer that appear to be tumour-specific, for example it is overexpressed in prostate cancer (Kelavkar *et al.*, 2001) but highly expressed in normal tissue compared to tumour tissue in breast, pancreas and colon (Jiang *et al.*, 2006b, Hennig *et al.*, 2007b, Shureiqi *et al.*, 1999). In our study, very low to negligible expression was determined in both normal adjacent and tumour samples. The lack of tumour expression is in concordance with previously published *in vitro* data and an immunohistochemical study of 15-LO-1 in oesophageal cancer specimens which showed absent protein expression in 87% of tumour samples (Shureiqi *et al.*, 2001). It must be noted however that in this study Shureiqi *et al.* observed strongly positive immuno-staining in the normal epithelium which we did not observe at the gene level. In contrast to malignancies such as breast cancer and prostate cancer where lipoxygenases have been found to be overexpressed at the gene level in tumour tissue compared to normal tissue (Jiang *et al.*, 2006a, Nie *et al.*, 1998), we observed significantly higher 5-LO and 12-LO in the macroscopically normal adjacent tissue compared to tumour tissue. Substantial 5-LO expression was found across the board in all isolated RNA samples, both normal adjacent and tumour, indicating that it may not be cancer specific. In the case of 12-LO, it was ultimately unexpressed at the gene level in tumour samples however strong expression was observed in the normal adjacent tissue. While unexpected it was consistent across all RNA biopsy samples and was further confirmed at the protein level in a subset of samples by western blot. Higher 12(S)HETE was also detected in the TCM from a very small cohort (n=3) of normal adjacent tissue compared to matched OAC tumour biopsies, thus providing further evidence. Granted the majority of publications in the literature suggest an upregulation of 12-LO in carcinogenesis, there are at least three cases where the opposite has been found in studies of cervical cancer, nasal polyposis and RCC (Nigam *et al.*, 1999, Ergin *et al.*, 2012, Gohara *et al.*, 2012). Given that 15-LO-1 has previously been shown to be expressed in the epithelium of histologically normal adjacent oesophageal tissue (Shureiqi *et al.*, 2001) and that 5-LO and 12-LO are known for a largely pro-tumourigenic role, our results of absent 15-LO-1 and high 5-LO and 12-LO in normal adjacent tissue are somewhat confounding. The finding of cytokeratin-8, (a maker of BO and gastric cardia (van Baal *et al.*, 2008) expression in the normal adjacent samples in this study may provide a rational for these findings. The presence this glandular marker suggests the normal adjacent tissue contains intestinal metaplasia or dysplasia and is possibly more representative of pre-cancerous tissue. This idea of a role of 5-LO at the pre-cancerous stage is supported by a previously published study which indicated an increased production of LTB4 by cultured erosive oesophagitis (stage 1-4) and BO biopsies compared to normal symptomatic controls

(Triadafilopoulos *et al.*, 1996). Therefore 5-LO and 12-LO may have a pre-cancerous role in driving tumour initiation in OAC. Crude biopsy RNA does not reveal the compartment specific expression of the enzymes, thus immunohistochemistry was used to provide further insight into the specific tissue localisation of 5-LO and 12-LO in OAC and OSCC specimens.

There are currently 3 published studies which discuss immunohistochemical 5-LO expression in oesophageal cancer and the data is conflicting with some suggesting epithelial specific expression (Chen *et al.*, 2004, Hoque *et al.*, 2005) and others describing stromal expression only (Boger *et al.*, 2012). Our larger immunohistochemical study has contributed another perspective to this debate: whilst epithelial expression was unquestionably observed in some 10% of the TMAs cores examined, the overwhelming majority of staining was stromal specific which is in agreement with Boger *et al.* While neutrophils and monocytes are major sources of immune 5-LO expression and activity (Cheon *et al.*, 2012, Boger *et al.*, 2012), we have shown a number of potentially interesting correlations with immune cell markers representing cells types that may have a novel role in 5-LO signalling for example the pro-tumourigenic immunosuppressive $CD8^+FOXP3^+$ T-cells and anti-tumour $CD8^+CD45RO^+$ IFN-γ producing T-cells. A novel contribution of this study was an examination of stromal 5-LO expression in relation to clinical parameters which was not addressed in previous studies. Excluding patients with neoadjuvant CRT, OSCC 5-LO stromal expression showed significant associations with absent lymph and venous involvement, presence of dysplasia and N-stage, while OAC was associated with a history of BO and a lower T-stage indicating an involvement of stromal 5-LO expression early in disease. The association of 5-LO stromal staining with a history of BO is of particular interest suggesting an involvement in the state of chronic inflammation that precedes OAC tumour initiation. This is supported by the fact that other eicosanoid signalling enzymes have been shown to be involved in the development and progression to OAC (Shirvani *et al.*, 2000). It was also noted that of the 10% of TMA cores showing epithelial staining, the largest areas of staining were found in benign gastric mucosa or glands with high grade dysplasia on a background of intestinal metaplasia which is in corroboration with observed higher 5-LO gene expression observed in the "normal" adjacent tissue. There were several cases of invasive carcinoma (i.e. glands in the muscle or fat in the TMA core) that stained positively for 5-LO. In these infrequent cases, staining tended to be restricted to the nucleus in low grade tumours while a weaker cytoplasmic staining was observed in high grade carcinoma cases. Due to the small number of positive staining cases no

clinical correlation proved significant, however epithelial 5-LO may be playing a relevant role in the small subset of patients expressing it. Our observations suggest that epithelial specific 5-LO may have a discrete expression pattern (both cytoplasmic and nuclear), depending on the grade of the tissue.

Another interesting research strand of this project involved investigating the emerging role of 5-LO in obesity (Neels, 2013), in the context of OAC, a cancer type thought to be strongly driven by an obese state (Renehan *et al.*, 2008). Previously in our department it was shown that 5-LO gene expression of the OAC cell line, OE33, was upregulated following co-culture with fragments of adipose tissue (unpublished data). In this project we found that 5-LO OAC gene expression was associated with VFA, the gold standard measurement of obesity status (Doyle *et al.*, 2013) and similarly, 5-LO protein stromal expression was significantly higher in obese CRT-naive patients by BMI. We investigated the circulating serums levels of LTB4 in OAC and a significantly higher level of LTB4 was associated with patients with an obese BMI (>30) compared to those considered to be a normal weight (BMI≤25). These results indicate that 5-LO expression and more specifically stromal 5-LO expression may be involved in obesity-driven OAC. While one previous study compared the expression of different LO isoforms in omental fat from bariatric patients this study notably did not include 5-LO (Dobrian *et al.*, 2010). Additionally, no study has investigated 5-LO expression in adipose tissue in the context of cancer, indicating the uniqueness of our study. We report here that 5-LO expression was present in both omental and subcutaneous adipose tissue derived from OAC patients and that 5-LO expression was significantly higher in the omental fat depot. Most interestingly we have shown that 5-LO expression is significantly higher in obese patients and that there is a positive correlation between 5-LO expression and increasing obesity status measured by VFA, BMI and WC, suggesting 5-LO may has a role in enhancing obesity-driven OAC. The idea of targeting the obesity-inflammatory-eicosanoid axis in the treatment of breast cancer has been recently reviewed (Vona-Davis and Rose, 2013), however this is the first study to show a link with OAC.

Although we did not identify 5-LO as a prognostic marker of oesophageal cancer it may still have potential as a therapeutic target in OAC considering its documented link with inflammation, tumour cell proliferation and in particular it role in the angiogenesis (Chatterjee *et al.*, 2013). In this project 5-LO gene expression was indicated to correlate with VEGF expression in OAC biopsies and an association between 5-LO stromal expression in OAC and hot spots of microvessels in TMA tumour, highlighting a

potential role of 5-LO in the modulation of OAC neo-angiogenesis. A similar association between 5-LO epithelial expression and microvessel density has been reported in sporadic colorectal cancer (Barresi *et al.*, 2008). In Chapter 5 and 6, using a novel class of 5-LO inhibitors based on a phenylenediamine scaffold (NIH4) we investigated the anti-angiogenic potential of targeting this pathway in models of angiogenesis and the anti-cancer effects using *in vitro* and *ex vivo* OAC models. Firstly, NIH4 did not affect *in vivo* angiogenesis in the zebrafish model, however as previously suggested, 5-LO inhibitors may only be effective in models of pathological angiogenesis (Yang *et al.*, 2014). It was noted however that NIH4 began to have morphological effects to the zebrafish at 25 μM, suggesting either toxic effects or potential involvement of zebrafish 5-LO in developmental processes as has been previously reported (Cannon *et al.*, 2013). The effect of NIH4 on apoptosis, proliferation, tubule formation and angiogenic gene expression and protein secretion in HUVECs, a cell model known not to express 5-LO was investigated. Unlike some of the 12-LO inhibitors assessed, NIH4 did not have any effect on tubule formation or apoptosis at the doses tested. NIH4 however significantly inhibited HUVEC proliferation and significantly downregulated secretion of the pro-angiogenic cytokine GRO-α. These findings indicate an anti-mitotic effect of this novel class of compound in endothelial cell that is independent of 5-LO expression and that may involve a suppression of GRO-α. Interestingly GRO-α is reportedly an essential autocrine growth factor in HUVECs (Fujisawa *et al.*, 1999) and thus this novel interaction of NIH4 raises important possibilities as an-angiogenic therapy. Given that a subset of oesophageal cancer patients had evident 5-LO epithelial expression in the TMA study and that the OAC cell line OE33 have high expression of the enzyme at both the gene and protein level we investigated the anti-cancer and anti-angiogenic effect of NIH4 *in vitro* and *ex vivo*. NIH4 was shown to significantly inhibit DNA synthesis of OE33 cells without inducing evident apoptosis suggesting specific anti-proliferative effects. At the same dose NIH4 was found to significantly decrease LTB4 synthesis suggesting this anti-proliferative effect is through a specific blockage of 5-LO. In our assessment of angiogenic secretions by OE33 cells in response to NIH4 treatment we unexpectedly observed a significant upregulation in VEGF. In contrary to other studies where 5-LO inhibition decreased VEGF expression (Ye *et al.*, 2004, Chatterjee *et al.*, 2013), our data may suggest that 5-LO is being regulated by VEGF. Alternatively, an upregulation of VEGF may be a compensatory mechanism in response to the downregulation of some other unknown signalling pathway targeted by NIH4. Possibly the most novel and interesting component of these inhibitory studies with the novel 5-LO inhibitor NIH4 was its effects to the 5-LO enzyme activity and angiogenic secretions of OAC biopsies treated *ex vivo*. Firstly, both NIH4 and the FDA

approved 5-LO inhibitor zileuton were found to significantly decrease LTB4 levels compared to untreated control, indicating the specificity of these inhibitors in an explant model of human OAC. In this 3D system containing both tumour cells and an intact tumour microenvironment NIH4 treatment was found to significantly decrease the major angiogenic regulator bFGF, PlGF, Flt-1 and the angiopoietin-Tie2 signalling pathway. Unlike other published studies (Chatterjee *et al.*, 2013) neither NIH4 nor zileuton appeared to decrease VEGF itself, suggesting that this phenomenon maybe be specific to the murine cancer model of the study published by Chatterjee *et al.* Instead NIH4 5-LO inhibition is eliciting effects by downregulating the VEGF receptor Flt-1 and other angiogenic signalling pathways that are independent of VEGF.

12-LO protein expression was investigated in the same cohort of patients used to perform the 5-LO staining. This is the first study of its kind to document the immunohistochemical expression of 12-LO in oesophageal cancer. Unlike 5-LO staining, 12-LO was shown to be expressed in the majority of epithelial and stromal components, with variable levels observed across the TMAs. We acknowledge that the high 12-LO staining in these tumour cores is somewhat conflicting with the previously discussed gene expression and western blot studies where negligible 12-LO mRNA and low 12-LO protein expression was noted compared to normal adjacent tissue. We note however that the western blot data study was carried out with a different antibody that was not suitable for IHC and that specificity of the IHC compatible antibody was confirmed by the western blot detection of recombinant 12-LO protein, thus both antibodies appear to be showing 12-LO specificity. Considering that platelet-type 12-LO research as a whole has not advanced to the same degree as that of other disease biomarkers, similar to the dearth of 12-LO specific inhibitors, there is a poor availability of reliable immuno-tools for the detection of human 12-LO. This is a limitation, particularly for clinical studies such as ours. In spite of the aforementioned discrepancies between our data sets, variable 12-LO staining was observed across the TMA and a number of clinical associations were found. Similar to 5-LO stromal protein expression in OAC, all observed significant associations between 12-LO expression, both epithelial and stromal, and clinical parameters indicate an association with a less aggressive form of OAC. Most notably epithelial and stromal 12-LO expression was significantly associated with lower T-stage and shorter tumour length. While not significant there was a trend for higher 12-LO expression to be associated with an improved prognosis, with patients expressing above median levels of 12-LO showing an increased survival time of at least 20 months. Assessment of the small subset of OSCC patients (n=25) in contrast revealed that epithelial 12-LO expression at the

invasive edge was associated with decreased prognosis. While 12-LO expression appears to be higher in earlier stages of OAC, suggesting a role in cancer initiation, 12-LO expression in OSCC appears to be associated with cancer progression and prognosis. While there are evidenced discrepancies between the previous qPCR and western blot data in OAC biopsies and the immunohistochemistry data for OAC with regards to tumour expression, taking both studies in isolation they both arrive at the same conclusion that 12-LO expression in OAC may play an early role in cancer development.

In Chapter 4 significant correlations between OAC 12-LO immunohistochemical expression and VEGF or VEGFR-2/KDR, and circulating 12(S)HETE levels and VEGF suggest a potential link between 12-LO and angiogenesis in this cancer. A major focus of Chapter 5 and 6 was to investigate the role of novel 12-LO inhibitors in angiogenic models and OAC models. Prior to this project, to our knowledge these novel inhibitors had only been assessed in a recombinant 12-LO qHTS assay, human platelets and human islets. Of the three different classes of novel 12-LO inhibitors, the unpublished oxadiazol-2-yl benzamide class of inhibitor was the only compound to show a significant effect to developmental angiogenesis in the zebrafish model, decreasing ISV formation by 35%. 8-hydroxquinoline-based NIH13 showed a consistent but non-significant 20% decrease in zebrafish vessel formation while the benzenesulfonamide class (GM5) showed no effect to either ISV formation or overall morphology of the zebrafish. Similar to the 5-LO inhibitors the utility of this model to test the anti-angiogenic effects of 12-LO inhibitors was questioned due to the abnormal form of 12-LO reportedly expressed by zebrafish. Regardless of this, the model had utility in testing the toxicity profile of the 12-LO inhibitors *in vivo* indicating that GM5 was the safest drug with no observed morphological defects up to a dose of 100 μM. In contrast the other two classes began to have morphological effects at the lower dose of 50 μM. Next the compounds were assessed for effects to HUVEC tubule formation, proliferation, apoptosis and HUVEC angiogenic gene expression and protein secretion. NIH13 was shown to have superior effects in all assays compared to the other two compound classes, significantly decreasing tubule formation, DNA synthesis, inducing early apoptosis at 48 hours and necrosis at 72 hours and showing the only validated alteration of a number of key angiogenic gene pathways. While other studies have indicated that blocking 12-LO in endothelial cells decreases tubule formation and VEGF expression (Nie *et al.*, 2000), this was the first study to screen the effect of 12-LO inhibitors on multiple angiogenic gene expression pathways. NIH13 was shown to significantly decrease *KDR* and *NRP1* expression of the VEGF signalling pathway and

what's more we observed significant downregulations in the angiopoietin-Tie system (*ANGPT1, TEK* and *TIE1*) and the pro-angiogenic and pro-inflammatory chemokine GRO-α (*CXCL1*) suggesting that inhibition of 12-LO activity in HUVECs is having effects beyond VEGF signalling. The significant gene downregulation of GRO-α by NIH13 was also confirmed at the secreted protein level, further validating this result. It was also noted that while GM5 failed to induce significant angiogenic gene alterations in HUVECs, a significant dose response decrease in GRO-α secreted level, similar to NIH13, was observed. While GM5 was the least potent of the novel 12-LO compounds investigated in the zebrafish and HUVEC model it interestingly showed specific anti-proliferative effects in OE33 cells at low doses. GM5 showed a lack of toxicity in the zebrafish model up to the high dose of 100 μM and it appeared to preferentially inhibit proliferation in cancer cells at lower doses than non-cancer cells, such as the HUVECs. These desirable drug features suggest GM5 may have efficacy as a potential anti-cancer agent, with minimal side effects. GM5 was found to inhibit 12(S)HETE production by OE33 cells, suggesting 12-LO specificity of the inhibitor while an additional significant decrease in secreted GRO-α similar to the HUVECs, suggests GRO-α is either regulated by 12-LO or that it is an alternate target of the benzenesulfonamide inhibitor class. In contrast a significant decrease in 12(S)HETE or GRO-α was not observed in the ex vivo OAC model however it was noted that there was substantial variability in the small patient subset and thus increasing the number of patients in the experimental set may provide a more conclusive result. The *ex vivo* OAC model provided the opportunity to investigate the effect of novel inhibitor treatment to tumour biopsy angiogenic secretions and we report here that of the three classes of 12-LO inhibitors, GM5 showed the greatest potency. GM5 caused broad anti-angiogenic effects through a downregulation of multiple key angiogenic factors and signalling pathways including bFGF, PlGF, Tie-2 and VEGF associated Flt1 and neuropilin-1. Although it caused fewer alterations to the angiogenic secretory profile of OAC biopsies, NIH13 was shown to downregulate neuropilin-1 secretion *ex vivo*, supporting the downregulation of *NRP1* gene expression in OE33 cells *in vitro*, and also decrease Tie-2.

In conclusion this thesis has shown 5-LO and 12-LO are involved in OAC and based on associations with clinical parameters both enzymes appear to be associated with an early stage of disease or tumour initiation rather than progression. An observed association between OAC tumour or omental adipose tissue derived 5-LO expression with patient obesity status may suggest a novel involvement in obesity-driven disease. Additionally, serum LTB4 levels showed a correlation with obesity status in OAC. While

LTB4 did not appear to differ significantly between cancer patients a small cohort of non cancer controls, 12(S)HETE was shown to be significantly upregulated in the cancer serums suggesting its potential as a biomarker of disease. Through pharmacological inhibitory studies a novel class of 8-hydroxyquinoline based 12-LO inhibitors showed robust effects to proliferation, apoptosis, tubule formation and alterations to the angiogenic gene profile of HUVECs, suggesting novel utility as an anti-angiogenic agent in oesophageal cancer or indeed other angiogenesis driven cancers and diseases. Assessment of novel 5-LO and 12-LO inhibitors classes in both *in vitro* and *ex vivo* models of OAC have indicated the involvement of these pathways in the regulation of cell growth, survival and apoptosis and angiogenesis. Therefore targeting 5-LO and 12-LO may be a therapeutic strategy in the treatment of OAC, particularly in respect to angiogenesis, in the subset of patients overexpressing these enzymes. Further studies are required to establish whether 5-LO and 12-LO are preferentially expressed early in the disease and at what point targeting these enzymes may have most efficacy.

7.2 Future directions

In this project we have shown a number of associations between 5-LO stromal expression and OAC, in a particular an association with a history of the BO metaplasia and with obese patients, thus indicating a potential involvement of 5-LO signalling in states of chronic inflammation. While 5-LO immune regulation has been investigated in pathologies such as asthma, COPD, cancer (Kilfeather, 2002, Tager *et al.*, 2003, Olkhanud *et al.*, 2011, Wejksza *et al.*, 2013) it has not been investigated in OAC specifically. 5-LO was also found to be higher in omental adipose tissue from obese patients, suggesting that fat may be a source of these 5-LO expressing immune cells. An obvious line of investigation for this work would be to isolate immune cell populations from digested OAC tumour and omental adipose tissue to investigate which immune cell types have 5-LO activity and whether they are responsive to 5-LO inhibition. Additionally, it would also be interesting to see what effect 5-LO inhibition has on the inflammatory secretion profile of adipose tissue or individual immune cell components. A correlation between 5-LO expression of the stromal compartment with immune markers suggestive of the immunosuppressive and pro-cancer cell phenotype ($CD8^+FOXP3^+$) and the anti-tumour immune cell phenotype ($CD8^+CD45RO^+$) were highlighted in our study, however to validate this correlation OAC tissue must be assessed for presence and percentages of these immune subtypes.

The identification of the glandular tissue marker cytokeratin-8 expression in normal adjacent oesophageal samples suggests the macroscopically normal adjacent samples used in this study more than likely represent abnormal pre-cancerous tissue. Considering the high expression of 5-LO and 12-LO in this adjacent tissue and the observed association of 5-LO and 12-LO expression with an earlier tumour phenotype, an obvious line of further investigation would be to investigate the role of these enzymes in the progressive sequence from normal to BO metaplasia to OAC. 5-LO associated protein FLAP gene expression was reported to be elevated and prognostic in breast cancer (Jiang *et al.*, 2006a). Boger *et al.* also reported significantly increased stromal FLAP protein levels in OAC tissue compared to normal tissue although the cohort was small. It would be interesting to investigate the level and tissue compartment location of FLAP and other 5-LO metabolites in a larger TMA cohort including normal samples. There has been criticism in the literature of the use of macroscopically normal adjacent tissue to represent the non-cancerous condition. This is because it is very likely that normal appearing tissue can undergo genetic changes in response to or in expectation of morphological cancer, in addition to the possible field effect surrounding a tumour (Chandran *et al.*, 2005). Thus, the absence of truly normal adjacent tissue as a control was a limitation in our gene study. Investigation of 5-LO and 12-LO expression in normal oesophageal squamous tissue derived from non-cancerous patients is a logical extension of this study.

In this project serum LTB4 levels showed a correlation with obesity status in OAC. While LTB4 did not appear to differ significantly between cancer patients a small cohort of non cancer controls, 12(S)HETE was shown to be significantly upregulated in the cancer serums suggesting its potential as a biomarker of disease. Due to limited reagents, only a limited number non-cancer control samples (n=6) could be run in these experiments. Given the elevated level of 12(S)HETE observed in OAC cancer serums it is critical that this experiment be repeated and devised to include a more even ratio of non-cancer controls to control serums. Although the cohort size was small it was highlighted previously in Chapter 4 that OSCC 12-LO epithelial expression was associated with a poorer patient survival. Serum 12(S)HETE levels of OSCC patients were not investigated in this study but clearly warrants investigation. Unfortunately in this study we were also not able to correlate tumour tissue-derived 5-LO or 12-LO and their corresponding serum metabolite levels because the two studies did not use the same cohort of patients. For future investigations of the biomarker potential of 12(S)HETE in particular, it would be important to select serum samples with FFPE blocks available to perform this correlation.

Given the discrepancies between our western blot and immunohistochemical 12-LO data and the limited availability of reliable and specific antibodies, it would be an invaluable and very informative exercise to perform a comparison of multiple 12-LO antibodies currently available to researchers, in tissue sections and isolated protein to investigate further issues with variability. The monoclonal western blot antibody and the polyclonal immunohistochemistry antibody used in this project both recognise a short region in the 12-LO protein and thus may not be as specific as 12-LO antibodies recognising the full length protein that are also available (JaŒKiewicz *et al.*, 2010). Given the opposing findings between the 3 currently published 5-LO immunohistochemical studies (Chen *et al.*, 2004, Hoque *et al.*, 2005, Boger *et al.*, 2012) and the fact that different antibody sources were used for each of these studies and our own work, it would be very interesting to perform an immunohistochemical comparison of all the antibodies involved using the same tissue specimen to address these discrepancies between our findings.

Our findings of significant alterations to major angiogenic factors and signalling pathways in tumour biopsies treated with novel 5-LO and 12-LO inhibitors, in addition to significant suppression of OE33 cell proliferation highlights a new area of exploration for OAC treatment. An *in vivo* xenograft murine model injected with 12-LO overexpressing cancer cells has previously demonstrated increased tumour growth and higher vessel numbers within the tumour mass and increased metastasis (Connolly and Rose, 1998, Nie *et al.*, 2003). It would be very interesting to see what effect overexpression of 5-LO and 12-LO enzymes in OAC cells injected into a mouse xenograft model has on tumour growth and whether the novel 5-LO and 12-LO inhibitors used in our studies could affect the size of the tumour mass, vessel formation or indeed the expression of angiogenic factor we have shown to be altered in our studies, such as bFGF. Additionally, considering associations of 5-LO and 12-LO with an early tumour phenotype and specifically the association of 5-LO expression with a history of BO, it would be interesting to see what effect 5-LO and 12-LO inhibitors have on progression to OAC in recently developed mouse models of BO (Quante *et al.*, 2012).

While the zebrafish model did reveal an anti-angiogenic hit with NIH15, the effects were modest in comparison to anti-angiogenic effects with multi-tyrosine kinase inhibitors (Chimote *et al.*, 2014). It has been suggested by a previous study that lipoxygenase inhibitors do not affect developmental angiogenesis in zebrafish embryos

(Yang *et al.*, 2014). However it was demonstrated that in a zebrafish cancer cell xenograft model, the induction of neoangiogenesis and the growth of new vessels towards the injected cancer cells could be suppressed by a lipoxygenase inhibitor. Thus it would be interesting to see if the anti-angiogenic effect of NIH15 is enhanced in a pathological xenograft zebrafish model of angiogenesis. NIH13 demonstrated potent anti-angiogenic effects to human endothelial cells *in vitro*, effecting proliferation, survival, apoptosis and numerous angiogenic gene pathways. A critical next phase in these studies would be to investigate the effect of these drugs, in particular NIH13, in a pathogenic model of tumour angiogenesis, such as a zebrafish xenograft model with injected with OAC cells.

Finally, given the potential of COX-2 as a prognostic marker (Prins *et al.*, 2012) and therapeutic target in OAC (Buttar *et al.*, 2002a, Souza *et al.*, 2000) and the evidenced shunting of AA between COX-2 and the 5-LO signalling pathways (Ganesh *et al.*, 2012, Park *et al.*, 2012) it would be very intriguing to investigate the dual targeting of COX-2/5-LO with the novel 5-LO inhibitor, NIH4 and selective COX-2 inhibitors. Using the OAC *ex vivo* model we could to explore what combined effect these inhibitors have on angiogenic and inflammatory secretions as a potential dual therapeutic approach for OAC.

References

ABDEL-LATIF, M. M., DUGGAN, S., REYNOLDS, J. V. & KELLEHER, D. 2009. Inflammation and esophageal carcinogenesis. *Curr Opin Pharmacol,* 9, 396-404.

ABDEL-LATIF, M. M., O'RIORDAN, J., WINDLE, H. J., CARTON, E., RAVI, N., KELLEHER, D. & REYNOLDS, J. V. 2004. NF-kappaB activation in esophageal adenocarcinoma: relationship to Barrett's metaplasia, survival, and response to neoadjuvant chemoradiotherapy. *Ann Surg,* 239, 491-500.

ABRAMOVITZ, M., WONG, E., COX, M. E., RICHARDSON, C. D., LI, C. & VICKERS, P. J. 1993. 5-lipoxygenase-activating protein stimulates the utilization of arachidonic acid by 5-lipoxygenase. *Eur J Biochem,* 215, 105-11.

ADACHI, Y., OHASHI, H., IMSUMRAN, A., YAMAMOTO, H., MATSUNAGA, Y., TANIGUCHI, H., NOSHO, K., SUZUKI, H., SASAKI, Y., ARIMURA, Y., CARBONE, D. P., IMAI, K. & SHINOMURA, Y. 2014. The effect of IGF-I receptor blockade for human esophageal squamous cell carcinoma and adenocarcinoma. *Tumour Biol,* 35, 973-85.

AGARWAL, S., ACHARI, C., PRAVEEN, D., ROY, K. R., REDDY, G. V. & REDDANNA, P. 2009. Inhibition of 12-LOX and COX-2 reduces the proliferation of human epidermoid carcinoma cells (A431) by modulating the ERK and PI3K-Akt signalling pathways. *Exp Dermatol,* 18, 939-46.

AKARASEREENONT, P. C., TECHATRAISAK, K., THAWORN, A. & CHOTEWUTTAKORN, S. 2002. The expression of COX-2 in VEGF-treated endothelial cells is mediated through protein tyrosine kinase. *Mediators Inflamm,* 11, 17-22.

AL-HUSEIN, B., ABDALLA, M., TREPTE, M., DEREMER, D. L. & SOMANATH, P. R. 2012. Anti-angiogenic therapy for cancer: An update. *Pharmacotherapy,* 32, 1095-111.

ALBERTI, K. G., ECKEL, R. H., GRUNDY, S. M., ZIMMET, P. Z., CLEEMAN, J. I., DONATO, K. A., FRUCHART, J. C., JAMES, W. P., LORIA, C. M. & SMITH, S. C., JR. 2009. Harmonizing the metabolic syndrome: a joint interim statement of the International Diabetes Federation Task Force on Epidemiology and Prevention; National Heart, Lung, and Blood Institute; American Heart Association; World Heart Federation; International Atherosclerosis Society; and International Association for the Study of Obesity. *Circulation,* 120, 1640-5.

ALLISON, K. H. & SLEDGE, G. W. 2014. Heterogeneity and cancer. *Oncology (Williston Park),* 28, 772-8.

ALVARO-GRACIA, J. M. 2004. Licofelone--clinical update on a novel LOX/COX inhibitor for the treatment of osteoarthritis. *Rheumatology (Oxford),* 43 Suppl 1, i21-5.

ARENBERG, D. A., POLVERINI, P. J., KUNKEL, S. L., SHANAFELT, A., HESSELGESSER, J., HORUK, R. & STRIETER, R. M. 1997. The role of CXC chemokines in the regulation of angiogenesis in non-small cell lung cancer. *J Leukoc Biol,* 62, 554-62.

ARNOLD, D., T., A. & BENNOUNA, J. 2012. Bevacizumab (BEV) plus chemotherapy (CT) continued beyond first progression in patients with metastatic colorectal cancer (mCRC) previously treated with BEV plus CT: Results of a randomized phase III intergroup study (TML study). *[abstract CRA3503] J Clin Oncol. 2012;30 [Available online at: http://meetinglibrary.asco.org/content/97866-114; cited July 13, 2013].*

AUGUSTIN, H. G., YOUNG KOH, G., THURSTON, G. & ALITALO, K. 2009. Control of vascular morphogenesis and homeostasis through the angiopoietin-Tie system. *Nat Rev Mol Cell Biol,* 10, 165-177.

AVRAAMIDES, C. J., GARMY-SUSINI, B. & VARNER, J. A. 2008. Integrins in angiogenesis and lymphangiogenesis. *Nat Rev Cancer,* 8, 604-17.

BACK, M., SULTAN, A., OVCHINNIKOVA, O. & HANSSON, G. K. 2007. 5-Lipoxygenase-activating protein: a potential link between innate and adaptive immunity in atherosclerosis and adipose tissue inflammation. *Circ Res,* 100, 946-9.

BAGUMA-NIBASHEKA, M., BARCLAY, C., LI, A. W., GELDENHUYS, L., PORTER, G. A., BLAY, J., CASSON, A. G. & MURPHY, P. R. 2007. Selective cyclooxygenase-2 inhibition suppresses basic fibroblast growth factor expression in human esophageal adenocarcinoma. *Mol Carcinog,* 46, 971-80.

BALKWILL, F. R., CAPASSO, M. & HAGEMANN, T. 2012. The tumor microenvironment at a glance. *J Cell Sci,* 125, 5591-6.

BANG, Y. J., KANG, Y. K., KANG, W. K., BOKU, N., CHUNG, H. C., CHEN, J. S., DOI, T., SUN, Y., SHEN, L., QIN, S., NG, W. T., TURSI, J. M., LECHUGA, M. J., LU, D. R., RUIZ-GARCIA, A. & SOBRERO, A. 2011. Phase II study of sunitinib as second-line treatment for advanced gastric cancer. *Invest New Drugs,* 29, 1449-58.

BANG, Y. J., VAN CUTSEM, E., FEYEREISLOVA, A., CHUNG, H. C., SHEN, L., SAWAKI, A., LORDICK, F., OHTSU, A., OMURO, Y., SATOH, T., APRILE, G., KULIKOV, E., HILL, J., LEHLE, M., RUSCHOFF, J. & KANG, Y. K. 2010. Trastuzumab in combination with chemotherapy versus chemotherapy alone for treatment of HER2-positive advanced gastric or gastro-oesophageal junction cancer (ToGA): a phase 3, open-label, randomised controlled trial. *Lancet,* 376, 687-97.

BARCLAY, C., LI, A. W., GELDENHUYS, L., BAGUMA-NIBASHEKA, M., PORTER, G. A., VEUGELERS, P. J., MURPHY, P. R. & CASSON, A. G. 2005. Basic fibroblast growth factor (FGF-2) overexpression is a risk factor for esophageal cancer recurrence and reduced survival, which is ameliorated by coexpression of the FGF-2 antisense gene. *Clin Cancer Res,* 11, 7683-91.

BARRESI, V., GROSSO, M., VITARELLI, E., TUCCARI, G. & BARRESI, G. 2007. 5-Lipoxygenase is coexpressed with Cox-2 in sporadic colorectal cancer: a correlation with advanced stage. *Dis Colon Rectum,* 50, 1576-84.

BARRESI, V., VITARELLI, E., TUCCARI, G. & BARRESI, G. 2008. Correlative study of microvessel density and 5-lipoxygenase expression in human sporadic colorectal cancer. *Arch Pathol Lab Med,* 132, 1807-12.

BEDNAR, W., HOLZMANN, K. & MARIAN, B. 2007. Assessing 12(S)-lipoxygenase inhibitory activity using colorectal cancer cells overexpressing the enzyme. *Food Chem Toxicol,* 45, 508-14.

BENARD, M., STRAAT, K., OMARSDOTTIR, S., LEGHMARI, K., BERTRAND, J., DAVRINCHE, C., DUGA-NEULAT, I., SODERBERG-NAUCLER, C., RAHBAR, A. & CASPER, C. 2014. Human cytomegalovirus infection induces leukotriene B4 and 5-lipoxygenase expression in human placentae and umbilical vein endothelial cells. *Placenta,* 35, 345-50.

BENDELL, J. C., MELUCH, A., PEYTON, J., RUBIN, M., WATERHOUSE, D., WEBB, C., BURRIS, H. A., 3RD & HAINSWORTH, J. D. 2012. A phase II trial of preoperative concurrent chemotherapy/radiation therapy plus bevacizumab/erlotinib in the treatment of localized esophageal cancer. *Clin Adv Hematol Oncol,* 10, 430-7.

BERGER, W., DE CHANDT, M. T. & CAIRNS, C. B. 2007. Zileuton: clinical implications of 5-Lipoxygenase inhibition in severe airway disease. *Int J Clin Pract,* 61, 663-76.

BERGERS, G. & HANAHAN, D. 2008. Modes of resistance to anti-angiogenic therapy. *Nat Rev Cancer,* 8, 592-603.

BERTAGNOLLI, M. M., EAGLE, C. J., ZAUBER, A. G., REDSTON, M., SOLOMON, S. D., KIM, K., TANG, J., ROSENSTEIN, R. B., WITTES, J., CORLE, D., HESS, T. M., WOLOJ, G. M., BOISSERIE, F., ANDERSON, W. F., VINER, J. L., BAGHERI, D., BURN, J., CHUNG, D. C., DEWAR, T., FOLEY, T. R., HOFFMAN, N., MACRAE, F., PRUITT, R. E., SALTZMAN, J. R., SALZBERG, B., SYLWESTROWICZ, T., GORDON, G. B. & HAWK, E. T. 2006. Celecoxib for the prevention of sporadic colorectal adenomas. *N Engl J Med,* 355, 873-84.

BIAN, X. W., JIANG, X. F., CHEN, J. H., BAI, J. S., DAI, C., WANG, Q. L., LU, J. Y., ZHAO, W., XIN, R., LIU, M. Y., SHI, J. Q. & WANG, J. M. 2006. Increased angiogenic capabilities of endothelial cells from microvessels of malignant human gliomas. *Int Immunopharmacol,* 6, 90-9.

BINATO, M., GURSKI, R. R., FAGUNDES, R. B., MEURER, L. & EDELWEISS, M. I. 2009. P53 and Ki-67 overexpression in gastroesophageal reflux disease--Barrett's esophagus and adenocarcinoma sequence. *Dis Esophagus,* 22, 588-95.

BITTO, A., MINUTOLI, L., DAVID, A., IRRERA, N., RINALDI, M., VENUTI, F. S., SQUADRITO, F. & ALTAVILLA, D. 2012. Flavocoxid, a dual inhibitor of COX-2 and 5-LOX of natural origin, attenuates the inflammatory response and protects mice from sepsis. *Crit Care,* 16, R32.

BJORK, J., HEDQVIST, P. & ARFORS, K. E. 1982. Increase in vascular permeability induced by leukotriene B4 and the role of polymorphonuclear leukocytes. *Inflammation,* 6, 189-200.

BLUFF, J. E., BROWN, N. J., REED, M. W. & STATON, C. A. 2008. Tissue factor, angiogenesis and tumour progression. *Breast Cancer Res,* 10, 204.

BLUMENSCHEIN, G. R., JR., GATZEMEIER, U., FOSSELLA, F., STEWART, D. J., CUPIT, L., CIHON, F., O'LEARY, J. & RECK, M. 2009. Phase II, multicenter, uncontrolled trial of single-agent sorafenib in patients with relapsed or refractory, advanced non-small-cell lung cancer. *J Clin Oncol,* 27, 4274-80.

BOADO, R. J., PARDRIDGE, W. M., VINTERS, H. V. & BLACK, K. L. 1992. Differential expression of arachidonate 5-lipoxygenase transcripts in human brain tumors: evidence for the expression of a multitranscript family. *Proc Natl Acad Sci U S A,* 89, 9044-8.

BOGER, P. C., SHUTT, J. D., NEALE, J. R., WILSON, S. J., BATEMAN, A. C., HOLLOWAY, J. W., PATEL, P. & SAMPSON, A. P. 2012. Increased expression of the 5-lipoxygenase pathway and its cellular localization in Barrett's adenocarcinoma. *Histopathology,* 61, 509-17.

BOONSTRA, J. J., VAN MARION, R., BEER, D. G., LIN, L., CHAVES, P., RIBEIRO, C., PEREIRA, A. D., ROQUE, L., DARNTON, S. J., ALTORKI, N. K., SCHRUMP, D. S., KLIMSTRA, D. S., TANG, L. H., ESHLEMAN, J. R., ALVAREZ, H., SHIMADA, Y., VAN DEKKEN, H., TILANUS, H. W. & DINJENS, W. N. M. 2010. Verification and Unmasking of Widely Used Human Esophageal Adenocarcinoma Cell Lines. *J Natl Cancer Inst,* 102, 271-4.

BRAAKHUIS, B. J., LEEMANS, C. R. & BRAKENHOFF, R. H. 2004. Using tissue adjacent to carcinoma as a normal control: an obvious but questionable practice. *J Pathol,* 203, 620-1.

BRESALIER, R. S., SANDLER, R. S., QUAN, H., BOLOGNESE, J. A., OXENIUS, B., HORGAN, K., LINES, C., RIDDELL, R., MORTON, D., LANAS, A., KONSTAM, M. A. & BARON, J. A. 2005. Cardiovascular events associated with rofecoxib in a colorectal adenoma chemoprevention trial. *N Engl J Med,* 352, 1092-102.

BROCK, T. G. 2005. Regulating leukotriene synthesis: the role of nuclear 5-lipoxygenase. *J Cell Biochem,* 96, 1203-11.

BROWN, J. R. & DUBOIS, R. N. 2004. Cyclooxygenase as a target in lung cancer. *Clin Cancer Res,* 10, 4266s-4269s.

BROWN, L. M., DEVESA, S. S. & CHOW, W. H. 2008. Incidence of adenocarcinoma of the esophagus among white Americans by sex, stage, and age. *J Natl Cancer Inst,* 100, 1184-7.

BRYANT, C. E., APPLETON, I. & MITCHELL, J. A. 1998. Vascular endothelial growth factor upregulates constitutive cyclooxygenase 1 in primary bovine and human endothelial cells. *Life Sci,* 62, 2195-201.

BU, J., BU, X., LIU, B., CHEN, F. & CHEN, P. 2015. Inhibition of metastasis of oral squamous cell carcinoma by anti-PLGF treatment. *Tumour Biol,* 36, 2695-701.

BUTTAR, N. S., WANG, K. K., ANDERSON, M. A., DIERKHISING, R. A., PACIFICO, R. J., KRISHNADATH, K. K. & LUTZKE, L. S. 2002a. The effect of selective cyclooxygenase-2 inhibition in Barrett's esophagus epithelium: an in vitro study. *J Natl Cancer Inst,* 94, 422-9.

BUTTAR, N. S., WANG, K. K., LEONTOVICH, O., WESTCOTT, J. Y., PACIFICO, R. J., ANDERSON, M. A., KRISHNADATH, K. K., LUTZKE, L. S. & BURGART, L. J. 2002b. Chemoprevention of esophageal adenocarcinoma by COX-2 inhibitors in an animal model of Barrett's esophagus. *Gastroenterology,* 122, 1101-12.

CALLE, E. E., RODRIGUEZ, C., WALKER-THURMOND, K. & THUN, M. J. 2003. Overweight, obesity, and mortality from cancer in a prospectively studied cohort of U.S. adults. *N Engl J Med,* 348, 1625-38.

CANNON, J. E., PLACE, E. S., EVE, A. M., BRADSHAW, C. R., SESAY, A., MORRELL, N. W. & SMITH, J. C. 2013. Global analysis of the haematopoietic and endothelial transcriptome during zebrafish development. *Mech Dev,* 130, 122-31.

CARMELIET, P. 2005. VEGF as a key mediator of angiogenesis in cancer. *Oncology,* 69 Suppl 3, 4-10.

CARMELIET, P. & JAIN, R. K. 2000. Angiogenesis in cancer and other diseases. *Nature,* 407, 249-57.

CASAK, S. J., FASHOYIN-AJE, I., LEMERY, S. J., ZHANG, L., JIN, R., LI, H., ZHAO, L., ZHAO, H., ZHANG, H., CHEN, H., HE, K., DOUGHERTY, M., NOVAK, R., KENNETT, S., KHASAR, S., HELMS, W., KEEGAN, P. & PAZDUR, R. 2015. FDA Approval Summary: Ramucirumab for Gastric Cancer. *Clin Cancer Res.*

CASTRO, C., BOSETTI, C., MALVEZZI, M., BERTUCCIO, P., LEVI, F., NEGRI, E., LA VECCHIA, C. & LUNET, N. 2014. Patterns and trends in esophageal cancer mortality and incidence in Europe (1980-2011) and predictions to 2015. *Ann Oncol,* 25, 283-90.

CATALANO, A. & PROCOPIO, A. 2005. New aspects on the role of lipoxygenases in cancer progression. *Histol Histopathol,* 20, 969-75.

CATHCART, J., PULKOSKI-GROSS, A. & CAO, J. 2015. Targeting Matrix Metalloproteinases in Cancer: Bringing New Life to Old Ideas. *Genes Dis,* 2, 26-34.

CATHCART, M., CAMPBELL, V., GATELY, K., KAY, E., PIDGEON, G. P. & O'BYRNE, K. J. 2011a. Examination of 12-lipoxygenase (12-LOX) as a therapeutic target in non-small cell lung cancer (NSCLC): Mechanisms controlling survival and induction of apoptosis following selective inhibition. *J Clin Oncol 29: 2011 (suppl; abstr 7068).*

CATHCART, M. C., LYSAGHT, J. & PIDGEON, G. P. 2011b. Eicosanoid signalling pathways in the development and progression of colorectal cancer: novel approaches for prevention/intervention. *Cancer Metastasis Rev,* 30, 363-85.

CHAI, J. & JAMAL, M. M. 2012. Esophageal malignancy: A growing concern. *World J Gastroenterol,* 18, 6521-6.

CHAKRABARTI, S. K., WEN, Y., DOBRIAN, A. D., COLE, B. K., MA, Q., PEI, H., WILLIAMS, M. D., BEVARD, M. H., VANDENHOFF, G. E., KELLER, S. R., GU, J. & NADLER, J. L. 2011. Evidence for activation of inflammatory lipoxygenase pathways in visceral adipose tissue of obese Zucker rats. *Am J Physiol Endocrinol Metab,* 300, E175-87.

CHAMBERLAIN, M. C. 2011. Bevacizumab for the Treatment of Recurrent Glioblastoma. *Clin Med Insights Oncol,* 5, 117-29.

CHANDRAN, U. R., DHIR, R., MA, C., MICHALOPOULOS, G., BECICH, M. & GILBERTSON, J. 2005. Differences in gene expression in prostate cancer, normal appearing prostate tissue adjacent to cancer and prostate tissue from cancer free organ donors. *BMC Cancer,* 5, 45.

CHAPUT, N., LOUAFI, S., BARDIER, A., CHARLOTTE, F., VAILLANT, J. C., MENEGAUX, F., ROSENZWAJG, M., LEMOINE, F., KLATZMANN, D. & TAIEB, J. 2009. Identification of CD8+CD25+Foxp3+ suppressive T cells in colorectal cancer tissue. *Gut,* 58, 520-9.

CHARLIER, C. & MICHAUX, C. 2003. Dual inhibition of cyclooxygenase-2 (COX-2) and 5-lipoxygenase (5-LOX) as a new strategy to provide safer non-steroidal anti-inflammatory drugs. *Eur J Med Chem,* 38, 645-59.

CHATTERJEE, M., DAS, S., ROY, K. & CHATTERJEE, M. 2013. Overexpression of 5-lipoxygenase and its relation with cell proliferation and angiogenesis in 7,12-dimethylbenz(alpha)anthracene-induced rat mammary carcinogenesis. *Mol Carcinog,* 52, 359-69.

CHEN, F. L., WANG, X. Z., LI, J. Y., YU, J. P., HUANG, C. Y. & CHEN, Z. X. 2008. 12-lipoxygenase induces apoptosis of human gastric cancer AGS cells via the ERK1/2 signal pathway. *Dig Dis Sci,* 53, 181-7.

CHEN, J., LI, T., WU, Y., HE, L., ZHANG, L., SHI, T., YI, Z., LIU, M. & PANG, X. 2011. Prognostic significance of vascular endothelial growth factor expression in gastric carcinoma: a meta-analysis. *J Cancer Res Clin Oncol,* 137, 1799-812.

CHEN, J., ZHOU, S. J., ZHANG, Y., ZHANG, G. Q., ZHA, T. Z., FENG, Y. Z. & ZHANG, K. 2013. Clinicopathological and prognostic significance of galectin-1 and vascular endothelial growth factor expression in gastric cancer. *World J Gastroenterol,* 19, 2073-9.

CHEN, M., CAI, E., HUANG, J., YU, P. & LI, K. 2012. Prognostic value of vascular endothelial growth factor expression in patients with esophageal cancer: a systematic review and meta-analysis. *Cancer Epidemiol Biomarkers Prev,* 21, 1126-34.

CHEN, X., WANG, S., WU, N., SOOD, S., WANG, P., JIN, Z., BEER, D. G., GIORDANO, T. J., LIN, Y., SHIH, W. C., LUBET, R. A. & YANG, C. S. 2004. Overexpression of 5-lipoxygenase in rat and human esophageal adenocarcinoma and inhibitory effects of zileuton and celecoxib on carcinogenesis. *Clin Cancer Res,* 10, 6703-9.

CHEN, Y., JIANG, T., MAO, A. & XU, J. 2014. Esophageal cancer stem cells express PLGF to increase cancer invasion through MMP9 activation. *Tumour Biol,* 35, 12749-55.

CHEN, Y. Q., DUNIEC, Z. M., LIU, B., HAGMANN, W., GAO, X., SHIMOJI, K., MARNETT, L. J., JOHNSON, C. R. & HONN, K. V. 1994. Endogenous 12(S)-HETE production by tumor cells and its role in metastasis. *Cancer Res,* 54, 1574-9.

CHEON, E. C., KHAZAIE, K., KHAN, M. W., STROUCH, M. J., KRANTZ, S. B., PHILLIPS, J., BLATNER, N. R., HIX, L. M., ZHANG, M., DENNIS, K. L., SALABAT, M. R., HEIFERMAN, M., GRIPPO, P. J., MUNSHI, H. G., GOUNARIS, E. & BENTREM, D. J. 2011. Mast cell 5-lipoxygenase activity promotes intestinal polyposis in APCDelta468 mice. *Cancer Res,* 71, 1627-36.

CHEON, E. C., STROUCH, M. J., KRANTZ, S. B., HEIFERMAN, M. J. & BENTREM, D. J. 2012. Genetic deletion of 5-lipoxygenase increases tumor-infiltrating macrophages in Apc(Delta468) mice. *J Gastrointest Surg,* 16, 389-93.

CHIMOTE, G., SREENIVASAN, J., PAWAR, N., SUBRAMANIAN, J., SIVARAMAKRISHNAN, H. & SHARMA, S. 2014. Comparison of effects of anti-angiogenic agents in the zebrafish efficacy-toxicity model for translational anti-angiogenic drug discovery. *Drug Des Devel Ther,* 8, 1107-23.

CHO, H., UEDA, M., TAMAOKA, M., HAMAGUCHI, M., AISAKA, K., KISO, Y., INOUE, T., OGINO, R., TATSUOKA, T., ISHIHARA, T. & *ET AL.* 1991. Novel caffeic acid derivatives: extremely potent inhibitors of 12-lipoxygenase. *J Med Chem,* 34, 1503-5.

CHOI, S. P., KIM, S. P., NAM, S. H. & FRIEDMAN, M. 2013. Antitumor effects of dietary black and brown rice brans in tumor-bearing mice: relationship to composition. *Mol Nutr Food Res,* 57, 390-400.

CHUNG, A. S., WU, X., ZHUANG, G., NGU, H., KASMAN, I., ZHANG, J., VERNES, J. M., JIANG, Z., MENG, Y. G., PEALE, F. V., OUYANG, W. & FERRARA, N. 2013. An interleukin-17-mediated paracrine network promotes tumor resistance to anti-angiogenic therapy. *Nat Med,* 19, 1114-23.

CONNOLLY, J. M. & ROSE, D. P. 1998. Enhanced angiogenesis and growth of 12-lipoxygenase gene-transfected MCF-7 human breast cancer cells in athymic nude mice. *Cancer Lett,* 132, 107-12.

CORLEY, D. A., KERLIKOWSKE, K., VERMA, R. & BUFFLER, P. 2003. Protective association of aspirin/NSAIDs and esophageal cancer: a systematic review and meta-analysis. *Gastroenterology,* 124, 47-56.

CORTES-BURGOS, L. A., ZWEIFEL, B. S., SETTLE, S. L., PUFAHL, R. A., ANDERSON, G. D., HARDY, M. M., WEIR, D. E., HU, G., HAPPA, F. A., STEWART, Z., MUTHIAN, S., GRANETO, M. J. & MASFERRER, J. L. 2009. CJ-13610, an orally active inhibitor of 5-lipoxygenase is efficacious in preclinical models of pain. *Eur J Pharmacol,* 617, 59-67.

COUSSENS, L. M. & WERB, Z. 2002. Inflammation and cancer. *Nature,* 420, 860-7.

CUI, Y., DONG, C., WU, B. Q., DUAN, X. C., SHI, G., GONG, M. & WANG, T. Y. 2015. Expression of cyclooxygenase-2, vascular endothelial growth factor, and epidermal growth factor receptor in Chinese patients with esophageal squamous cell carcinoma. *J Cancer Res Ther,* 11 Suppl, c44-8.

DANIEL, T. O., LIU, H., MORROW, J. D., CREWS, B. C. & MARNETT, L. J. 1999. Thromboxane A2 is a mediator of cyclooxygenase-2-dependent endothelial migration and angiogenesis. *Cancer Res,* 59, 4574-7.

DAWSON, S. J., MICHAEL, M., BIAGI, J., FOO, K. F., JEFFORD, M., NGAN, S. Y., LEONG, T., HUI, A., MILNER, A. D., THOMAS, R. J. & ZALCBERG, J. R. 2007. A phase I/II trial of celecoxib with chemotherapy and radiotherapy in the treatment of patients with locally advanced oesophageal cancer. *Invest New Drugs,* 25, 123-9.

DE FALCO, S. 2012. The discovery of placenta growth factor and its biological activity. *Exp Mol Med,* 44, 1-9.

DES GUETZ, G., UZZAN, B., NICOLAS, P., CUCHERAT, M., MORERE, J. F., BENAMOUZIG, R., BREAU, J. L. & PERRET, G. Y. 2006. Microvessel density and VEGF expression are prognostic factors in colorectal cancer. Meta-analysis of the literature. *Br J Cancer,* 94, 1823-32.

DESCHAMPS, J. D., KENYON, V. A. & HOLMAN, T. R. 2006. Baicalein is a potent in vitro inhibitor against both reticulocyte 15-human and platelet 12-human lipoxygenases. *Bioorg Med Chem,* 14, 4295-301.

DEVERY, A. M., WADEKAR, R., BOKOBZA, S. M., WEBER, A. M., JIANG, Y. & RYAN, A. J. 2015. Vascular endothelial growth factor directly stimulates tumour cell proliferation in non-small cell lung cancer. *Int J Oncol.*

DHAKAL, H. P., NAUME, B., SYNNESTVEDT, M., BORGEN, E., KAARESEN, R., SCHLICHTING, E., WIEDSWANG, G., BASSAROVA, A., HOLM, R., GIERCKSKY, K. E. & NESLAND, J. M. 2012. Expression of vascular endothelial growth factor and vascular endothelial growth factor receptors 1 and 2 in invasive breast carcinoma: prognostic significance and relationship with markers for aggressiveness. *Histopathology,* 61, 350-64.

DI GENNARO, A., KENNE, E., WAN, M., SOEHNLEIN, O., LINDBOM, L. & HAEGGSTROM, J. Z. 2009. Leukotriene B4-induced changes in vascular permeability are mediated by

neutrophil release of heparin-binding protein (HBP/CAP37/azurocidin). *FASEB J,* 23, 1750-7.

DI TOMASO, E., LONDON, N., FUJA, D., LOGIE, J., TYRRELL, J. A., KAMOUN, W., MUNN, L. L. & JAIN, R. K. 2009. PDGF-C induces maturation of blood vessels in a model of glioblastoma and attenuates the response to anti-VEGF treatment. *PLoS One,* 4, e5123.

DILLY, A. K., EKAMBARAM, P., GUO, Y., CAI, Y., TUCKER, S. C., FRIDMAN, R., KANDOUZ, M. & HONN, K. V. 2013. Platelet-type 12-lipoxygenase induces MMP9 expression and cellular invasion via activation of PI3K/Akt/NF-kappaB. *Int J Cancer,* 133, 1784-91.

DING, X. Z., IVERSEN, P., CLUCK, M. W., KNEZETIC, J. A. & ADRIAN, T. E. 1999. Lipoxygenase inhibitors abolish proliferation of human pancreatic cancer cells. *Biochem Biophys Res Commun,* 261, 218-23.

DING, X. Z., TONG, W. G. & ADRIAN, T. E. 2003. Multiple signal pathways are involved in the mitogenic effect of 5(S)-HETE in human pancreatic cancer. *Oncology,* 65, 285-94.

DOBRIAN, A. D., LIEB, D. C., MA, Q., LINDSAY, J. W., COLE, B. K., MA, K., CHAKRABARTI, S. K., KUHN, N. S., WOHLGEMUTH, S. D., FONTANA, M. & NADLER, J. L. 2010. Differential expression and localization of 12/15 lipoxygenases in adipose tissue in human obese subjects. *Biochem Biophys Res Commun,* 403, 485-90.

DOYLE, S. L., BENNETT, A. M., DONOHOE, C. L., MONGAN, A. M., HOWARD, J. M., LITHANDER, F. E., PIDGEON, G. P., REYNOLDS, J. V. & LYSAGHT, J. 2013. Establishing computed tomography-defined visceral fat area thresholds for use in obesity-related cancer research. *Nutr Res,* 33, 171-9.

DOYLE, S. L., DONOHOE, C. L., FINN, S. P., HOWARD, J. M., LITHANDER, F. E., REYNOLDS, J. V., PIDGEON, G. P. & LYSAGHT, J. 2012. IGF-1 and its receptor in esophageal cancer: association with adenocarcinoma and visceral obesity. *Am J Gastroenterol,* 107, 196-204.

DRAGOVICH, T., MCCOY, S., FENOGLIO-PREISER, C. M., WANG, J., BENEDETTI, J. K., BAKER, A. F., HACKETT, C. B., URBA, S. G., ZANER, K. S., BLANKE, C. D. & ABBRUZZESE, J. L. 2006. Phase II trial of erlotinib in gastroesophageal junction and gastric adenocarcinomas: SWOG 0127. *J Clin Oncol,* 24, 4922-7.

DRUKER, B. J. 2009. Perspectives on the development of imatinib and the future of cancer research. *Nat Med,* 15, 1149-52.

DU, L., WANG, H., HE, L., ZHANG, J., NI, B., WANG, X., JIN, H., CAHUZAC, N., MEHRPOUR, M., LU, Y. & CHEN, Q. 2008. CD44 is of functional importance for colorectal cancer stem cells. *Clin Cancer Res,* 14, 6751-60.

DUCHARME, Y., BLOUIN, M., BRIDEAU, C., CHATEAUNEUF, A., GAREAU, Y., GRIMM, E. L., JUTEAU, H., LALIBERTE, S., MACKAY, B., MASSE, F., OUELLET, M., SALEM, M., STYHLER, A. & FRIESEN, R. W. 2010. The discovery of setileuton, a potent and selective 5-lipoxygenase inhibitor. *ACS Med Chem Lett,* 1, 170-4.

DUTTON, S. J., FERRY, D. R., BLAZEBY, J. M., ABBAS, H., DAHLE-SMITH, A., MANSOOR, W., THOMPSON, J., HARRISON, M., CHATTERJEE, A., FALK, S., GARCIA-ALONSO, A., FYFE, D. W., HUBNER, R. A., GAMBLE, T., PEACHEY, L., DAVOUDIANFAR, M., PEARSON, S. R., JULIER, P., JANKOWSKI, J., KERR, R. & PETTY, R. D. 2014. Gefitinib for oesophageal cancer progressing after chemotherapy (COG): a phase 3, multicentre, double-blind, placebo-controlled randomised trial. *Lancet Oncol,* 15, 894-904.

DVORAK, H. F. 1986. Tumors: wounds that do not heal. Similarities between tumor stroma generation and wound healing. *N Engl J Med,* 315, 1650-9.

EBERHART, C. E., COFFEY, R. J., RADHIKA, A., GIARDIELLO, F. M., FERRENBACH, S. & DUBOIS, R. N. 1994. Up-regulation of cyclooxygenase 2 gene expression in human colorectal adenomas and adenocarcinomas. *Gastroenterology,* 107, 1183-8.

EL-RAYES, B. F., ZALUPSKI, M., BEKAI-SAAB, T., HEILBRUN, L. K., HAMMAD, N., PATEL, B., URBA, S., SHIELDS, A. F., VAISHAMPAYAN, U., DAWSON, S., ALMHANNA, K., SMITH, D. & PHILIP, P. A. 2010. A phase II study of bevacizumab, oxaliplatin, and docetaxel in locally advanced and metastatic gastric and gastroesophageal junction cancers. *Ann Oncol,* 21, 1999-2004.

ELLIS, L. M. 2006. The role of neuropilins in cancer. *Mol Cancer Ther,* 5, 1099-107.

ENNIS, D. P., PIDGEON, G. P., MILLAR, N., RAVI, N. & REYNOLDS, J. V. 2010. Building a bioresource for esophageal research: lessons from the early experience of an academic medical center. *Dis Esophagus,* 23, 1-7.

ENZINGER, P. C., *ET AL.* 2015. Multicenter phase 2: Capecitabine (CAP) + oxaliplatin (OX) + bevacizumab (BEV) + trastuzumab (TRAS) for patients (pts) with metastatic esophagogastric cancer (MEGCA). *J Clin Oncol 33, 2015 (suppl; abstr 4038, 2015 ASCO Annual Meeting).*

ENZINGER, P. C., MAMON, H., CHOI, N., BUENO, R., KULKE, M. H. & FIDIAS, P., *ET AL.* 2004. Phase II cisplatin, irinotecan, celecoxib and concurrent radiation therapy followed by surgery for locally advanced esophageal cancer. *American Society of Clinical Oncology Chicago, IL, USA, 2004: Abstract 35.*

ENZINGER, P. C., RYAN, D. P., REGAN, E. M., LEHMAN, N., ABRAMS, T. A., HEZEL, A. F., FIDIAS, P., SEQUIST, L. V., BLASZKOWSKY, L. S. & AND FUCHS, C. S. 2008. Phase II trial of docetaxel, cisplatin, irinotecan, and bevacizumab in metastatic esophagogastric cancer [abstract 97]. *J Clin Oncol (Meeting Abstracts) May 2008 vol. 26 no. 15_suppl 4552.*

ERGIN, V., YILMAZ, A., CELENK, F., USLU, S., ILERI, F. & MENEVSE, A. 2012. [The role of COX-2, ALOX12 and iNOS genes in nasal polyposis]. *Kulak Burun Bogaz Ihtis Derg,* 22, 254-8.

ESCUDIER, B., PLUZANSKA, A., KORALEWSKI, P., RAVAUD, A., BRACARDA, S., SZCZYLIK, C., CHEVREAU, C., FILIPEK, M., MELICHAR, B., BAJETTA, E., GORBUNOVA, V., BAY, J. O., BODROGI, I., JAGIELLO-GRUSZFELD, A. & MOORE, N. 2007. Bevacizumab plus interferon alfa-2a for treatment of metastatic renal cell carcinoma: a randomised, double-blind phase III trial. *Lancet,* 370, 2103-11.

EVANS, J. F., FERGUSON, A. D., MOSLEY, R. T. & HUTCHINSON, J. H. 2008. What's all the FLAP about?: 5-lipoxygenase-activating protein inhibitors for inflammatory diseases. *Trends Pharmacol Sci,* 29, 72-8.

FAIVRE, S., DELBALDO, C., VERA, K., ROBERT, C., LOZAHIC, S., LASSAU, N., BELLO, C., DEPRIMO, S., BREGA, N., MASSIMINI, G., ARMAND, J. P., SCIGALLA, P. & RAYMOND, E. 2006. Safety, pharmacokinetic, and antitumor activity of SU11248, a novel oral multitarget tyrosine kinase inhibitor, in patients with cancer. *J Clin Oncol,* 24, 25-35.

FAN, F., WEY, J. S., MCCARTY, M. F., BELCHEVA, A., LIU, W., BAUER, T. W., SOMCIO, R. J., WU, Y., HOOPER, A., HICKLIN, D. J. & ELLIS, L. M. 2005. Expression and function of vascular endothelial growth factor receptor-1 on human colorectal cancer cells. *Oncogene,* 24, 2647-53.

FEINMARK, S. J. & CANNON, P. J. 1986. Endothelial cell leukotriene C4 synthesis results from intercellular transfer of leukotriene A4 synthesized by polymorphonuclear leukocytes. *J Biol Chem,* 261, 16466-72.

FERLAY, J., SHIN, H. R., BRAY, F., FORMAN, D., MATHERS, C. & PARKIN, D. M. 2010. Estimates of worldwide burden of cancer in 2008: GLOBOCAN 2008. *Int J Cancer,* 127, 2893-917.

FERLAY J, S. I., ERVIK M, DIKSHIT R, ESER S, MATHERS C, REBELO M, PARKIN DM, FORMAN D, BRAY, F. 2012. GLOBOCAN 2012 v1.0, Cancer Incidence and Mortality Worldwide. *IARC CancerBase No. 11 [Internet].*

Lyon, France: International Agency for Research on Cancer; 2013. Available from: http://globocan.iarc.fr, accessed on 23/07/2015.

FERRARA, N., GERBER, H. P. & LECOUTER, J. 2003. The biology of VEGF and its receptors. *Nat Med,* 9, 669-76.

FILLIES, T., WERKMEISTER, R., PACKEISEN, J., BRANDT, B., MORIN, P., WEINGART, D., JOOS, U. & BUERGER, H. 2006. Cytokeratin 8/18 expression indicates a poor prognosis in squamous cell carcinomas of the oral cavity. *BMC Cancer,* 6, 10.

FISCHER, A. S., METZNER, J., STEINBRINK, S. D., ULRICH, S., ANGIONI, C., GEISSLINGER, G., STEINHILBER, D. & MAIER, T. J. 2010. 5-Lipoxygenase inhibitors induce potent anti-proliferative and cytotoxic effects in human tumour cells independently of suppression of 5-lipoxygenase activity. *Br J Pharmacol,* 161, 936-49.

FISCHER, L., HORNIG, M., PERGOLA, C., MEINDL, N., FRANKE, L., TANRIKULU, Y., DODT, G., SCHNEIDER, G., STEINHILBER, D. & WERZ, O. 2007. The molecular mechanism of the inhibition by licofelone of the biosynthesis of 5-lipoxygenase products. *Br J Pharmacol,* 152, 471-80.

FITZGERALD, R. C., DI PIETRO, M., RAGUNATH, K., ANG, Y., KANG, J. Y., WATSON, P., TRUDGILL, N., PATEL, P., KAYE, P. V., SANDERS, S., O'DONOVAN, M., BIRD-LIEBERMAN, E., BHANDARI, P., JANKOWSKI, J. A., ATTWOOD, S., PARSONS, S.

L., LOFT, D., LAGERGREN, J., MOAYYEDI, P., LYRATZOPOULOS, G. & DE CAESTECKER, J. 2014. British Society of Gastroenterology guidelines on the diagnosis and management of Barrett's oesophagus. *Gut,* 63, 7-42.

FLAHERTY, K. T., PUZANOV, I., KIM, K. B., RIBAS, A., MCARTHUR, G. A., SOSMAN, J. A., O'DWYER, P. J., LEE, R. J., GRIPPO, J. F., NOLOP, K. & CHAPMAN, P. B. 2010. Inhibition of mutated, activated BRAF in metastatic melanoma. *N Engl J Med,* 363, 809-19.

FOLCO, G. & MURPHY, R. C. 2006. Eicosanoid transcellular biosynthesis: from cell-cell interactions to in vivo tissue responses. *Pharmacol Rev,* 58, 375-88.

FOLKMAN, J. 1971. Tumor angiogenesis: therapeutic implications. *N Engl J Med,* 285, 1182-6.

FOLKMAN, J. 1995. Angiogenesis in cancer, vascular, rheumatoid and other disease. *Nat Med,* 1, 27-31.

FRIEDMAN, H. S., PRADOS, M. D., WEN, P. Y., MIKKELSEN, T., SCHIFF, D., ABREY, L. E., YUNG, W. K., PALEOLOGOS, N., NICHOLAS, M. K., JENSEN, R., VREDENBURGH, J., HUANG, J., ZHENG, M. & CLOUGHESY, T. 2009. Bevacizumab alone and in combination with irinotecan in recurrent glioblastoma. *J Clin Oncol,* 27, 4733-40.

FUCHS, C. S., TOMASEK, J., YONG, C. J., DUMITRU, F., PASSALACQUA, R., GOSWAMI, C., SAFRAN, H., DOS SANTOS, L. V., APRILE, G., FERRY, D. R., MELICHAR, B., TEHFE, M., TOPUZOV, E., ZALCBERG, J. R., CHAU, I., CAMPBELL, W., SIVANANDAN, C., PIKIEL, J., KOSHIJI, M., HSU, Y., LIEPA, A. M., GAO, L., SCHWARTZ, J. D. & TABERNERO, J. 2014. Ramucirumab monotherapy for previously treated advanced gastric or gastro-oesophageal junction adenocarcinoma (REGARD): an international, randomised, multicentre, placebo-controlled, phase 3 trial. *Lancet,* 383, 31-9.

FUJISAWA, N., HAYASHI, S., KURDOWSKA, A., CARR, F. K. & MILLER, E. J. 1999. Inhibition of GROalpha-induced human endothelial cell proliferation by the alpha-chemokine inhibitor antileukinate. *Cytokine,* 11, 231-8.

FUNK, C. D., FUNK, L. B., FITZGERALD, G. A. & SAMUELSSON, B. 1992. Characterization of human 12-lipoxygenase genes. *Proc Natl Acad Sci U S A,* 89, 3962-6.

GAKIOPOULOU-GIVALOU, H., NAKOPOULOU, L., PANAYOTOPOULOU, E. G., ZERVAS, A., MAVROMMATIS, J. & GIANNOPOULOS, A. 2003. Non-endothelial KDR/flk-1 expression is associated with increased survival of patients with urothelial bladder carcinomas. *Histopathology,* 43, 272-9.

GANESH, R., MARKS, D. J., SALES, K., WINSLET, M. C. & SEIFALIAN, A. M. 2012. Cyclooxygenase/lipoxygenase shunting lowers the anti-cancer effect of cyclooxygenase-2 inhibition in colorectal cancer cells. *World J Surg Oncol,* 10, 200.

GAO, X., GRIGNON, D. J., CHBIHI, T., ZACHAREK, A., CHEN, Y. Q., SAKR, W., PORTER, A. T., CRISSMAN, J. D., PONTES, J. E., POWELL, I. J. & *ET AL.* 1995. Elevated 12-lipoxygenase mRNA expression correlates with advanced stage and poor differentiation of human prostate cancer. *Urology,* 46, 227-37.

GASPARINI, G. 2000. Prognostic value of vascular endothelial growth factor in breast cancer. *Oncologist,* 5 Suppl 1, 37-44.

GATELY, S. & LI, W. W. 2004. Multiple roles of COX-2 in tumor angiogenesis: a target for antiangiogenic therapy. *Semin Oncol,* 31, 2-11.

GEH, J. I., CRELLIN, A. M. & GLYNNE-JONES, R. 2001. Preoperative (neoadjuvant) chemoradiotherapy in oesophageal cancer. *Br J Surg,* 88, 338-56.

GENENTECH INC. 2011. Avastin [package insert]. *In:* GENENTECH, I. S. S. F., CA (ed.).

GHANEM, M. A., VAN STEENBRUGGE, G. J., SUDARYO, M. K., MATHOERA, R. B., NIJMAN, J. M. & VAN DER KWAST, T. H. 2003. Expression and prognostic relevance of vascular endothelial growth factor (VEGF) and its receptor (FLT-1) in nephroblastoma. *J Clin Pathol,* 56, 107-13.

GHOSH, J. & MYERS, C. E. 1998. Inhibition of arachidonate 5-lipoxygenase triggers massive apoptosis in human prostate cancer cells. *Proc Natl Acad Sci U S A,* 95, 13182-7.

GIANTONIO, B. J., CATALANO, P. J., MEROPOL, N. J., O'DWYER, P. J., MITCHELL, E. P., ALBERTS, S. R., SCHWARTZ, M. A. & BENSON, A. B., 3RD 2007. Bevacizumab in combination with oxaliplatin, fluorouracil, and leucovorin (FOLFOX4) for previously treated metastatic colorectal cancer: results from the Eastern Cooperative Oncology Group Study E3200. *J Clin Oncol,* 25, 1539-44.

GOHARA, A., ELTAKI, N., SABRY, D., MURTAGH, D., JR., JANKUN, J., SELMAN, S. H. & SKRZYPCZAK-JANKUN, E. 2012. Human 5-, 12- and 15-lipoxygenase-1 coexist in

kidney but show opposite trends and their balance changes in cancer. *Oncol Rep,* 28, 1275-82.

GOLD, P. J., GOLDMAN, B., IQBAL, S., LEICHMAN, L. P., ZHANG, W., LENZ, H. J. & BLANKE, C. D. 2010. Cetuximab as second-line therapy in patients with metastatic esophageal adenocarcinoma: a phase II Southwest Oncology Group Study (S0415). *J Thorac Oncol,* 5, 1472-6.

GONDEK, T., SZAJEWSKI, M., SZEFEL, J., ALEKSANDROWICZ-WRONA, E., SKRZYPCZAK-JANKUN, E., JANKUN, J. & LYSIAK-SZYDLOWSKA, W. 2014. Evaluation of 12-lipoxygenase (12-LOX) and plasminogen activator inhibitor 1 (PAI-1) as prognostic markers in prostate cancer. *Biomed Res Int,* 2014, 102478.

GOODWIN, A. M. 2007. In vitro assays of angiogenesis for assessment of angiogenic and anti-angiogenic agents. *Microvasc Res,* 74, 172-83.

GOUNARIS, E., ERDMAN, S. E., RESTAINO, C., GURISH, M. F., FRIEND, D. S., GOUNARI, F., LEE, D. M., ZHANG, G., GLICKMAN, J. N., SHIN, K., RAO, V. P., POUTAHIDIS, T., WEISSLEDER, R., MCNAGNY, K. M. & KHAZAIE, K. 2007. Mast cells are an essential hematopoietic component for polyp development. *Proceedings of the National Academy of Sciences,* 104, 19977-19982.

GOUNARIS, E., HEIFERMAN, M. J., HEIFERMAN, J. R., SHRIVASTAV, M., VITELLO, D., BLATNER, N. R., KNAB, L. M., PHILLIPS, J. D., CHEON, E. C., GRIPPO, P. J., KHAZAIE, K., MUNSHI, H. G. & BENTREM, D. J. 2015. Zileuton, 5-lipoxygenase inhibitor, acts as a chemopreventive agent in intestinal polyposis, by modulating polyp and systemic inflammation. *PLoS One,* 10, e0121402.

GOVINDAN, R., MCLEOD, H., MANTRAVADI, P., FINEBERG, N., HELFT, P., KESLER, K., HANNA, N., STONER, C., ANSARI, R. & FOX, E. 2004. Cisplatin, fluorouracil, celecoxib, and RT in resectable esophageal cancer: preliminary results. *Oncology (Williston Park),* 18, 18-21.

GREENE, E. R., HUANG, S., SERHAN, C. N. & PANIGRAHY, D. 2011. Regulation of inflammation in cancer by eicosanoids. *Prostaglandins Other Lipid Mediat,* 96, 27-36.

GUIU, B., PETIT, J. M., BONNETAIN, F., LADOIRE, S., GUIU, S., CERCUEIL, J. P., KRAUSE, D., HILLON, P., BORG, C., CHAUFFERT, B. & GHIRINGHELLI, F. 2010. Visceral fat area is an independent predictive biomarker of outcome after first-line bevacizumab-based treatment in metastatic colorectal cancer. *Gut,* 59, 341-7.

GUO, C. A. N., D. 2012. Are Lipoxygenases Valid Targets of Cancer Prevention and Treatment? *J Carcinogen Mutagen 2012, S1.*

GUO, P., FANG, Q., TAO, H. Q., SCHAFER, C. A., FENTON, B. M., DING, I., HU, B. & CHENG, S. Y. 2003. Overexpression of vascular endothelial growth factor by MCF-7 breast cancer cells promotes estrogen-independent tumor growth in vivo. *Cancer Res,* 63, 4684-91.

GUO, Y. & NIE, D. 2014. Tumor-suppressing 15-lipoxygenase-2: time for prime time? *Cell Cycle,* 13, 1836-7.

GUO, Y., WANG, X., ZHANG, X., SUN, Z. & CHEN, X. 2011. Ethanol promotes chemically induced oral cancer in mice through activation of the 5-lipoxygenase pathway of arachidonic acid metabolism. *Cancer Prev Res (Phila),* 4, 1863-72.

GUO, Y., ZHANG, X., TAN, W., MIAO, X., SUN, T., ZHAO, D. & LIN, D. 2007. Platelet 12-lipoxygenase Arg261Gln polymorphism: functional characterization and association with risk of esophageal squamous cell carcinoma in combination with COX-2 polymorphisms. *Pharmacogenet Genomics,* 17, 197-205.

GUPTA, S., SRIVASTAVA, M., AHMAD, N., SAKAMOTO, K., BOSTWICK, D. G. & MUKHTAR, H. 2001. Lipoxygenase-5 is overexpressed in prostate adenocarcinoma. *Cancer,* 91, 737-43.

GURIEC, N., LE JOSSIC-CORCOS, C., SIMON, B., IANOTTO, J. C., TEMPESCUL, A., DREANO, Y., SALAUN, J. P., BERTHOU, C. & CORCOS, L. 2014. The arachidonic acid-LTB4-BLT2 pathway enhances human B-CLL aggressiveness. *Biochim Biophys Acta,* 1842, 2096-105.

HAAS, U., RASCHPERGER, E., HAMBERG, M., SAMUELSSON, B., TRYGGVASON, K. & HAEGGSTROM, J. Z. 2011. Targeted knock-down of a structurally atypical zebrafish 12S-lipoxygenase leads to severe impairment of embryonic development. *Proc Natl Acad Sci U S A,* 108, 20479-84.

HAGMANN, W., KAGAWA, D., RENAUD, C. & HONN, K. V. 1993. Activity and protein distribution of 12-lipoxygenase in HEL cells: induction of membrane-association by

phorbol ester TPA, modulation of activity by glutathione and 13-HPODE, and Ca(2+)-dependent translocation to membranes. *Prostaglandins,* 46, 471-7.
HANAHAN, D. & WEINBERG, R. A. 2000. The hallmarks of cancer. *Cell,* 100, 57-70.
HANAHAN, D. & WEINBERG, R. A. 2011. Hallmarks of cancer: the next generation. *Cell,* 144, 646-74.
HANAWA, M., SUZUKI, S., DOBASHI, Y., YAMANE, T., KONO, K., ENOMOTO, N. & OOI, A. 2006. EGFR protein overexpression and gene amplification in squamous cell carcinomas of the esophagus. *Int J Cancer,* 118, 1173-80.
HARRIS, R. R., CARTER, G. W., BELL, R. L., MOORE, J. L. & BROOKS, D. W. 1995. Clinical activity of leukotriene inhibitors. *Int J Immunopharmacol,* 17, 147-56.
HARVEY, J. M., CLARK, G. M., OSBORNE, C. K. & ALLRED, D. C. 1999. Estrogen receptor status by immunohistochemistry is superior to the ligand-binding assay for predicting response to adjuvant endocrine therapy in breast cancer. *J Clin Oncol,* 17, 1474-81.
HASHIMOTO, N., INAYAMA, M., FUJISHIMA, M. & SHIOZAKI, H. 2007. Clinicopathologic significance of expression of cyclooxygenase-2 in human esophageal squamous cell carcinoma. *Hepatogastroenterology,* 54, 758-60.
HASHIZUME, H., FALCON, B. L., KURODA, T., BALUK, P., COXON, A., YU, D., BREADY, J. V., OLINER, J. D. & MCDONALD, D. M. 2010. Complementary actions of inhibitors of angiopoietin-2 and VEGF on tumor angiogenesis and growth. *Cancer Res,* 70, 2213-23.
HECHT, J. R., TRARBACH, T., HAINSWORTH, J. D., MAJOR, P., JAGER, E., WOLFF, R. A., LLOYD-SALVANT, K., BODOKY, G., PENDERGRASS, K., BERG, W., CHEN, B. L., JALAVA, T., MEINHARDT, G., LAURENT, D., LEBWOHL, D. & KERR, D. 2011. Randomized, placebo-controlled, phase III study of first-line oxaliplatin-based chemotherapy plus PTK787/ZK 222584, an oral vascular endothelial growth factor receptor inhibitor, in patients with metastatic colorectal adenocarcinoma. *J Clin Oncol,* 29, 1997-2003.
HEGDE, P.S., JUBB, A.M., CHEN, D., LI, N.F., MENG, G.Y., BERNAARDS, C., ELLIOTT, R., SCHERER, S.J. & CHEN D.S. 2014. Predictive Impact of Circulating Vascular Endothelial Growth Factor in Four Phase III Trials Evaluating Bevacizumab. *Clin Cancer Res*, 19, 929-37.
HENNIG, R., DING, X. Z., TONG, W. G., SCHNEIDER, M. B., STANDOP, J., FRIESS, H., BUCHLER, M. W., POUR, P. M. & ADRIAN, T. E. 2002. 5-Lipoxygenase and leukotriene B(4) receptor are expressed in human pancreatic cancers but not in pancreatic ducts in normal tissue. *Am J Pathol,* 161, 421-8.
HENNIG, R., GRIPPO, P., DING, X. Z., RAO, S. M., BUCHLER, M. W., FRIESS, H., TALAMONTI, M. S., BELL, R. H. & ADRIAN, T. E. 2005a. 5-Lipoxygenase, a marker for early pancreatic intraepithelial neoplastic lesions. *Cancer Res,* 65, 6011-6.
HENNIG, R., KEHL, T., NOOR, S., DING, X. Z., RAO, S. M., BERGMANN, F., FURSTENBERGER, G., BUCHLER, M. W., FRIESS, H., KRIEG, P. & ADRIAN, T. E. 2007a. 15-lipoxygenase-1 production is lost in pancreatic cancer and overexpression of the gene inhibits tumor cell growth. *Neoplasia,* 9, 917-26.
HENNIG, R., KEHL, T., NOOR, S., DING, X. Z., RAO, S. M., BERGMANN, F., FÜRSTENBERGER, G., BÜCHLER, M. W., FRIESS, H., KRIEG, P. & ADRIAN, T. E. 2007b. 15-Lipoxygenase-1 Production is Lost in Pancreatic Cancer and Overexpression of the Gene Inhibits Tumor Cell Growth. *Neoplasia,* 9, 917-26.
HENNIG, R., VENTURA, J., SEGERSVARD, R., WARD, E., DING, X. Z., RAO, S. M., JOVANOVIC, B. D., IWAMURA, T., TALAMONTI, M. S., BELL, R. H., JR. & ADRIAN, T. E. 2005b. LY293111 improves efficacy of gemcitabine therapy on pancreatic cancer in a fluorescent orthotopic model in athymic mice. *Neoplasia,* 7, 417-25.
HERRERA, L. J., EL-HEFNAWY, T., QUEIROZ DE OLIVEIRA, P. E., RAJA, S., FINKELSTEIN, S., GOODING, W., LUKETICH, J. D., GODFREY, T. E. & HUGHES, S. J. 2005. The HGF Receptor c-Met Is Overexpressed in Esophageal Adenocarcinoma. *Neoplasia,* 7, 75-84.
HIRASHIMA, K., BABA, Y., WATANABE, M., KARASHIMA, R., SATO, N., IMAMURA, Y., HIYOSHI, Y., NAGAI, Y., HAYASHI, N., IYAMA, K. & BABA, H. 2010. Phosphorylated mTOR expression is associated with poor prognosis for patients with esophageal squamous cell carcinoma. *Ann Surg Oncol,* 17, 2486-93.
HOELDER, S., CLARKE, P. A. & WORKMAN, P. 2012. Discovery of small molecule cancer drugs: Successes, challenges and opportunities. *Mol Oncol,* 6, 155-76.

HOOBLER, E. K., RAI, G., WARRILOW, A. G., PERRY, S. C., SMYRNIOTIS, C. J., JADHAV, A., SIMEONOV, A., PARKER, J. E., KELLY, D. E., MALONEY, D. J., KELLY, S. L. & HOLMAN, T. R. 2013. Discovery of a novel dual fungal CYP51/human 5-lipoxygenase inhibitor: implications for anti-fungal therapy. *PLoS One,* 8, e65928.

HOQUE, A., LIPPMAN, S. M., WU, T. T., XU, Y., LIANG, Z. D., SWISHER, S., ZHANG, H., CAO, L., AJANI, J. A. & XU, X. C. 2005. Increased 5-lipoxygenase expression and induction of apoptosis by its inhibitors in esophageal cancer: a potential target for prevention. *Carcinogenesis,* 26, 785-91.

HORRILLO, R., GONZALEZ-PERIZ, A., MARTINEZ-CLEMENTE, M., LOPEZ-PARRA, M., FERRE, N., TITOS, E., MORAN-SALVADOR, E., DEULOFEU, R., ARROYO, V. & CLARIA, J. 2010. 5-lipoxygenase activating protein signals adipose tissue inflammation and lipid dysfunction in experimental obesity. *J Immunol,* 184, 3978-87.

HOWLADER N, N. A., KRAPCHO M, GARSHELL J, NEYMAN N, ALTEKRUSE SF, KOSARY CL, YU M, RUHL J, TATALOVICH Z, CHO H, MARIOTTO A, LEWIS DR, CHEN HS, FEUER EJ, CRONIN KA (EDS). 2012. SEER Cancer Statistics Review. National Cancer Institute. Bethesda, MD, http://seer.cancer.gov/csr/1975_2010/, based on November 2012 SEER data submission, posted to the SEER web site, April 2013.

HUANG, D., DING, Y., ZHOU, M., RINI, B. I., PETILLO, D., QIAN, C. N., KAHNOSKI, R., FUTREAL, P. A., FURGE, K. A. & TEH, B. T. 2010. Interleukin-8 mediates resistance to antiangiogenic agent sunitinib in renal cell carcinoma. *Cancer Res,* 70, 1063-71.

HUANG, J., BAE, J. O., TSAI, J. P., KADENHE-CHIWESHE, A., PAPA, J., LEE, A., ZENG, S., KORNFELD, Z. N., ULLNER, P., ZAGHLOUL, N., IOFFE, E., NANDOR, S., BUROVA, E., HOLASH, J., THURSTON, G., RUDGE, J., YANCOPOULOS, G. D., YAMASHIRO, D. J. & KANDEL, J. J. 2009. Angiopoietin-1/Tie-2 activation contributes to vascular survival and tumor growth during VEGF blockade. *Int J Oncol,* 34, 79-87.

HUANG, Y. J., QI, W. X., HE, A. N., SUN, Y. J., SHEN, Z. & YAO, Y. 2013. Prognostic value of tissue vascular endothelial growth factor expression in bladder cancer: a meta-analysis. *Asian Pac J Cancer Prev,* 14, 645-9.

HURWITZ, H., FEHRENBACHER, L., NOVOTNY, W., CARTWRIGHT, T., HAINSWORTH, J., HEIM, W., BERLIN, J., BARON, A., GRIFFING, S., HOLMGREN, E., FERRARA, N., FYFE, G., ROGERS, B., ROSS, R. & KABBINAVAR, F. 2004. Bevacizumab plus irinotecan, fluorouracil, and leucovorin for metastatic colorectal cancer. *N Engl J Med,* 350, 2335-42.

HUSSAIN, H., SHORNICK, L. P., SHANNON, V. R., WILSON, J. D., FUNK, C. D., PENTLAND, A. P. & HOLTZMAN, M. J. 1994. Epidermis contains platelet-type 12-lipoxygenase that is overexpressed in germinal layer keratinocytes in psoriasis. *Am J Physiol,* 266, C243-53.

HWANG, C. & HEATH, E. I. 2010. Angiogenesis inhibitors in the treatment of prostate cancer. *J Hematol Oncol,* 3, 26.

HWANG, J., J., , IYER, R., V., & MULLIGAN, M. 2014. Cancer Management, Esophageal Cancer. - *See more at: http://www.cancernetwork.com/esophageal-cancer/page/2/0?gid=All&domain_id=All#sthash.X8TtFqiy.dpuf.*

IDELEVICH, E., KASHTAN, H., KLEIN, Y., BUEVICH, V., BARUCH, N. B., DINERMAN, M., TOKAR, M., KUNDEL, Y. & BRENNER, B. 2012. Prospective phase II study of neoadjuvant therapy with cisplatin, 5-fluorouracil, and bevacizumab for locally advanced resectable esophageal cancer. *Onkologie,* 35, 427-31.

IKEGUCHI, M., MAETA, M. & KAIBARA, N. 2001. Bax expression as a prognostic marker of postoperative chemoradiotherapy for patients with esophageal cancer. *Int J Mol Med,* 7, 413-7.

IMDAHL, A., BOGNAR, G., SCHULTE-MONTING, J., SCHOFFEL, U., FARTHMANN, E. H. & IHLING, C. 2002. Predictive factors for response to neoadjuvant therapy in patients with oesophageal cancer. *Eur J Cardiothorac Surg,* 21, 657-63.

IZZEDINE, H., MASSARD, C., SPANO, J.P., GOLDWASSER, F., KHAYAT, D. & SORIA, J.C. 2010. VEGF signalling inhibition-induced proteinuria: Mechanisms, significance and management. *Eur J Cancer,* 46, 439-48.

IZZO, J. G., MALHOTRA, U., WU, T. T., ENSOR, J., LUTHRA, R., LEE, J. H., SWISHER, S. G., LIAO, Z., CHAO, K. S., HITTELMAN, W. N., AGGARWAL, B. B. & AJANI, J. A. 2006. Association of activated transcription factor nuclear factor kappab with chemoradiation resistance and poor outcome in esophageal carcinoma. *J Clin Oncol,* 24, 748-54.

JACKSON, S. E. & CHESTER, J. D. 2015. Personalised cancer medicine. *Int J Cancer,* 137, 262-6.
JAIN, R. K. 2005. Normalization of tumor vasculature: an emerging concept in antiangiogenic therapy. *Science,* 307, 58-62.
JANKOWSKI, J. A. 2012. Aspirin Chemoprevention in Barrett Esophagus: Is the Risk Worth the Benefit? *Gastroenterol Hepatol (N Y),* 8, 831-3.
JANKUN, J., ALEEM, A. M., MALGORZEWICZ, S., SZKUDLAREK, M., ZAVODSZKY, M. I., DEWITT, D. L., FEIG, M., SELMAN, S. H. & SKRZYPCZAK-JANKUN, E. 2006. Synthetic curcuminoids modulate the arachidonic acid metabolism of human platelet 12-lipoxygenase and reduce sprout formation of human endothelial cells. *Mol Cancer Ther,* 5, 1371-82.
JAŒKIEWICZ, K., IŻYCKA-ŒWIESZEWSKA, E., JANIAK, M., ŁYSIAK-SZYDŁOWSKA, W., ADRYCH, K., REINARTZ, J., JANKUN, J. & SKRZYPCZAK-JANKUN, E. 2010. Platelet 12-lipoxygenase and stem cells in Barrett's esophagus. *Oncol Lett,* 1, 789-91.
JARDIM, D. L., DE MELO GAGLIATO, D., FALCHOOK, G. S., JANKU, F., ZINNER, R., WHELER, J. J., SUBBIAH, V., PIHA-PAUL, S. A., FU, S., MURPHY, M. B., AJANI, J., TANG, C., HESS, K., HAMILTON, S. R., ROY-CHOWDHURI, S., KURZROCK, R., MERIC-BERNSTAM, F. & HONG, D. S. 2014. MET aberrations and c-MET inhibitors in patients with gastric and esophageal cancers in a phase I unit. *Oncotarget,* 5, 1837-45.
JIANG, W. G., DOUGLAS-JONES, A. & MANSEL, R. E. 2003. Levels of expression of lipoxygenases and cyclooxygenase-2 in human breast cancer. *Prostaglandins Leukot Essent Fatty Acids,* 69, 275-81.
JIANG, W. G., DOUGLAS-JONES, A. G. & MANSEL, R. E. 2006a. Aberrant expression of 5-lipoxygenase-activating protein (5-LOXAP) has prognostic and survival significance in patients with breast cancer. *Prostaglandins Leukot Essent Fatty Acids,* 74, 125-34.
JIANG, W. G., WATKINS, G., DOUGLAS-JONES, A. & MANSEL, R. E. 2006b. Reduction of isoforms of 15-lipoxygenase (15-LOX)-1 and 15-LOX-2 in human breast cancer. *Prostaglandins Leukot Essent Fatty Acids,* 74, 235-45.
JOSHI, Y. B. & PRATICO, D. 2014. The 5-lipoxygenase pathway: oxidative and inflammatory contributions to the Alzheimer's disease phenotype. *Front Cell Neurosci,* 8, 436.
KAAMAN, M., RYDEN, M., AXELSSON, T., NORDSTROM, E., SICARD, A., BOULOUMIE, A., LANGIN, D., ARNER, P. & DAHLMAN, I. 2006. ALOX5AP expression, but not gene haplotypes, is associated with obesity and insulin resistance. *Int J Obes (Lond),* 30, 447-52.
KAMANGAR, F., CHOW, W. H., ABNET, C. C. & DAWSEY, S. M. 2009. Environmental causes of esophageal cancer. *Gastroenterol Clin North Am,* 38, 27-57, vii.
KANAOKA, Y. & BOYCE, J. A. 2004. Cysteinyl leukotrienes and their receptors: cellular distribution and function in immune and inflammatory responses. *J Immunol,* 173, 1503-10.
KANG Y, O. A., VAN CUTSEM E, *ET AL.* 2010. AVAGAST: A randomized, double-blind, placebo-controlled, phase III study of first-line capecitabine and cisplatin plus bevacizumab or placebo in patients with advanced gastric cancer (AGC) *J Clin Oncol;28 18 suppl:950S.*
KELAVKAR, U. P. & COHEN, C. 2004. 15-lipoxygenase-1 expression upregulates and activates insulin-like growth factor-1 receptor in prostate cancer cells. *Neoplasia,* 6, 41-52.
KELAVKAR, U. P., NIXON, J. B., COHEN, C., DILLEHAY, D., ELING, T. E. & BADR, K. F. 2001. Overexpression of 15-lipoxygenase-1 in PC-3 human prostate cancer cells increases tumorigenesis. *Carcinogenesis,* 22, 1765-73.
KENYON, V., RAI, G., JADHAV, A., SCHULTZ, L., ARMSTRONG, M., JAMESON, J. B., 2ND, PERRY, S., JOSHI, N., BOUGIE, J. M., LEISTER, W., TAYLOR-FISHWICK, D. A., NADLER, J. L., HOLINSTAT, M., SIMEONOV, A., MALONEY, D. J. & HOLMAN, T. R. 2011. Discovery of potent and selective inhibitors of human platelet-type 12-lipoxygenase. *J Med Chem,* 54, 5485-97.
KHAN, R., SPAGNOLI, V., TARDIF, J. C. & L'ALLIER, P. L. 2015. Novel anti-inflammatory therapies for the treatment of atherosclerosis. *Atherosclerosis,* 240, 497-509.
KHURANA, R., SIMONS, M., MARTIN, J. F. & ZACHARY, I. C. 2005. Role of angiogenesis in cardiovascular disease: a critical appraisal. *Circulation,* 112, 1813-24.
KILFEATHER, S. 2002. 5-lipoxygenase inhibitors for the treatment of COPD. *Chest,* 121, 197S-200S.

KIM, D. W., LU, B. & HALLAHAN, D. E. 2004. Receptor tyrosine kinase inhibitors as anti-angiogenic agents. *Curr Opin Investig Drugs,* 5, 597-604.

KIM, G. Y., LEE, J. W., CHO, S. H., SEO, J. M. & KIM, J. H. 2009. Role of the low-affinity leukotriene B4 receptor BLT2 in VEGF-induced angiogenesis. *Arterioscler Thromb Vasc Biol,* 29, 915-20.

KIM, H. S., MOON, H. G., HAN, W., YOM, C. K., KIM, W. H., KIM, J. H. & NOH, D. Y. 2012. COX2 overexpression is a prognostic marker for Stage III breast cancer. *Breast Cancer Res Treat,* 132, 51-9.

KIM, M. A., LEE, H. S., LEE, H. E., JEON, Y. K., YANG, H. K. & KIM, W. H. 2008. EGFR in gastric carcinomas: prognostic significance of protein overexpression and high gene copy number. *Histopathology,* 52, 738-46.

KLAMPFL, T., BOGNER, E., BEDNAR, W., MAGER, L., MASSUDOM, D., KALNY, I., HEINZLE, C., BERGER, W., STÄTTNER, S., KARNER, J., KLIMPFINGER, M., FÜRSTENBERGER, G., KRIEG, P. & MARIAN, B. 2012. Up-regulation of 12(S)-lipoxygenase induces a migratory phenotype in colorectal cancer cells. *Experimental Cell Research,* 318, 768-778.

KLASA-MAZURKIEWICZ, D., JARZAB, M., MILCZEK, T., LIPINSKA, B. & EMERICH, J. 2011. Clinical significance of VEGFR-2 and VEGFR-3 expression in ovarian cancer patients. *Pol J Pathol,* 62, 31-40.

KLENKE, F. M., GEBHARD, M. M., EWERBECK, V., ABDOLLAHI, A., HUBER, P. E. & SCKELL, A. 2006. The selective Cox-2 inhibitor Celecoxib suppresses angiogenesis and growth of secondary bone tumors: An intravital microscopy study in mice. *BMC Cancer,* 6, 9.

KLIL-DRORI, A. J. & ARIEL, A. 2013. 15-Lipoxygenases in cancer: A double-edged sword? *Prostaglandins Other Lipid Mediat,* 106, 16-22.

KNAB, L. M., GRIPPO, P. J. & BENTREM, D. J. 2014. Involvement of eicosanoids in the pathogenesis of pancreatic cancer: The roles of cyclooxygenase-2 and 5-lipoxygenase. *World J Gastroenterol,* 20, 10729-10739.

KNORR, B., MATZ, J., BERNSTEIN, J. A., NGUYEN, H., SEIDENBERG, B. C., REISS, T. F. & BECKER, A. 1998. Montelukast for chronic asthma in 6- to 14-year-old children: a randomized, double-blind trial. Pediatric Montelukast Study Group. *JAMA,* 279, 1181-6.

KOH, Y. J., KIM, H. Z., HWANG, S. I., LEE, J. E., OH, N., JUNG, K., KIM, M., KIM, K. E., KIM, H., LIM, N. K., JEON, C. J., LEE, G. M., JEON, B. H., NAM, D. H., SUNG, H. K., NAGY, A., YOO, O. J. & KOH, G. Y. 2010. Double antiangiogenic protein, DAAP, targeting VEGF-A and angiopoietins in tumor angiogenesis, metastasis, and vascular leakage. *Cancer Cell,* 18, 171-84.

KOZLOWSKI, M., LAUDANSKI, W., MROCZKO, B., SZMITKOWSKI, M., MILEWSKI, R. & LAPUC, G. 2013. Serum tissue inhibitor of metalloproteinase 1 (TIMP-1) and vascular endothelial growth factor A (VEGF-A) are associated with prognosis in esophageal cancer patients. *Adv Med Sci,* 58, 227-34.

KREISL, T. N., KIM, L., MOORE, K., DUIC, P., ROYCE, C., STROUD, I., GARREN, N., MACKEY, M., BUTMAN, J. A., CAMPHAUSEN, K., PARK, J., ALBERT, P. S. & FINE, H. A. 2009. Phase II trial of single-agent bevacizumab followed by bevacizumab plus irinotecan at tumor progression in recurrent glioblastoma. *J Clin Oncol,* 27, 740-5.

KRISHNAMOORTHY, S., JIN, R., CAI, Y., MADDIPATI, K. R., NIE, D., PAGES, G., TUCKER, S. C. & HONN, K. V. 2010. 12-Lipoxygenase and the regulation of hypoxia-inducible factor in prostate cancer cells. *Exp Cell Res,* 316, 1706-15.

KUBAVAT, A. H., KHIPPAL, N., TAK, S., RIJHWANI, P., BHARGAVA, S., PATEL, T., SHAH, N., KSHATRIYA, R. R. & MITTAL, R. 2013. A randomized, comparative, multicentric clinical trial to assess the efficacy and safety of zileuton extended-release tablets with montelukast sodium tablets in patients suffering from chronic persistent asthma. *Am J Ther,* 20, 154-62.

KUHN, H., BANTHIYA, S. & VAN LEYEN, K. 2015. Mammalian lipoxygenases and their biological relevance. *Biochim Biophys Acta,* 1851, 308-30.

KUHN, H., WALTHER, M. & KUBAN, R. J. 2002. Mammalian arachidonate 15-lipoxygenases structure, function, and biological implications. *Prostaglandins Other Lipid Mediat,* 68-69, 263-90.

KULKE, M. H., ODZE, R. D., MUELLER, J. D., WANG, H., REDSTON, M. & BERTAGNOLLI, M. M. 2004. Prognostic significance of vascular endothelial growth factor and

cyclooxygenase 2 expression in patients receiving preoperative chemoradiation for esophageal cancer. *J Thorac Cardiovasc Surg,* 127, 1579-86.

KUSMARTSEV, S. 2012. Enhanced 15-lipoxygenase activity and elevated eicosanoid production in kidney tumor microenvironment contribute to the inflammation and immune suppression. *Oncoimmunology,* 1, 249-251.

LANDEN, C. N., JR., GOODMAN, B., KATRE, A. A., STEG, A. D., NICK, A. M., STONE, R. L., MILLER, L. D., MEJIA, P. V., JENNINGS, N. B., GERSHENSON, D. M., BAST, R. C., JR., COLEMAN, R. L., LOPEZ-BERESTEIN, G. & SOOD, A. K. 2010. Targeting aldehyde dehydrogenase cancer stem cells in ovarian cancer. *Mol Cancer Ther,* 9, 3186-99.

LANE, B. R., LIU, J., BOCK, P. J., SCHOLS, D., COFFEY, M. J., STRIETER, R. M., POLVERINI, P. J. & MARKOVITZ, D. M. 2002. Interleukin-8 and growth-regulated oncogene alpha mediate angiogenesis in Kaposi's sarcoma. *J Virol,* 76, 11570-83.

LAROCHELLE, P., KOLLMANNSBERGER, C., FELDMAN, R.D., SCHIFFRIN, E.L., POIRIER, L., PATENAUDE, F., RUETHER, D., MYERS, M. & BJARNASON, G. 2012. Hypertension management in patients with renal cell cancer treated with anti-angiogenic agents. *Current Oncology*, 19, 202-208.

LEE, S. H., JEONG, D., HAN, Y. S. & BAEK, M. J. 2015. Pivotal role of vascular endothelial growth factor pathway in tumor angiogenesis. *Ann Surg Treat Res,* 89, 1-8.

LI, B., WANG, C., ZHANG, Y., ZHAO, X. Y., HUANG, B., WU, P. F., LI, Q., LI, H., LIU, Y. S., CAO, L. Y., DAI, W. M., FANG, W. G., SHANG, D. S., CAO, L., ZHAO, W. D. & CHEN, Y. H. 2013a. Elevated PLGF contributes to small-cell lung cancer brain metastasis. *Oncogene,* 32, 2952-62.

LI, P., OH DA, Y., BANDYOPADHYAY, G., LAGAKOS, W. S., TALUKDAR, S., OSBORN, O., JOHNSON, A., CHUNG, H., MAYORAL, R., MARIS, M., OFRECIO, J. M., TAGUCHI, S., LU, M. & OLEFSKY, J. M. 2015. LTB4 promotes insulin resistance in obese mice by acting on macrophages, hepatocytes and myocytes. *Nat Med,* 21, 239-47.

LI, S., ZHAO, X., WU, Z., LI, Y., ZHU, L., CUI, B., DONG, X., TIAN, S., HU, F. & ZHAO, Y. 2013b. Polymorphisms in arachidonic acid metabolism-related genes and the risk and prognosis of colorectal cancer. *Fam Cancer,* 12, 755-65.

LI, T., ZHU, Y., QIN, C. Y., YANG, Z., FANG, A., XU, S. & REN, W. 2012. Expression and prognostic significance of vascular endothelial growth factor receptor 1 in hepatocellular carcinoma. *J Clin Pathol,* 65, 808-14.

LIAGRE, B., VERGNE, P., RIGAUD, M. & BENEYTOUT, J. L. 1997. Expression of arachidonate platelet-type 12-lipoxygenase in human rheumatoid arthritis type B synoviocytes. *FEBS Lett,* 414, 159-64.

LIU, B., MAHER, R. J., HANNUN, Y. A., PORTER, A. T. & HONN, K. V. 1994. 12(S)-HETE enhancement of prostate tumor cell invasion: selective role of PKC alpha. *J Natl Cancer Inst,* 86, 1145-51.

LIU, X., LI, P., ZHANG, S. T., YOU, H., JIA, J. D. & YU, Z. L. 2008. COX-2 mRNA expression in esophageal squamous cell carcinoma (ESCC) and effect by NSAID. *Dis Esophagus,* 21, 9-14.

LIU, X. H., CONNOLLY, J. M. & ROSE, D. P. 1996a. The 12-lipoxygenase gene-transfected MCF-7 human breast cancer cell line exhibits estrogen-independent, but estrogen and omega-6 fatty acid-stimulated proliferation in vitro, and enhanced growth in athymic nude mice. *Cancer Lett,* 109, 223-30.

LIU, X. H., CONNOLLY, J. M. & ROSE, D. P. 1996b. Eicosanoids as mediators of linoleic acid-stimulated invasion and type IV collagenase production by a metastatic human breast cancer cell line. *Clin Exp Metastasis,* 14, 145-52.

LIU, X. H., KIRSCHENBAUM, A., YAO, S., LEE, R., HOLLAND, J. F. & LEVINE, A. C. 2000. Inhibition of cyclooxygenase-2 suppresses angiogenesis and the growth of prostate cancer in vivo. *J Urol,* 164, 820-5.

LLOVET, J. M., RICCI, S., MAZZAFERRO, V., HILGARD, P., GANE, E., BLANC, J. F., DE OLIVEIRA, A. C., SANTORO, A., RAOUL, J. L., FORNER, A., SCHWARTZ, M., PORTA, C., ZEUZEM, S., BOLONDI, L., GRETEN, T. F., GALLE, P. R., SEITZ, J. F., BORBATH, I., HAUSSINGER, D., GIANNARIS, T., SHAN, M., MOSCOVICI, M., VOLIOTIS, D. & BRUIX, J. 2008. Sorafenib in advanced hepatocellular carcinoma. *N Engl J Med,* 359, 378-90.

LODDENKEMPER, C., SCHERNUS, M., NOUTSIAS, M., STEIN, H., THIEL, E. & NAGORSEN, D. 2006. In situ analysis of FOXP3+ regulatory T cells in human colorectal cancer. *J Transl Med,* 4, 52.

LOGES, S., SCHMIDT, T. & CARMELIET, P. 2010. Mechanisms of Resistance to Anti-Angiogenic Therapy and Development of Third-Generation Anti-Angiogenic Drug Candidates. *Genes Cancer,* 1, 12-25.

LU-EMERSON, C., SNUDERL, M., KIRKPATRICK, N. D., GOVEIA, J., DAVIDSON, C., HUANG, Y., RIEDEMANN, L., TAYLOR, J., IVY, P., DUDA, D. G., ANCUKIEWICZ, M., PLOTKIN, S. R., CHI, A. S., GERSTNER, E. R., EICHLER, A. F., DIETRICH, J., STEMMER-RACHAMIMOV, A. O., BATCHELOR, T. T. & JAIN, R. K. 2013. Increase in tumor-associated macrophages after antiangiogenic therapy is associated with poor survival among patients with recurrent glioblastoma. *Neuro Oncol,* 15, 1079-87.

LU, K. V. & BERGERS, G. 2013. Mechanisms of evasive resistance to anti-VEGF therapy in glioblastoma. *CNS Oncol,* 2, 49-65.

LUCI, D. K., JAMESON, J. B., 2ND, YASGAR, A., DIAZ, G., JOSHI, N., KANTZ, A., MARKHAM, K., PERRY, S., KUHN, N., YEUNG, J., KERNS, E. H., SCHULTZ, L., HOLINSTAT, M., NADLER, J. L., TAYLOR-FISHWICK, D. A., JADHAV, A., SIMEONOV, A., HOLMAN, T. R. & MALONEY, D. J. 2014. Synthesis and structure-activity relationship studies of 4-((2-hydroxy-3-methoxybenzyl)amino)benzenesulfonamide derivatives as potent and selective inhibitors of 12-lipoxygenase. *J Med Chem,* 57, 495-506.

LUCIO-ETEROVIC, A. K., PIAO, Y. & DE GROOT, J. F. 2009. Mediators of glioblastoma resistance and invasion during antivascular endothelial growth factor therapy. *Clin Cancer Res,* 15, 4589-99.

MACARRON, R., BANKS, M. N., BOJANIC, D., BURNS, D. J., CIROVIC, D. A., GARYANTES, T., GREEN, D. V., HERTZBERG, R. P., JANZEN, W. P., PASLAY, J. W., SCHOPFER, U. & SITTAMPALAM, G. S. 2011. Impact of high-throughput screening in biomedical research. *Nat Rev Drug Discov,* 10, 188-95.

MAGNUSSON, C., LIU, J., EHRNSTROM, R., MANJER, J., JIRSTROM, K., ANDERSSON, T. & SJOLANDER, A. 2011. Cysteinyl leukotriene receptor expression pattern affects migration of breast cancer cells and survival of breast cancer patients. *Int J Cancer,* 129, 9-22.

MAGNUSSON, C., MEZHYBOVSKA, M., LORINC, E., FERNEBRO, E., NILBERT, M. & SJOLANDER, A. 2010. Low expression of CysLT1R and high expression of CysLT2R mediate good prognosis in colorectal cancer. *Eur J Cancer,* 46, 826-35.

MAIER, T. J., TAUSCH, L., HOERNIG, M., COSTE, O., SCHMIDT, R., ANGIONI, C., METZNER, J., GROESCH, S., PERGOLA, C., STEINHILBER, D., WERZ, O. & GEISSLINGER, G. 2008. Celecoxib inhibits 5-lipoxygenase. *Biochem Pharmacol,* 76, 862-72.

MAKINO, T., YAMASAKI, M., TAKENO, A., SHIRAKAWA, M., MIYATA, H., TAKIGUCHI, S., NAKAJIMA, K., FUJIWARA, Y., NISHIDA, T., MATSUURA, N., MORI, M. & DOKI, Y. 2009. Cytokeratins 18 and 8 are poor prognostic markers in patients with squamous cell carcinoma of the oesophagus. *Br J Cancer,* 101, 1298-306.

MANCINI, J. A., ABRAMOVITZ, M., COX, M. E., WONG, E., CHARLESON, S., PERRIER, H., WANG, Z., PRASIT, P. & VICKERS, P. J. 1993. 5-lipoxygenase-activating protein is an arachidonate binding protein. *FEBS Lett,* 318, 277-81.

MAPP, P. I. & WALSH, D. A. 2012. Mechanisms and targets of angiogenesis and nerve growth in osteoarthritis. *Nat Rev Rheumatol,* 8, 390-398.

MARU, D., VENOOK, V.P. 7 ELLIS, L.M. 2013. Predictive biomarkers for bevacizumab: are we there yet? *Clin Cancer Res*, 19, 2824-7.

MASFERRER, J. L., LEAHY, K. M., KOKI, A. T., ZWEIFEL, B. S., SETTLE, S. L., WOERNER, B. M., EDWARDS, D. A., FLICKINGER, A. G., MOORE, R. J. & SEIBERT, K. 2000. Antiangiogenic and antitumor activities of cyclooxygenase-2 inhibitors. *Cancer Res,* 60, 1306-11.

MASFERRER, J. L., ZWEIFEL, B. S., HARDY, M., ANDERSON, G. D., DUFIELD, D., CORTES-BURGOS, L., PUFAHL, R. A. & GRANETO, M. 2010. Pharmacology of PF-4191834, a novel, selective non-redox 5-lipoxygenase inhibitor effective in inflammation and pain. *J Pharmacol Exp Ther,* 334, 294-301.

MATSUO, Y., TAKEYAMA, H. & GUHA, S. 2012. Cytokine network: new targeted therapy for pancreatic cancer. *Curr Pharm Des,* 18, 2416-9.

MATSUYAMA, M., HAYAMA, T., FUNAO, K., KAWAHITO, Y., SANO, H., TAKEMOTO, Y., NAKATANI, T. & YOSHIMURA, R. 2007. Overexpression of cysteinyl LT1 receptor in prostate cancer and CysLT1R antagonist inhibits prostate cancer cell growth through apoptosis. *Oncol Rep,* 18, 99-104.

MATSUYAMA, M., YOSHIMURA, R., MITSUHASHI, M., HASE, T., TSUCHIDA, K., TAKEMOTO, Y., KAWAHITO, Y., SANO, H. & NAKATANI, T. 2004. Expression of lipoxygenase in human prostate cancer and growth reduction by its inhibitors. *Int J Oncol,* 24, 821-7.

MATSUYAMA, M., YOSHIMURA, R., MITSUHASHI, M., TSUCHIDA, K., TAKEMOTO, Y., KAWAHITO, Y., SANO, H. & NAKATANI, T. 2005. 5-Lipoxygenase inhibitors attenuate growth of human renal cell carcinoma and induce apoptosis through arachidonic acid pathway. *Oncol Rep,* 14, 73-9.

MCCABE, N. P., SELMAN, S. H. & JANKUN, J. 2006. Vascular endothelial growth factor production in human prostate cancer cells is stimulated by overexpression of platelet 12-lipoxygenase. *Prostate,* 66, 779-87.

MEDINA, V. A. & RIVERA, E. S. 2010. Histamine receptors and cancer pharmacology. *Br J Pharmacol,* 161, 755-67.

MEHTA, S., BODDY, A., JOHNSON, I. T. & RHODES, M. 2006. Systematic review: Cyclo-oxygenase-2 in human oesophageal adenocarcinogenesis. *Aliment Pharmacol Ther,* 24, 1321-31.

MENG, Z., CAO, R., YANG, Z., LIU, T., WANG, Y. & WANG, X. 2013. Inhibitor of 5-lipoxygenase, zileuton, suppresses prostate cancer metastasis by upregulating E-cadherin and paxillin. *Urology,* 82, 1452 e7-14.

MEUNIER-CARPENTIER, S., DALES, J. P., DJEMLI, A., GARCIA, S., BONNIER, P., ANDRAC-MEYER, L., LAVAUT, M. N., ALLASIA, C. & CHARPIN, C. 2005. Comparison of the prognosis indication of VEGFR-1 and VEGFR-2 and Tie2 receptor expression in breast carcinoma. *Int J Oncol,* 26, 977-84.

MICHIE, C. A., MCLEAN, A., ALCOCK, C. & BEVERLEY, P. C. 1992. Lifespan of human lymphocyte subsets defined by CD45 isoforms. *Nature,* 360, 264-5.

MIDDLETON, M. K., ZUKAS, A. M., RUBINSTEIN, T., JACOB, M., ZHU, P., ZHAO, L., BLAIR, I. & PURE, E. 2006. Identification of 12/15-lipoxygenase as a suppressor of myeloproliferative disease. *J Exp Med,* 203, 2529-40.

MIKULE, K., GATLIN, J. C., DE LA HOUSSAYE, B. A. & PFENNINGER, K. H. 2002. Growth cone collapse induced by semaphorin 3A requires 12/15-lipoxygenase. *J Neurosci,* 22, 4932-41.

MILES, D. W., CHAN, A., DIRIX, L. Y., CORTES, J., PIVOT, X., TOMCZAK, P., DELOZIER, T., SOHN, J. H., PROVENCHER, L., PUGLISI, F., HARBECK, N., STEGER, G. G., SCHNEEWEISS, A., WARDLEY, A. M., CHLISTALLA, A. & ROMIEU, G. 2010. Phase III study of bevacizumab plus docetaxel compared with placebo plus docetaxel for the first-line treatment of human epidermal growth factor receptor 2-negative metastatic breast cancer. *J Clin Oncol,* 28, 3239-47.

MIOCINOVIC, R., MCCABE, N. P., KECK, R. W., JANKUN, J., HAMPTON, J. A. & SELMAN, S. H. 2005. In vivo and in vitro effect of baicalein on human prostate cancer cells. *Int J Oncol,* 26, 241-6.

MITTAL, K., KOON, H., ELSON, P., TRIOZZI, P., DOWLATI, A., CHEN, H., BORDEN, E. C. & RINI, B. I. 2014. Dual VEGF/VEGFR inhibition in advanced solid malignancies: clinical effects and pharmacodynamic biomarkers. *Cancer Biol Ther,* 15, 975-81.

MIZUKAMI, Y., JO, W. S., DUERR, E. M., GALA, M., LI, J., ZHANG, X., ZIMMER, M. A., ILIOPOULOS, O., ZUKERBERG, L. R., KOHGO, Y., LYNCH, M. P., RUEDA, B. R. & CHUNG, D. C. 2005. Induction of interleukin-8 preserves the angiogenic response in HIF-1alpha-deficient colon cancer cells. *Nat Med,* 11, 992-7.

MOBIUS, C., STEIN, H. J., SPIESS, C., BECKER, I., FEITH, M., THEISEN, J., GAIS, P., JUTTING, U. & SIEWERT, J. R. 2005. COX2 expression, angiogenesis, proliferation and survival in Barrett's cancer. *Eur J Surg Oncol,* 31, 755-9.

MOHAMMAD, A. M., ABDEL, H. A., ABDEL, W., AHMED, A. M., WAEL, T. & EIMAN, G. 2006. Expression of cyclooxygenase-2 and 12-lipoxygenase in human breast cancer and their relationship with HER-2/neu and hormonal receptors: impact on prognosis and therapy. *Indian J Cancer,* 43, 163-8.

MOTZER, R. J., HUTSON, T. E., TOMCZAK, P., MICHAELSON, M. D., BUKOWSKI, R. M., RIXE, O., OUDARD, S., NEGRIER, S., SZCZYLIK, C., KIM, S. T., CHEN, I., BYCOTT,

P. W., BAUM, C. M. & FIGLIN, R. A. 2007. Sunitinib versus interferon alfa in metastatic renal-cell carcinoma. *N Engl J Med,* 356, 115-24.

MULLIN, B. H., SPECTOR, T. D., CURTIS, C. C., ONG, G. N., HART, D. J., HAKIM, A. J., WORTHY, T. & WILSON, S. G. 2007. Polymorphisms in ALOX12, but not ALOX15, are significantly associated with BMD in postmenopausal women. *Calcif Tissue Int,* 81, 10-7.

MURASE, H., INOKUCHI, M., TAKAGI, Y., KATO, K., KOJIMA, K. & SUGIHARA, K. 2014. Prognostic significance of the co-overexpression of fibroblast growth factor receptors 1, 2 and 4 in gastric cancer. *Mol Clin Oncol,* 2, 509-17.

NAIR, K. S., NAIDOO, R. & CHETTY, R. 2005. Expression of cell adhesion molecules in oesophageal carcinoma and its prognostic value. *J Clin Pathol,* 58, 343-51.

NANOBASHVILI, J., JOZKOWICZ, A., NEUMAYER, C., FÜGL, A., SPORN, E., POLTERAUER, P. & HUK, I. 2003. Comparison of Angiogenic Potential of Human Microvascular Endothelial Cells and Human Umbilical Vein Endothelial Cells. *European Surgery,* 35, 214-219.

NARDONE, P. A., SLOTMAN, G. J. & VEZERIDIS, M. P. 1988. Ketoconazole: a thromboxane synthetase and 5-lipoxygenase inhibitor with antimetastatic activity in B16-F10 melanoma. *J Surg Res,* 44, 425-9.

NASSAR, A., RADHAKRISHNAN, A., CABRERO, I. A., COTSONIS, G. & COHEN, C. 2007. COX-2 expression in invasive breast cancer: correlation with prognostic parameters and outcome. *Appl Immunohistochem Mol Morphol,* 15, 255-9.

NATARAJAN, R., ESWORTHY, R., BAI, W., GU, J. L., WILCZYNSKI, S. & NADLER, J. 1997. Increased 12-lipoxygenase expression in breast cancer tissues and cells. Regulation by epidermal growth factor. *J Clin Endocrinol Metab,* 82, 1790-8.

NATIONAL CANCER REGISTRY 2011. Cancer Trends No 8. Cancers of oesophagus and stomach *National Cancer Registry.*

NATIONAL CANCER REGISTRY 2013. Cancer in Ireland 2013: Annual Report. National Cancer Registry.

NCT00357682 2006. A Phase III, Randomized, Study of Aspirin and Esomeprazole Chemoprevention in Barrett's Metaplasia (AspECT).

AstraZeneca. NCT00357682. https://clinicaltrials.gov/ct2/show/NCT00357682 (available 05/08/15).

NCT01130688 2010. Safety of Zileuton (Zyflo) in Combination With Imatinib Mesylate (Gleevec) in CML.

NCT01130805 2014. A study of pazopanib with CAPEOX in AGC patients. *[cited 2014 June 22]. Available online: http://clinicaltrials.gov/ct2/show/NCT01130805*

NCT01503372 2014. FLO +/- pazopanib as first-line treatment in advanced gastric cancer (PaFLO). *[cited 2014 June 22]. Available online: http://clinicaltrials.gov/ct2/show/NCT01503372.*

NEELS, J. G. 2013. A role for 5-lipoxygenase products in obesity-associated inflammation and insulin resistance. *Adipocyte,* 2, 262-5.

NG, M., FLEMING, T., ROBINSON, M., THOMSON, B., GRAETZ, N., *et al.* 2014. Global, regional, and national prevalence of overweight and obesity in children and adults during 1980-2013: a systematic analysis for the Global Burden of Disease Study 2013. *Lancet,* 384, 766-81.

NGUYEN, D. M., CHEN, G. A., REDDY, R., TSAI, W., SCHRUMP, W. D., COLE, G., JR. & SCHRUMP, D. S. 2004. Potentiation of paclitaxel cytotoxicity in lung and esophageal cancer cells by pharmacologic inhibition of the phosphoinositide 3-kinase/protein kinase B (Akt)-mediated signaling pathway. *J Thorac Cardiovasc Surg,* 127, 365-75.

NIE, D., HILLMAN, G. G., GEDDES, T., TANG, K., PIERSON, C., GRIGNON, D. J. & HONN, K. V. 1998. Platelet-type 12-lipoxygenase in a human prostate carcinoma stimulates angiogenesis and tumor growth. *Cancer Res,* 58, 4047-51.

NIE, D., KRISHNAMOORTHY, S., JIN, R., TANG, K., CHEN, Y., QIAO, Y., ZACHAREK, A., GUO, Y., MILANINI, J., PAGES, G. & HONN, K. V. 2006. Mechanisms regulating tumor angiogenesis by 12-lipoxygenase in prostate cancer cells. *J Biol Chem,* 281, 18601-9.

NIE, D., NEMETH, J., QIAO, Y., ZACHAREK, A., LI, L., HANNA, K., TANG, K., HILLMAN, G. G., CHER, M. L., GRIGNON, D. J. & HONN, K. V. 2003. Increased metastatic potential in human prostate carcinoma cells by overexpression of arachidonate 12-lipoxygenase. *Clin Exp Metastasis,* 20, 657-63.

NIE, D., TANG, K., DIGLIO, C. & HONN, K. V. 2000. Eicosanoid regulation of angiogenesis: role of endothelial arachidonate 12-lipoxygenase. *Blood,* 95, 2304-11.

NIGAM, S., KUMAR, G. S., SUTHERLAND, M., SCHEWE, T., IKAWA, H., YAMASAKI, Y., UEDA, N. & YAMAMOTO, S. 1999. Metabolic suppression of platelet-type 12-lipoxygenase in human uterine cervix with invasive carcinoma. *Int J Cancer,* 82, 827-31.

NITHIPATIKOM, K., ISBELL, M. A., SEE, W. A. & CAMPBELL, W. B. 2006. Elevated 12- and 20-hydroxyeicosatetraenoic acid in urine of patients with prostatic diseases. *Cancer Lett,* 233, 219-25.

NIXON, J. B., KIM, K. S., LAMB, P. W., BOTTONE, F. G. & ELING, T. E. 2004. 15-Lipoxygenase-1 has anti-tumorigenic effects in colorectal cancer. *Prostaglandins Leukot Essent Fatty Acids,* 70, 7-15.

OHBU, M., SAEGUSA, M., KOBAYASHI, N., TSUKAMOTO, H., MIENO, H., KAKITA, A. & OKAYASU, I. 1997. Expression of bcl-2 protein in esophageal squamous cell carcinomas and its association with lymph node metastasis. *Cancer,* 79, 1287-93.

OHD, J. F., NIELSEN, C. K., CAMPBELL, J., LANDBERG, G., LOFBERG, H. & SJOLANDER, A. 2003. Expression of the leukotriene D4 receptor CysLT1, COX-2, and other cell survival factors in colorectal adenocarcinomas. *Gastroenterology,* 124, 57-70.

OHGAMI, R. S., MA, L., REN, L., WEINBERG, O. K., SEETHARAM, M., GOTLIB, J. R. & ARBER, D. A. 2012. DNA methylation analysis of ALOX12 and GSTM1 in acute myeloid leukaemia identifies prognostically significant groups. *Br J Haematol,* 159, 182-90.

OHTSU, A., SHAH, M. A., VAN CUTSEM, E., RHA, S. Y., SAWAKI, A., PARK, S. R., LIM, H. Y., YAMADA, Y., WU, J., LANGER, B., STARNAWSKI, M. & KANG, Y. K. 2011. Bevacizumab in combination with chemotherapy as first-line therapy in advanced gastric cancer: a randomized, double-blind, placebo-controlled phase III study. *J Clin Oncol,* 29, 3968-76.

OKINES, A. F., LANGLEY, R. E., THOMPSON, L. C., STENNING, S. P., STEVENSON, L., FALK, S., SEYMOUR, M., COXON, F., MIDDLETON, G. W., SMITH, D., EVANS, L., SLATER, S., WATERS, J., FORD, D., HALL, M., IVESON, T. J., PETTY, R. D., PLUMMER, C., ALLUM, W. H., BLAZEBY, J. M., GRIFFIN, M. & CUNNINGHAM, D. 2013. Bevacizumab with peri-operative epirubicin, cisplatin and capecitabine (ECX) in localised gastro-oesophageal adenocarcinoma: a safety report. *Ann Oncol,* 24, 702-9.

OLITHSELVAN, A., GORARD, D. A. & MCINTYRE, A. S. 2007. A surveillance programme for Barrett's oesophagus in a UK general hospital. *Eur J Gastroenterol Hepatol,* 19, 305-9.

OLKHANUD, P. B., DAMDINSUREN, B., BODOGAI, M., GRESS, R. E., SEN, R., WEJKSZA, K., MALCHINKHUU, E., WERSTO, R. P. & BIRAGYN, A. 2011. Tumor-evoked regulatory B cells promote breast cancer metastasis by converting resting CD4(+) T cells to T-regulatory cells. *Cancer Res,* 71, 3505-15.

OLSSON, A. K., DIMBERG, A., KREUGER, J. & CLAESSON-WELSH, L. 2006. VEGF receptor signalling - in control of vascular function. *Nat Rev Mol Cell Biol,* 7, 359-71.

OZDEMIR, F., AKDOGAN, R., AYDIN, F., REIS, A., KAVGACI, H., GUL, S. & AKDOGAN, E. 2006. The effects of VEGF and VEGFR-2 on survival in patients with gastric cancer. *J Exp Clin Cancer Res,* 25, 83-8.

PACE, E., PROFITA, M., MELIS, M., BONANNO, A., PATERNO, A., MODY, C. H., SPATAFORA, M., FERRARO, M., SIENA, L., VIGNOLA, A. M., BONSIGNORE, G. & GJOMARKAJ, M. 2004. LTB4 is present in exudative pleural effusions and contributes actively to neutrophil recruitment in the inflamed pleural space. *Clin Exp Immunol,* 135, 519-27.

PAN, Q., CHANTHERY, Y., LIANG, W. C., STAWICKI, S., MAK, J., RATHORE, N., TONG, R. K., KOWALSKI, J., YEE, S. F., PACHECO, G., ROSS, S., CHENG, Z., LE COUTER, J., PLOWMAN, G., PEALE, F., KOCH, A. W., WU, Y., BAGRI, A., TESSIER-LAVIGNE, M. & WATTS, R. J. 2007. Blocking neuropilin-1 function has an additive effect with anti-VEGF to inhibit tumor growth. *Cancer Cell,* 11, 53-67.

PANDOLFINO, J. E., EL-SERAG, H. B., ZHANG, Q., SHAH, N., GHOSH, S. K. & KAHRILAS, P. J. 2006. Obesity: a challenge to esophagogastric junction integrity. *Gastroenterology,* 130, 639-49.

PARK, S. W., HEO, D. S. & SUNG, M. W. 2012. The shunting of arachidonic acid metabolism to 5-lipoxygenase and cytochrome p450 epoxygenase antagonizes the anti-cancer effect of cyclooxygenase-2 inhibition in head and neck cancer cells. *Cell Oncol (Dordr),* 35, 1-8.

PENG, J., SHAO, N., PENG, H. & CHEN, L. Q. 2013. Prognostic significance of vascular endothelial growth factor expression in esophageal carcinoma: a meta-analysis. *J BUON,* 18, 398-406.

PETERS-GOLDEN, M., GLEASON, M. M. & TOGIAS, A. 2006. Cysteinyl leukotrienes: multi-functional mediators in allergic rhinitis. *Clin Exp Allergy,* 36, 689-703.

PETERS-GOLDEN, M. & HENDERSON, W. R., JR. 2007. Leukotrienes. *N Engl J Med,* 357, 1841-54.

PETERS, C. J. & FITZGERALD, R. C. 2007. Systematic review: the application of molecular pathogenesis to prevention and treatment of oesophageal adenocarcinoma. *Aliment Pharmacol Ther,* 25, 1253-69.

PICARDO, S. L., O'BRIEN, M. P., FEIGHERY, R., O'TOOLE, D., RAVI, N., O'FARRELL, N. J., O'SULLIVAN, J. N. & REYNOLDS, J. V. 2015. A Barrett's esophagus registry of over 1000 patients from a specialist center highlights greater risk of progression than population-based registries and high risk of low grade dysplasia. *Dis Esophagus,* 28, 121-6.

PIDGEON, G. P., KANDOUZ, M., MERAM, A. & HONN, K. V. 2002. Mechanisms controlling cell cycle arrest and induction of apoptosis after 12-lipoxygenase inhibition in prostate cancer cells. *Cancer Res,* 62, 2721-7.

PIDGEON, G. P., LYSAGHT, J., KRISHNAMOORTHY, S., REYNOLDS, J. V., O'BYRNE, K., NIE, D. & HONN, K. V. 2007. Lipoxygenase metabolism: roles in tumor progression and survival. *Cancer Metastasis Rev,* 26, 503-24.

PIDGEON, G. P., TANG, K., CAI, Y. L., PIASENTIN, E. & HONN, K. V. 2003. Overexpression of platelet-type 12-lipoxygenase promotes tumor cell survival by enhancing alpha(v)beta(3) and alpha(v)beta(5) integrin expression. *Cancer Res,* 63, 4258-67.

PIOTROWSKA, M., SZEFEL, J., SKRZYPCZAK-JANKUN, E., LYSIAK-SZYDLOWSKA, W., SZAJEWSKI, M., ALEKSANDROWICZ-WRONA, E. & JANKUN, J. 2013. The concentration of 12-lipoxygenase in platelet rich plasma as an indication of cancer of the prostate. *Contemp Oncol (Pozn),* 17, 389-93.

PLEIN, A., FANTIN, A. & RUHRBERG, C. 2014. Neuropilin regulation of angiogenesis, arteriogenesis, and vascular permeability. *Microcirculation,* 21, 315-23.

POCH, E. 2003. Role of lipoxygenase metabolites in cardiovascular disease. *Curr Hypertens Rep,* 5, 1-2.

POMMERY, N., TAVERNE, T., TELLIEZ, A., GOOSSENS, L., CHARLIER, C., POMMERY, J., GOOSSENS, J. F., HOUSSIN, R., DURANT, F. & HENICHART, J. P. 2004. New COX-2/5-LOX inhibitors: apoptosis-inducing agents potentially useful in prostate cancer chemotherapy. *J Med Chem,* 47, 6195-206.

PRESTA, M., DELL'ERA, P., MITOLA, S., MORONI, E., RONCA, R. & RUSNATI, M. 2005. Fibroblast growth factor/fibroblast growth factor receptor system in angiogenesis. *Cytokine Growth Factor Rev,* 16, 159-78.

PRESTON, I. R., HILL, N. S., WARBURTON, R. R. & FANBURG, B. L. 2006. Role of 12-lipoxygenase in hypoxia-induced rat pulmonary artery smooth muscle cell proliferation. *Am J Physiol Lung Cell Mol Physiol,* 290, L367-74.

PRINS, M. J., VERHAGE, R. J., TEN KATE, F. J. & VAN HILLEGERSBERG, R. 2012. Cyclooxygenase isoenzyme-2 and vascular endothelial growth factor are associated with poor prognosis in esophageal adenocarcinoma. *J Gastrointest Surg,* 16, 956-66.

QUANTE, M., ABRAMS, J. A., LEE, Y. & WANG, T. C. 2012. Barrett esophagus: what a mouse model can teach us about human disease. *Cell Cycle,* 11, 4328-38.

RADES, D., GOLKE, H., SCHILD, S. E. & KILIC, E. 2008. Impact of VEGF and VEGF receptor 1 (FLT1) expression on the prognosis of stage III esophageal cancer patients after radiochemotherapy. *Strahlenther Onkol,* 184, 416-20.

RADES, D., SETTER, C., DUNST, J., DAHL, O., SCHILD, S. E. & NOACK, F. 2010. Prognostic impact of VEGF and VEGF receptor 1 (FLT1) expression in patients irradiated for stage II/III non-small cell lung cancer (NSCLC). *Strahlenther Onkol,* 186, 307-14.

RAIMONDI, C. & RUHRBERG, C. 2013. Neuropilin signalling in vessels, neurons and tumours. *Semin Cell Dev Biol,* 24, 172-8.

RAO, C. V., JANAKIRAM, N. B. & MOHAMMED, A. 2012. Lipoxygenase and Cyclooxygenase Pathways and Colorectal Cancer Prevention. *Curr Colorectal Cancer Rep,* 8, 316-324.

RASO, E., DOME, B., SOMLAI, B., ZACHAREK, A., HAGMANN, W., HONN, K. V. & TIMAR, J. 2004. Molecular identification, localization and function of platelet-type 12-lipoxygenase

in human melanoma progression, under experimental and clinical conditions. *Melanoma Res,* 14, 245-50.

RAUT, C. P., NAWROCKI, S., LASHINGER, L. M., DAVIS, D. W., KHANBOLOOKI, S., XIONG, H., ELLIS, L. M. & MCCONKEY, D. J. 2004. Celecoxib inhibits angiogenesis by inducing endothelial cell apoptosis in human pancreatic tumor xenografts. *Cancer Biol Ther,* 3, 1217-24.

RECK, M., VON PAWEL, J., ZATLOUKAL, P., RAMLAU, R., GORBOUNOVA, V., HIRSH, V., LEIGHL, N., MEZGER, J., ARCHER, V., MOORE, N. & MANEGOLD, C. 2010. Overall survival with cisplatin-gemcitabine and bevacizumab or placebo as first-line therapy for nonsquamous non-small-cell lung cancer: results from a randomised phase III trial (AVAiL). *Ann Oncol,* 21, 1804-9.

REICHELT, U., DUESEDAU, P., TSOURLAKIS, M., QUAAS, A., LINK, B. C., SCHURR, P. G., KAIFI, J. T., GROS, S. J., YEKEBAS, E. F., MARX, A., SIMON, R., IZBICKI, J. R. & SAUTER, G. 2007. Frequent homogeneous HER-2 amplification in primary and metastatic adenocarcinoma of the esophagus. *Mod Pathol,* 20, 120-9.

REN, Y., CAO, B., LAW, S., XIE, Y., LEE, P. Y., CHEUNG, L., CHEN, Y., HUANG, X., CHAN, H. M., ZHAO, P., LUK, J., VANDE WOUDE, G. & WONG, J. 2005. Hepatocyte growth factor promotes cancer cell migration and angiogenic factors expression: a prognostic marker of human esophageal squamous cell carcinomas. *Clin Cancer Res,* 11, 6190-7.

RENEHAN, A. G., TYSON, M., EGGER, M., HELLER, R. F. & ZWAHLEN, M. 2008. Body-mass index and incidence of cancer: a systematic review and meta-analysis of prospective observational studies. *Lancet,* 371, 569-78.

REYNOLDS, J. V., DONOHOE, C. L., MCGILLYCUDDY, E., RAVI, N., O'TOOLE, D., O'BYRNE, K. & HOLLYWOOD, D. 2012. Evolving progress in oncologic and operative outcomes for esophageal and junctional cancer: lessons from the experience of a high-volume center. *J Thorac Cardiovasc Surg,* 143, 1130-1137 e1.

REYNOLDS, J. V., MCGILLYCUDDY, E., RAVI, N., DONOHOE, C., O'TOOLE, D., O'BYRNE, K. & HOLLYWOOD, D. 2011. Modern oncologic and operative outcomes for oesophageal cancer treated with curative intent. *Ir Med J,* 104, 235-8.

REYNOLDS, J. V., MULDOON, C., HOLLYWOOD, D., RAVI, N., ROWLEY, S., O'BYRNE, K., KENNEDY, J. & MURPHY, T. J. 2007. Long-term outcomes following neoadjuvant chemoradiotherapy for esophageal cancer. *Ann Surg,* 245, 707-16.

RIABOV, V., GUDIMA, A., WANG, N., MICKLEY, A., OREKHOV, A. & KZHYSHKOWSKA, J. 2014. Role of tumor associated macrophages in tumor angiogenesis and lymphangiogenesis. *Front Physiol,* 5, 75.

RICE, T. W. 2015. Esophageal Cancer Staging. *Korean J Thorac Cardiovasc Surg,* 48, 157-63.

ROBERT, N. J., DIERAS, V., GLASPY, J., BRUFSKY, A. M., BONDARENKO, I., LIPATOV, O. N., PEREZ, E. A., YARDLEY, D. A., CHAN, S. Y., ZHOU, X., PHAN, S. C. & O'SHAUGHNESSY, J. 2011. RIBBON-1: randomized, double-blind, placebo-controlled, phase III trial of chemotherapy with or without bevacizumab for first-line treatment of human epidermal growth factor receptor 2-negative, locally recurrent or metastatic breast cancer. *J Clin Oncol,* 29, 1252-60.

ROBINSON, E.S., KHANKIN, E.V., KARUMANCHI, S.A. & HUMPHREYS, B.D. 2010. Hypertension Induced by VEGF Signaling Pathway Inhibition: Mechanisms and Potential Use as a Biomarker. *Seminars in nephrology*, 30, 591-601.

ROBSON, T. & JAMES, I. F. 2012. The therapeutic and diagnostic potential of FKBPL; a novel anticancer protein. *Drug Discov Today,* 17, 544-8.

RODRIGUEZ-BLANCO, G., BURGERS, P. C., DEKKER, L. J., IJZERMANS, J. J., WILDHAGEN, M. F., SCHENK-BRAAT, E. A., BANGMA, C. H., JENSTER, G. & LUIDER, T. M. 2014. Serum levels of arachidonic acid metabolites change during prostate cancer progression. *Prostate,* 74, 618-27.

RODRIGUEZ, P. C., QUICENO, D. G., ZABALETA, J., ORTIZ, B., ZEA, A. H., PIAZUELO, M. B., DELGADO, A., CORREA, P., BRAYER, J., SOTOMAYOR, E. M., ANTONIA, S., OCHOA, J. B. & OCHOA, A. C. 2004. Arginase I production in the tumor microenvironment by mature myeloid cells inhibits T-cell receptor expression and antigen-specific T-cell responses. *Cancer Res,* 64, 5839-49.

ROMANO, M., CATALANO, A., NUTINI, M., D'URBANO, E., CRESCENZI, C., CLARIA, J., LIBNER, R., DAVI, G. & PROCOPIO, A. 2001. 5-lipoxygenase regulates malignant mesothelial cell survival: involvement of vascular endothelial growth factor. *FASEB J,* 15, 2326-36.

ROMANO, M. & CLARIA, J. 2003. Cyclooxygenase-2 and 5-lipoxygenase converging functions on cell proliferation and tumor angiogenesis: implications for cancer therapy. *FASEB J,* 17, 1986-95.

ROSE, D. P. & CONNOLLY, J. M. 2000. Regulation of tumor angiogenesis by dietary fatty acids and eicosanoids. *Nutr Cancer,* 37, 119-27.

ROSENGREN, S., OLOFSSON, A. M., VON ANDRIAN, U. H., LUNDGREN-AKERLUND, E. & ARFORS, K. E. 1991. Leukotriene B4-induced neutrophil-mediated endothelial leakage in vitro and in vivo. *J Appl Physiol (1985),* 71, 1322-30.

RUNDHAUG, J. E. 2005. Matrix metalloproteinases and angiogenesis. *J Cell Mol Med,* 9, 267-85.

RYAN, A. M., DUONG, M., HEALY, L., RYAN, S. A., PAREKH, N., REYNOLDS, J. V. & POWER, D. G. 2011. Obesity, metabolic syndrome and esophageal adenocarcinoma: epidemiology, etiology and new targets. *Cancer Epidemiol,* 35, 309-19.

RYAN, A. M., ROWLEY, S. P., FITZGERALD, A. P., RAVI, N. & REYNOLDS, J. V. 2006. Adenocarcinoma of the oesophagus and gastric cardia: male preponderance in association with obesity. *Eur J Cancer,* 42, 1151-8.

SAFRAN, H. E. A. 2015. RTOG 1010: A Phase III Trial Evaluating the Addition of Trastuzumab to Trimodality Treatment of Her2-Overexpressing Esophageal Adenocarcinoma. *https://www.rtog.org/ClinicalTrials/ProtocolTable/StudyDetails.aspx?study=1010 [updated 11/05/14, accessed 30/07/15].*

SAHARINEN, P., EKLUND, L., PULKKI, K., BONO, P. & ALITALO, K. 2011. VEGF and angiopoietin signaling in tumor angiogenesis and metastasis. *Trends Mol Med,* 17, 347-62.

SAIF, M. W., OETTLE, H., VERVENNE, W. L., THOMAS, J. P., SPITZER, G., VISSEREN-GRUL, C., ENAS, N. & RICHARDS, D. A. 2009. Randomized double-blind phase II trial comparing gemcitabine plus LY293111 versus gemcitabine plus placebo in advanced adenocarcinoma of the pancreas. *Cancer J,* 15, 339-43.

SAIJO, N. 2012. Present Status and Problems on Molecular Targeted Therapy of Cancer. *Cancer Res Treat,* 44, 1-10.

SALAMA, P., PHILLIPS, M., GRIEU, F., MORRIS, M., ZEPS, N., JOSEPH, D., PLATELL, C. & IACOPETTA, B. 2009. Tumor-infiltrating FOXP3+ T regulatory cells show strong prognostic significance in colorectal cancer. *J Clin Oncol,* 27, 186-92.

SALMELA, M. T., KARJALAINEN-LINDSBERG, M. L., PUOLAKKAINEN, P. & SAARIALHO-KERE, U. 2001. Upregulation and differential expression of matrilysin (MMP-7) and metalloelastase (MMP-12) and their inhibitors TIMP-1 and TIMP-3 in Barrett's oesophageal adenocarcinoma. *Br J Cancer,* 85, 383-92.

SAMUELSSON, B. & FUNK, C. D. 1989. Enzymes involved in the biosynthesis of leukotriene B4. *J Biol Chem,* 264, 19469-72.

SANDLER, A., GRAY, R., PERRY, M. C., BRAHMER, J., SCHILLER, J. H., DOWLATI, A., LILENBAUM, R. & JOHNSON, D. H. 2006. Paclitaxel-carboplatin alone or with bevacizumab for non-small-cell lung cancer. *N Engl J Med,* 355, 2542-50.

SAPIEHA, P., STAHL, A., CHEN, J., SEAWARD, M. R., WILLETT, K. L., KRAH, N. M., DENNISON, R. J., CONNOR, K. M., ADERMAN, C. M., LICLICAN, E., CARUGHI, A., PERELMAN, D., KANAOKA, Y., SANGIOVANNI, J. P., GRONERT, K. & SMITH, L. E. 2011. 5-Lipoxygenase metabolite 4-HDHA is a mediator of the antiangiogenic effect of omega-3 polyunsaturated fatty acids. *Sci Transl Med,* 3, 69ra12.

SARVESWARAN, S., THAMILSELVAN, V., BRODIE, C. & GHOSH, J. 2011. Inhibition of 5-lipoxygenase triggers apoptosis in prostate cancer cells via down-regulation of protein kinase C-epsilon. *Biochim Biophys Acta,* 1813, 2108-17.

SCHMITT, J. M., SOMMERS, S. R., FISHER, W., ANSARI, R., ROBIN, E., KONERU, K., MCCLEAN, J., LIU, Z., TONG, Y. & HANNA, N. 2012. Sunitinib plus paclitaxel in patients with advanced esophageal cancer: a phase II study from the Hoosier Oncology Group. *J Thorac Oncol,* 7, 760-3.

SCHROEDER, C. P., YANG, P., NEWMAN, R. A. & LOTAN, R. 2007. Simultaneous inhibition of COX-2 and 5-LOX activities augments growth arrest and death of premalignant and malignant human lung cell lines. *J Exp Ther Oncol,* 6, 183-92.

SCHWARTZ, G. K., WEITZMAN, A., O'REILLY, E., BRAIL, L., DE ALWIS, D. P., CLEVERLY, A., BARILE-THIEM, B., VINCIGUERRA, V. & BUDMAN, D. R. 2005. Phase I and pharmacokinetic study of LY293111, an orally bioavailable LTB4 receptor antagonist, in patients with advanced solid tumors. *J Clin Oncol,* 23, 5365-73.

SCHWENK, U. & SCHRODER, J. M. 1995. 5-Oxo-eicosanoids are potent eosinophil chemotactic factors. Functional characterization and structural requirements. *J Biol Chem,* 270, 15029-36.

SEKIYA, K. & OKUDA, H. 1982. Selective inhibition of platelet lipoxygenase by baicalein. *Biochem Biophys Res Commun,* 105, 1090-5.

SEO, J. M., CHO, K. J., KIM, E. Y., CHOI, M. H., CHUNG, B. C. & KIM, J. H. 2011. Up-regulation of BLT2 is critical for the survival of bladder cancer cells. *Exp Mol Med,* 43, 129-37.

SHAH, C. H., VIKTORSSON, K., KANTER, L., SHERIF, A., ASMUNDSSON, J., ROSENBLATT, R., LEWENSOHN, R. & ULLEN, A. 2014. Vascular endothelial growth factor receptor 2, but not S100A4 or S100A6, correlates with prolonged survival in advanced urothelial carcinoma. *Urol Oncol,* 32, 1215-24.

SHAH, M. A., ILSON, D. H., RAMANATHAN, R. K., LEVNER, A., D'ADAMO, D., SCHWARTZ, L., CASPER, E., SCHWARTZ, G. K. & AND KELSEN, D. P. 2005. A multicenter phase II study of irinotecan (CPT), cisplatin (CIS), and bevacizumab (BEV) in patients with unresectable or metastatic gastric or gastroesophageal junction (GEJ) adenocarcinoma. *Proc Am Soc Clin Oncol 2005;23:16s.*

SHAH, M. A., JHAWER, M., ILSON, D. H., LEFKOWITZ, R. A., ROBINSON, E., CAPANU, M. & KELSEN, D. P. 2011. Phase II study of modified docetaxel, cisplatin, and fluorouracil with bevacizumab in patients with metastatic gastroesophageal adenocarcinoma. *J Clin Oncol,* 29, 868-74.

SHAKED, Y., CIARROCCHI, A., FRANCO, M., LEE, C. R., MAN, S., CHEUNG, A. M., HICKLIN, D. J., CHAPLIN, D., FOSTER, F. S., BENEZRA, R. & KERBEL, R. S. 2006. Therapy-induced acute recruitment of circulating endothelial progenitor cells to tumors. *Science,* 313, 1785-7.

SHANG, L., LIU, H. J., HAO, J. J., JIANG, Y. Y., SHI, F., ZHANG, Y., CAI, Y., XU, X., JIA, X. M., ZHAN, Q. M. & WANG, M. R. 2014. A panel of overexpressed proteins for prognosis in esophageal squamous cell carcinoma. *PLoS One,* 9, e111045.

SHARMA-WALIA, N., CHANDRAN, K., PATEL, K., VEETTIL, M. V. & MARGINEAN, A. 2014. The Kaposi's sarcoma-associated herpesvirus (KSHV)-induced 5-lipoxygenase-leukotriene B4 cascade plays key roles in KSHV latency, monocyte recruitment, and lipogenesis. *J Virol,* 88, 2131-56.

SHARMA, P. 2009. Clinical practice. Barrett's esophagus. *N Engl J Med,* 361, 2548-56.

SHENG, H., SHAO, J., MORROW, J. D., BEAUCHAMP, R. D. & DUBOIS, R. N. 1998. Modulation of apoptosis and Bcl-2 expression by prostaglandin E2 in human colon cancer cells. *Cancer Res,* 58, 362-6.

SHEPPARD, K. A., GREENBERG, S. M., FUNK, C. D., ROMANO, M. & SERHAN, C. N. 1992. Lipoxin generation by human megakaryocyte-induced 12-lipoxygenase. *Biochim Biophys Acta,* 1133, 223-34.

SHI, H. Y., LV, F. J., ZHU, S. T., WANG, Q. G. & ZHANG, S. T. 2011. Dual inhibition of 5-LOX and COX-2 suppresses esophageal squamous cell carcinoma. *Cancer Lett,* 309, 19-26.

SHIH, C. H., OZAWA, S., ANDO, N., UEDA, M. & KITAJIMA, M. 2000. Vascular endothelial growth factor expression predicts outcome and lymph node metastasis in squamous cell carcinoma of the esophagus. *Clin Cancer Res,* 6, 1161-8.

SHIMIZU, D., VALLBOHMER, D., KURAMOCHI, H., UCHIDA, K., SCHNEIDER, S., CHANDRASOMA, P. T., SHIMADA, H., DEMEESTER, T. R., DANENBERG, K. D., PETERS, J. H., DEMEESTER, S. R. & DANENBERG, P. V. 2006. Increasing cyclooxygenase-2 (cox-2) gene expression in the progression of Barrett's esophagus to adenocarcinoma correlates with that of Bcl-2. *Int J Cancer,* 119, 765-70.

SHIOZAKI, A., NAKASHIMA, S., ICHIKAWA, D., FUJIWARA, H., KONISHI, H., KOMATSU, S., KUBOTA, T., OKAMOTO, K., IITAKA, D., SHIMIZU, H., NAKO, Y., TAKEMOTO, K., KISHIMOTO, M. & OTSUJI, E. 2013. Prognostic significance of p21 expression in patients with esophageal squamous cell carcinoma. *Anticancer Res,* 33, 4329-35.

SHIRVANI, V. N., OUATU-LASCAR, R., KAUR, B. S., OMARY, M. B. & TRIADAFILOPOULOS, G. 2000. Cyclooxygenase 2 expression in Barrett's esophagus and adenocarcinoma: Ex vivo induction by bile salts and acid exposure. *Gastroenterology,* 118, 487-96.

SHUREIQI, I., CHEN, D., DAY, R. S., ZUO, X., HOCHMAN, F. L., ROSS, W. A., COLE, R. A., MOY, O., MORRIS, J. S., XIAO, L., NEWMAN, R. A., YANG, P. & LIPPMAN, S. M. 2010. Profiling lipoxygenase metabolism in specific steps of colorectal tumorigenesis. *Cancer Prev Res (Phila),* 3, 829-38.

SHUREIQI, I., WOJNO, K. J., POORE, J. A., REDDY, R. G., MOUSSALLI, M. J., SPINDLER, S. A., GREENSON, J. K., NORMOLLE, D., HASAN, A. A., LAWRENCE, T. S. & BRENNER, D. E. 1999. Decreased 13-S-hydroxyoctadecadienoic acid levels and 15-lipoxygenase-1 expression in human colon cancers. *Carcinogenesis,* 20, 1985-95.

SHUREIQI, I., XU, X., CHEN, D., LOTAN, R., MORRIS, J. S., FISCHER, S. M. & LIPPMAN, S. M. 2001. Nonsteroidal anti-inflammatory drugs induce apoptosis in esophageal cancer cells by restoring 15-lipoxygenase-1 expression. *Cancer Res,* 61, 4879-84.

SHUTT, J. D., BOGER, P., NEALE, J. R., PATEL, P. & SAMPSON, A. P. 2012. Activity of the leukotriene pathway in Barrett's metaplasia and oesophageal adenocarcinoma. *Inflamm Res.*

SIEHL, J. & THIEL, E. 2007. C-kit, GIST, and imatinib. *Recent Results Cancer Res,* 176, 145-51.

SINGH, A. K., KANT, S., PARSHAD, R., BANERJEE, N. & DEY, S. 2011. Evaluation of human LOX-12 as a serum marker for breast cancer. *Biochem Biophys Res Commun,* 414, 304-8.

SIVAMANI, R. K. 2014. Eicosanoids and Keratinocytes in Wound Healing. *Adv Wound Care (New Rochelle),* 3, 476-81.

SNUDERL, M., BATISTA, A., KIRKPATRICK, N. D., RUIZ DE ALMODOVAR, C., RIEDEMANN, L., WALSH, E. C., ANOLIK, R., HUANG, Y., MARTIN, J. D., KAMOUN, W., KNEVELS, E., SCHMIDT, T., FARRAR, C. T., VAKOC, B. J., MOHAN, N., CHUNG, E., ROBERGE, S., PETERSON, T., BAIS, C., ZHELYAZKOVA, B. H., YIP, S., HASSELBLATT, M., ROSSIG, C., NIEMEYER, E., FERRARA, N., KLAGSBRUN, M., DUDA, D. G., FUKUMURA, D., XU, L., CARMELIET, P. & JAIN, R. K. 2013. Targeting placental growth factor/neuropilin 1 pathway inhibits growth and spread of medulloblastoma. *Cell,* 152, 1065-76.

SOBHANI, I. & LE GOUVELLO, S. 2009. Critical role for CD8+FoxP3+ regulatory T cells in colon cancer immune response in humans. *Gut,* 58, 743-4.

SOKER, S., TAKASHIMA, S., MIAO, H. Q., NEUFELD, G. & KLAGSBRUN, M. 1998. Neuropilin-1 is expressed by endothelial and tumor cells as an isoform-specific receptor for vascular endothelial growth factor. *Cell,* 92, 735-45.

SOUZA, R. F., SHEWMAKE, K., BEER, D. G., CRYER, B. & SPECHLER, S. J. 2000. Selective inhibition of cyclooxygenase-2 suppresses growth and induces apoptosis in human esophageal adenocarcinoma cells. *Cancer Res,* 60, 5767-72.

SPECHLER, S. J. 2013. Barrett esophagus and risk of esophageal cancer: a clinical review. *JAMA,* 310, 627-36.

SPINOZZI, F., RUSSANO, A. M., PIATTONI, S., AGEA, E., BISTONI, O., DE BENEDICTIS, D. & DE BENEDICTIS, F. M. 2004. Biological effects of montelukast, a cysteinyl-leukotriene receptor-antagonist, on T lymphocytes. *Clin Exp Allergy,* 34, 1876-82.

SPITE, M., HELLMANN, J., TANG, Y., MATHIS, S. P., KOSURI, M., BHATNAGAR, A., JALA, V. R. & HARIBABU, B. 2011. Deficiency of the leukotriene B4 receptor, BLT-1, protects against systemic insulin resistance in diet-induced obesity. *J Immunol,* 187, 1942-9.

STATON, C. A., STRIBBLING, S. M., TAZZYMAN, S., HUGHES, R., BROWN, N. J. & LEWIS, C. E. 2004. Current methods for assaying angiogenesis in vitro and in vivo. *Int J Exp Pathol,* 85, 233-48.

STEINHILBER, D. & HOFMANN, B. 2014. Recent advances in the search for novel 5-lipoxygenase inhibitors. *Basic Clin Pharmacol Toxicol,* 114, 70-7.

STOCK, N. S., BAIN, G., ZUNIC, J., LI, Y., ZIFF, J., ROPPE, J., SANTINI, A., DARLINGTON, J., PRODANOVICH, P., KING, C. D., BACCEI, C., LEE, C., RONG, H., CHAPMAN, C., BROADHEAD, A., LORRAIN, D., CORREA, L., HUTCHINSON, J. H., EVANS, J. F. & PRASIT, P. 2011. 5-Lipoxygenase-activating protein (FLAP) inhibitors. Part 4: development of 3-[3-tert-butylsulfanyl-1-[4-(6-ethoxypyridin-3-yl)benzyl]-5-(5-methylpyridin-2-y lmethoxy)-1H-indol-2-yl]-2,2-dimethylpropionic acid (AM803), a potent, oral, once daily FLAP inhibitor. *J Med Chem,* 54, 8013-29.

STRATTON, M. R., CAMPBELL, P. J. & FUTREAL, P. A. 2009. The cancer genome. *Nature,* 458, 719-24.

STURM, I., PETROWSKY, H., VOLZ, R., LORENZ, M., RADETZKI, S., HILLEBRAND, T., WOLFF, G., HAUPTMANN, S., DORKEN, B. & DANIEL, P. T. 2001. Analysis of p53/BAX/p16(ink4a/CDKN2) in esophageal squamous cell carcinoma: high BAX and p16(ink4a/CDKN2) identifies patients with good prognosis. *J Clin Oncol,* 19, 2272-81.

SUD'INA, G. F., PUSHKAREVA, M. A., SHEPHARD, P. & KLEIN, T. 2008. Cyclooxygenase (COX) and 5-lipoxygenase (5-LOX) selectivity of COX inhibitors. *Prostaglandins Leukot Essent Fatty Acids,* 78, 99-108.

SUGIURA, K., OZAWA, S., KITAGAWA, Y., UEDA, M. & KITAJIMA, M. 2007. Co-expression of aFGF and FGFR-1 is predictive of a poor prognosis in patients with esophageal squamous cell carcinoma. *Oncol Rep,* 17, 557-64.

SUISSA, S., DENNIS, R., ERNST, P., SHEEHY, O. & WOOD-DAUPHINEE, S. 1997. Effectiveness of the leukotriene receptor antagonist zafirlukast for mild-to-moderate asthma. A randomized, double-blind, placebo-controlled trial. *Ann Intern Med,* 126, 177-83.

SUN, W., POWELL, M., O'DWYER, P. J., CATALANO, P., ANSARI, R. H. & BENSON, A. B., 3RD 2010. Phase II study of sorafenib in combination with docetaxel and cisplatin in the treatment of metastatic or advanced gastric and gastroesophageal junction adenocarcinoma: ECOG 5203. *J Clin Oncol,* 28, 2947-51.

SUNPAWERAVONG, P., SUNPAWERAVONG, S., PUTTAWIBUL, P., MITARNUN, W., ZENG, C., BARON, A. E., FRANKLIN, W., SAID, S. & VARELLA-GARCIA, M. 2005. Epidermal growth factor receptor and cyclin D1 are independently amplified and overexpressed in esophageal squamous cell carcinoma. *J Cancer Res Clin Oncol,* 131, 111-9.

SUNTHARALINGAM, M., WINTER, K. & ILSON, D. H. 2014. The initial report of RTOG 0436: A phase III trial evaluating the addition of cetuximab to paclitaxel, cisplatin, and radiation for patients with esophageal cancer treated without surgery. *2014 Gastrointestinal Cancers Symposium. Abstract LBA6. Presented January 16, 2014.*

SURANENI, M. V., MOORE, J. R., ZHANG, D., BADEAUX, M., MACALUSO, M. D., DIGIOVANNI, J., KUSEWITT, D. & TANG, D. G. 2014. Tumor-suppressive functions of 15-Lipoxygenase-2 and RB1CC1 in prostate cancer. *Cell Cycle,* 13, 1798-810.

SUZUKI, H., UEDA, T., JURANEK, I., YAMAMOTO, S., KATOH, T., NODE, M. & SUZUKI, T. 2000. Hinokitiol, a selective inhibitor of the platelet-type isozyme of arachidonate 12-lipoxygenase. *Biochem Biophys Res Commun,* 275, 885-9.

TAGER, A. M., BROMLEY, S. K., MEDOFF, B. D., ISLAM, S. A., BERCURY, S. D., FRIEDRICH, E. B., CARAFONE, A. D., GERSZTEN, R. E. & LUSTER, A. D. 2003. Leukotriene B4 receptor BLT1 mediates early effector T cell recruitment. *Nat Immunol,* 4, 982-90.

TAGER, A. M. & LUSTER, A. D. 2003. BLT1 and BLT2: the leukotriene B(4) receptors. *Prostaglandins Leukot Essent Fatty Acids,* 69, 123-34.

TAKAHASHI, Y., TUCKER, S. L., KITADAI, Y., KOURA, A. N., BUCANA, C. D., CLEARY, K. R. & ELLIS, L. M. 1997. Vessel counts and expression of vascular endothelial growth factor as prognostic factors in node-negative colon cancer. *Arch Surg,* 132, 541-6.

TAKIKITA, M., HU, N., SHOU, J. Z., WANG, Q. H., GIFFEN, C., TAYLOR, P. R. & HEWITT, S. M. 2009. Biomarkers of apoptosis and survival in esophageal squamous cell carcinoma. *BMC Cancer,* 9, 310.

TAN, B. T., PARK, C. Y., AILLES, L. E. & WEISSMAN, I. L. 2006. The cancer stem cell hypothesis: a work in progress. *Lab Invest,* 86, 1203-7.

TAN, W., WU, J., ZHANG, X., GUO, Y., LIU, J., SUN, T., ZHANG, B., ZHAO, D., YANG, M., YU, D. & LIN, D. 2007. Associations of functional polymorphisms in cyclooxygenase-2 and platelet 12-lipoxygenase with risk of occurrence and advanced disease status of colorectal cancer. *Carcinogenesis,* 28, 1197-201.

TANG, D. G., DIGLIO, C. A. & HONN, K. V. 1994. Activation of microvascular endothelium by eicosanoid 12(S)-hydroxyeicosatetraenoic acid leads to enhanced tumor cell adhesion via up-regulation of surface expression of alpha v beta 3 integrin: a posttranscriptional, protein kinase C- and cytoskeleton-dependent process. *Cancer Res,* 54, 1119-29.

TANG, D. G., GROSSI, I. M., CHEN, Y. Q., DIGLIO, C. A. & HONN, K. V. 1993. 12(S)-HETE promotes tumor-cell adhesion by increasing surface expression of alpha V beta 3 integrins on endothelial cells. *Int J Cancer,* 54, 102-11.

TARDIF, J. C., L'ALLIER P, L., IBRAHIM, R., GREGOIRE, J. C., NOZZA, A., COSSETTE, M., KOUZ, S., LAVOIE, M. A., PAQUIN, J., BROTZ, T. M., TAUB, R. & PRESSACCO, J. 2010. Treatment with 5-lipoxygenase inhibitor VIA-2291 (Atreleuton) in patients with recent acute coronary syndrome. *Circ Cardiovasc Imaging,* 3, 298-307.

TARUI, T., MAJUMDAR, M., MILES, L. A., RUF, W. & TAKADA, Y. 2002. Plasmin-induced migration of endothelial cells. A potential target for the anti-angiogenic action of angiostatin. *J Biol Chem,* 277, 33564-70.

TERSEY, S. A., BOLANIS, E., HOLMAN, T. R., MALONEY, D. J., NADLER, J. L. & MIRMIRA, R. G. 2015. Minireview: 12-Lipoxygenase and Islet beta-Cell Dysfunction in Diabetes. *Mol Endocrinol,* 29, 791-800.

TEW, W. P., KELSEN, D. P. & ILSON, D. H. 2005. Targeted therapies for esophageal cancer. *Oncologist,* 10, 590-601.

TEWARI, K. S., SILL, M. W., LONG, H. J., 3RD, PENSON, R. T., HUANG, H., RAMONDETTA, L. M., LANDRUM, L. M., OAKNIN, A., REID, T. J., LEITAO, M. M., MICHAEL, H. E. & MONK, B. J. 2014. Improved survival with bevacizumab in advanced cervical cancer. *N Engl J Med,* 370, 734-43.

TIMAR, J., RASO, E., DOME, B., LI, L., GRIGNON, D., NIE, D., HONN, K. V. & HAGMANN, W. 2000. Expression, subcellular localization and putative function of platelet-type 12-lipoxygenase in human prostate cancer cell lines of different metastatic potential. *Int J Cancer,* 87, 37-43.

TIMAR, J., RASO, E., HONN, K. V. & HAGMANN, W. 1999. 12-lipoxygenase expression in human melanoma cell lines. *Adv Exp Med Biol,* 469, 617-22.

TONG, W. G., DING, X. Z., WITT, R. C. & ADRIAN, T. E. 2002. Lipoxygenase inhibitors attenuate growth of human pancreatic cancer xenografts and induce apoptosis through the mitochondrial pathway. *Mol Cancer Ther,* 1, 929-35.

TORRE, L. A., BRAY, F., SIEGEL, R. L., FERLAY, J., LORTET-TIEULENT, J. & JEMAL, A. 2015. Global cancer statistics, 2012. *CA Cancer J Clin,* 65, 87-108.

TRIADAFILOPOULOS, G., KACZYNSKA, M. & IWANE, M. 1996. Esophageal mucosal eicosanoids in gastroesophageal reflux disease and Barrett's esophagus. *Am J Gastroenterol,* 91, 65-74.

TSUJII, M., KAWANO, S., TSUJI, S., SAWAOKA, H., HORI, M. & DUBOIS, R. N. 1998. Cyclooxygenase regulates angiogenesis induced by colon cancer cells. *Cell,* 93, 705-16.

URONIS, H. E., BENDELL, J. C., ALTOMARE, I., BLOBE, G. C., HSU, S. D., MORSE, M. A., PANG, H., ZAFAR, S. Y., CONKLING, P., FAVARO, J., ARROWOOD, C. C., CUSHMAN, S. M., MEADOWS, K. L., BRADY, J. C., NIXON, A. B. & HURWITZ, H. I. 2013. A phase II study of capecitabine, oxaliplatin, and bevacizumab in the treatment of metastatic esophagogastric adenocarcinomas. *Oncologist,* 18, 271-2.

UZUNOGLU, F. G., KOENIG, A. M. & IZBICKI, J. R. 2014. The potential for targeting HER2 therapeutically in esophageal cancer - a grasp at straws? *Expert Opin Ther Targets,* 18, 1421-6.

VALLBOHMER, D., PETERS, J. H., KURAMOCHI, H., OH, D., YANG, D., SHIMIZU, D., DEMEESTER, S. R., HAGEN, J. A., CHANDRASOMA, P. T., DANENBERG, K. D., DANENBERG, P. V. & DEMEESTER, T. R. 2006. Molecular determinants in targeted therapy for esophageal adenocarcinoma. *Arch Surg,* 141, 476-81; discussion 481-2.

VAN BAAL, J. W., BOZIKAS, A., PRONK, R., TEN KATE, F. J., MILANO, F., RYGIEL, A. M., ROSMOLEN, W. D., PEPPELENBOSCH, M. P., BERGMAN, J. J. & KRISHNADATH, K. K. 2008. Cytokeratin and CDX-2 expression in Barrett's esophagus. *Scand J Gastroenterol,* 43, 132-40.

VAN CUTSEM, E., BAJETTA, E., VALLE, J., KOHNE, C. H., HECHT, J. R., MOORE, M., GERMOND, C., BERG, W., CHEN, B. L., JALAVA, T., LEBWOHL, D., MEINHARDT, G., LAURENT, D. & LIN, E. 2011. Randomized, placebo-controlled, phase III study of oxaliplatin, fluorouracil, and leucovorin with or without PTK787/ZK 222584 in patients with previously treated metastatic colorectal adenocarcinoma. *J Clin Oncol,* 29, 2004-10.

VAN CUTSEM, E., DE HASS, S., KANG, Y.K., OHTSU, A., TEBBUTT, N.C., MING XU, J. YONG, W.P., LANGER, B., DELMAR, P, SCHERER, S.J., & SHAH, M.A. 2012. Bevacizumab in combination with chemotherapy as first-line therapy in advanced gastric cancer: a biomarker evaluation from the AVAGAST randomized phase III trial. *J Clin Oncol*, 30, 2119–27.

VAN HAGEN, P., HULSHOF, M. C. C. M., VAN LANSCHOT, J. J. B., STEYERBERG, E. W., HENEGOUWEN, M. I. V. B., WIJNHOVEN, B. P. L., RICHEL, D. J., NIEUWENHUIJZEN, G. A. P., HOSPERS, G. A. P., BONENKAMP, J. J., CUESTA, M. A., BLAISSE, R. J. B., BUSCH, O. R. C., TEN KATE, F. J. W., CREEMERS, G.-J., PUNT, C. J. A., PLUKKER, J. T. M., VERHEUL, H. M. W., BILGEN, E. J. S., VAN DEKKEN, H., VAN DER SANGEN, M. J. C., ROZEMA, T., BIERMANN, K., BEUKEMA, J. C., PIET, A. H. M., VAN RIJ, C. M., REINDERS, J. G., TILANUS, H. W. & VAN DER

GAAST, A. 2012. Preoperative Chemoradiotherapy for Esophageal or Junctional Cancer. *New England Journal of Medicine,* 366, 2074-2084.

VASUDEV, N. S. & REYNOLDS, A. R. 2014. Anti-angiogenic therapy for cancer: current progress, unresolved questions and future directions. *Angiogenesis,* 17, 471-94.

VERHEUL, H. M. & PINEDO, H. M. 2007. Possible molecular mechanisms involved in the toxicity of angiogenesis inhibition. *Nat Rev Cancer,* 7, 475-85.

VON RAHDEN, B. H., STEIN, H. J., PUHRINGER, F., KOCH, I., LANGER, R., PIONTEK, G., SIEWERT, J. R., HOFLER, H. & SARBIA, M. 2005. Coexpression of cyclooxygenases (COX-1, COX-2) and vascular endothelial growth factors (VEGF-A, VEGF-C) in esophageal adenocarcinoma. *Cancer Res,* 65, 5038-44.

VONA-DAVIS, L. & ROSE, D. P. 2013. The obesity-inflammation-eicosanoid axis in breast cancer. *J Mammary Gland Biol Neoplasia,* 18, 291-307.

WADDELL, T., CHAU, I., CUNNINGHAM, D., GONZALEZ, D., OKINES, A. F., OKINES, C., WOTHERSPOON, A., SAFFERY, C., MIDDLETON, G., WADSLEY, J., FERRY, D., MANSOOR, W., CROSBY, T., COXON, F., SMITH, D., WATERS, J., IVESON, T., FALK, S., SLATER, S., PECKITT, C. & BARBACHANO, Y. 2013. Epirubicin, oxaliplatin, and capecitabine with or without panitumumab for patients with previously untreated advanced oesophagogastric cancer (REAL3): a randomised, open-label phase 3 trial. *Lancet Oncol,* 14, 481-9.

WAINBERG, Z. A., LIN, L. S., DICARLO, B., DAO, K. M., PATEL, R., PARK, D. J., WANG, H. J., ELASHOFF, R., RYBA, N. & HECHT, J. R. 2011. Phase II trial of modified FOLFOX6 and erlotinib in patients with metastatic or advanced adenocarcinoma of the oesophagus and gastro-oesophageal junction. *Br J Cancer,* 105, 760-5.

WAJCHENBERG, B. L. 2000. Subcutaneous and visceral adipose tissue: their relation to the metabolic syndrome. *Endocr Rev,* 21, 697-738.

WAKATSUKI, K., SHO, M., YAMATO, I., TAKAYAMA, T., MATSUMOTO, S., TANAKA, T., MIGITA, K., ITO, M., HOTTA, K. & NAKAJIMA, Y. 2013. Clinical impact of tumor-infiltrating CD45RO(+) memory T cells on human gastric cancer. *Oncol Rep,* 29, 1756-62.

WALKER, J. L., LOSCALZO, J. & ZHANG, Y. Y. 2002. 5-Lipoxygenase and human pulmonary artery endothelial cell proliferation. *Am J Physiol Heart Circ Physiol,* 282, H585-93.

WANG, B., YU, S. C., JIANG, J. Y., PORTER, G. W., ZHAO, L. T., WANG, Z., TAN, H., CUI, Y. H., QIAN, C., PING, Y. F. & BIAN, X. W. 2011a. An inhibitor of arachidonate 5-lipoxygenase, Nordy, induces differentiation and inhibits self-renewal of glioma stem-like cells. *Stem Cell Rev,* 7, 458-70.

WANG, C. H., CHIOU, S. H., CHOU, C. P., CHEN, Y. C., HUANG, Y. J. & PENG, C. A. 2011b. Photothermolysis of glioblastoma stem-like cells targeted by carbon nanotubes conjugated with CD133 monoclonal antibody. *Nanomedicine,* 7, 69-79.

WANG, D. & DUBOIS, R. N. 2010. Eicosanoids and cancer. *Nat Rev Cancer,* 10, 181-93.

WANG, D., WANG, H., BROWN, J., DAIKOKU, T., NING, W., SHI, Q., RICHMOND, A., STRIETER, R., DEY, S. K. & DUBOIS, R. N. 2006. CXCL1 induced by prostaglandin E2 promotes angiogenesis in colorectal cancer. *J Exp Med,* 203, 941-51.

WASILEWICZ, M. P., KOLODZIEJ, B., BOJULKO, T., KACZMARCZYK, M., SULZYC-BIELICKA, V., BIELICKI, D. & CIEPIELA, K. 2010. Overexpression of 5-lipoxygenase in sporadic colonic adenomas and a possible new aspect of colon carcinogenesis. *Int J Colorectal Dis,* 25, 1079-85.

WEIS, S. M. & CHERESH, D. A. 2011. Tumor angiogenesis: molecular pathways and therapeutic targets. *Nat Med,* 17, 1359-70.

WEJKSZA, K., LEE-CHANG, C., BODOGAI, M., BONZO, J., GONZALEZ, F. J., LEHRMANN, E., BECKER, K. & BIRAGYN, A. 2013. Cancer-produced metabolites of 5-lipoxygenase induce tumor-evoked regulatory B cells via peroxisome proliferator-activated receptor alpha. *J Immunol,* 190, 2575-84.

WELTI, J. C., GOURLAOUEN, M., POWLES, T., KUDAHETTI, S. C., WILSON, P., BERNEY, D. M. & REYNOLDS, A. R. 2011. Fibroblast growth factor 2 regulates endothelial cell sensitivity to sunitinib. *Oncogene,* 30, 1183-93.

WEN, Z., LIU, H., LI, M., LI, B., GAO, W., SHAO, Q., FAN, B., ZHAO, F., WANG, Q., XIE, Q., YANG, Y., YU, J. & QU, X. 2014. Increased metabolites of 5-lipoxygenase from hypoxic ovarian cancer cells promote tumor-associated macrophage infiltration. *Oncogene.*

WERNER, D., ATMACA, A., PAULIGK, C., PUSTOWKA, A., JAGER, E. & AL-BATRAN, S. E. 2013. Phase I study of everolimus and mitomycin C for patients with metastatic esophagogastric adenocarcinoma. *Cancer Med,* 2, 325-33.

WHITMAN, S., GEZGINCI, M., TIMMERMANN, B. N. & HOLMAN, T. R. 2002. Structure-activity relationship studies of nordihydroguaiaretic acid inhibitors toward soybean, 12-human, and 15-human lipoxygenase. *J Med Chem,* 45, 2659-61.

WILKE, H., VAN CUTSEM, E. & OH, S. C. E. A. RAINBOW: A global, phase 3, randomized, double-blind study of ramucirumab plus paclitaxel versus placebo plus paclitaxel in the treatment of metastatic gastric adenocarcinoma following disease progression on first-line platinum- and fluoropyrimidine-containing combination therapy: Results of a multiple Cox regression analysis adjusting for prognostic factors. *J Clin Oncol 32:5s, 2014 (suppl; abstr 4076).*

WILKINSON, N. W., BLACK, J. D., ROUKHADZE, E., DRISCOLL, D., SMILEY, S., HOSHI, H., GERADTS, J., JAVLE, M. & BRATTAIN, M. 2004. Epidermal growth factor receptor expression correlates with histologic grade in resected esophageal adenocarcinoma. *J Gastrointest Surg,* 8, 448-53.

WINER, I., NORMOLLE, D. P., SHUREIQI, I., SONDAK, V. K., JOHNSON, T., SU, L. & BRENNER, D. E. 2002. Expression of 12-lipoxygenase as a biomarker for melanoma carcinogenesis. *Melanoma Res,* 12, 429-34.

WONG, B. C., WANG, W. P., CHO, C. H., FAN, X. M., LIN, M. C., KUNG, H. F. & LAM, S. K. 2001. 12-Lipoxygenase inhibition induced apoptosis in human gastric cancer cells. *Carcinogenesis,* 22, 1349-54.

WONG, S. & WITTE, O. N. 2004. The BCR-ABL story: bench to bedside and back. *Annu Rev Immunol,* 22, 247-306.

WOODS, J. W., COFFEY, M. J., BROCK, T. G., SINGER, II & PETERS-GOLDEN, M. 1995. 5-Lipoxygenase is located in the euchromatin of the nucleus in resting human alveolar macrophages and translocates to the nuclear envelope upon cell activation. *J Clin Invest,* 95, 2035-46.

WRIGHT, L., TUDER, R. M., WANG, J., COOL, C. D., LEPLEY, R. A. & VOELKEL, N. F. 1998. 5-Lipoxygenase and 5-lipoxygenase activating protein (FLAP) immunoreactivity in lungs from patients with primary pulmonary hypertension. *Am J Respir Crit Care Med,* 157, 219-29.

XI, H., BALDUS, S. E., WARNECKE-EBERZ, U., BRABENDER, J., NEISS, S., METZGER, R., LING, F. C., DIENES, H. P., BOLLSCHWEILER, E., MOENIG, S., MUELLER, R. P., HOELSCHER, A. H. & SCHNEIDER, P. M. 2005. High cyclooxygenase-2 expression following neoadjuvant radiochemotherapy is associated with minor histopathologic response and poor prognosis in esophageal cancer. *Clin Cancer Res,* 11, 8341-7.

XU, L., STEVENS, J., HILTON, M. B., SEAMAN, S., CONRADS, T. P., VEENSTRA, T. D., LOGSDON, D., MORRIS, H., SWING, D. A., PATEL, N. L., KALEN, J., HAINES, D. C., ZUDAIRE, E. & ST CROIX, B. 2014a. COX-2 inhibition potentiates antiangiogenic cancer therapy and prevents metastasis in preclinical models. *Sci Transl Med,* 6, 242ra84.

XU, X. L., LING, Z. Q., CHEN, S. Z., LI, B., JI, W. H. & MAO, W. M. 2014b. The impact of E-cadherin expression on the prognosis of esophageal cancer: a meta-analysis. *Dis Esophagus,* 27, 79-86.

XU, X. M., YUAN, G. J., DENG, J. J., GUO, H. T., XIANG, M., YANG, F., GE, W. & CHEN, S. Y. 2012. Inhibition of 12-lipoxygenase reduces proliferation and induces apoptosis of hepatocellular carcinoma cells in vitro and in vivo. *Hepatobiliary Pancreat Dis Int,* 11, 193-202.

YAKKUNDI, A., BENNETT, R., HERNANDEZ-NEGRETE, I., DELALANDE, J. M., HANNA, M., LYUBOMSKA, O., ARTHUR, K., SHORT, A., MCKEEN, H., NELSON, L., MCCRUDDEN, C. M., MCNALLY, R., MCCLEMENTS, L., MCCARTHY, H. O., BURNS, A. J., BICKNELL, R., KISSENPFENNIG, A. & ROBSON, T. 2015. FKBPL is a critical antiangiogenic regulator of developmental and pathological angiogenesis. *Arterioscler Thromb Vasc Biol,* 35, 845-54.

YAMAMOTO, S., KATSUKAWA, M., NAKANO, A., HIRAKI, E., NISHIMURA, K., JISAKA, M., YOKOTA, K. & UEDA, N. 2005. Arachidonate 12-lipoxygenases with reference to their selective inhibitors. *Biochem Biophys Res Commun,* 338, 122-7.

YANG, X., CUI, W., YU, S., XU, C., CHEN, G., GU, A., LI, T., CUI, Y., ZHANG, X. & BIAN, X. 2014. A synthetic dl-nordihydroguaiaretic acid (Nordy), inhibits angiogenesis, invasion

and proliferation of glioma stem cells within a zebrafish xenotransplantation model. *PLoS One,* 9, e85759.

YAO, L., LIU, F., HONG, L., SUN, L., LIANG, S., WU, K. & FAN, D. 2011. The function and mechanism of COX-2 in angiogenesis of gastric cancer cells. *J Exp Clin Cancer Res,* 30, 13.

YE, Y. N., LIU, E. S., SHIN, V. Y., WU, W. K. & CHO, C. H. 2004. Contributory role of 5-lipoxygenase and its association with angiogenesis in the promotion of inflammation-associated colonic tumorigenesis by cigarette smoking. *Toxicology,* 203, 179-88.

YE, Y. N., WU, W. K., SHIN, V. Y., BRUCE, I. C., WONG, B. C. & CHO, C. H. 2005a. Dual inhibition of 5-LOX and COX-2 suppresses colon cancer formation promoted by cigarette smoke. *Carcinogenesis,* 26, 827-34.

YE, Y. N., WU, W. K., SHIN, V. Y. & CHO, C. H. 2005b. A mechanistic study of colon cancer growth promoted by cigarette smoke extract. *Eur J Pharmacol,* 519, 52-7.

YI, J. H., LEE, J., LEE, J., PARK, S. H., PARK, J. O., YIM, D. S., PARK, Y. S., LIM, H. Y. & KANG, W. K. 2012. Randomised phase II trial of docetaxel and sunitinib in patients with metastatic gastric cancer who were previously treated with fluoropyrimidine and platinum. *Br J Cancer,* 106, 1469-74.

YOSHIMURA, R., INOUE, K., KAWAHITO, Y., MITSUHASHI, M., TSUCHIDA, K., MATSUYAMA, M., SANO, H. & NAKATANI, T. 2004. Expression of 12-lipoxygenase in human renal cell carcinoma and growth prevention by its inhibitor. *Int J Mol Med,* 13, 41-6.

YOUNUS, J., VERMA, S., FRANEK, J. & COAKLEY, N. 2010. Sunitinib malate for gastrointestinal stromal tumour in imatinib mesylate–resistant patients: recommendations and evidence. *Curr Oncol,* 17, 4-10.

YU, G., WANG, J., CHEN, Y., WANG, X., PAN, J., LI, G., JIA, Z., LI, Q., YAO, J. C. & XIE, K. 2009. Overexpression of phosphorylated mammalian target of rapamycin predicts lymph node metastasis and prognosis of chinese patients with gastric cancer. *Clin Cancer Res,* 15, 1821-9.

ZHAN, P., WANG, J., LV, X. J., WANG, Q., QIU, L. X., LIN, X. Q., YU, L. K. & SONG, Y. 2009. Prognostic value of vascular endothelial growth factor expression in patients with lung cancer: a systematic review with meta-analysis. *J Thorac Oncol,* 4, 1094-103.

ZHANG, B., WANG, C. L., ZHAO, W. H., LV, M., WANG, C. Y., ZHONG, W. X., ZHOU, W. Y., YU, W. S., ZHANG, Y. & LI, S. 2008. Effect of 5-LOX/COX-2 common inhibitor DHDMBF30 on pancreatic cancer cell Capan2. *World J Gastroenterol,* 14, 2494-500.

ZHANG, H. Z., JIN, G. F. & SHEN, H. B. 2012. Epidemiologic differences in esophageal cancer between Asian and Western populations. *Chin J Cancer,* 31, 281-6.

ZHANG, Y., KANG, S., FANG, W., HONG, S., LIANG, W., YAN, Y., QIN, T., TANG, Y., SHENG, J. & ZHANG, L. 2015. Impact of smoking status on EGFR-TKI efficacy for advanced non-small-cell lung cancer in EGFR mutants: a meta-analysis. *Clin Lung Cancer,* 16, 144-151 e1.

ZHI, H., WANG, L., ZHANG, J., ZHOU, C., DING, F., LUO, A., WU, M., ZHAN, Q. & LIU, Z. 2006. Significance of COX-2 expression in human esophageal squamous cell carcinoma. *Carcinogenesis,* 27, 1214-21.

ZHI, H., ZHANG, J., HU, G., LU, J., WANG, X., ZHOU, C., WU, M. & LIU, Z. 2003. The deregulation of arachidonic acid metabolism-related genes in human esophageal squamous cell carcinoma. *Int J Cancer,* 106, 327-33.

Appendices

Appendix I: 84 genes on Human Angiogenesis Pathway Finder Array and raw Ct basal expression levels in wild-type HUVEC and OE33 cells

Unigene	Refseq	Symbol	HUVEC Ct	OE33 Ct
Hs.525622	NM_005163	AKT1	22.81	23.4
Hs.283749	NM_001145	ANG	28.36	28.87
Hs.369675	NM_001146	ANGPT1	28.76	UD
Hs.583870	NM_001147	ANGPT2	22.8	28.7
Hs.9613	NM_001039667	ANGPTL4	27.74	25.91
Hs.1239	NM_001150	ANPEP	21.47	UD
Hs.194654	NM_001702	BAI1	UD	UD
Hs.54460	NM_002986	CCL11	UD	UD
Hs.303649	NM_002982	CCL2	22.58	34.29
Hs.76206	NM_001795	CDH5	21.19	UD
Hs.517356	NM_030582	COL18A1	24.03	27.38
Hs.570065	NM_000091	COL4A3	32.73	UD
Hs.410037	NM_001901	CTGF	17.79	28.5
Hs.708652	NM_001511	CXCL1	24.65	23.63
Hs.632586	NM_001565	CXCL10	UD	UD
Hs.89714	NM_002994	CXCL5	29.91	UD
Hs.164021	NM_002993	CXCL6	29.22	26.49
Hs.77367	NM_002416	CXCL9	UD	UD
Hs.713645	NM_001955	EDN1	20.38	26.23
Hs.516664	NM_182685	EFNA1	24.19	24.73
Hs.149239	NM_004093	EFNB2	25.14	24.55
Hs.419815	NM_001963	EGF	UD	UD
Hs.76753	NM_000118	ENG	20.46	24.72
Hs.437008	NM_004444	EPHB4	24.16	23.2
Hs.446352	NM_004448	ERBB2	28.66	22.57
Hs.62192	NM_001993	F3	29.14	19.87
Hs.483635	NM_000800	FGF1	28.45	UD
Hs.284244	NM_002006	FGF2	25.38	UD
Hs.1420	NM_000142	FGFR3	31.29	26.21
Hs.11392	NM_004469	FIGF	29.23	UD
Hs.594454	NM_002019	FLT1	22.44	UD
Hs.203717	NM_002026	FN1	17.97	21.67
Hs.396530	NM_000601	HGF	31.81	UD
Hs.719495	NM_001530	HIF1A	21.71	23.37
Hs.44227	NM_006665	HPSE	27.02	25.69

Hs.504609	NM_002165	ID1	23.89	22.18
Hs.37026	NM_024013	IFNA1	33.21	UD
Hs.856	NM_000619	IFNG	UD	UD
Hs.160562	NM_000618	IGF1	33.91	UD
Hs.126256	NM_000576	IL1B	30.75	29.54
Hs.654458	NM_000600	IL6	24.2	32.69
Hs.624	NM_000584	IL8	23.83	23.23
Hs.436873	NM_002210	ITGAV	22.52	23.43
Hs.218040	NM_000212	ITGB3	24.18	UD
Hs.626544	NM_000214	JAG1	23.77	24.02
Hs.479756	NM_002253	KDR	22.35	UD
Hs.421391	NM_007015	LECT1	UD	UD
Hs.194236	NM_000230	LEP	33.67	UD
Hs.82045	NM_002391	MDK	29.07	27.26
Hs.2399	NM_004995	MMP14	24.6	28.24
Hs.513617	NM_004530	MMP2	21.78	UD
Hs.297413	NM_004994	MMP9	33.55	UD
Hs.647092	NM_000603	NOS3	25.7	27.96
Hs.436100	NM_004557	NOTCH4	23.8	30.58
Hs.653996	NM_003873	NRP1	21.41	22.91
Hs.471200	NM_003872	NRP2	23.45	23.65
Hs.535898	NM_002607	PDGFA	23.29	25.96
Hs.376675	NM_000442	PECAM1	23.99	UD
Hs.81564	NM_002619	PF4	31.36	UD
Hs.252820	NM_002632	PGF	22.44	UD
Hs.77274	NM_002658	PLAU	24.74	22.53
Hs.143436	NM_000301	PLG	28.61	29.35
Hs.528665	NM_021935	PROK2	UD	UD
Hs.201978	NM_000962	PTGS1	24.9	33.64
Hs.154210	NM_001400	S1PR1	22.81	UD
Hs.713079	NM_000602	SERPINE1	17.6	28.44
Hs.532768	NM_002615	SERPINF1	28.69	29.24
Hs.68061	NM_021972	SPHK1	23.99	28.83
Hs.89640	NM_000459	TEK	23.64	UD
Hs.628298	NM_003236	TGFA	32.14	23.87
Hs.645227	NM_000660	TGFB1	21.82	23.68
Hs.133379	NM_003238	TGFB2	24.39	25.49
Hs.494622	NM_004612	TGFBR1	25.51	24.04
Hs.164226	NM_003246	THBS1	17.41	27.18

Hs.371147	NM_003247	THBS2	24.28	25.19
Hs.78824	NM_005424	TIE1	22.46	UD
Hs.522632	NM_003254	TIMP1	22.17	23.71
Hs.633514	NM_003255	TIMP2	21.33	23.71
Hs.644633	NM_000362	TIMP3	23.46	UD
Hs.241570	NM_000594	TNF	34.9	33.78
Hs.730607	NM_001953	TYMP	28.5	27.43
Hs.73793	NM_003376	VEGFA	24.46	23.64
Hs.732095	NM_003377	VEGFB	22.99	23.11
Hs.435215	NM_005429	VEGFC	23.17	UD

Appendix II: Representative BSA standard curve used in BCA protein quantification assay

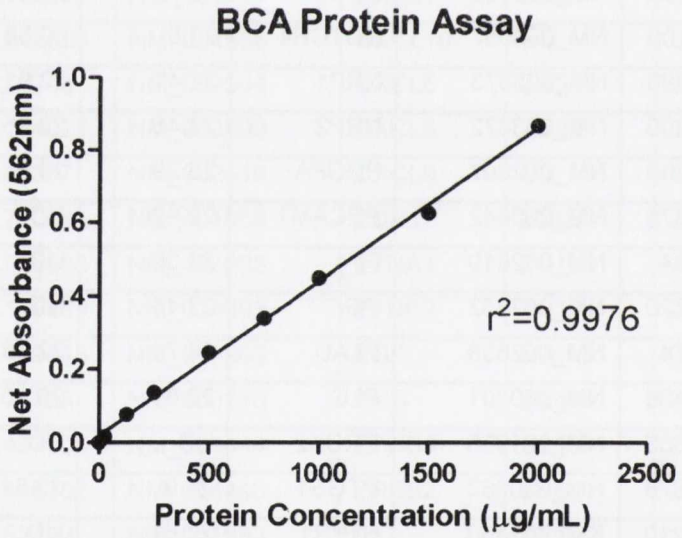

Appendix III: Representative images of tubule formation assay quantification

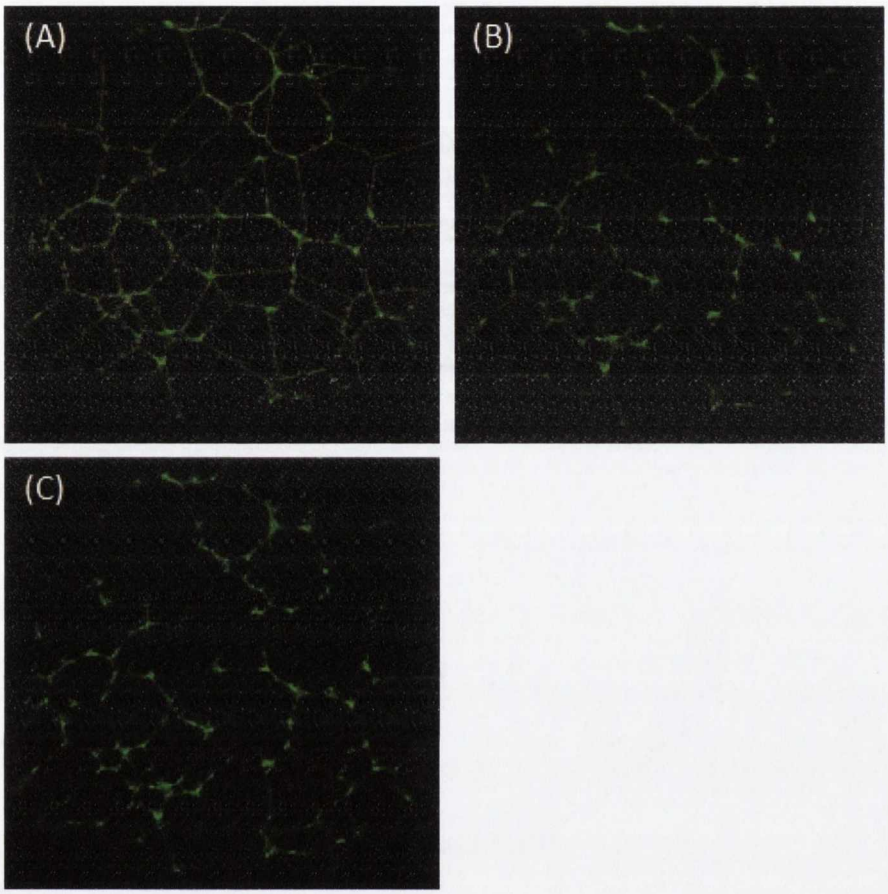

Appendix III: Tubule formation assay: (A) tubule length was measured in pixels using a line tool. (B) Loops regions (indicated by blue 1s) and (C) branch points (indicated by turquoise 2s) were totalled using a cell counter tool. Measurements were made using ImageJ software.

Appendix IV :pcDNA3.1(+) parent vector used for 12-LO overexpression studies

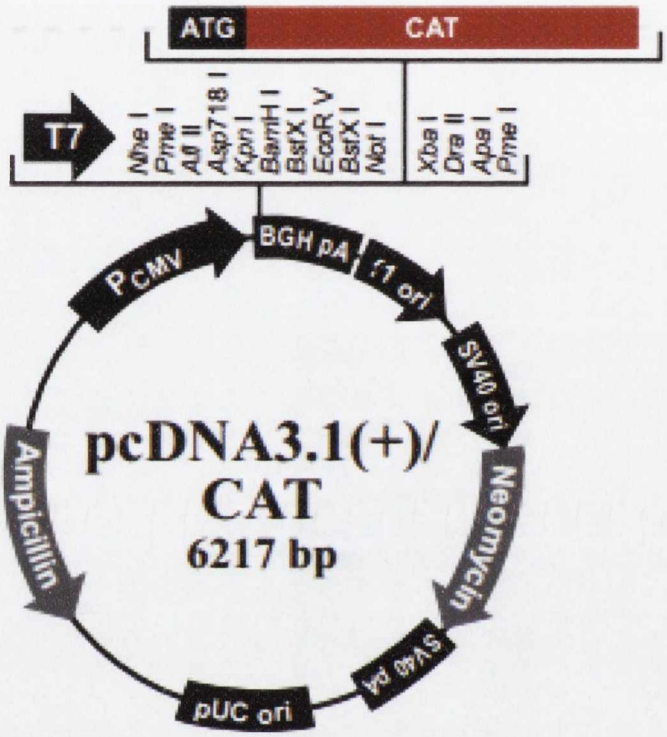

Appendix IV: pcDNA3.1(+) expression plasmid: The full-length cDNA encoding human 12-LO was subcloned into the EcoRI/Xbal site of pcDNA3.1(+) from pCMV (porcine cytomegalovirus) -12-LOX, gifted from Dr. Kenneth Honn (Wayne State University, MI, USA). Image source: www.invitrogen.com

Appendix V: Immune cell markers and cytokines that were stained and scored in the oesophageal cancer TMA and available for correlations with 5-LO and 12-LO IHC staining

Immune marker or cytokine	Function
CD8	T-cell marker
CD69	Lymphocyte activation marker, proliferation/activation of T-cells
CD56	NK cell marker
IL-10	Anti-inflammatory cytokine, suppresses macrophage cytokine release
TGF-β	Regulatory cytokine, regulates lymphocyte proliferation, differentiation and survival
IFN-γ	Pro-inflammatory cytokine, macrophage activation
IL-4	Cytokine, stimulates Th2 differentiation
FoxP3	Immunosuppressive marker
IL-17	Pro-inflammatory cytokine, monocyte and/or neutrophil recruitment
CD68	Macrophage homing marker
CD3	T-cell marker (all T-cells)
CD45RO	regulator of T- and B-cell antigen receptor signalling
CD107A	Degranulation marker (i.e. basophils, NK cells and cytotoxic T-cell)

Appendix VI Novel 5-LO and 12-LO inhibitor names and corresponding chemical structures

Drug name	Structural backbone	Registration I.D.	Structure
NIH1	Phenylenediamine	NCGC00241581-01	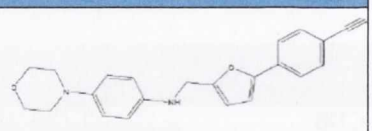
NIH2	Phenylenediamine	NCGC00241585-01	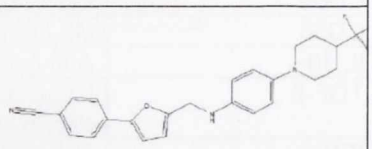
NIH3	Phenylenediamine	NCGC00187923-01	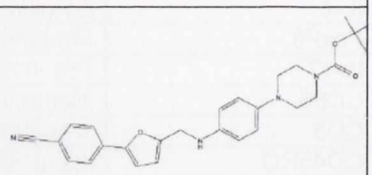
NIH4	Phenylenediamine	NCGC00241580-01	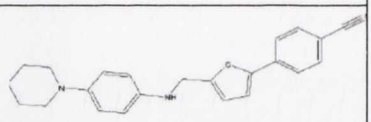
NIH5	8-hydroxyquinoline	NCGC00188868-01	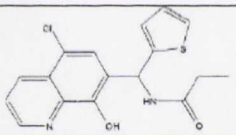
NIH6	8-hydroxyquinoline	NCGC00182956-06	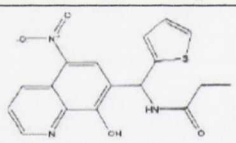
NIH7	Oxadiazol-2-yl benzamide	NCGC00249860-01	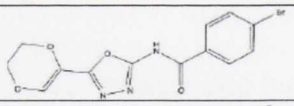
NIH8	Oxadiazol-2-yl benzamide	NCGC00250240-01	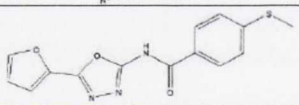
NIH9	Oxadiazol-2-yl benzamide	NCGC00249679-01	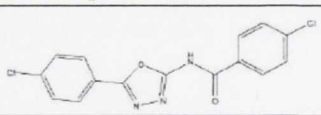
NIH10	8-hydroxyquinoline	NCGC00188369-02	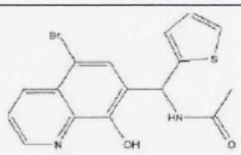
NIH11	8-hydroxyquinoline	NCGC00188370-03	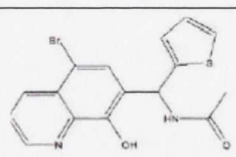

NIH12	Oxadiazol-2-yl benzamide	NCGC00249881-01	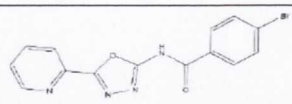
NIH13	8-hydroxyquinoline	NCGC00183685-03	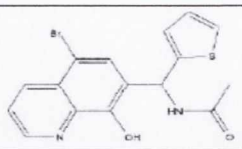
NIH14	Oxadiazol-2-yl benzamide	NCGC00250250-01	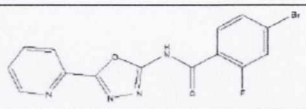
NIH15	Oxadiazol-2-yl benzamide	NCGC00182932-04	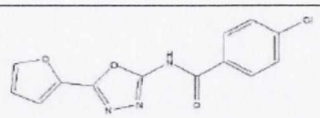
GM1	Benzenesulfonamide	NCGC00345009-05	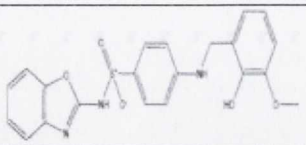
GM2	Benzenesulfonamide	NCGC00263773-08	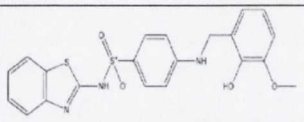
GM3	Benzenesulfonamide	NCGC00263323-01	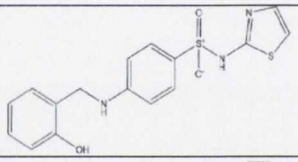
GM4	Benzenesulfonamide	NCGC00319012-03	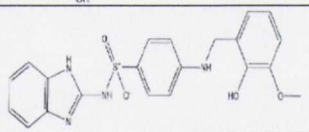
GM5	Benzenesulfonamide	NCGC00346865-01	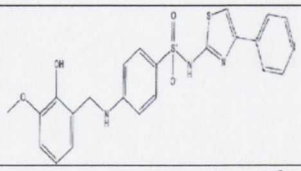
GM6	Benzenesulfonamide	NCGC00263709-01	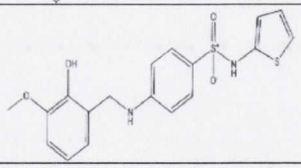
GM7	Benzenesulfonamide	NCGC00262831-01